ANNUAL REVIEW

INSTITUTE FOR MOLECULAR SCIENCE

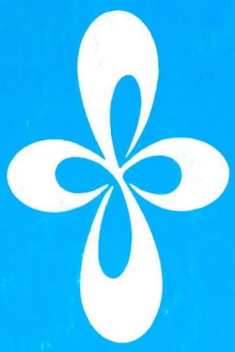

1989

ANNUAL REVIEW

INSTITUTE FOR MOLECULAR SCIENCE

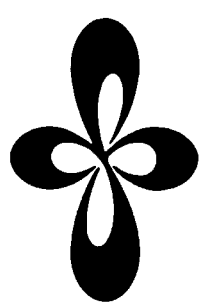

1989

Published by
Institute for Molecular Science
Okazaki National Research Institutes
Myodaiji, Okazaki 444, Japan
Phone 0564-54-1111
Telex 4537-475 KOKKEN J

IMS 1989

Research activities at IMS have progressed favorably in 1989. The subjects worthy of special mention are as follows: (1) The Graduate University for Advanced Studies has opened, and as one of the constituents of the University the Institute for Molecular Science has accepted 11 doctor-course graduate students, (2) two new laboratories, faculty members of which are appointed for a two year term, are operating, and (3) a new laboratory building, called the South Laboratory Building, has been constructed. The improvement of the graduate educational system will not only strengthen the research at IMS and increase the circulation of researchers, but also help to maintain the activities of the Institute in the years to come.

The circulation of researchers continues apace. Many researchers and technical associates at IMS have been promoted and/or have moved to positions at universities and research institutes all over Japan. New researchers and technical associates have been appointed to fill the vacancies at IMS.

The newly established laboratories mentioned above are the Laboratory for Surface Molecular Science and the Laboratory for Physical Organic Chemistry. In the former, surface science will be studied using the UVSOR synchrotron radiation facility, for the first two years by the staff moved from the Catalyst Chemistry Center of Hokkaido University. Associate Professors T. Matsushima and S. Sato have been appointed to the positions of this laboratory. The Laboratory for Physical Organic Chemistry has been established to strengthen cooperation between researchers in the fields of organic chemistry and molecular science. Professor Y. Tsuno and Associate Professor J. Inanaga from Kyushu University have been appointed.

The Laboratory for Functional Coordination Chemistry has been recently established within the Coordination Chemistry Laboratories.

Professor Robert G. Parr, who contributed greatly as a foreign member of the IMS Council, resigned from the position. Professor John C. Polanyi of the University of Toronto has accepted our invitation to become a foreign member, and I hope to receive advice concerning the future plans of the Institute from him.

September, 1989

H. Inokuchi

Hiroo INOKUCHI

CONTENTS

ORGANIZATION AND STAFF

Organization

The Institute for Molecular Science comprises twenty one research laboratories – each staffed by a professor, and associate professor, two research associates and a few technical associates –, two research laboratories with foreign visiting professors, and six research facilities. The laboratories are grouped into five departments and one facility for coordination chemistry:

Department of Theoretical Studies	Theoretical Studies I
	Theoretical Studies II
	Theoretical Studies III[1)]
Department of Molecular Structure	Molecular Structure I
	Molecular Structure II[1)]
	Molecular Dynamics
Department of Electronic Structure	Excited State Chemistry
	Excited State Dynamics
	Electronic Structure[1)]
	Molecular Energy Conversion[2)]
Department of Molecular Assemblies	Solid State Chemistry
	Photochemistry
	Molecular Assemblies Dynamics
	Interface Molecular Science
	Molecular Assemblies[1)]
	Synchrotron Radiation Research[2)]
Department of Applied Molecular Science	Applied Molecular Science I
	Applied Molecular Science II[1)]
	Physical Organic Chemistry
Coordination Chemistry Laboratories	Synthetic Coordination Chemistry
	Complex Catalysis
	Functional Coordination Chemistry
	Coordination Bond[1)]

Research facilities are:

Computer Center
Chemical Materials Center
Instrument Center
Low-Temperature Center
Equipment Development Center
Ultraviolet Synchrotron Orbital Radiation (UVSOR) Facility.

1) Professors and associate professors are adjunct professors from universities.

2) Research Laboratories with foreign visiting professors.

Scientific Staff

Hiroo INOKUCHI	**Professor, Director-General**

Department of Theoretical Studies

Theoretical Studies I

Keiji MOROKUMA	Professor
Iwao OHMINE	Associate Professor
Koichi YAMASHITA	Research Associate
Masaki SASAI	Research Associate
Mutsumi AOYAGI	Technical Associate (–November '89)[1)]
Osamu KITAO	Technical Associate (–July '89)[2)]
Yoshiaki AMATATSU	Technical Asscociate (January '89–)
Andrea DORIGO	Post-doctoral Fellow (–July '89), JSPS Post-doctoral Fellow (August '89–)
Simon MATHIEU	JSPS Post-doctoral Fellow (March '89–)
Yanbo DING	Visiting Scientist (April–September '89), Graduate Student (October '89–)
Keiichiro SAMESHIMA	Graduate Student from Hoshi College of Pharm.* (–March '89)
Kyoichi SAWABE	Graduate Student from Univ. of Tokyo*
Hiroo FUKUNAGA	Visiting Research Fellow from Fuji Photo Film Co.
Hiroshi KAWAMURA	Visiting Research Fellow from Sumitomo Chemical Co.
Jun ENDO	Visiting Research Fellow from Mitsubishi Petrochemical Co.
Tadahiro OZAWA	Visiting Research Fellow from Kao Corp.

Theoretical Studies II

Hiroki NAKAMURA	Professor
Keiichiro NASU	Associate Professor
Masahiro IWAI	Research Associate
Hidemitsu HAYASHI	Research Associate (–September '89)
Akihiko OHSAKI	Technical Associate
Jun-ichi TAKIMOTO	Technical Associate (–February '89)
Kaoru IWANO	IMS Fellow (April '89–)
Masato SUZUKI	Graduate Student from Hiroshima Univ.* (April '89–)

Theoretical Studies III

Akira IMAMURA	Adjunct Professor from Hiroshima Univ. (–March '89)
Michio MATSUZAWA	Adjunct Professor from The University of Electro-Communications (April '89–)
Kazuo KITAHARA	Adjunct Associate Professor form Tokyo Inst. of Tech. (–March '89)
Yuzo SHINOZUKA	Adjunct Associate Professor from Yamaguchi University (April '89–)
Nobuaki KOGA	Research Associate
Kiyohiko SOMEDA	Research Associate

Department of Molecular Structure

Molecular Structure I

Eizi HIROTA	Professor
Norio MORITA	Associate Professor

Chikashi YAMADA	Research Associate
Toshifumi SUZUKI	Research Associate (–December '88)
Asuka FUJII	Research Associate (September '89–)
Toshinori SUZUKI	Technical Associate (–March '89)
Mitsutaka KUMAKURA	Technical Associate (October '88–)
Edward A. COHEN	Visiting Scientist (–December '88)
Wyn LEWIS-BEVAN	Visiting Scientist (July '89–)
Haruhiko ITO	JSPS Post-doctoral Fellow (–December '88)
Masaharu FUJITAKE	Graduate Student from Hiroshima Univ.* (–March '89) JSPS Post-doctoral Fellow (April '89–August '89)[3]

Molecular Structure II

Akifumi UENO	Adjunct Professor from Toyohashi Univ. of Tech. (–March '89)
Takashi KUSHIDA	Adjunct Professor from Osaka Univ. (April '89–)
Yasuki ENDO	Adjunct Associate Professor from Univ. of Tokyo
Kentarou KAWAGUCHI	Research Associate (–December '88)[4]
Takashi OGURA	Research Associate
Toshinori SUZUKI	Research Associate (April '89–)

Molecular Dynamics

Teizo KITAGAWA	Professor
Yasuo UDAGAWA	Associate Professor
Keiji KAMOGAWA	Research Associate
Kazuyuki TOHJI	Research Associate
Takanori MIZUSHIMA	Technical Associate
Shin'ichiro SATO	Technical Associate
Eleni ANNI	EC Post-doctoral Fellow (–October '89)
Scott L. ANDERSON	Visiting Scientist (August '89–February '90)
Shoji KAMINAKA	JSPS Post-doctoral Fellow (April '89–)
Masashi NAKAGAWA	JSPS Post-doctoral Fellow (April '89–December '89)
Tsuyoshi EGAWA	Graduate Student from Tokyo Metropolitan Univ.*
Takeshi MIKI	Graduate Student from Toyohashi Univ. of Tech.*
Naoyuki TAKAHASHI	Graduate Student from Toyohashi Univ. of Tech.*
Hisashi HAYASHI	Graduate Student (April '89–)
Yasuhisa MIZUTANI	Graduate Student (April '89–)
Yoshinao SAKAN	Graduate Student (April '89–)
Satoshi TAKAHASHI	Graduate Student (April '89–)

Department of Electronic Structure

Excited State Chemistry

Keitaro YOSHIHARA	Professor
Tadayoshi SAKATA	Associate Professor (–May '89)[5]
Hrvoje PETEK	Research Associate
Kazuhito HASHIMOTO	Research Associate (–August '89)[6]
Tohru KOBAYASHI	Technical Associate
Masashi AZUMA	Technical Associate (–March '89)[7]
Stephen R. MEECH	Visiting Scientist (–Dec. '88, July '89–)
Robert PANSU	Visiting Scientist (July '88–August '89)
Klaus KEMNITZ	Visiting Scientist (Sept. '88–Feb. '89)
Ayyakkannu MANIVANNAN	Visiting Scientist (Sept. '88–)

Excited State Dynamics

Ichiro HANAZAKI	Professor
Nobuyuki NISHI	Associate Professor
Masao TAKAYANAGI	Research Associate
Minoru SUMITANI	Research Associate
Kazuhiko OHASHI	Research Associate (October '89–)
Teruhiko NISHIYA	Technical Associate
Kazunori YAMAMOTO	Technical Associate
Yoshihito MORI	Technical Associate (April '89–)
Hiroshi OHOYAMA	IMS Fellow (–May '89)[8]
Fuminori MISAIZU	Graduate Student from the Univ. of Tokyo (–May '89)*
Paul HOUSTON	Visiting Scientist (Feb. '89–April '89)
Prem K. SRIVASTAVA	Visiting Scientist (April '89–)
Kazuhiro HONDA	Graduate Student

Electronic Structure

Koichi ITO	Adjunct Professor form Osaka City Univ.
Haruo ABE	Adjunct Associate Professor from Inst. of Phys. and Chem. Res. (–March '89)
Masaharu OKAZAKI	Adjunct Professor from Government Industrial Research Institute, Nagoya
Ryoichi NAKAGAKI	Research Associate
Hiromi OKAMOTO	Research Associate

Molecular Energy Conversion

John H. D. ELAND	Visiting Professor from Oxford Univ., U.K. (Jan. '89–)
Vlastimil FIDLER	Visiting Associate Professor from Charlus Univ., Czechoslovakia (–August '89)

Department of Molecular Assemblies

Solid State Chemistry

Kyuya YAKUSHI	Professor
Inosuke KOYANO	Associate Professor
Takashi IMAMURA	Research Associate
Akito UGAWA	Research Associate
Shinzo SUZUKI	Technical Associate
Takashi IDA	Technical Associate
Ken-ichi IMAEDA	Technical Associate
Hitoshi FUJIMOTO	Toyota Rikagaku Kenkyusho Post-doctoral Fellow (April '88–January '89)
Takashi IMAJO	IMS Fellow (April '87–March '89)[9]
Kohji KAMIYA	JSPS Post-doctoral Fellow (April '88–July '89) IMS Fellow (August '89–)
Hideo YAMAKADO	Graduate Student of Graduate Univ. for Advanced Studies*

Photochemistry

Katsumi KIMURA	Professor
Kosuke SHOBATAKE	Associate Professor
Kiyohiko TABAYASHI	Research Associate
Katsuhiko OKUYAMA	Research Associate
Masahiko TAKAHASHI	Technical Associate
Hitoshi FUJIMOTO	Technical Associate (February–September '89)[10]
Takato HIRAYAMA	IMS Fellow (December '87–December '88)[11]

Hiroyuki OZEKI	Graduate Student of Graduate Univ. for Advanced Studies (April '89–)
Kunikazu KONDOW	Graduate Student from Nagoya Univ.* (October '88–)
Haruhiko OHASHI	Graduate Student from Toyohashi Univ. of Technology* (April '88–)
Toshiyasu TSUBOUCHI	Graduate Student from Toyohashi Univ. of Technology* (April '89–)
Yasuhiro IWANO	Graduate Student from Toyohashi Univ. of Technology* (April '89–)

Molecular Assemblies Dynamics

Yusei MARUYAMA	Professor
Masatoshi SATO	Associate Professor
Tamotsu INABE	Research Associate
Masashige ONODA	Research Associate
Masafumi SERA	Research Associate
Hajime HOSHI	Technical Associate
Shin-ichi SHAMOTO	Technical Associate
Toshifumi TERUI	Graduate Student from Muroran Inst. of Technology* (November '87–March '89), Graduate Student (April '89–)
Isabelle GAUTIER-LUNEAU	Graduate Student (April '89–)
Shin-ich YAMAGATA	Graduate Student from Nagoya Univ.* (October '88–)
Yoichiro KAWAI	Visiting Research Fellow from Toyota Motor Co., Ltd. (April '87–March '89)
Shinji KONDOH	Visiting Research Fellow from Asahi Glass Co., Ltd. (June '87–May '89)
Yoshiyasu ANDO	Visiting Research Fellow from Nippon Soken, INC. (November '87–March '89)
Chikako NAKANO	Visiting Research Fellow (September '87–)
Hiromichi YAMAMOTO	Visiting Research Fellow (April '88–April '89)[12]

Interface Molecular Science

Shinri SATO	Associate Professor (May '89–)
Tatsuo MATSUSHIMA	Associate Professor (May '89–)
Tadayoshi OHMORI	Research Associate (May '89–)
Yuichi OHNO	Research Associate (May '89–)

Molecular Assemblies

Koji KAYA	Adjunct Professor from Keio Univ. (April '87–March '89)
Ichimin SHIROTANI	Adjunct Associate Professor from Muroran Inst. of Technology (April '87–March '89)
Yuuji OHASHI	Adjunct Professor from Ochanomizu Univ. (April '89–)
Youji ACHIBA	Adjunct Associate Professor from Tokyo Metropolitan Univ. (April '89–)
Takehiko MORI	Research Associate
Shin-ichi NAGAOKA	Research Associate

Synchrotron Radiation Research

Robert J. FLEMING	Visiting Professor from Monash Univ., Australia (Jan. '89–)
Ellak I. VON NAGY-FELSOBUKI	Visiting Associate Professor from Univ. of Newcastle, Australia (Jan. '89–)

Department of Applied Molecular Science

Applied Molecular Science I

Kazuhiro NAKASUJI	Professor
Kiyoshi ISOBE	Associate Professor
Koshiro TORIUMI	Research Associate
Yoshiki OZAWA	Research Associate
Yoshihito HAYASHI	Technical Associate
Jiro TOYODA	Technical Associate (April '89–)
Keisuke UMAKOSHI	IMS Fellow (–March '89)
Toshikazu KITAGAWA	IMS Fellow (January '89–)
Ken-ichi SUGIURA	Graduate Student (April '89–)

Applied Molecular Science II

Kazuhiro MARUYAMA	Adjunct Professor from Kyoto Univ. (–March '89)
Hideki SAKURAI	Adjunct Professor from Tohoku Univ. (April '89–)
Hiroharu SUZUKI	Adjunct Associate Professor from Tokyo Inst. of Tech. (–March '89)
Eiichi NAKAMURA	Adjunct Associate Professor from Tokyo Inst. of Tech. (April '89–)
Hiroki OSHIO	Research Associate

Physical Organic Chemistry

Yuho TSUNO	Professor (May '89–)
Junji INANAGA	Associate Professor (September '89–)
Masaaki MISHIMA	Research Associate (May '89–)
Hiroshi IMAHORI	Graduate Student from Kyoto Univ.* (June '89–)

Coordination Chemistry Laboratories

Hitoshi OHTAKI	Director

Synthetic Coordination Chemistry

Eiichi KIMURA	Professor
Ryuichi IKEDA	Associate Professor
Chinthia J. BURROWS	JSPS Visiting Associate Professor from State Univ. of New York (August '89–February '90)
Hideki MASUDA	Research Associate
Mitsuhiko SHIONOYA	Research Associate
Hiromasa KUROSAKI	Graduate Student from Hiroshima Univ. (–February '89) Technical Associate (March '89–)
Yasuhisa KUROGI	Graduate Student from Hiroshima Univ.*
Senji WADA	Graduate Student from Hiroshima Univ.*
Takeshi SHIOTA	Graduate Student from Hiroshima Univ.*
Matsuo NISHIYAMA	Graduate Student from Hiroshima Univ.*
Atsushi ISHIKAWA	Graduate Student from Nagoya Univ.*

Complex Catalysis

Hitoshi OHTAKI	Professor
Georg JOHANSSON	Adjunct Professor from Royal Inst. of Technology in Sweden (October '89–July '90)
Toshikatsu YOSHIDA	Adjunct Professor from Univ. Osaka Pref.
Reiko KURODA	Adjunct Associate Professor from Univ. of Tokyo
Kiyohiko NAKAJIMA	Research Associate
Atsushi YAGASAKI	Technical Associate (August '89–)

Hiromasa TAMURA	IMS Fellow (July '89–)
Kwang O. KOH	Visiting Research Fellow from Soonchunhyang Univ. in Korea (January–August '89, December '89–February '90)
Dominique N. LUNEAU	JSPS Post-doctoral Fellow (–December '89)
Nobuhiro FUKUSHIMA	Graduate Student from Tokyo Inst. of Tech.*
Kenji WAIZUMI	Graduate Student from Tohoku Univ.* (April '89–)

Functional Coordination Chemistry

Coordination Bond

Masanobu HIDAI	Adjunct Professor from Univ. of Tokyo (April '89–)
Toshio YAMAGUCHI	Adjunct Associate Professor from Fukuoka Univ. (April '89–)

Research Facilities

Computer Center

Keiji MOROKUMA	Director
Hiroshi KASHIWAGI	Associate Professor (–April '89)[13]
Kazuo KITAURA	Associate Professor (July '89–)
Umpei NAGASHIMA	Research Associate
Shigeyoshi YAMAMOTO	Technical Associate
Yuji MOCHIZUKI	Graduate Student from Hokkaido Univ.* (–October '89)[14]

Chemical Materials Center

Kazuhiro NAKASUJI	Director (June '89–)
Yoshiro YAMASHITA	Associate Professor (January '89–)
Shoji TANAKA	Research Associate (April '89–)
Masaaki TOMURA	Technical Associate (August '89–)

Instrument Center

Ichiro HANAZAKI	Director
Kiyokazu FUKE	Associate Professor (November '88–)
Keisaku KIMURA	Research Associate
Fuminori MISAIZU	Research Associate (June '89–)

Low-Temperature Center

Yusei MARUYAMA	Director
Kunio AWAGA	Research Associate

Equipment Development Center

Teizo KITAGAWA	Director
Tadaoki MITANI	Associate Professor
Yoshihiro TAKAGI	Research Associate
Hiroshi OKAMOTO	Research Associate
Kaoru OKANIWA	Graduate Student

Ultraviolet Synchrotron Orbital Radiation Facility

Katsumi KIMURA	Director
Makoto WATANABE	Associate Professor
Toshio KASUGA	Associate Professor (–February '89)[15]
Shun-ichi NAOÉ	Adjunct Associate Professor from Kanazawa Univ. (April '87–March '89)[16]
Kazuhiko SEKI	Adjunct Associate Professor from Hiroshima Univ. (–April '89)

Hiroto YONEHARA	Research Associate
Kazutoshi FUKUI	Research Associate
Atsunari HIRAYA	Research Associate

Technical Staff

Akira UCHIDA	Technical Division Head
Keiichi HAYASAKA	Technical Section Chief
Kusuo SAKAI	Technical Section Chief
Satoshi INA	Computer Center (Unit Chief)
Fumio NISHIMOTO	Computer Center
Fumitsuna TESHIMA	Computer Center
Takaya YAMANAKA	Instrument Center
Shunji BANDOW	Instrument Center
Kiyonori KATO	Low-Temperature Center (Unit Chief)
Takashi TAKAYAMA	Low-Temperature Center
Kazuo HAYAKAWA	Equipment Development Center (Unit Subchief)
Hisashi YOSHIDA	Equipment Development Center
Masashi NAGATA	Equipment Development Center
Kouichi UCHIYAMA	Equipment Development Center
Toshio HORIGOME	Equipment Development Center (Unit Subchief)
Norio OKADA	Equipment Development Center
Mitsukazu SUZUI	Equipment Development Center
Nobuo MIZUTANI	Equipment Development Center
Shinji KATO	Equipment Development Center
Osamu MATSUDO	UVSOR Facility (Unit Chief)
Toshio KINOSHITA	UVSOR Facility
Masami HASUMOTO	UVSOR Facility
Jun-ichiro YAMAZAKI	UVSOR Facility
Eiken NAKAMURA	UVSOR Facility

* Carries out graduate research of IMS on the Cooperative Education Programs of IMS with graduate schools.

1) Present Address: Chemistry Division, Argonne National Laboratory, 9700 South Cass Avenue, Argonne, Illinois 60439, U.S.A.
2) Present Address: Dept. of Industrial Chemistry, Faculty of Engineering, Kyoto Univ., Kyoto 606
3) Present Address: Dept. of Physics, Faculty of Science, Kanazawa Univ. 1-1 Marunouchi, Kanazawa 920
4) Present Address: Nobeyama Radio Observatory, Minami-Saku, Nagano 384-13
5) Present Address: Dept. of Elect. Chem., The Grad. School at Nagatsuda, Tokyo Inst. of Tech., Nagatsuda 4259, Midori-ku, Yokohama 227
6) Present Address: Faculty of Engineering, Tokyo Univ., Hongo 7-3-1, Bunkyo-ku, Tokyo 113
7) Present Address: Dept. of Appl. Chem., Osaka Inst. of Tech., Ohmiya 5-16-1, Asahi-ku, Osaka 535
8) Present Address: Faculty of Science, Osaka Univ., Machikaneyama 1-1, Toyonaka Osaka 560
9) Present Address: Dept. of Chemistry, Kyushu Univ., 6-10-1, Hakozaki, Higashi-ku, Fukuoka 812
10) Present Address: Dept. of Chemistry, Kumamoto Univ., 2-39-1, Kurokami, Kumamoto 860
11) Present Address: Dept. of Physics, Faculty of Science, Gakushuin Univ., 1-5-1, Mejiro, Toshima-ku, Tokyo 171
12) Present Address: New Material Laboratory, Nippon Petrochemical Co. Ltd., Kawasaki, Kawasaki, Kanagawa 210
13) Present Address: Dept. of Biochemical Engineering & Science, Faculty of Computer Science & Systems Engineering, Kyushu Inst. of Tech., Kawazu, Iizuka, Fukuoka 820
14) Present Address: Dept. of Chemistry, Faculty of Science, Hokkaido Univ., Kita-ku, Sapporo 060
15) Present Address: Faculty of Science, Hiroshima Univ., 1-1-89, Higashi-Senda, Naka-ku, Hiroshima 730
16) Present Address: College of Liberal Arts, Kanazawa Univ., 1-1, Marunouchi, Kanazawa 920

Foreign Visiting Staff

Y.S. Kong	Chonbuk Natl. Univ., Korea	–Aug. 1988 Jan.–Mar. 1989
H. Sun	Pusan Natl. Univ., Korea	Aug. 1988 Dec. 1988–Feb. 1989
W. T. Borden	Univ. of Washington, USA	Sep.–Nov. 1988
L. Zhang	Inst. Chem., Acad. Sin., China	–Nov. 1988
C. Zhang	Inst. Chem., Acad. Sin., China	–Dec. 1988
X. Ying	Fudan Univ., China	Dec. 1988–Apr. 1989
S. N. Rai	North Eastern Hill Univ., India	Jan. 1989–
S. C. Park	Kangweon Natl. Univ., Korea	Feb. 1989
F. Maseras	Univ. of Barcelona, Spain	Apr. 1989–
A. J. Dann	Univ. of Nottingham, UK	–May 1989
J. Lee	Seoul Natl. Univ.	Jun. 1989–
A. V. de Miguel	Univ. of Alecala de Henares, Spain	Jun. 1989–
M. R. Fahy	Univ. of Nottingham, UK	–Jul. 1989
J. Hudeček	Visiting Scientist from Charlus Univ., Czechoslovakia	Jul. 1989–
B. J. Yoon	Kangreung Natl. Univ., Korea	Jul. 1989–

COUNCIL

Hiroo INOKUCHI **Director-General**

Councillors

Chairman	Kenichi FUKUI	President, Institute for Fundamental Chemistry
Vice-Chairman	Yutaka TOYOZAWA	Professor, Chuo University
	Hirotugu AKAIKE	President, The Institute of Statistical Mathematics (June '89–)
	Hiroaki BABA	Professor Emeritus, Hokkaido University (–May '89)
	Hideaki CHIHARA	Professor, Osaka University (June '89–)
	Eiichi FUJITA	President, Osaka University of Pharmaceutical Sciences
	Sachio HAYAKAWA	President, Nagoya University
	Ryuichi HIRANO	Professor Emeritus, University of Tokyo (–May '89)
	Namio HONDA	President, Toyohashi University of Technology
	Sho ITO	Professor, Tokushima Bunri University
	Kouzou KUCHITU	Professor, Nagaoka University of Technology
	Michio KURATA	Professor Emeritus, Kyoto University
	Haruo NISHIHARA	President, Waseda University
	Akira MIKAZUKI	Professor Emeritus, University of Tokyo (June '89–)
	Masatoshi MORITA	Chief Executive Officer, Toyota Central Research & Development Laboratories, INC
	Minoru ODA	President, Institute of Physical and Chemical Research (–May '89)
	Kazuo SAITO	Professor, International Christian University (June '89–)
	Yoshihiko SAITO	Professor, Keio University (–May '89)
	Kenji TAMARU	Professor, Science University of Tokyo
	Ikuzou TANAKA	President, Tokyo Institute of Technology
	Teijiro YONEZAWA	Professor, Kinki University (June '89–)
	Manfred EIGEN	Head of Department, Max-Planck Institute of Physical Chemistry and Professor, Technical University of Gottingen (–May '89)
	Robert G. PARR	Professor, University of Northcarolina (–May '89)
	John C. POLANYI	Professor, University of Toronto (June '89–)
	Heinz A. STAAB	President, Max-Planck Society for The Advancement of Science, F.R.G.

The Council is the advisory board for the Director-General. Two of the councillors are selected among distinguished foreign scientists.

Distinguished Research Consultants

Masao KOTANI	Professor Emeritus, University of Tokyo
Kenichi FUKUI	President, Institute for Fundamental Chemistry; Professor Emeritus, Kyoto University
Yonezo MORINO	Professor Emeritus, University of Tokyo; Director and Supreme Consultant, Sagami Chemical Research Center
Saburo NAGAKURA	President, The Graduate University for Advanced Studies
Yasutada UEMURA	Professor, Science University of Tokyo (June '89–)

Administration Bureau

Shousuke WAKISAKA	Director-General, Administration Bureau (–August '89)
Toshio UENO	Director-General, Administration Bureau (August '89–)
Yukio OHMURA	Director, General Affairs Department (–January '89)
Satoshi HUZISAWA	Director, General Affairs Department (April '89–)
Jitsuo SUZUKI	Director, Finance and Facilities Department
Nobuaki SHIMIZU	Head, General Affairs Division
Junsaku NAGATA	Head, Personnel Division
Minoru AKIMOTO	Head, Research Cooperation and International Affairs Division (–April '89)
Tsunetaka GIMA	Head, Research Cooperation and International Affairs Division (April '89–)
Takashi TAKIKAWA	Head, Budget Division (–August '89)
Kaoru KATO	Head, Accounts Division
Michitaro MATUI	Head, Construction Division (–April '89)
Masakazu SASAKI	Head, Construction Division (April '89–)
Motokazu FURUYA	Head, Equipment Division

BUILDINGS AND CAMPUS

The IMS campus covering 62,343 m^2 is located on a low hill in the middle of Okazaki City. The inequality in the surface of the hill and growing trees are preserved as much as possible, and low-storied buildings are adopted for conservation of the environment. The buildings of IMS are separated according to their functions as shown in the map. The Research Office Building and all Research Facilities except for the Computer Center are linked organically to the Main Laboratory Building by corridors. Computer Center, Library, and Administration Buildings are situated between IMS and the neighboring National Institute for Basic Biology and National Institute for Physiological Sciences, because the latter two facilities are common to these three institutes.

The lodging facility of IMS called Yamate Lodge, located within 10 min walk, has sleeping accommodations for 19 guests and two families. Since June 1, 1981 a new lodging facility called Mishima Lodge has been opened. Mishima Lodge, located within four minutes' walk east of IMS can accommodate 68 guests and ten families. Scientists who visit IMS as well as the two other institutes can make use of these facilities. Foreign visiting scientists can also live at these lodgings with their families during their stays.

The Institute for Molecular Science

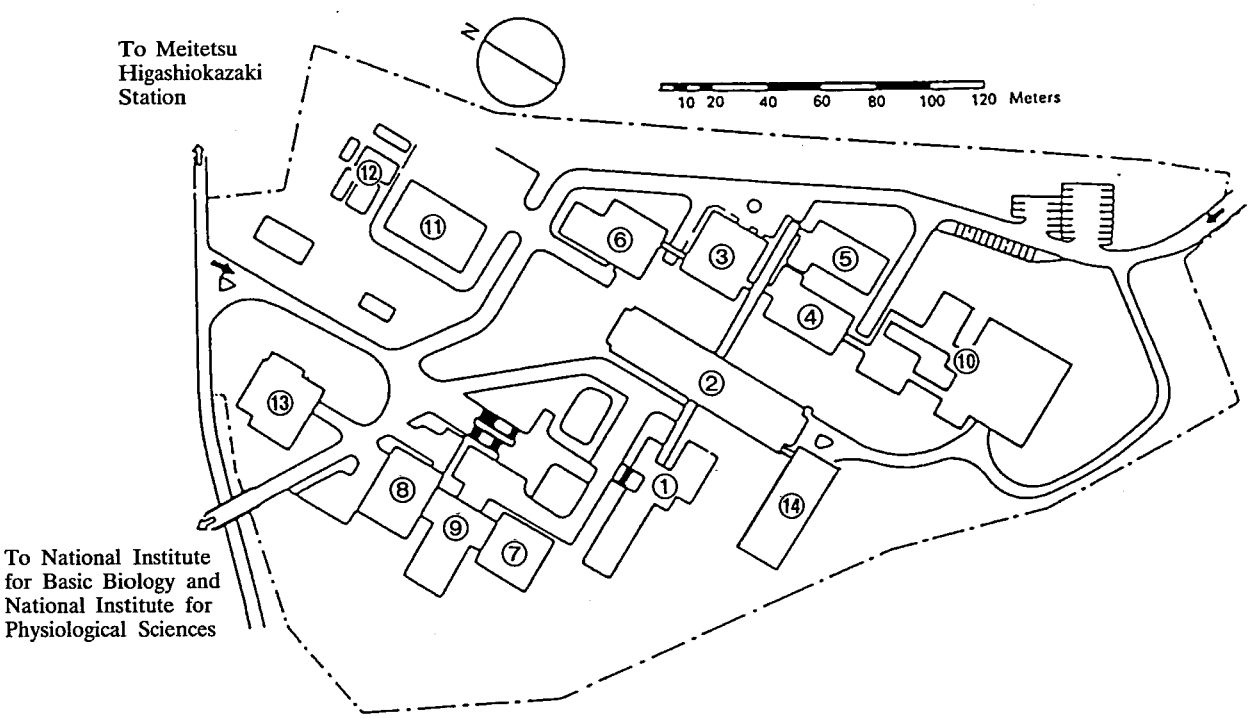

1. Research Office Building
2. Main Laboratory Building
3. Equipment Development Center
4. Instrument Center
5. Chemical Materials Center
6. Low-Temperature Center
7. Computer Center
8. Library
9. Central Administration
10. UVSOR Facility
11. Power Station
12. Waste-Water Disposition Facilities
13. Faculty Club
14. South Laboratory Building

Okazaki (population 300,000) is 260 km southwest of Tokyo, and can be reached by train in about 3 hours from Tokyo via New Tokaido Line (Shinkansen) and Meitetsu Line.
The nearest large city is Nagoya, about 40 km west of Okazaki.

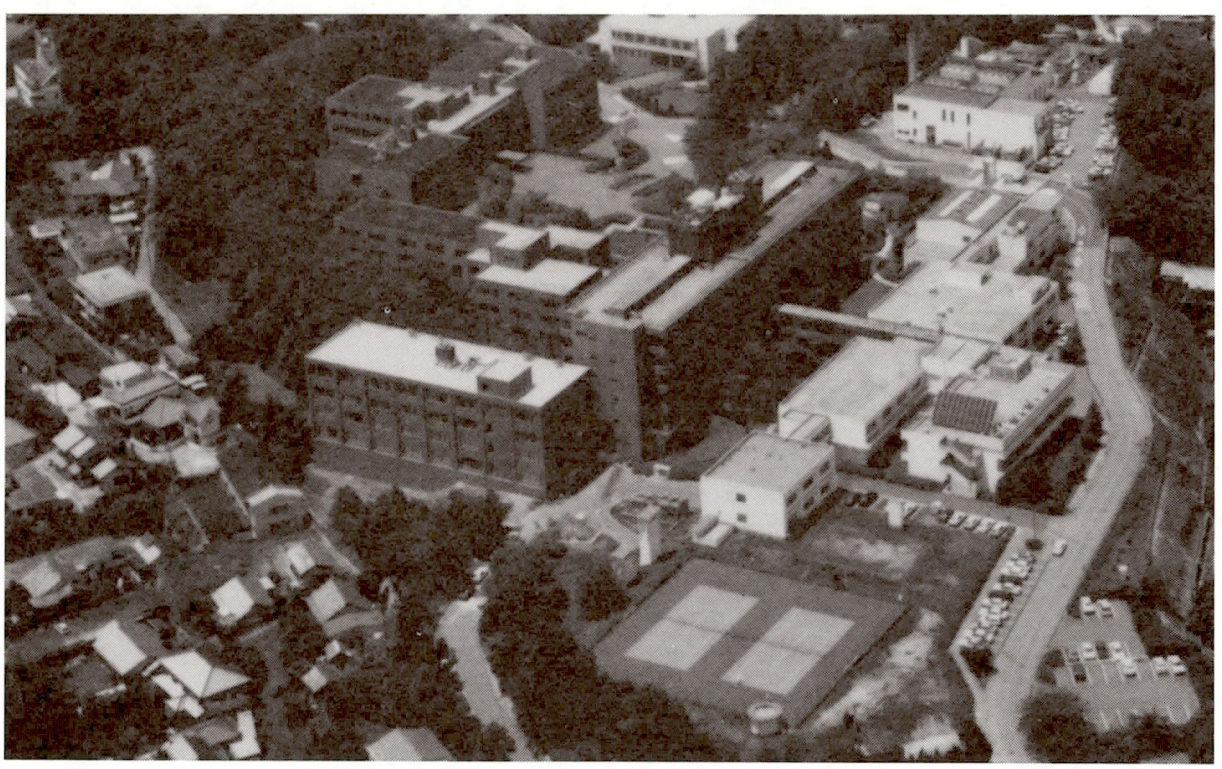

RESEARCH ACTIVITIES I
Department of Theoretical Studies

I–A Potential Energy Surfaces and Dynamics of Elementary Chemical Reactions

The ab initio theoretical calculation and characterization of potential energy surfaces of chemical reactions and their application to reaction dynamics calculation has been one of the continuing central themes of the Morokuma group since its initiation at IMS in 1977. The main emphasis in the last several years has been placed on reactions involving more than one potential energy surfaces. Dr. Koichi Yamashita, Research Associate in the group, has been the principal driving force in the project in the recent years. Mr. Yoshiaki Amatatsu joined the group in January 1989 as a Technical Associate and is also involved in this project.

I-A-1 Theoretical Study of Potential Energy Curves and Dynamics of NaCl, NaBr and NaI Photodissociation

Koichi YAMASHITA, Keiji MOROKUMA and Peter J. KNOWLES *(Univ. of Sussex, UK)*

We performed the ab initio potential energy curves and dynamics calculations related to the "femtosecond transition state spectroscopy" of NaCl, NaBr and NaI photodissociation. The potential energy curves of the lowest two states were determined by the state averaged CASSCF and internally contracted MRCI method for the repulsive as well as the ionic-covalent curve-crossing regions. Basis sets used are the TZP augmented with an f function. A diabatic description of the two states were obtained by diagonalizing the adiabatic dipole matrix. Simple classical dynamics calculations for NaBr and NaI using the ab initio potential energy curves and the diabatic coupling constants reproduced the principal features recently observed by Zewail et al.[1)]

Reference

1) T.S. Rose, M.J. Rosker and A.H. Zewail, *J. Chem. Phys.* **88**, 6672 (1988); M.J. Rosker, T.S. Rose and A.H. Zewail, *Chem. Phys. Lett.* **146**, 175 (1988).

I-A-2 Potential Energy Surfaces and Photodissociation Dynamics of Methyl Iodide

Yoshiaki AMATATSU, Satoshi YABUSHITA *(IMS and Hiroshima Univ.)* **and Keiji MOROKUMA**

The photodissociation dynamics of methyl iodide has been extensively studied from the theoretical and experimental point of view. However, Powis and Black have found that methyl fragment produced in the $I(^2P_{3/2})$-channel is rotating around an axis perpendicular to the methyl top axis (1), which could not be explained by the previous pseudo-triatomic model. Spin Orbit Configuration Interaction (SOCI) calculations are performed to obtain the potential energy surfaces of excited states of methyl iodide, varying six internal coordinates except for three C-H bond distances. In the present calculations, first, the required diagonal terms are calculated by performing large scale spin free CI and then, small dimensional matrices, which are composed of these diagonal terms and off-diagonal terms including SO interactions, are diagonalized to get adiabatic energies. The energy differences between ground and excited states are almost same as those in our previous large scale SOCI calculations (2). The transformations from adiabatic to diabatic basis are performed so as to minimize the overlaps among two singlet states and a triplet state. The six diabatic terms are expressed by functions with respect to six internal coordinates. Singlet diagonal diabatic terms decrease monotonically with respect to the distance between C and I atoms. On the other hand, a triplet diagonal diabatic term has a shallow well

outside of the conical intersection region. Classical trajectory calculations are now in progress.

References
1) J.F. Black and I. Powis, *J. Chem. Phys.* **89**, 3986 (1988).
2) S. Yabushita and K. Morokuma, *Chem. Phys. Lett.* **153**, 517 (1988).

I-A-3 The Effect of Reagent Excitation on Reactivity of the Ground State Na + HCl Reaction

Koichi YAMASHITA, Ying XIE *(IMS and Fudan Univ., China)* **and Keiji MOROKUMA**

We studied the effect of reagent excitation in the gas phase Na + HCl reaction. Dependences of reaction cross section on vibration, rotation and translation excitations in the ground state reagents were investigated by using quasiclassical trajectory calculations on the ab initio potential surface fitted to the Murrell-Sorbie function. The potential energies were calculated at over 500 geometries by using the MRSD-CI method with the DZP valence basis set and the Na and Cl effective core potentials by Wadt and Hay. Vibrational enhancement seen in the calculated cross section was consistently interpreted in terms of the "late" barrier surface of the reaction. In the case of rotational excitation the reaction cross section initially decreased with increase in the rotational quantum number J, reached a minimum and then increased as J increased further. The decrease was identified as an "orientation" effect and the increase as an "energy" effect. These features agree well with the experimental observation.[1)]

Reference
1) F.E. Bartoszek, B.A. Blackwell, J.C. Polanyi, and J.J. Sloan, *J. Chem. Phys.* **74**, 3400 (1981); B.A. Blackwell, J.C. Polanyi and J.J. Sloan, *Chem. Phys.* **30**, 299 (1978).

I–B Theoretical Studies of Structure and Spectroscopy

We have enjoyed active collaboration with visiting scientists in this project. Prof. Pavel Rosmus spent a month in the summer of 1989 and carried out, in collaboration with Dr. Yamashita, a substantial calculation on the high resolution vibrational and rotational spectra of several triatomic molecules. Mr. Fukunaga, a trainee from Fuji Photo Film Co., spent a year in the group, studying the solvent effect on the absorption spectra using the ab initio MO and Monte Carlo simulation method.

I-B-1 Theoretical Rotationally Resolved Spectra for the X^1A_1 and a^3B_1 States of SiH_2

Koichi YAMASHITA, Pavel ROSMUS *(Frankfurt Univ., FRG)* **and Keiji MOROKUMA**

Three-dimensional potential energy and electric dipole moment functions for the X^1A_1 and a^3B_1 states of SiH_2 have been calculated from highly correlated CEPA electronic wavefunctions. The analytic representations of these functions have been used to evaluate rotation-vibration spectra by perturbation theory and by variational approach, which fully accounted for anharmonicity and rotational-vibrational coupling effects. The quartic force fields in normal coordinates have been employed in the calculation of the equilibrium spectroscopic constants for SiH_2, SiD_2 and SiHD. Absolute line positions and intensities for several low-lying vibrational states (up to $J'' = 11$) have been evaluated. The results for the $1\nu_2$ band of the singlet state agree well with the recent spectral data.[1)] The strongly overlapping $1\nu_2$, $1\nu_3$ and $2\nu_2$ bands[2)] were analyzed by means of the theoretical rotational-vibrational line positions and intensity patterns. To date, there are no high resolution data known for the $^3B_1$ state. Hence, the theoretical ro-vibrational spectra may alleviate the experimental search for bands characterizing this electronic state.

References
1) C. Yamada, H. Kanamori, E. Hirota, N. Nishiwaki, N. Itabashi, K. Kato and T. Goto, *J. Chem. Phys.* in press.
2) C. Yamada, H. Kanamori, E. Hirota, N. Nishiwaki, N. Itabashi, K. Kato and T. Goto, in preparation.

I-B-2 The A-X Electronic Band Systems of the CCC, CCN^+ and CNC^+ Molecules

Koichi YAMASHITA, Philip R. BUNKER *(NRCC, Canada)* **and Keiji MOROKUMA**

CCN^+ and CNC^+ might be important constituents of interstellar gas clouds, but their spectra have not yet been discovered in the laboratory. The isoelectronic neutral molecule CCC has a strong electronic band system, the A-X band system, in the 4050 Å region, and CCN^+ and CNC^+ may have analogous band systems. We therefore calculated the T_e values for these bands as an aid to their experimental discovery. We used the MOLPRO program with the triple-zeta plus double polarization basis functions and performed internally contracted CASSCF-MRCI (+ Davidson correction) calculations for the X and A electronic states of the three molecules. For CCC we obtained $T_e(A)$ = 3.25 eV and $R_e(CC)$ = 2.450 bohr to be compared with the experimental values of 3.06 eV and 2.413 bohr. For CNC^+ the ground (Σ_g^+) state R_e values were calculated as 2.354 bohr and for the excited (Π_u) state as 2.367 bohr. The $T_e(A)$ value was calculated as 4.24 eV. For CCN^+ the ground (Σ^+) state geometry was obtained as $R_e(CC)$ = 2.606 and $R_e(CN)$ = 2.253 bohr and for the excited (Π) state $R_e(CC)$ = 2.383 and R_e (CN) = 2.404 bohr. The $T_e(A)$ value was calculated as 2.84 eV. If these values follow the same trend as for CCC, they would suggest experimental $T_e(A)$ values of 4.0 and 2.6 eV respectively for CNC^+ and CCN^+.

I-B-3 Solvent Effect on Vibrational Structure in (n, π^*) Transition of Formaldehyde

Hiroo FUKUNAGA *(Fuji Photo Film Co. and IMS)* **and Keiji MOROKUMA**

Intermolecular potential functions between formaldehyde in the ground and excited (n, π^*) state and a water molecule have been based on ab initio molecular orbital calculations with the DZP basis set. SCF and electron-hole potential methods have been employed for calculation of the formaldehyde-water complex in the ground and excited state, respectively. Interaction energies for 393 configurations are fit to analytic forms expressed by terms in r^{-1}, r^{-3}, r^{-6} and r^{-12}. The transition dipole moment of the complex has also been calculated and fit into a functional form. Both potential and transition dipole moment functions have been determined not only for the equilibrium geometry but also for distortions along the normal coordinates of the ground state formaldehyde. These functions are being used for simulation of the (n, π^*) absorption spectrum of formaldehyde in liquid water.

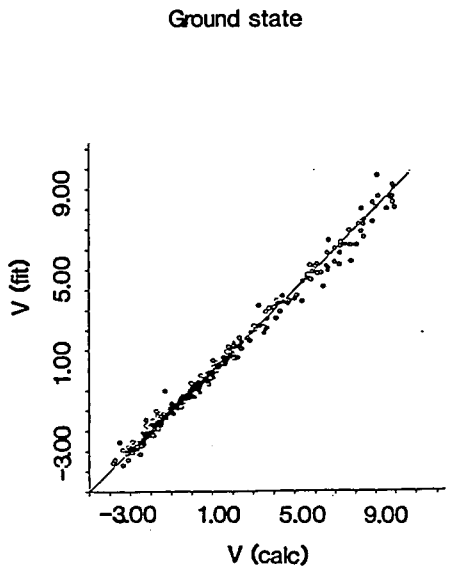

Figure 1. Correlation between the calculated interaction energies and those from the fitted function.

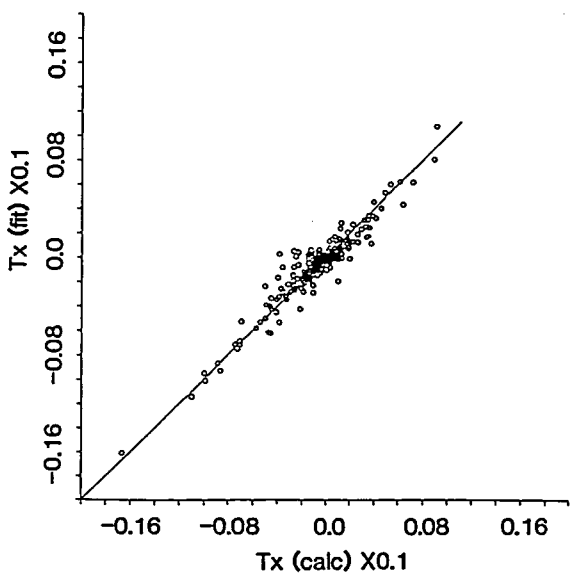

Figure 2. Correlation between the calculated transition dipole moments and those from the fitted function.

I–C Theoretical Studies of Reaction Mechanisms and Structure of Organic Compounds

Dr. Simon Mathieu, a PhD in organic and theoretical chemistry from Toulouse, France, has joined the Morokuma group in March 1989 as a JSPS Postdoctoral Fellow, and has been actively involved in MO studies of structure and reactivity of hypervalent compounds. Dr. Andrea Dorigo in his second year of a Postodoctoral Fellowship has been working hard mainly on the diastereoselectivity in varieties of reactions on a C=C double bond. We hope to maintain a high activity in this project.

I-C-1 Theoretical Studies of the Role of Complexation in the Conjugate Addition of Dialkylcuprates to Electron-Deficient Double Bonds. Influence on the Stereochemistry of the Reaction

Andrea E. DORIGO and Keiji MOROKUMA

[*J. Chem. Soc. Chem. Commun.*, in press]

Ab initio molecular orbital calculations suggest that dialkylcuprates add to the C=C bond of C=C–ZZ′ systems (Z = CHO, Z′ = H; Z = CN, Z′ = H; Z = Z′ = CN) *via* a mechanism which involves precomplexation of the copper center with the double bond. This implies an acute angle of attack onto the C=C bond; this should in turn be responsible for the opposite stereoselectivites observed in the reaction of dialkylcuprates on the one hand and of alkylcopper reagents (and other conventional nucleophiles) on the other. The approach of the cuprate reagent causes the conformation at the γ-carbon to be staggered with respect to the forming C_β-Cu bond. An acute angle of approach implies that the least hindered position is the one *anti* to the cuprate molecule, with the *outside* position being more crowded and the *inside* position being the most hindered for an alkyl or aryl group, due to the encumbrance of the copper center. Thus, a phenyl (or large) group occupies the *anti* position, an alkyl (medium-sized group) the *outside* position, and a hydrogen (small) atom the *inside* position. The diastereoselectivity predicted by this model is in agreement with the results obtained experimentally. These considerations do not apply to small groups having electron-donating atoms (such as OR groups) which may coordinate to the metal.

I-C-2 Theoretical Studies of Nucleophilic Additions of Simple Anions to α, β-Unsaturated Carbonyl Compounds. Diastereoselectivities of the Addition to Chiral Substrates.

Andrea E. DORIGO and Keiji MOROKUMA

The addition of some simple nucleophiles (OH^-, NH_2^-) to acrolein, *E*-crotonalydehyde, and *E*-4-hydroxy-2-pentenal has been studied. Transition states have been located at the HF/3-21G level, with diffuse functions added to the nucleophilic center and the C=C–C=O atoms. The third substrate serves as a model for chiral systems, which have been previously studied experimentally. In all cases the transition states are "early", but the conformational preferences of the allylic substituents are nonetheless quite different in the transition states and in the reactants. An electron-withdrawing group (such as OH or OR) prefers the *anti* position, which is unfavorable for an electron-donating group. The latter prefers the relatively unhindered *inside* position over the *outside* position. These results are opposite to those obtained for the addition reactions of alkylcopper reagents (Dorigo, A.E.; Morokuma, K., *J. Am. Chem. Soc.*, **111**, 6524 (1989)), and are more representative of the behavior of "free" nucleophiles. These results thus suggest that a carbanionic nucleophile which is stable enough to add as a free nucleophile should give the opposite stereoselectivity to that observed for alkylcopper reagents. Work is now in progress to test this hypothesis with simple carbon nucleophiles.

I-C-3 Theoretical Studies of the S_N2' Reaction of Dialkylcuprates with Chiral Allylic Halides. Influence of Pre-Complexation on the Reaction Stereochemistry

Andrea E. DORIGO and Keiji MOROKUMA

Ab initio molecular orbital calculations suggest that the complexation of dialkylcuprates with the double bond of allyl chloride is an important first step in the S_N2' reaction. The chlorine atom prefers to be *anti* to the cuprate molecule, with the *inside* and *outside* positions being disfavored by 0.8 kcal/mol and 3.41 kcal/mol, respectively. In the S_N2' reaction of cuprates with cyclic systems, such as cyclohexenyl acetates, the *inside* position is necessarily occupied by a carbon atom of the ring. The leaving group thus strongly favors the *anti* over the *outside* position. Thus results provides a rationale for the preference for *anti* attack observed in these reactions of cuprates with good leaving groups, where the transition state is expected to strongly resemble the π-complex.

The reaction with chiral substrates having formula $CH(R)(OR)-CH=CH-CH_2Cl$ has also been studied. Here the source of chirality is the asymmetric γ-carbon. The stereoselectivity of the reaction with *E*-substrates may be explained in terms of the conformational preference of the substituents at C_γ in the π-complex. Thus, a methyl (or alkyl) goup is found to prefer the *anti* position, while an oxygen atom prefers to take up the *inside* position where it can coordinate to the copper center of the cuprate. The somewhat hindered *outside* position is occupied by a hydrogen atom. The diastereoselectivity predicted by the model based on these calculations is in agreement with the experimental results. Further work is now in progress to extend these considerations to the *Z* substrates, which give the same diastereoselectivity (at least qualitatively) as the *E* isomers.

I-C-4 Ab Initio Theoretical Study of the Structure, Stability and Reactivity of XH_n Neutral and Ionic Hypervalent Molecules (X = S, Se, Te; n = 2 to 6)

Simon MATHIEU and Keiji MOROKUMA

Periodic trends have been examined by studying the properties of selected title compounds with elements from group 16 as a function of atomic number. These comparative studies on the structure, stability and reactivity have been carried out by means of ab initio molecular orbital calculations using an effective core potential on the central atom. In order to establish the factors which can favor hypervalency in such systems, we have first analysed the role of polarization functions. Full geometry optimizations have then been carried out at the HF level without and with such orbitals using valence basis sets of double zeta quality. The use of polarization functions has been found to be very important in giving meaningful results for geometric parameters as well as for energetics in the case of hypervalent structures. The main qualitative role of such functions is to reinforce the bonding and to strongly stabilize the HOMO in these structures. Diffuse functions have also given a noticeable improvement of the description of anionic systems. The correlation energy of the stationary points optimized using polarization and diffuse functions on all atomic centers was calculated at the MP2 level. Among the trends observed for stability and reactivity, selenium represents a case intermediate between S and Te. The endothermicity of the following hydrogenation reactions:

$$XH_2 + H_2 \rightarrow XH_4 \qquad (1)$$

$$XH_4 + H_2 \rightarrow XH_6 \qquad (2)$$

has been found to increase in going from Te to S by 20.3 kcal/mol (reaction 1) and by 11.0 kcal/mol (reaction 2). This result can give an insight on the ability for hypervalency which increases going down the periodic table. The isomerization of tetra-, penta- and hexacoordinated compounds has been investigated to test the flexibility of these molecules. No substantial barriers have been found for the Berry pseudorotation of XH_5^+ species. XH_4 molecules exhibit stronger structural preference for the C_{4v} symmetry, the D_{4h} structure being energetically higher up to 14 kcal/mol in the case of Te. In sharp contrast, XH_6 octahedral molecules are non-flexible and present a large barrier for the trigonal twist distortion through a D_{3h} prismatic transition state, going from 46 in the case of Te to 71 kcal/mol for S. Correlation orbital diagrams and considerations of Pauli repulsions are useful to under-

stand the differences observed for these three symmetry allowed processes.

Further work is now in progress on fluorinated derivatives to establish the importance of the nature of the ligands.

I-C-5 Theoretical Studies of Hypervalency at Sulfur on the Effect of Ligand Proximity on the Stability and Nature of the Ligand-Sulfur Bonds in Organic Molecules

Andrea E. DORIGO and Keiji MOROKUMA

Ab initio M.O. calculations have been performed on some unusually stable organic molecules containing hypervalent main group atoms. Thus, the 6a-thiapentalenes possess the C_{2v}-symmetric structure **1a** (X = S and/or NH) in solution. Calculations showed that, at the HF/3-21G* level, **1a** is 8.67 (0.85) kcal/mol *higher* in energy than the monocyclic form 1b for X = S (NH). However, at the MP2/6-31G*//HF/3-21G* level, **1a** was found to be more stable than **1b** by 5.43 kcal/mol (X = S) and 3.30 kcal/mol (X = NH). These calculations stress the importance of electron correlation in the analysis of hypervalent species. Model calculations further suggest that the close contact between non-bonded S and X atoms contributes significantly to the destabilization of **1b**.

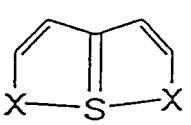

1a

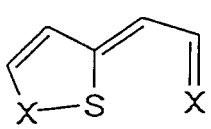

1b

A related case concerns the sulfonium ion **2a**, which is isomeric with the alkyl-ammonium cation **2b**. HF/3-21G* calculations on two model systems, $[(NH_3)S(CH_3)_3]^+$ and the complex between $^+NH_3-CH_3$ and $(CH_3)_2S$, showed that the latter is favored by 6.58 kcal/mol. The calculated preference for **2d** over **2c** is actually stronger (17.14 kcal/mol); nevertheless, **2c** is a local minimum, since it exists in a puckered conformation which is drastically different from the chair-boat conformation of 2d. Interconversion between the two isomers thus involves ring flip as well as R migration, and is therefore expected to have a sizeable barrier. The calculation also suggests the presence of significant bonding between the N and S atoms of **2c**.

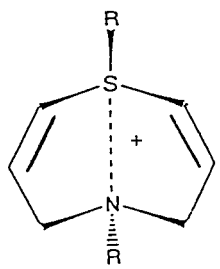

2a:R=CH_3
2c:R=H

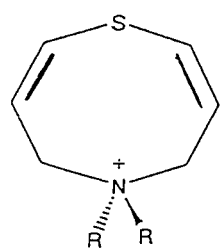

2b:R=CH_3
2d:R=H

I-C-6 Parallel and Cross Cycloaddition of Triplet 1,4-Pentadiene. An *ab initio* MO Study.

Masaru OHSAKU *(Hiroshima Univ.)* **and Keiji MOROKUMA**

[*J. Chem. Soc. Perkin Trans.* 2, in press]

Ab initio UHF molecular orbital calculations using the 3-21G through 6-31G* basis sets and including spin projection and electron correlation (APUMP2) have been carried out to investigate the photosensitized cycloaddition reactions of 1,4-pentadiene. Two forms of triplet 1,4-pentadiene, cis-trans and envelope, with nearly equal energy but with excitation localized on different bonds, are the starting points for the transition state TS1 of cross closure and TS2 of parallel closure, respectively. TS2 has a barrier of 14 kcal/mol, about 22 kcal/mol lower than TS1, supporting the experimental dominance of parallel closure. The transition states have the structures where a significant ring strain has already developed, and the TS1 − TS2 energy difference is mainly dictated by the strain energy difference of the cyclic triplet product intermediates.

I-D Structure and Reactions of Transition Metal Complexes

We continue to work very actively in the field of theoretical organometallic and inorganic chemistry. Dr. Nobuaki Koga, Research Associate in the Morokuma group, has been the principal figure behind the activity. He has had a very fruitful collaboration with Mr. Yanbo Ding, a Visiting Scientist from Beijing Normal University, Mr. Feliu Maseras from the University of Barcelona, and two trainees from industrial laboratories, Mr. Kawamura of Sumitomo Chemical Co. and Mr. Endo of Mitsubishi Petrochemical Co.

I-D-1 Ab Initio Potential Energy Surface and Electron Correlation Effect in CH Activation of CH_4 by Coordinatively Unsaturated $RhCl(PH_3)_2$

Nobuaki KOGA and Keiji MOROKUMA

[*J. Phys. Chem.*, in press]

Ab initio molecular orbital (MO) study of a model 'CH activation' reaction, oxidative addition of CH_4 to coordinatively unsaturated $RhCl(PH_3)_2$, is presented. We have found that the reaction proceeds through a bifurcated (η^2) CH_4 complex, $(CH_4)RhCl(PH_3)_2$, and a three-centered transition state. At the highest level of calculation, MP4SDTQ, the reaction is exothermic by 24 kcal/mol relative to the isolated reactants and by 7 kcal/mol relative to the CH_4 complex from which the activation barrier required is 3 kcal/mol. The CH_4 complex is stabilized by the CH $\rightarrow$ Rh d donation supplemented significantly by Rh $\rightarrow$ CH_4 back-donation as well as intermolecular (dispersion) and intramolecular electron correlation. The electron correlation is found to change the heat of reaction by 37 kcal/mol, thus shifting the location of transition state earlier and lowering the activation barrier drastically. The effect of electron correlation on the heat of reaction and activation energy is analyzed in detail using the MP2 method with the localized orbitals. The electron correlation related to the newly formed RhH and RhC bonds in the product is so large due to their covalency and large d character as to make the reaction very exothermic.

I-D-2 Activation of Ethylene C-H Bond by Organometallic Complexes. Is the π Complex an Intermediate of the Reaction?

Feliu MASERAS *(Univ. of Autonoma de Barcelona and IMS)*, **Nobuaki KOGA and Keiji MOROKUMA**

In the last few years, the important elementary process of C-H activation by organometallic complexes has been characterized in several experiments, both for saturated and unsaturated substrates. The present work is focused on the activation of the ethylene C-H bond by $MCp(PR_3)$ complexes to give vinyl hydride complexes $MCp(PR_3)(C_2H_3)H$, which has recently been subject to an extensive experimental study.[1] Our ab initio RHF geometry oprimization with M = Rh and R = H shows the existence of two deep and clearly different minima on the potential energy surface, corresponding to the π complex and the vinyl hydride. The π complex is more stable than the vinyl hydride by 21.8 kcal/mol at the MP2 level and has a specially strong bond to the metal, as indicated by the long C-C distance of 1.42 Å. A path connecting directly the reactants and the vinyl hydride passing through a weak σ complex and a transition state has been determined. The π complex is deep in a dead-end valley and seems to have no direct path to the product. This unusual uninvolvement of π complexation in the C-H activation may be connected to the fact that the orbitals of the metal fragment responsible for the π complexation are the same as those playing leading role in the C-H activation. Thus, a substantial weakening of π complex bond may be required before the π complex can spare its orbital interaction with C-H activation.

Reference

1) P.O. Stoutland and R.G. Bergman, *J. Am. Chem. Soc.*, **110**, 5732 (1988).

I-D-3 Potential Energy Surface of Olefin Hydroformylation by Rhodium Complex Catalyst $HRh(CO)_2(PR_3)$

Yanbo DING *(IMS and Beijing Normal University)*, **Nobuaki KOGA and Keiji MOROKUMA**

The catalytic cycle of hydroformylation by a rhodium complex $HRh(CO)_2(PR_3)$ is believed to be represented by the series of reaction steps shown in Fig. 1. In our previous work,[1] we studied with the ab initio MO method the potential energy surface of ethylene coordination to $HRh(CO)_2(PH_3)$ (step B) and intramolecular rearrangement through Berry pseudorotation and olefin insertion of $HRh(C_2H_4)(CO)_2(PH_3)$ (step C). In order to obtain the potential energy profile of full catalytic cycle, in the present study we have carried out similar calculations with the ab initio method for the following steps: the PH_3 coordination to $Rh(C_2H_5)(CO)_2(PH_3)$ to form $Rh(C_2H_5)(CO)_2(PH_3)_2$ (step D), the intramolecular CO insertion in $Rh(C_2H_5)(CO)_2(PH_3)_2$ to form $Rh(COC_2H_5)(CO)(PH_3)_2$ (step E), the H_2 oxidative addition to form $H_2Rh(COC_2H_5)(CO)(PH_3)_2$ (step F) and the C_2H_5CHO reductive elimination from $H_2Rh(COC_2H_5)(CO)(PH_3)_2$ to give $HRh(CO)(PH_3)_2$ (step G).

There are many isomeric species for intermediates and consequently many isomeric transition states. We have optimized at the RHF level the structures of some low energy intermediates and transition states. We found that the energy barriers of CO insertion and H_2 oxidative addition are around 19 and 31 kcal/mol, respectively. However, a preliminary calculation for the C_2H_5CHO reductive elimination from the hexacoordinate complex shows a very high barrier, suggesting that some other mechanism might be in operation in this step.

Reference

1) N. Koga, S.Q. Jin and K. Morokuma, *J. Am. Chem. Soc.*, **110**, 3417 (1988).

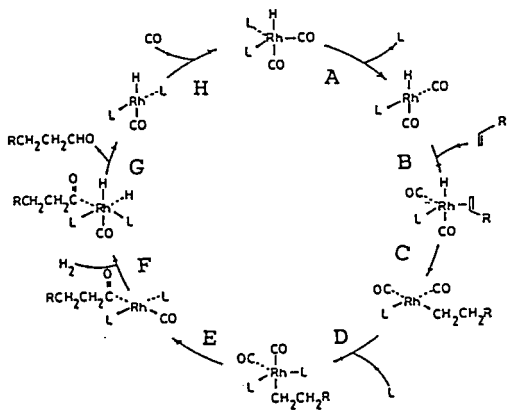

Figure 1. The full catalytic cycle of olefin hydroformylation

I-D-4 A Theoretical Study of the Structure of $CpRu(\mu\text{-}H)_4RuCp$

Nobuaki KOGA and Keiji MOROKUMA

The structure and bonding nature of $CpRu(\mu\text{-}H)_4RuCp$, **1**, have been studied by using an ab initio molecular orbital method with the double zeta basis functions for Ru and hydrides, the STO-3G minimal basis functions for Cp rings and the effective core potential replacing the core electrons of Ru. The optimized structural parameters of **1** except for the positions of the hydrides are in good agreement with the experimental X-ray values of $Cp^*Ru(\mu\text{-}H)_4RuCp^*$, **2**,[1] as shown in Figure 1. The four hydrides are found to be almost equivalent and the calculated HH distances of 1.88 Å are much longer than the X-ray values (0.88 – 0.94 Å). These structural features, however, support the conclusion based on the IR and NMR spectra of **2**.[1] The detailed analysis of the electronic structure shows that between the two Ru atoms there exist four hydride bridged (three-center two-electron) bonds but no direct Ru-Ru bond. At the RHF level of calculation, we also found an H_2 complex, $CpRu(\mu\text{-}H)_2(H_2)RuCp$ (**3**) and the transition state connecting **1** and **3** (Figure 1). **3** is only 3 kcal/mol higher in energy than **1** at the RHF level. At the MP2 level, however, the electron correlation stabilizes **1** very much; **1** is 25 kcal/mol lower in energy than **3**. Consequently the transition state disappears and **3** is not the equilibrium structure any more. For a delocalized bond such as the

three-center two-electron bond in **1**, the electron correlation must be taken into account.

Reference

1) H. Suzuki, H. Omori, D.H. Lee, Y. Yoshida, and Y. Moro-oka, *Organometallics*, **7**, 2243 (1988).

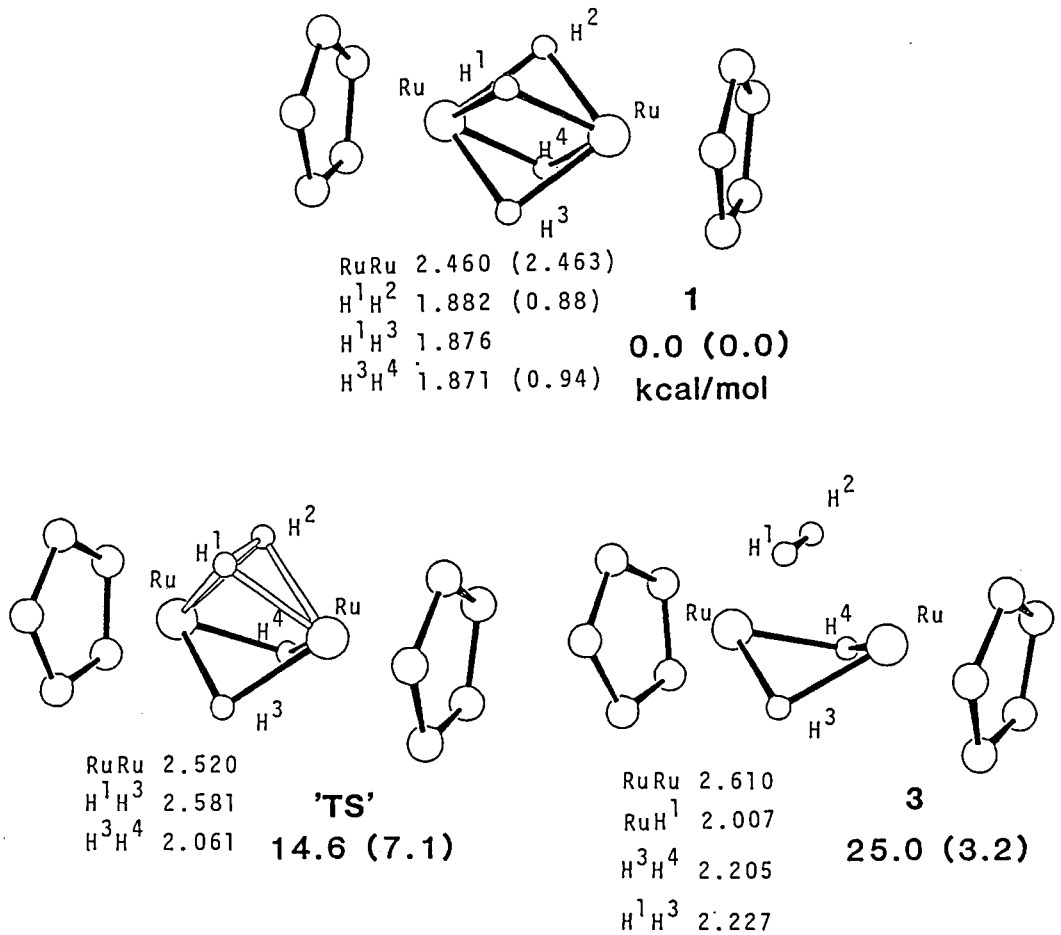

Figure 1. RHF optimized structures of $CpRu(\mu\text{-}H)_4RuCp$, **1**, $CpRu(\mu\text{-}H)_2(H_2)RuCp$, **3**, and the transition state between **1** and **3**. The numbers in parentheses for **1** are experimental values of **2**. The relative energies in kcal/mol are at the MP2 level and those in parentheses at the RHF level.

I-D-5 A Theoretical Study on Olefin Insertion into a Ti-Me Bond

Hiroshi KAWAMURA *(Sumitomo Chemical Co. and IMS)*, **Nobuaki KOGA and Keiji MOROKUMA**

We studied the mechanism of insertion reaction (1) of ethylene and propylene with an ab initio MO methods, as a model propagation step in the Ziegler-Natta polymerization.

$$CH_3TiCl_2^+ + C_2H_3R \rightarrow CH_3TiCl_2(C_2H_3R)^+ \rightarrow C_3H_6RTiCl_2^+ \quad (1)$$

The fully optimized structures of olefin complex, transition state and alkyl complex for ethylene insertion were obtained at the RHF/3-21G(Ti:MIDI4) level. The enegetics with the 6-31G(*) basis depends sensitively on electron correlation. This model reaction should take place easily, with no activation barrier at the PUMP2 level. The four-centered transition state is slightly non-planar (~10°) presumably to avoid eclipsing of CH bond (See Figure 1). In the product, the $C^{\beta}C^{\gamma}$ agostic interaction takes place, due to electron donation from the $C^{\beta}C^{\gamma}$ bond to a Ti vacant orbital. Of four transition states of propylene insertion, which are obtained by replacing each hydrogen atom of C_2H_4 by a standard CH_3, those for primary (head-to-tail) insertion are lower in energy than those for secondary

(tail-to-head) insertion. The non-planarity of the transition state gives rise to a 2 kcal/mol energy difference between two stereomeric primary insertion processes, suggesting the stereoselectivity favoring isotactic propagation.

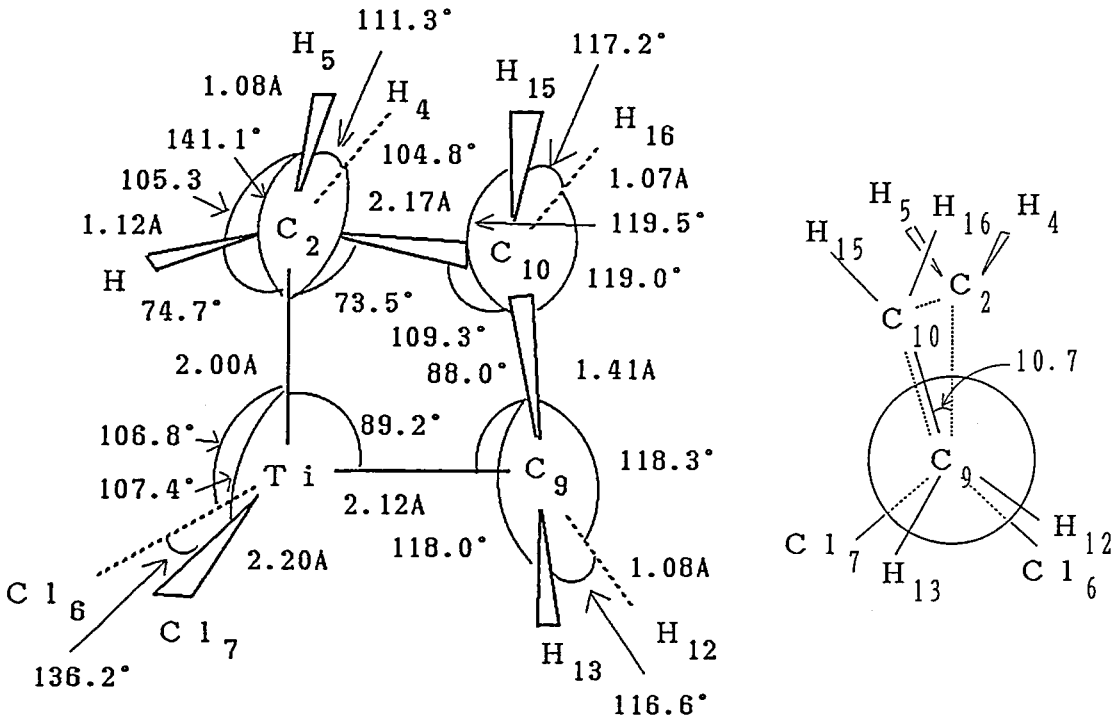

Figure 1. The optimized geometry of the transition state (in Å and degree) at the RHF/3-21G(Ti:MIDI4)

I-D-6 A Theoretical Study on Hydrozirconation

Nobuaki KOGA, Jun ENDO *(Mitsubishi Petrochemical Co. and IMS)* **and Keiji MOROKUMA**

Hydrozirconation, one of the elementary reactions in organometallic chemistry, is utilized for organic synthesis and is also considered to be the model process of olefin polymerization by zirconocene/methylalminoxane catalyst system. In order to understand the mechanism of this important process, we have performed ab initio MO calculations for the model reaction (1) using the effective core potential approximation. There are two possible approaches of ethylene to zirconocene; the one site is trans to Cl and cis to H and the other is between H and Cl. We have so far studied the former approach.

$(Cp)_2Zr(H)Cl + C_2H_4 \rightarrow (Cp)_2Zr(C_2H_5)Cl$ (1)

Although an ethylene complex has sometimes been considered to be an intermediate, extensive search starting from various initial guess geometries have showed that ethylene does not coordinate to zirconocene; the interaction leads directly to a four-centered transition state. Although the product, an ethyl complex, is electron deficient, no agostic interaction between the zirconium atom and any hydrogen atom of the ethyl ligand takes place. The reaction is calculated to be 17 kcal/mol exothermic with the activation energy of 28 kcal/mol at the HF level. This activation barrier is much higher than those for the other olefin insertions we have previously studied. A large energy required for deformation of crowded $(Cp)_2Zr(H)Cl$ from its equilibrium structure to the transition state structure is considered to be responsible for the high activation barrier.

I-E Theoretical Studies of Chemical Reactions on Solid Surfaces

The electronic structural study of chemisorption and chemical reactions on solid surfaces is a new project we just started in April 1988, when Mr. Kyoichi Sawabe, a PhD student of University of Tokyo, joined the Morokuma group from the experimental group of Prof. Iwasawa. We are now studying the potential energy surface for dissociative chemisorption reaction of molecular hydrogen and the mechanism of hydrogen exchange reaction on magnesium oxide clusters. We hope to broaden the scope of our theoretical studies in this area, as we become more familiar with the field.

I-E-1 An Ab Initio MO Study of Hydrogen Chemisorption on Low Coordinate Site of MgO Surface. $(MgO)_4$ Cluster Model.

Kyoichi SAWABE *(Univ. of Tokyo and IMS)*, **Nobuaki KOGA, Yasuhiro IWASAWA** *(Univ. of Tokyo)* **and Keiji MOROKUMA**

The reactivity of low coordination sites of the MgO surface was investigated with the ab initio method. We adopted the $(MgO)_4$ cluster as the surface site model. For hydrogen chemisorption onto $(MgO)_4$, all structures of complexes, transition state and chemisorbed product were optimized at the RHF/6-31+(H,O)G level with the Mg-O bond length fixed at 2.106 Å.

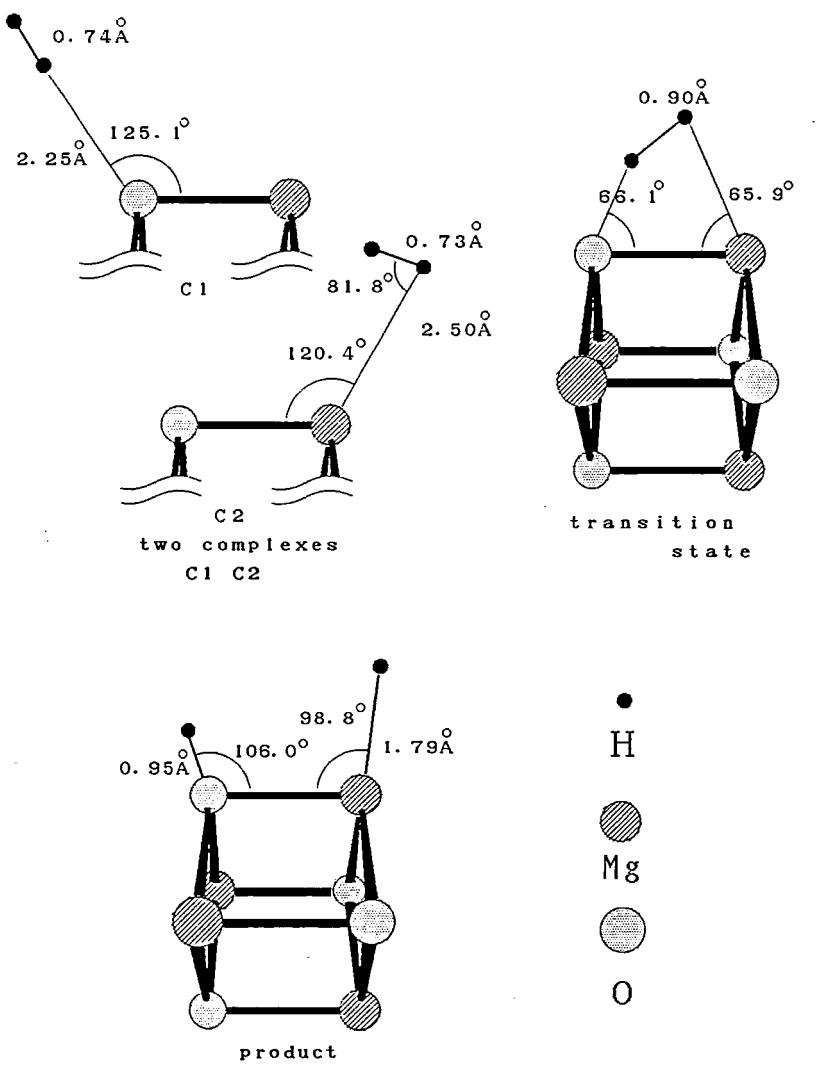

Figure 1. Optimized geometries of $(H_2)(MgO)_4$ complexes (C1, C2), transition state and product $(H)_2(MgO)_4$.

Effects of basis functions and electron correlation were studied as well.

We have found two complexes in which H_2 is adsorbed molecularly; one is an end-on complex on the oxygen site (C1 in Figure 1) and the other a side-on complex on the Mg site (C2). These complexes are led to a common transition state (TS) of dissociative chemisorption, the reaction paths from the complexes joining together before the transition state. A substantial polarization ($H^{+\delta}H^{-\delta}$) of hydrogen charges has taken place already at the TS. From the TS, the dissociative chemisorption proceeds ionically. The energies of the TS and the product relative to the isolated reactants are 5.6 kcal/mol and −15.0 kcal/mol, respectively, at RMP2/6-311+(H,O)G level.

Addition of many point charges surrounding the cluster as a model of Madelung potential has been found to enhance the ionicity of the surface. This results in an increase in the product exothermicity by several kcal/mol, though it has little effect on the activation barrier height.

I-E-2 An Ab Initio MO Study of Site Dependency of Hydrogen Chemisorption on MgO Surface. $(MgO)_6$ and $(MgO)_8$ Cluster Models

Kyoichi SAWABE *(Univ. of Tokyo and IMS)*, **Nobuaki KOGA, Yasuhiro IWASAWA** *(Univ. of Tokyo)* **and Keiji MOROKUMA**

Experimentally, varieties of hydrogen adsorption sites are thought to exist on the MgO surface. Using the cluster of $(MgO)_6$ and $(MgO)_8$, we investigated the site dependency of H_2 chemisorption. Fixing the cluster geometries, the positions of dissociatively chemisorbed hydrogen atoms were optimized at the RHF/3-21+ (H, O)G level.

We have found that a pair of dissociatively adsorbed hydrogen atoms are the most stable on the Mg_{3c}-O_{3c} site, followed by the Mg_{3c}-O_{4c} sites and that no other sites have a positive binding energy. Here Mg_{3c}-O_{4c} denotes the adjacent three-coordinate (i.e. corner) Mg and four-coordinate (i.e. edge) O site. In addition, we have found that the stabilization energy depends also on the coordination number of the nearest neighbor atoms. The most favorable is Mg_{3c44}-O_{3c44}, where the subscripts following c denote the coordination numbers of the nearest neighbors.

Models for hydrogen exchange reactions on the MgO surface were also studied. For the exchange reaction through neutral intermediates, the models of co-adsorption of two hydrogen molecules were examined. It has been found that the Mg_{4c}-O_{3c} site, which is inactive for H_2 chemisorption, become active after the adjacent Mg_{3c}-O_{4c} site are occupied with hydrogen atoms. The possibility of hydrogen exchange through such co-adsorption of two H_2 molecules, as well as through ionic intermediates, is under investigation.

I−F Structures and Reactions of Manybody Chemical Systems

Electronic structure and dynamical behavior of large systems such as liquids and polymers are investigated theoretically. (a) Collective motions and fluctuations in liquid and clusters (b) Chemical reactions and energy relations in liquid and clusters, and (c) Electronic structures and dynamical behaviors of polyenes and polyacetylenes, are analyzed.

I-F-1 Potential Energy Surfaces for Water Dynamics; Reaction Coordinates, Transition States and Normal Mode Analyses

Hideki TANAKA *(Kyoto Univ.)* **and Iwao OHMINE**

[*J. Chem. Phys.*, **91**, 6318 (1989)]

Dynamics of water binding structure reorganization is investigated by analyzing the potential energy surfaces involved. The water structures in a trajectory are quenched to their local minima, called the inherent structures. The reaction coordinates, which connect the inherent structures successively visited by the system,

are determinded. It is found that the energy barrier heights, the transition state energies, along the reaction coordinates are mostly distributed in the range of 0.2 ~ 6 kcal/mole. The classification of inherent structures is made to groups of "overall-inherent structures"; successive inherent structures are most often not so geometrically distinct. It is found that transitions between the overall-inherent structures, involving large collective motions, occurs in the sub-pico time scale. Individual molecular motions in these collective motions are strongly correlated, not yielding large transition energies. The transition state energy sometimes reaches up to 20 kcal/mole, when the system goes through the ridge between deep minima, yielding ballistic dynamical behavior. Temperature dependence of the collective motions is also investigated.

I-F-2 A Theoretical Study of Liquid Argon Dynamics; Reaction Coordinates and Transition States

Y.S. KONG *(Chonbuk National Univ. and IMS)* **and I. OHMINE**

Molecular dynamics calculation is performed by using the standard method for 108 atomic system. The periodic boundary condition used. Quenching is performed by using the steepest descent method solving the first order differential equations. The trajectory is quenched in a certain intervals (10fs) to local minima, called inherent structures. The transition states and reaction coordinates connecting among the inherent structures successively visited by the system are determined by the new technique, which is obtained by modefying the Elber and Karplus method. We found that there are essentially two energy domains; the higher energy domain and the low energy domain. The configuration at high energy inherent structure is a random amorphous structure. On the other hand, the low energy inherent structure yields the very ordered crystal-like structure. It is found that energy barrier heights from a structure to the next are fairly low for transitions in the high energy region; they are less than 0.1 kJ/atom. On the other hand, the energy barriers in low energy region are larger than ~0.3 kJ/atom. This fact indicates that the dynamics there must be a ballistic process.

I-F-3 Vibrational Energy Relaxation Processes in Liquid and Clusters

Osamu KITAO and Iwao OHMINE

We have investigated relaxation processes of optically excited molecules in liquid and clusters. It was found that the energy relaxation shows strong frequency matching dependence. For $\omega_v \gg \omega_t$ (ω_v is the excited molecular internal vibrational frequency, and ω_t is the translational mode frequency of the excited molecule in a solvent cage), the energy relaxation is governed purely by "hard impulsive collisions", the energy discipation takes place only if the vibrational amplitude exceeds a certain threshold. On the other hand, for $\omega_b \lesssim \omega_t$, the relation process becomes "resonance" type; the dissipation occurs for any amplitude of motion. Energy relaxation in clusters is also investigated. The reaction coordinates and transition state barrier neights connecting among inherent structures are being determined for surface and core modes of clusters to understand the energy transfer and evapolation mechanisms.

I-F-4 The Frequency Increase of the C = C a_g Stretch Mode of Polyenes in the $2^1A_g^-$ state: Ab Initio MOSCF Study of Butadiene, Hexatriene and Octatetraene

Mutsumi AOYAGI, Iwao OHMINE and Bryan E. KOHLER *(Univ. of California, Riverside)*

[*J. Phys. Chem.*, in press]

The harmonic force field in the ground (1^1A_g) and lowest energy excited singlet ($2^1A_g^-$) states of *trans*-butadiene, hexatriene, and octatetraene have been computed using the *ab initio* MCSCF method. The effect of mode mixing was analyzed using the Wilson GF matrix formalism. Although the calculated frequencies for the C=C symmetric stretch mode are uniformly 15% too high, the relative increase in the frequency of this mode on going from the ground (1^1A_g) to the excited ($2^1A_g^-$) state as well as the dependence of this relative increase on chain length agrees well with the experimental results. In these calculations, the frequency increase of the C=C symmetric stretch comes primarily from couplings between this mode and the C-C single bond stretches and C-C-H bends.

I-F-5 Instability of Supercooled Liquid Water

Masaki SASAI

Liquid water exhibits many anomalous properties such as the density maximum at 4°C, large heat capacity, increase of the compressibility by lowering temperature, and so on. These anomalies become more evident when the liquid water is supercooled below 0°C. At about −45°C, the heat capacity and the compressibility become critically large and water becomes unstable.

We consider that the statistics of the hydrogen bond network among water molecules is responsible for this instability. We develop the field theory model of the network by applying the techniques of de Gennes and des Cloiseaux, which are popular in polymer science. The field quantity $\phi(x)$ corresponds to the "half of" hydrogen bond and the order-parameter $<\phi>$ is proportional to the density of dangling sites. $<\phi^*(x)\phi(x)>$ is the density of hydrogen bonds and $<\phi^*(x)\phi(y)>$ is the correlation function of bonds in separate positions. Using the mean-field approximation, we investigate the instability of the network and divergence of the thermodynamic quantities. Effects of the variation of pressure and effects of the solute molecules are also studied.

I-F-6 Nonlinear Phase Excitations in the PPP Model of Polyacetylene

Masaki SASAI

[*Int. J. of Quantum Chem.* in press]

Effects of the electron-electron Coulomb interaction on polyacetylene are studied with the Pariser-Parr-Pople (PPP) model by using the unrestricted Hartree-Fock (UHF) and time-dependent Hartree-Fock (TDHF) mehods. We show that the UHF and TDHF solutions of polyacetylene are described by the amplitude and phase variables. Solitons in the PPP model are phase excitations with the almost constant amplitude. This is in a sharp contrast to solitons in the Su-Schrieffer-Heeger (SSH) model, which are pure amplitude excitations. We derive the effective Hamiltonian to describe the phase excitations in the PPP model. The effective phase Hamiltonian has a family of new soliton solutions which corresponds to the exciton and magnon in polyacetylene.

References

1) J. Takimoto and M. Sasai, *Phys. Rev. B*, **39**, 8511 (1989); J. Takimoto and M. Sasai, *Synth. Metals*, **28**, D427 (1989).
2) M. Sasai and H. Fukutome, *Prog. Theor. Phys.* **73**, 1 (1985).

I-G Theoretical Studies of Chemical Reaction Dynamics

The purposes of the theoretical reaction dynamics studies are to understand the effects of potential energy hypersurface topography and mass combination of reactants on the dynamics, and also to clarify the role of each internal degree of freedom or of the internal energy in each degree of freedom. The basic idea we employ is a separate treatment of vibrational transition and rotational transition. This is reasonable, because the mechanisms of the vibrational transitions in reaction are different from those of the rotational transitions. As for vibrational transition, the sudden and adiabatic approximations reformulated in terms of the hyperspherical coordinates have been applied to various reaction systems. For rotational transition, the IOS-DW and the independent events approximations have been proposed and applied to some systems. The reaction mechanisms can be clarified by these treatments.

I-G-1 Hyperspherical Coordinate approach to Atom-Diatom Chemical Reactions in the Sudden and Adiabatic Approximations

Akihiko OHSAKI and Hiroki NAKAMURA

[*Physics Reports*, in press]

The methodology and the basic physical idea of the sudden and the adiabatic approximations to deal with atom-diatom chemical reactions are reviewed. This paper is intended not to give a thorough review either on the applications of these approximations in the Jacobi coordinate approach or on the hyperspherical coordinate approach to reactions, but to introduce the reformulation of these approximations in terms of the hyperspherical coordinates as a practically useful method and to discuss how the reaction mechanisms can be clarified by these approaches, mainly by referring to our own numerical applications to some practical reaction systems. It is particularly emphasized that the potential ridge, the watershed dividing the reactant and product valleys, plays very important role in "reactive transition", different from the role played by the transition state. The power of the hyperspherical coordinate approach is also emphasized and demonstrated. Comparison with quasiclassical trajectory calculations clearly reveals the quantum mechanical tunneling effects. A new approach to rotational transition in reaction is also discussed briefly.

I-G-2 Rotational Transitions in Atom-Diatom Chemical Reactions

Masato NAKAMURA and Hiroki NAKAMURA

Considering the fact that the mechanisms of the rotational transitions in reaction are different from those of the vibrational transitions and that they are induced by the three consecutive processes, the rotationally inelastic half collisions in the initial and final channels and the transition induced by the particle rearrangement in the reaction zone, we have proposed a rather compact analytical theory, called IOS-DW, and also the most naive method, called independent events approximations [*J. Chem. Phys.*, **90**, 4835 (1989)]. These methods are applied to $H+H_2$ and its isotopically substituted variants and are found to work acceptably well for the simplicity of the methods.

I-G-3 Quantum Mechanical Studies of Atom-Diatom Chemical Reactions in the Sudden and Adiabatic Approximations

Akihiko OHSAKI, Seung. C. PARK *(Kangweon National Univ., Korea)* **and Hiroki NAKAMURA**

Hyperspherical coordinate approach in the sudden and adiabatic approximations are employed to investigate the reactions $O(^3P) + HCl \rightarrow OH + Cl$, $Cl + H_2 \rightarrow HCl + H$, and their isotopically substituted variants. The reaction cross sections and the rate constants are calculated. Comparisons are made with experiments and quasiclassical trajectory calculations. Quantum mechanical tunneling effects are clearly manifested at low collision energies (low temperatures). As is expected, the adiabatic (sudden) approximation works well for the light(heavy)-atom-transfer reactions. The following various aspects of the above reactions are discussed and clarified: isotope effect, tunneling effect, effect of surface topography, and steric effect.

I–H Theoretical Studies of Highly Excited States of Atoms and Molecules

Highly (electronically or vibrationally) excited states show various intriguing properties and participate in a variety of dynamic processes. We believe that they will open a new challenging world of science. The ultimate purpose of our studies is to find and understand the new collective motions in these states and their isomorphism among the various systems of different kinds. We also want to have a unified view of the various dynamic processes involving the highly excited states.

I-H-1 Generator Coordinate Representation of the O(4) Supermultiplets of Doubly Excited States

Masahiro IWAI and Hiroki NAMAMURA

[*Phys. Rev.* **A40**, 2247 (1989)]

The O(4) supermultiplets of doubly excited states of atoms are analyzed and reexpressed in a generator coordinate representation. It is explicitly shown that a complete separation of the collective and internal motions is realized in the high excitation limit. A new explicit expression for the collective vibration in terms of quasi-spin operators is also derived. Particular emphasis is laid on the close relation between the group theoretical supermultiplet classification and the mean-field theoretical approach.

I-H-2 Cranking Model of Collective Rotational Motion of Atomic Electrons

Masahiro IWAI and Hiroki NAKAMURA

[*Phys. Rev.* **A**, in press]

Collective rotational motion of strongly correlated atomic electrons is investigated by using the self-consistent cranking model. The intrinsic wave function and the moment of inertia are analyzed as a function of angular velocity of rotation. Origin of the "rotational contraction" is ascribed to the effect of quantum-mechanical shell structure.

I-H-3 Superexcited States of Molecules —Their Dynamic Processes and Quantum Defect Theory—

Hiroki NAKAMURA and Hidekazu TAKAGI *(Kitasato Univ.)*

[*Butsuri* (in Japanese), in press]

Superexcited states of molecules are classified into the following two: (1) doubly excited states embedded in the electronic continuum, and (2) rovibrationally excited Rydberg states. The autoionization mechanisms of these states are clarified. A brief review of the multichannel quantum defect theory is presented, and it is shown that the various dynamic processes can be treated in a unified way by this theory. Thoeretical analysis of the multiphoton ionization of NO and the dissociative recombination of electrons with hydrogen molecular ions are discussed as examples.

I–I Theory for High-T_c Superconductivity

To clarify the physical and chemical natures of metal-oxide type high-temperature superconductors, we theoretically study a microscopic electronic structure of this type materials. We are mainly interested in the origin of pairing attraction in this type materials.

I-I-1 BCS Pairing Mediated by Double Excitation of Triplet in Two-Band System with Intermediate Electron Correlations

Keiichiro NASU

[*Physica*, in press]

A two band system, composed of a half-filled insulating band and a metallic band, with no hybridization in between, is studied as a model for Cu-O type high-Tc ceramics. In the case of hole-type ceramics, these two bands correspond to the 3d band of Cu and the 2p band of O, while, in the case of electron-type newly found ceramics, they correspond to the 3d and 4s bands of Cu. The intraband electron-electron repulsions are assumed to be intermediate strength, while the interband repulsion V is assumed to be weak. It is shown, however, that this V results in an attraction between electrons in the metallic band, through a virtual excitation of two triplet excitons (or two magnons) which are low lying excitations in the correlation gap of the half-filled band. Because of its

retardation effect, this attraction can overcome the direct coulombic repulsion between electrons, only at around the Fermi level, and can give Tc of about 50K ~ 100K. A large damping of this excitation due to the ferromagnetic interband exchange is also obtained, in agreement with experimental results.

I-I-2 N-Band Hubbard Models for Doped Transition Metal Oxides -Cooperation of Charge and Spin Fluctuations for the High-Tc Superconductivity-

Kizashi YAMAGUCHI*, Hideo NAMIMOTO*, Takayuki FUENO* *(*Osaka Univ.)*, **Shigeyoshi YAMAMOTO and Keiichiro NASU**

[*Physica*, in press]

The N-band Hubbard models for doped cooper oxides and related species were investigated in order to elucidate the populations of doped holes and spin densities, and lower-lying electronic excitations. The implications of these results are discussed in relation to the cooperation of charge and spin fluctuations for the high-Tc superconductivity.

I-J Nonlinear Excitations in Halogen-Bridged Mixed-Valence Metal Complexes

To clarify the nature of nonlinear excitations in one dimensional charge density wave state, we study solitons, excitons and polarons in one-dimensional halogen-bridged mixed-valence metal complexes.

I-J-1 Pair-Creation Path of Charged Soliton through Photoexcitation in Halogen-Bridged Metal Complexes

Akiomi MISHIMA *(Kanazawa Inst. of Technology)* **and Keiichiro NASU**

[*Synthetic Metals* **29**, F175 (1989)]

To clarify the lattice relaxation paths of the photogenerated charge transfer excitation in halogen-bridged mixed-valence metal complexes, we study the ground and excited states of a one-dimensional Peierls-Hubbard model with half-filled electrons. A pair of charged solitons is shown to be the lowest excited states and causes a photo-induced absorption (PIA) with an energy of about a half of the gap, while a distant pair of polarons is shown to give the three PIA bands observed by Kurita et al. The self-trapped exciton is shown to be the next lowest excited state separated from this soliton pair only by a small barrier in agreement with the recent experiments.

I-J-2 A Formation Process of a Bipolaron and New Light Absorption Bands in Halogen-Bridged Mixed-Valence Metal Complexes

Akiomi MISHIMA *(Kanazawa Inst. of Technology)* **and Keiichiro NASU**

[*Phys. Rev.* **B40**, 5593 (1989)]

A formation process of a singlet bipolaron from doped two polarons in halogen-bridged mixed-valence metal complexes is studied, by using a one-dimensional extended Peierls-Hubbard model with N(≫1) lattice sites and N+2 electrons. The ground and the excited states of this system are calculated within the unrestricted Hartree-Fock theory for electrons, and by the adiabatic approximation for phonons. Doped two polarons are shown to make a singlet bound state as the result of competition between the Coulombic repulsion and the phonon-mediated attraction, and its interpolaron distance becomes a few times of the lattice constant. A new light absorption band due to this bound state is also shown to appear at the energy of about 50% of the intrinsic gap. These theoretical results agree well with the recent optical and ESR experiments. A pair of solitons is also studied, and is shown to have no bound state.

I–K Theory for Nonadiabatic Electron-Transfer at Solid Surface

To clarify the dynamics of the electron transfer or the energy transfer from a molecule to solids at its surface, we study a time evolution of an electron using the Fano-Anderson type model. Our main interest is to clarify the nonadiabatic transfer rate of an electron from a molecule to a conduction band of solids.

I-K-1 Dynamics of Charge Transfer between Semiconductor Surface and Molecule: Numerical Calculations for Nonadiabatic Transition to Continuum State

Masato SUZUKI *(Hiroshima Univ. and IMS)* **and Keiichiro NASU**

[*J.C.P.*, in press]

The dynamical process wherein electrons or holes transfer from molecules to continuum states of solids, appears in various experiments of surface-molecule systems, as their elementary process. In this study, the nonadiabatic charge transfer from a molecular level to a conduction band of a semiconductor is investigated by using the Fano-Anderson type model Hamiltonian. The numerical solutions of this Hamiltonian are analyzed as a function of real time by using the Trotter formula.

New concepts for the nonadiabatic electron transition from a descrite to a continuum are explicated, especially, in connection with the effects of the band width on the transition rate. When the band width is comparatively narrow, the transition rate increases as this width increases, since the irreversibility of the electron at the final state increases. In the case of the wide band width, on the other hand, the transition rate decreases with the increase of this width. The decrease in this region is mainly caused by the decrease of the substantial surface-molecule interaction. Thus, the maximum of the transition rate is shown to be realized in the case of intermediate band-width.

It is also shown that the quantum interference effect between the back and forth motions of the wave packet is very important to determine the transition rate.

I–L Collison Dynamics of Atoms in Doubly Excited States

To elucidate correlation effects in collision dynamics, we theoretically investigate collision processes involving He atoms in high-lying doubly excited states in collisions with charged and neutral particles and try to understand the physical meaning of the propensity rules obtained based on the interpretation of the rovibrational models of the collective motion of two atomic electrons.

I-L-1 Electron Impact Excitation of Atoms in High-Lying Doubly Excited States: Correlation Effects in Collision Dynamics

Takashi MOTOYAMA *(Univ. of Electro-Comm.)*, **Naoto KOYAMA** *(Univ. of Electro-Comm.)* **and Michio MATSUZAWA** *(Univ. of Electro-Comm. and IMS)*

[*Phys. Rev. A.*, **38**, 670 (1988)]

Based on the hyperspherical approach, we have calculated the generalized oscillator strengths and the electron-impact-excitation Born cross sections from the initial $^1S^e$ high-lying doubly excited states to the final $^1P^e$ and $^1D^e$ high-lying doubly excited ones. Together with the previous results on the $^1S^e$-$^1S^e$ excitation processes, we have found a simple propensity rule that the excitation processes with $\Delta n_2 = 0$ are most likely to take place within each manifold, i.e., the S-S, S-P, or S-D excitation process where n_2 is the radial bending quantum number, i.e., the number of the nodes of the bending vibrational wave functions on the body fixed

frame based on the rovibrator model of the doubly excited states. There propensity rules are interpreted based on the rovibrator model of collective motion of two atomic electrons.

I-L-2 High-Lying Doubly Excited States of H^- and He: II. $^1P^o$ States

Naoto KOYAMA *(Univ. of Electro-Comm.)*, **Atsuko TAKAFUJI** *(Univ. of Electro-Comm.)* **and Michio MATSUZAWA** *(Univ. of Electro-Comm. and IMS)*

[*J. Phys. B At. Mol. Opt. Phys.* **22**, 553 (1989)]

We present the energy levels of the doubly excited $^1P^o$ states of H^- and He which belong to the manifolds of the $N = 3-7$ threshold of H and He^+, respectively. We calculate these energies using the hyperspherical coordinates method with a set of basis functions of 100 terms. The energy levels obtained are specified in terms of the supermultiplet classification based on the collective representation of the rovibrator model for the doubly excited states. Our calculated energies are found to be in agreement with other *ab initio* calculations available at present within an accuracy of a few per cent.

I-L-3 Collision of He in Doubly Excited States with Ar: Correlation Effects in Collision Dynamics

Naoto KOYAMA *(Univ. of Electro-Comm.)*, **Atsuko TAKAFUJI** *(Univ. of Electro-Comm.)* **and Michio MATSUZAWA** *(Univ. of Electro-Comm. and IMS)*

[*Chinese J. Phys.*, in press]

To understand the collisional properties of atoms in doubly excited states, we have theoretically investigated the excitation processes of doubly excited He atoms by collisions with Ar, paying particular attention to the correlated motion of the two excited electron. The doubly excited states of He are described in hyperspherical coordinates and in terms of the supermultiplet classification scheme based on the rovibrator model of the collective motion of XYX triatomic molecules. We employ the impluse approximation to describe collision processes. We have neglected the He^{++}-Ar interaction and made use of experimental data on e-Ar elastic scattering cross-sections to describe the e-Ar interaction. Evaluating the cross-sections from some initial states to various final states, we have found some systematic trends, i.e. "propensity rules", in the excitation processes between the doubly excited states. A set of simple propensity rules is presented for the excitation processes form the $^1S^e$ to the $^1S^e$ and $^1P^o$ doubly excited states of He and interpreted based on the rovibrator model. The results are briefly compared with those previously obtained for electron impact excitation processes.

I-L-4 Electron-Impact Excitation of Atoms in High-Lying Doubly Excited States: Single Electron Excitation between Doubly Excited States

Michio MATSUZAWA *(Univ. of Electro-Comm. and IMS)*, **Tohru ATSUMI** *(Univ. of Electro-Comm.)* **and Naoto KOYAMA** *(Univ. of Electro-Comm.)*

It is theoretically pointed out that, even between the strongly correlated doubly excited states, there exist single-electron type transitions in electron impact excitation processes of He atoms in doubly excited states under the condition $\Delta L=0$ where L is the total orbital angular momentum of the atom. The propensity rules found for the $^1P^o-^1P^o$ and $^1D^e-^1D^e$ double excitation processes are also presented and discussed based on the rovibrational interpretation of the collective motion of the two atomic electrons.

I–M Electronic Properties and Structural Change in Condensed Matter

We study the effect of the electron correlation and the electron-lattice interaction to understand the variety in electronic properties in condensed matter (metal, semiconductor and insulator) and the transition between them.

I-M-1 Self-Trapping in Mixed Crystal. II: A Mean-Field Approach

Yuzo SHINOZUKA *(Yamaguchi Univ. and IMS)*

[*J. Phys. Soc. Jpn.*, in press]

We study self-trapping of a Frenkel exciton in binary mixed crystal A_xB_{1-x} with randomness in exciton atomic (ε_i) and transfer (t_{ij}) energies, and short range exciton-lattice interaction D_i. The energies of relaxed excitons are calculated for self-trapped (S_i) state at i=A or B site and free (F) state with the use of the coherent potential approximation. Extrinsic self-trapping and F-S transition are discussed with the phase diagrams obtained for various parameters $\Delta=\varepsilon_B-\varepsilon_A$, D_i, exciton band width T_i (i=A, B) and the concentration x. The results are compared with recent experiments on mixed ionic crystals and II-VI compound semiconductors.

I-M-2 Theory for Intrinsic Electronic States and Lattice Relaxation Processes in Amorphous Semiconductors

Yuzo SHINOZUKA *(Yamaguchi Univ. and IMS)*

In order to understand various electronic-atomic processes in amorphous semiconductors, especially in a-Si, we study a simple two-site model, which represents one of Si-Si bonds consists of two sp^3 orbitals. We calculate the ground and excited states of one, two and three electrons in the system, depending on the Fermi level. With the aid of the adiabatic potentials for these states, we can dicuss various physical properties and electronic-atomic processes, including the density of states in the gap, optical and thermal excitation energy, relaxation and recombination of an electron and a hole, creation and annihilation of dangling bond pair.

RESEARCH ACTIVITIES II
Department of Molecular Structure

II-A High Resolution Spectroscopy of Transient Molecules and Ions

During the course of chemical reactions many transient molecules and ions appear as intermediates. Because of their high reactivities, i.e. their short lifetimes, these transient species have remained to be explored and some of them have even escaped detection. Many of these molecules have open-shell electronic structure, which characterizes them as free radicals. Unpaired electrons in a molecule cause splittings in high resolution spectra of such species through fine and hyperfine interactions, and, when properly analyzed, these splittings provide us with information on the electronic properties of the molecule which is not obtainable for molecules without unpaired electrons. High resolution spectroscopy not only provides molecular constants of transient molecules at very high precision, but also allows us to unambiguously identify chemical species occuring in reaction systems and to unravel the details of reaction mechanisms, in particular, when it is combined with some time-resolved detection methods. The present project will also be of some significance in related fields such as astrophysics and environmental sciences, and even in semiconductor fabrication.

II-A-1 Microwave Spectroscopy of Dichlorosilylene in Excited Vibrational States

Masaharu FUJITAKE and Eizi HIROTA

The microwave spectrum of $^{28}Si^{35}Cl_2$ has been observed for the ν_2, $2\nu_2$, ν_1, and ν_3 states and analyzed to yield rotational and centrifugal distortion constants in each state. For ν_1 and ν_3, the Coriolis interaction has been taken into account explicitly. Table I summarizes the rotational constants thus determined together with the ν_1/ν_3 Coriolis parameters D and F and the energy difference E_1–E_3. The equilibrium rotational constants were thus derived as A_e = 14755.506, B_e = 2832.060, and C_e = 2376.090 MHz, which led to the residual inertial defect of $\Delta_e = -0.006$ uÅ^2. The equilibrium molecular structure was calculated from A_e, B_e, and C_e to be r_e(Si-Cl) = 2.0653(1) Å and θ_e(Cl-Si-Cl) = 101°20(1)′. Harmonic force field was derived from the Coriolis coupling constant and the vibrational frequencies, and was checked by calculating centrifugal distortion constants to be compared with the observed values. The vibration-rotation constants were then employed to derive third-order anharmonic potential constants: $F_{rrr} = -11.7$ md/Å^2, $F_{rrr'} = -0.21$ md/Å^2, $F_{rr\theta} = -0.44$ md/Å, $F_{rr'\theta} = -0.47$ md/Å, $F_{r\theta\theta} = -1.16$ md, and $F_{\theta\theta\theta} = -2.80$ mdÅ.

Table I. Rotational Constants of $^{28}Si^{35}Cl_2$ in Excited Vibrational States (MHz)[a]

	ν_2	$2\nu_2$	ν_1	ν_3
A	14 906.915(24)	15 035.030(99)	14 817.674(72)	14 669.809(75)
B	2 818.422(5)	2 814.365(38)	2 810.282(14)	2 819.236(22)
C	2 361.333(6)	2 356.093(62)	2 357.888(18)	2 361.008(19)
D			2 834.46(26)	
F			[−17.464][b]	
E_1–E_3/cm^{-1}			5.402 46(19)	

a. Values in parentheses denote three standard deviations and apply to the last digits of the constants.
b. Fixed. This value was calculated from the force field derived.

II-A-2 Coriolis Interaction between the ν_1 and $\nu_2+\nu_3$ States of DBO

Yoshiyuki KAWASHIMA *(Kanagawa Tech. Univ.)*, **Kentarou KAWAGUCHI, Toshinori SUZUKI, Masaharu FUJITAKE, and Eizi HIROTA**

We have observed rotational and vibrational-rotational transitions of HBO and DBO and have derived equilibrium structure and harmonic and anharmonic (third-order) potential constants precisely.[1] However, the spectra involving the ν_1 state of DBO have eluded detection. This failure is probably due to a

Coriolis interaction between ν_1 and $\nu_2+\nu_3$; the latter state is expected to be very close to the ν_1 state in $D^{11}B^{16}O$. Therefore, a careful search was carried out for the ν_1 band of DBO in 2220 to 2300 cm^{-1} with an infrared diode laser spectrometer. The discharge in BCl_3(60 mTorr) + O_2(trace) + D_2(120 mTorr) + He (3 Torr) was employed to generate DBO. Twelve lines thus observed could be fitted, if we took into account the Coriolis interaction with $\nu_2+\nu_3$. Using this result, we predicted pure rotational transitions of DBO in the ν_1 state and observed three transitions at the predicted frequencies. All the observed data were then subjected to a least-squares analysis to yield molecular constants listed in Table I. The Coriolis constant thus determined agrees with the value 0.107 calculated from the force field.

Reference

1) Y. Kawashima, Y. Endo, and E. Hirota, *J. Mol. Spectrosc.*, **133**, 116 (1989) and earlier references cited therein.

Table I. Molecular Constants of $D^{11}B^{16}O$ in the ν_1 and $\nu_2+\nu_3$ States[a]

Constant	ν_1	$\nu_2+\nu_3$
B_v	1.039 598(30)	[1.046 734 56][b]
10^6D	[1.761][b]	[1.716][b]
ν_0	2253.528 7(10)	2263.[c]
10^3q_{2+3}		[4.807 96][b]
$\zeta_{1,2+3}$	0.110 70(56)	

a. In cm^{-1}, except for $\zeta_{1,2+3}$, which is dimensionless. The values in parentheses denote three standard deviations and apply to the last digits of the constants.
b. Fixed.
c. Not included in the fit, but adjusted in 1 cm^{-1} step so as to get a best fit.

II-A-3 Infrared Diode Laser Kinetic Spectroscopy of the Vinyl Radical

Hideto KANAMORI, Yasuki ENDO, and Eizi HIROTA

A c-type band was observed at around 895 cm^{-1} by infrared diode laser kinetic spectroscopy combined with the excimer laser photolysis of vinyl halides at 193 nm and was assigned to the CH_2 wagging mode of the vinyl radical. The band was found to consist of two component bands separated by 0.0541 (11) cm^{-1}. Both component bands showed clearly the statistical weight in an alternative way, that is, if one shows the weight 1:3 for even: odd K_a levels, the other exhibits 3:1, indicating that the radical is of C_{2v} effective symmetry, executing a double-minimum motion probably associated with the C-H in-plane rocking vibration. The upper states of the two bands were found to be perturbed weakly, possibly by a Coriolis interaction with the first overtone state of the C-H rocking mode.

II-A-4 Diode Laser Spectroscopy of C_3: the $\nu_2+\nu_3-\nu_2$, $2\nu_2+\nu_3-2\nu_2$, and $2\nu_2+\nu_3$ Bands

Kentarou KAWAGUCHI, Keiji MATSUMURA *(Seinan Gakuin Univ.)*, **Hideto KANAMORI, and Eizi HIROTA**

[*J. Chem. Phys.*, **91**, 1953 (1989)]

The ν_3 hot bands (011)–(010), (021)–(020), and the combination band (021)–(000) of C_3 were observed by a diode laser spectroscopic method. The C_3 molecule was produced by the photolysis of allene or by the discharge in cyclopropane or furan. Analysis gave molecular constants in each vibrational state and also the energy difference between (020) and (000). The derived vibrational frequencies were compared with the result of a Morse oscillator-rigid bender internal dynamics (MORBID) calculation by Jensen.

II-A-5 Detection of the Silylene ν_2 Band by Infrared Diode Laser Kinetic Spectroscopy

Chikashi YAMADA, Hideto KANAMORI, Eizi HIROTA, Nobuki NISHIWAKI *(Nagoya Univ.)*, **Naoshi ITABASHI** *(Nagoya Univ.)*, **Kozo KATO** *(Nagoya Univ.)*, **and Toshio GOTO** *(Nagoya Univ.)*

[*J. Chem. Phys.*, **91**, 4582 (1989)]

The ν_2 band of the silylene SiH_2 molecule in $\tilde{X}^1A_1$ was observed for the first time in the gas phase by using infrared diode laser kinetic spectroscopy. Silylene molecules were generated by the photolysis of phenylsilane at 193 nm. The observed spectrum was analyzed to determine the rotational and centrifugal distortion constants in the ground and $\nu_2=1$ states and the band origin ν_0=998.6241 (3) cm^{-1} with one standard deviation in parentheses. The significance of the derived parameters was discussed in detail.

II-A-6 Diffusion Coefficient and Reaction Rate Constant of the SiH_3 Radical in Silane Plasma

Naoshi ITABASHI *(Nagoya Univ.)*, **Kozo KATO** *(Nagoya Univ.)*, **Nobuki NISHIWAKI** *(Nagoya Univ.)*, **Toshio GOTO** *(Nagoya Univ.)*, **Chikashi YAMADA, and Eizi HIROTA**

[*Jpn. J. Appl. Phys.*, **28**, L325 (1989)]

By using infrared diode laser absorption spectroscopy, the rotational temperature and the number density of the SiH_3 ($\tilde{X}^2A_1$) radical were measured in a pulsed SiH_4/H_2 discharge. The decay of the absorption intensity was also measured as a function of the filling gas pressure for the line Q(6,6) ($1^- \leftarrow 0^+$) of the SiH_3 ν_2 fundamental band to determine the effective diffusion coefficients (D(SiH_3 in H_2) and D(SiH_3 in SiH_4)) and the reaction rate constant (k) of the SiH_3 radical.

II-A-7 Infrared Diode Laser Spectroscopy of SCl Generated by the Photolysis of S_2Cl_2 and SCl_2

Eberhard TIEMANN *(Univ. Hannover and IMS)*, **Hideto KANAMORI, and Eizi HIROTA**

[*J. Mol. Spectrosc.*, **137**, 278 (1989)]

The photolysis of S_2Cl_2 and SCl_2 with excimer laser radiation at 248 nm yields the SCl radical in its electronic ground state $X^2\Pi_{3/2}$. By infrared diode laser kinetic spectroscopy the vibrational bands v=1–0 and 2–1 are observed up to high rotational levels ($J \leqq 59.5$) and the isotopes $^{32}S^{35}Cl$ and $^{32}S^{37}Cl$ are assigned. The spectrum is fitted to a few molecular parameters using isotope relations. It cannot be ruled out that the hot band (2–1) should be assigned to the missing $X^2\Pi_{1/2}$ state.

II-A-8 Infrared Diode Laser Spectroscopy of the LiO Radical

Chikashi YAMADA and Eizi HIROTA

The fundamental vibrational band of the ^{7}LiO radical ($X^2\Pi_i$) has been observed by infrared diode laser spectroscopy. The lithium monoxide radical was generated in a high temperature cell by the reaction of lithium metal vapor with N_2O. Absorption signal was detected with diode lasers which covered a range of 720 to 850 cm^{-1} and were frequency modulated. The present result was analyzed, together with those of radio frequency and microwave spectroscopy, to yield a precise value for the band origin. The spin-orbit interaction constants of v=0 and v=1 have been improved in accuracy.

II-A-9 Microwave Spectrum of the RbO Radical

Chikashi YAMADA, Masaharu FUJITAKE, and Eizi HIROTA

As an extension of our studies on alkali monoxides, we have investigated the rubidium monoxide radical with microwave spectroscopy. We have shown that LiO, NaO, and KO have the $^2\Pi$ ground electronic state, but previous electron spin resonance and *ab initio* theoretical studies concluded that the $^2\Sigma^+$ state was the real ground state for RbO. We attempted to use the alkali metal and N_2O reaction which was successfully employed to produce LiO, NaO, and KO, but found it difficult to handle Rb metal, because its melting point is 38°C. Therefore, we first generated Rb by the reaction RbCl + Li → Rb + LiCl; we loaded Li metal and RbCl in a microwave absorption cell. At 350°C absorption lines started to appear and reached an optimum condition at 500°C. The region 103–380 GHz was scanned, and, as expected, $^2\Sigma^+$ type spectra were observed for the v = 0 and 1 states of ^{85}RbO and the v = 0 state of ^{87}RbO. Least-squares analysis of the observed spectra yields molecular constants listed in Table I. The equilibrium bond length was calculated from B_e to be 2.254 195 Å and the harmonic vibrational frequency was estimated using D_e to be 388.4 cm^{-1}.

Table I. Molecular Constants of the RbO Radical (MHz)[a]

Constant	$^{85}Rb^{16}O$ v=0	$^{85}Rb^{16}O$ v=1	$^{87}Rb^{16}O$ v=0
B	7 356.7244(39)	7 291.5432(37)	7 329.9930(20)
D	0.012 617(33)	0.014 043(32)	0.012 540(56)
γ	−1 072.51(12)	−2 051.38(13)	−1 068.13(12)
γ_D	0.046 26(63)	0.151 66(65)	0.046 22(21)
b	180.39(60)	175.16(56)	604.1(40)
c	44.7(21)	53.4(18)	167 (12)
eQq	−26.6(34)	−35.2(30)	−24 (13)
C_I	0.007(16)	[0.0][b]	0.050(44)

a. Values in parentheses denote standard deviation and apply to the last digits of the constants.
b. Fixed.

II-A-10 The Millimeter- and Submillimeter-Wave Spectrum of Dichlorocarbene CCl_2: Electronic Structure Estimated from the Nuclear Quadrupole Coupling Constants

Masaharu FUJITAKE and Eizi HIROTA

[*J. Chem. Phys.*, **91**, 3426 (1989)]

The pure rotational spectrum of CCl_2 in the ground state was observed for the first time in the millimeter- and submillimeter-wave region. The CCl_2 molecule was generated directly in a free space cell by a dc glow discharge in CCl_4. Several transitions showed hyperfine splittings arising from the nuclear quadrupole coupling of two Cl atoms. Analysis of the observed spectrum yielded the rotational, centrifugal distortion, and nuclear quadrupole coupling constants of the $C^{35}Cl_2$ species. The r_0 structure was derived from the rotational constants to be r_0(C-Cl) = 1.7157 Å and θ_0(ClCCl) = 109.2°. The ionic and π character of the C-Cl bond were estimated from the nuclear quadrupole coupling constants to be 0.26 and 0.32, respectively.

II-A-11 The Microwave Spectrum of the AlO Radical

Chikashi YAMADA, Edward A. COHEN *(Jet Propulsion Lab. and IMS)*, **Masaharu FUJITAKE, and Eizi HIROTA**

The rotational spectrum of the aluminum monoxide radical in the ground electronic state $X^2\Sigma^+$ was observed in the millimeter- and submillimeter-wave region. Aluminum monoxide radicals were generated directly in a flow reactor absorption cell by the reaction of N_2O with aluminum vaporized from a high-temperature crucible. The observed spectrum was analyzed to yield molecular constants including the rotational constant, centrifugal distortion constant, spin-rotation interaction constant, magnetic hyperfine interaction constants, and nuclear quadrupole coupling constant, as listed in Table I. The b and c hyperfine constants were interpreted in terms of two configurations $Al^{++}O^{--}$ and AlO which contributed 19.1 and 67.8%, respectively, leaving 13.1% for Al^+O^-.

Table I. Molecular Constants of the AlO Radical (MHz)[a]

B	19 141.574 1(11)	b	681.6(14)
D	0.033 120 5(65)	c	169.18(25)
γ	51.660(38)	C_I	−0.014 3(39)
γ_D	0.003 43(17)	eQq	−26.08(69)

a. Values in parentheses denote standard deviation and apply to the last digits of the constants.

II-A-12 The $CH_4 + O(^1D) \rightarrow CH_3 + OH$ Reaction Investigated by Infrared Diode Laser Kinetic Spectroscopy

Toshinori SUZUKI and Eizi HIROTA

The reaction in the title is one of the most fundamental reactions among those induced by $O(^1D)$. It has been studied by monitoring OH with laser induced fluorescence, but CH_3 radicals simultaneously produced have not been examined because of the lack of spectroscopic methods suitable for CH_3. In the present study we applied infrared diode laser kinetic spectroscopy to CH_3 radicals to clarify their dynamical behavior in the reaction system. We generated $O(^1D)$ by the photolysis of N_2O at 193 nm. The sample was a mixture of N_2O and methane, which was flowed through a cell with the total pressure maintained at 500 mTorr. The $^qQ_N(N)$ with N=1–9 of v_2=3–2 and a few R lines of v_2=1–0 and 2–1 of CH_3 and lines of J=19.5 to 24.5 of OH in $^2\Pi_{1/2}$ and $^2\Pi_{3/2}$ were observed. Methyl radicals seem to attain the equilibrium rotational distribution within 2 μs after the excimer laser was fired, and thus their lines will reflect the vibrational

distribution. Figure 1 shows the time profiles of the v = 3 ← 2 $^qQ_6(6)$ and v = 1 ← 0 $^qR_5(6)$ lines of CH_3. Oxygen in ^3P was generated by the photolysis of SO_2 at 193 nm. In this case CH_3 radicals were detected, but no OH lines were observed.

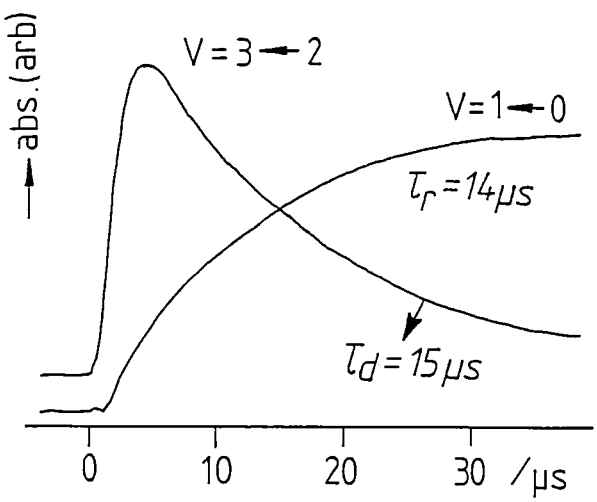

Figure 1. Time profiles of $v_2 = 3 \leftarrow 2$ $^qQ_6(6)$ and $v_2 = 1 \leftarrow 0$ $^qR_5(6)$ of CH_3 generated by the 193 nm photolysis of N_2O in a CH_4: N_2O = 2:1 mixture with the total pressure of 500 mTorr.

II-A-13 Microwave Spectrum of the SSCl Radical

Masaharu FUJITAKE and Eizi HIROTA

The S_2Cl radical has been known to arise from photochemical and thermal decompositions of and from reactions with alkali metals of S_2Cl_2. Electronic absorption spectroscopy in the gas phase and infrared spectroscopy in low-temperature matrices[1] have been carried out, in addition to an electron spin resonance study, which concluded the spin density to be localized at the terminal S atom[2]. We generated S_2Cl radicals directly in a microwave absorption cell by a dc glow discharge in an S_2Cl_2/Ar or SCl_2/Ar mixture; the optimum condition was S_2Cl_2 of 6 mTorr mixed with Ar of 15 mTorr, discharged with the current of 35 mA. An external microwave discharge also yielded S_2Cl, indicating the radical to be of relatively long lifetime. The rotational spectrum was observed in 170 to 380 GHz, and the Zeeman effect was of great use in discriminating S_2Cl lines against diamagnetic lines of S_2Cl_2. Figure 1 illustrates an example of the observed spectrum. The Cl hyperfine structure has not been resolved. Both a-type and b-type transitions were observed with nearly equal intensities, as shown in Figure 1. The lines of the ^{37}Cl species were also detected, giving further support to ascribing the observed paramagnetic lines to S_2Cl. Least-squares analysis yielded A = 18 319.67(10), B = 2 827.582(16), C = 2 445.941(10), ε_{aa} = −1334.8(21), ε_{bb} = −120.81(44), ε_{cc} = 1.79(19), and $|\varepsilon_{ab}+\varepsilon_{ba}|/2$= 27.9(89) MHz with three standard deviations in parentheses.

References

1) M. E. Jacox, *J. Phys. Chem. Ref. Data*, **17**, 269 (1988).
2) F. G. Herring, C. A. McDowell, and J. C. Tait, *J. Chem. Phys.*, **57**, 4564 (1972).

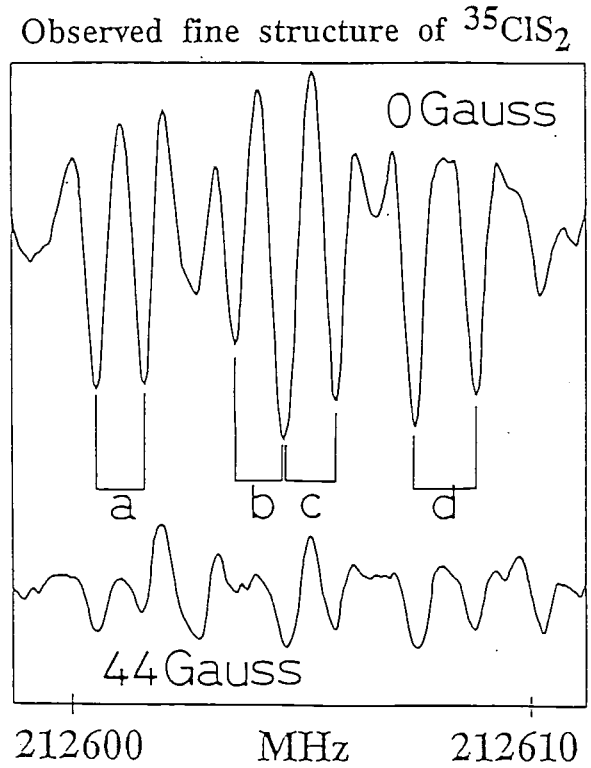

Figure 1. Observed spectra of $^{35}ClS_2$; a $43_{0,43} \leftarrow 42_{1,42}$, b $43_{1,43} \leftarrow 42_{1,42}$, c $43_{0,43} \leftarrow 42_{0,42}$, and d $43_{1,43} \leftarrow 42_{0,42}$. The lower trace was recorded with a magnetic field of 44 G.

II-A-14 Diffusion Coefficient of the CF Radical

Mitsuo MAGANE *(Nagoya Univ.)*, **Naoshi ITABASHI** *(Nagoya Univ.)*, **Nobuki NISHIWAKI** *(Nagoya Univ.)*, **Toshio GOTO** *(Nagoya Univ.)*, **Chikashi YAMADA, and Eizi HIROTA**

In order to facilitate understanding etching processes taking place in fabricating electronics material, we have been developing a method of measuring the abundance of active species present in discharge plasma. In the present study we focused attention to CF radicals generated by a dc discharge in a CF_4/H_2 mixture and determined their concentration as a function of time. For a sample consisting of CF_4 and H_2 with the partial pressures of 41.7 and 258.3 mTorr, respectively, and flowed with a rate of 105 sccm, both the rotational and spin temperatures were found to be 320±20 K and the abundance of CF in $X^2\Pi$ was determined to be $1.33(6)\times10^{12}$ cm^{-3}. The decay curve of a CF line, $R_2(4.5)$ of the fundamental band, was then measured while varying the pressures of CF_4 and H_2. The dc discharge pulse employed was of 1.1 ms width with the peak current of 1 A and the repetition rate of 9 Hz. The decay profile was found to be of single exponential with the time constant increasing linearly with the total pressure as well as the H_2 partial pressure, indicating that the process was determined mainly by diffusion. The diffusion constant was determined to be 630(30) and 230(10) $cm^2Torr\ s^{-1}$ for CF in H_2 and CF_4, respectively.

II-A-15 Reactions of Excimer-Laser Generated Oxygen Atoms with Unsaturated Hydrocarbons Investigated by Microwave Kinetic Spectroscopy

Seiichiro KODA *(Univ. Tokyo)*, **Yasuki ENDO** *(Univ. Tokyo and IMS)*, **Soji TSUCHIYA** *(Univ. Tokyo)*, **Chikashi YAMADA, and Eizi HIROTA**

We have previously investigated the reaction of $O(^3P)$ with ethylene by monitoring vinoxy, formyl, and formaldehyde with microwave spectroscopy[1]. In this experiment $O(^3P)$ was generated by the Hg-sensitized decomposition of N_2O. As a result the time scale of $O(^3P)$ generation was rather long; the Hg-lamp emitted a light pulse 4 ms long with about 0.2 ms rise and fall times. In the present experiment the $O(^3P)$ source was replaced by the excimer laser photolysis of SO_2 at 193 nm. The microwave kinetic spectroscopic method employed was described previously[2]. The ratio of ethylene or propylene and SO_2 was chosen to be either 2:1 or 1:2 with the total pressure lower than 30 mTorr. The time profiles measured for the three species are shown in Figures 1(a) and 1(b) for the C_2H_4 and C_3H_6 cases, respectively. The branching ratio (1b)/(1a) for $C_2H_4 + O \rightarrow CH_2CHO + H$ (1a) and $HCO + CH_3$ (1b) was determined to be 1.15±0.20, in good agreement with the previous result 1.2±0.23[1]. For $C_3H_6 + O$, the ratio (2b)/(2a) was obtained to be about 1.5 by assuming only $CH_2CHO + CH_3$ (2a) and $HCO + C_2H_5$ (2b) to be dominant.

References

1) Y. Endo, S. Tsuchiya, C. Yamada, E. Hirota, and S. Koda, *J. Chem. Phys.*, **85**, 4446 (1986).
2) Y. Endo, H. Kanamori, and E. Hirota, *Laser Chem.*, **7**, 61 (1987).

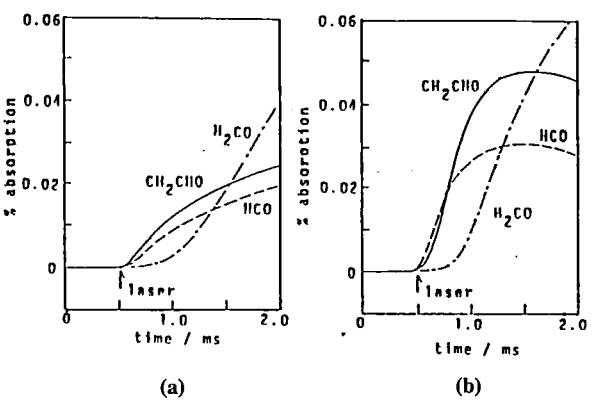

Figure 1. Time profiles of vinoxy, formyl, and formaldehyde generated by the reactions (a) $C_2H_4 + O$ and (b) $C_3H_6 + O$.

II-A-16 The O + SiH_4 Reaction Investigated by Infrared Diode Laser Kinetic Spectroscopy

Shinsuke SUGA *(Univ. Tokyo)*, **Seiichiro KODA** *(Univ. Tokyo)*, **Toshinori SUZUKI, Chikashi YAMADA, and Eizi HIROTA**

Little has been known on the reaction of $O(^1D)$ with silane, in sharp contrast with the case of the ground-state oxygen $O(^3P) + SiH_4$, for which several reports have been published. In the present study we generated

$O(^1D)$ by the photolysis of N_2O at 193 nm. The sample consisted of SiH_4 diluted to 10% with Ar, N_2O, and He with the total pressure of 1 to 1.5 Torr. Figure 1 shows an example of the observed time-resolved spectra, which consists of six Q-branch lines of the $v_2 = 1^- - 0^+$ band of the SiH_3 radical and two R-branch lines of OH in the $v=2$ state. The spectrum indicates clearly that SiH_3 radicals are prepared initially in excited states and relax gradually to the ground state, whereas OH radicals nascently populate the $v=2$ state, although they disappear within 10 μs or so. A semiquantitative analysis of the time profiles observed for SiH_3 and OH indicates that $O(^1D) + SiH_4 \rightarrow SiH_3^{\dagger} + OH$ is plausible as the initial process of the reaction, where $SiH_3^{\dagger}$ denotes the radicals being prepared in excited states.

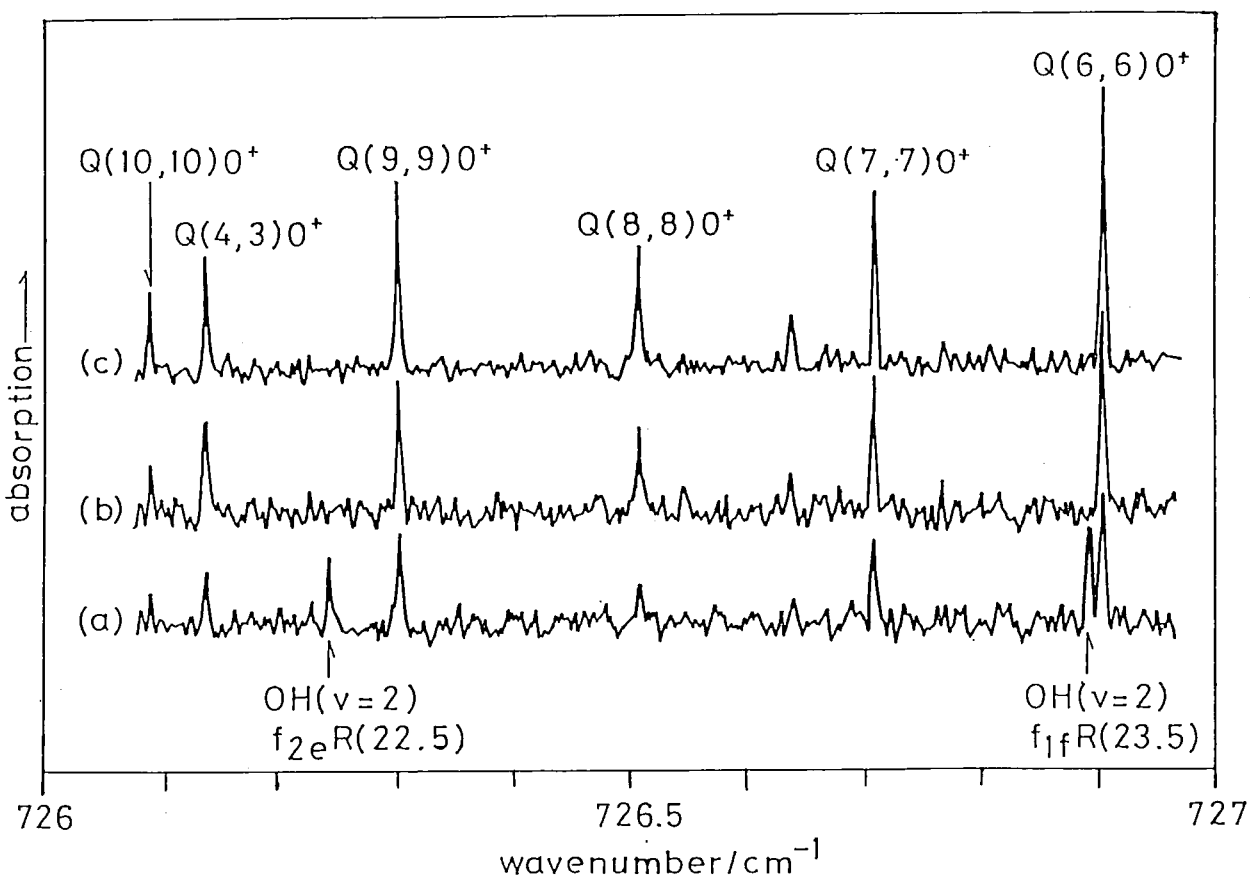

Figure 1. Time resolved spectra of SiH_3 and OH generated by the reaction $O(^1D)+SiH_4$: (a) for 2–12 μs, (b) for 12–24 μs, and (c) for 24–46 μs. The sample was a mixture of SiH_4 of 65 mTorr and N_2O of 200 mTorr diluted with Ar and He to the total pressure of 1 Torr.

II–B Development of New Instruments and New Experimental Methods for High Resolution Spectroscopy

The scope of a research is limited by the techniques and the capabilities of instruments available to a researcher. This is particularly true for spectroscopic investigations of simple molecules, free radicals, and ions, which are main research themes this Department is interested in. The high precision with which we determine molecular parameters often unravels new features of molecular structure which have previously escaped experimental observation. The

diversity of molecular systems which we can detect and analyze is often limited by the sensitivity of the spectrometer employed. It is thus imperative for us to steadily improve our research facilities and to develop equipments of radically new conceptual design. The rewards of these efforts will include not only the detailed knowledge of the molecules under investigation, but also contributions to related fields. Various technical problems need to be solved to attain these goals. In this respect the collaboration of the Equipment Development Center is indispensable. New instruments developed in this program promise to open new research area in the field of molecular science.

II-B-1 A Laser Induced Fluorescence Spectrometer for Detection of Transient Molecules

Haruhiko ITO and Eizi HIROTA

The spectrometer is equipped with two chambers, one for observing the spectra of simple free radicals generated by a microwave or DC discharge and the other for recording the high-resolution spectra of polyatomic transient molecules produced by photolysis and other means and cooled in a supersonic beam. The first chamber is illustrated in Figure 1. It is a 4" stainless steel chamber, which is pumped by a 110 m^3/hr mechanical booster pump followed by a 600 *l*/m rotary pump. Care was taken to reduce scattering of laser light by using a series of baffles, and a variable slit was placed in the optical path collecting fluorescence. The laser source, which is used commonly to the two chambers, consists of a Lambda Physik FL 2002E dye laser pumped by a Lambda Physik EMG 103 MSC excimer laser. The laser induced fluorescence signal is recorded by a Stanford Research SR 250 gated integrator. The second chamber is a 12" stainless steel one, which is pumped by a 10" oil diffusion pump of 2400 *l*/s or the mechanical booster pump mentioned above. It is equipped with a pulse nozzle.

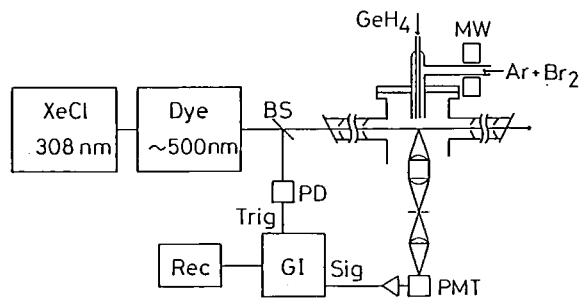

Figure 1. Blockdiagram of a laser induced fluorescence spectrometer designed to detect simple free radicals generated by a discharge.

II-C High Resolution Spectroscopy of Molecules of Fundamental Importance

The need for high quality spectroscopic data has recently been increasing, especially for molecules of fundamental importance. Perhaps such spectroscopic data have been accumulated in the past because of interest in precise molecular structure determination. However, research activities in other related fields such as reaction kinetics, environmental sciences, plasma chemistry and physics, astronomy, and semiconductor technology have recently been advanced such that precise spectroscopic data are indispensable as a means of monitoring molecules. Spectroscopic data which are available at present are not necessarily good enough and must often be replaced by new data that meet necessary requirements. Such spectroscopic data on chemically stable molecules of fundamental importance will be presented in this section.

II-C-1 Microwave Spectrum of *cis*-Cyclobutane-1,2-d_2 Perturbed by the Puckering Vibration

Eizi HIROTA, Masaharu FUJITAKE, and James S. CHICKOS *(Univ. Missouri)*

The present study aims at obtaining detailed information on the molecular structure of cyclobutane which is the simplest molecule executing a puckering vibration. Because the molecule is nonpolar, we have

focussed attention to deuterated species and have investigated them with microwave spectroscopy. The result on *trans*-1,2-d_2 and also a preliminary analysis of *cis*-1,2-d_2 have been reported[1]. The latter species shows complications in its spectra which are caused by coupling between molecular asymmetry and puckering. In the present study this coupling is analyzed by introducing the off-diagonal terms of the form $[(R_x/2) - (R_{xx}/2)J^2][J_x,J_y]_+ - (R_{xz}/4)[J_z^2, [J_x, J_y]_+]_+ - (R_{xy}/4)[(J_x^2-J_y^2), [J_x, J_y]_+]_+ + (R_z/2)[J_y,J_z]_+$, where z denotes an axis nearly perpendicular to the molecular "plane", whereas x and y stand for the "in-plane" coordinates, only y being antisymmetric to the puckering. We have also extended the observation and have succeeded in detecting transitions between symmetric and antisymmetric states, which allowed us to calculate the puckering splitting in some rotational states without assuming any model. Molecular parameters obtained from a least-squares analysis are given in Table I.

Reference

1) E. Hirota, Y. Endo, M. Fujitake, E. W. Della, P. E. Pigou, and J. S. Chickos, *J. Mol. Struct.*, **190**, 235 (1988).

Table I. Molecular Constants of *cis*-Cyclobutane-1,2-d_2 (MHz)[a]

A	9765.104(28)	ΔE	86.21(40)
B	[A−14.5]	R_x	362.70(19)
C	5912.965(36)	R_z	[0.0]
Δ_J	0.004 64(11)	R_{xx}	0.002 05(66)
Δ_{JK}	−0.006 11(21)	R_{xz}	−0.000 08(12)
Δ_K	0.002 29(19)	R_{xy}	0.000 14(28)
δ_J	[0.004 41]		
δ_K	[−0.015 19]		
Φ_J	−0.000 000 02(15)		
Φ_{JK}	−0.000 000 78(41)		
Φ_{KJ}	0.000 000 43(50)		
Φ_K	−0.000 000 53(36)		

a. Values in parentheses denote standard deviation and apply to the last digits of the constants. Values in square brackets are fixed. Constants not listed in the table are constrained to zero.

II−D Experimental and Theoretical Studies of High-Lying Doubly Excited States of Atoms

A doubly excited state of an atom is one of the interesting problems in atomic physics, because it is a typical model for the quantum-mechanical three-body problem, in which a strong electron correlation effect is expected to play an important role and to cause a cooperative electronic motion. In He-like atoms consisting of two electrons and of a bare nucleus, understanding of the electronic behaviors has greatly been developed for the past two decades. In other atoms, however, in which two electrons are necessarily governed by a non-Coulombic field of the ionic core, we have only a poor knowledge about their electronic behaviors. For this reason, by using Ca atom, we have experimentally and theoretically been studying the electron correlation effect in this type of atoms.

II-D-1 Laser Spectroscopic Observation and Large-Scale Configuration-Interaction Calculation of Doubly Excited *msns* $^1S^e$ States of Ca Atoms

Norio MORITA and Toshifumi SUZUKI

[*Phys. Rev. A*, in press]

With multistep laser excitation, doubly excited *msns* $^1S^e$ states of Ca atoms have been observed, and their energy levels have been obtained. A large-scale configuration-interaction calculation for Ca atoms has also been executed using a discrete two-electron basis set, in which a frozen Ca^{2+} core is assumed and the total number of the bases is 1714. The calculated energy levels are in good agreement with the observed ones. Based on the good agreement, charge density plots have been drawn for the *nsns* states ($4 \leq n \leq 10$), using the calculated eigenvectors. In all the *nsns* states investigated, a reasonably large part of the charge density has been seen to be localized on the Wannier's potential ridge and to show a fairly strong angular correlation. In lower *nsns* states, the angular correlation pattern has been found to support the moleculelike picture, though an unusual pattern has been seen in a smaller radial region. In higher states, two types of unusual angular correlation have been seen. In particu-

lar, one of them is suggestive of a bent structure of the charge density distribution, in spite of the zero angular momentum states. The cause of this correlation has been discussed from a viewpoint of configuration-mixing.

II-D-2 R-Matrix Calculation of Doubly Excited $^1S^e$ States of Ca Atom below the 6s Threshold

Norio MORITA

[*J. Phys. B*, in press]

By an eigenchannel R-matrix calculation of the final-state multichannel quantum-defect parameters in *LS* coupling, the photoexcitation spectrum of doubly excited $^1S^e$ states of atomic calcium from the 4p threshold up to the 6s threshold has been obtained with the initial state fixed to the 4s4p state. The spectrum has been calculated in both ways using the length- and velocity-form dipole-matrix elements, and an agreement between both results is good enough to support the correctness of the calculation. Furthermore, using the isolated-core-excitation formula, excitation spectra of the 6s*n*s Rydberg series from the 4s*n*'s states have been calculated and compared with the experimentally observed ones. A good agreement has been seen between the calculated and observed ones except in the lowest observed state, i.e. 6s9s. The latter disagreement has been discussed under a consideration of strong channel interactions.

II-D-3 Laser Multiphoton Excitation of Doubly Excited *msn*d and *mdn*d States of Ca Atom

Norio MORITA and Toshifumi SUZUKI

Doubly excited *mln*d ($12 \leq n \leq 20$ for *ml*=8s and 7d; $11 \leq n \leq 19$ for *ml*=9s and 8d; $16 \leq n \leq 17$ for *ml*=10s and 9d) states of Ca atom have been produced by a three-step four-photon laser excitation via various 4s*n*'d one-electron Rydberg states, and they have been observed by detecting photoionization current of Ca^{2+} ions yielded from the doubly excited states. Energy levels and quantum defects of those states have been obtained and discussed. In both *msn*d and *mdn*d states, similar to the case of the *msn*s states, the *m*-dependence of the quantum defects of the $m \ll n$ states has been found to be linear. Though this dependence can be predicted by a theoretical calculation assuming the independent electron model, the slope of the linear increase is different between the experimental and observed quantum defects. This difference has been explained by an electron correlation effect existing still in the $m \ll n$ states. The reason why it is more difficult to observe the $m \approx n$ states in the *msn*d and *mdn*d series than in the *msn*s series has also been discussed based on the fact that there are more interacting channels than in the latter case.

II-E Raman Spectroscopy and Its Application

Raman spectroscopy reveals a vibrational spectrum, which is sensitive to a geometrical structure and an electronic state of a molecule. We have applied this technique to study the following projects; 1) elucidation of activation mechanism of oxygen by enzymes and of the electron- and proton-transfer mechanism through protein, 2) structure of transient species, and 3) solution structure. For (1) and (2), we take advantage of resonance enhancement of Raman intensity when the excitation wavelength comes into the absorption band. This resonance effect enables us to observe the vibrational spectra of chromophores of large molecules selectively with a small amount of dilute solution. Various kinds of hemeproteins, retinoid proteins, metalloproteins, and their model compounds have been investigated. Currently we focus our attention to reaction intermediates of bacteriorhodopsin, cytochrome *c* oxidase, peroxidase, and cytochrome P-450. We have also investigated photoreduction of hemeproteins and iron porphyrins by visible light. Recently we succeeded in observing resonance Raman spectra excited in the ultraviolet region (200–240 nm) and thus in observing some vibrations of aromatic residues of proteins. In order to determine a molecular structure in transient states with a time resolution of $10^{-7} - 10^{-11}$ sec, the pump-probe technique with two pulsed lasers are used. Currently, photoreduction and dynamics of protein structure are investigated. We also

developed an improved method for fluorescence rejection by using a gated diode array detector. The project (3) intends to evaluate relative magnitudes of solvent-solvent and solvent-solute interactions and their properties for various binary mixtures. A Raman difference spectrometer was constructed for this purpose and has been applied to detect a frequency shift upon isotope mixing.

II-E-1 Resonance Raman Characterization of Hog Thyroid Peroxidase: A SERRS Study

Shinji HASHIMOTO, Ryo NAKAJIMA *(Hokkaido Univ.)*, **Isao YAMAZAKI** *(Hokkaido Univ.)*, **Tomio KOTANI** *(Miyazaki Medical College)*, **Sachiya OHTAKI** *(Miyazaki Medical College)*, **and Teizo KITAGAWA**

[*FEBS Lett.* **248**, 205 (1989)]

Resonance Raman (RR) spectra of hog thyroid peroxidase (TPO) were observed for the first time and compared with those of lactoperoxidase (LPO) and horseradish peroxidase (HRP). Since TPO purified with the monoclonal antibody-assisted immunoaffinity chromatography was very fluorescent, the surface enhancement effect upon adsorption on Ag colloid was used for the oxidized form, but ordinary RR spectra could be obtained for the reduced form. The RR spectra of TPO were distinct from that of HRP in both the oxidized and reduced states and indicated the presence of a hexa-coordinated iron-protoporphyrin.

II-E-2 Time-Resolved Ultraviolet Resonance Raman Study of the Photolysis of Carbonmonoxy Hemoglobin; Relaxation of the Globin Structure

Shoji KAMINAKA, Takashi OGURA, and Teizo KITAGAWA

[*J. Am. Chem. Soc.* in press]

Dynamical features of quaternary structure change of carbonmonoxy hemoglobin (COHb) after photolysis were followed by observing resonance enhanced Raman bands of the aromatic residues in ultraviolet excitation. The Raman scattering was excited by 10-ns pulses at 218 nm, which were obtained from the second H_2-Raman shift of the fourth harmonic of a Nd:YAG laser, while CO was photodissociated by 10-ns pulses at 419 nm generated by a nitrogen-laser-pumped dye laser or by pulses at 436 nm generated from the first H_2-Raman shift of the second harmonic of the Nd:YAG laser. The delay time (Δt_d) from the photolysis pulse to the Raman probe pulse was varied from $-100\ \mu s$ to $500\ \mu s$. The observed spectra obtained for $\Delta t_d = -100\ \mu s$ and 10 ns were the same as each other and as that obtained without the pump beam, contrary to expectations based on the reported 7 ns change of the protein structure, but the spectral pattern did change when Δt_d changed from 10 to 20 μs; the bands at 1613 and 1011 cm^{-1} decreased in intensity and the band at 878 cm^{-1} shifted to 883 cm^{-1}. These spectral changes appeared as a smooth monotonous function of time, suggesting the absence of an intermediate around $\Delta t_d = 10\ \mu s$. A similar spectral change was also observed upon addition of an effector (inositol hexaphosphate) to metHb fluoride. Accordingly, the observed changes of the UV resonance Raman spectra were attributed to a quaternary structure change, presumably to a status change of β37-Trp and α42-Tyr at the α_1–β_2 subunit interface.

II-E-3 Raman-Absorption Simultaneous Measurements for Cytochrome Oxidase Compound A at Room Temperature with a Novel Flow Apparatus

Takashi OGURA, Shinya YASHIKAWA *(Himeji Inst. of Tech.)*, **and Teizo KITAGAWA**

[*Biochemistry*, **28**, 8022 (1989)]

A novel flow apparatus for continuously producing reaction intermediates of cytochrome oxidase was constructed and applied successfully to observe the transient absorption and resonance Raman spectra in its reaction with oxygen. Time-resolved difference absorption spectra in 500–650 nm region clearly indicated the formation of compound A upon photolysis of the fully reduced CO-bound form at 5 °C and at this stage electrons were not transferred from cytochrome *c*

to cytochrome oxidase. However, at the stage of formation of compound B, cytochrome *c* was oxidized. Resonance Raman spectra of these intermediates measured simultaneously with the absorption spectra are also reported.

II-E-4 Manipulation of Hemoglobin Function by Protein Engineering

Kiyohiro IMAI *(Osaka Univ.)*, **Koichiro ISHIMORI** *(Kyoto Univ.)*, **Kenzo FUSHITANI** *(Dokkyo Univ.)*, **Gentaro MIYAZAKI** *(Osaka Univ.)*, **Teizo KITAGAWA, Hideki MORIMOTO** *(Osaka Univ.)*, **Isao MORISHIMA** *(Kyoto Univ.)*, **D. SHIH** *(MRC, Cambridge)*, **J. TAME** *(MRC, Cambridge)*, **and Kiyoshi NAGAI** *(MRC, Cambridge)*

In order to test the functional roles of amino acid residues which are proposed to be crucial for cooperative oxygen binding by normal hemoglobin, we synthesized three mutant hemoglobins, Hb Y42αF (Tyr-42α->Phe), Hb Y42αH (Tyr-42α->His) and Hb Y145βF (Tyr-145β->Phe), by protein engineering. Hb Y42αF exhibited oxygen binding properties which are characterized by a very high affinity and absence of cooperativity, whereas Hb Y42αH and Hb Y145βF exhibited considerably high affinities and moderately diminished cooperativity. The protein-conformational probes including UV difference spectroscopy, proton NMR, and resonance Raman scattering determined the quaternary structure at the α1–β2 interface and tertiary structure at the proximal His and heme contact residues. These probes demonstrated that all the three mutant Hbs are in the R state when oxygenated whereas upon deoxygenation Hb Y42αF remains predominantly in the R state and two other Hbs undergo a transition to the T state to some extent. These results are fully consistent with the oxygenation properties of the mutants. The present study revealed that Tyr-42α which forms a hydrogen bond with Asp-99β at the α1–β2 interface is vital to Hb function and that the hydrogen bond between Tyr-145β and the Val-98β carbonyl group also makes a considerable contribution to stabilization of the T structure and hence to cooperative oxygen binding.

II-E-5 A New Device for Raman Difference Spectroscopy and Its Application to Observe Frequency Shifts due to Isotope Mixing

Keiji KAMOGAWA and Teizo KITAGAWA

[*J. Phys. Chem.* in press]

A new double beam device was developed for Raman difference spectroscopy (RDS). The device intends to measure Raman spectra of two samples simultaneously by using the branched bundles of optical fibers and a multichannel detector, and thus to avoid the time drift of Raman band positions on the diode array detector. The accuracy of the frequency shift ($\Delta\nu$) of a Raman band observed upon mixing of two liquids was raised to 0.01 cm^{-1} from 0.05 cm^{-1} of the previous measurements. The device was applied to explore the frequency shifts due to isotopic dilution of C_6H_6/C_6D_6 and CH_3CN/CD_3CN pairs as a function of concentration. The symmetric C-H and C-D stretching modes exhibited a linear dependence on a mole fraction of the probe species (χ_A) except for very dilute solution of C_6D_6 in C_6H_6 ($\chi_A<0.1$). A few other bands gave the $\Delta\nu$–χ_A curves which seem to involve a saturation effect. The results are discussed on the basis of vibrational resonance coupling and difference between polarizabilities and volumes of isotope molecules.

II-E-6 Photoreduction of Fe-porphyrin Alcohol Complexes

Vlatimil FIDLER, Takashi OGURA, Shin-ichiro SATO, and Teizo KITAGAWA

We reported previously that photoreduction of Fe(OEP) (OEP: octaethylporphyrin) in organic solvents is a ligand-aided process in which coordination of 2-methylimidazole (2-MeIm) is needed, but here we demonstrate that a further complex-forming ligand, e.g. aliphatic alcohol is necessary for the photoreduction to occur. Fe(OEP)(2-MeIm) in the distilled CH_2Cl_2 did not exhibit photoreduction but it did in the presence of a small amount of MeOH. The photoreduction proceeded effectively in the presence of a few % of EtOH, 1-propanol or 2-propanol but not with t-BuOH.

For the complex of Fe(OEP) with 1-MeIm, photoreduction did not take place at all with any alcohol. Active alcohols gave a new absorption band around 585 nm and a new Raman band around 525 cm^{-1} when it was added to the Fe(OEP)(2-MeIm) solution. The 524 cm^{-1} band of the MeOH complex exhibited a frequency shift upon ^{54}Fe, CD_3OD and CD_3OH substitutions and its excitation profile reproduced the 585 nm absorption band. Therefore, the Raman band was assigned to the Fe-MeOH stretching mode and the new absorption band was assigned to the MeOH->Fe charge transfer band. The resonance Raman spectra of the MeOH-coordinated complex were analysed on the basis of the observed shifts upon the ^{15}N and meso-D isotope substitutions. It is emphasized that unexpectedly, the photoreduction does not occur upon laser illumination within the CT band. Upon 441.6 nm excitation, the photoreduction was clearly seen in the absence of O_2 but apparently not in the presence of O_2. Transient absorption measurements indicated that photoreduction itself occurs in the ns time scale but reoxidation of the photoreduced species by O_2 takes place in a ms scale. Pump/probe time-resolved Raman experiments are in progress.

II-E-7 Solution Structures of Aqueous Fluoroalcohol Systems and the Phase Separation as Studied by Raman and NMR Spectra

Yasuhisa MIZUTANI *(Kyoto Univ.)*, **Keiji KAMOGAWA, Teizo KITAGAWA, Akio SHIMIZU** *(Ritsumeikan Univ.)*, **Koichiro NAKANISHI** *(Kyoto Univ.)*, **and Yoshihiro TANIGUCHI** *(Ritsumeikan Univ.)*

The Static and dynamic structures of aqueous solutions of 2-propanol (IPA), 1,1,1-trifluoro-2-propanol (TFP), and 1,1,1,3,3,3-hexafluoro-2-propanol (HFP) were investigated with Raman and ^{13}C-NMR spectroscopy to understand the phase separation of the TFP solution at intermediate concentrations. Frequency shifts of the C-H stretching vibrations of the alcohols were observed with the Raman difference technique and analyzed in terms of the homogeneous ($\Delta\nu_{AA}$) and heterogeneous ($\Delta\nu_{AB}$) interaction factors proposed previously. For the IPA- and HFP-water systems, $\Delta\nu_{AA}$ showed zero at first and then decreased upon dilution by water similar to those of other organic molecules in water. For the TFP-water system, however, phase separation took place in the concentration region where $\Delta\nu_{AA}$ decreased for IPA- and HFP-systems and accordingly the formation of a micelle-like aggregation is suggested. The dynamic as well as static structures are discussed on the basis of the rotational correlation times of alcohols which were obtained from the spin-lattice relaxation times of ^{13}C and the nuclear Overhauser enhancements. The present results suggest that the repulsion between the C-H and C-F groups prohibits TFP from forming a micelle-like aggregate and thus results in phase separation.

II-E-8 Resonance Raman Study on Oxidation Process of Ferrous Porphyrin

Yasuhisa MIZUTANI, Shinji HASHIMOTO *(Tohoku Univ.)*, **Yoshitaka TATSUNO** *(Osaka Univ.)*, **and Teizo KITAGAWA**

Resonance Raman (RR) spectra of ferrous oxy (Fe^{II}-O_2) and ferryl oxo (Fe^{IV}=O) tetramesitylporphyrin (TMP) complexes were investigated. The toluene solution of (TMP)FeO_2 at −100°C exhibited the O=O stretching [$\nu(O_2)$] and Fe-O_2 stretching [ν(Fe-O_2)] bands at 1171 and 522 cm^{-1}, respectively. This is the first simultaneous observation of the $\nu(O_2)$ and ν(Fe-O_2) modes for the Fe^{II}-O_2 porphyrin complex. The frequency of $\nu(O_2)$ indicates that dioxygen coordinates to the metal in the end-on fashion. As for (TMP)FeO, which was obtained from thermal decomposition of (TMP)FeO_2 at −70°C, the intensity of the band at 843 cm^{-1} decreased as the laser power was raised. This band was assigned to the Fe=O stretching mode owing to its 33 cm^{-1} downshift and 4 cm^{-1} upshift upon $^{16}O/^{18}O$ and $^{56}Fe/^{54}Fe$ isotopic substitutions, respectively. Since the laser power dependences of Raman bands at 1570 and 1368 cm^{-1} were similar to each other and also to that of the 843 cm^{-1} band, these bands were assigned to the ferryl oxo complex. The ferryl oxo complex was much more stable in toluene-d_8 than in toluene-h_8, suggesting that the reduction of ferryl oxo complex involves hydrogen subtraction from solvent.

II-E-9 Resonance Raman Study on Ferryloxo Porphyrin π Cation Radical

Shinji HASHIMOTO *(Tohoku Univ.)*, **Yasuhisa MIZUTANI, Yoshitaka TATSUNO** *(Osaka Univ.)*, **and Teizo KITAGAWA**

Resonance Raman (RR) spectra of ferryloxo tetramesitylporphyrin π cation radical, $(TMP^{\cdot})Fe^{IV}=O$, which was obtained by reacting $(TMP)Fe^{III}Cl$ with *m*-chloroperoxybenzoic acid in CH_2Cl_2 at $-80°C$, were investigated. The $Fe^{IV}=O$ stretching mode ($\nu_{Fe=O}$) was observed at 831 and 802 cm^{-1} in the presence and absence of methanol, respectively. When *i*-Pr alcohol or *t*-Bu alcohol was used instead of methanol, the $\nu_{Fe=O}$ band was observed at 802 cm^{-1}, The π cation radical derived in ethylacetate also gave the $\nu_{Fe=O}$ band at 802 cm^{-1}. These facts suggest that the Raman band at 831 cm^{-1} arises from an alcohol-coordinated $(TMP^{\cdot})Fe^{IV}=O$. In order to assign the vibrational modes, the cation radical species were derived from ^{15}N and ^{13}C substituted $TMPFe^{III}Cl$. The C_α-N stretching mode (ν_4) was identified at 1332 cm^{-1} while the C_β-C_β stretching modes were observed at 1578 (ν_2) and 1561 cm^{-1} (ν_{11}). The ν_2 mode is upshifted whereas the ν_4 mode is downshifted in the cation radical compared with those of ferryloxo neutral porphyrin. This feature is the same as the observation for several a_{1u} radical cations of octaethylporphyrins, but the shift direction for ν_2 is opposite to those of tetraphenylporphyrins.

II-E-10 Resonance Raman Studies on Mutant Cytochromes P-450 Derived with Site-Directed Mutagenesis

Tsuyoshi EGAWA, Yoshio IMAI *(Osaka Univ.)*, **Takashi OGURA, and Teizo KITAGAWA**

Resonance Raman spectra were measured for mutants of rabbit liver microsomal cytochromes P-$450_{\omega-1}$ prepared with the site-directed mutagenesis using yeast. Mutations were directed to distal Thr (Thr-301), which is proposed to be crucial in the P-450 catalysis. T301S (Thr-301 -> Ser) and T301V (Thr-301 -> Val) have the ω-1 oxidation activity of capric acid (C_{10}) as large as 104 and 0 %, respectively, of that of the wild type. The Fe-CO stretching mode (ν_{Fe-CO}) was measured for the CO adduct of mutants as well as of the wild type and it was found that the ν_{Fe-CO} frequency of T301V (476 cm^{-1}) was higher than those of the wild type (473 cm^{-1}) and T301S (473 cm^{-1}). This finding suggests that Thr-301 plays an important role to maintain the environment around the sixth ligand of the heme iron of P-450. Increases of the ν_{Fe-CO} frequency was observed for binding of capric or longer acid (480 cm^{-1} for both T301V and wild type) but not for shorter one, although the binding of these substrates was evident from the absorption spectra. The intensity of the Raman spin-state markers in the high frequency region indicated that a partial spin transition from the low- to high-spin states upon binding of the substrate, and this trend was most prominent with capric acid; capric acid(C_{10})>lauric acid(C_{12})>pelargohic acid(C_9)>caprilic acid(C_8). This is almost consistent with the observations in absorption spectroscopy.

II-F Structure of Noncrystalline Solids by EXAFS

Catalysts are very important in chemistry and chemical engineering, and the catalytic properties are closely related to their structures. EXAFS (extended x-ray absorption fine structure) is best suited to determine structures of catalysts, because it can determine the local structures around a selected element irrespective of the phase. In this laboratory efforts to develop EXAFS spectroscopy has been continued as well as EXAFS studies on the structures of amorphous materials, especially supported catalysts.

In the past year, a new, improved double crystal spectrometer was constructed which made EXAFS measurements of heavy elements much easier. By the use of the new spectrometer EXAFS studies on the catalyst under reaction conditions have been attempted with an in situ cell, and morphology changes of very small Ru clusters

by CO adsorption have been observed. EXAFS studies on other catalysts have been continued and extended to try to make relationship between catalyst structure and catalytic activity. A possibility of x-ray Raman spectroscopy as a complementary method for EXAFS has also been pursued, and anisotropic effects on x-ray Raman spectra have been observed for the first time.

The followings are the abstracts of the manuscripts submitted to several journals in the past year.

II-F-1 Anisotropic Effect in X-ray Raman Scattering from Graphite

Kazuyuki TOHJI, Yasuo UDAGAWA, Tadashi MATSUSHITA*, Masaharu NOMURA*, and Tetsuya ISHIKAWA* *(*Photon Factory, KEK)*

[submitted to *J. Chem. Phys*]

Very recently we have reported for the first time EXAFS-like wiggles in x-ray Raman spectra of graphite and diamond and showed that the equation employed for EXAFS analysis of isotropic materials can be used to extract structural parameters[1,2]. For anisotropic materials additional information can be obtained, since the momentum transfer or scattering vector **s** is expected to play the same role as the polarization vector in absorption.

We have observed for the first time anisotropy effects in extended x-ray Raman spectra with a single crystal graphite. The c-axis of graphite is perpendicular to the ring plane; transitions in the plane are forbidden for **c**//**s**, while those perpendicular to the plane are forbidden for **c** ⊥ **s**. Figure 1 shows the x-ray Raman spectra from graphite with the scattering vector **s** parallel as well as perpendicular to the c-axis. Significant anisotropy effects are clear in the figure; different edge shift and prominent differences in the extended fine structure. The former indicates that the first transitions are to π^* states and the transition to σ^* states starts at about 6 eV higher in energy. Analyses of the latter by the use of Fourier transform for each spectrum yields interatomic distances between intra- and inter-layer carbons, respectively.

References

1) K. Tohji and Y. Udagawa, *Phys. Rev.* **B36**, 9410 (1987).
2) K. Tohji and Y. Udagawa, *Phys. Rev.* **B39**, 7590 (1989).

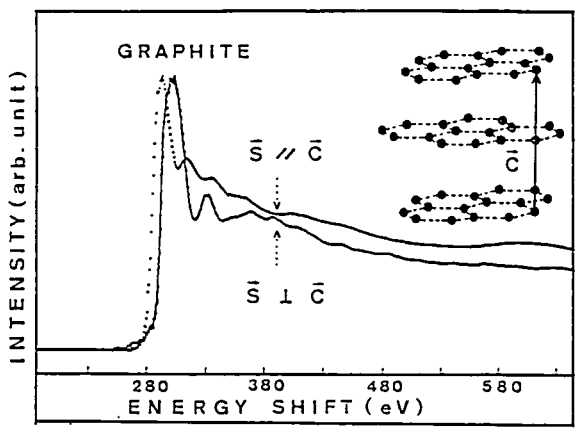

Figure 1. X-ray Raman scattering spectra of graphite with the scattering vector s//c and s⊥c.

II-F-2 An EXAFS Study on the CO Adsorption Induced Morphology Change of Ru Cluster Supported on Alumina

Takanori MIZUSHIMA, Kazuyuki TOHJI, Yasuo UDAGAWA, and Akifumi UENO* *(*Toyohashi Univ. Technology)*

[submitted to *J. Phys. Chem.*]

Highly dispersed Ru/Al_2O_3 catalysts were prepared from $Ru_3(CO)_{12}$. EXAFS (Extended X-ray Absorption Fine Structuer) study shows that all the Ru atoms in the catalyst are in small metal clusters. The Ru clusters are so small that the oxygen atoms at the cluster-support interface have a significant contribution to the EXAFS signal. Adsorption of CO completely changes the structure of this small metal cluster as is evidenced from EXAFS oscillation; Ru-Ru bonds are disrupted and Al-O-Ru-$(CO)_n$ (n=1–2) species are formed, as shown in Figure 1. By raising the temperature Ru atoms agglomerate and small metal clusters are recovered. Infrared spectroscopic observations support the conclusion obtained from EXAFS.

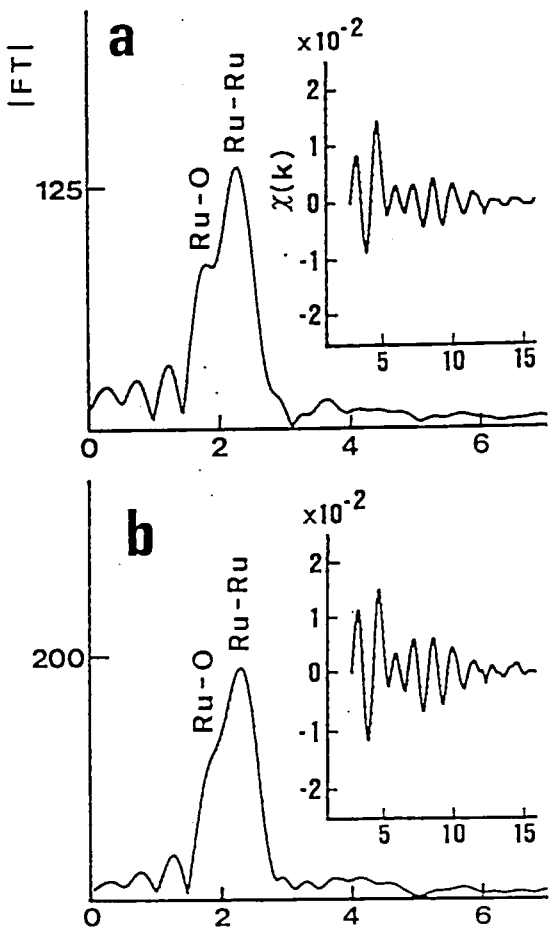

Figure 1. Extracted Ru K EXAFS oscillations and the associated k^3-weighted Fourier transforms of (a) 2 wt% and (b) 4 wt% Ru/Al_2O_3 catalyst after admission of 200 Torr of CO.

II-F-3 Characterization of Iron Oxide Thin Film Prepared by Sol-Gel Method

N. TAKAHASHI*, N. KAKUTA*, A. UENO*, K. YAMAGUCHI*, T. MIZUSHIMA, and Y. UDAGAWA
*(*Toyohashi Univ. Technology)*

[submitted to *J. Materials Sci.*]

Thin films consisting of γ-Fe_2O_3 particles were prepared by a spin-on process using a solution of iron(III) nitrate dissolved in ethylene glycol. Film thickness was observed to be controlled by the solution viscosity as well as the revolution of spinner. Local structures around iron ions in the solution were studied by EXAFS and the formation of $(FeO_x)_n$ cluster was deduced. A film thus prepared was confirmed to consist of finely divided γ-Fe_2O_3 particles by TEM observations. Magnetic and optical properties of the films were briefly discussed.

II-F-4 Preparation and Characterization of Aluminum-doped SiO_2:Sm^{3+} Phosphor

H. OKUMURA*, N. KAKUTA*, A. UENO*, R. MORIMO*, T. MIZUSHIMA, Y. UDAGAWA, and H. NAMIKAWA** *(*Toyohashi Univ. Technology, **Nihon Sanso Co.)*

[*Chem. Lett.* **1989**, 829]

Samarium ions in Al-doped SiO_2:Sm^{3+} phosphor were revealed to be atomically dispersed in small Al_2O_3 crystallites by forming Sm-O-Al bonding, which contributes to improvements in the fluorescent intensity of SiO_2:Sm^{3+} phosphor.

II-F-5 Construction of a New Double Crystal Spectrometer for Laboratory EXAFS Spectroscopy

Kazuyuki TOHJI, Takanori MIZUSHIMA, and Yasuo UDAGAWA

[*Advances in X-ray Chemical Analysis*, in press]

Previously we have reported a double crystal spectrometer for EXAFS spectroscopy at high energy region (Annual Review 1988 p163 and ref. 1). Last year a new, improved version of double crystal monochromator was constructed. It consists of two bent Johansson crystal monochromators with Rowland circles of 320 mm in the (+,+) arrangement. It features a perfect elimination of contaminations of undesired reflections or scattering, high mechanical stability, and high throughput. Combined with a 18 kW rotating anode x-ray generator, this new system can supply almost an order of magnitude more intense x-ray fluxes than the old version. Photon numbers available at several energies are shown in Figure 1 as a function of applied voltages to the x-ray source.

Reference

1) K. Tohji, Y. Udagawa, T. Kawasaki, and K. Mieno, *Rev. Sci. Instrum.* **59**, 1127 (1989).

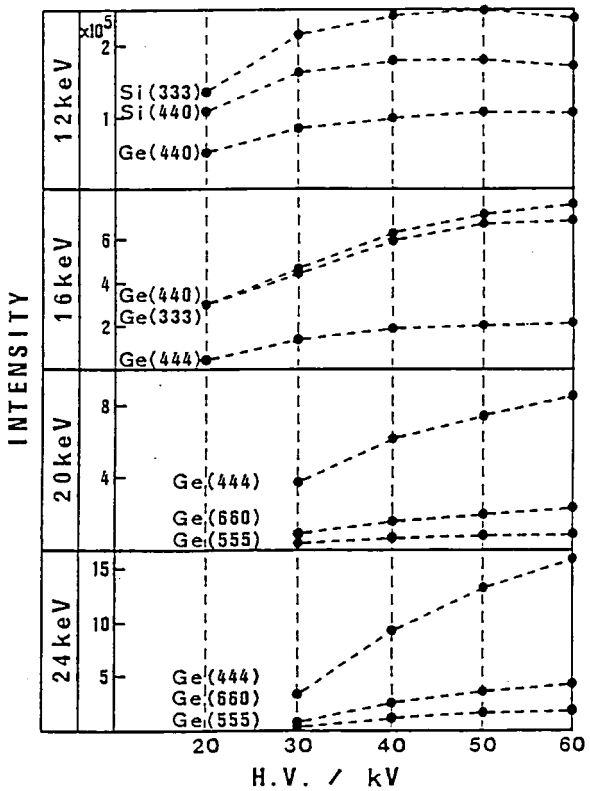

Figure 1. Photon number in counts/sec obtained by the use of various crystals at several energies as a function of the source voltages. Current is kept to be 300 mA.

RESEARCH ACTIVITIES III
Department of Electronic Structure

III–A Photochemical Isomerization of Stilbenes in Clusters and under Isolated Conditions

The photochemical isomerization of stilbene has been a paradigm for cis-trans isomerization reactions. cis-Stilbene is of particular interest because it can isomerize to form either trans-stilbene or dihydrophenantrene. We have demonstrated that cis-stilbene, which is non-fluorescent at room temperature due to ultrafast isomerization, becomes fluorescent in rare gas and organic clusters in supersonic jet conditions. This observation was interpreted as evidence for a minimum in the S_1 state of cis-stilbene, which contradicts commonly held belief that cis-stilbene isomerization is a barrierless process. We have continued investigation of cis-stilbene dynamics in order to identify the processes responsible for the non-radiative decay, and to determine the role of the cluster environment in arresting them. We present new data on trans-stilbene isomerization product detection, and its rate of formation measurement using picosecond pump-probe techniques. Also, spectroscopic and dynamical measurements on 1,2-diphenylcycloalkenes, cis-stilbene analogs that cannot cis-trans isomerize, provide new information on the cis-stilbene S_1 state structure and the dihydrophenantrene isomerization channel.

III-A-1 cis-Stilbene Isomerization in Ar Clusters: Detection of trans-Stilbene Product Under Non-Linear Excitation Conditions

Hrvoje PETEK and Keitaro YOSHIHARA

In this work emission from cis-stilbene: Ar clusters is observed as a function of excitation laser fluence. Strong emission from cis-stilbene: Ar clusters indicates that significant fraction of cis-stilbene molecules excited to S_1 state decay radiatively. Since isomerization is a dark process, the extent of isomerization is not known. Excitation of cis-stilbene: Ar clusters with an intense 266 nm pulse, which is resonant with both cis- and trans-stilbene S_1 states, offers the possibility of detecting the trans-stilbene product if the isomerization rate is faster than the laser pulse duration.

The emission spectra from cis-stilbene: Ar clusters following excitation by a 5 ns 266 nm pulse are shown in Figure 1 for laser fluences between 0.04 and 10 mJ/cm^2. At low fluence only structureless cis-stilbene emission is observed. The structured trans-stilbene emmision intensity increases quadratically with laser fluence indicating that trans-stilbene emission is produced by a two photon process. This observation confirms the previous assertion that in an Ar cluster friction is not sufficient to prevent cis-trans isomerization,[1] and in fact the isomerization quantum yeild is significant.

References

1) H. Petek, Y. Fujiwara, and K. Yoshihara, *J. Am. Chem. Soc.* **110**, 6269 (1988).

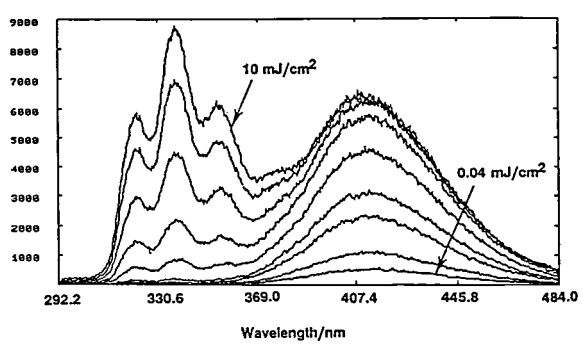

Figure 1. The emission spectra from cis-stilbene: Ar clusters for several laser fluences. The structureless fluorescence with a maximum at 417 nm that dominates the spectrum at low intensities is due to cis-stilbene. The structured fluorescence in near uv that is observed under non-linear excitation conditions is due to the trans-stilbene isomerization product.

III-A-2 Picosecond Pump-Probe Measurement of trans-Stilbene Formation Rate in cis-Stilbene: Ar Clusters

Hrvoje PETEK and Keitaro YOSHIHARA

In the above report it has been shown that cis-stilbene in Ar clusters isomerizes in S_1 state to form

trans-stilbene in less than 5 ns. With a newly developed high power picosecond laser system, we have measured for the first time the rate of isomerization in a cluster. The laser system consisting of a cw modelocked Nd: YAG laser, a synchronously pumped dye laser, a regenerative YAG amplifier, and a dye amplifier, produces tunable (620–570 nm) 1 mJ, 1 ps pulses at 10 Hz repetition rate. 600 nm laser pulses are doubled in a KDP crystal, split into two by a 50% beam splitter, and recombined inside a vacuum chamber at the intersection with the cluster beam. The two pulses are separated in time so that the pump pulse induces cis-trans isomerization and the probe pulse excites trans-stilbene fluorescence. The trans-stilbene isomerization rate is measured by changing the delay between pump and probe pulses.

The trans-stilbene emission intensity as a function of delay between pump and probe pulses is shown in Figure 1. The trans-stilbene is detected in <5 ps after the excitation pulse. This rate may either correspond to the true isomerization rate or to the rate of vibrational relaxation of initially produced vibrationally hot trans-stilbene. The measured rate is considerably slower than the isomerization rate of 1.35 ps that has been measured from the cis-stilbene S_1 state decay in room temperature solution.[1] Detailed picosecond measurements of cis-stilbene isomerization and trans-stilbene vibrational relaxation rates, as well as other photochemical problems of fundamental importance will be measured in rare gas and organic clusters in the future.

Reference

1) F.E. Doany, R.M. Hochstrasser, B.I. Greene, and R.R. Millard, *Chem. Phys. Lett.* **118**, 1 (1985).

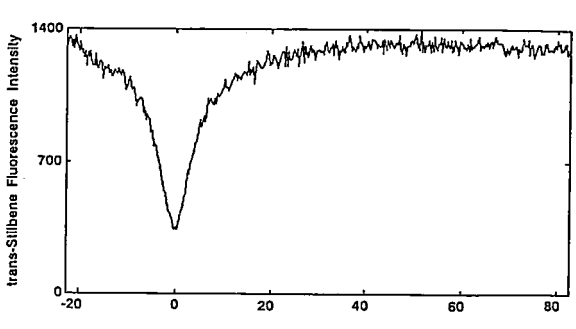

Figure 1. trans-Stilbene emission intensity as a function of delay from excitation of cis-stilbene: Ar clusters with 1 ps, 300 nm laser pulse. The signal is symmetric with zero delay decause pump and probe pulses are identical. Each point represents an average of 80 laser pulses.

III-A-3 Photophysics of 1,2-Diphenylcycloalkenes in Supersonic Beams Under Isolated Conditions and in Clusters

Hrvoje PETEK, Yoshihisa FUJIWARA *(Kanazawa Univ.)*, **John H. PENN** *(West Virginia Univ.)*, **and Keitaro YOSHIHARA**

At room temperature the quantum yield for isomerization of cis-stilbene (I) to form trans-stilbene is 35%, and to form dihydrophenantrene (II) it is 10%.[1] Because very little is known about the involvement of dihydrophenantrene (DHP) channel in non-radiative decay of S_1 state of cis-stilbene, we have investigated the photophysical properties of several 1,2-diphenylcycloalkanes (see below), which are cis-stilbene analogues that can only isomerize to form DHP.

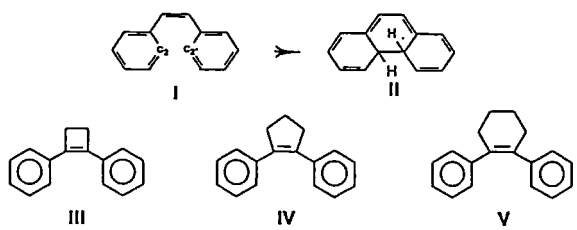

Consistent with previous solution results,[2] III is fluorescent under isolated conditions and in clusters, IV is only fluorescent in clusters, and V is non-fluorescent. The ethylenic ring size can have a profound effect on non-radiative rates because it controls the phenyl ring conformations and specifically the σ interaction between p orbitals on C_2 and C_2'. This interaction, which is repulsive in HOMO and attractive in LUMO, is responsible for low or no barrier to DHP isomerization in S_1 state.[2]

One important conclusion from this work is that the fluorescence properties of IV closely resemble those of cis-stilbene, therefore the DHP channel may be the cause of cis-stilbene non-radiative decay.

Reference

1) T. Wismonski-Knittel, G. Fischer, and E. Fischer, *J. C. S. Perkin II*, 1930 (1974).
2) G. Hohlneicher, et al., *J. Am. Chem. Soc.* **110**, 4483 (1988).

III-A-4 The Fluorescence Excitation Spectrum of 1,2-Diphenylcyclobutene

Hrvoje PETEK, Yoshihisa FUJIWARA *(Kanazawa Univ.)*, **John H. PENN** *(West Virginia Univ.)*, **and Keitaro YOSHIHARA**

The molecular structure of cis-stilbene in S_1 state is of great interest in relation to isomerization dynamics, but because the absorption spectrum is structureless no structural information can be obtained. The resonance Raman spectrum of cis-stilbene shows evidence of changes in the ethylenic bond angle with respect to the ground state.[1] 1,2-Diphenylcyclobutene (DPC-4), a cis-stilbene analogue (see above), is fluorescent and it has sharp vibrational structure (Figure 1), therefore the structural changes with respect to the ground state for a cis-stilbene like molecule can be deduced from its fluorescence excitation spectrum.

In the spectrum shown in Figure 1, >95% of the observed transitions can be assigned to fundamentals, overtones and combination bands of 23.7 and 151.4 cm^{-1} vibrational modes. These long progressions (up to 36 quanta) indicate that most of the structural changes are along these two normal modes. According to the calculations by Warshel,[2] the 23.7 cm^{-1} mode can be assigned to the phenyl twisting vibration. The higher frequency mode could correspond to the ethylenic C = C twisting vibration identified in the resonance Raman spectrum of cis-stilbene,[1] or to the C - C - Φ bending motion, which is the most prominent progression in the trans-stilbene absorption and emission spectra. The observation of large change in the phenyl twisting angle is important because it is evidence for structural changes that result in dihydrophenatrene formation in cis-stilbene like molecules.

References

1) A.B. Myers, and R.A. Mathies, *J. Chem. Phys.* **81**, 1552 (1984).
2) A. Warshel, *J. Chem. Phys.* **62**, 214 (1975).

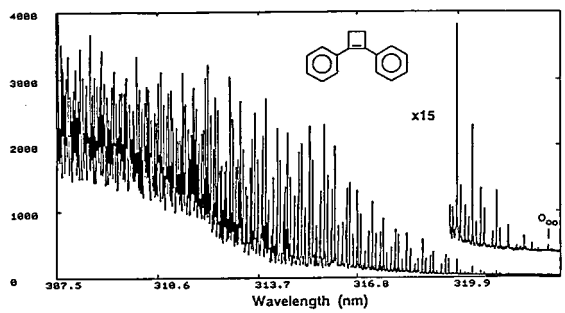

Figure 1. The fluorescence excitation spectrum of 1,2-diphenylcyclobutene in He supersonic expansion.

III–B Excited State Dynamics and Photochemistry of Adsorbed Dyes on Various Substrates

In the past few years we have been studying picosecond dynamics of adsorbed dyes on substrates like organic single crystals, inorganic semiconductors, and glasses. By controlling substrate materials, surface qualities, and dye coverages, we can observe surface energy transfer, electron transfer between dye and substrate, site- and aggregate-dependent fluorescence dynamics. For electron transfer reactions, the system serves as a fixed donor-acceptor with diffusionless semi-rigid character. We have elucidated the electron exchange matrix element, reorganization energy, intramolecular and intermolecular coupling, and successfully explained these parameters and their temperature dependence with quantum mechanical theory. In this issue we firstly report on the spectral sensitization in photography on the basis of electron transfer of J-aggregates of cyanine dye to AgBr single crystals. We secondly describe nonradiative decays of cyanine and triphenylmethane dye monomers in the adsorbed state and explain these with uni-directional photochemistry on surfaces. All of the above studies were performed by time-resolved fluorescence (TRF) method. Recently we have introduced time-resolved surface second harmonic generation (TRSSHG) as a truly surface specific optical method. TRSSHG permits studies of the reaction dynamics in adsorbates with picosecond time resolution. Finally we describe a test of TRSSHG in comparison to TRF and its application to picosecond isomerization in adsorbates.

III-B-1 Short and Excitation-Independent Fluorescence Lifetimes of J-Aggregates Adsorbed on AgBr and SiO_2

Klaus KEMNITZ, Keitaro YOSHIHARA, and Tadaaki TANI *(Fuji Photo Film Co.)*

[*J. Phys. Chem.*, in press]

We compared fluorescence decays of J-aggregates adsorbed on the AgBr electron-transfer system with those from J-aggregates adsorbed on an inert silica gel reference system in order to obtain additional information on the electron transfer in the former system. The fluorescence decays in both systems had lifetimes between 25 and 5 ps at 298 K and were independent of excitation intensity down to a photon density of 3×10^9 photons cm^{-2} $pulse^{-1}$. We attributed these fast fluorescence decays to the radiative decay channel and were able to correlate the fluorescence dynamics with the size of the J-aggregate, which itself was obtained from spectroscopic and kinetic data. The strong temperature dependence observed in the SiO_2 system was explained by a thermally activated nonradiative decay channel and various mechanisms were discussed for its explanation. A comparison of kinetic data of the AgBr system with corresponding data on the efficiency of sensitization in dependence of the J-aggregate size, yielded information concerning the mechanism of electron transfer involved, important results being shown in Figure 1.

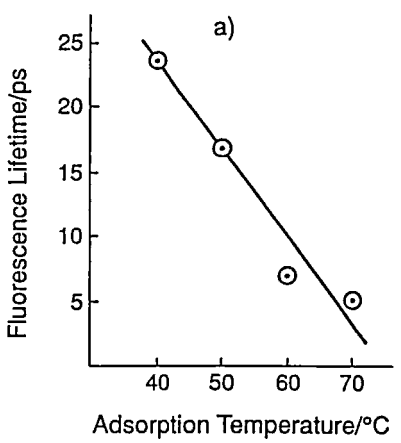

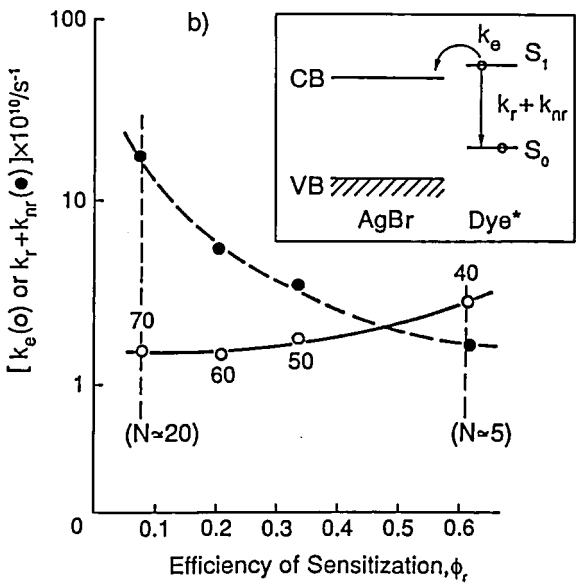

Figure 1. Dependence of J-aggregate fluorescence lifetime on adsorption temperature T_{ads} for octahedral AgBr microcrystals (a), and plot of k_e and $(k_r + k_{nr})$ vs. Φ_r (b), using experimental values of Φ_r and k_{obs}, where $k_{obs} = k_e + k_r + k_{nr}$. N indicates approximate number of molecules in a J-aggregate.

III-B-2 Nonradiative Decay of Cyanine and Triphenylmethane Dye Monomer in the Adsorbed State

Klaus KEMNITZ and Keitaro YOSHIHARA

The temperature dependence in the range from 298 to 4 K of the monomer fluorescence lifetimes of a thiacarbocyanine, pseudoisocyanine, and malachite green adsorbed on silica gel and on quartz has been examined. The fluorescence lifetimes at 298 K are about 20 times longer than the corresponding lifetimes in low viscosity solvents. Weakly activated or completely activationless behaviour of the rate constants of internal conversion have been observed. Asymmetric potential surfaces, induced by unidirectional forces exerted by the surface, are proposed as shown in Figure 1 which can explain the observed temperature dependences. The fluorescence lifetimes at 4 K are substantially shorter than the corresponding ones in rigid matrix and are attributed to a large free-volume effect in the absorbed state.

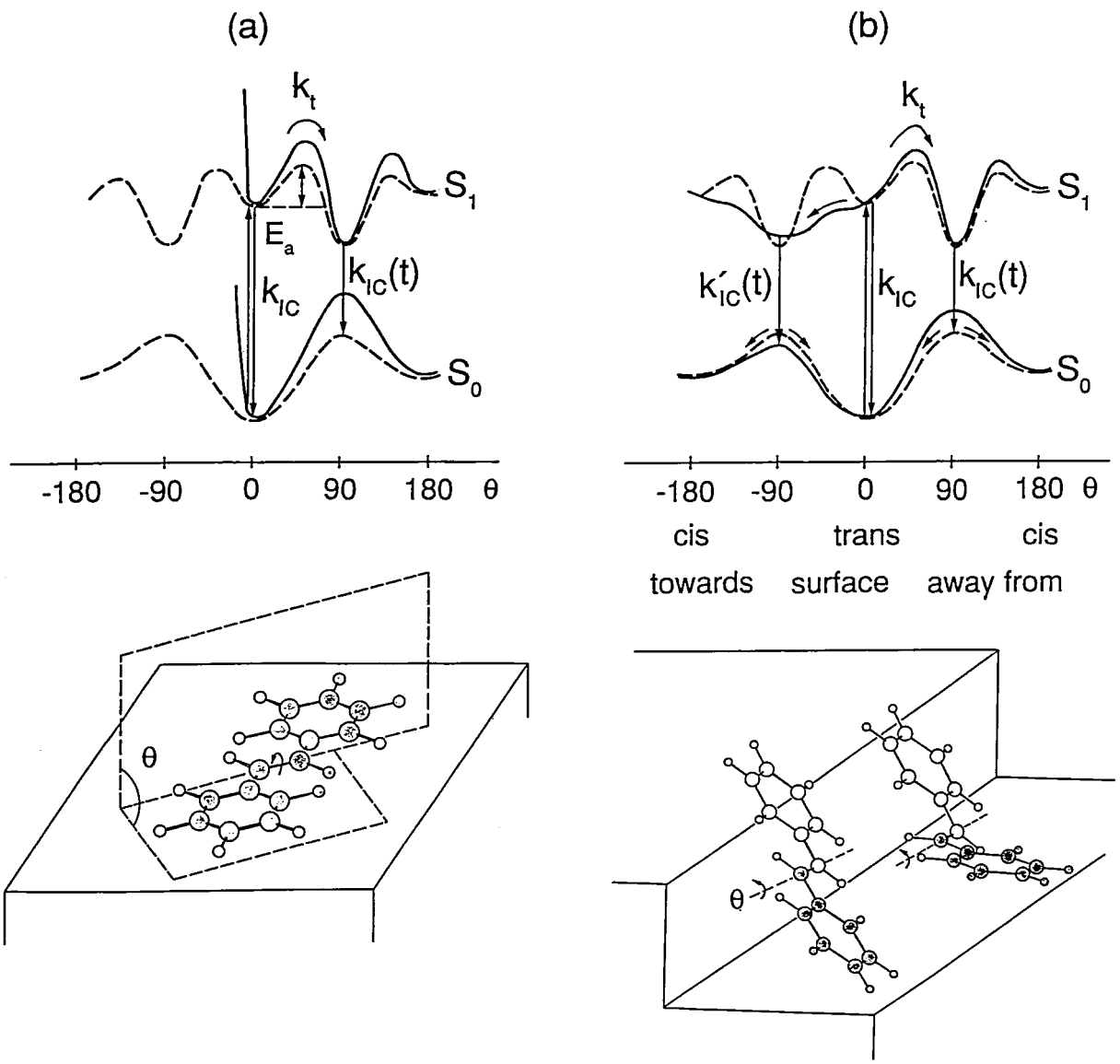

Figure 1. Ground and excited state potential surfaces for molecules adsorbed at (a) planar sites and (b) at distorted sites or for molecules not adsorbed in a flat way. The lower figures show stilbene, which is taken as model compound for isomerization, adsorbed at planar and distorted sites and demonstrate the "free volume" effect possible at distorted sites. The depicted configuration of the adsorbed molecule is, as is the geometry of the distorted site, one possibility among many others, conceivable.

III-B-3 Time Resolved Surface Second Harmonic Generation (TRSSHG): A Test of the Method and its Application to Picosecond Isomerisation in Adsorbates

Stephen R. MEECH and Keitaro YOSHIHARA

A test of the TRSSHG method has been performed. The decay dynamics of a submonolayer of a dye adsorbed on quartz were determined by both the TRSSHG and TR fluorescence methods. It can be shown that TRSSHG is essentially a surface specific transient "absorption" experiment, except that the hyperpolarisability, rather than absorbance, is measured. When the laser is resonant with a dye's $S_1 \leftarrow S_0$ transition the ground state recovery time will be recorded. In TR fluorescence the excited state decay time is measured. The two are directly comparable in

the case of a two level system. A molecule which approximates this is malachite green. A comparison of the two signals is shown in Figure 1. As can be seen the agreement is quite good. However, the TRSSHG signal recovers slightly faster than the fluorescence. Two other adsorbates gave similar results. The small difference between the traces can be explained by the heterogeneity of the surface. Essentially different orientations of adsorbates contribute different intensities in the two experiments.

The method has been used to study excited state isomerization dynamics in adsorbates. The results show that inramolecular motion can occur on a picosecond timescale in molecules adsorbed on solid surfaces, where diffusional motion is frozen. A comparison with the dynamics measured in solution shows that the details of the adsorbate interaction determine the relaxation rates.

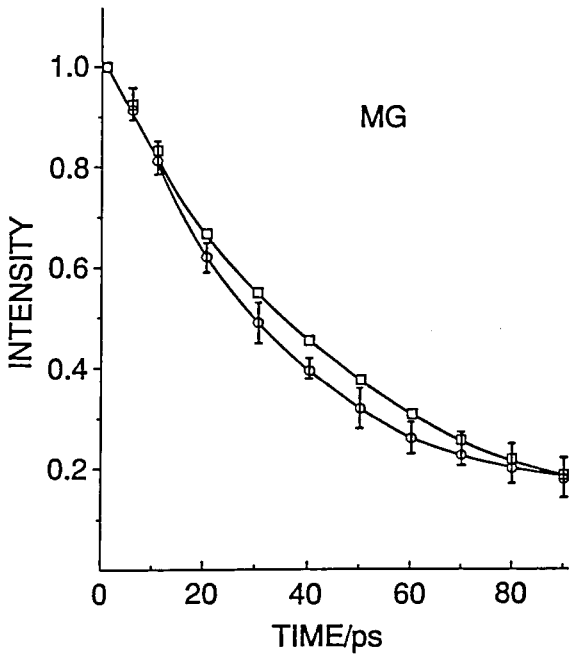

Figure 1. A comparison of the $E(2\omega)(t)$ (○) and $I_f(t)$ (□) results for malachite green (0.4 monolayer) as a function of time. The $E(2\omega)(t)$ data are the average of four traces.

III–C Development of Femtosecond Laser System for Observation of Ultrafast Molecular Processes

It is generally recognized that many elementary processes in chemical reactions fall into femtosecond timescale, and development of laser science enables us to measure these phenomena directly. We have constructed two independent femtosecond laser systems for time-resolved coherent anti-Stokes Raman spectroscopy (time-resolved CARS) and for time-resolved fluorescence spectroscopy. Two different research subjects are currently underway, namely i) studies on vibrational relaxation and energy transfer in the ground and the excited electronic state in condensed phases and ii) studies on intra- and inter-molecular energy transfer and elementary photochemical reactions of dyes in the electronic excited states in condensed phases. These researches have been supported in part by the Special Research Project of IMS.

III-C-1 Construction of a Femtosecond Time-Resolved CARS Measurement System for the Research of Ultrafast Molecular Processes

Hiromi OKAMOTO and Keitaro YOSHIHARA

Recent development in laser technique enables us to obtain coherent light pulses in the femtosecond time domain. The time scale corresponds to the period of a molecular vibration (100 fs = 333 cm^{-1}, for example). We have constructed a femtosecond time-resolved CARS system (Figure 1) for the research of ultrafast vibrational relaxation. The second harmonic of a home made CW mode-locked Nd:YAG laser (532 nm, pulse width 70 ps, repetition rate 81 MHz) excites two dye lasers. The linear cavity hybridly mode-locked dye laser[1] produces ultrashort light pulses (585 nm, pulse width as short as 80 fs). Another ordinary synchronously pumped dye laser (pulse width about 5 ps) oscillates at longer wavelengths (tunable between 600 and 700 nm). The fs laser radiation is divided into two parts

("pump" and "probe" beams). After a variable optical delay line between "pump" and "probe", these radiations are focused into the sample together with the ps radiation ("Stokes" beam) to satisfy a proper anti-Stokes phase matching condition. Polarization rotator is used for the "pump" and/or "probe" beams if necessary. The generated anti-Stokes radiation is detected by a cooled photomultiplier tube. The intensity of the anti-Stokes signal is recorded as a function of the delay time.

Reference

1) M.D. Dawson, T.F. Boggess, D.W. Garvey and A.L. Smirl, *Opt. Commun.* **60**, 79 (1986).

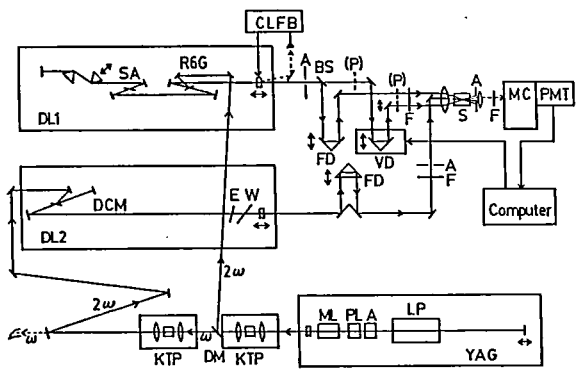

Figure 1. Block diagram of the femtosecond time-resolved CARS measurement system. YAG: CW-ML Nd:YAG laser, ML: mode-locker, PL: polarizer, A: aperture, LP: laser pot, DM: dichroic mirror, DL1: femtosecond dye laser, SA: saturable absorber, CLFB: cavity length feed back system, DL2: picosecond dye laser, W: tuning wedge, E: etalon, FD: fixed delay, VD: variable delay, BS: beam splitter, P: half-wave plate, F: filter, S; sample, MC: monochromator, PMT: cooled photomultiplier.

III-C-2 Observation of Femtosecond Time-Resolved CARS Signals of Liquid Samples with Various Polarization Conditions and the Autocorrelation Measurements by the Non-Resonant Background

Hiromi OKAMOTO and Keitaro YOSHIHARA

Femtosecond time-resolved CARS signal of liquid samples are observed for three different polarization conditions: Stokes polarization parallel to (//) pump polarization and probe polarization // pump polarization (abbreviated as [//,//]), Stokes // pump and probe perpendicular to ($\perp$) pump ([//, $\perp$]) and Stokes $\perp$ pump and probe // pump ([$\perp$,//]). The left-hand side of Figure 1 shows the anti-Stokes intensities of 992 cm^{-1} vibrational transition of liquid benzene as a function of the delay time between pump and probe pulses. Dephasing of the vibrational level is directly observed as the decay of the anti-Stokes signals. The previous observations by Zinth et al.[1] correspond to the [//, $\perp$] condition. A very fast dephasing process (τ = 0.39 ps) is newly observed in the [$\perp$,//] condition, in addition to the slow decay component (τ = 2.4 ps).[1] The right-hand side of Figure 1 shows the non-resonant background signal (the energy difference between the pump and the Stokes radiation is set at about 1800 cm^{-1} where no Raman transition is observed) as a function of the delay time, which corresponds to the autocorrelation of the fs pulse. This shows that we can obtain an autocorrelation trace in much better signal to noise ratio if we adopt the [//,//] condition, compared with the [//, $\perp$] condition.[1]

Reference

1) W. Zinth, R. Leonhardt, W. Holzapfel and W. Kaiser, *IEEE J. Quantum Elec.* **24**, 455 (1988).

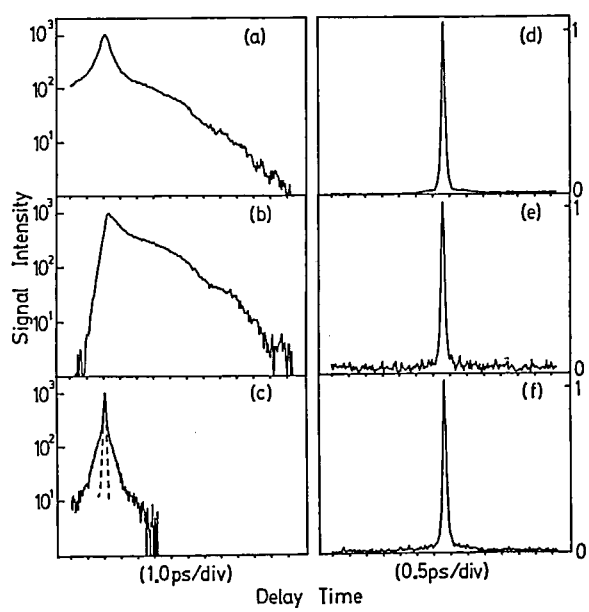

Figure 1. Anti-Stokes signals obtained for the 992 cm^{-1} Raman transition (a)–(c) and the nonresonant background (d)–(f) of neat benzene. Polarization conditions are: [//,//] for (a) and (d), [//, $\perp$] for (b) and (e) and [$\perp$,//] for (c) and (f). The broken curve in (c) shows the system response function. The intensity scale is different in each panel.

III-C-3 Observation of Femtosecond Time-Resolved Pre-Resonance and Resonance CARS Signals of Dye Solutions

Hiromi OKAMOTO and Keitaro YOSHIHARA

It is expected that time-resolved resonance CARS experiment provides detailed information about vibrational relaxations in the electronically excited state in resonance, in addition to that in the ground state. We performed measurements of femtosecond time-resolved CARS in pre-resonance and resonance conditions. β-carotene and DQOCI (1,3'-diethyl-4,2'-quinolyloxacarbocyanine iodide) were used as the test samples for pre-resonance and resonance conditions, respectively. β-carotene shows the 0-0 absorption maximum at 493 nm in benzene solution and is known for its non-fluorescent character and strong Raman intensities. Figure 1(a) shows the anti-Stokes intensity of β-carotene benzene solution (10^{-3}M) with [//,//] polarization as a function of the delay time. The energy difference of the pump and the Stokes light ($\omega_p - \omega_s$) was set at ca. 1150 cm^{-1}. The anti-Stokes intensity (and the non-resonant background) was greatly enhanced because of the resonance effect. The vibrational dephasing time is found to be 0.5 ps. The shoulder on the both sides of the main peak may be due to beating of vibrational modes. The similar plot for DQOCI methanol solution (10^{-4} M) is given in Figure 1(b). DQOCI has the absorption maximum at 593 nm in methanol. $\omega_p - \omega_s$ was set at ca. 1300 cm^{-1}. The anti-Stokes signal decays with a time constant of 0.3 ps and shows beating structure. The very fast decay time constant even in the rigorous resonance condition suggests the existence of very fast dephasing processes in the electronically excited state.

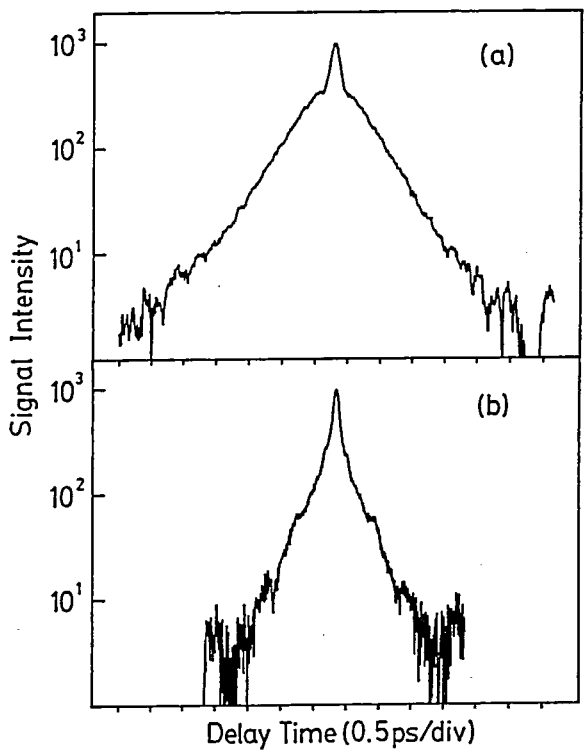

Figure 1. Anti-Stokes signals obtained for (a) benzene solution of β-carotene (10^{-3} M) and (b) methanol solution of DQOCI (10^{-4} M). The intensity scale is different in each panel.

III-C-4 Theoretical Considerations on Time-Resolved Resonance CARS as a New Method for the Reserarch of Vibrational Relaxation Pathways in the Electronically Excited States

Hiromi OKAMOTO and Keitaro YOSHIHARA

Time-resolved resonance CARS is formulated by a simple density-matrix method. Model calculations demonstrate that the anti-Stokes signals may rise and decay in rigorous resonance conditions, and that the information on the vibrational relaxation pathway in the electronically excited state is included in the vibrational mode dependence of the rise time of the anti-Stokes signals.

III-C-5 Construction of Femtosecond Laser System for Fluorescence Studies

Tohru KOBAYASHI, Yoshihiro TAKAGI and Keitaro YOSHIHARA

A mode-locked YAG laser (COHERENT Antares 76s) which produces 532 nm light pulses with 70 ps duration and 76 MHz repetition has been used as a pump source of a dye laser. For a femtosecond dye laser cavity, we adopted hybridly mode-locked synchronously pumped linear cavity with two Brewster prisms to compensate for group velocity dispersion[1] (Figure 1(a)). It consists of two dye jets, one for gain dye (Rhodamine 6G) and the other for saturable dye (DQOCI+DODCI). With two Brewster angled quartz prisms, we could produce orange pulses with duration of 80 fs and peak power of 10 kW. We further modified the cavity to use cavity dumper in order to get high peak power of output laser pulse and to synchronize output pulses to pulses from copper vapor laser for amplification. Inclusion of cavity dumper brought about longer pulse duration (around 0.4 ps) but higher peak power around 15 kW. Cavity dumped pulse was next introduced into pulse compressor which compressed the pulse width to 80 fs as shown in Fig. 1 (b). After amplification, we will get pulses with peak power around 20 MW.

Reference

1) M.D. Dawson, T.F. Boggess, D.W. Garvey and A.L. Smirl, *Optics Comn.* **60**, 79 (1986).

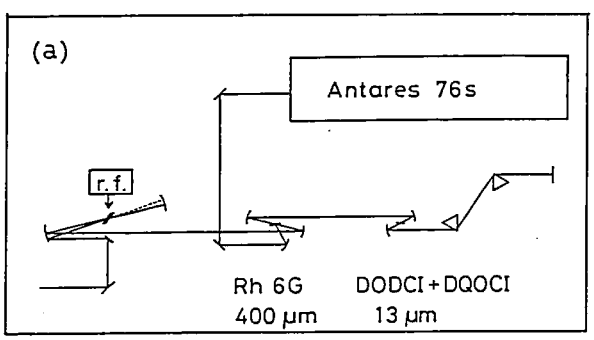

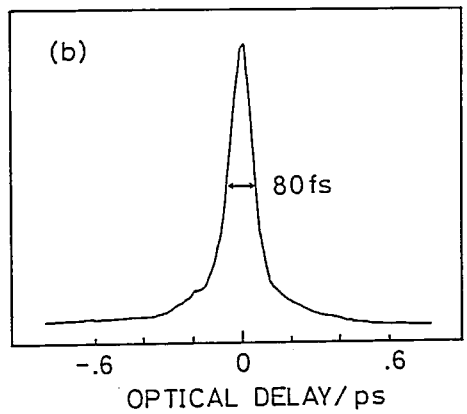

Figure 1. (a) Comfiguration of cavity dumped dye laser system. Combination and thickness of two dye jets are indicated in the figure. (b) Autocorreleation trace of compressed laser pulse. Actual pulse width is calculated by assuming $sech^2$ pulse shape.

III-C-6 Subpicosecond Fluorescence Sampling Using Up-Conversion Method

Tohru KOBAYASHI, Yoshihiro TAKAGI and Keitaro YOSHIHARA

Because of the poor response time of electronic instruments, it is not yet possible to observe ultrafast phenomena directly. For this reason, we have constructed fluorescence up-conversion apparatus to measure fluorescence decay with time resolution close to the pulse width of the excitation laser.

Figure 1 shows the fluorescence decay of nile blue observed at two different wavelengths. As clearly seen in the figure, short wavelength fluorescence shows rapid rise (equal to the laser pulse) and slow decay. In contrast with this behavior, long wavelength fluorescence shows different decay profile. It has long rise time which corresponds to the decay time of the short wavelength fluorescence. It indicates that the long wavelength fluorescence comes from the state which is produced after the relaxation from initially prepared state. The results are in consistent with the fluorescence decay dynamics previously observed.[1] Thus we could reproduce the experimental result using our new laser system. We are now amplifing the dye laser output with copper vapor laser. By using second harmonic of the amplified pulse, it will be possible to apply this system to various molecular systems in future.

Reference
1) A. Mokhtari, J. Chesnoy and A. Laubereau, *Chem. Phys. Lett.* **155**, 593 (1989).

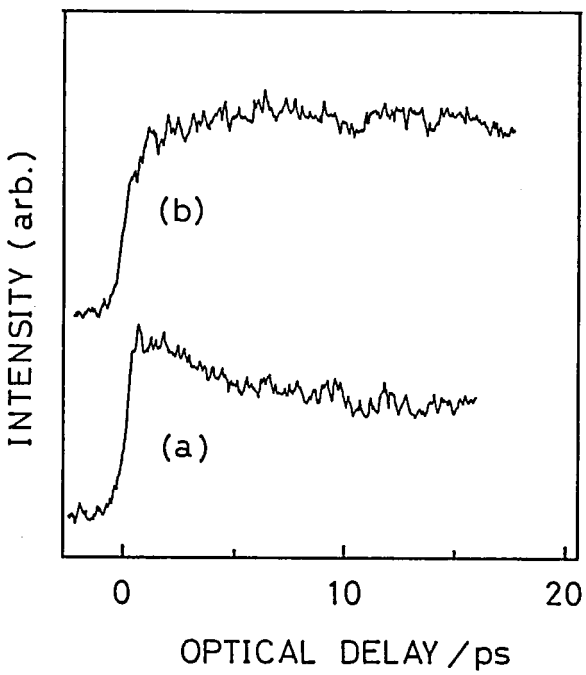

Figure 1. Up-conversion signal vs. optical delay time. (a) decay of 640 nm emission; (b) decay of 675 nm emission.

III–D Dynamic Behavior of Electronic Excited States

Optical excitation of molecules to electronically excited states causes a variety of dynamical behavior, depending upon the nature of electronic structures and environments, such as energy transfer, proton transfer, chemical reaction, radiationless transition, ionization, and others. Most of these processes fall into the nanosecond, picosecond and femtosecond timescales. Firstly, we discuss the nanosecond and picosecond kinetics of excited-state isomerization and ionization of cis-and tras-1,2-bis(1-methyl-4-pyridino)ethylene, and the effect of charge transfer in cis-trans isomerization. Secondly, we discuss the excited-state diffusion of bianthryl in microheterogeneous systems like vesicles, membranes, and micelles.

III-D-1 Charge Transfer and Cis-Trans Photoisomerization

Thomas W. EBBESEN *(Notre Dame Univ.)*, **Katsumi TOKUMARU** *(Tsukuba Univ.)*, **Minoru SUMITANI, and Keitaro YOSHIHARA**

[*J. Phys. Chem.* **93**, 5453 (1989)]

The photophysical and photochemical properties of cis- and trans-1,2-bis(1-methyl-4-pyridino) ethylene dication (BPE^{2+}) in acetonitrile are examined. These properties are significantly altered by the charge-transfer complexation in the ground state. The free olefins undergo cis-trans photoisomerization with a quantum yield of ca. 0.3. The cis isomer does not

fluoresce unlike the trans isomer ($\Phi_F = 0.01$, $\tau_F = 5 \times 10^{-11}$s). The fluorescence of the trans isomer is quenched by complexation with iodide ions in the ground state. In addition, static quenching occurs within a 16-Å radius. Upon excitation in the charge-transfer absorption band, the trans iodide complex gives the trans radical with a quantum yield of 0.06. The cis iodide complex leads not only to the formation of the cis radical isomer with a quantum yield of 0.02 but also to the trans isomer dication (quantum yield 0.05). The latter reaction can be interpreted either as a geminate pair catalyzed event or as isomerization in the excited charge-transfer state from the results of the nanosecond and picosecond laser flash photolysis experiments. The results are summerized in Table 1.

Table I Properties of *cis*- and *trans*-BPE^{2+} in Different States

	uncomplexed species (BPE^{2+})			charge-transfer complexes ($BPE^{2+}I^-$)			radical species[a] ($BPE^{\cdot+}$)
	Φ_{iso}	Φ_F	τ, S	K_1, M^{-1}	Φ_R	Φ_{iso}	Φ_{iso}
cis	0.3	0.00		1.6	0.02	0.05	0.2
trans	0.35	0.01	5×10^{-11}	4.6	0.06	0.00	0.0

Reference

a. T.W. Ebbesen, C.W. Previtali, T. Karatsu, T. Arai, K. Tokumaru, *Chem. Phys. Lett.* **119**, 489 (1985).

III-D-2 Excited State Diffusion of Bianthryl in Microheterogeneous Systems

Robert PANSU and Keitaro YOSHIHARA

The diffusion and trapping of bianthryl excited state has been studied in various microheterogeneous media in order to determine bianthryl localisation and the transverse viscosity in these media. Bianthryl is known to be an apolar molecule but its excited state emission depends on the polarity of the solvent. From what is known in homogeneous phase, it can be expected that bianthryl is localised in the middle of the membrane; the excited state diffuses and reaches the water phase where it is trapped. The membrane and trap population have been measured by monitoring the fluorescence intensity. The media studied include DMPC (dimeristoyl-phosphatidyl-choline) vesicles, DODAC (dioctadecyl-dimethyl-ammonium chloride) membranes, CTAC (cethyl-trimethyl-ammonium chloride) and SDS (sodium dodecylsulfate micelles), and bianthryl microcrystal suspensions. The surfactant suspensions were obtained by sonication and filtration using standard preparation protocols[1]. The fluorescence decay curves where registered with the picosecond time correlated single photon counting method using the synchronously pumped dye laser system at the instrument center.

Time resolved emission spectra (Figure 1a) reveal that the spectrum shifts to the red as time elapses. The existence of an isobestic point shows the existence of only two solvatation sites for bianthryl. The analysis of the polar site (trap) emission indicates that these molecules are actually produced by the disactivation of the apolar population and that their decay is an exponential.

In membrane systems (DMPC, DODAC), the decay of the membrane population has the form of exp $(-k\sqrt{t})$. This decay shape is typical of a diffusion process to randomly distributed traps (Figure 1b). Furthermore in membrane systems the depolarisation of the emission is rapid and much shorter than the expected rotational relaxation time. Both observations can be rationalized if we assume that bianthryl molecules form micro domains in the membrane and that exciton diffusion and trapping occurs via a resonant energy transfer.

In micellar systems the fluorescence depolarisation lifetime indicates that physical diffusion occurs. In CTAC micelles bianthryl appears to be close to the surface whereas in SDS micelles bianthryl is deeper in the micelle.

Reference

1) R. Pansu, S. Baer, B. Arrio, J. Roncin, J. Faure, *Nouv. J. Chem.* in press.
R. Pansu, L. Lane, B. Arrio, J. Roncin, J. Faure, *J. Phys. Chem.* in press.

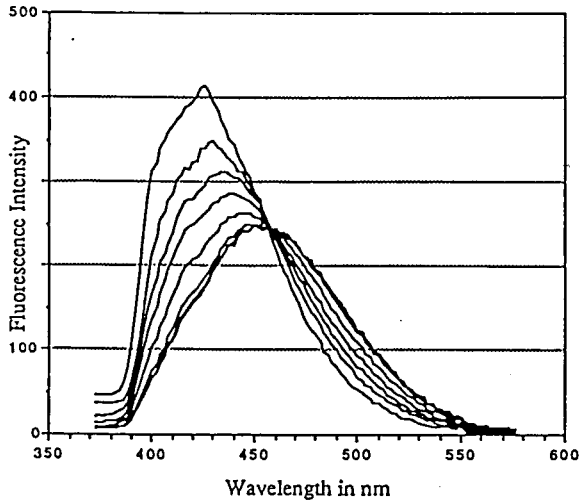

Figure 1a. Transient emission spectra of bianthryl in DODAC. A red shift is observed as time increases. The spectra have been normalised to the same area. Delay times in ns: 0, 0.4, 1.2, 3.8, 5.8, 12.2, and 20.0. Excitation wavelength is 353 nm.

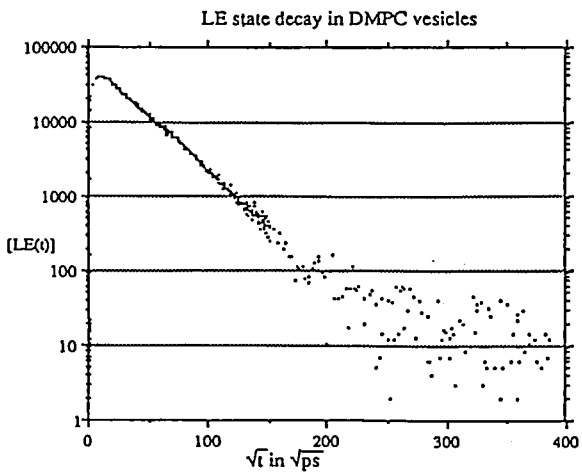

Figure 1b. Decay of the membrane population. DMPC is 10^{-2} mol/l, bianthryl molar frac. is 10^{-2}. Room temperature. λ_{exc} = 313 nm.

III–E Solar Energy Conversion by Using Photocatalytic Effects of Semiconductors and Dyes — Decomposition of Water and Application to Organic Synthesis —

III-E-1 Electrochemical Reduction of Carbon Dioxide on Various Metal Electrodes in Low-Temperature Aqueous Media

Masashi AZUMA, Kazuhito HASHIMOTO, Masahiro HIRAMOTO, Masahiro WATANABE *(Yamanashi Univ.)*, **and Tadayoshi SAKATA***

[*J. Electroanal. Chem.* **260**, 441 (1989)]

Electrochemical CO_2 reduction was investigated on 32 metal electrodes, that are usable in the electrochemical system, by measuring the amounts of several reduction products after potentiostatic electrolysis in the aqueous medium. The current efficiency of CO_2 reduction on Ni, Ag, Pb and Pd increases significantly with lowering the temperature. The ratio of reduction products are also changed by lowering temperature. Potential dependence of HCOOH and H_2 on a Hg electrode supports the electron transfer mechanism for HCOOH production. Formation of methane and ethylene is observed on alsmost all metal electrodes used, though the efficiency is mostly very low except for Cu. Figure 1 is the periodic table for CO_2 reduction in a CO_2-saturated 0.05 mol dm^{-3} $KHCO_3$ solution at 0°C. This figure clearly shows that most of light transition metals are not so effective for CO_2 reduction except Ti. Light metals in the III B or IV B group are not effective also. Heavy metals in II B, III B and IV B group are not effective also. Heavy metals in II B, III B and IV B group reduce CO_2 into HCOOH effectively. Some of VIII and I B metals are effective for CO production. It should be noticed that Cu metal, which has very high electrocatalytic activity for CO_2 reduction into hydrocarbons, is located between metals effective for CO and HCOOH production.

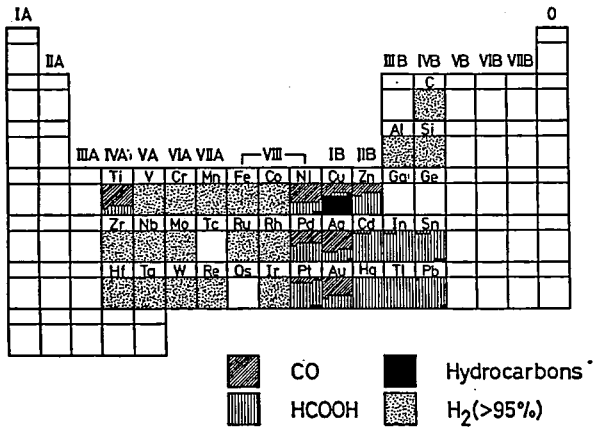

Figure 1. Periodic table for CO_2 reduction products at −2.2 V vs. SCE in low temperature 0.05 mol dm^{-3} $KHCO_3$ aqueous solution.

III-E-2 Semiconductor Effect on the Selective Photocatalytic Reaction of α-Hydroxycarboxylic Acids

Hisashi HARADA *(Meisei Univ.)*, **Toyotoshi UEDA** *(Meisei Univ.)*, **and Tadayoshi SAKATA**

[*J. Phys. Chem.* **93**, 1542 (1989)]

Photocatalytic and photoelectrochemical reactions of lactic acid and other α-hydroxycarboxylic acids (glycolic acid and 2-hydroxy-3-methylbutyric acid) were compared for various types of semiconductor electrodes (TiO_2, CdS, $SrTiO_3$, and ZnO) and suspension of particulate semiconductors (TiO_2, CdS, MoS_2, and ZnS). These reactions were found to depend strongly on the type of semiconductor studied. The reaction products from lactic acid-water solution are shown in Table 1. In the cases of Pt/CdS and ZnS photocatalysts, the hydroxy group of the acids was oxidized selectively into the corresponding keto acids, whereas in the cases of Pt/TiO_2, decarboxylation took place in addition to dehydrogenation. The same dependence was observed in the photoelectrochemical reactions with semiconductor single-crystal electrodes. For the TiO_2 electrode, the reation depends strongly on pH, whereas it does not for CdS. The results of pH effects, electrochemical reaction with various metal electrodes, and Fenton reaction in a homogeneous solution suggest the importance of adsorption of the reactants on the semiconductor and metal surfaces for the selective reaction.

Table 1. Photocatalytic and photoelectrochemical reaction products from lactic acid-water (1:10v/v) solution[a].

catalyst[b] (electrode)	irrad. time/h	product/μmol				
		H_2	CO_2	H_2S	CH_3CHO	$CH_3COCOOH$
Pt/TiO_2	4	1210	1430		1080	20
Pt/CdS	4	1200	15			800
Pt/MoS_2[c]	4		36		33	
ZnS[d]	13	218		35		30
(TiO_2)[e]					37	6
(TiO_2)[ef]					7	30
(CdS)[e]						45
(CdS)[ef]						37

[a]Irradiated with 500-W or 1-kW Xenon lamp (under 500-W operation). [b]300mg of photocatalyst was used. [c]With Ag^+ (electron acceptor). [d]Colloidal ZnS. [e]Gaseous reaction products were not analyzed. Applied potential was 0–1.0V vs. SCE. Amount of electricity was 9.65coulomb. [f]Electrolyte was sodium lactate solution (pH 13).

III-E-3 Observation of Fast Electroluminescence (EL) Rise Time Transients at Semiconductor/Electrolyte Interface

***Ayyakkannu MANIVANNAN, Kazuhito HASHIMOTO, Tadayoshi SAKATA and *Akira FUJISHIMA** *(*Univ. of Tokyo)*

Study of the dynamics of Electrochemical Luminescence (EL) is of importance in understanding the transport of charge carriers at semiconductor/liquid junctions. The use of transient techniques in EL studies provide useful information on the charge transfer processes at the interface. Moreover, the kinetics of heterogeneous reactions occurring are normally determined by a sequence of steps involving both transport through the solution phase and the transfer of charge at the interface. In the present study, a dynamic potential pulse technique has been employed to explore the controlling factors of the charge transfer mechanism. For this, we employed a pulse generator which supplies potential pulses with nanosecond rise times. The experiments were all carried out at n- SiC single crystals in various electrolytes as given in Figure 1. The spectral distribution and the other preliminary parameters are described elsewhere. The EL rise times were found to

be in the order of microseconds. Basically, the EL transients have a dead zone and a rising zone. The dead zone seems to be the time needed to charge the semiconductor space charge and it varies with the change in the cathodic potential limit. The rising zone seems to be controlled by the solution species and it is clear from Figure 1 that the rising behaviour of the EL transients for an n-SiC electrode are different for various electrolyte species.

References

(1) A. Manivannan and A. Fujishima, *J. Luminescence* **42**, 43 (1988).

(2) A. Manivannan, G.V. Subba Rao, and A. Fujishima, *Ber. Bunsenges. Phy. Chem.* **92**, 1522 (1988).

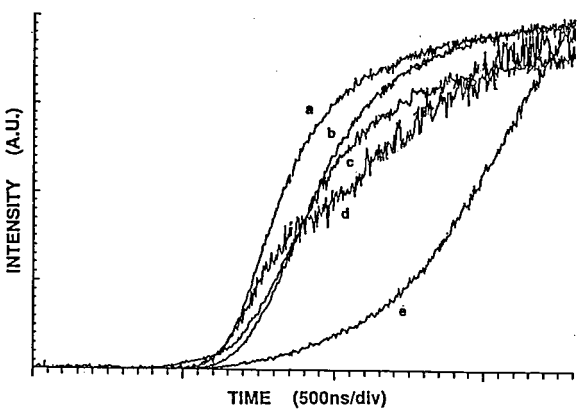

Figure 1. EL rise behaviour obtained at a n-SiC electrode pulsed at 833Hz with a bias of −8.0V vs Pt in a.) $Na_2S_2O_8$ b.)H_2O_2 c.) HSO_5^- d.) $K_3Fe(CH)_6$ e.) $NaBrO_3$ (all prepared as 0.5M with 0.5M H_2SO_4).

III-E-4 Picosecond Dynamics of Photocatalytic Reactions with Powdered Semiconductor Studied by Transient Absorption. (I) CdS

Kazuhito HASHIMOTO and Tadayoshi SAKATA

Charge transfer at the interface between semiconductor and electrolyte is an initial, important step for photoelectrochemistry, photocatalysis, etc. In order to determine both the charge transfer rate and intermediate products, transient absorption measurement is one of the most powerful methods. We built an equipment for picosecond transient absorption with which two-dimensional information (time and wavelength) can be obtained simultaneously. The equipment is schematically illustrated in Fig. 1. Time resolution is *ca.* 10 *ps* and absorbance of more than 10^{-3} can be detected. Transient absorption can be, however, applied only to transparent samples such as colloidal systems, although semiconductor photocatalysts are usually powdered opaque samples. We, therefore, used powdered semiconductors supported on porous Vycor glass (PVG, surface area: 200 m^2/g), which is transparent and stable in most solvents, and also *in vacuo*. In this report we show the study of CdS supported on PVG. When CdS is excited, photobleaching occurs just below the absorption edge. This is considered to be caused by excited electrons in the conduction band, and recombines with a hole in valence band. Therefore it is expected that the recovery time of the photobleaching becomes faster and slower in the presence of electron acceptor and electron donor, respectively. Actually, the rate was found to become larger with methylviologen or oxygen. On the contrary it became smaller with triethylamine. From those data, it is suggested that hole transfer is in general slower than electron transfer.

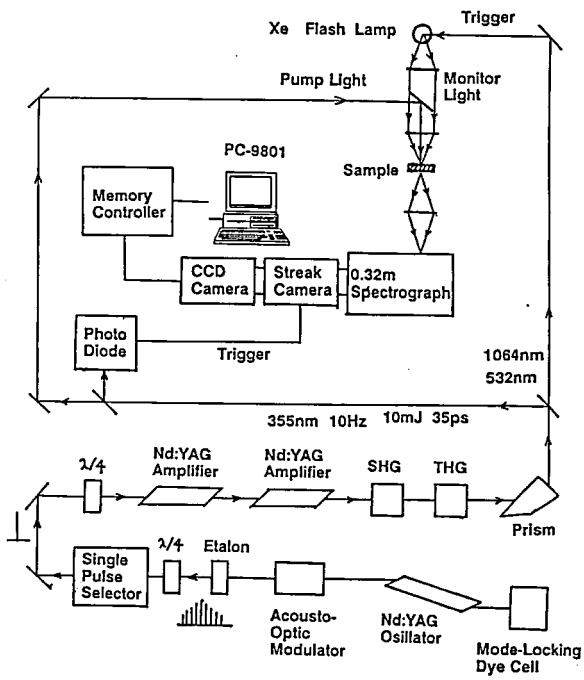

Figure 1. Schematic illustration of two-dimensional picosecond time resolved absorption measurement.

III-E-5 Picosecond Dynamics of Photocatalytic Reactions with Powdered Semiconductor Studied by Transient Absorption. (II) TiO_2

Kazuhito HASHIMOTO and Tadayoshi SAKATA

When TiO_2 is photoexcited, a broad absorption (peak wavelength: *ca.* 600 nm) due to trapped electron is observed. These trapped electrons recombine with free and trapped holes. This process competes with both the electron-transfer and hole-transfer processes to adsorbed molecules; electron acceptors will shorten the lifetime of the trapped electron, and electron donors will prolong it. Therefore the charge-transfer rates can be estimated by the measurements of lifetime of the trapped electron. In this paper our study was focused on the oxidation process of the adsorbed molecule (hole transfer), and TiO_2 small particle (r=60 Å) adsorbed on porous Vycor glass was used. In Figure 1 time behavior of the transient absorption in cyclohexane, water, ethanol and benzene is shown. The initial decay rate in cyclohexane is almost the same as that *in vacuo*. This is reasonable because the oxidation potential of cyclohexane is so positive that it cannot be oxidized by photogenerated hole in TiO_2. The dacay rates in water, ethanol and benzene, however, are smaller than that in cyclohexane. By analyzing those decay curves, the hole transfer rate, k_{et}, could be estimated. k_{et} for water is almost equivalent to that for ethanol, *ca.* 5×10^9 sec^{-1}. k_{et} for benzene is, however, *ca.*1.3×10^{10} sec^{-1}, larger than that for water and ethanol.

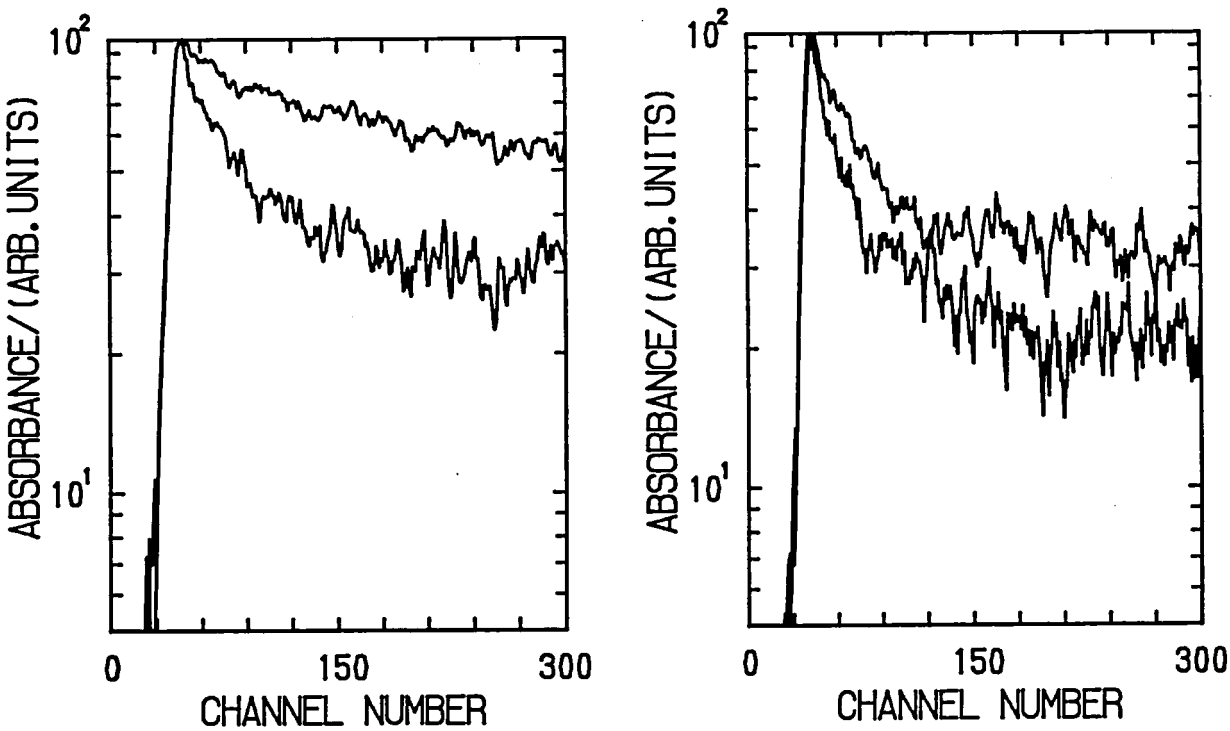

Figure 1. Time behavior of the transient absorption of TiO_2/PVG observed around 600 nm. Time scale: 11.2 ps/channel. (a) Upper curve: in benzene, lower curve: in ethanol. (b) Upper curve: in water, lower curve: in cyclohexane.

III–F Dynamical Processes in Electronically- and/or Vibrationally-Excited Molecules

Fundamental molecular aspects of chemical reactions and energy transfer processes in the electronically or vibrationally excited states have been studied. Particular interests have been directed to the dynamics of vibrationally-excited weakly-coupled complexes such as van der Waals and hydrogen-bonded complexes and the "disproportionation" reaction caused by UV irradiation of complexes. Dynamics of highly-excited vibrational states (local modes) and chemical reaction induced by their excitation have also been subjects of research. This year we have also started the study of non-linear self-organizing chemical processes which exhibit temporal chemical oscillation and spatial pattern formation.

III-F-1 Chemical Reaction of Weakly Bound Complexes: $HI{\cdot}N_2O + h\nu \rightarrow OH + N_2 + I$

Hiroshi OHOYAMA *(Osaka Univ.)*, **Masao TAKAYANAGI, Kazuhiro HONDA** *(Grad. Univ. Adv. Studies)*, **Teruhiko NISHIYA and Ichiro HANAZAKI**

[*Chem. Phys. Lett.*, **162**, 1 (1989)]

The title reaction was studied in a supersonic jet. The nascent rotational distribution of OH was determined by the LIF technique to give two or more Boltzmann distributions, corresponding to different isomers and more than one reaction channels. Measurements were also made for the corresponding bulb reaction ($H + N_2O \rightarrow OH + N_2$) to compare the results with those for the jet reaction under various stagnation pressure. Figure 1 shows the nozzle stagnation pressure dependence of the rotational distribution of OH obtained from the R_{11} transition. It is seen that the rotational population depends drastically on the stagnation pressure. The results were explained in terms of the existence of two geometrically isomeric complexes.

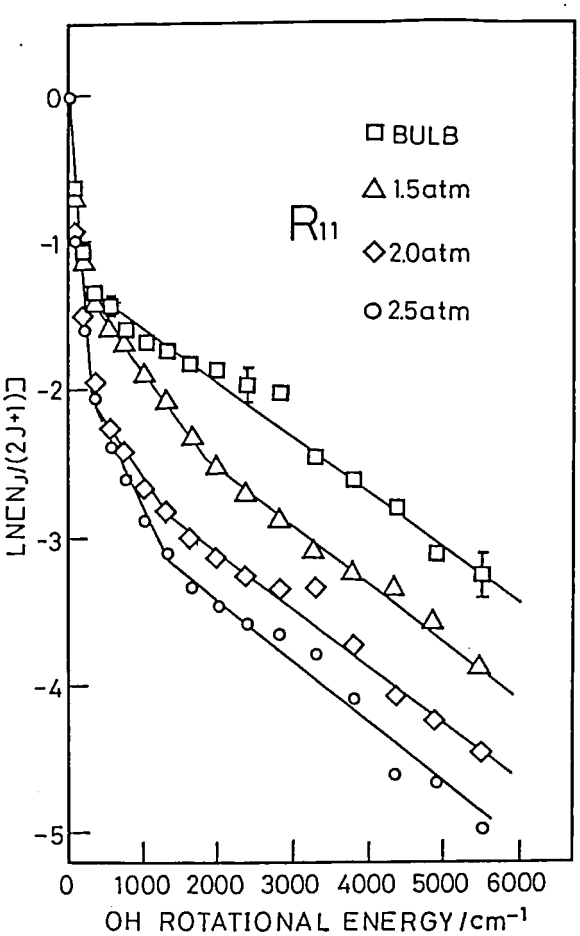

Figure 1. Boltzmann plot for the R-branch rotational distribution of OH in the v″=0 state for bulb and jet experiments. Each distribution is normalized separately at rotational energy=0.

III-F-2 Velocity Slip and Delayed Formation of $(HI)_n(N_2O)_m$ Clusters in the Pulsed Supersonic Jet

Hiroshi OHOYAMA *(Osaka Univ.)*, **Masao TAKAYANAGI, Kazuhiro HONDA** *(Grad. Univ. Adv. Studies)*, **Teruhiko NISHIYA and Ichiro HANAZAKI**

$(HI)_n(N_2O)_m$ complexes were generated by the supersonic expansion of He containing 2.6% HI and 4.4% N_2O through a conventional pulsed valve of 0.8mm diameter. The time profiles of $(HI)_n(N_2O)_m$ clusters were measured at 50 cm downstream using a quadrupole mass spectrometer. Figure 1 shows a time profile of several clusters. The cluster species appeared after a significant delay from the rise of the monomer signal with a shorter duration. A large velocity slip was observed. The delay was also dependent on the cluster size (e.g. $HI\cdot(N_2O)_2$ signal appeared after $(HI)_2$), indicating that it is not only due to the difference of velocity but also to the delayed formation of higher-order cluster species during the expansion. This result shows that a mass selection of neutral clusters is possible and enables us to study the chemical reaction of binary complexes with no contribution from higher-order clusters. The study of chemical reaction of higher-order clusters is also possible. Such a study is being undertaken in our laboratory.

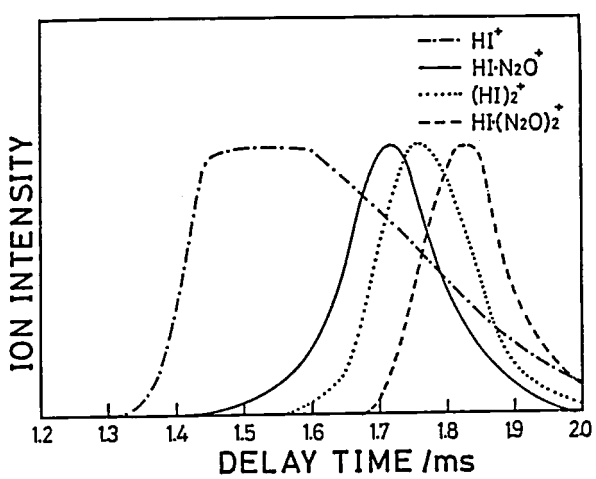

Figure 1. Time profile of $(HI)_n(N_2O)_m$ clusters generated by the supersonic expansion at the stagnation pressure of 2.0 atm. Abscissa is the delay time of ion signal from the trigger pulse to the pulsed valve.

III-F-3 Rotational Distribution of OH Produced by the 355 nm Irradiation of the NO_2 + H_2S System

Kazuhiro HONDA *(Grad. Univ. Adv. Studies)*, **Hiroshi OHOYAMA** *(Osaka Univ.)*, **Masao TAKAYANAGI, Teruhiko NISHIYA and Ichiro HANAZAKI**

We have studied the photochemical reaction in NO_2 + H_2S in a flow system. The reaction consists of two processes:

$$NO_2 \xrightarrow{h\nu} O(^3P) + NO \quad (1)$$

$$O(^3P) + H_2S \rightarrow OH + HS : \Delta H = -48.4 \text{ kcal/mol} \quad (2)$$

The rotational distribution of OH produced in the second process was measured by the LIF (laser-induced fluorescence) technique. The 355 nm pulse (third harmonic of a Nd:YAG laser, Quanta-Ray DCR2A) was used to photodisociate NO_2. The LIF probe pulse was provided by the second harmonic of a dye laser (LAMBDA PHYSIK FL 3002) pumped by a XeCl excimer laser (LUMONICS HE-420-SM-B). The probe light was delayed by 200 ns, so the effect of the 355 nm scattering could be avoided and the rotational relaxation of OH was negligible. The LIF spectrum corresponding to the OH $v''=0$ state is shown in Figure 1, which suggests the rotational state distribution with relatively low rotational temperature. The analysis of the spectrum is being undertaken to determine the rotational distribution of OH. It is also planned to measure the rotational distribution of HS and NO for the purpose of elucidating a detailed mechanism of the process.

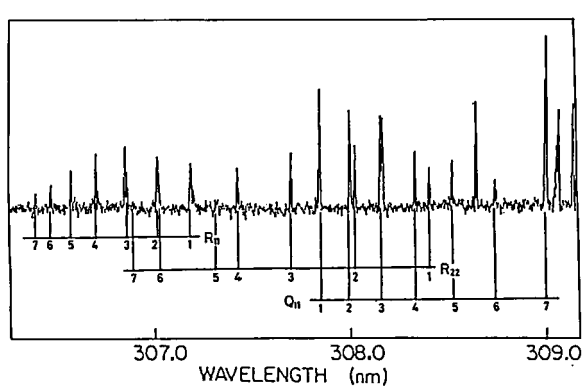

Figure 1. The OH $A^2\Sigma$-$X^2\Sigma$ (0,0) LIF spectra. Total pressure is 16 mTorr (H_2S:8 mTorr, NO_2:8 mTorr).

III-F-4 Investigation of Vibrationally Excited States by Tunable-IR/UV-REMPI Double-resonance Method

Teruhiko NISHIYA, Masao TAKAYANAGI, and Ichiro HANAZAKI

Several groups have revealed the SEP method to be a valuable tool for the investigation of highly vibrationally excited states. However, the stretching overtones are difficult to observe because of poor Franck-Condon factors to the intermediate states. We applied the tunable-IR/UV-REMPI double-resonance method to 0.1 Torr flowing NH_3 and investigated the relaxation from the stretching overtone states.

YAG pumped dye laser (Quantel) output was frequency converted by a H_2 Raman cell (2^{nd} Stokes line of OX 720 dye output) and used to excite a rotational-vibrational state ($\nu_1+\nu_3$ mode) of NH_3. The excited NH_3 was then selectively detected with (2+1) REMPI transition via the $\tilde{B}$ Rydberg state using a UV laser (Lumonics excimer pumped Lambda Physik dye laser: PTP or DMQ dye). Background signals due to hot bands were subtracted on a boxcar averager (Stanford Research System).

Figure 1 shows double-resonance REMPI signals at different delay times between IR and UV lasers. UV laser was set at 349.22 nm. Pronounced band at 6610 cm^{-1} corresponds to the Q branch head of the $\nu_1+\nu_3$ mode of NH_3. Considering the band intensity dependence on the delay time, we can conclude that other bands appear as a result of relaxation from the IR-pumped state to the 6610 cm^{-1} state which is being monitored. The pseudo first-order collisional lifetime of the monitored state is ≈100 ns in pure NH_3.

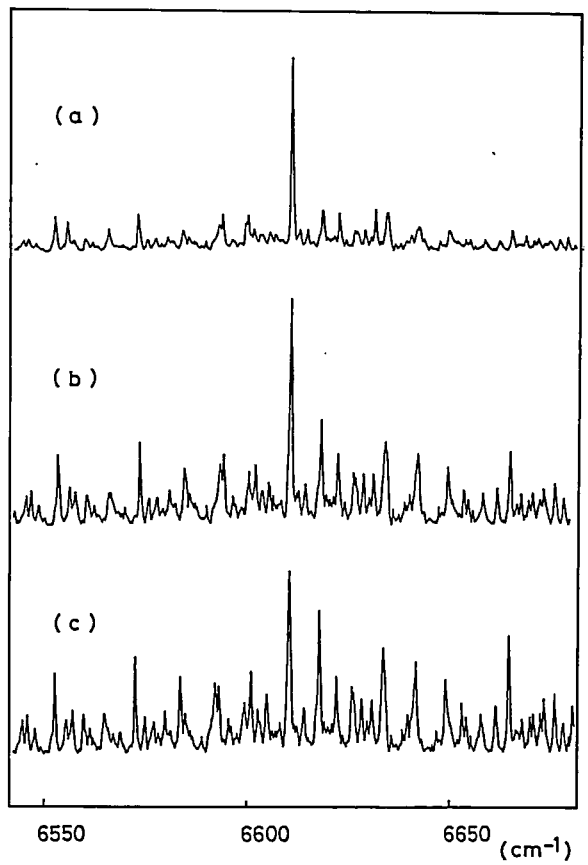

Figure 1. Double-resonance REMPI signals at different delay times between IR and UV lasers. UV laser was set at 349.22 nm. Delay times are (a) Δt=20 ns, (b) 60 ns, and (c) 100 ns, respectively.

III-F-5 Observation of Stretching Vibrational Modes in the $\tilde{B}$ Rydberg State of Ammonia

Teruhiko NISHIYA, Masao TAKAYANAGI, and Ichiro HANAZAKI

NH_3 is pyramidal in its ground state, and its Rydberg states are all planar. Therefore, a long progression of the out-of-plane bending mode (ν_2) appears in the VUV absorption spectrum of NH_3 and little is known about the excited-state stretching vibrations. Tunable-IR/UV-REMPI double-resonance method can provide excitation spectra of the intermediate states. Especially, excitation of vibrational modes in the ground state can change the Franck-Condon factor to the intermediate states and can provide information on unobserved vibrational modes in the excited states. We applied it to 0.1 Torr flowing NH_3 to observe

stretching vibrational modes in the $\tilde{B}$ Rydberg state of NH_3.

Figure 1 shows double-resonance REMPI spectrum. IR laser was tuned to 6610 cm^{-1} (Q branch head of $\nu_1+\nu_3$ mode). Delay time between IR and UV lasers was 20 ns. Pronounced band at 349.22 nm was assigned to $\nu_3+\nu_4$ mode in the $\tilde{B}$ Rydberg state. Although the bands around 6610 cm^{-1} in the ground state are of $\nu_1+\nu_3$ character, the molecular constants obtained by high-resolution spectroscopy suggests that they couple with the $\nu_1+2\nu_4$, $\nu_3+2\nu_4$ modes (ν_1, $\nu_3 \approx 2\nu_4$)[1], which may enhance the Franck-Condon transition from $\nu_1''+\nu_3''$ to $\nu_3'+\nu_4'$ mode in the $\tilde{B}$ state. We also obtained signals in the ν_4, $\nu_1+\nu_3$, and other regions. More detailed rovibrational analysis is now under way.

Reference

1) K. Nakagawa and T. Shimizu, private communication.

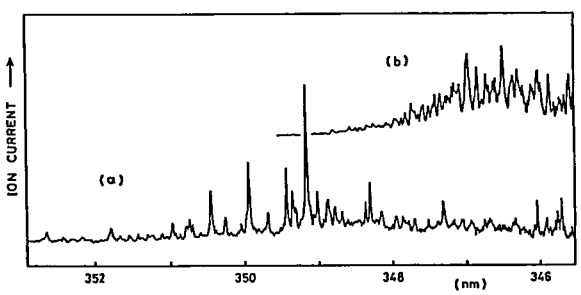

Figure 1. (a) Double-resonance REMPI spectrum. IR laser was tuned at 6610 cm^{-1} (Q branch head of $\nu_1+\nu_3$ mode). Delay time between IR and UV lasers was 20 ns. (b) Background signal due to hot bands measured without IR pumping. It has been subtracted in the double-resonance spectrum shown in (a).

III-F-6 Detection of Vibrationally Excited Species in Molecular Beam by SEP-Probe Spectroscopy

Masao TAKAYANAGI, Teruhiko NISHIYA, Hiroshi OHOYAMA *(Osaka Univ.)* **and Ichiro HANAZAKI**

An apparatus for measuring SEP-probe spectra was constructed. The apparatus contains a pulsed molecular beam equipment, three dye laser systems, a timing circuit, and a fluorescence detection system. The system has been used to investigate the dynamics of vibrationally excited species (molecules and van der Waals complexes) in molecular beams.

Molecules under investigation were vibrationally excited in the ground electronic state by SEP (stimulated emission pumping). Two UV lasers (frequency-doubled outputs of dye lasers pumped by second harmonics of Nd:YAG laser) were used for the SEP. Vibrational excitations could be monitored by fluorescence dip spectra measured with the two lasers. LIF spectra of the vibrationally excited species were measured with the third laser (the second harmonic of a dye laser excited by an excimer laser). The products generated by the reaction and/or relaxation of the vibrationally excited species can also be probed if their populations are sufficient for LIF measurements.

In the present measurements, we obtained LIF spectra with hot bands caused by the species in the vibrational states to which they were initially excited. An example of the SEP-probe measurement is shown in Figures 1(a) and 1(b), which correspond, respectively, to the LIF measurements of benzonitrile with and without the laser irradiation for the 460 cm^{-1}-SEP process. In Figrue 1(a), a hot band caused by the excitation from v=1 in S_0 to v=0 in S_1 can be observed: On the other hand, no hot band can be observed in Figure 1(b).

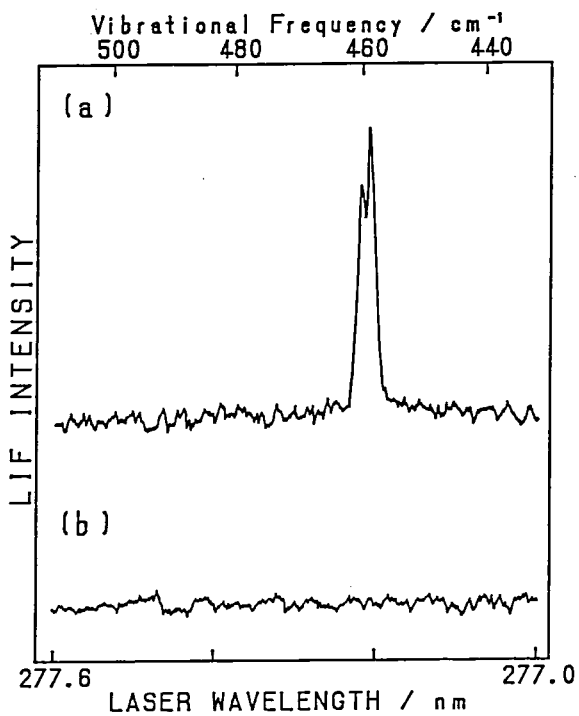

Figure 1. LIF spectra of benzonitrile (a) with and (b) without SEP excitation. The former is an example of SEP-probe spectrum.

III-F-7 SEP-Probe Spectra of van der Waals Complexes Containing Benzonitrile

Masao TAKAYANAGI and Ichiro HANAZAKI

SEP-probe spectra of benzonitrile (C_6H_5CN) and some van der Waals complexes (benzonitrile dimer, C_6H_5CN·Ar and C_6H_5CN·H_2O) in pulsed molecular beams were obtained. The lifetimes of excited vibrational states of these species were compared.

Each species was pumped to an excited vibrational state (460 cm^{-1} mode or 1000 cm^{-1} mode) in the ground electronic state by SEP. Vibrational excitation was confirmed by fluorescence dip spectra. Vibrationally excited species were probed with a delay of 100-600 ns after the excitation.

We could observe vibrationally excited monomers by the probe laser as hot bands in LIF spectra. However, we could not detect vibrationally excited dimers. The vibrational energy in the dimer seems to dissipate very quickly to the van der Waals intermolecular modes. The vibrationally relaxed species, where the intermolecular modes are excited, can hardly be observed by LIF method because of their small Franck-Condon factors and low population.

The LIF signals caused by the vibrationally hot C_6H_5CN·Ar and C_6H_5CN·H_2O could be measured but the signal was very weak. A careful analysis is now under way to obtain further information on the rate of the vibrational relaxation.

III-F-8 Oscillation of Fluorescence Intensity in the Aqueous Solution of Eriochrome Black T. I. Observation

Yoshihito MORI, Prem K. SRIVASTAVA, and Ichiro HANAZAKI

Temporal oscillation of fluorescence intensity has been observed in the aqueous solution of eriochrome black T containing 10% acetone. The fluorescence of the solution in an unstoppered cell (1 × 1 × 4.5 cm) was excited at 309 nm in a fluorometer (Shimazu RF-5000). Figure 1a shows the time profile of fluorescence taken at 410 nm. The oscillation started after an induction period and continued for more than 2 hrs. No oscillation was observed when the solution was stirred (Figure 1b) or it was in a stoppered cuvette. This indicates that the convective motion plays an important role. It is also to be noted that the fluorescence increased suddenly after the induction period and the overall time profile was the same as that for the oscillating case. It can therefore be concluded that the autocatalytic production of the fluorescent species gives rise to instability in the system which results in a chemical oscillation.

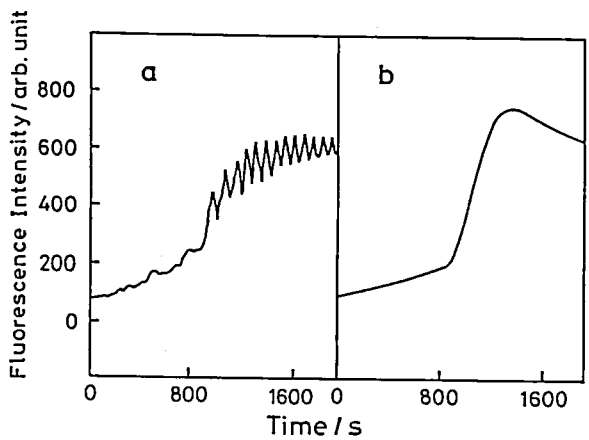

Figure 1. Typical oscillation of fluorescence intensity in the aqueous solution containing 0.033 mM eriochrome black T and 10% acetone. (a) without stirring, (b) with stirring. Fluorescence intensity at 410 nm (slit width 5 nm) was monitored by exciting the system at 309 nm (slit width 20 nm).

III-F-9 Oscillation of Fluorescence Intensity in the Aqueous Solution of Eriochrome Black T. II. Mechanistic Considerations

Yoshihito MORI, Prem K. SRIVASTAVA, and Ichiro HANAZAKI

We propose here a possible mechanism for the temporal oscillation of fluorescence intensity described in Part I of this report, where it is suggested that eriochrome black T yields a fluorescent species photochemically in a non-linear (autocatalytic) manner and that a convection in the solution plays an important role. However the combination of these two processes are not sufficient to understand the peculiar phenomenon of oscillating fluorescence. It seems to be essential to assume that a local domain of the solution first starts the sudden increase of the fluorescent

species probably due to a statistical fluctuation (stage (a)→(b) in Figure 1), while the other part of the irradiated solution, as well as the non-irradiated part, remains in the induction period. As the reaction proceeds in this domain, the heat of reaction and/or the excess energy provided by photons will dissipate heat to result in a local heating of the domain. If it moves out of the irradiated zone by convection, the fluorescence would decrease suddenly (stage (c) in Figure 1). Meanwhile another domain is formed in the irradiated zone to repeat the above process. Thus the combination of a local reaction domain, which is characteristic of the autocatalytic reaction, with the convective motion would explain the observed phenomenon.

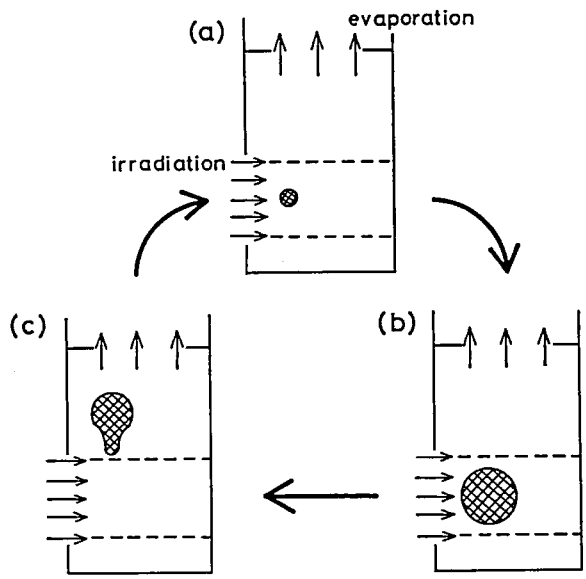

Figure 1. A mechanistic model of oscillatory fluorescence. The zone between broken lines is irradiated. The meshed area represents the local reaction domain.

III–G Molecular Association and Cluster Formation in Aqueous Environments Studied by Mass-spectrometry of Liquid Fragments

Molecular association, which leads to generate highly ordered structures of solute and/or solvent complexes in aqueous solutions, is a basic and quite important subject of chemistry in the relation to biological roles of molecules in aqueous environment. There exist many models of molecular associates which explain the structures of lipid bilayer membranes or hydrophobic bonding in protein conformation. In order to examine the reality of those models and ideas, the direct observation of such molecular associates must be highly indispensable. Isolation of strongly bound molecular associates from aqueous solution was performed by expanding fine liquid jets into vacuum. On the changes of liquid temperature and solute concentration, mass-spectral pattern sensitively varied suggesting that molecular association in aqueous solution is dependent on temperature as well as molar fraction of solute species. Extension of mass range up to m/e=2000 enabled us to detect large molecular clusters with multiple solute species and unforeseen structural anomalies.

III-G-1 Ethanol-Monohydrate Polymers?: Molecular Composition of Large Ethanol-Water Binary Clusters in Mixed Solutions

Nobuyuki NISHI, Toshiya FURUSAWA*, Masaru SAITA*, Kiichi NISHIMURA*, Kazunori YAMAMOTO, Kunimasa KOGA*, Kenzo NAGAMI* *(*Suntory Research Center)*

About 40 years ago, Brewer and Palmer reported the formation of cubic crystal formed at −72°C from aqueous solutions of ca. 70% ethanol and suggested that these possibly consisted of "ethanol monohydrate". The low mass spectra of thick ethanol-water solutions did not provide any clue solving this problem. Figure 1-a shows the mass spectra of 43% ethanol

solution (X_1=0.19) in high mass region (m/e=500 ~ 1000). The main sequence of $H^+(C_2H_5OH)_n$ with an interval of mass 46, which appeared in a lower mass region, suddenly end at n=9 and hydrate cluster signals become quite dominant in the high mass region. Intensity maxima in the respective ethanol m-mer hydrate sequences were seen for $H^+(C_2H_5OH)_9(H_2O)_1$, $H^+(C_2H_5OH)_{10}(H_2O)_2$, $H^+(C_2H_5OH)_{11}(H_2O)_{2,3}$, $H^+(C_2H_5OH)_{12}(H_2O)_4$ and so on. Namely, $n'_{max} = m-8$ or $m-7$ for $6<m<14$, and $n'_{max} = m-6$ for $14\leq m<21$, where n'_{max} is the hydration number of the strongest ion. The parent cluster giving the strongest ion is expressed by $(C_2H_5OH)_{5+k}(C_2H_5OH-H_2O)_{n(max)}$, where n(max) = n'_{max} + 1 or n'_{max} + s (s=2,3,...), and k=0 for m≥14. The smallest hydrate ion of ethanol m-mer is expressed simply by $(C_2H_5OH)_9(H_2O)(C_2H_5OH - H_2O)_t$, where m = 9+t. Figrue 1-b shows an example of the three dimensional cluster with a molecular composition $(C_2H_5OH)_6(C_2H_5OH - H_2O)_{10}$, which has an Ice-I like hydrogen bonding network formed by the water-chain fasteners connecting the two sides of a cyclic ethanol 16-mer. In this cluster, ethyl groups are situated close to each other forming hydrophobic layers on top and bottom.

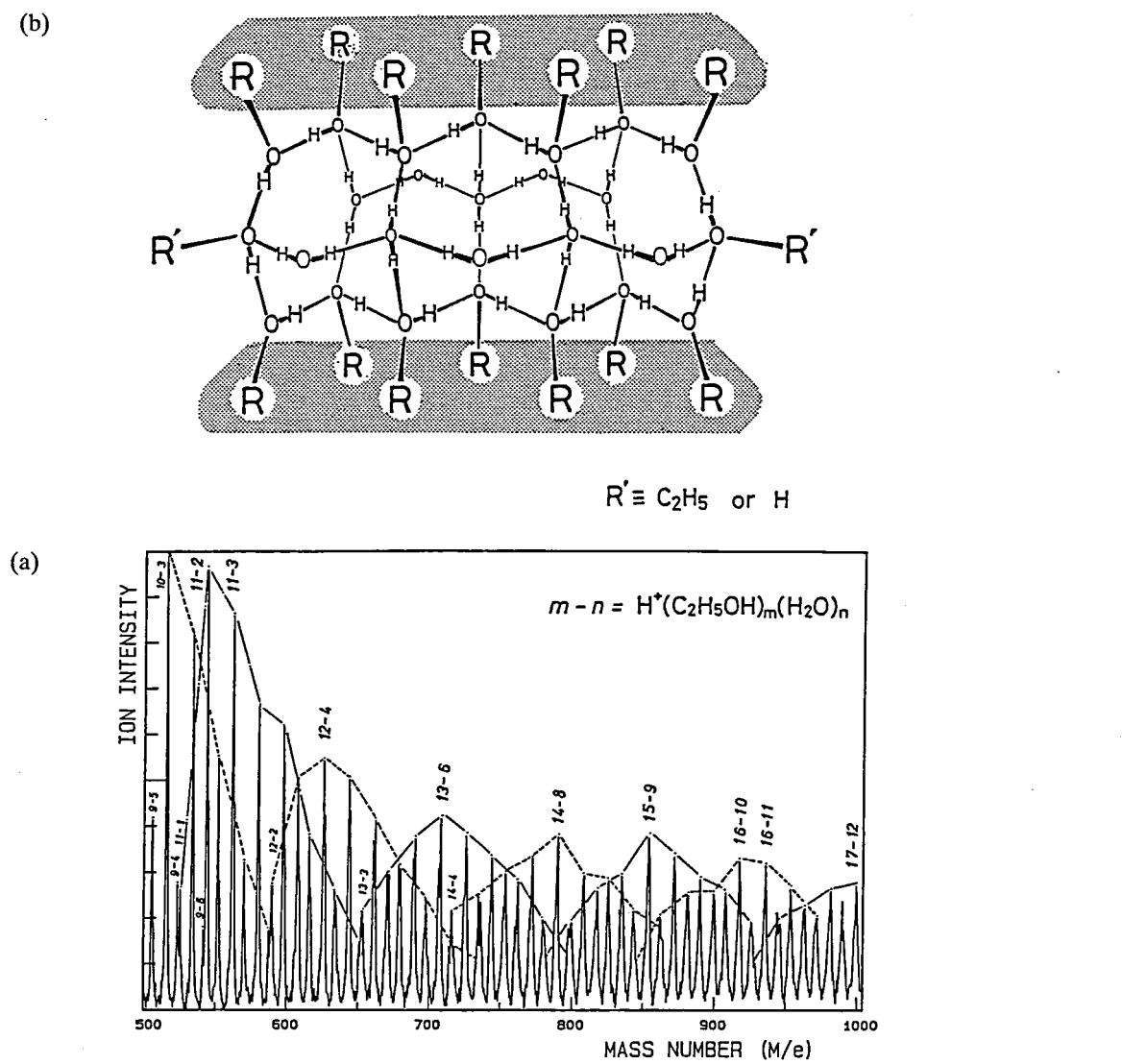

Figure 1. (a): Mass spectrum of ethanol (43%)-water binary solution in mass region 500≤m/e≤1000. (b): A model of an ethanol hydrate cluster $(C_2H_5OH)_m(C_2H_5OH\text{-}H_2O)_n$ with m=6 and n=10. A cyclic ethanol 16-mer is rigidified by the two water-side-chains which bridge the ring ethanol molecules from both sides of the ellipsoidal ring plane forming a cylindrical structure.

III-G-2 Origin of the Stability of Hydrates of Various Carboxylic Acids in Aqueous Solution

Kazunori YAMAMOTO and Nobuyuki NISHI

[*J. Am. Chem. Soc.* in press]

Carboxylic compounds have large affinities for water due to strong hydrogen bond formation between the carboxyl group and water molecules. For water molecules, however, these solute species are alien substances because carboxyl groups destroy pure water-cluster networks. On the other hand, it is well-known that some hydrocarbons such as methane form clathrate hydrates; this kind of interaction is called as hydrophobic hydration. Thus carboxylic acids with alkyl chains are expected to show large affinity for water molecules. In order to obtain quantitative data on the hydration, we performed mass-spectrometrical analysis of the fragments from the aqueous solutions. The spectral pattern of the cluster signals changed sensitively with increasing temperature of the solutions. The analysis was done by assuming the association-dissociation equilibrium between the solute species (A) and water molecules in the final liquid state of the superheated droplets: $A + (H_2O)_n = A(H_2O)_{n-1} + H_2O$. $\varkappa_1$ is defined as stability constant of monomer hydrate clusters: $\varkappa_1 = ([H^+A(H_2O)_{n-1}]/[H^+(H_2O)_n])(1/(n+n_0))(\chi_2/\chi_1)$, where χ_1 and χ_2 are mole fractions of solute and solvent, respectively. Figure 1 displays van't Hoff plots of $\varkappa_1$ values of five carboxylic compounds. The plots provided enthalpy and entropy changes (ΔH_1 and ΔS_1, respectively) for the exchange process. ΔH_1 for HCOOH, CH_3COOH, C_2H_5COOH, C_3H_7COOH, C_4H_9COOH, and $C_5H_{11}COOH$ were +1.1, −2.3, −3.3, −4.5, −6.1, −9.7 kcal/mol, respectively; ΔS_1 was +7.1, −2.7, −3.0, −4.0, −5.4, −8.6 cal/mol·K, respectively. These values indicate that hydration of formic acid is due to entropic effect while the hydration of alkyl carboxylic acids is due to enthalpic effect caused by hydrophobic hydration.

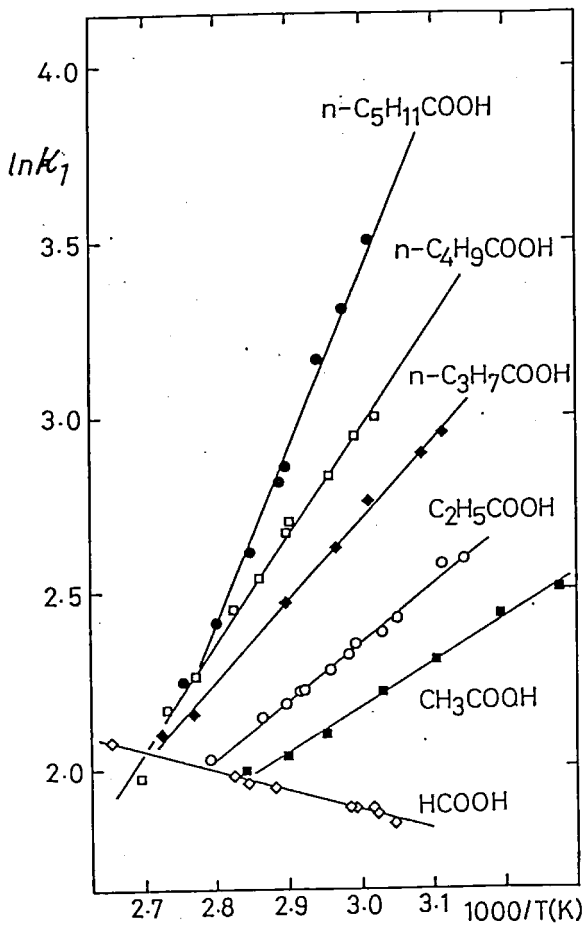

Figure 1. Logarithmic plots of $\varkappa_1$ (stability constants for monomer hydrates) of six carboxylic acids as function of T^{-1}.

III-G-3 Carboxylic Acid Dimer Formation and Hydrophobic Interaction in Aqueous Solution

Kazunori YAMAMOTO and Nobuyuki NISHI

[*J. Am. Chem. Soc.* in press]

In nonpolar liquids such as CCl_4 and C_6H_6, dimerization constants of the alkyl carboxylic acids are almost independent of the chain length of the alkyl residue. The results have been interpreted in terms of a cyclic dimer with two hydrogen bonds between the two solutes. On the other hand, the dimerization in aqueous solution seems markedly different from those in the nonaqueous solvents. It was found that the dimerization constants for a homologous series of carboxylic acids in water are much smaller than the

corresponding values in nonpolar solvents. We analyzed the following dimerization process in aqueous solution: $RCOOH(H_2O)_n + RCOOH(H_2O)_{n'-1} \rightleftarrows (RCOOH)_2(H_2O)_{n-1} + (H_2O)_{n'}$. Stability constant of the dimer hydrates $\varkappa_{D'}$ enthalpy and enthropy changes of the above process, $\Delta\bar{H}_{D'}$ and $\Delta\bar{S}_{D'}$ respectively, were obtained from cluster mass spectra of aqueous solutions of 6 carboxylic acids. $\varkappa_D$ values (at 70°C) of HCOOH, CH_3COOH, C_2H_5COOH, C_3H_7COOH, C_4H_9COOH, and $C_5H_{11}COOH$ were 0.9, 1.2, 1.3, 1.4, 1.5, 1.8, respectively. $\Delta\bar{H}_D$ was 0.0, 0.0, 0.3, 0.5, 0.7, 1.1 kcal/mol, respectively; and $\Delta\bar{S}_D$ was −0.4, 0.4, 1.4, 2.2, 2.9, 4.2 cal/mol·K, respectively, in the order of increasing alkyl-chain length. The increase of entropy exceeds the contribution of the endothermic enthalpy change to the free energy for propionic, N-butyric, N-valeric and N-caproic acids. Thus, the equilibrium shifts to the right direction for all alkyl carboxylic acids. The fact that alkyl carboxylic acids have the tendency of self-association in aqueous solution has been thought due to the "hydrophobic interaction" between the alkyl groups. Figure 1 shows our model of a carboxylic acid dimer in aqueous solution which explains the observed thermodynamical quantities.

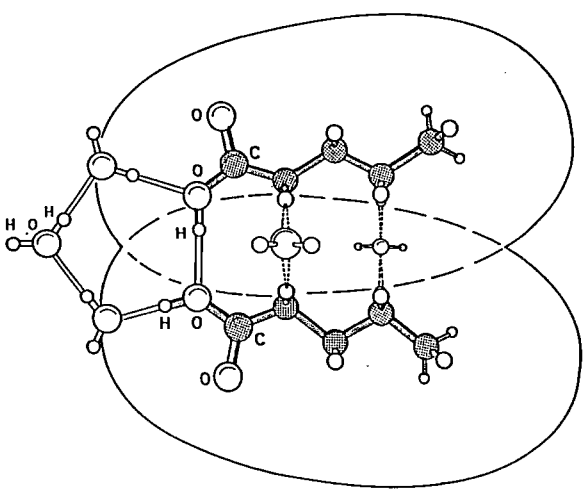

Figure 1. A model of aliphatic carboxylic acid dimer in aqueous solution. The two carboxylic groups may form a pentagonal ring with three water molecules. Hydrophobic hydration region surrounding alkyl group is shown by ellipsoidal circles.

III-G-4 Estimation of Conventional Dimerization Constants of Propionic Acids in Aqueous Solutions

Kazunori YAMAMOTO and Nobuyuki NISHI

[*J. Am. Chem. Soc.*, in press]

Aqueous solutions of propionic acid with acid molar fractions of 0.0005~0.005 were converted to neutral cluster beams in vacuum and investigated by mass spectrometrical analysis. Figure 1 shows typical mass spectra of clusters generated from the solutions. The intensity of acid monomer-hydrate clusters, $H^+A(H_2O)_n$(where $A=C_2H_5COOH$), varied linearly with the change of acid molar fraction. More exactly, the cluster population ratio, $[H^+A(H_2O)_{n-1}]/[H^+(H_2O)_n]$, was actually found to be proportional to the molar ratio of acid to water (χ_1/χ_2) only in the concentration region of $\chi_1/\chi_2 \leq 0.00125$. At higher concentrations the cluster population ratio, $[H^+A(H_2O)_{n-1}]/[H^+(H_2O)_n]$ showed smaller values than expected from the concentration. The decrease was explained by acid-acid association. Acid dimer-hydrate clusters, $H^+A_2(H_2O)_{n'}$ were actually observed in the mass spectra of $C_2H_5COOH:H_2O$ =1:400(Figure 1-B). Since no acid trimer-hydrate clusters were seen at $\chi_1/\chi_2=0.0025$, the decrease in the ratio $[H^+A(H_2O)_{n-1}]/[H^+(H_2O)_n]$ is attributed to the formation of the dimer species only. The conventional dimerization constant K_D for the equilibrium $2A \rightleftarrows A_2$ was derived from those population ratios. The present K_D value obtained from the cluster distribution (log $K_D=-0.4$) is close to the values obtained by the other measurement such as potentiometric titration of bulk aqueous solution. The coincidence of dimerization constants of propionic acid both in bulk solution and in the isoltated clusters confirmed that the composition of the clusters separated from aqueous solutions reflects the association properties of the molecules in the original solutions.

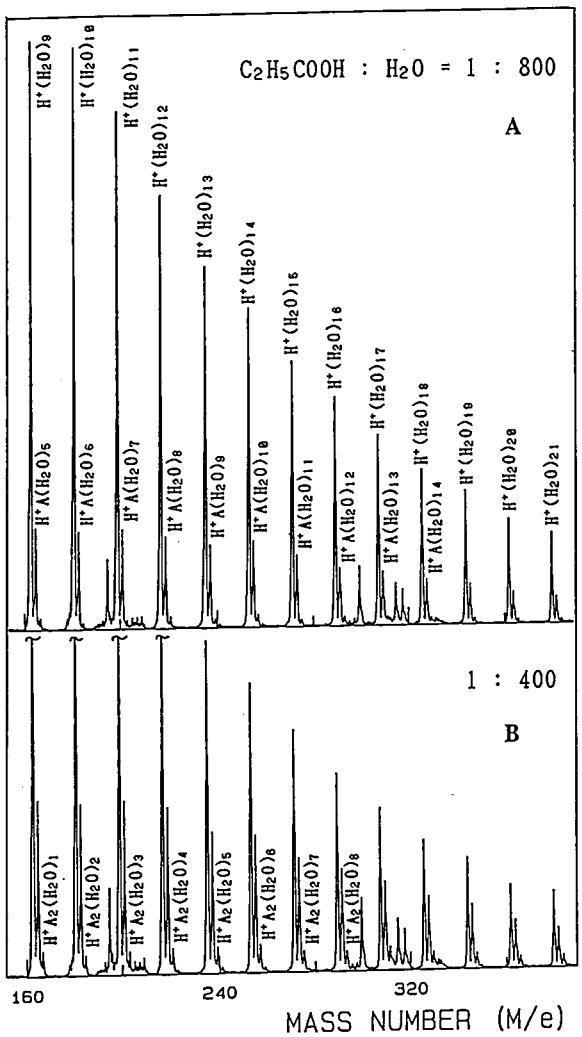

Figure 1. Concentration change of mass spectral pattern of propionic acid aqueous solutions at 70°C with molar ratios of $C_2H_5COOH:H_2O$ = 1:800(A) and 1:400(B). Electron impact ionization energy = 40eV.

III–H Excited State Dynamics and Ion Appearance Potential of Molecular Clusters

Cluster-specific excited state dynamics is explored with the aid of two-color Resonance Enhanced Two-Photon Ionization technique. Molecular clusters show reactions either in the intermediate excited state located around 6 eV or in an excited (or sometimes ground) state of the ion species. Reaction pathways may change depending on the excess internal energies or relative molecular configuration of the clusters. Here we report a finding of the excimer state of benzene clusters, reactions induced in the benzene-chlorine binary complexes, and ionization-dissociation mechanisms in ammonia clusters.

III-H-1 Excited State Lifetimes and Appearance Potentials of Benzene Dimer and Trimer

Hisanori SHINOHARA *(Mie Univ.)* **and Nobuyuki NISHI**

[*J. Chem. Phys.* **91**, 6743 (1989)]

Van der Waals clusters of benzene are formed in a supersonic jet, subjected to two-color resonance-enhanced two-photon ionization (2C-RE2PI) via the S_2 state, and analyzed in a time-of-flight mass spectrometer. The observed lifetime data of the dimer and trimer show a biexponential decay, which corresponds to the lifetimes of the lowest singlet $^1B_{1g}$ state of a parallel spaced benzene excimer and an excited S_1-van der Waals dimer state. The two excited states are likely to be separated by a shallow potential barrier. The observed lifetimes of the parallel stacked lowest singlet excimer and the vibrationally excited S_1-van der Waals states of the benzene dimer are 122 and 24 ns, respectively. These excited states are produced as a result of the internal conversion from an optically excited S_2-van der Waals dimer state. Because of the large excess energy produced upon the vertical S_2 excitation of the dimer, the excited van der Waals state (which has a large Franck-Condon factor with the ground state) spontaneously collapses, over the barrier, to the deeply bound $^1B_{2g}$ excimer state which, in turn, internally converts to the lowest $^1B_{1g}$ excimer state (see Figure 1). It is therefore likely that the second component of our two-color RE2PI signal of the benzene dimer corresponds to the decay of this lowest singlet $^1B_{1g}$ excimer state or, more specifically, to the lifetime of a vibrationally excited $^1B_{1g}$ excimer state. The photoionization curves of the dimer and trimer in the threshold region show very slow rise at 8.53 ± 0.03 eV and 8.54 ± 0.03 eV, respectively. The observed photoionization thresholds are much lower than those reported previously.

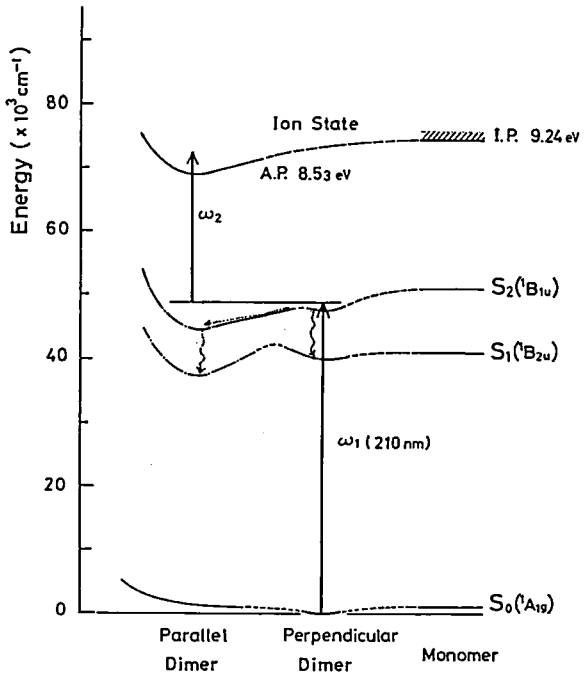

Figure 1. Schematic energy level diagram pertinent to resonance-enhanced two-photon ionization processes of benzene dimer via the second excited singlet S_2 state. Owing to geometrical similarities, Franck-Condon factors for the ionizing transition ω_2 are much more favorable than those of ω_1 and of one-photon ionization.

III-H-2 Resonance-Enhanced Multiphoton Ionization Processes of Benzene-Chlorine Binary Clusters

Kazuhiko OHASHI and Nobuyuki NISHI

Ionization processes and intracluster reactions of benzene-chlorine binary clusters are studied by two-color resonance-enhanced multiphoton ionization method. The time-of-flight mass spectra of the binary clusters are shown in Figure 1. The clusters are resonantly excited by the first laser (λ_1 = 210 nm) and ionized by the delayed second laser (λ_2 = 460 nm (a), 339 nm (b)). At λ_1 = 210 nm the binary clusters are excited to the S_2 state of benzene. In addition to pure benzene cluster ions, $(C_6H_6)_m^+$, chlorine-substituted cluster ions, $(C_6H_6)_m$ $(C_6H_5Cl)_n^+$, are seen in Figure 1 (a) and (b), which are indicative of intracluster reactions. On the other hand simple binary cluster ions, $(C_6H_6)_m$ $(Cl_2)_n^+$, or chlorine cluster ions, $(Cl_2)_n^+$ (n>1), are not observed. Another interesting feature is

the appearance of Cl_2^+ ion when more intense λ_1 is introduced.

When λ_2 is set at 339 nm (absorption band of chlorine molecule), elimination of hydrogen atom from benzene cluster ions occurs much more extensively than the ionization with λ_2 = 460 nm. This is probably due to the hydrogen abstraction by the dissociated chlorine atoms. Moreover cracking of the benzene ring is more pronounced with λ_2 = 339 nm and the cracking pattern is dissimilar to the case of pure benzene clusters. The difference may be ascribed to the change of the character of the electronic state of benzene molecule caused by the strong charge-transfer interaction whith chlorine molecules.

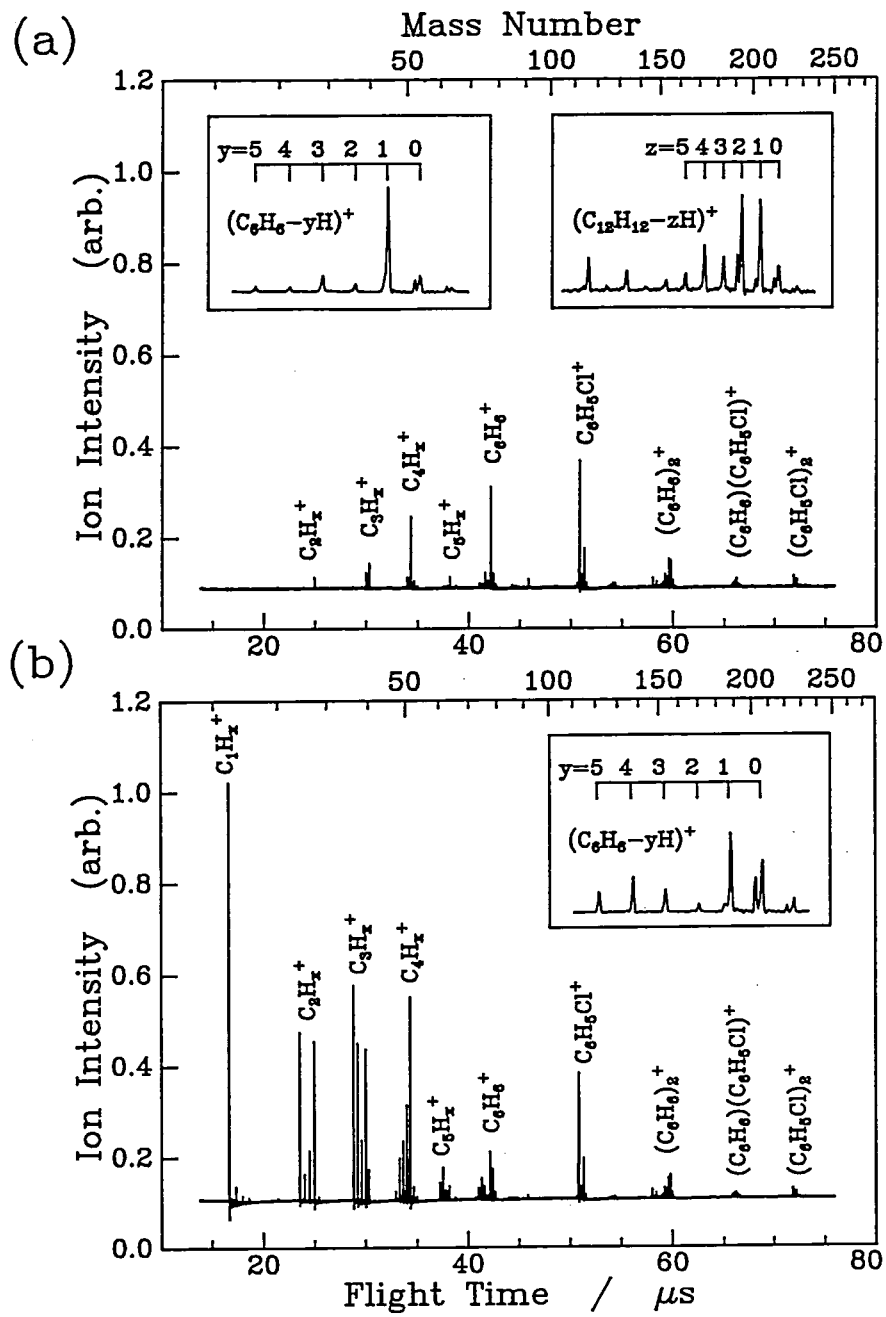

Figure 1. Time-of-flight mass spectra of benzene-chlorine binary clusters obtained by two-color resonance-enhanced multiphoton ionization method. The wavelength of the first laser is 210 nm, and that of the second laser is 460 nm (a) or 339 nm (b). The mass regions around $C_6H_6^+$ and $(C_6H_6)_2^+$ are expanded in the insets.

III-H-3 The Dissociation Dynamics and Multiphoton Ionization Mechanism of Ammonia Clusters

Fuminori MISAIZU, Paul L. HOUSTON *(Cornell Univ. and IMS)*, **Nobuyuki NISHI, Hisanori SHINOHARA** *(Mie Univ.)*, **Tamotsu KONDOW** *(Univ. of Tokyo)*, **and Minoru KINOSHITA** *(ISSP, Univ. of Tokyo)*

[*J. Phys. Chem.*, **93**, 7041 (1989)]

Two-color, two-photon ionization has been used to investigate the ionization and dissociation mechanism of ammonia clusters. Ion signal, which is mass-selected by an angular reflectron TOF mass spectrometer, is monitored as a function of the delay time between the two laser pulses. Figure 1 displays sections of the mass spectra of deuterated ammonia clusters as a function of the delay time. As the time between the two lasers increased, the signals corresponding to ND_3^+, ND_4^+, and $(ND_3)_2^+$ were found to decrease rapidly, within 20–30 ns, while the signal of $(ND_3)_2D^+$, as well as those for ions of higher mass, remain high, even out to several μs. Qualitatively similar data were obtained for NH_3.

A central question in the dynamics of ammonia cluster ionization concerns the sequence of the absorption, dissociation, and ionization steps. It was observed that $(NH_3)_2^+$ and NH_4^+ displayed the same behavior with respect to the two-laser delay time. This suggests that the step which competes with the production of $(NH_3)_2^+$ and the step that competes with the production of NH_4^+ are the same steps, as required in the absorption-ionization-dissociation mechanism. By contrast, the long lifetime for the intermediate to formation of $(NH_3)_{n-1}H^+$ for n>2, might be explained by the mechanism that the dissociation occurs between the absorption of the first and second photons.

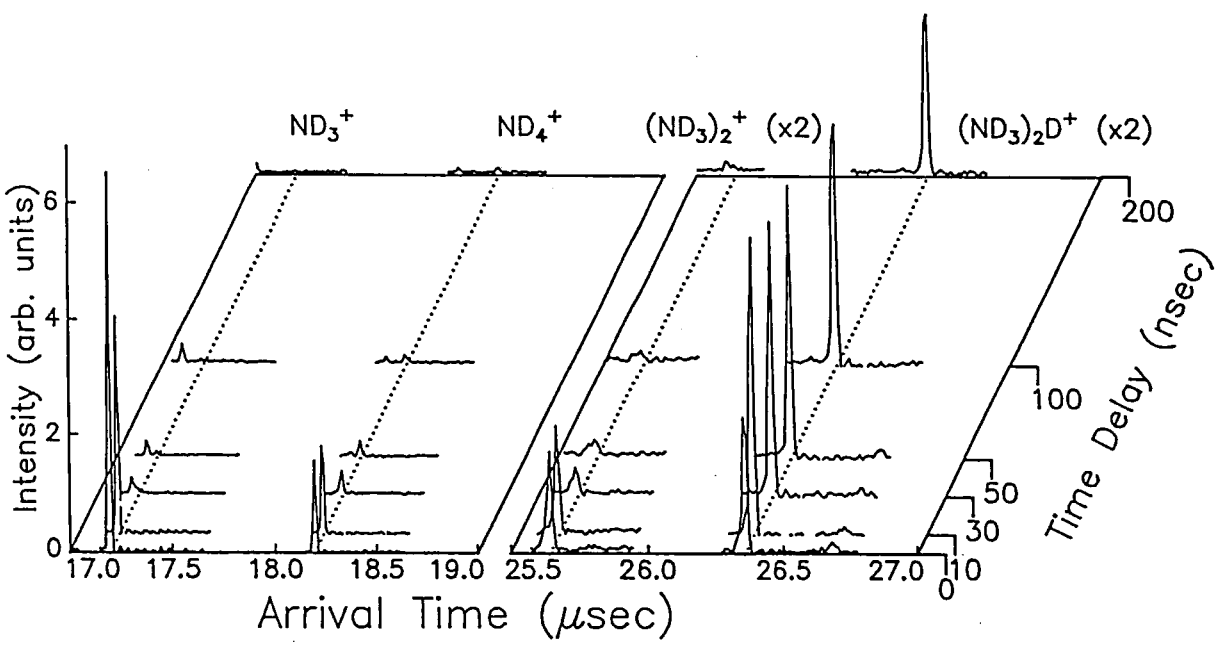

Figure 1. Portions of the mass spectrum of ammonia clusters as a function of the delay time between the two laser pulses used to ionize the clusters. The arrival time is measured from the firing of the second laser (272.5 nm). The small peaks falling to the left of the dotted lines are due to background one-color two-photon ionization by the first laser (211 nm).

III-H-4 Observation of Evaporating Benzene Cluster Ions

Hisanori SHINOHARA *(Mie University)*, **Masahiko MIWA** *(Mie University)*, **Hiroyasu SATO** *(Mie University)*, **Fuminori MISAIZU, and Nobuyuki NISHI**

Van der Waals clusters of benzene in a supersonic jet are resonantly two-photon ionized (RE2PI) via the second excited singlet state S_2 (corresponding to the $^1B_{1u}$ state of benzene) by using tunable pulsed UV dye lasers, and the resultant cluster ions are subjected to reflectron time-of-flight (TOF) mass analysis.[1] Benzene cluster ions with an energy content of 0.1 eV – 1.5 eV are produced via a two-color RE2PI technique. By energy analysis of the daughter ions produced by a metastable decay both in the field-free drift and the acceleration regions of a reflectron TOF mass spectrometer, we are able to determine all the major dissociation channels for each benzene cluster ion.

Figure 1 shows an appearance of metastable benzene cluster ions. By lowering the applied voltages of an ion reflector (so as to remove stable parent ions), the metastable ions begin to emerge in the spectrum (Figures 1a and b). Further reducing the voltages, one obtains a "pure" metastable TOF spectrum of the benzene clusters (Figure 1c). The obtained TOF spectra indicate that the dominant metastable decay channel is a loss of one benzene molecule and that evaporation of more than one benzene unit is found to be a minor process. Furthermore the metastable decay rate constants for the major process are determined.

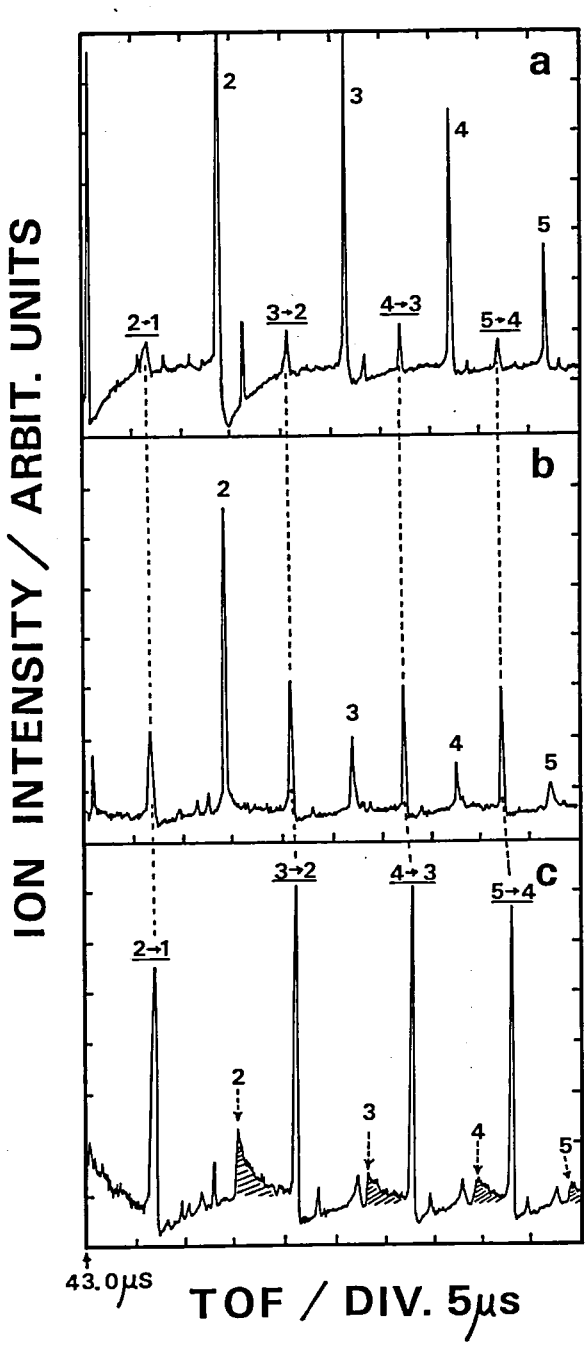

Figure 1. Resonance-enhanced (1+1)-photon-ionization mass spectra of both stable and metastable benzene cluster ions. Dotted lines indicate the positions of the metastable ions. The notation n → n-1 shows the metastable decay of the reaction $(C_6H_6)_n^+ \rightarrow (C_6H_6)_{n-1}^+$. The shaded peaks correspond to the metastable decay for a loss of two benzene molecules.

Reference

1) H. Shinohara and N. Nishi, *Chem. Phys.* **129**, 149 (1989).

III–I Resonance Enhanced Two-Photon Ionization Study of Intramolecular Non-radiative Processes

III-I-1 Resonance-Enhanced Two-Photon Ionization Spectra of Benzene in the Third Channel Region

Teijiro ICHIMURA *(Tokyo Ins. Tech.)*, **Hisanori SHINOHARA** *(Mie Univ.)*, **and Nobuyuki NISHI**

Resonance-enhanced two-photon ionization (RE2PI) process of the S_1 state of benzene was investigated by time-of-flight (TOF) mass-spectrometric technique. Benzene is resonantly ionized to yield $C_6H_6^+$ ions which are subjected to efficient fragmentation. However, low power (<20 μJ/pulse) laser irradiation depresses the fragmentation and under such conditions excitation spectra of the mass-selected ion ($C_6H_6^+$) intensity were measured. The relative ion intensity determined from the excitation spectra and the corresponding S_1 absorption spectra revealed that the transient population in vibronic levels above the channel three threshold decreases due to non-radiative processes. Excitation of the $6^1\,1^3$ or $6^1\,1^2$ band under carefully controlled low laser powers has revealed the fact that the relative intensity of the 6^11^3 band (above the 3rd channel) to that of the $6^1\,1^2$ band (below 3rd channel) decreases with decreasing the excitation laser power. The result indicates that the ionizing process following the resonant first photon pumping at the channel three band is competing with the nonradiative relaxation processes at the resonant state. High-resolution excitation spectra of the parent ion have been measured for the $6^1\,1^n$ progression (n=0,1,2,3) under warm molecular beam conditions. For the wavelength region 241.5–243.1 nm, covering the two specific vibronic bands, $6^1\,1^3$ and 7^1, similar experiments have been carried out under cold beam conditions. The relative ion intensity for the 7^1 band resonance excitation was found to be much higher than that of the $6^1\,1^3$ band and to be even more than twice as large as that of the $6^1\,1^2$ band.

III–J External Magnetic Field Effects upon Chemical Reactions

Magnetic field effects upon chemical reactions provide us with useful methods for elucidation of reaction mechanisms and techniques for controlling reaction rates and product yields. Magnetic isotope effects can be used for enrichment of a certain nucleus through the difference in hyperfine interaction. In the recent decade, the magnetic field effects upon photochemical reactions have been extensively studied by a variety of methods, *e.g.*, magnetic-field-modulated fluorescence measurement, kinetic spectroscopy of reaction intermediates by laser photolysis and its modification two-step laser excitation, and chemical analysis of photoproducts obtained by steady-state irradiation. In particulalr, photochemistry of aromatic carbonyl compounds and bichromophoric chain species in the solution phase has been investigated in some detail. In addition, we have also examined the magnetic field effects on afterglow activated by a microwave discharge and the mechanism of magnetic quenching of CS_2 fluorescence in the gaseous state.

III-J-1 Magnetic Field Effects upon Photochemistry of Bichromophoric Chain Molecules Containing 4-Nitrophenoxyl and Anilino Chromophores

Ryoichi NAKAGAKI, Kiyoshi MUTAI *(Univ. of Tokyo)*, **and Saburo NAGAKURA** *(Grad. Univ. for Adv. Studies)*

We have observed magnetic field effects on photoredox reaction yields for a bifunctional chain species. A-$(CH_2)_n$-D with A=4-nitrophenoxyl, D=N-benzylanilino, and n=12. Two different cage and two different escape processes have been identified through product analysis by means of high performance liquid chromatography. The major process is hydrogen (H) abstraction at the benzylic position of N-benzylanilino

moiety. Another process is H abstraction from the methylene group adjacent to the anilino nitrogen. Since two kinds of magnetic field effects are observed on the redox yields, two different biradicals are involved in the intramolecular reaction. The branching process is shown in Figure 1. Magnetic field effects on the cage product formation via BR-2 biradical were enhanced on the substitution of carbon-13 for a normal carbon at α-position in the benzyl radical.

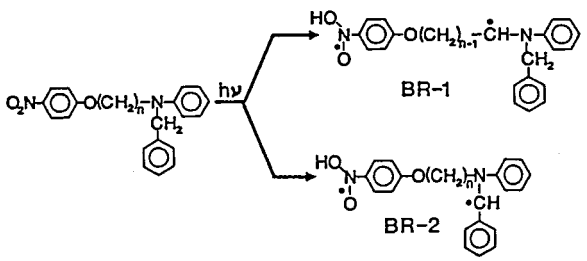

Figure 1. Photochemical biradical formation from a bifunctional chain molecule containing nitro-aromatic and anilino moieties.

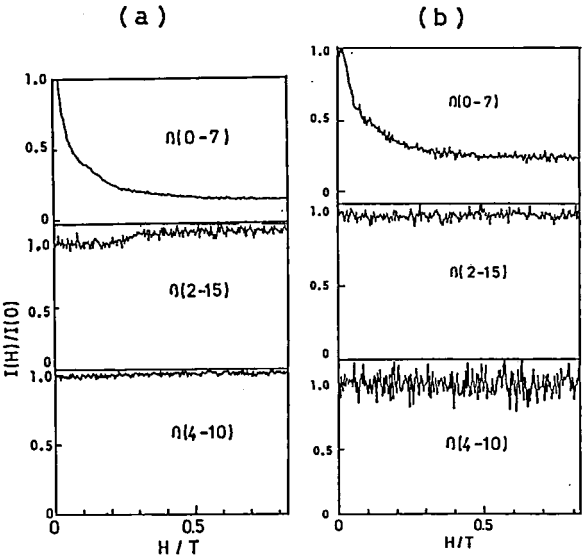

Figure 1. Magnetic field dependence (I(H)/I(O)) of each vibrational level of $B^2\Pi$ state. (a): NO is produced from the N + O → NO reaction. (b): NO is produced from the N_2O + N → NO + N_2 reaction. The same magnetic effects were observed in the case of the energy transfer reaction.

III-J-2 External Magnetic Effect on the Emission of NO β band

Minoru SUMITANI, Haruo ABE *(Inst. of Phys. and Chem. Res.)*, **and Saburo NAGAKURA** *(Grad. Univ. for Adv. Studies)*

Magnetic field effects of the fluorescence from NO β band, which was produced by three reaction methods, were studied. As shown in Figure 1, the fluorescence from the v'=0 level was quenched with a magnetic field, and this effect did not depend on the reaction process. The magnetic field effect of the fluorescence from the v'=2 level was dependent on the reaction process. The magnetic field did not give an effect on the fluorescence from the v'=4 level. These magnetic field effects can be explained with the magnetic induced interaction between the $B^2\Pi$ state and the $a^4\Pi$ or the $b^4\Sigma$ state.

RESEARCH ACTIVITIES IV
Department of Molecular Assemblies

IV-A Microwave and dc Conductivity of Organic Conductors

Frequency dependence of electrical conductivity is the fundamental quantity which reflects the response of materials to the external electromagnetic wave. It involves microscopic information about the transport mechanism in solid state as well as about the vibrational and electronic structures. The need for this method has been increasing especially to the study of low-dimensional conductors characterized by the strong electron-electron correlation, strong anisotropy, and disorder. As a part of ongoing program of gathering the data of frequency-dependent conductivity from dc to ultraviolet frequency, we have set up instruments to obtain dc and microwave (9.4 GHz) conductivity. This section describes the construction of instruments and the application of the techniques to the highly conductive radical salts of phthalocyanines and DCNQI's.

IV-A-1 Construction of the Instruments to measure Microwave and dc Conductivity

Akito UGAWA, Hideo YAMAKADO, Takashi IDA, and Kyuya YAKUSHI

We have designed the instrument to measure dc conductivity by four probe method and thermoelectric power, and almost completed the construction. The temperature has been stably lowered down to 1.5 K. The sample chamber, which contains four samples, is doubly shielded by copper walls, the space between which is evacuated by oil diffusion pump. Because of this thermal insulation, it is possible to measure the electrical resistivity both in the cooling and heating processes.

We have designed and constructed a microwave conductivity measurement system. The block diagram is shown in Figure 1. The microwave cavity is placed in the double-wall container for thermal insulation. The data acquisition and analysis is fully controlled by a microcomputer. This technique is useful in particular for fragile or unstable samples, because electric contact is not necessary. This system is designed for an easy improvement to measure the frequency dependence, which is planned in near future.

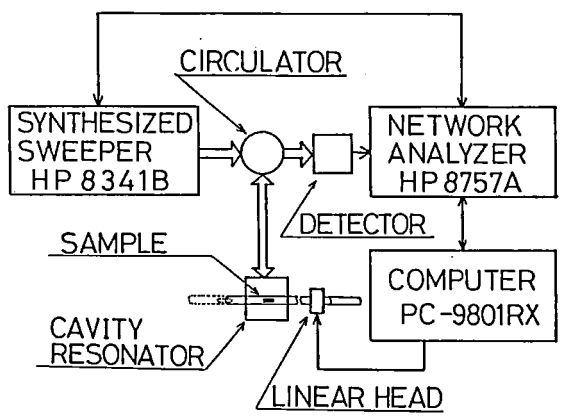

Figure 1. Block diagram of the microwave-conductivity measurement system.

IV-A-2 Microwave Conductivity of $MPc(X)_{0.5}$ and $M(R_1, R_2\text{-DCNQI})_2$

Hideo YAMAKADO, Akito UGAWA, Takashi IDA, and Kyuya YAKUSHI

Microwave conductivity at 9.4 GHz is measured on the single crystals of $NiPc(AsF_6)_{0.5}$, $PtPc(ClO_4)_{0.5}$, and $CoPc(AsF_6)_{<0.5}$ from room temperature to 4.2 K. They have almost the same tetragonal structure. $NiPc(AsF_6)_{0.5}$ and $PtPc(ClO_4)_{0.5}$ are metallic at room temperature and undergo metal-insulator transition at around 40 K and 150 K, respectively. The conductivity of $CoPc(AsF_6)_{<0.5}$ is an order of magnitude lower than the former salts, showing semiconductive behavior around room temperature. The characteristics of these

materials in the semiconductive phase is the small activation energy (<10 meV) and large dielectric constant at low temperature. The diffuse X-ray scattering due to the generation of CDW is not observed in these salts.

Microwave conductivity of $M(R_1, R_2\text{-DCNQI})_2$ (M=Cu, Ag, Na, and Li; R_1 and R_2=Me, Br, and Cl) is found to almost coincide with the dc conductivity.

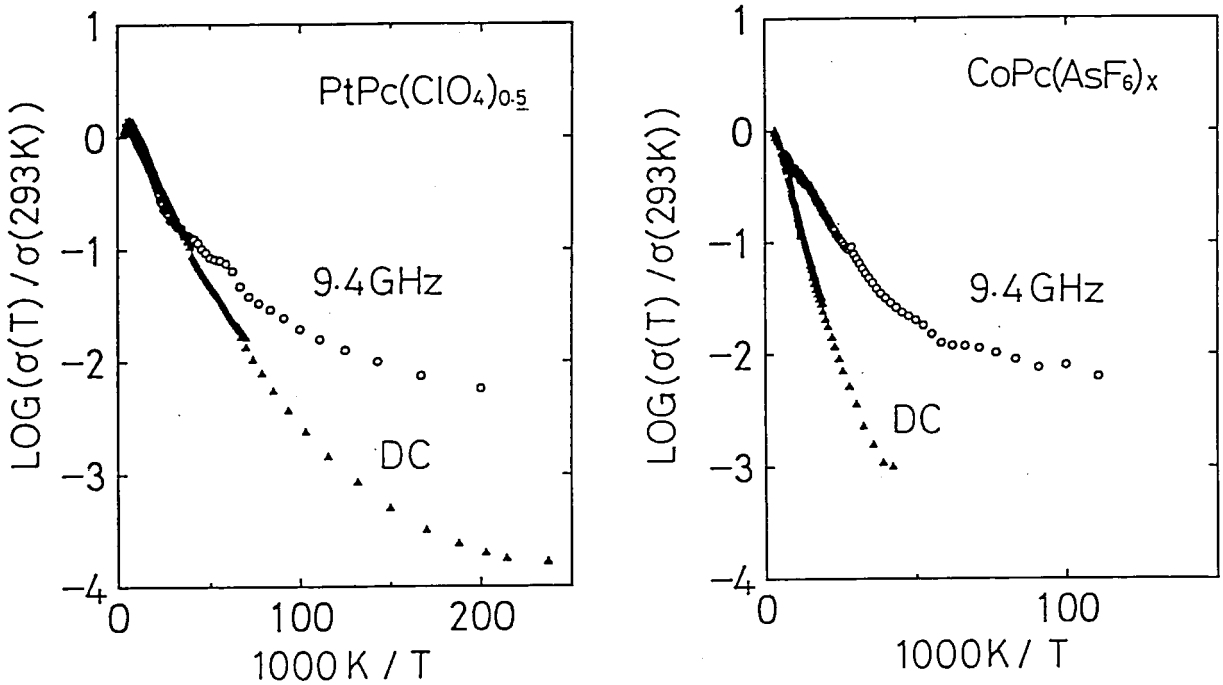

Figure 1. Temperature dependence of the dc and microwave conductivities of $PtPc(ClO_4)_{0.5}$ and $CoPc(AsF_6)_{<0.5}$.

IV-B Synthesis and Characterization of Phthalocyanine Salts

Some phthalocyanine molecules contain *d*-electrons in the conjugated π-electron system. Most importantly the highest occupied molecular orbital is not hybridized with the d_{z^2} orbital although they are energetically close to each other. Owing to this special nature, the partially oxidized phthalocyanine salts in solid state may possibly have distinct natures from conventional organic conductors, say a double-channel structure, coupling with exciton, or coexistence of conduction electrons and localized spins. To search for such a new type of conductor or superconductor, we have synthesized and characterized partially oxidized phthalocyanine salts and related compounds.

IV-B-1 Electrochemical Preparation and Characterization of the Radical Salts of (Phthalocyaninato) nickel, $NiPc(SbF_6)_{0.5}$, and $NiPc(AsF_6)_{0.5}$

Kyuya YAKUSHI, Hideo YAMAKADO*, Michiko YOSHITAKE*, Nobuhiro KOSUGI*, Haruo KURODA*, Tadashi SUGANO, Minoru KINOSHITA**, Atsushi KAWAMOTO***, and Jiro TANAKA*****
*(*Univ. of Tokyo, **ISSP, ***Nagoya Univ.)*

[*Bull. Chem. Soc. Jpn.*, **62**, 687 (1989)]

The single crystal of $NiPc(SbF_6)_{0.5}$ and $NiPc(AsF_6)_{0.5}$ were prepared by means of an electrochemical method. The electrical, magnetic, optical and structural properties of these crystals were examined. These crystals are isostructural to each other, and exhibit a metallic behavior at least above 200 K. The *g*-values of the ESR signals remarkably depend upon temperature. By the aid of the low temperature experiments of XANES and reflectance spectrum, the temperature dependence is explained by the model

based on the interaction between the small amount of local spins on the Ni atoms and the conduction electrons on the ligand chain. In addition, a sample dependence was found on the ESR properties of the crystals of $NiPc(AsF_6)_{0.5}$. This is attributed to the sample dependence of the concentration of the local spins on Ni atoms. From these considerations, we concluded that the ligand part is mainly oxidized in these partially oxidized salts, in other words the conduction electrons are located on the ligand chain. The bandwidth of the conduction band was estimated to be about 1 eV.

IV-B-2 Preparation and Characterization of the Cation Radical Salts of Phthalocyanine and Tetrabenzoporphyrin

Kyuya YAKUSHI, Hideo YAMAKADO*, Michiko YOSHITAKE*, Nobuhiro KOSUGI*, Haruo KURODA*, Atsushi KAWAMOTO, Jiro TANAKA**, Tadashi SUGANO***, Minoru KINOSHITA***, and S. HINO****** *(*Univ. of Tokyo, **Nagoya Univ., ***ISSP, ****Chiba Univ.)*

[*Synth. Met.*, **29**, F95 (1989)]

The radical salts of NiPc, PtPc and NiTBP were prepared by the method of electrochemical oxidation. The radical salts of NiPc and PtPc have 2:1 chemical composition and are metallic, the crystal structure being composed of tetragonally packed molecular columns with the metal-over-metal stacking mode. On the other hand, the radical salts of NiTBP with tetrahedral and octahedral counter anions have 3:2 chemical composition and are semiconductive, the crystal structure being composed of hexagonally packed molecular columns including a periodic unit of NiTBP trimer. All these materials have predominantly oxidized macrocycles, a small on-site Coulomb energy, and a small electron-phonon interaction.

IV-B-3 Preparation, Crystal Structure, and Solid State Properties of Highly Conductive (Phthalocyaninato) platinum Radical Salts: $PtPc(ClO_4)_{0.5}$ and $PtPc(AsF_6)_x$

Hideo YAMAKADO*, Kyuya YAKUSHI, Nobuhiro KOSUGI*, Haruo KURODA*, Atsushi KAWAMOTO, Jiro TANAKA**, Tadashi SUGANO***, Minoru KINOSHITA***, and Shojun HINO****** *(*Univ. of Tokyo, **Nagoya Univ., ***ISSP, ****Chiba Univ.)*

[*Bull. Chem. Soc. Jpn.*, **62**, 2267 (1989)]

New conducting salts of (phthalocyaninato) platinum (PtPc), $PtPc(ClO_4)_{0.5}$ belong to a tetragonal system with a space group of *P4/mcc*, the lattice constants being a=14.062(1)Å, c=6.510(1)Å, and Z=2. They are metallic at least down to 120 K, the room-temperature conductivity being $\sigma=10^2-10^3$ Scm^{-1}. XPS indicates that the conduction pathway is located mainly at the ligand chain due to a partial oxidation of the ligand-centered HOMO. ESR experiments have also strongly supported this conclusion. The bandwidth of the ligand-centered conduction band has been estimated to be 1.2 eV from the plasma frequency, $\hbar\omega_p$=0.87 eV, which is obtained by the polarized reflectance spectrum.

IV-C Studies of Electronic Structures of Highly Conducting BEDT-TTF Salts by means of Microspectrophotometric Technique

The band structure of an organic conductor is entirely sensitive to the arrangement of molecules, so that a subtle change of crystal structure brings about a variety of band structure. Owing to this nature and the presence of a large number of crystal modifications, BEDT-TTF salts show a variety of solid state properties. Polarized reflectance spectrum in the infrared and visible regions yields a wealth of information about the electronic structures of such anisotropic organic conductors. This project was designed in the University of Tokyo 7 years ago, and recently succeeded by IMS in collaboration with the University of Tokyo. We have focused our research activities to the

systematic study on the relationship between the crystal structure and band structure through the optical spectra of BEDT-TTF salts.

IV-C-1 Relation between the Dimensionality of electronic Structure and the Correlation Effect in the (BEDT-TTF)$_2X$ System

Akito UGAWA, Kyuya YAKUSHI, and Haruo KURODA *(Univ. of Tokyo)*

The optical properties of (BEDT-TTF)$_2X$ (α-, β-, β'-, β''-, δ-, and $\varkappa$-types) were studied to elucidate the relationship between the crystal structure and the electronic structure in these charge-transfer salts. Although there is a two-dimensional network of mutually interacting BEDT-TTF molecules in all these salts, the two-dimensional character markedly varies depending on the crystal type. It was found that the correlation effect strongly appears when the system is of one-dimensional character, and that the screening of electron correlation becomes more efficient on increasing the dimensionality of electronic structure.

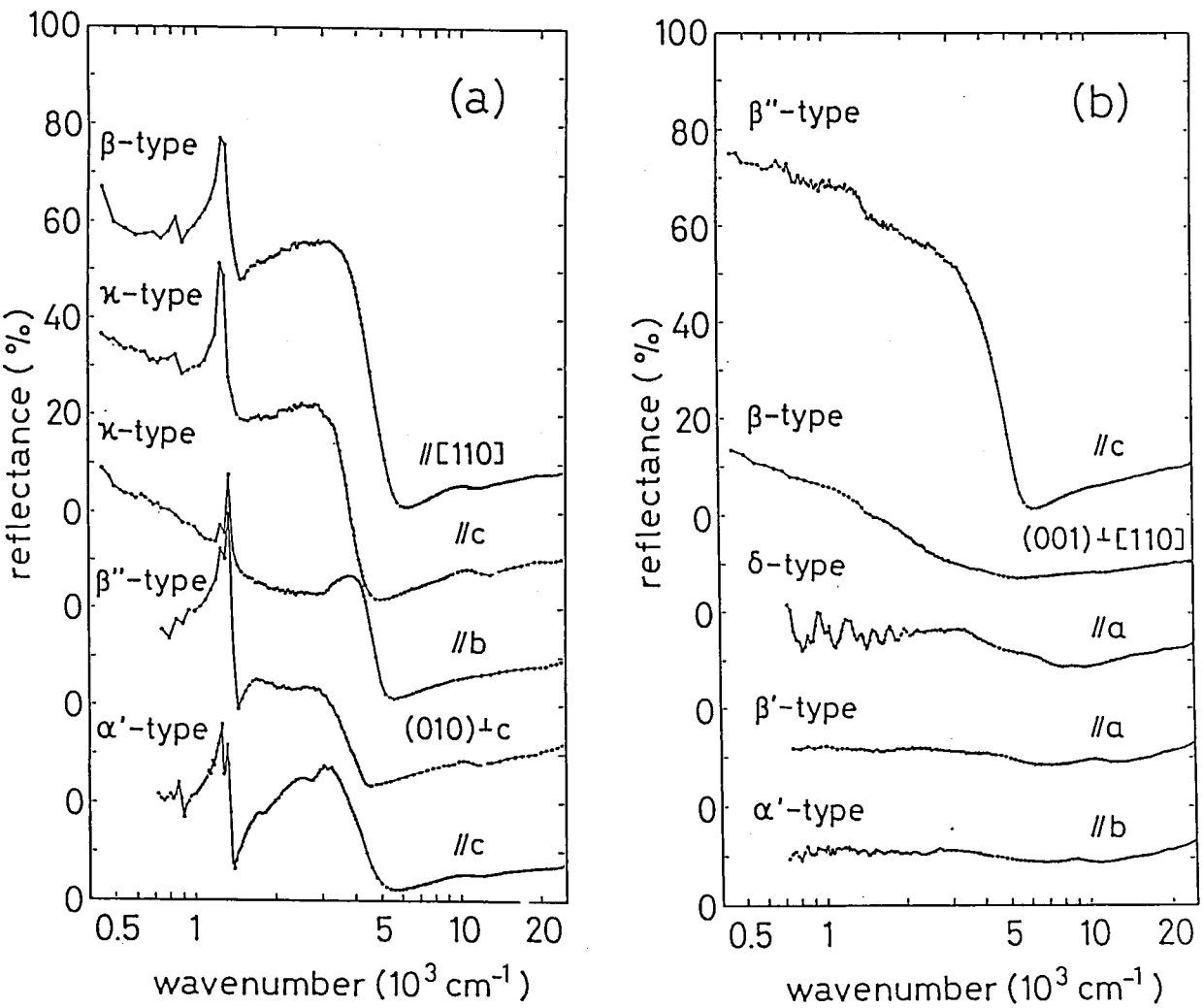

Figure 1. Polarized reflectance spectra of (BEDT-TTF)$_2X$, for the polarization (a) parallel to the dimeric arrangement direction and (b) parallel to the regular arrangement direction of BEDT-TTF.

IV-C-2 Physical Properties of β''-(BEDT-TTF)$_2$ICl$_2$

Akito UGAWA*, Yuji OKAWA*, Kyuya YAKUSHI, Haruo KURODA*, Atsushi KAWAMOTO, Jiro TANAKA**, Masanori TANAKA*, Yoshio NOGAMI*, Seiichi KAGOSHIMA*, Keizo MURATA***, and Takehiko ISHIGURO***** *(*Univ. of Tokyo, **Nagoya Univ., ***ETL)*

[*Synth. Met.*, **27**, A407 (1988)]

A single crystal of β''-(BEDT-TTF)$_2$ICl$_2$ was synthesized electrochemically, and the crystal structure was determined by X-ray analysis. This β''-type crystal was characterized by means of the electrical resistivity, electron spin resonance, X-ray diffraction, and polarized reflectance spectrum. The temperature dependence of the electrical resistivity which was proportional to T down to 10 K shows a typical metallic behavior. The ESR spectrum exhibited a Dysonian line-shape. The intensity of the spin susceptibility abruptly decreased at 17 K, although the electrical resistivity and the Bragg diffraction intensity showed no discontinuous change: this indicates the occurrence of a magnetic phase transition. The reflectance spectrum for the $\| c$ polarization showed a Drude-like dispersion already at room temperature. The anisotropic two-dimensional electronic structure was examined by the reflectance spectrum analysis.

IV-C-3 Reflectance Spectra of β-, θ-, $\varkappa$-(BEDT-TTF)$_2$I$_3$, and β'-, β''-(BEDT-TTF)$_2$ICl$_2$: Relation between the Interband Transition and the Dimeric Structure

Haruo KURODA*, Kyuya YAKUSHI, Hiroyuki TAJIMA*, Akito UGAWA*, Masafumi TAMURA*, Yuji OKAWA*, Akiko KOBAYASHI*, Reizo KATO, Hayao KOBAYASHI**, and Gunji SAITO***** *(*Univ. of Tokyo, **Toho Univ., ***ISSP),*

[*Synth. Met.*, **27**, A491 (1988)]

The polarized reflectance spectra of the single crystals of the title compounds were measured at room and low temperatures. The correlation was found between the appearance of the extra electronic transitions overlapped on the Drude-tail and the dimeric arrangement of BEDT-TTF. From this relation, this extra transition was assigned to the interband transition between the split band due to the strong dimeric interaction. The Drude parameters were determined by analyzing the low temperature spectra taking account of the interband transition.

IV-C-4 Optical and Electrical Properties of an Organic Superconductor, (BEDT-TTF)$_2$[Cu(SCN)$_2$]

Akito UGAWA*, Gen OJIMA*, Kyuya YAKUSHI, and Haruo KURODA* *(*Univ. of Tokyo)*

[*Phys. Rev.*, **B38**, 5122 (1988)]

A single crystal of (BEDT-TTF)$_2$[Cu(SCN)$_2$] was prepared, and its reflectance spectrum and electrical resistivity were investigated. The optical anisotropy was found to be very small. The spectrum in the infrared region was concluded to be dominated by the interband transitions for the directions parallel to both b and c. From the analysis of the spectra measured at 25 K, the effective masses were estimated to be m^*_b=5.5m_e and m^*_c=4.1m_e, respectively. The material was proved to be metallic over the temperature range from 300 K down to 10 K, and become superconductive at 11 K.

IV-C-5 Spectroscopic Evidence for the Inter-chain Charge-Transfer Interaction in Copper-bis (2,5-dimethyl-*N*, *N'*-dicyanoquinonediimine), Cu(2,5-DM-DCNQI)$_2$

Kyuya YAKUSHI, Gen OJIMA*, Akito UGAWA*, and Haruo KURODA* *(*Univ. of Tokyo)*

[*Chem. Lett.*, **1988**, 95]

Polarized reflectance spectra of the single crystals of Cu(2,5-DM-DCNQI)$_2$ and Na(2,5-DM-DCNQI)$_2$ were measured at room temperature. The spectrum of Cu(2,5-DM-DCNQI)$_2$ clearly indicated the inter-chain interaction through the coordinate bonds, whereas the spectrum of Na(2,5-DM-DCNQI)$_2$ showed a typical one-dimensional feature along the stacking direction.

IV–D Study of the Pressure Dependence of the Charge-Transfer State

The technique of microspectrophotometry under high pressure has been developed by use of diamond anvil cell in collaboration with the University of Tokyo. Pressure dependence of the charge-transfer band was measured on the single crystal of mixed-stacked type charge-transfer complex for the first time.

IV-D-1 Pressure dependence of the polarized reflectance spectrum of the solid charge-transfer complex, perylene-TCNQ: Estimation of microscopic parameters

Takashi IDA, *(Univ. of Tokyo)* **Kyuya YAKUSHI, and Haruo KURODA** *(Univ. of Tokyo)*

[*J. Chem. Phys.* **91,** 3450 (1989)]

The polarized reflectance spectrum of perylene-TCNQ complex has been measured at high pressure up to 27 kbar using a diamond anvil cell incorporated into a microspectrophotometer. The degree of charge transfer (ρ), the transfer integral (t) and the site-energy difference (Δ) are estimated at each pressure from analysis of the charge-transfer band. The pressure dependences of t and Δ are found to be $d\ln t/dP = +2.3\%$ kbar^{-1} and $d\Delta/dP = -6.4$ meV·kbar^{-1}, respectively. It is shown that the observed pressure dependence of the stabilization energy of the chrage-transfer excited state is mainly attributable to the change in the electrostatic energy accompanying the lattice contraction.

IV–E Studies of Ion-Molecule Reactions by a Threshold Electron-Secondary Ion Coincidence (TESICO) Technique

The knowledge of the microscopic reaction cross sections for evolution of a system in a single reactant quantum state (translational, rotational, vibrational, and electronic) to a single product quantum state is essential for a complete understanding of a chemical reaction. Ion-Molecule reactions are particularly suited for studying such microscopic cross sections since ions can readily be prepared in various internal states in the initial ionization processes, such as photoionization, and the emitted photoelectrons provide information on the distribution among these states.

In this project, we study state-selected ion-molecule reactions by the use of a photoionization technique which utilizes the threshold photoelectron-secondary ion coincidence. The technique allows direct determination of $\sigma(i,v)$, i.e., the reaction cross section as a function of the internal and collisional energies of reactants. The selection of electronic, vibrational, rotational, and fine-structure states are possible by this technique.

IV-E-1 The Study of the Internal and Collision Energy Dependence for Two Microscopic Reaction Mechanisms in the Reaction $MH^+ + MH \rightarrow MH_2^+ + M$ (MH = CH_3F, CH_3Cl, CH_4)

Shinzo SUZUKI and Inosuke KOYANO

The ion-molecule reactions of the type $MH^+ + MH \rightarrow MH_2^+ + M$ (MH = CH_3Cl, CH_3F, CH_4) have been investigated using the TESICO technique. Two peaks were found in the time-of-flight coincidence spectra of the product ions MH_2^+ at higher collision energies. These peaks have been interpreted as corresponding to the hydrogen abstraction and proton transfer mechanisms for the MH_2^+ formation. Relative cross sections

have been determined for each of the two microscopic reaction mechanisms as a function of the total energy of the reactants. The results seem to indicate that there are two distinct types of the (MH^+ + MH) reaction in terms of the behavior of its microscopic cross sections. In one of these (MH = CH_4, CH_3F), the proton transfer dominates over hydrogen atom abstraction and the relative importance of the former increases as the total energy is increased, whereas in the other (MH = CH_3Cl) both mechanisms have nearly equal contribution and their relative importance does not change much as the total energy is varied.

To explain these results, a hypothesis has been presented that the hydrogen abstraction is actually a proton transfer following an electron hopping in the entrance channel, and that the above two types are caused by the difference in the efficiency of this electron hopping. An *ab initio* estimate of the upper limit of the barrier height for the charge hopping in the entrance channel supported this model.

IV-E-2 Dynamics of the Reaction $D_2^+ + D_2$: Separation of Charge Transfer Products from Reactant Ions Using TOF Coincidence Technique

Shinzo SUZUKI and Inosuke KOYANO

Over the last few years, we have been investigating the ion-molecule reactions of the type $MH^+ + MH \rightarrow MH_2^+ + M$ by use of the TESICO technique. The two peaks appearing in the TOF coincidence spectra of the product ion MH_2^+ have been interpreted as corresponding to the hydrogen atom abstraction and proton transfer mechanisms of the MH_2^+ formation (see IV-E-1). Through these studies, a hypothesis has been presented that an electron transfer process in the entrance channel plays an important role in the phenomenological hydrogen atom abstraction mechanism. To further corroborate this hypothesis, we have measured the TOF coincidence spectra for the primary and secondary ions of the reaction ($D_2^+ + D_2$). This system is known to belong to the type of the reaction in which the contributions of the two direct mechanisms are almost equal. The equal contribution is attributed to the very efficient charge transfer process in the entrance channel. In such a system, the charge transfer product should also be detectable with almost the same intensity as that of the hydrogen abstraction product.

Figure 1 shows that the TOF spectrum for the D_2^+ ion also has two peaks, corresponding to the reactant ions (faster one) and the charge transfer products (slower one). The intensity of the latter peak is comparable with those of the TOF peaks for the product ions D_3^+, supporting the above hypothesis.

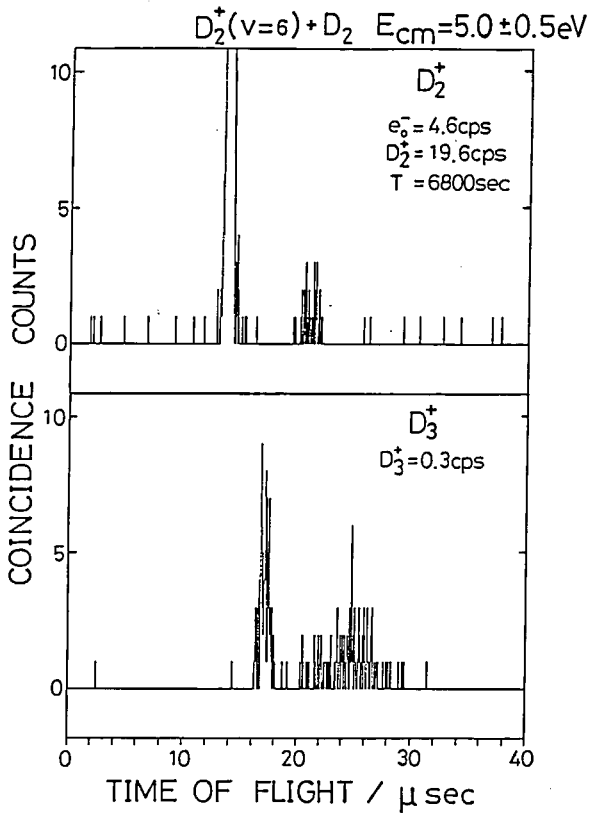

Figure 1. Typical TOF spectra for the D_2^+ and D_3^+ ions for ($D_2^+ + D_2$) system at the center-of-mass collision energy E_{cm} of 5.0 ± 0.5 eV

IV-E-3 Time-of-Flight Analysis of the $C_3H_3^+$ Ions Produced by the Reaction $C_3H_4^+ + C_3H_4$

Teruhiko OGATA *(Sizuoka Univ.)*, **Shinzo SUZUKI, and Inosuke KOYANO**

The $C_3H_3^+$ ion, an ubiquitous molecular ion in the mass spectra of hydrocarbons, is considered to play an important role in the formation of the interstellar molecules. The time-of-flight coincidence spectra of

$C_3H_3^+$ have been investigated using the TESICO technique. The reactions studied include all combinations of reactant ions and neutrals from allene, cyclopropene, and allene-d_4. The collisions of $C_3H_4^+$ with argon produced no $C_3H_3^+$ ions, indicating that no collision induced dissociation occurred. Less $C_3H_3^+$ ions were produced by the reactions of allene ion than by those of cyclopropene ion regardless of the neutral reactant, and much less $C_3H_3^+$ ions were created by the reaction of allene-d_4^+ ions. The sepctra of $C_3H_3^+$ ion were found to be abnormally broad and spread over the whole range between the TOF peaks of the reactant ion $C_3H_4^+$ and product ion $C_6H_7^+$, as shown in Figure 1 for the case of $C_3H_3^+$ produced by the reaction of cyclopropene ion with cyclopropene. In most cases, the spectrum of $C_3H_3^+$ consists of at least two broad peaks. (The sharp peak near 45 μs corresponds to the ions produced in the ionization chamber and disappears after the extraction of the back ground signals.) These two broad peaks were observed even in the spectrum of the $C_3H_3^+$ ions produced by the reaction $C_3H_4^+ + C_3D_4$, where $C_3H_3^+$ was only possible to be produced by H-atom transfer, and are considered to correspond to the two isomers of $C_3H_3^+$, probably those having cyclic and linear structures.

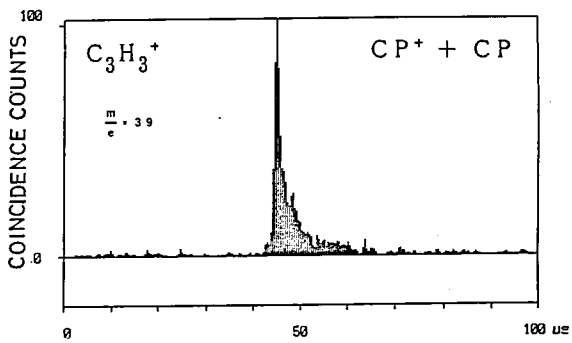

Figure 1. TOF coincidence spectrum of the $C_3H_3^+$ ions produced by the reaction of cyclopropene ion with cyclopropene.

IV–F Studies of Photo-Induced Ion-Molecule Reactions

Exploration of chemical reactions coupled with radiation field has paved the way for a deeper understanding of the structure and potential energy surfaces of interacting systems. In this project, we attempt to investigate the ion-molecule reactions induced by the resonant and/or non-resonant laser irradiation to obtain some information on the intermediate states of reactions, as well as on the reactions of excited ions. Detection of stimulated transitions in colliding systems induced by the non-resonant laser irradiation might provide new information of the reaction path and potential energy surfaces. Collision induced deactivation processes of electronically excited ions are also aimed at since they are expected to provide new aspects which are different from those of the neutral molecules, especialy in connection with the existence of the charge.

IV-F-1 Collisional Quenching Rates for Electronically Excited Ions: $CO^+A^2\Pi(v'=0-2)$

Takashi IMAMURA, Takashi IMAJO and Inosuke KOYANO

[*Chem. Phys. Lett.*, **160**, 143 (1989)]

Collisional removal rates of electronically excited CO^+ ions by He, Ne, Ar, N_2 and CO have been measured by a flowing afterglow/time-resolved laser induced fluorescence technique. CO^+ is generated by reacting metastable helium atoms produced in a DC hollow cathode discharge with CO reactant added downstream and excited to some vibrational level in the first excited $A^2\Pi$ state. The overall quenching rate constants of each vibronic level ($v'=0$, 1, 2) were obtained from the Stern-Volmer plots and are summarized in Table 1. The quenchers Ar, N_2, and CO deactivate all vibronic levels of CO^+ measured very efficiently with the rate constants of the same order of magnitude as the Langevin rate constants, in contrast with the cases of He and Ne, for which the quenching is

inefficient. The ionization potentials of the former group molecules are smaller than and those of the latter group molecules are larger than the recombination energy of CO^+ $A^2\Pi$. Furthermore, the quenching rate constants by Ar, N_2 and CO are almost independent of the vibrational level of CO^+ $A^2\Pi$. (In the case of He, k_q for v'=2 is ca. 60 times larger than that for v'=0.) The charge transfer reaction must be a major channel of the quenching of the $A^2\Pi$ state of CO^+ by Ar, N_2 and CO.

Table I Collisional quenching rate constants for the $A^2\Pi(v'=0-2)$ levels of CO^+.

quencher	V'=0	V'=1	V'=2	k_L^a
He	<0.001 (0.0001)[b]	0.0009±0.0001 (0.0011)[b]	0.0059±0.0004 (0.0065)[b]	0.56
Ne	<0.01	0.013±0.001	0.067±0.004	0.43
Ar	0.8±0.1	1.1±0.1	0.8±0.2	0.74
N_2	1.4±0.1	1.9±0.1	1.6±0.2	0.83
CO	0.9±0.1	1.5±0.1	1.5±0.3	0.87

The unit is 10^{-9} cm^3 $molec^{-1}s^{-1}$.
a) Langevin rate constant
b) Reported by D.H. Katayama and J.A. Welsh in *J. Chem. Phys.* **79**, 3627 (1983).

IV-G Studies of Unimolecular Decomposition of Energy/State Selected Molecular Ions

The TEPSICO and the TEPSICO-II apparatus which we have developed for the study of state selected ion-molecule reactions (see **IV-E** above and *IMS Ann. Rev.* 1984, **IV-F-4**) are also applicable to the study of unimolecular decomposition of molecular ions. In this technique, ions can be prepared in a specified internal state or with a defined amount of internal energy and their subsequent decomposition is investigated. In the present project, we study unimolecular decomposition of complex molecular ions mainly following valence and inner valence photoionization. Both laboratory and synchrotron light sources are used. Dissociation of excited neutrals into ion-pairs is also included.

IV-G-1 Unimolecular Fragmentation of Energy Selected Metastable Ions in Formaldehyde

Takae TAKEUCHI *(Nara Women's Univ.)*, **Masao YAMAMOTO** *(Nara Women's Univ.)*, **Shinzo SUZUKI and Inosuke KOYANO**

The fragmentation behavior of internal-energy-selected formaldehyde CX_2O^+(X=H or D) molecular cations has been explored using the threshold electron-photoion coincidence technique. The metastable transition:

$$X_2CO^{+\cdot} \rightarrow XCO^+ + X^\cdot \quad (X= H \text{ or } D) \qquad (1)$$

from H_2CO and D_2CO is investigated in the energy region from 12 to 14.5 eV.

The branching ratio of the molecular ion, b, i.e. the number of molecular ions detected after a time of flight t relative to the number of molecular ions initially generated, has been measured as a function of energy. These data can be converted into lifetime τ, assuming a simple exponential decay, by

$$\tau=-t/\ln b, \qquad k=\tau^{-1}.$$

The rate constants k thus obtained are shown in Figure 1. As can be seen in Figure 1, there is a large isotope effect on the rate constant in the excited state $\tilde{A}$. On the other hand, the isotope effect in the ground state $\tilde{X}$

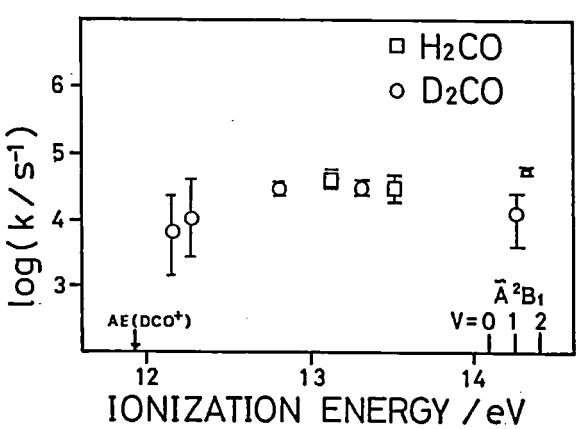

Figure 1. Rate constant of raction $X_2CO^{+\cdot} \rightarrow XCO^+ + X^\cdot$(X=H or D).

is smaller. The rate constant increases with energy in the $\tilde{X}$ state. The particularly small rate constant for D_2CO in the $\tilde{A}$ state is interpreted as being due to the slow internal conversion of D_2CO^+ from $\tilde{A}^2B_1$ to $\tilde{X}^2B_2$, from which the dissociation takes place.

IV-G-2 Dissociation of Energy-Selected $HCOOCH_3^+$ and $HCOOCD_3^+$ Ions

Seiji TOBITA *(Gunma Coll. of Tech.)*, **Susumu TAJIMA** *(Gunma Coll. of Tech.)*, **Shinzo SUZUKI, Takashi IMAMURA and Inosuke KOYANO**

Unimolecular dissociation processes of the energy-selected $HCOOCH_3^+$ and $HCOOCD_3^+$ ions have been investigated using the PEPICO technique. The experimental breakdown diagram of $HCOOCH_3^+$ gave the relative intensities of individual ions as a function of internal energy of the molecular ion. The low-energy dissociation channels of the methyl formate ions and their threshold energies were obtained as shown in Table 1. Deuterium labeling experiments clearly showed the production of isomeric ions, CD_3O^+ and CD_2OH^+. The latter ion is thermochemically more stable but its appearance energy was higher than that of CD_3O^+. This implies that the CD_2OH^+ is produced by loss of a D atom from the primary fragment ion CD_3OH^+

Table 1. Appearance energies for the dissociation processes of methyl formate

$HCOOCH_3^+$	$HCOOCD_3^+$
CH_3OH^++CO (11.27 eV)	CD_3OH^++CO (11.37 eV)
CH_3O^++HCO (11.92 eV)	CD_3O^++HCO (11.48 eV)
	CD_2OH^++D +CO (12.04 eV)
HCO^++CH_3O (12.78 eV)	HCO^++CD_3O (12.27 eV)

IV-G-3 Dissociation Processes of Keto- and Enol-Forms of Molecular Ions of 1,3-Diketone Compounds

Seiji TOBITA *(Gunma Coll. of Tech.)*, **Susumu TAJIMA** *(Gunma Coll. of Tech.)* **Shinzo SUZUKI, Takashi IMAMURA and Inosuke KOYANO**

Unimolecular dissociation processes of the parent ions of acetylacetone (AA), trifluoroacetylacetone (TFAA) and hexafluoroacetylacetone (HFAA) have been investigated by using the TESICO technique[1] and reversed-geometry mass spectrometry[2]. Dominant fragmentation processes of their enol-forms at low internal energy were found to be the loss of CH_3 or CF_3, whereas the diketo-form of AA preferentially eliminated the CO molecule with a relatively large kinetic energy release (KER). The potential energy profiles of the low energy dissociation processes of AA and TFAA were clarified by measuring the photoionization efficiency curves. The appearance energy (AE) and the activation energy (E_a) for each dissociation process were obtained as shown in Table 1. These results show the fragmentation characteristics of keto- and enol-tautomers of 1,3-diketone molecular ions.

References
1) I. Koyano and K. Tanaka, *J. Chem. Phys.* **72**, 4858 (1980).
2) S. Tobita, K. Ogino, S. Ino and S. Tajima, *Int. J. Mass Spectrom. Ion Processes* **85**, 31 (1988).

Table 1. Thermochemistry for ion fragmentations at 298K

Compound	IE (eV)	Neutral lost	KER (meV)	AE (eV)	E_a (kJ/mol)
AA (enol)	8.81	CH_3	23.4	9.92	107
AA (diketo)	9.41	CO	77.8	9.82	40
TFAA (enol)	9.42	CF_3	181	10.16	71
		(CH_3	—	10.97	150)
HFAA (enol)	10.55	CF_3	27.5	11.2	63

IV-G-4 Measurement of Photoionization Efficiency Curves for Negative Ions from OCS, CO_2, and N_2O by Using Synchrotron Radiation

Koichiro MITSUKE *(Univ. of Tokyo)*, **Shinzo SUZUKI, Takashi IMAMURA, and Inosuke KOYANO**

There has been only a little amount of information about ion pair formation processes induced by vacuum UV photoabsorption of triatomic molecules. We have measured photoionization efficiency curves of S^- and O^- from OCS, O^- from CO_2, and O^- from N_2O. A molecular beam apparatus was installed on the beam line BL3B of UVSOR. The beam of OCS was produced by expanding the sample gas from a sonic nozzle and intersected at 90° with the monochroma-

tized light in the ionization region. The negative ions formed were mass-analyzed by a quadrupole mass spectrometer and detected by a channel electron multiplier. The photoionization efficiency curve of S^- from OCS shows an onset at 819Å (15.14 eV). This accords with the thermochemical threshold of 15.08 eV for the formation of $S^-(^2P_u)$ + $CO^+(\tilde{X}^2\Sigma^+)$. Several peaks at ~780Å (~15.9 eV) is assigned as resulting from the following two processes: (i) transition to the OCS ($^1\Sigma^+$, $^1\Pi$) excited states belonging to the Rydberg series converging to $OCS^+(\tilde{B}^2\Sigma^+)$, and (ii) subsequent predissociation into $S^-(^2P_u)$ + $CO^+(\tilde{X}^2\Sigma^+)$. In the efficiency curve of O^- from OCS, the ion signal starts to appear at 735Å (16.87 eV), which conceivably corresponds to the formation of $O^-(^2P_u)$ + $CS^+(\tilde{X}^2\Sigma^+)$ (thermochemical threshold = 16.76 eV). The efficiency curve of O^- from N_2O displays progressions of peaks due to predissociation from the Rydberg levels converging to $N_2O^+(\tilde{A}^2\Sigma^+$, and $\tilde{C}^2Z^+)$ (see Figure 1). In particular, two Rydberg series ($nd\sigma$ and $nd\pi$) converging to the $\tilde{C}$ state can be observed most prominently.

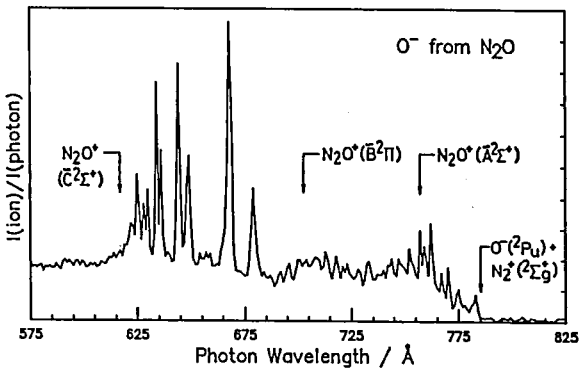

Figure 1. Ionization efficiency curve of O^- produced from N_2O. The thermochemical threshold for the formation of $O^-(^2P_u)$ + N_2^+ $(\tilde{X}^2\Sigma_g^+)$, and the ionization limits for the three N_2O^+ (v'=0, 0, 0) excited states are indicated.

IV–H Investigation of Ionic Fragmentation Following Core Level Ionization in the Vapor Phase Using Synchrotron Radiation

Shallow valence-level ionization and subsequent fragmentation of molecules have been studied extensively using various kinds of light source in recent years. However, the investigation of processes following core level excitation have not been so extensive, because, for the purpose of such investigation, the conventional light sources are insufficient both in photon energy and intensity. Synchrotron radiation is expected to provide a powerful means to obtain information about the core level excitation. In contrast to the case of the valence electrons delocalized over the molecule, the core electrons in a molecule are localized near the atom to which they belonged originally. As a result, the photoionization from the core levels is expected to produce dissociation pathways quite different from those following valence photoionization.

IV-H-1 Ionic Fragmentation Following the 3d Core Excitation of $Sn(CH_3)_4$ by Soft X-Ray

Kiyoshi UEDA *(Tohoku Univ.)*, **Eiji SHIGEMASA** *(Tohoku Univ.)*, **Yukinori SATO** *(Tohoku Univ.)*, **Shin-ichi NAGAOKA, Inosuke KOYANO, Akira YAGISHITA** *(National Lab. High Energy Phys.)*, **Tetsuo NAGATA** *(Meisei Univ.)*, **and Tatsuji HAYAISHI** *(Univ. of Tsukuba)*

[*Chem. Phys. Lett.* **154**, 357 (1989)]

Ionic fragmentation following the core-level photoionization of $Sn(CH_3)_4$ has been studied in the photon energy region between 400 and 600 eV by use of monochromatized synchrotron radiation and time-of-flight mass spectrometry. The production of small ionic fragments Sn^+, $CH_m^+(m=0-2)$, and H^+ is strongly enhanced by Sn 3d photoionization above 500 eV. Fragmentation processes yielding such small ions are interpreted as decomposition of the multiply charged ion $Sn(CH_3)_4^{q+}(q=3-5)$ produced by the vacancy cascade via Auger and/or Coster-Kronig transitions following Sn:3d photoionization.

IV-H-2 Site-Specific Fragmentation Following Inner-Core Level Excitation of $Pb(CH_3)_4$ in the Vapor Phase

Shin-ichi NAGAOKA, Inosuke KOYANO, Kiyoshi UEDA *(Tohoku Univ.)*, **Eiji SHIGEMASA** *(Tohoku Univ.)*, **Yukinori SATO** *(Tohoku Univ.)*, **Akira YAGISHITA** *(Natural Lab. High Energy Phys.)*, **Tetsuo NAGATA** *(Meisei Univ.)*, **and Tatsuji HAYAISHI** *(Univ. of Tsukuba)*

[*Chem. Phys. Lett.* **154**, 363 (1989)]

Ionic fragmentation following inner-shell (Pb:5p and 4f, C:1s) excitation of $Pb(CH_3)_4$ has been studied in the vapor phase by use of synchrotron radiation and time-of-flight mass spectrometry. The C:1s ionization is followed by a KVV Auger process and the fragmentation proceeds by way of the doubly charged parent ion. The Pb:5p or 4f ionization is followed by a cascade of Auger events, and the fragmentation proceeds by way of the triply or higher multiply charged parent ions. The fragmentation pattern changes significantly depending on the site of the core electrons excited (Pb or C).

IV-H-3 Dissociation of Doubly Charge Parent Ions of $Al(CH_3)_3$ produced by Valence and Al:2p Core Level Photoexcitation

Shin-ichi NAGAOKA, Inosuke KOYANO, and Toshio MASUOKA *(Osaka City Univ.)*

Dissociation processes following double photoionization of $Al(CH_3)_3$ have been studied in the range of valence and Al:2p core-level ionization by means of the photoelectron-photoion and photoion-photoion coincidence methods. The double-ionization threshold and the Al:2p core-ionization threshold are estimated to be about 30 and 80 eV, respectively. The variation of the fragmentation pattern with photon energy is discussed in conjunction with the relevant electronic states. The relative yields of the H^+-Al^+ and $H^+-CH_m{}^+(m'=0-3)$ ion-pairs are enhanced around the Al:2p core-ionization threshold.

IV-H-4 Ionic Fragmentation Following Core-Level Photoionization of $Sn(CH_3)_4$ by Soft X-Rays

Kiyoshi UEDA *(Tohoku Univ.)*, **Eiji SHIGEMASA** *(Tohoku Univ.)*, **Yukinori SATO** *(Tohoku Univ.)*, **Shin-ichi NAGAOKA, Inosuke KOYANO, Akira YAGISHITA,** *(National Lab. High Energy Phys.)*, **Tatsuji HAYAISHI** *(Univ. of Tsukuba)*

[*Chem. Phys. Lett.* submitted]

Ionic fragmentation following the photoionization of $Sn(CH_3)_4$ (TMT) has been studied in the photon energy range of 60–600 eV using synchrotron radiation and time-of-flight mass spectrometry. Each of the Sn:4d, 4p, 3d and C:1s photoionization leads to a type of ionic fragmentation characteristic of the ionized core. The Sn:4d photoionization above 60 eV predominantly produces doubly-charged TMT which dissociate into two singly-charged ions and some neutral fragments. The ions produced in this pathway are CH_3^+, $C_2H_3^+$, $C_2H_5^+$, $SnCH_m^+$ and/or Sn^+. The Sn:4p photoionization produces triply-charged TMT and enhances the production of H^+, $CH_m{}^+(m'=0-3)$ and Sn^+ significantly. The Sn:3d photoionization produces multiply-charged TMT with the numbers of the charges of 3–5 and enhances the production of H^+, $CH_m{}^+(m'=0$ and 1) and Sn^+ significantly. The C:1s photoionization produces doubly-charged TMT via the KVV Auger transition and enhances the production of CH_3^+, $C_2H_3^+$, $SnCH_m^+$ and/or Sn^+.

IV-H-5 Ionic Fragmentation Following the 3p and 3s Core Excitation of $Ga(CH_3)_3$ by Soft X-ray

Kiyoshi UEDA *(Tohoku Univ.)*, **Yukinori SATO** (Tohoku Univ.), **Shin-ichi NAGAOKA, Inosuke KOYANO, Akira YAGISHITA** *(National Lab. High Energy Phys.)*, **and Tatsuji HAYAISHI** *(Univ. of Tsukuba)*

Ionic fragmentation following core-level photoionization of $Ga(CH_3)_3$ has been studied in the photon energy region between 90–260 eV by use of monochromatized synchrotron radiation and time-of-flight mass spectrometry. Kinetic energies released by fragmentation are estimated to be about 3 eV for $CH_m^+(m=0-3)$ and 5.5 eV for H^+. The production of H^+ is enhanced significantly by the Ga:3p and 3s photoionization.

IV–I Studies of Dissociative Double Photoionization of Polyatomic Molecules

Molecular Dications have long been believed to be unstable with respect to dissociation because the Coulomb repulsion between the two positive charges usually exceeds the bond dissociation energy. Recently, however, several stable molecular dications, both diatomic and polyatomic, have been observed with the advent of new sophisticated experimental techniques. This aroused a great deal of interest in the study of structure and stability of molecular dications, as well as their dissociation mechanism. In the present project, we aim at an extensive study of the dissociation mechanisms of polyatomic dications produced by valence double photoionization. Emphasis is placed on the relation between the electronic states and dissociation pathways. Synchrotron radiation and the angle-resolved PIPICO (Photoion–photoion coincidence) technique are utilized.

IV-I-1 Dissociation of Methyl Fluoride Dication CH_3F^{2+}

Toshio MASUOKA *(Osaka City Univ.)* **and Inosuke KOYANO**

Using the new photoionization apparatus developed for the measurements of angle resolved photoelectrons and photoions, we have performed a series of studies on the dissociation of polyatomic dications. Reported here is the result on the methyl fluoride dication CH_3F^{2+} in the energy range 35–125 eV.

Stable CH_3F^{2+} was not observed in all the energy range studied. A photoion–photoion coincidence (PIPICO) spectrum measured at 100 eV showed that at least the following four types of dissociation process take place at this photon energy.

$$CH_3F^{2+} \rightarrow H^+ + CH_nF^+ + \text{n.f. } (n=0-2) \quad (1)$$
$$\rightarrow H_2^+ + CHF^+ \quad (2)$$
$$\rightarrow H^+ + CH_n^+ + \text{n.f. } (n=0-2) \quad (3)$$
$$\rightarrow H^+ + F^+ + \text{n.f.} \quad (4)$$

Here, n.f. stands for neutral fragments. At low energies below about 40 eV, only the four pathways are open, i.e., the C-H bond breakage (1) and rearrangement reaction (2). These two types of processes are due to two-electron ejection from the outermost 2e orbital. The fragmentation $H^+ + CH_n^+$ (the C-F as well as C-H bond breakage) starts to occur at about 40.5 eV because of two electron ejection such as $(5a_1 2e)^{-1}$ and $(1e2e)^{-1}$. The observed dissociation pathways are correlated with the electronic states of CH_3F^{2+} calculated by the Green's function method.[1] shown in Figure 1 is an example of the PIPICO spectrum.

Reference

1) C. M. Liegener, *Chem. Phys. Lett.* **151**, 83 (1988).

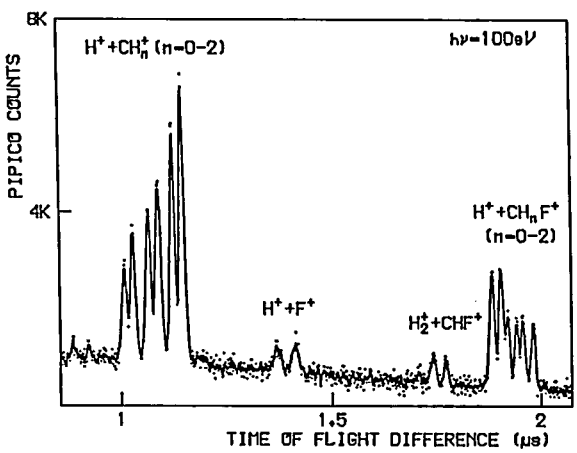

Figure 1. An example of PIPICO spectrum of methyl fluoride.

IV–J Application of Excited-State Photoelectron Spectroscopy to Photophysics and Photochemistry

Pulse Laser photoelectron spectroscopy for studying excited molecules in the gas phase has been developed in this Institute by K. Kimura and his coworkers since 1980 [*IMS Annual Review* (1980–89); *Adv. Chem. Phys.* **60**, 161

(1985); *Intern. Rev. Phys. Chem.* **6**, 195 (1987)]. Since any electronically excited states can in principle be ionized by an appropriate pulse laser, the laser photoelectron spectroscopic technique is especially powerful for studying the dynamic behavior of radiative and nonradiative excited states. The laser photoelectron technique is also useful for finding new ionic states of molecules. In this project, we have been further improving the technique and applying it for various molecular excited states associated with photophysical and photochemical processes.

IV-J-1 Dynamic Aspect of Excited-State Photoelectron Spectroscopy: Some Small Molecules

Katsumi KIMURA

Combination of a nanosecond tunable UV/visible laser with a photoelectron spectroscopic technique has made it possible to observe excited-state photoelectron spectra according to resonant multiphoton ionization (MPI) or stepwise ionization. With this technique it is possible to study dynamic behavior of excited states. The dynamic aspect of the laser photoelectron spectroscopy is in striking contrast to the VUV photoelectron spectroscopy which is mostly concerned with static aspect of ground-state molecules. In this sense, laser photoelectron spectroscopy provides a useful technique for studying the dynamic behavior of excited state molecules.

The author has recently reviewed the several following applications of excited-state photoelectron spectroscopy recently studied in this laboratory: one-photon forbidden excited states; autoionization; and small van der Waals molecules and photodissociation.[1)]

Reference

1) K. Kimura, "Dynamic Aspect of Excited-State Photoelectron Spectroscopy. Some Small Molecules", In, *"The Structure of Small Molecules and Ions,"* ed. by R. Naaman and Z. Vager, Plenum, New York, (1988), p. 173.

IV-J-2 Autoionization Mechanism of NO Molecule: Calculation of Quantum Defect and Theoretical Analysis of REMPI Experiment

Keiji NAKASHIMA *(IMS and Kyushu Univ.)*, **Hiroki NAKAMURA, Yohji ACHIBA** *(IMS and Tokyo Met. Univ.)*, **and Katsumi KIMURA**

[*J. Chem. Phys.* **91** 1603 (1989)]

Quantum defects of NO at the $\ell\lambda$-Rydberg states (ℓ=s,p,d; $\lambda=\sigma,\pi,\delta$) have been calculated by SCF and CI methods at various internuclear distances. Using the multichannel quantum defect theory (MQDT), the photoelectron spectra of resonant multiphoton ionization (REMPI) of NO have been analyzed in terms of calculated quantum defects. The analysis was made particularly on the autoionization of vibrationally excited Rydberg states of σ- and δ-symmetry.

From the present study, it has been concluded that the autoionization is dominated by the two-step electronic mechanism in which dissociative superexcited state plays a role of intermediate state. Potential curves and electronic coupling strengths of the relevant dissociative states ($B'^2\Delta$ and $I^2\Sigma$) have been estimated from this analysis, providing us with useful information to investigate various dynamic processes involving these superexcited states. Importance of dissociative superexcited state has been emphasized in reference to the various dynamic processes.

IV-J-3 Measurements of Threshold Photoelectron Spectra of Excited-State Molecules by Means of A Laser MPI Technique

M. Takahashi, K. Okuyama and K. Kimura

In order to study the vibrational structure of ions produced by photoionization from molecular excited states, we have developed a new capillary-type threshold electron analyzer for nanosecond laser photoelectron measurements with a resolution of 2-4 meV. The analyzer is similar in design to that earlier reported.[1)] Using a two-color REMPI technique, we measured a photoelectron spectrum for the lowest excited state (S_1) of, for example, aniline. The wavelength of the first laser was fixed to a specific vibronic level of S_1, while that of the second laser was scanned to produce threshold electrons which correspond to the Franck-Condon-allowed vibronic levels of the ion. A threshold photoelectron spectrum thus

obtained here for the aniline S_1 state is shown in Figure 1. Our best resolution (FWHM) is now 30 cm^{-1} (≃4 meV).

The advantage of the method is the following. 1) Ionic states unfavorable from the neutral ground state in Franck-Condon factors can be produced via a special S_1 vibronic level. 2) The photoelectron energy scale can be determined only from the laser wavelength. 3) Correct Franck-Condon factors can be obtained from relative photoelectron vibrational-band intensities. 4) The photoelectron collecting efficiency is independent of the photon energy and very high (solid angel 4π).

Reference

1) R. Spohr, P. M. Guyon, W. A. Chupka, and J. Berkowitz, *Rev. Sci. Instrum.* **42**, 1872 (1971).

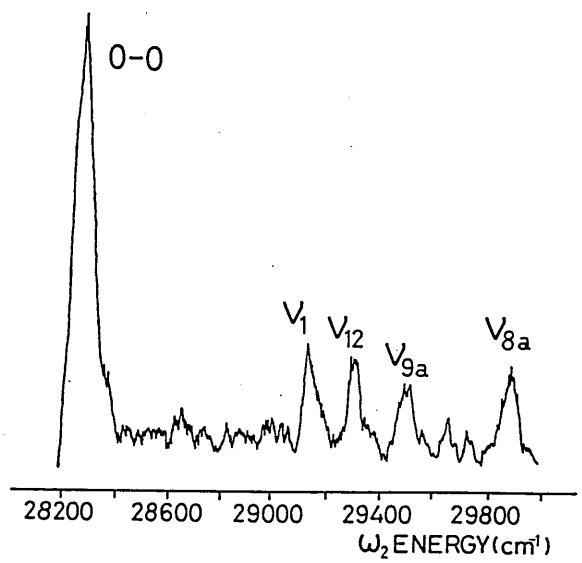

Figure 1. The threshold photoelectron spectrum of the S_1 (0_0^0) state of aniline in a supersonic jet.

IV-J-4 MPI Spectra of *p*-Phenylenediamine and Its Methyl Derivatives

Hiroyuki OZEKI, Katsuhiko OKUYAMA, Masahiko TAKAHASHI, and Katsumi KIMURA

p-Phenylenediamine (PD), *N,N*-dimethylphenylenediamine (DMPD), and *N,N,N',N'*-tetramethylphenylenediamine (TMPD) are important electron donating molecules, forming charge transfer complexes with various acceptor molecules. In order to study dynamic behavior of these donor molecules in their excited S_1 states, we have obtained their one-color MPI ion-current spectra under jet-cooled conditions in the region of the $S_1 \leftarrow S_0$ transition.

The MPI ion-current spectrum obtained here for PD shows well-resolved structure, the 0-0 peak appearing at 29821 cm^{-1}, as shown in Figure 1(a), its spectral feature being similar to those of typical benzene derivatives. However, it has been found that the MPI spectra of DMPD and TMPD (Figure 1b and 1c, respectively) show anomalous spectral features. In the spectrum of DMPD, its 0-0 band is broader (FWHM – 6.8 cm^{-1}) than in PD, shifting to the red side from the origin of PD by 478 cm^{-1}, and the vibronic structure becomes unresolved as increasing excess energy (see Figure 1b). Furthermore, in the spectrum of TMPD, no resolved structure has been observed, and the appearance energy is nearly 500 cm^{-1} lower than the origin of DMPD.

From these experimental facts, it has been suggested that there should be some rapid relaxation processes in the S_1 states of DMPD and TMPD. The relaxation process of TMPD should be much faster than that of DMPD.

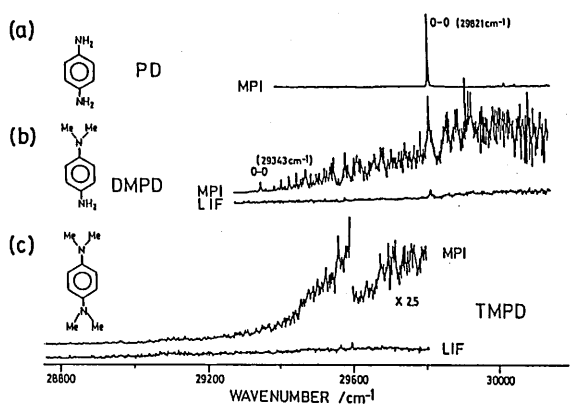

Figure 1. One-color MPI ion-current spectra of PD, DMPD, and TMPD in supersonic jets in the 331-347 nm region.

IV-J-5 Vibrational Assignment of the "LB" Excited State of Molecular Oxygen by MPI Photoelectron Spectroscopy

Shunji KATSUMATA *(Iwaki Meisei Univ.)*, **Katsuhiko OKUYAMA, Masahiko TAKAHASHI, and Katsumi KIMURA**

There are a series of well-known excited states of O_2 molecule, which are called LB (*longest band;* 9.970 eV), SB (*second band;* 10.288 eV), and TB (*third band;* 10.576 eV) in several electron-impact energy-loss studies.[1] The spectral assignment of these excited states has not been established yet;[2] some theoretical studies suggest that these excited states belong to the second excited state of $3p\pi_u{}^3\Sigma_u{}^-$ at different vibronic levels, but some others suggest different assignments.

In the present work, we have studied the LB state by means of laser MPI (ion-current and photoelectron) techniques. A (3+1) MPI ion-current spectrum was obtained in the laser wavelength region 574–575 nm, whose four-photon energy corresponds to the LB state. A photoelectron spectrum was observed at 574.65 nm, showing the vibrational peaks due to $O_2{}^+$ ($X^1\Pi_g$) as shown in Figure 1.

Figure 1. A photoelectron spectrum of the LB excited state of O_2 in a supersonic jet, obtained by (3+1) MPI.

Reference

1) For example, T. A. York and J. Commer, *J. Phys. B: At. Mol. Phys.* **16**, 3627 (1983).
2) P.J. Miller, L.C. Li, W.A. Chupka and S.D. Colson *J. Chem. Phys.* **88**, 2972 (1988) D.H. Katayama, *J. Chem. Phys.*, **89** 5349 (1988).

IV–K Synchrotron Radiation Researches of Molecules and Molecular Clusters: Photoionization and Photoelectron Spectroscopy

The use of synchrotron radiation is attractive for studying photoionization and photoelectron spectroscopy of gaseous molecules and molecular clusters produced in supersonic jets. For this purpose, recently we have constructed two kinds of photoionization apparatuses, using synchrotron radiation from the 750-MeV electron storage ring called UVSOR in this Institute. One is a molecular-beam apparatus on beamline BL2B2, using a multi-stage differential pumping system not to use any window materials between the molecular-beam apparatus and the storage ring. The other is a PEPECO apparatus on beamline 3A2, using undulator radiation. The PEPECO apparatus has been constructed to study doubly charge ions of gasous atoms and molecules as well as to perform coincidence measurements of two photoelectrons.

IV-K-1 Photoionization Studies of HCOOH, CH_3COOH, CH_3OH, C_2H_5OH and the Respective Dimers

Ellak I. VON NAGY-FELSOBUKI *(Univ. of Newcatle and IMS)* and Katsumi KIMURA

Photoionization studies of simple organic acids and bases provides information on appearance potentials, and so directly yields information of intracluster excess energy dissipation processes. In the present work, the photoionization experiments were performed in the energy region 106-140 nm, using the molecular beam apparatus on the beam line BL2-B2 at UVSOR.

A lithium fluoride window was used to filter out the higher-order light. A Q-pole mass filter (ULVAC Model MSQ-400) was used for analysis and detection. Figure 1 shows the photoionization efficiency (PIE) curves of $(HCOOH)^+$ and $(HCOOH)H^+$ as representative examples of the work completed thus far. PIE curves were also measured of $(CH_3COOH)^+$, $(CH_3COOH)H^+$, $(CH_3COOH)_2^+$, $(CH_3COOH)_2H^+$, $(HCOOH)_2^+$, $(HCOOH)_2H^+$, $(CH_3OH)^+$, $(CH_3OH)H^+$, $(CH_3OH)_2H^+$, $(C_2H_5OH)^+$, $(C_2H_5OH)H^+$, and $(C_2H_5OH)_2H^+$. The photoionization of clusters of these simple molecules gives rise to the following intercluster reaction,

$$[(HA)^+_n]^*_{VIP} \rightarrow (HA)_{n-k}H^+ + A + (k-1)\ HA$$

where VIP represents the vertically ionized point.

In the case of methanol and ethanol, the photoionization studies revealed the absence of unprotonated cluster ions, thereby indicating that the potential minima of the neutral and ionic states are significantly displaced from each other yielding poor Franck-Condon overlaps.

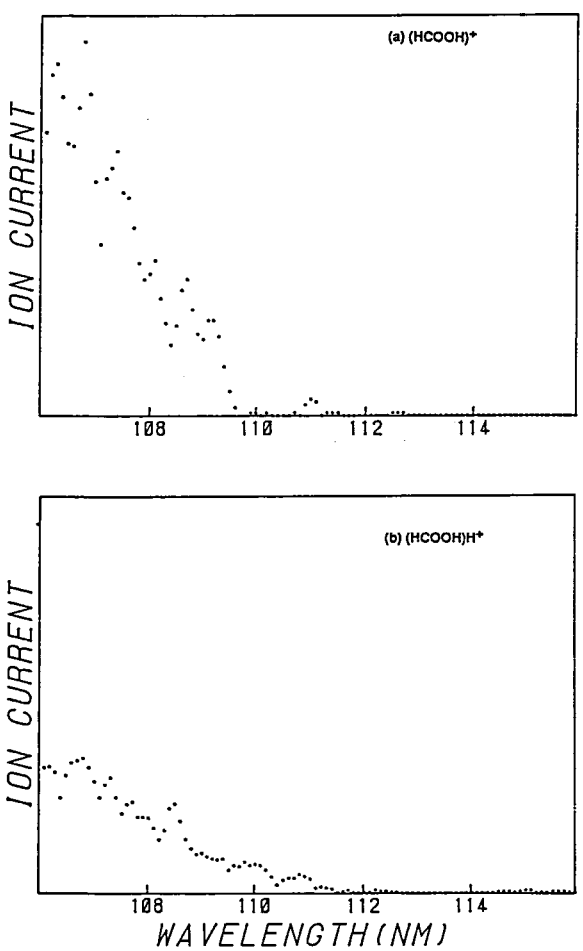

Figure 1. PIE curves of producing $(HCOOH)^+$ and $(HCOOH)H^+$.

IV-K-2 Ab Initio Proton Affinities of HCOOH, CH_3COOH, CH_3OH and C_2H_5OH

Ellak I. VON NAGY-FELSOBUKI *(Univ. of Newcastle and IMS)* **and Katsumi KIMURA**

Simple organic acids and bases are electron sparse enough to enable relative proton affinities to be calculated at the Hartree-Fock level using a variety of different quality bases sets, thereby testing the severity of using tractable models. Ab initio molecular orbital calculations using the STO-3G, STO-3G**, 3-21G and 6-31G** bases sets have been performed for the series HCOOH, CH_3COOH, CH_3OH and C_2H_5OH. Structural calculations of the neutrals and predictions of the structure of the respective cations are discussed and reported. Relative proton affinities have been calculated. Only at the 6-31G//6-31G Hartree-Fock level of theory are the relative proton affinities and trend for this simple organic acid/base series in agreement with experiment. Of the other models the STO-3G//STO-3G model is the most effective.

IV-K-3 Construction of Photoelectron-photoelectron Coincidence Apparatus by using the Magnetic Bottle Electron Spectrometer

Katushiko OKUYAMA, John H. D. ELAND *(Oxford Univ. and IMS)*, **and Katsumi KIMURA**

The formation of doubly-charged cations of atoms or molecules in the gas phase upon VUV one-photon excitation has become of interest in recent year. In a study of such double ionization, it is important to measure the kinetic-energy distribution for a pair of two electrons ejected from an atom or molecule. In order to identify correlated electron pairs, it is essential to use a photoelectron-photoelectron coincidence (PEPECO) technique, although the direct double ionization is much weaker compared with the ordinary photoionization. In previous PEPECO experiments by two groups at Orsay and Oxford, it has been shown that the signal-accumulating time takes at least 24 hours for deriving each spectrum.

The use of a magnetic bottle electron analyzer in PEPECO experiments should have a great advantage, because of its large acceptance angle of 2 steradian. With such a bright electron analyzer, it is possible to measure a PEPECO spectrum in the order of minutes.

In the present work, therefore we have constructed a new PEPECO apparatus using a commercial magnetic-bottle electron spectrometer, as shown in Figure 1, for performing our PEPECO experiments with synchrotron radiation at the Beamline 3A2 of UVSOR.

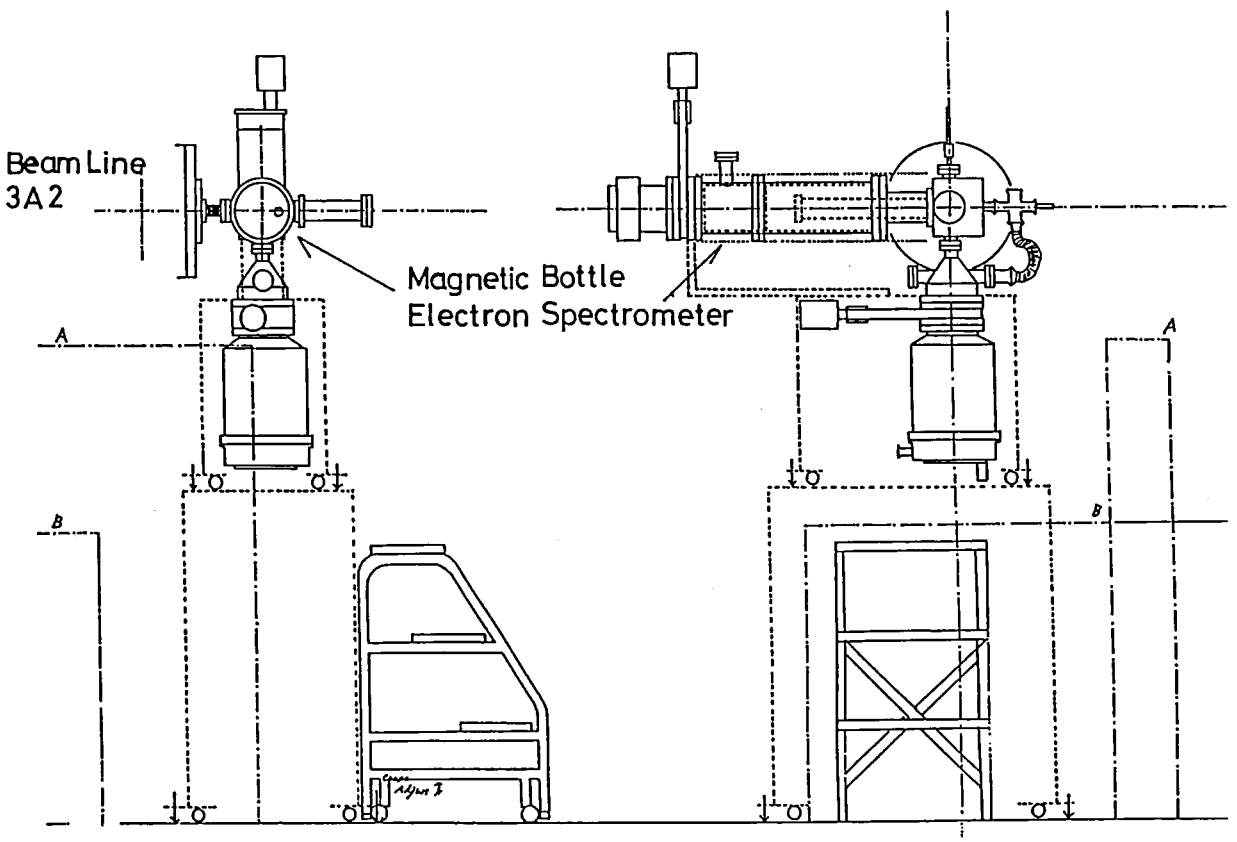

Figure 1. Schematic drawing of the PEPECO apparatus with a magnetic bottle electron analyzer.

IV-K-4 First Three-Dimensional PEPECO Spectra Measured Using A New TOF-TOF Coincidence Double Electron Energy Analyzer at UVSOR

J. H. D. ELAND *(Oxford Univ. and IMS)*, **Katsuhiko OKUYAMA and Katsumi KIMURA**

By using the newly installed magnetic bottle analyzer with two independent electron flight paths on the line 3A2 at UVSOR with undulator radiation we have made the first three-dimensional PEPECO (photoelectron-photoelectron coincidence) measurements on a gas. The spectra show how Xe atoms can

lose two electrons to form Xe^{++} in different states after a hole has been created in the 4d shell. These initial experiments demonstrate that the new technique can become a powerful tool for spectroscopy of doubly-charge ions, and especially for the study of multiple electron ejection dynamics.

The magnetic bottle analyzer is a commercial unit, modified by the addition of a second electron detector to provide a time-of-flight analyzer of short path length in addition to the existing 50cm drift tube. The detection of one electron from a double ionization event within the period of UVSOR in single bunch mode allows us to identify the particular light pulse on which ionization occurred, and thus to measure the flight time of the second electron in the longer analyzer although it is much more than one period of the light source. Two electrons ejected simultaneously from a single atom are thus energy analyzed, and the energy of the final state of the doubly-charged target species is deduced by subtracting both electron energies from the photon energy. Because all electron energies are measured all the time the technique is fully multiplex, and complete two-parameter (three-dimensional) spectra are produced. Details of the spectra show whether double ionization is direct or involves intermediate states of the single-charge ion. We find that the decay of the $4d^9 5s^2 5p^6 6p\ ^2D$ state of Xe to Xe^{++} is indeed indirect but the intermediate states have not yet been identified. Figure 1 shows a plot of intensity versus the two times of flight of electrons from the excited state of Xe mentioned above.

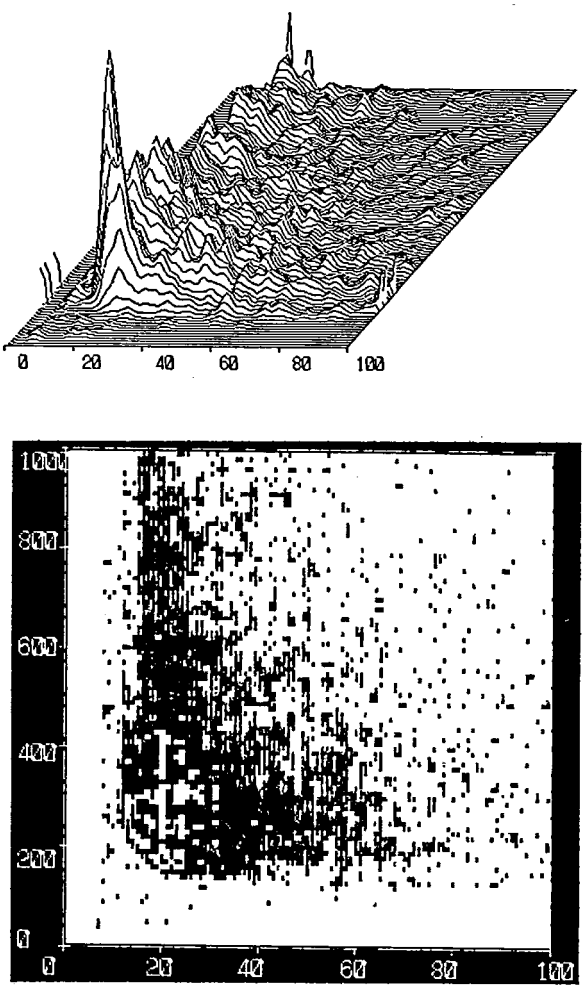

Figure 1. A three-dimensional PEPECO spectrum obtained by the undulator radiation (190.4 A; 65.1 eV), showing a plot of intensity versus the two times of flight of electrons from the above-mentioned excited state of Xe.

IV–L Production, Characterization, and Spectroscopic Studies of Molecular Complexes and Clusters

There are several techniques to investigate physics and chemistry of molecular complexes and clusters. One of the most powerful techniques for producing such weakly bound complexes is supersonic expansion of a high pressure gas through a small nozzle hole, by which one can produce a large numbers of exotic molecules. However, quantitative characterization of van der Waals complexes is hard because of its weak bonding character.

In this project we apply laser induced fluorescence spectroscopy combined with a nanosecond time resolved fluorescence technique to study dynamics of electronically excited rare gas clusters and solvated molecules of substituted anthracenes produced in a free jet expansion.

IV-L-1 Vibrational Predissociation of Rare-Gas van der Waals Complexes of 9-Methoxyanthracene

Satoshi HIRAYAMA *(Kyoto Inst. of Tech.)*, **Fujio TANAKA** *(Univ. of Osaka Prefecture)*, **and Kosuke SHOBATAKE**

[*J. Chem. Soc. Jpn.* **1989**, 1217 (1989)]

The results of an investigation of the photodissociation of the rare-gas van der Waals complexes of 9-Methoxyanthracene (MEOA), obtained by the use of both kinetic and spectroscopic techniques, are reported. The non-exponential decays which are recorded for the fragmented molecules show clearly that the dissociation from the vibronic level of 12_0^2 results in relatively high yields of vibrationless MEOA. The short-lived component becomes dominant upon increasing the excess energy of excitation. A comparison of the relative fluorescence quantum yields, calculated by using the fluorescence decay parameters, with the relative band intensities suggests that dissociation of the Ar and Kr complexes occurs in much shorter periods of time than the radiative lifetimes of the corresponding complexes. However, an appreciable fraction of the Xe lifetimes decays from the 8_0^1 vibronic level via a nonradiative pathway in which dissociation does not occur. The substantial reduction in the fluorescence lifetime of the insufficiently cooled states of MEOA, together with the data obtained for the photodissociation of complexes of 9,10-dimethoxyanthracene with rare-gas atoms, indicates that the residual energies of the vibrational predissociation are not distributed significantly among optically inactive modes.

IV-L-2 Microscopic Solvent Effects on the S_1-T_2 Intersystem Crossing of 9,10-Diphenylanthracene in Supersonic Free Jets

Fujio TANAKA *(Univ. of Osaka Prefecture)*, **Satoshi HIRAYAMA** *(Kyoto Inst. of Tech.)*, **and Kosuke SHOBATAKE**

Fluorescence excitation spectra and fluorescence decays were measured for isolated 9,10-diphenylanthracene (DPA) and its van der Waals (vdW) complexes with Ar and Xe atoms. The fluorescence lifetime of DPA at the S_1 origin is significantly shorter than the pure radiative lifetime. In contrast to the condensed phase, the intersystem crossing from S_1 to T_2 occurs in the isolated state because S_1 is located above T_2 as a result of the absence of solvation. However, it is proposed that S_1 lies below T_2 when the number of Xe atoms coordinated to DPA is increased, since the heavy-atom effect of Xe on the fluorescence lifetime which is observed for the 1:1 vdW complex disappears in the highly coordinated complexes.

IV-L-3 Electronic Relaxation in Isomers of 9,10-Dimethoxyanthracene and their Rare-Gas Complexes

Satoshi HIRAYAMA *(Kyoto Inst. of Tech.)*, **Fujio TANAKA** *(Univ. of Osaka Prefecture)*, **and Kosuke SHOBATAKE**

[*J. Phys. Chem.* (in press)]

Two types of red shift observed upon complexation of the title compound (DMEOA) with rare-gas atoms (Ar, Kr, and Xe) have revealed the existence of two stereo-isomers (cis and trans) of DMEOA. The main vibronic bands of the uncomplexed DMEOA in the range 25790 to 28630 cm^{-1} can be classified to either isomer and the fluorescence decay features and rare-gas complex stability associated with these bands examined in detail. The fluorescence lifetime of the uncomplexed molecule is 28.1 ± 0.1 ns in the electronic origin of S_1 and is rather insensitive to the excess energy, and even at the excess energy of 2835 cm^{-1} it is as long as 1.9 ± 0.1 ns. For the 12_0^1 band DMEOA exhibits isomer-dependent fluorescence lifetimes but, for the other higher vibronic levels, there is no significant difference in τ_f and 1:1 complex-band intensity between the two isomers. However, less feasible formation of higher coordination complexes is suggested for the cis-isomer. In contrast to 9-methoxyanthracene (MEOA), all the rare-gas complexes have fluorescence lifetimes between 25–33 ns and no external heavy atom effect is found at any main vibronic levels examined. photodissociation of the vdW complex and energy redistribution after dissociation are also discussed in relation to the greatly shortened fluorescence decays in partially cooled states of

DMEOA and rather insensitive excess-energy dependence of the fluorescence lifetimes when it is supercooled.

IV-L-4 Natural Radiative Lifetimes of Anthracene Derivatives and their Dependence on Refractive Index

Satoshi HIRAYAMA*, Yutaka IUCHI* *(*Kyoto Inst. of Tech.)*, **Fujio TANAKA** *(Univ. of Osaka Prefecture)*, **and Kosuke SHOBATAKE**

Fluorescence lifetimes of the electronic origins of S_1 are measured in supersonic free jets for nine anthracene derivatives. For most of the meso-di-substituted derivatives, these lifetimes are virtually equal to the natural radiative lifetimes in vacuum and they are satisfactorily related to the radiative lifetimes determined in n-hexane through a factor of n^2 (n: refractive index). This unambiguous relationship found for the anthracene derivatives will bring a long-standing debate on the refractive-index dependence of the radiative lifetime to an end. It will also provide a basis for the discussion of the dependence of the radiative lifetime on single vibronic levels.

IV-M Molecular Beam Studies of Photodissociation and Bimolecular Reaction Dynamics

In this project we investigate the dynamics of (1) photodissociation of molecules at 193 nm and (2) dissociative excitation transfer reactions involving metastable rare gas atoms. For the study of photodissociation dynamics of molecules a crossed molecular beams apparatus (MBC-I) with a rotatable mass spectrometer detector is used. For the studies of the latter project chemiluminescence spectroscopy is applied.

IV-M-1 Photodissociation Dynamics of Ethylene Sulfide at 193 nm Studied by Photofragment TOF-Mass Spectroscopy

Kiyohiko TABAYASHI and Kosuke SHOBATAKE

Photodissociation dynamics of ethylene sulfide C_2H_4S has been studied by photofragment time-of-flight (TOF) mass spectroscopy. Photofragments S (at m/e=32) and SH (at m/e=33) from the following dissociative processes, $C_2H_4S + h\nu \rightarrow S(^1D) + C_2H_4$ (1), and $\rightarrow SH + C_2H_3$ (2) have been detected. The center-of-mass (C.M.) translational energy E_t distribution of the S fragment shown in Figure 1 was found to have two (low energy (A) and high energy (B)) components, indicating that the S fragments are produced via two different dissociation mechanisms, i.e. a long lived near-statistical and a direct dissociation mechanism. The C.M. polarization dependences obtained for these components also confirm the view that the excited intermediate states dissociate with two different lifetimes.

The translational energy and angular distributions of the SH fragment are accounted for in term of a near-statistical behavior, which is consistent with the dissociation of C_2H_4S via the migration of a hydrogen

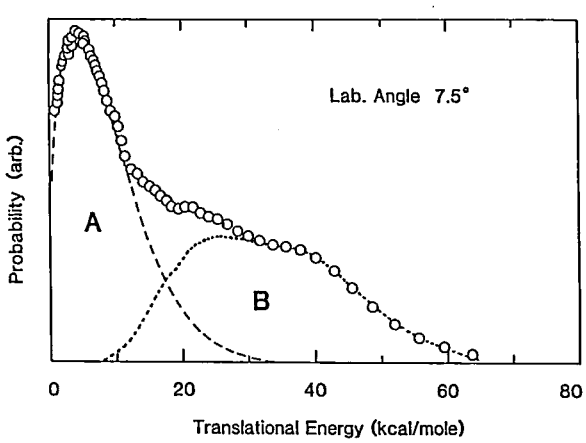

Figure 1. The C.M. translational energy distribution for the process, $C_2H_4S + h\nu \rightarrow C_2H_4 + S(^1D)$ decomposed into two components. The dashed curve represents a parametric fit of RRK-type distribution to the low energy component (A); the dotted curve shows the high energy component obtained by subtracting the lower one from the observed distribution.

atom followed by the ring opening. The total energy flows leading to products S and SH are also discussed upon laser excitation of ethylene sulfide to ($4p \leftarrow$ n) Rydberg state at 193 nm.

IV-M-2 Crossed Laser-Molecular Beam Study of Allene Photofragmentation at 193 nm

Kiyohiko TABAYASHI and Kosuke SHOBATAKE

Photofragmentation of allene at 193 nm has been investigated using a crossed laser-molecular beam apparatus equipped with a mass spectrometer detector rotatable in the plane of the two beams. Taking advantage of the present set-up which enables us to detect low recoil-velocity fragments at low laboratory scattering angles, the TOF spectra have been measured at masses (m/e) = 39 and 38. The TOF spectra measured at mass m/e = 39 and the translational energy (E_t) distributions for the main fragmentation step,

$$C_3H_4 + h\nu \rightarrow C_3H_3 + H \qquad (1)$$

are shown in Figure 1. From the appearance threshold of the TOF signals the bond dissociation energy is determined to be 100.8 ± 5.6 kcal/mole. Since the Et distribution appears to be relatively relaxed, it is fitted to an RRK-type function as is illustrated in Figure 1b.

The minor fragment mass $C_3H_2^+$ (m/e = 38) detected may be originated from either molecular H_2 elimination from the excited C_3H_4 or successive H detachment from C_3H_3 formed in step (1). The examination of the maximum recoil energy available for C_3H_2 favors the molecular H_2 elimination mechanism.

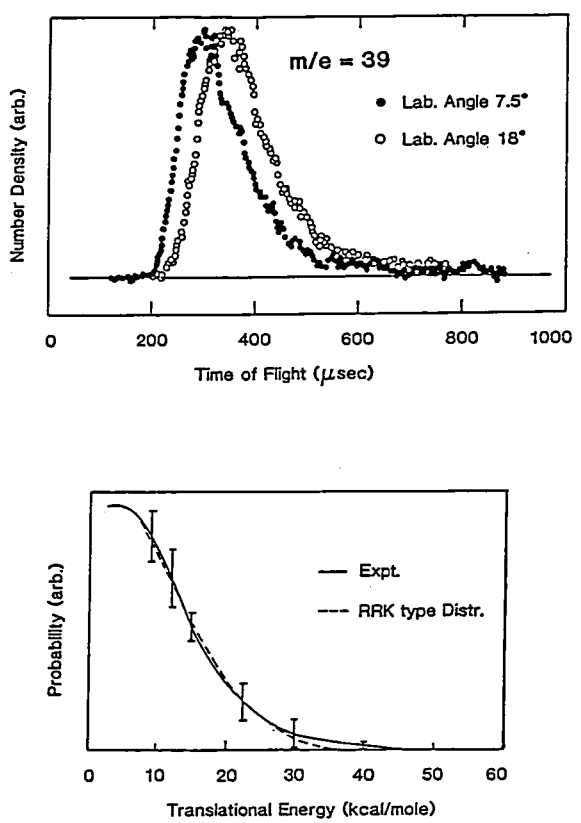

Figure 1. (a) Time-of-flight spectra of the fragment mass $C_3H_3^+$ (m/e = 39) observed at two laboratory scattering angles, 7.5° (•) and 18° (o). (b) The C.M. flux-translational energy distribution determined from the photofragment spectra measured at mass $C_3H_3^+$. The dashed curve represents a best-fit RRK-type distribution to the observed.

IV-M-3 Dissociative Excitation of Silane by Metastable Rare Gas Atoms

Kiyohiko TABAYASHI and Kosuke SHOBATAKE

Dissociative excitation processes of silane in collision with metastable rare gas atoms (Ar*, Ne*, Kr*) have been studied using crossed beam chemiluminescence technique in the collision energy range 0.08 ~ 0.25 eV. In addition to the emission arising from SiH($A^2\Delta$), those from both triplet and singlet Si* atoms have been

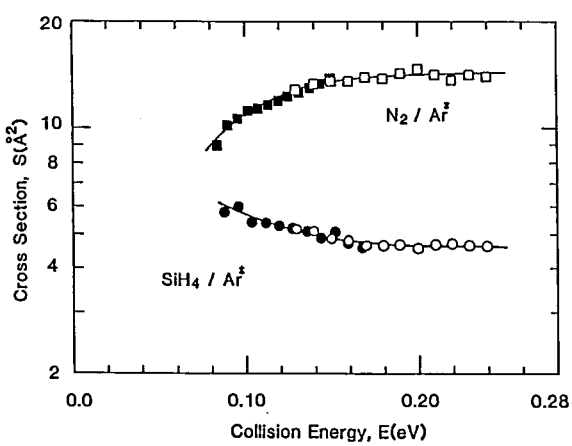

Figure 1. Figure 1. Integral cross-section S vs. collision energy for the dissociative excitation process: Ar* + $SiH_4 \rightarrow$ SiH($A^2\Delta$) + H + H_2. Each symbol corresponds to the data obtained under the same Ar* beam condition. The results for the reference Ar* + N_2 reaction are also shown.

observed with excitation of Ar* and Ne* collision. With Kr* excitation, however, no atomic emission was found. Relative intensities of the singlet/triplet atomic emission indicate the importance of the spin conservation routes for both the collisional excitation and following dissociation processes of the silane molecule.

As for a main radiative process, $Ar^* + SiH_4 \rightarrow SiH(A^2\Delta) + H + H_2$, the collision energy dependence of the integral cross section were determined using TOF energy selection method. The dissociative excitation cross-section is found to decrease as $E^{-0.26}$ over the collision energy range studied.

IV–N Vacuum UV Photochemistry of Molecules and Clusters

Photochemistry by vacuum UV (VUV) light has recently become a very active field owing to the rapid progress in and the relatively easy access to the VUV light sources such as synchrotron orbital radiation (SR) and VUV laser as well as conventional atomic resonance lines. In the present project we seek to obtain more detailed information about, 1) photodissociation dynamics of simple molecules, 2) production of emitting species from highly excited molecules, 3) excited states of clusters formed in a supersonic free-jet, and 4) excimer formation reactions in the electronically excited van der Waals molecules and clusters, applying absorption and fluorescence (polarization) spectroscopy by means of the tunable, stable, and polarized VUV light from UVSOR.

IV-N-1 Photoabsorption Spectra and Photodissociation of S_2Cl_2 in the Vacuum Ultraviolet

Ikuo TOKUE *(Niigata Univ.)*, **Atsunari HIRAYA** *(UVSOR)*, **and Kosuke SHOBATAKE**

[*Chem. Phys. Lett.* **153**, 346 (1988)]

The photoabsorption cross section and fluorescence excitation spectrum of S_2Cl_2 vapor were measured in the range 110–200 nm using synchrotron radiation. A number of broad bands observed in the 120–170 nm region are assigned as Rydberg transitions. The fluorescence which starts to appear at 155.0 ± 1.6 nm is attributed to the S_2 ($B^3\Sigma_u^- - X^3\Sigma_g^-$) band. As for the formation of emitting species, the process of $S_2(B)$ +2Cl is predominant for excitation in the 120–155 nm region, whereas another emission appears below 130 nm.

IV-N-2 Photoexcitation of Dimethyl Sulfide and Dimethyl Disulfide in the Vacuum Ultraviolet Region: Rydberg States and Photofragment Emissions

Ikuo TOKUE *(Niigata Univ.)*, **Atsunari HIRAYA** *(UVSOR)*, **and Kosuke SHOBATAKE**

[*Chem. Phys.* **130**, 401 (1989)]

Photoabsorption cross section and fluorescence excitation spectra of dimethyl sulfide (DMS) and dimethyl disulfide (DMDS) vapors have been studied in the 110–220 nm region using synchrotron radiation. For DMS, a new Rydberg series originating from the ns orbital is identified. A number of broad bands from DMDS are assigned as Rydberg transitions. Emissions from DMS and DMDS are assigned as the $CH_3(\tilde{A}\text{-}\tilde{X})$ band. For DMDS, another emission which is attributable to the S_2(B-X) band appears in the excitation below 125 nm. Photodissociation processes forming the excited fragments are discussed.

IV-N-3 Photoabsorption spectrum and CCl_2 ($\tilde{A}^1B_1$) Radical Formation in the VUV Excitation of C_2Cl_6

Toshio IBUKI *(Kyoto Univ.)*, **Atsunari HIRAYA** *(UVSOR)*, **and Kosuke SHOBATAKE**

[*Chem. Phys. Lett.* **157**, 521 (1989)]

The photoabsorption cross section and fluorescence excitation spectra of C_2Cl_6 have been investigated in the 105–200 nm region using synchrotron radiation as a light source. The absorption bands observed are assigned as the Rydberg excitations. The fluorescence yield starts at about 160 nm and increases to $\Phi = 0.18$

at 111.5 nm. The emitting species is $CCl_2(\tilde{A}^1B_1 \rightarrow \tilde{X}^1A_1)$; its radiative lifetime was determined to be 1.83 ± 0.02 μs.

IV-N-4 Formation of NH($c^1\Pi$), NH($A^3\Pi$) and NCO($A^2\Sigma$) in the VUV Photolysis of HNCO

Kenkichi UNO*, Takumi HIKIDA* *(*Tokyo Inst. of Tech.)*, **Atsunari HIRAYA** *(UVSOR)*, **and Kosuke SHOBATAKE**

[*Chem. Phys. Lett.* (in press)]

Photodissociative excitation processes of gaseous HNCO are studied in the wavelength region of 107 and 180 nm using synchrotron radiation as a light source. Fluorescence excitation spectra of photofragments, NH($c^1\Pi$, $A^3\Pi$) and NCO($A^2\Sigma$) have been measured under near collision-free conditions. The quantum yields for formation of these radicals are also determined.

IV-N-5 Vacuum Ultraviolet Absorption Spectra of Thiirane and Thietane

Ikuo TOKUE *(Niigata Univ.)*, **Atsunari HIRAYA** *(UVSOR)*, **and Kosuke SHOBATAKE**

[*J. Chem. Phys.* **91**, 2808 (1989)]

Photoabsorption cross-sections of cyclic S containing compounds, thiirane (C_2H_4S) and thietane (C_3H_6S) in the vapor phase have been studied in the 110–240 nm region using synchrotron radiation. A number of peaks from thiirane and thietane are arranged into four and five Rydberg series, respectively, converging to the first ionization potential. For both molecules many Rydberg peaks which possess vibronic progressions are observed. The vibrational progressions from thietane are assigned to the CH_2 wagging(ν_4) and CS sym. stretching (ν_5) modes. For thietane, the CH_2 wagging (ν_5) and CS sym. stretching (ν_7) modes of the excited states are discussed on the basis of *ab initio* calculations.

IV-N-6 Quenching of the HCl($2^1\Sigma^+$) Ion-Pair State by Xe

Atsunari HIRAYA, Kosuke SHOBATAKE, Teiichiro ICHIMURA *(Tokyo Inst. of Tech.)*, **and Robert J. DONOVAN** *(IMS and Univ. of Edinburgh)*

The formation of XeCl*(B) in the reaction between HCl* ($2^1\Sigma^+$) and Xe (reaction 1) was found to be difficult in the laser two-photon excitation techniques, comparing with the reaction between HCl and Xe* (reaction 2). We report the use of tunable vacuum ultraviolet synchrotron radiation for one-photon excitation of HCl($2^1\Sigma^+$ state) and the study of its quenching by Xe in a jet. By monitoring emission from XeCl(B→X) after eliminating emission from HCl($2^1\Sigma^+$), we were able to detect only very low levels of emission from XeCl*(B) following excitation of HCl($2^1\Sigma^+$), whilst large signals were observed following excitation of Xe, under the same conditions (se Figure 1). After allowing for the relative excitation efficiencies for HCl and Xe, we estimate that the

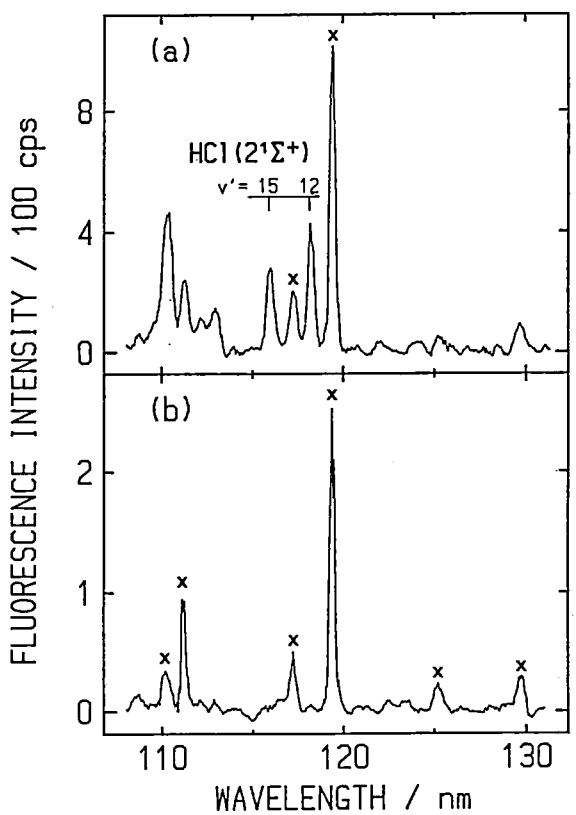

Figure 1. Emission excitation spectra of HCl and Xe mixture (a) with and (b) without filter (UV-D35, band-path 270–440 nm). Xe lines are indicated by crosses. Mixing condition: HCl/Xe = 1.1 (total stagnation pressure = 140 Torr).

cross-section for reaction (1) is less than 0.04 smaller than that for reaction (2). This result is surprising in view of the very large cross-section observed for noble gas halide formation from reactions involving halogen and interhalogen ion-pair states and Xe. The only plausible explanation that we can offer at this time is that the dominant quenching process for $HCl(2^1\Sigma^+)$ by Xe involve intramolecular energy transfer, possibly leading to dissociation of HCl or, less likely, excitation transfer to Xe.

IV–O Synchrotron Orbital Radiation-Assisted Surface Reactions

Synchrotron orbital radiation (SR) is still a new light source from the viewpoint of promoting chemical reactions on solid surfaces although lithography of resist materials by means of SOR has been known for about a decade. In this project we explore the possibilities of promoting surface reactions, such as etching reactions, or making new types of thin films using SR as a light source, and furthermore seek to clarify the mechanisms of photochemical reactions which occur on solid surfaces. The experiments are done using an apparatus for photochemical surface reactions installed on the Beam Line BL8A or BL31 at the UVSOR facility. when the apparatus is connected to the beam line BL8A, unfocused synchrotron radiation is irradiated upon the solid sample at 5.85 m from the source point. On the beam line BL3A1 pseudo-monochromatic undulator radiation is used for the etching reactions as well as photochemical vapor deposition.

IV-O-1 Synchrotron Radiation-Assisted Etching of SiO_2 With SF_6 Using Undulator Radiation.

Kosuke SHOBATAKE, Haruo OHASHI, Akira Yoshida *(Tech. Univ. of Toyohashi)*, **Nobuo HAYASAKA** *(Toshiba Corp.)*, **Hiroshi KUME** *(Niigata Univ.)*, **Kazutoshi Fukui*, Makoto Watanabe*, and Atsunari HIRAYA*** *(*UVSOR)*

The photo-assisted etching reaction of SiO_2 surface is studied using undulator light from beam line BL3A1. We have obtained the pressure and wavelength dependences of the etch rates of SiO_2 with SF_6 gas using undulator radiation (UR), because it provides pseudo-monochrotamic light, which simplifies the interpretation of the results. Figure 1 illustrates the etch rates of SiO_2 by SF_6 against the SF_6 pressure for the UR at 251 and 143 Å. It is noted that the pressure dependence of etch rate reflects the light intensity profile irradiated upon the SiO_2 surface through 4.9 cm SF_6 gas path length. The rate of F atom production gives somewhat different pressure dependence from that of the irradiated light upon the surface. From these results one can conclude that surface excitation by UR is a very important step in the etching reaction of SiO_2.

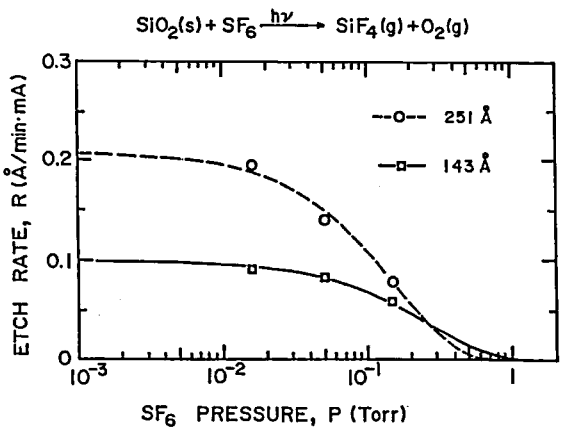

Figure 1. Etch rate as a function of SF_6 pressure for undulator radiation at 142 and 251 Å. The curves correspond to the calculated transparent light intensity irradiated upon the SiO_2 surface fitted to the experiment.

IV-O-2 Synchrotron Radiation-Assisted Etching Reactions of Semiconductor Materials: Polycrystalline Silicons Using Undulator Radiation

Kosuke SHOBATAKE, Haruo OHASHI, Nobuo HAYASAKA *(Toshiba Corp.)*, **Hiroshi KUME** *(Niigata Univ.)*, **and Atsunari HIRAYA** *(UVSOR)*

In this study the photo-assisted etching reactions of various polycrystalline Si surfaces are studied using undulator light as a light source. For most of the present experiments was used the undulator radiation from the beam line BL3A1 for the gap lengths 70 mm (142 Å) and 33 mm (wavelength of the 1st order light: 251 Å. We have measured the pressure and wavelength dependences of the etch rates of polycrystalline Si samples with Cl_2 gas. Figure 1 shows the etch rates versus Cl_2 pressure in the range from 0.016 to 1.0 Torr at 251 Å for six polycrystalline samples, three P-doped n-type, two B-doped p-type, and undoped poly-Si samples. The pressure dependence of the etch rate differs quite a lot from one sample to another. We find that the etch rate decreases with decreasing free electron density in the Si sample.

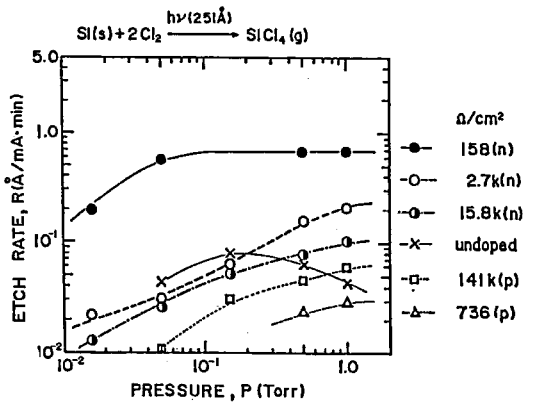

Figure 1. Etch rate vs. Cl_2 pressure for the SR-assisted etching reaction of polycrystalline Si samples.

IV–P Synthesis and Electrical Properties of Organic Conductors

In order to obtain the knowledge required for the further development of new organic conductors, charge-transfer complexes and radical salts of OCNAQ and phthalocyanines have been prepared and their structural and electrical properties have been studied.

IV-P-1 Charge Transfer Complexes Based on the Twin-TCNQ-Type Acceptor 11,11,12,12,13,13,-14,14-Octacyano-1,4:5,8-anthradiquinotetramethane (OCNAQ)

Tamotsu INABE, Tsutomu MITSUHASHI *(Univ. of Tokyo)*, **and Yusei MARUYAMA**

[*Bull. Chem. Soc. Jpn.*, **61**, 4215 (1988)]

Charge transfer complexes of OCNAQ with pyrene, PT (phenothiazine), TMTTF (tetramethyltetrathiafulvalene), TTT (5,6:11,12-bis(epidithio)naphthacene), and TTF (tetrathiafulvalene) have been prepared. The pyrene and PT complexes are electrically insulating and the ground state is neutral. In most of the other complexes OCNAQ is fully charged. One of the TTT complexes, $(TTT)_2OCNAQ(DMF)$, where DMF is *N,N*-dimethylformamide, has been found to show metallic conductivity. A structural study has revealed that short S···N contacts exist between TTT and OCNAQ, in addition to one-dimensional TTT stacks. This transverse interaction has been demonstrated by the small anisotropy of the conductivity. The 2:1 TTF complex is also metallic down to 43 K, at which point a metal-to-insulator transition occurs. A structure analysis and thermoelectric power data suggest that the charge conduction in this crystal takes place not only through the TTF stacks but also through a two-dimensional network of the OCNAQ molecules.

IV-P-2 Crystal Structure of the Electrochemical Product of Potassium Dicyanophthalocyaninatocobalt(III). Novel Two-Dimensional Stacking Interaction of Phthalocyanine

Tamotsu INABE and Yusei MARUYAMA

[*Chem. Lett.*, **1989**, 55]

The crystal obtained by electrocrystallization of potassium dicyanophthalocyaninatocobalt(III), $K[Co(Pc)(CN)_2]$, in acetonitrile has been found to be a cation deficient salt, $K[Co(Pc)(CN)_2]_2(CH_3CN)_5$. The structural study has indicated that partly overlapped phthalocyanine rings form a two-dimensional sheet.

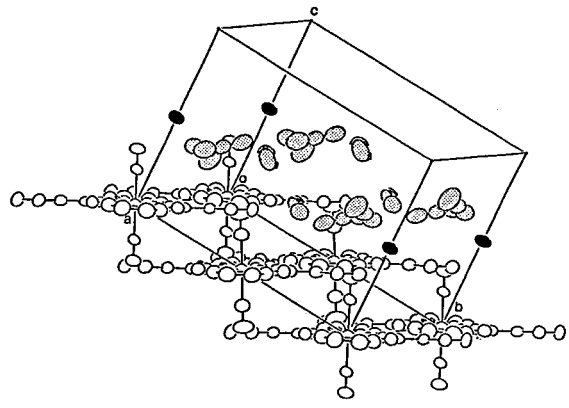

Figure 1. Crystal structure of $K[Co(Pc)(CN)_2]_2(CH_3CN)_5$.

IV-Q Synthesis and Characterization of Proton-Transfer/ Charge-Transfer System

Hydrogen-bonded systems, in which the proton transfer is coupled with the π-electron configurational change, are studied. If the interaction between molecules is sufficiently strong in the crystalline state, the proton transfer is expected to modulate the solid-state properties, especially expected is the coupling between the electronic properties and proton motion. In order to examine such a possibility, compounds which have a framework of salicylideneaniline have been synthesized as the intramolecular proton transfer system. The similar possibilities are examined for the intermolecular hydrogen-bonded systems of the charge transfer complexes based on 1,6-pyrenediamine.

IV-Q-1 Structure and Optical Properties of a Thermochromic Schiff Base. Low-Temperature Structural Studies of the *N,N'*-Disalicylidene-*p*-phenylenediamine and *N,N'*-Disalicylidene-1,6-pyrenediamine Crystals

Tamotsu INABE, Naomi HOSHINO *(Hokkaido Univ.)*, Tadaoki MITANI, and Yusei MARUYAMA

[*Bull. Chem. Soc. Jpn.*, **62**, 2245 (1989)]

The crystal structure of *N,N'*-disalicylidene-*p*-phenylenediamine (BSP) has been determined at 108 K. This compound shows a thermochromic-type behavior in the crystalline state; this chromism has been interpreted in terms of an intramolecular proton transfer from the hydroxyl oxygen to the imine nitrogen through the O-H···N hydrogen bond. In comparison with the room-temperature structure, no significant differences in the molecular structure and the molecular packing in the lattice have been observed. The room-temperature and low-temperature structures of another *N*-salicylideneaniline derivative, *N,N'*-disalicylidene-1,6-pyrenediamine (DSPY), have also been determined. In contrast to BSP, the absence of a thermal proton-transfer process in DSPY is suggested by optical measurements. Comparative studies of these two compounds indicate that a conjugation system which is not included in a π-electron configurational change by the proton transfer must be coplanar with the hydrogen-bonded chelate ring for the thermal proton transfer.

IV-Q-2 Reversible Self-Isomerization Induced by Proton Transfer: Correlation between the Structures and Optical Properties

Tamotsu INABE, Naomi HOSHINO *(Hokkaido Univ.)*, **Tadaoki MITANI, Hiroshi OKAMOTO, Isabelle GAUTIER-LUNEAU, and Yusei MARUYAMA**

N-Salicylideneaniline derivativies and their charge transfer complexes have been prepared, and subjected to structural and optical studies. It is demonstrated that the intramolecular proton transfer is strongly influenced by the electronic state of the molecule, suggesting possibilities to create a novel type of electrical conduction system.

IV-Q-3 Structure and Optical Properties of a Thermochromic Schiff Base. Effect of Charge Transfer Interaction on the Proton Transfer

Tamotsu INABE, Isabelle GAUTIER-LUNEAU, Naomi HOSHINO *(Hokkaido Univ.)*, **Kaoru OKANIWA, Hiroshi OKAMOTO, Tadaoki MITANI, and Yusei MARUYAMA**

N-Tetrachlorosalicylideneaniline and *N*-tetrachlorosalicylidene-1-pyrenylamine have been synthesized and subjected to structural and optical studies in the crystalline state. Although both compounds are derivatives of salicylideneaniline, the thermochromic behaviors are modified by the introduction of electronegative substituents on the salicylaldehyde site. The former crystals show a thermochromic-type behavior; the color change is observed as a shift of the absorption edge by temperature. On the other hand, the latter crystals exhibit only a slight change in the absorption spectra by temperature. The crystallographic studies indicate that the intermolecular charge transfer interaction operates only in the latter crystals. This CT interaction is supposed to cause the different behavior in thermochromism.

IV-Q-4 Charge Transfer Complexes of Salicylideneaniline Derivatives with Various Acceptors. The Influence on Proton Transfer

Tamotsu INABE, Naomi HOSHINO *(Hokkaido Univ.)*, **Isabelle GAUTIER-LUNEAU, Hiroshi OKAMOTO, Kaoru OKANIWA, Tadaoki MITANI, and Yusei MARUYAMA**

Some salicylideneaniline derivatives have been employed as a donor component to form charge transfer complexes with various acceptors. In most of the cases the equilibrium position of the proton changes from the oxygen side to the nitrogen side upon the complex formation. One exceptional case, DSPY-TCNQ, has been found and the structural relationship is now being studied. The possibility of coupling between the proton transfer and the π-electron systems, especially conduction electron systems, is continuously investigated.

IV-Q-5 Charge Transfer Complexes with Intermolecular Hydrogen-Bonds

Tamotsu INABE, Hiroshi OKAMOTO, Kaoru OKANIWA, Tadaoki MITANI, and Yusei MARUYAMA

In order to examine the possibility of coupling between the proton motion and the conduction electron system in the intermolecular hydrogen-bonded systems, charge transfer complexes of pyrenediamine are prepared and subjected to structural, electrical, and optical studies. The complexes so far structurally studied are two forms of 1,6-pyrenediamine(DAP)-*p*-chloranil, two forms of DAP-*p*-bromanil, and DAP-TCNQ. All of them have a hydrogen-bond network in the lattice. The relationship between the hydrogen-bond structure and the electrical properties is now investigated.

IV-R Ultra-Thin Organic Film Systems Prepared by Molecular Beam Epitaxy Technique

As a strategy for the development of new types of organic materials, we have undertaken the fabrication of ultra-thin organic multi-layer film systems with an "MBE" technique. We are expecting new types of charge transfer compounds and/or intercalation compounds (hybrid compounds), and also the realization of novel 2-dimensional materials in such systems. As an initial step of the study, we have prepared ultra-thin well-oriented monolayers on several substrates.

IV-R-1 The Structure and Properties of Phthalocyanine Films Grown by Molecular Beam Epitaxy Technique
Part I. Preparation and Characterisation

Anthony John DANN *(Univ. of Nottingham and IMS)*, **Hajime HOSHI, and Yusei MARUYAMA**

[*J. Appl. Phys.* in press]

Ultra-thin films of the cofacially stacked F-bridged Al-phthalocyanine polymer, $(AlPcF)_n$, have been grown using the highly controlled technique of MBE. A parallel orientation of the polymer backbone to the substrate surface occurs in films on silicon and quartz, but epitaxy is not apparent. On single crystal alkali-halide substrates, the backbone is perpendicular to the substrate surface and an epitaxial relationship exists which is influenced by the interaction between the substrate and phthalocyanine molecule. The TEM studies indicate that the most highly ordered films are produced on KBr(100) which have good continuity and unidirectional crystallite orientation.

IV-R-2 The Structure and Properties of Phthalocyanine Films Grown by Molecular Beam Epitaxy Technique
Part II. UV/Visible Spectroscopy Study

Hajime HOSHI, Anthony John DANN *(Univ. of Nottingham and IMS)*, **and Yusei MARUYAMA**

[*J. Appl. Phys.* in press]

Ultra-thin films of F-bridged Al-phthalocyanine polymer, $(AlPcF)_n$, grown by the MBE technique show unusual spectroscopic properties which can be described by the possibility of pseudomorphic layer formation at the thin film/substrate interface. A change in the electronic structure of the molecules of this layer is presumed to occur. The existence of the layer is directly related to the degree of epitaxy.

IV-R-3 Epitaxial Growth of Lu-(Phthalocyanine)$_2$ Film on (Al-phthalocyanine -F)$_n$ Film by MBE

Hajime HOSHI, Anthony DANN *(Univ. of Nottingham and IMS)*, **and Yusei MARUYAMA**

A unidirectionally well-oriented film of $(AlPcF)_n$ can be formed on a KBr single crystal substrate. In the case of $Lu(Pc)_2$, however, the film on KBr is found to be bidirectional. If we evaporate $Lu(Pc)_2$ on a unidirectional $(AlPcF)_n$ film on KBr, it forms a unidirectionally well-oriented film. This fact means that the structure of films is epitaxially controllable depending on the substrate film. This type of films could be a relevant system to prepare multi-layered organic films.

IV–S Black Phosphorus

Black phosphorus is a layered structure semiconductor. We have prepared iodine intercalated compounds of black phosphorus and revealed their metallic character. Recently, inclusion or doping of silicon or germanium to black phosphorus has been undertaken.

IV-S-1 Electrical Conductivity of Black Phosphorus-Germanium Compounds

Yusei MARUYAMA, Tamotsu INABE, Lin HE *(General Institute for Colored Metal, Beijing, and IMS)*, **Ichimin SHIROTANI** *(Muroran Inst. of Technology and IMS)*, **and Martin Richard WILLIS** *(Univ. of Nottingham)*

A new material, black phosphorus-germanium, has been prepared, and the temperature dependence of electrical resistivity has been measured at low temperature region. Germanium was introduced in black phosphorus by two ways. One is the inclusion in the course of black phosphorus crystal preparation by a bismuth-flux method, and the other is ion-implantation to the surface of black phosphorus single crystals

prepared by a high pressure technique. The former crystals apparently show a metallic behavior done to 1.5 K, but the latter ones always have a fairly high rise (but not semiconductive) in the resistivity below about 50 K. Inclusion of germanium was confirmed by ICP analysis for the former and by RBS for the latter. Further analysis of the structure and properties are now under way.

IV–T Preparation and Characterization of Metal Oxide High T_c Superconductor Films

After the discovery of novel high T_c superconductors, a lot of works including the film preparation have been carried out. We have started to fabricate thin films of such superconductors by a sputtering method and an electron-beam evaporation technique with the purpose of searching for new composition, structures, and elements in high T_c superconductors.

IV-T-1 Preparation of $(Bi_{1-x},Pb_x)_2Sr_2Ca_3Cu_4O_y$ Superconducting Film by a Single Composite Target Sputtering Method

Yoichiro KAWAI *(Toyota Motor Corp. and IMS)*, **Toshifumi TERUI, and Yusei MARUYAMA**

Thin films of the $(Bi_{1-x},Pb_x)_2Sr_2Ca_3Cu_4O_y$ phase which is difficult to be realized in bulk specimens have been prepared by a single composite target sputtering method. Although the obtained film seems to be of a single phase by an X-ray analysis, the residual resistivity at low temperature has still a semiconducting character below the sharp drop near 86 K.

IV-T-2 Tunneling Spectroscopic Study of Y-Ba-Cu-O and Bi-Sr-Ca-Cu-O Films Prepared by Sputtering Method

Yoichiro KAWAI *(Toyota Motor Corp. and IMS)*, **Yusei MARUYAMA, Toshifumi TERUI, and Tamotsu INABE**

Thin films of $YBa_{2.1}Cu_{2.9}O_y$ and $Bi_{2.3}Sr_{2.0}CaCu_{1.9}O_y$ have been prepared by RF-magnetron sputtering with using simple targets which are composed of mixed powder of each component oxide material. Both films show high *c*-axis orientation and superconductivity as deposited condition. A tunneling spectroscopic study has also revealed the superconducting parameters, such as gap energy, 2Δ, of both films.

IV-T-3 La-Sr-Cu-O Superconducting Thin Films Preparation by MBE with Multi Electron-Beam Gun Sources

Toshifumi TERUI, Yoichiro KAWAI *(Toyota Motor Corp. and IMS)*, **Robert John FLEMING** *(Monash Univ. and IMS)*, **and Yusei MARUYAMA**

La-Sr-Cu-O system seems to have crucially important physical aspects in the study of high T_c metal oxides superconductors. In this point of view, we have undertaken to construct various kinds of La-Sr-Cu-O system, especially focusing to $La_2SrCu_2O_6$ series, by MBE technique with multi electron-beam gun sorces. The equipment has been already set up and the preparation and characterization are now under way.

IV–U High Temperature Oxide Superconductors

At the very beginning of the study on the high-T_c oxides, we felt through the electron tunneling experiment and the estimation of the coherence length, almost all of their superconducting characteristics except for the very high

transition temperatures could be explained within the framework of BCS's mean field description, that is, the qualitative superconducting behaviors did not depend on the origins of the electron-electron pairing force. Therefore, for the assignment of the mechanism of the superconductivity or the origin of the attractive force, it was necessary to first accumulate various data on the detailed properties of the systems. Then, continuous effort has been made in this field. We have studied the transport, thermal, magnetic and optical properties. Structure determination by X-ray diffraction and neutron inelastic scattering to clarify the dynamical properties of the spins at the Cu sites have also been carried out. We also paid much attention to the correct characterization of the used specimens, where electron probe micro analyzer (EPMA) and SQUID magnetometer were quite powerful. As the result of these studies, the electronic natures and other characteristic properties have essentially been, at least experimentally, understood and now, we feel that on the basis of these knowledge, we are moving to the new stage, where we have to clarify in what kinds of the behaviors, the clear difference can be found between usual superconductors and the high-T_c oxides. In this respect, our recent studies seem to have actually revealed certain difference of the superconducting properties between them. Along the same line, detailed and careful experiments are underway. Below, the abstract of the published papers and the preprints are mainly shown.

IV-U-1 Neutron Scattering Study of Soft Optical Phonon in $La_{2-x}Sr_xCuO_{4-y}$

T.R. THURSTON*, R.J. BIRGENEAU*, D.R. GABBE*, H.P. JENSSEN*, M.A. KASTNER*, P.J. PICONE*, N.W, PREYER*, J.D. AXE, P. BONI**, G. SHIRANE**, M. SATO, K. FUKUDA and S. SHAMOTO** *(*Massachusetts Institute of Technology, **Brookhaven National Laboratory)*

[*Phys. Rev.* **B39** 4327 (1989)]

The soft optical phonons associated with the tetragonal-to-orthorhombic structural phase transition in $La_{2-x}Sr_xCuO_{4-y}$ have been investigated using inelastic-neutron-scattering techniques. Single crystals with Sr concentrations of x=0, 0.08, and 0.14 were studied. Both branches of the doubly degenerate X-point phonon which go soft at the tetragonal-to-orthorhombic transition have been observed in the orthorhombic phase. In all three samples one branch hardens, while the other remains relatively soft with behavior indicative of a further incipient structural phase transition. We identify the hard and soft branches of the orthorhombic phase as zone-center and zone-boundary phonons, respectively. The zone-center mode has A_g symmetry and is, consequently, Raman active. The relation of these measurements to other structural properties and to the superconductivity in $La_{2-x}Sr_xCuO_{4-y}$ is discussed.

IV-U-2 Neutron Scattering Studies of Magnetic Excitations in $La_{2-x}Sr_xCuO_4$

M.A. KASTNER*, A. AHARONY, R.J. BIRGENEAU*, Y. ENDOH†, K. FUKUDA, D.R. GABBE*, Y. HIDAKA††, H.P. JENSSEN*, T. MURAKAMI††, M. ODA††, P.J. PICONE*, M. SATO, S. SHAMOTO, G. SHIRANE§, M. SUZUKI††, T.R. THURSTON* and K. YAMADA†** *(*Massachusetts Institute of Technology, ** Tel Aviv Univ., † Tohoku Univ., ††NTT Electrical Communication Laboratory)*

[*International Symposium on the Electronic Structure of High-T_c Superconductors, Rome*]

The results of recent neutron scattering studies on $La_{2-x}Sr_xCuO_4$ are reviewed. For x=0 the material is an antiferromagnetic insulator, and the spins in the CuO_2 sheets are well-described by the 2D S=1/2 square lattice Heisenberg model. With increasing x the Néel state is destroyed and is replaced at low temperatures, at least for samples which are nonmetallic or have low superconducting T_c's, by a spin glass. The instantaneous correlations as well as those of the glass are incommensurate with the crystal lattice. The spin-spin correlation length in the doped CuO_2 sheets equals the average separation between the holes which ultimately carry the supercurrent.

IV-U-3 Recent Experimental Studies on High-T_c Oxides at IMS

M. SATO, M. SERA, S. SHAMOTO, M. ONODA, S. KONDOH, K. FUKUDA and Y. ANDO

[*Proc. 2nd NEC Conf. Hakone*, 1988, *Springer Verlag* p275]

In this article, the absence of the T-linear term in the low temperature specific heat of $Bi_4Sr_3Ca_3Cu_4O_y$, which first cleared out the long time belief of the existence of the contribution of the low energy spin excitations in the high-T_c oxides was reported. It also reported the anisotropic thermoelectric power of La- and Y- systems. The electronic nature of $(Ba,K)BiO_3$ was also discussed and the clear difference between the magnetic properties of the Bi and the Cu oxides was pointed out.

IV-U-4 Transport and Magnetic Anomalies at the Structural Transition to the New Low Temperature Phase in $La_{2-x}Ba_xCuO_4$

M. SERA, Y. ANDO, S. KONDOH, K. FUKUDA, M. SATO, I. WATANABE*, S. NAKASHIMA* and K. KUMAGAI* *(*Hokkaido Univ.)*

[*Solid State Commun.* **69** 851 (1989)]

Electrical resistivity, Hall coefficient, thermoelectric power and magnetic susceptibility of $La_{2-x}Ba_xCuO_4$ have been measured. In all these quantities, drastic anomalies have been found below $\sim 60K$ in a narrow Ba concentration region around $x=0.12$, where the superconducting transition temperature is reported by Moodenbaugh et al. to have a significant dip as a function of x. The anomalies are associated with the structural transition to the new low temperature phase recently reported by Axe et al. The electronic state in the new phase is very different from that in the high temperature orthorhombic phase and the superconducting transition temperature is largely suppressed.

IV-U-5 NORMAL STATE PROPERTIES OF $La_{2-x}Sr_xCUO_4$ and $La_2SrCu_2O_y$

Y. ANDO, M. SERA, S. YAMAGATA, S. KONDOH, M. ONODA and M. SATO

[*Solid State Commun.* **70** 303 (1989)]

Electrical resistivities, magnetic susceptibilities, Hall coefficients and thermoelectric powers of the $La_{2-x}Sr_xCuO_4$ ($0.15<x<0.50$) system and $La_2SrCu_2O_y$ have been measured. For $La_{2-x}Sr_xCuO_4$, qualitative natures of these quantities in the region of $x<0.3$, where the high-T_c superconductivity occurs, are quite different from those in $x=0.3$, where the compounds are metallic but do not exhibit the superconductivity. These differences are discussed in relation to the x-dependence of the electronic state of the system. The behaviors of these quantities of $La_2SrCu_2O_y$ which does not exhibit superconductivity are quite similar to those of $La_{2-x}Sr_xCuO_4$ with $x>0.30$. The inverse of R_H has been found to be linear in temperature T, which gives us an evidence that the relation $R_H^{-1} \propto T$ is not characteristic of high-T_c oxide superconductors.

IV-U-6 Crystal Structure of Superconducting $LnBaAeCu_3O_y$ (Ln=La, Nd: Ae=Ca, Sr)

H. FUJISHITA*, S. SHAMOTO, M. ONODA and M. SATO *(*Kanazawa Univ.)*

[*Jpn. J. Appl. Phys.* **28** 754 (1989)]

Crystal structures of $LaBaCaCu_3O_y$, $NdBaCaCu_3O_y$ and $LaBaSrCu_3O_y$ were analyzed by powder X-ray Rietvelt profile analysis method. Their chemical formulae were different from the compositions of the raw materials due to the formation of impurities. They were obtained as $La_{1.23}Ba_{1.23}Ca_{0.54}Cu_3O_y$, $Nd_{1.26}Ba_{1.26}Ca_{0.48}Cu_3O_y$ and $La_{1.14}Ba_{1.14}Sr_{0.72}Cu_3O_y$, respectively. Ca^{2+} or Sr^{2+} ions were found to enter not only Ba^{2+} sites but La^{3+} or Nd^{3+} sites as well. The occupancy of Ca^{2+} or Sr^{2+} at La^{3+} or Nd^{3+} sites was found to correlate with their ionic radii.

IV-U-7 Origins of the Electronic States near the Fermi Level in High-T_c Superconductors

A. FUJIMORI*, H. EISAKI, H. TAKAGI**, S. UCHIDA** and M. SATO** *(*Department of Physics, Univ. of Tokyo, **Engineering Research Institute, Univ. of Tokyo)*

[*Phys. Rev.* **B40** 7303 (1989)]

We have studied superconducting and insulating Cu-oxide systems by photoemission spectroscopy. The emission feature near the Fermi level (E_F) for $Bi_2(Sr,Ca)_3Cu_2O_{8+\delta}$ remains unchanged when hole carriers are depleted by Y-substitution for Ca. A similar feature is observed also for insulating $Sr_2CuO_2Cl_2$. These facts suggest that the feature near E_F in the Bi compounds are due to states which are split of out of the oxygen p band, possibly through hybridization with Cu d^8 states, and cannot be due to a Kondo-type resonance and resulting renormalized heavy-electron band states. Other origins for the states near E_F in $La_{2-x}Sr_xCuO_4$ and $YBa_2Cu_3O_{7-\delta}$ are also discussed.

IV-U-8 Normal State Properties and Oxygen Isotope Effect of (Ba,K)BiO_3

S. KONDOH, M. SERA, Y. ANDO and M. SATO

[*Physica* **C157** 469 (1989)]

Experimental results of Hall effect, thermoelectric power and magnetic susceptibility of the Cu-free high-T_c oxides, (Ba,K) BiO_3 are presented. It is shown that the electronic nature of (Ba,K)BiO_3 is quite different from those of high-T_c oxides with CuO_2 planes. One of the remarkable differences between the Bi and Cu systems is that the charge carriers of the former are electrons with small effective mass, while the charge carriers of the latter are holes with large effective mass. We also measured the effect of oxygen isotope substitution on its T_c, where we first synthesized BaO_2, KO_2 and Bi_2O_3 by using ^{16}O and ^{18}O in parallel, and then the superconducting oxide (Ba,K)BiO_3 was synthesized from these oxides, which guaranteed the complete substitution of ^{16}O by ^{18}O. A large oxygen isotope effect (α=0.35) suggests that the usual phonon mediated pairing mechanism is working in the present system.

IV-U-9 EPR Study on Dynamics of Electrons in Superconducting and Normal Metallic $(La_{2-x}Sr_x)_2CuO_{4-\delta}$ System

M. ONODA and M. SATO

[*Solid State Commun.* **70** 309 (1989)]

An EPR study was carried out for high-T_c superconducting and normal metallic $(La_{1-x}Sr_x)_2CuO_{4-\delta}$ system, where magnetic Mn ions were doped as a microscopic probe. A distinct change of the relaxation rates was found at the transition from the superconducting to normal metallic phase with increasing x. It is attributable to the difference between the magnitudes of spin fluctuation in these phases. The Korringa relation seems to hold for the normal metallic phase.

IV-U-10 Oxygen Isotope Effect of Superconducting $(Nd_{1-x}Ce_x)_2CuO_{4-\delta}$ System

M. ONODA, S. KONDOH and M. SATO

[*Solid State Commun.* **70** 1141 (1989)]

The effect of oxygen isotope substitution on the transition temperature T_c of a superconducting $(Nd_{1-x}Ce_x)_2CuO_{4-\delta}$ system was studied, where the special synthetic method was taken to minimize ambiguous factors on the oxygen concentration and to guarantee the complete substitution of ^{16}O by ^{18}O. The isotope exponent α in the relationship of $T_c \propto 1/M^{\alpha}$ was estimated to be less than 0.15 by magnetic susceptibility measurements.

IV-U-11 Physical Properties of (Ba,K)BiO_3

M. SATO, S. KONDOH and M. SERA

[*Proc. IBM-Japan Symposium on Strong Correlation and Superconductivity* 1989, *Hakone, Springer Verlag* p341]

In order to see if the mechanism of the superconductivity of (Ba,K)BiO_3 is common to that of Cu-oxide systems, the transport and magnetic properties of (Ba,K)BiO_3 were measured and the oxygen isotope effect was also studied. All these results suggest that the superconductivity can be explained by the classical phonon-mediated mechanism, which seems to be unable to explain the high temperature superconductivity of the Cu-oxides.

IV-U-12 Neutron Scattering Study of Magnetic Excitations in $YBa_2Cu_3O_{6+x}$

J. M. TRANQUADA*, G. SHIRANE*, B. KEIMER†, S. SHAMOTO and M. SATO (*BNL, †MIT)

[*Phys. Rev.* **B40** 4503 (1989)]

Inelastic neutron scattering has been used to study magnetic excitations in several single crystals of $YBa_2Cu_3O_{6+x}$. In particular, an extensive study of spin waves in a large crystal with $x = 0.3$ has been performed. As in La_2CuO_4, a very large superexchange is found within the CuO_2 layers, with $J_{\parallel}=80^{+60}_{-30}$ meV. The optical mode spin-wave energies are higher than 30 meV, indicating that $J_{\perp 1}$, the coupling between nearest-neighbor CuO_2 planes, is $\gtrsim$2 meV. From the dispersion and splitting of the acoustic modes, we obtain values of 0.020±0.005 meV for the effective exchange between next-nearest-neighbor layers, $J_{\perp 2}$, and 0.035±0.005 meV for the anisotropy parameter D. The weak anisotropy gives the planes an XY-like symmetry; no evidence has been found for any in-plane anisotropy. The CuO_2 bilayers remain strongly correlated well above T_N, and dispersion of the acoustic modes appears 30° above T_N. The decrease of the magnetic order parameter below 30 K in the $x = 0.3$ crystal is interpreted as the onset of an incoherent ordering of Cu moments in the oxygen-deficient CuO_x layers. Low-energy inelastic scattering associated with the transition is also observed. Searches for low-energy magnetic fluctuations in several superconducting single crystals have so far been unsuccessful.

IV-U-13 Magnon and Phonon Raman Scattering in $Bi_2Sr_2Ca_{1-x}Y_xCu_2O_{8+y}$

S. SUGAI* and M. SATO *(*Osaka Univ.)*

[*Phys. Rev.* **B40** 9292 (1989)]

From Raman scattering experiments on $Bi_2Sr_2Ca_{1-x}Y_xCu_2O_{8+y}$ antiferromagnetism and lattice vibrations are investigated. The exchange integral is estimated as 1140 cm^{-1} at x=0.5. The energies of the vibrating modes of the O atoms on the CuO_2 layers show drastic change with the decrease of hole concentration, while the modes of O atoms at the apexes of CuO_5 pyramids do not, which is inverse to the case of $YBa_2Cu_3O_{7-y}$. It indicates that the doped holes enter O sites on the CuO_2 layers in $Bi_2Sr_2Ca_{1-x}Y_xCu_2O_{8+y}$ and at the apexes in $YBa_2Cu_3O_{7-y}$.

IV-U-14 Phonon Raman Spectroscopy in $Bi_2Sr_2Ca_{1-x}Y_xCu_2O_{8+y}$

S. SUGAI* and M. SATO *(*Osaka Univ.)*

[*Jpn. J. Appl. Phys.* **28** 1361 (1989)]

The hole concentration dependence of the lattice vibrations in $Bi_2Sr_2Ca_{1-x}Y_xCu_2O_{8+y}$ was investigated by Raman spectroscopy. The full assignment of the vibrational modes in CuO_5 pyramidal layers was made. The anisotropy between x and y is large for the phonon energies. On decreasing the hole concentration, the energy shifts of the vibrational modes of layered O atoms are larger than those of apical O atoms, which indicates the doped holes enter the layered O sites. The resonant enhancement of the A_g modes at 141 and 187 cm^{-1} and the B_{1g} mode at 326 cm^{-1} indicates the strong electron-phonon interactions.

IV-U-15 Anomaly of Magnetoresistance in Normal State of $(Nd_{1-x}Ce_x)_2CuO_4$ System

M. ONODA, S. YAMAGATA, S. SHAMOTO and M. SATO

[*Solid State Commun.* to be published]

The magnetoresistance was measured in $(Nd_{1-x}Ce_x)_2CuO_4$ single crystals with x=0.11 which were annealed in oxygen atmosphere. An anomalous behavior which may be attributed to the antiferro-

magnetic spin ordering of Nd^{3+} ions was observed below 5K and thus the finite coupling between magnetism and transport properties in this system was suggested.

IV-U-16 Comparison of the Normal State Properties between the Superconducting and the Nonsuperconducting Metallic Phases in $La_{2-y}Sr_yCu_{1-x}Ni_xO_4$

H. FUJISHITA* and M. SATO *(*Kanazawa Univ.)*

[*Solid State Commun.* to be published]

Structural, transport and magnetic properties have been studied for $La_{2-y}Sr_yCu_{1-x}Ni_xO_4$ with varying x for several fixed y-values of 0.1, 0.15, 0.22, 0.32 and 0.45. For x=0, the superconductivity appears, as is already known, in the region of $y<y_c\simeq0.3$. For every value of y studied here, x_c is defined as the concentration of x where the resistivity upturn with decreasing T becomes appreciable due to the electron localization. For $y<y_c$, T_c disappears at $x\simeq x_c$, where the Hall coefficient R_H does not have any significant change, while the temperature dependence of the magnetic susceptibility changes qualitatively. The x_c was found to be a smooth function of y through y_c, which may suggest that the electronic natures in the superconducting ($y<y_c$) and the nonsuperconducting metallic ($y>y_c$) phases are not largely different from each other.

IV-U-17 Small Electronic Specific Heat in the Electron Doped Cu-Oxide Superconductors

M. SERA, S. SHAMOTO and M. SATO

[*Solid State Commun.* **72** 749 (1989)]

The specific heat of the electron doped high-T_c Cu-oxides, $Nd_{1.85}Ce_{0.15}CuO_4$ and $Pr_{2-x}Ce_xCuO_4$ ($0<x<0.25$) has been studied, where the attention was focussed on the behaviors around the superconducting transition temperature T_c in the former and at low temperatures in the latter. The specific heat of $Nd_{1.85}Ce_{0.15}CuO_4$ shows a very small jump at T_c from which the electronic specific heat coefficient γ was estimated to be ~1.2mJ/mol K^2 by assuming $\Delta C/T_c=1.43\gamma$. The γ value of $Pr_{2-x}Ce_xCuO_4$ was estimated from the low temperature specific heat data obtained in the normal state near the metallic region as ~2mJ/mol K^2 for $x\simeq0.15$, which is rather small compared to those of the hole doped Cu-oxide superconductors $La_{2-x}M_xCuO_4$ (M=Ba or Sr). This indicates that the effective mass m^* of the carriers in the electron doped system is smaller than those in the hole doped systems.

IV-U-18 Electronic Specific Heat in the Normal Metallic Region in $La_{2-x}Sr_xCuO_4$

M. SERA and M. SATO

The low temperature specific heat has been measured for $La_{2-x}Sr_xCuO_4$ with $0.35\leqq x\leqq0.55$, where the compounds are metallic but do not exhibit superconductivity. All the samples were prepared by the sintering in the high pressure oxygen atmosphere to avoid the introduction of the oxygen deficiency. The electronic specific heat coefficient γ decreases from 7 mJ/mol.K^2 for x = 0.35 to 4.7 mJ/mol.K^2 for x = 0.5. As the carrier number increases with x, the results indicate that the effective mass m^* of the carriers decrease with increasing x. We have not observed any discontinuous change in γ at the boundary between the superconducting and the nonsuperconducting phases.

IV-U-19 Anomalous Behaviors of the diamagnetic Moment in High-T_c Oxides

M. SATO, S. SHAMOTO, M. SERA and H. FUJISHITA* *(*Kanazawa Univ.)*

Anomalous temperature dependence has been observed in the lower critical field H_{c1} of La and Y based high-T_c oxides. The diamagnetic moment M (<0) measured with increasing temperature under the constant magnetic field H also exhibits anomalous behavior, where $|M|$ increases in certain region of $H_{c1}<H<H_{c2}$, the higher critical field. We have found the experimental evidence for the fact that these two anomalies have the same physical origin. Of course, these anomalies cannot be easily understood by the usual BCS theory and seem to present an unique example of the difference of the physical properties

between the high-T_c oxides and usual superconductors. It is, we believe, quite important to further study this kind of qualitative characteristics of the high-T_c superconductivity to get the key information to understand its mechanism.

IV-U-20 Crystal Growth of High-T_c Oxides

S. SHAMOTO and M. SATO

Large single crystals of $YBa_2Cu_3O_x$ for neutron inelastic measurements have been successfully obtained by using CuO and BaO excess condition. For this measurements, following requirements should be satisfied. (i) The mosaic spread should be smaller than 2 degrees. (ii) The crystal volume should be larger than 0.1 cm^3. (iii) The flux inclusion should be less than a few percents. After the detailed trials, we finally found that the composition of the starting mixtures, crystal growing temperature, and the cooling rate should be carefully chosen to achieve the requirements mentioned above. The obtained crystals were annealed in various atmospheres and at various temperatures to control the oxygen number x or the hole concentration in the crystals, on which the magnetic properties or the magnetic excitation spectra depend in a sensitive way. For the case of the present ingot crystals, the x value can be controlled homogeneously within the whole volume of the rather large crystals. As the results of this success, the interesting x dependence of the magnetic dynamical structure factor has been obtained, which elucidates the relationship between the magnetism and the high-T_c superconductivity.

IV-V Development of Surface Molecular Dynamics Sensitive to the Structure of Reaction Sites

The structure of reaction sites on solid surfaces is one of the most important pieces of information for designing new functional catalysts. This project is aimed at a new approach to the reaction site through analysis of dynamic properties of surface processes. It is based on the crystal azimuth dependence of the angular distribution of the product desorption. The model reactions utilized are the oxidation of carbon monoxide over well-defined surfaces of platinum metals and also the dissociation and desorption of simple admolecules. We have succeeded in observing the anisotropy in the desorption flux of carbon dioxide produced on Pd(110) and Pt(110)(1×2) reconstructed surfaces. This anisotropy is well correlated with the reaction site symmetry.

IV-V-1 Anisotropic Angular Distribution of Desorption of CO_2 Produced on Pd(110) Surfaces

Tatsuo MATSUSHIMA

[*Chem. Phys. Letters*, **155**, 313 (1989)]

The angular distribution of CO_2 produced on Pd(111) depends on the local configuration of adsobates around the reaction sites[1]. The collimation of the desorption along the surface normal was suggested to be caused by the collision of desorbing CO_2 with surrounding adsorbates, as well as by the repulsive force exerted on nascent CO_2 by the surface. This consideration led to the idea that product desorption would show anisotropic angular distribution based on a crystal azimuth. This idea was examined for the CO oxidation on Pd(110).

The desorption of CO_2 produced by the interaction of oxygen adatoms and CO admolecules on Pd(110), which was generated by reactive thermal desorption, was analyzed in angle-resolved form. The adsorption temperature was 200K. Four peaks of CO_2 formation appeared in the different coverage and temperature range. The desorption flux of each CO_2 shows sharp angular distribution in the [00$\bar{1}$] direction (perpendicular to the surface trough), and broader distribution in the [$\bar{1}$10] direction (along the trough).

This is the first finding of anisotropic angular distribution in the desorption of surface reaction products.

Reference
1) T. Matsushima and H. Asada, *J. Chem. Phys.*, **85**, 1658 (1986).

IV-V-2 Angular Distribution of the Desorption of Carbon Monoxide and the Exchange Reaction over Alkali-Covered Noble Metal Surfaces

Tatsuo MATSUSHIMA

[*Z. Phys. Chem. Neue Folge* **162**, 1 (1989)]

Sharp angular distributions of the desorption flux of surface reaction products (non-equilibrium desorption) have been reported for several recombinative processes[1]. In such desorptions the molecules that are produced are likely to be pushed out along the surface normal. Thus, we expect a correlation between the sharp angular distribution and the progress of the isotope exchange between CO admolecules, since both are characteristic of combinative desorption processes. This correlation was examined for the desorption of CO adsorbed on alkali-covered Pt(111), Pd(111), Rh(111), Ni(111), Ru(001) and Ir(pol) surfaces. It was studied with angle-resolved thermal desorption, isotope tracer and low energy electron diffraction. The sharp angular distribution was observed on Ni(111), Ru(001) and Ir(pol). On these surfaces the isotope exchange takes place. On the other hand, a simple cosine distribution and negligible progress of the isotope exchange were found on the other surfaces.

Reference
1) T. Matsushima, *Z. Phys. Chem. Neue Folge* **158**, 175 (1988).

IV-V-3 Adsorption and Dissociation of Oxygen Molecules on Palladium (110) Surfaces at Low Temperatures

Tatsuo MATSUSHIMA

[*Surface Sci.*, **217**, 155 (1989)]

Oxygen is adsorbed molecularly and dissociatively on noble metal surfaces around 100K. The dissociation energy of the O-O bond is significantly reduced on metal surfaces from that of the double bond in free O_2. The degree of dissociation of admolecules depends strongly on the structure of the surface plane[1]. This molecule may play a role as a probe in examining the surface reactivity. However, this degree of dissociation was determined on only a few metals. We previously proposed thermal desorption combined with isotope tracer which allowed a differentiation of the dissociation at the adsorption temperature from that during subsequent heating procedures. This method was applied to the dissociation on Pd(110) surface. Around 110K, part of the admolecules dissociates and yields sites for molecular adsorption. The degree of both dissociations during exposure at 110K and subsequent thermal desorption were estimated. New molecular adsorption was found on surfaces covered with a well-ordered c(2×4)-O lattice.

Reference
1) T. Matsushima, *Surface Sci.*, **157**, 297 (1985).

IV-V-4 The Crystal Azimuth Dependence of the Angular Distribution of the Desorption Flux of Carbon Dioxide Produced on Palladium (110) Surfaces

Tatsuo MATSUSHIMA

[*J. Chem. Phys.*, in press]

The reaction of adsorbed CO and oxygen adatoms on Pd(110) was studied with low energy electron diffraction and angle-resolved thermal desorption. Heating the co-adlayer prepared at 100K produces five peaks in the CO_2 formation; P_1-CO_2 at 460-430K, P_2-CO_2 at 390-350K, P_3-CO_2 around 320K, P_4-CO_2 at 270-230K and P_5-CO_2 around 160K. The angular distribution of each is different. The distribution becomes sharper as the density of the co-adlayer is increased. The azimuthal dependence of the desorption flux of P_1-CO_2 and P_4-CO_2 at fixed desorption angles is summarized in Figure 1. ϕ is the crystal azimuth, θ the desorption angle (polar angle) and θ_o the oxygen coverage. Both CO_2 show sharp angular distributions in the $[00\bar{1}]$ direction and broader in the $[\bar{1}10]$ direction. The correlation between the anisotropy in the angular distribution and the structure around the reaction site is discussed. It is suggested that the azimuth dependence

originates from the anisotropic momentum distribution in the parallel vibration of the whole product molecule immediately prior to the desorption.

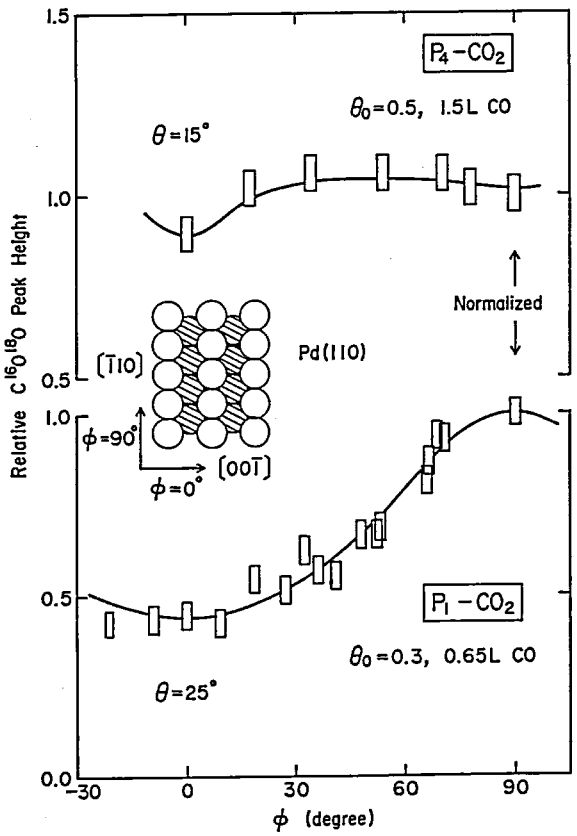

Figure 1. Crystal azimuth dependence of the desorption flux of (a) P_1-CO_2 and (b) P_4-CO_2 at fixed desorption angles. The signal intensity was normalized to the value at ϕ=90 degrees. The CO_2 formation was generated by heating the surface covered with ^{18}O(a) and $C^{16}O$(a) at a rate of 17K/s. 1L(Langmuir)=1×10^{-6} Torr sec.

IV-V-5 Crystal Azimuth Dependence of the Desorption Flux of Carbon Dioxide Produced on Palladium (110) and (111) Surfaces

Tatsuo MATSUSHIMA

[submitted to *Vacuum*]

The correlation between the reaction site symmetry and the crystal azimuth dependence of the desorption flux of products was examined for the CO oxidation on Pd(111) and Pd(110) surfaces, by using angle-resolved thermal desorption and low energy electron diffraction. On Pd(111), CO and oxygen form separate domains. The domains are compressed with the increasing coverages and three CO_2 formation peaks appeared in the subsequent heating. No azimuth dependence was found for all CO_2 desorption on this plane. On the other hand, the azimuth dependence on Pd(110) is well correlated with the symmetry of reaction sites. Five CO_2 peaks were observed on this plane. The distribution of CO_2 produced in the dilute co-adlayer is sharp in the [00$\bar{1}$] direction and broad in the [$\bar{1}$10] direction.

IV-V-6 Determination of Dissociation Temperature of Oxygen Admolecules on Pt(110)(1×2) Reconstructed Surfaces

Yuichi OHNO and Tatsuo MATSUSHIMA

[submitted to *Surface Sci.*]

Clean platinum (110) surfaces are unstable and are easily reconstructed to form a Pt(110)(1×2) structure. This consists of patches of (111) structure declined ±35 degrees from the bulk surface plane. It is interesting whether this plane is characteristic of (111) structure for the reactivity towards simple molecules. The desorption and dissociation of oxygen admolecules were studied on this surface at low temperatures by using thermal desorption combined with an isotope tracer method. The dissociation temperature was estimated from the difference in the isotope fraction between the admolecules and the adatoms, when the surface exposed to $^{18}O_2$ and $^{16}O_2$ sequentially was heated. The desorption phenomena are quite different from those on Pt(111) surfaces. The desorption from the molecular adsorption state forms two peaks at 180K and 200K. The dissociation was confirmed to occur in the temperature range of the latter peak.

IV-W Photochemistry on Solid Surfaces – Light-to-Chemical Energy Conversion and Application to Catalyst Preparation

Photoelectrochemical reactions over powdered metal-oxide semiconductors have been studied in view of their potential for light-to-chemical energy conversion. In our study, a fairly high quantum yield was obtained in water photodecomposition as well as in hydrogen or oxygen photoevolution in the presence of sacrificial electron donors or acceptors. The yield depended sensitively upon impurity, particle size, carrier density, band structure of semiconductor and upon experimental conditions. Thin film of titanium dioxide prepared by CVD showed a photochemical property similar to the particulate system.

Photodecomposition of adsorbed metal carbonyls on metal oxide powders was carried out to investigate reaction intermediates which are catalytically active. The decomposition process was monitored with FTIR in transmission mode. To study surface photochemistry in detail, an apparatus for polarization-modulation FTIR reflection-absorption spectroscopy is under construction.

IV-W-1 Photochemical Properties of Ultrathin TiO_2 Films Prepared by CVD

Shinri SATO, A. SOBCZYNSKI*, J.M. WHITE*, A.J. BARD*, A. CAMPION*, M.A. FOX*, T.E. MALLOUK*, and S.E. WEBBER* *(* Univ. Texas at Austin)*

[*J. Photochem. Photobiol. A: Chem.*, in press]

Thin films of TiO_2 were prepared on fused silica and Ti substrates by chemical vapor deposition (CVD) using $Ti[OCH(CH_3)_2]_4$ under conditions of anatase formation. The UV-visible transmission spectrum of the film deposited on the fused silica substrate showed an absorption edge 30 nm shorter than that of anatase powder. This blue shift may be attributed to size quantization, i.e., the film may consist of extremely small TiO_2 particles. The absorption edge shifted to slightly longer wavelength upon heating the film in air at high temperatures. Photocatalytic property of the film was examined using the photodeposition reaction of Ag from aqueous $AgNO_3$. The Ag photodeposition rate increased with calcination temperature, maximizing at around 400°C and then decreasing at higher temperature. To compare the photocatalytic property with photoelectrochemical property, photocurrents were measured in a KOH solution using the films deposited on the Ti substrate. They decreased after calcination at temperatures above 400°C. Compared to bulk TiO_2, the wavelength dependence of the current was shifted to considerably shorter wavelengths, in agreement with the absorption spectrum.

IV-W-2 Photoevolution of Oxygen from a Suspension of Metal Oxide Semiconductors in Aqueous Silver-Salt Solutions

Shinri SATO and Toru KADOWAKI *(Catalysis Res. Center, Hokkaido Univ.)*

[*Denki Kagaku*, **57**, 1151 (1989)]

Oxygen photoevolution from a suspension of metal oxide semiconductor in aqueous silver-salt solutions was studied to investigate factors influencing its yield as well as reaction mechanism. Among commercial semiconductor powders, TiO_2, ZnO, WO_3, and $BaTiO_3$ were active for the oxygen evolution from $AgNO_3$ solution. For the TiO_2 as supplied, rutile was, on the whole, more active than anatase. The activity of most TiO_2 samples was significantly enhanced upon hydrogen reduction, while most active rutile samples were not affected. Pt loading followed by hydrogen treatment at low temperatures also enhanced the activity. These results were discussed in terms of a reaction mechanism.

IV-W-3 Mechanism and Quantum Yield of Hydrogen Photoevolution from a Suspension of Pt/TiO_2 in Sacrificial Electron-Donor Solutions

Shinri SATO

[*Shokubai (Catalyst)*, **31**, 469 (1989)]

Quantum yield of the hydrogen photoevolution from a suspension of Pt/TiO_2 in various electron-donor solutions was measured. In dialcoholic solutions, the quantum yield exceeded 100%, indicating that a current doubling effect is operative in semiconductor photocatalysis. Although anatase has ca. 0.1 eV more negative conduction band than rutile, they gave a similar yield in alcoholic and EDTA solutions, while anatase showed higher photoactivity in the other electron-donor solutions. This result was discussed in relation to the results of IR spectroscopic and photoluminescence experiments, in which a direct reaction of holes with adsorbed electron donor and strong adsorption of alcohol on TiO_2 were observed. It seems reasonable to conclude that a direct, irreversible reaction of holes with adsorbed alcohol makes Pt/TiO_2 particle potential so negative that electrons are inevitably used for hydrogen evolution, and as a result, the difference in the conduction band position gives little effect on the yield.

IV-W-4 Photodecomposition of Metal Carbonyls Adsorbed on Alumina, Silica, PVG, and Magnesia

Shinri SATO and Tadayoshi OHMORI

Metal carbonyl such as $Fe(CO)_5$ adsorbed on metal oxide powders is often used as a photocatalyst, in which unsaturated coordinate sites formed by illumination are thought to play an important role as a thermal catalyst. In the present study, we investigate the photodecomposition process of adsorbed metal carbonyls on alunima, silica, PVG, and magnesia using FTIR and to prepare active catalysts even in dark.

IV-W-5 Construction of an Apparatus of Polarization-Modulation FTIR Reflection-Absorption Spectroscopy

Shinri SATO, Makoto WATANABE, and Tadayosi OHMORI

Since surface photochemical reactions occur in adsorbed layer on illuminated surface, a surface-sensitive analytical method is required to observe their intermediates and products. IR reflection-absorption spectroscopy (IR-RAS) has been employed to study the molecular structure of adsorbed species on metal, and the use of FTIR improves the sensitivity of RAS. Because only *p*-wave gives the information of surface species, polarization-modulation (PM) method enables us not only to improve the sensitivity but to take RAS even in the presence of gas-phase species. PM-FTIR-RAS involving ultrahigh vacuum system is now under construction.

IV-X Photoelectron Spectroscopy of Organic Solids in Vacuum Ultraviolet Region

Ultraviolet photoelectron spectroscopy (UPS) of organic solids has been carried out and also UPS with synchrotron radiation (UVSOR-UPS) was applied to observe the electronic and band structure of various kinds of organic/inorganic materials.

IV-X-1 Ultraviolet Photoelectron Spectroscopic Study of Perfluorinated Carboxylic Acid Monomolecular Films Prepared by Vacuum Deposition

Munehisa MITSUYA *(Hitachi Ltd.)*, **Kazuhiko SEKI** *(Hiroshima Univ. and IMS)*, **and Hiroo INOKUCHI**

[*J. Appl. Phys.*, **64**, 4150 (1988)]

Ultraviolet photoelectron spectra have been measured for monomolecular films of perfluorinated carboxylic acids prepared by vacuum deposition. Their threshold ionization potentials were determined to be 8.5 eV and their work functions larger than those for other organic compounds. The escape depth of photoelectrons through the perfluorocarbon chain was evalu-

ated at 2.3 nm. These results are interpreted in relation to the large electronegativity of constituent fluorine atoms.

IV-X-2 Band Structure of $Bi_2Sr_2CaCu_2O_8$ Studied by Angle-Resolved Photoemission

Takashi TAKAHASHI*, Hiroyoshi MATSUYAMA*, Hiroshi KATAYAMA-YOSHIDA*, Yutaka OKABE*, Shoichi HOSOYA* *(*Tohoku Univ.)*, **Kazuhiko SEKI** *(Hiroshima Univ. and IMS)*, **Hitoshi FUJIMOTO, Masatoshi SATO, and Hiroo INOKUCHI**

[*Phys. Rev.* **B, 39**, 6636 (1989)]

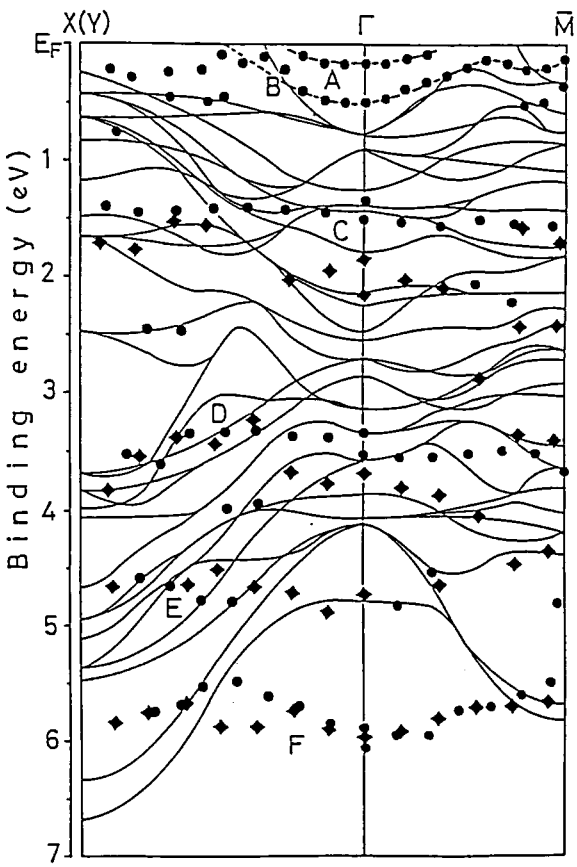

Figure 1. Band structure of $Bi_2Sr_2CaCu_2O_8$ determined by the present angle-resolved photoemission study with $h\nu$=18 eV (circles) and 40 eV (squares). Note that the energy position of band C and D are slightly different between $h\nu$=18 eV and 40 eV, probably because of the difference in the cross-section amplitude. A possible connection of the experimental points for bands A and B is shown by broken lines. A representative-band structure calculation (Reference 1) is shown by thin solid lines for comparison.

Angle-resolved photoemission measurement with synchrotron radiation has been performed on single-crystal $Bi_2Sr_2CaCu_2O_8$. Two dispersive bands intersecting the Fermi level midway between the Γ point and the Brillouin-zone boundary were observed (see Figure 1). The other bands with higher binding energy are almost dispersionless in contrast with the band-structure calculation. The present experimental result indicates the existence of a Fermi surface and Fermi-liquid states in the high-T_c superconductor as well as band renormalization due to the strong electron correlation.

Reference

1) S. Massida, J . Yu, and A. J . Freemann, *Physica C*, **52**, 251 (1988).

IV-X-3 Electronic Structure of Thiacyanine Dyes in the Solid State

Tong Bor TANG *(Hong Kong Baptist College and IMS)*, **Hiromichi YAMAMOTO, Kenichi IMAEDA, Hiroo INOKUCHI. Kazuhiko SEKI** *(Hiroshima Univ. and IMS)*, **M. Okazaki* and Tadaaki TANI*** *(*Fuji Photo Film Co.)*

[*J. Phys. Chem.*, **93**, 3970 (1989)]

The solid-state electronic structures of 12 thiacyanine dyes with four different central methine chain lengths and three counterions (Br^-, ClO_4^-, and p-toluenesulfonate) have been investigated by using ultraviolet photoelectron spectroscopy. The measured ionization threshold energies decrease with increasing methine chain length and are ascribed to the ionization from the highest occupied molecular orbitals of the cyanine cations. A small anion dependence of ionization threshold was observed. Comparison of these thresholds with electrochemical oxidation potentials and molecular orbital calculations with Hückel methods revealed a good correlation among these quantities for each series with a common anion. These results are discussed in terms of various factors in the solid and the solution, such as polarization energy, Madelung energy, and solvation energy. The contrast with the results from merocyanine dyes points to a different correlation between ionization threshold and oxidation potential, calling for caution in estimating solid-state properties of a different class of compounds from electrochemical measurements.

IV-Y Electrical Conduction of Organic Solids

We have observed the electrical properties of tetrakis alkylchalcogeno substituted tetrathiafulvalene extensively as functions of their molecular packings and solid-solid phase changes.

IV-Y-1 Crystal Structures and Electrical Properties of Tetrakis (methylseleno) tetrathiafulvalene ($TSeC_1$-TTF) and Two Phase of ($TSeC_1$-TTF)I_3

Ping WANG *(Inst. Chem. Academia Sinica, China and IMS)*, **Tamotsu INABE, Chikako NAKANO, Yusei MARUYAMA, Hiroo INOKUCHI, Naoko IWASAWA*, and Gunzi SAITO*** *(*ISSP, Univ. of Tokyo)*

[*Bull. Chem. Soc. Jpn.*, **62**, 2252 (1989)]

The crystal structure and the electrical property of $TSeC_1$-TTF as well as those of the new complex ($TSeC_1$-TTF)I_3 with two kinds of phase are reported. The crystal structure of $TSeC_1$-TTF was determined to be monoclinic, space group $P2_1/a$, a=7.728(1), b=20.952(4), c=5.315(l)Å, and β=90.57(2)° having a unit cell volume of 860.6(3)Å. By an electrochemical method and a diffusion method, $TSeC_1$-TTF gave two forms of single crystals of ($TSeC_1$-TTF)I_3. The crystal data of one form; monoclinic, space group $P2_1/n$, a=24.359(1), b=11.831(3), c=7.842(6)Å, β=96.71(4)°, V=2244(l)Å and those of the other; monoclinic, space group $P2_1/a$, a=23.174(5), b=11.727(3), c=8.960(5)Å, β=110.54(2)°, V=2280(l)Å. The former complex has lower resistivity, $4.1\times10^4\Omega$cm, compared with the latter one, $1.1\times10^8\Omega$cm. The dimerization is more noticeable in the latter complex than in the former one.

IV-Y-2 Charge-Carrier Drift Mobilities and Phase Transition in Tetrakis (octhylthio) tetrathiafulvalene, TTC_8-TTF, Crystal

Yongfang LI, Chikako NAKANO, Kenichi IMAEDA, Hiroo INOKUCHI, Yusei MARUYAMA, Naoko IWASAWA*, and Gunzi SAITO* *(*ISSP, Univ. of Tokyo)*

Temperature dependence of the charge-carrier mobility in tetrakis (octhylthio) tetrathiafulvalene crystals has been observed in the temperature range of −100 to 45°C by a time-of-flight measurement of transient photo-carriers. It shows a clear correlation with the crystal phase transition around 33°C.

IV-Y-3 Thermal and Electrical Properties of Tetrakis(alkylseleno)tetrathiafulvalenes ($TSeC_n$-TTF, n=1−18)

Ping WANG, Toshiaki ENOKI *(Tokyo Institute of Technology)*, **Kenichi IMAEDA, Naoko IWASAWA*, Hideki YAMOCHI*, Hatsumi URAYAMA*, Gunzi SAITO*** *(*ISSP, Univ. of Tokyo)*, **and Hiroo INOKUCHI**

[*J. Phys. Chem.*, **93**, 5947 (1989)]

Thermal and electrical properties have been investigated for tetrakis(alkylseleno)tetrathiafulvalenes, ($TSeC_n$-TTF (n=1−18)). The linear n dependences of the enthalpy and entropy changes at the melting point, ΔH_m and ΔS_m are observed, which is consistent with the usual behavior of flexible molecules. The n dependence of the melting points, in addition to those of ΔH_m and ΔS_m, suggests that the series of $TSeC_n$-TTF's is divided into two subgroups with respect to n. In one subgroup with smaller n, n<6, the intermolecular interactions between adjacent selenium-substituted TTF moieties dominate the crystal structures, while, in the other subgroup with $n\geq6$, the van der Waals intermolecular interaction associated with alkyl chain groups works to reduce the interplanar distances between adjacent TTF moieties in the crystal, and consequently, in the latter subgroup, it is also suggested that the electrical conductivities are enhanced by the increased overlaps between adjacent TTF π systems through the reduction of the interplanar distances.

IV-Z Electron Transport in Cytochromes

The electrical conduction of solid proteins has been reported by many investigators with interest in the carrier transport in biological systems. We have already found an enormously large conductivity of cytochrome c_3. Using surface-enhanced resonance Raman (SERR) method, we found direct evidence that the physiological function of cytochrome c_3 and hydrogenase in bulk are preserved in the adsorbed state (See II-F). Recently, we found more peculiar conductive behaviour of cytochrome c and are analyzing their detailed mechanisms.

IV-AA Physics and Chemistry of Graphite Intercalation Compounds

We are investigating the properties of graphite intercalation compounds by means of measurements of ultraviolet photoelectron spectra and positron anihilation spectra.

IV-AB Organic Metals

In an attempt to develop new organic superconductors and to explore the related phenomena, several new organic charge-transfer complexes are prepared, and their structural and physical properties are investigated.

IV-AB-1 Thermoelectric Power of Organic Superconductors – Calculation on the Basis of the Tight-Binding Theory

Takehiko MORI and Hiroo INOKUCHI

[*J. Phys. Soc. Jpn.*, **57**, 3674 (1988)]

Thermoelectric power of organic superconductors, β-(BEDT-TTF)$_2$I$_3$ and (BEDT-TTF)$_2$Cu(NCS)$_2$ (BEDT-TTF: bis(ethylenedithio)tetrathiafulvalene) is calculated by the integration of the Boltzmann equation on the basis of the two-dimensional tight-binding band models. This calculation provides the interpretation of the observed complicated temperature dependence and anisotropy of the thermoelectric power and a tool estimating the transfer integrals (Figure 1).

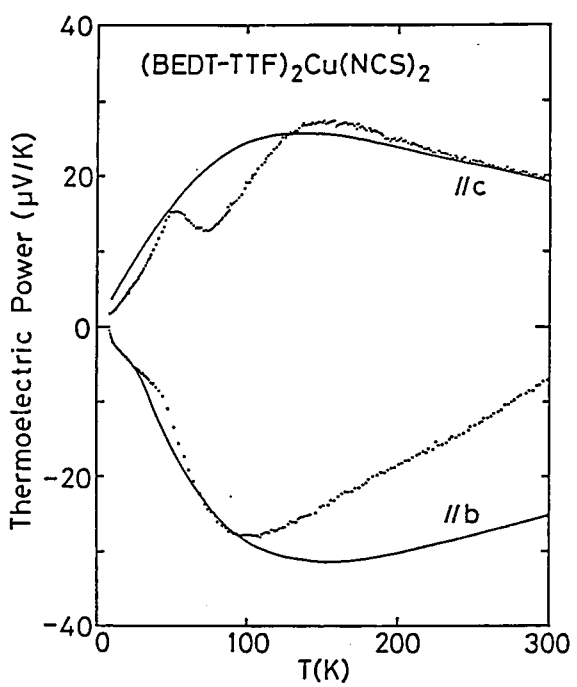

Figure 1. Temperature dependence of thermoelectric power of (BEDT-TTF)$_2$Cu(NCS)$_2$. The dots from the experiment,[1] and the solid curves from the theory.

Reference

1) H. Urayama, H. Yamochi, G. Saito, T. Sugano, M. Kinoshita, T. Inabe, T. Mori, Y. Maruyama, and H. Inokuchi, *Chem. Lett.*, **1988**, 1057.

IV-AB-2 Metal-to-Semiconductor Transition of an Organic Metal, $(EDT\text{-}TTF)_2AuBr_2$

Takehiko MORI and Hiroo INOKUCHI

[*Solid State Commun.*, **70**, 823 (1989)]

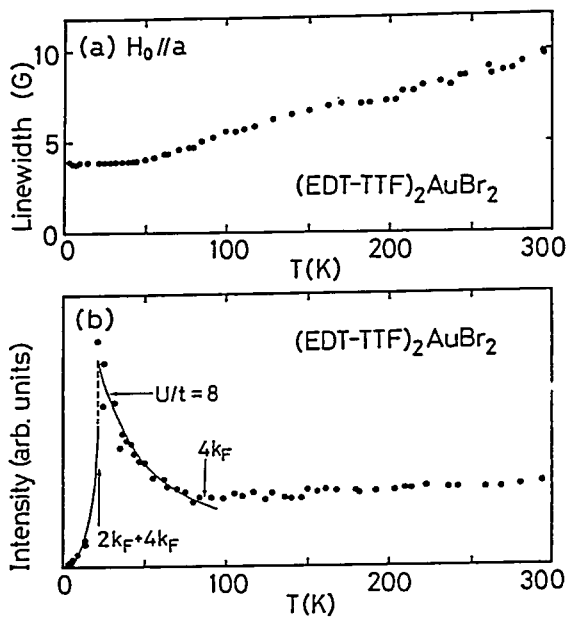

Figure 1. ESR results of $(EDT\text{-}TTF)_2AuBr_2$. (a) The temperature dependence of the peak-to-peak linewidth. (b) The temperature dependence of the ESR intensity. The solid curve designates a theoretical prediction.

A new organic conductor, $(EDT\text{-}TTF)_2AuBr_2$, where EDT-TTF is an unsymmetrical donor, ethylenedithiotetrathiafulvalene, exhibits an SDW-like metal-to-semiconductor transition at 20 K. Above this transition, a considerable Curie-like enhancement of the spin susceptibility is observed (Figure 1). There are reported the crystal structure, the energy band calculation, the resistivity under pressure, the thermoelectric power, and the ESR data.

IV-AB-3 Electrical and Magnetic Properties of $(BEDT\text{-}TTF)_4Ni(CN)_4$ Complex

Masashi TANAKA*, Hideo TAKEUCHI*, Mitsuru SANO* *(*Nagoya Univ.)*, **Toshiaki ENOKI**, Kazuya SUZUKI**** *(**Tokyo Inst. Tech.)*, **and Kenichi IMAEDA**

[*Bull. Chem. Soc. Jpn.*, **62**, 1432 (1989)]

The electrical conductivity and the ESR spectra of the single crystal of $(BEDT\text{-}TTF)_4Ni(CN)_4$ complex were measured. This crystal exhibits a metal-insulator transition at 160 K. The ESR signals show the presence of the $[Ni(III)(CN)_4]^-$ anion in addition to the BEDT-TTF cation radical. The spin concentration of Ni(III) ion was estimated to be 0.01 of the total Ni ions from the temperature dependence of the spin susceptibility of these components. The X-ray photoelectron spectra were also taken.

RESEARCH ACTIVITIES V
Department of Applied Molecular Science

V–A New Multi-Stage Redox Systems

Multi-stage redox systems, which transfer electrons by multi-stage manners, are an important class of organic molecules to explore new organic materials having interesting solid state properties, such as electrical, magnetic, and optical properties. Recently, we have designed and synthesized two classes of new multi-stage redox systems, such as peri-condensed Weitz type donors and amphoteric multi-stage redox systems. The former is designed by replacing two of the sp^2 carbon atoms in a polycyclic arene by two sulfur atoms. Such condensed type heterocycles have produced new organic molecular metals which contain non-TTF and non-TCNQ type components. The latter is designed so as to decrease the difference between the oxidation and the reduction potentials of a molecule. We already reported the conjugated hydrocarbons with the highest amphotericity. Design and synthesis of new type of multi-stage redox systems are actively continued.

V-A-1 New Multi-Stage Redox Systems and New Organic Molecular Metals

Kazuhiro NAKASUJI

[*Pure Appl. Chem.*, in press]

Exploration of new multi-stage redox systems and realization of new organic molecular metals are reviewed. New multi-stage redox systems, "peri-condensed Weitz type donors", have been designed. As basic skeletons, 3,9-, 1,7-, and 3,10-dithiaperylene (DTPR) and 1,6-dithiapyrene (DTPY) were synthesized. As chemical modifications for multi-dimensionality, alkylthio groups were introduced on the DTPY skeleton. Thus, 2,7-, and 3,8-methylthio derivatives (MTDTPY) and an ethylenedithio derivative (ETDTPY) were synthesized. All these donors showed reversible two-stage redox behavior with potentials comparable to that of TTF. Among charge transfer complexes prepared, 2,7-MTDTPY has produced new organic molecular metals which contain neither a TTF nor a TCNQ type framework.

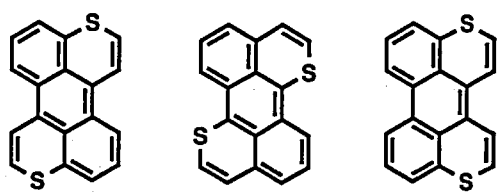

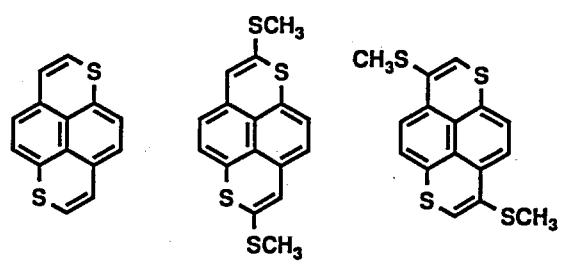

V-A-2 Synthesis and Properties of 1,7-Dithiaperylene: A New Peri-Condensed Weitz Type Donor

Kazuhiro NAKASUJI, Akio ODA[a], Ichiro MURATA[a], Kenichi IMAEDA, and Hiroo INOKUCHI *([a] Osaka Univ.)*

[*J. Chem. Soc. Chem. Commun.*, in press]

1,7-Dithiaperylene (DTPR), a new peri-condensed Weitz type donor, has been synthesized from anthracene-9,10-dithiolate anion through six steps and characterized. The key step of the reaction scheme is the final hydro-alkoxy-elimination reaction. The cyclic voltammetry showed two-stage redox behavior with relatively low oxidation potentials at +0.39 and +0.82 V (vs SCE). In accord with the low oxidation potentials, the dicationic species of 1,7-DTPR could be generated simply dissolving in concentrated D_2SO_4. Charge transfer complexes of 1,7-DTPR with various organic and inorganic acceptors were prepared. Among them, the NO_3 complex is showed high conductivity (14 Scm^{-1}).

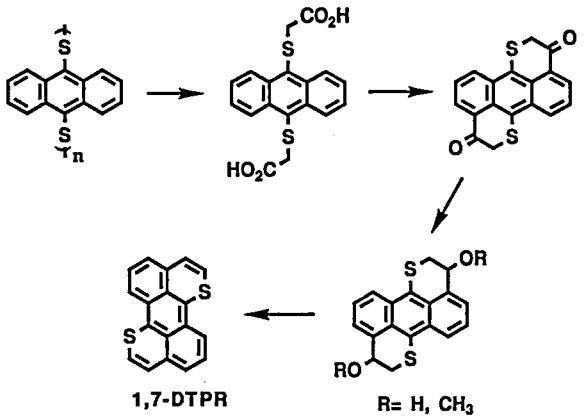

V–B New Stable Neutral Conjugated Radicals and Their Redox States

Recently, we have been engaged in design and synthesis of new stable neutral conjugated radicals to explore new organic conductors, for example single component conductors, and magnetically interesting materials. For synthetic chemists, exploration of totally new molecules are always important, but chemical modifications for known electronic systems are also important. First, we have utilized the phenalenyl system as the basic skeleton of nutral radicals and modified the skeleton by introducing donor and acceptor substituents. Such modifications are sometimes applied in physical organic chemistry to stabilized unstable electronic systems.

V-B-1 Synthesis and Isolation of Phenalenyl Cations Having Donor and Acceptor Substituents

Kazuhiro NAKASUJI, Masakazu YAMAGUCHI[a], and Ichiro MURATA[a] *([a]Osaka Univ.)*

The precursor of phenalenyl cations having donor and acceptor substituents were prepared from the cyanonaphthalene derivative by several steps. The cationic species were isolated as orange to violet solids by treatment of the cyanonaphthalene with trityl perchlorate. These salts are stable on drying, and constitute rare examples of the isolable carbocations containing the cyano group. Their structures were confirmed by ^1H- and ^{13}C-NMR spectra. Furthermore, the most stable cation salt with perchlorate gave the satisfactory elemental analysis as 1:1 stoicheometry. The reduction potentials of the cations were measured by cyclic voltammetry. The observed potentials are less positive for the first reduction and less negative for the second one than the corresponding values reported for the unsubstituted cation. This indicates that both the cation and the anion states interact to larger extent with the donor and acceptor substituents, respectively. Therefore, the amphoteric redox nature of the radicals generated by cyclic voltammetry in solution are enhanced.

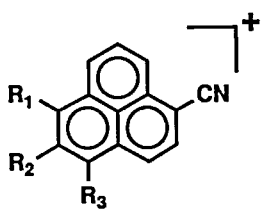

Phenalenyl Cations

	R_1	R_2	R_3
a	OCH_3	H	H
b	OCH_3	H	OCH_3
c	OCH_3	OCH_3	OCH_3
d	SCH_3	H	H

V–C New Cooperative Electronic Systems for Hydrogen-Electron Transfer

Recent discovery of a new phase transition in quinhydrone under pressure has opened an interdisciplinary area between organic chemistry and solid state physics to explore new materials having potentially interesting solid state properties. Molecular level considerations for such a cooperative phenomena in solids lead to new molecular design strategies. Thus, as a first step, we design and synthesize the donor and acceptor substituted quinones and hydroquinones. The extended conjugated quinhydrones, for example, naphthoquinhydrones were also prepared. Furthermore, the exploration of the stable neutral radicals having hydrogen bonding networks also important to realize new cooperative electronic systems for hydrogen-electron transfer.

V-C-1 Synthesis and Physical Properties of the Donor and Acceptor Substituted Benzoquinones and Hydroquinones

Hiroshi YAMAMOTO[a], Ichiro MURATA[a], Toshikazu KITAGAWA, and Kazuhiro NAKASUJI *([a]Osaka Univ.)*

In order to examine the basic effects of the donor and acceptor substituents on the quinhydrones, in particular, on HOMO and LUMO energies, we prepared the quinones substituted with methyl, methoxy, hydroxy, methylthio, amino, and dimethylamino groups as donors and fluoro and chloro groups as acceptors. The reduction potentials measured by cyclic voltammetry showed a linear correlation with Hammett's σ-constants. Interestingly, we found a linear correlation between the oxidation potentials of the quinones and Hammett's σ-constants.

V-C-2 Synthesis and Physical Properties of the Extended Quinhydrones: 1,5-Dihalo-2,6-naphthoquinones

Kazuhiro NAKASUJI, Hiroshi YAMAMOTO[a], Ichiro MURATA[a], Hiroshi OKAMOTO, and Tadaoki MITANI *([a]Osaka Univ.)*

For the component molecules of the extended quinhydrones, we prepared 1,5-dichloro, 1,5-dibromo-, and 1,5-bismethylthio-2,6-naphthoquinones and their hydroquinone derivatives. The acceptor strength of these quinones estimated from reduction potentials are almost comparable with that of chloranil. Bismethylthionaphthoquinone showed the oxidation potential. From these components, 1,5-dichloro and 1,5-dibromo derivatives of 2,6-naphthoquinhydrones were prepared as the first extended quinhydrones. These charge transfer complexes showed the charge transfer transitions around 700-800 nm which exist at the lower energy region than that of simple quinhydrone. The electric and optical properties are now in investigation.

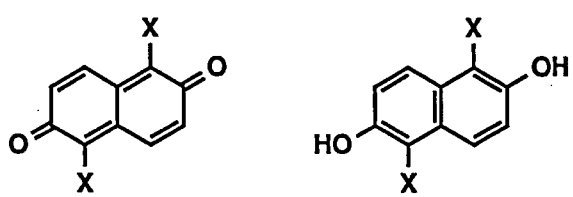

X = Cl, Br

V–D New Types of Transition Metal Cluster Compounds

We have recently synthesized integrated cubane type of clusters under some control of condensation of oxometalates and thiometalates. These clusters may prove to be a good model for surfaces of transition metal oxides and sulfides.

We have found that the clusters show interesting reactivities and physicochemical properties such as site selective oxygen exchange, organometallic group substitution reaction, multielectron transfer, and nonlinear optical properties.

V-D-1 Oxidation of Cyclohexene with t-Butyl Hydroperoxide Catalyzed by Transition Metal Oxide Clusters

Cuiju ZHANG, Yoshiki OZAWA, Yoshihito HAYASHI, and Kiyoshi ISOBE

[*J. Organomet. Chem.*, **373**, C21 (1989)]

Organometallic oxide clusters $[(RhCp^*)_4V_6O_{19}]$ ($Cp^*=\eta^5-C_5Me_5$) **1** was recently prepared, and has approximately T_d symmetry.[1] $[(RhCp^*)Cl(CH_3CN)_2]_2[Mo_6O_{19}]$ **2** has been newly obtained from the reaction of the triple cubane-type cluster $[(RhCp^*)MoO_4]_4$[2] with excess t-BuOOH in 1,2-dichloroethane at 70 °C. Single crystal X-ray diffraction has revealed that **2** is an ionic compound consisting of the $[(RhCp^*)Cl(CH_3CN)_2]^+$ cation and the $[Mo_6O_{19}]^{2-}$ anion in a cage-like structure.

Cluster **1** and **2** catalyze the oxidation of cyclohexene with t-butyl hydroperoxide (eq 1) to give allylic oxidation products mainly and epoxycylohexane selectively, respectively.

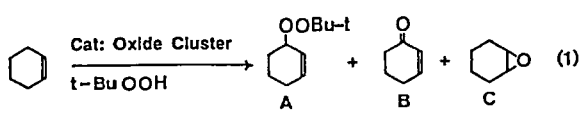

References

1) Y. Hayashi, Y. Ozawa, and K. Isobe, *Chem. Lett.*, **1989**, 425.
2) Y. Hayashi, K. Toriumi, and K. Isobe, *J. Am. Chem. Soc.*, **110**, 3666 (1988).

V-D-2 Isolation of $[(RhCp^*)_{4-m}(IrCp^*)_mV_6O_{19}]$ ($0 \leqq m \leqq 4$)

Yoshihito HAYASHI, Yoshiki OZAWA, and Kiyoshi ISOBE

The ^{1}H-NMR of $[(RhCp^*)_4V_6O_{19}]$ in D_2O shows several peaks as the acidity of the solution is increased. The bridging oxygen atoms in the cluster are protonated in an acidic aqueous solution and this protonation causes the $(RhCp^*)^{2+}$ groups to dissociate (eq 1).

$$[(RhCp^*)_4V_6O_{19}] + 2mHBF_4 \longrightarrow H_{2m}[(RhCp^*)_{4-m}V_6O_{19}] + m[(RhCp^*)(H_2O)_3](BF_4)_2 \quad (1)$$

The distribution of the resulting $[(RhCp^*)_{4-m}V_6O_{19}]^{2m-}$ species depends on the pH of the solution.

We have found that this dissociation reaction is useful for introduction of other organometallic groups into the cluster framework. The (IrCp*) dication was added to an acidic solution of $[(RhCp^*)_4V_6O_{19}]$ with HBF_4 to form a mixture of clusters $[(RhCp^*)_{4-m}(IrCp^*)_mV_6O_{19}]$ ($0 \leqq m \leqq 4$) which were separated with a silica gel column. The ^{51}V-NMR spectra of these substituted complexes show the difference in magnetic environment of the vanadium atoms. When one RhCp* group is substituted for an IrCp* group the resulting $[(RhCp^*)_3(IrCp^*)V_6O_{19}]$ has two equally intense signals (Figure 1, d) corresponding to two kinds of vanadiums in different environments. In cases of di- and tri-substituted clusters, three (c) and two signals (b) are observed due to the number of different chemical environments around vanadium atoms, respectively. These intensities of the signals are proportional to the number of the vanadium atoms. These data indicate that the vanadiums on the rhodium-located site resonate at a higher field than those on the iridium-one.

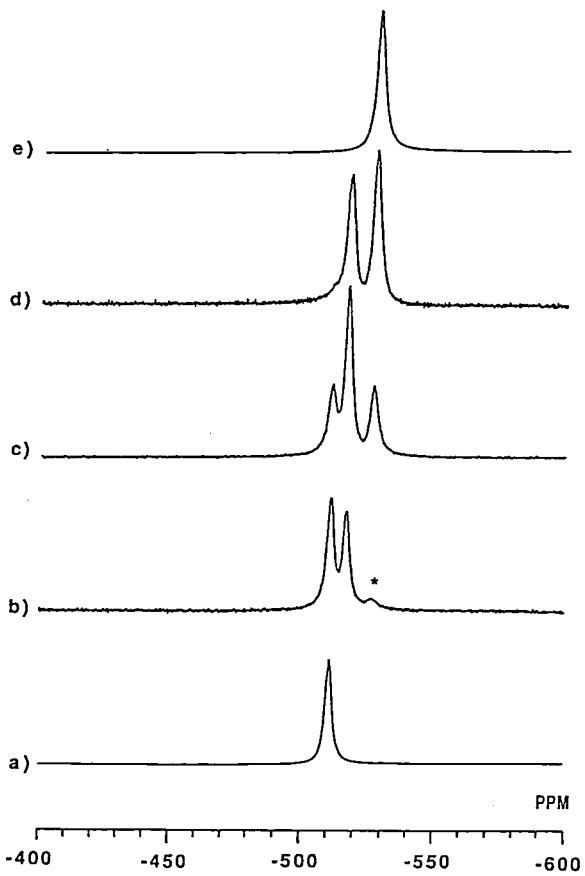

Figure 1. ^{51}V NMR Spectra of $[(RhCp^*)_{4-m}(IrCp^*)_m V_6O_{19}]$ $(0 \leq m \leq 4)$ in $CDCl_3$; a) m=4, b) m=3, c) m=2, d) m=1, e) m=0.

V-D-3 Site-Selective Oxygen Exchange of $[(RhCp^*)_4V_6O_{19}]$ with Water

Yoshihito HAYASHI, Yoshiki OZAWA, and Kiyoshi ISOBE

Although ^{17}O-NMR spectroscopy has been established as the most powerful technique for a structural probe of polyanions, exchange reaction of oxygen in water at polyanions is difficult to observe by ^{17}O-NMR due to the experimental problems associated with a large signal of water. We have used selective excitation methods and the temperature dependence of the ^{17}O resonance intensity of the ^{17}O enriched $[(RhCp^*)_4V_6O_{19}]$, **1** in water to analyze oxygen exchange reaction.

The cluster **1** contains three magnetical nonequivalent oxygen atoms: terminal, bridging, and centered oxygen atoms. The centered oxygen possessing a high symmetry (O_h), has a rather narrow line width because its quadruple relaxation time is longer than that of the other oxygen atoms. Figure 1 shows the time-dependent ^{17}O-NMR spectra of the ^{17}O-enriched cluster in water at 60 °C at pH 7.0. The only intensity of the bridging oxygen signal decreases with time, therefore this observation suggests clearly that the bridging oxygens are selectively exchanged with those in the bulk of water.

$$[(RhCp^*)_4V_6\ {}^{17}O^c\ {}^{17}O_6{}^t\ {}^{17}O_{12}{}^b] + H_2{}^{16}O \rightleftharpoons [(RhCp^*)_4V_6\ {}^{17}O^c\ {}^{17}O_6{}^t\ {}^{17}O_{11}{}^b\ {}^{16}O^b] + H_2{}^{17}O \quad (1)$$

Pseudo-first order rate constants of eq 1 at different temperatures were obtained and the activation parameters were derived from them as $\log_{10}A=5.92$, $E_a=62$ kJ mol^{-1}.

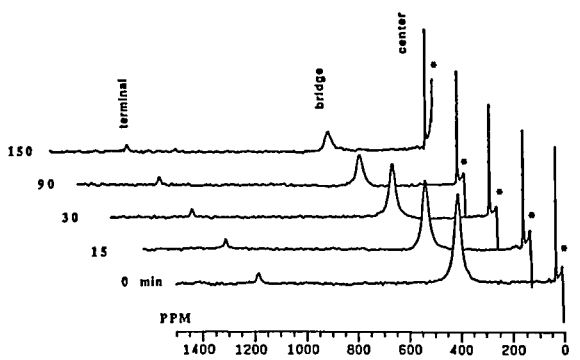

Figure 1. Time-dependent ^{17}O NMR spectra of the ^{17}O enriched $[(RhCp^*)_4V_6O_{19}]$ in water at 60 °C.

V-D-4 Synthesis and Molecular Structure of High-Valent Transition Metal Sulfide Cluster

Yoshiki OZAWA, Yoshihito HAYASHI, and Kiyoshi ISOBE

The reactions of tetrathio-molybdate or -tungstate with organometals give various heteronuclear clusters which display unique stereochemistries and electrochemical properties. In most of these clusters, Mo and W atoms are in low oxidation states (2+~4+) and have

d-electrons provided for metal-metal direct interactions. There have been few examples with higher oxidation states like polyoxometalates with no d-electron. We have synthesized novel type sulfide clusters of high-valent Mo or W with organo-rhodium or -iridium which have few metal-metal bondings.

Compound $[(Cp^*Rh)_3W_2O(\mu_3\text{-}S)_3(\mu_3\text{-}S_2)(\mu\text{-}S)_2(S_4)]$ ($Cp^*=\eta^5\text{-}C_5(CH_3)_5$) was prepared by the reaction of $[Cp^*RhCl_2]_2$ with $(NH_4)_2WS_4$ refluxed in acetonitrile. Black crystals were obtained from the reaction mixture kept under air atmosphere. X-ray crystal structure analysis reveals a distorted cubane-like framework which is made of three Rh^{III} and a W^V atoms linked by S and (S_2) atoms. Crystallographic data: monoclinic, space group $P2_1/c$, a=19.264(2), b=21.847(6), c=11.336(2) Å, β=94.15(1)°, V=4758(2) Å^3, Z=4, Dc=2.14 g cm^{-3}. Metal-metal short contact is only found in W(1)-W(2) bond length (2.84 Å). Other W-Rh and Rh-Rh bond distances within the cubane core in the range of 2.96-3.98 Å show no direct metal-metal bondings.

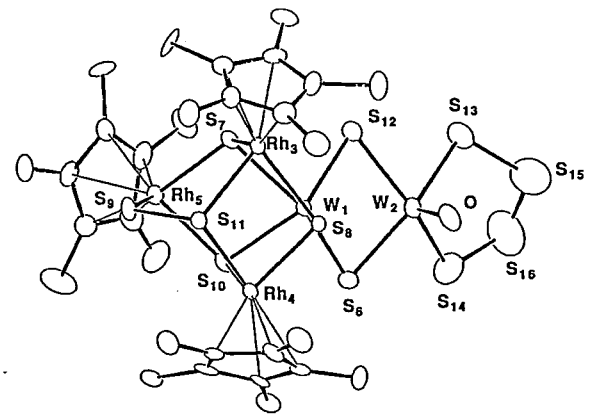

Figure 1. Molecular structure of $[(Cp^*Rh)_3W_2O(\mu_3\text{-}S)_3(\mu_3\text{-}S_2)(\mu\text{-}S)_2(S_4)]$ with ORTEP drawing. Selected metal-metal interatomic distances are given as follows: W(1)-W(2) 2.838(2), W(1)-Rh(3) 2.958(2), W(1)-Rh(4) 2.981(2), W(1)-Rh(5) 3.698(2), Rh(3)-Rh(4) 3.531(3), Rh(3)-Rh(5) 3.974(3), Rh(4)-Rh(5) 3.975(3) Å.

V–E Synthesis and Properties of Organo-palladium (II) and -molybdenum (V)

M-C, M=O, and M-H bonds in organometallic compounds have been frequently used for hydrocarbon transformation due to C-C coupling, oxidation, and hydride transfer, respectively.

We have synthesized new organopalladium(II) complexes containing carbon-bonded heterocycles and organo-mloybdenum(V) containing Mo=O and Mo-Cl bonds.

V-E-1 Preparation and Properties of the σ-Picolyl Complexes of Palladium(II), $[\{PdCl(C_5H_4N\text{-}2\text{-}CH_2)PPh_{3-n}Me_n\}_2]$ (n=0, 1 and 2)

Kiyoshi ISOBE, Yukio NAKAMURA *(Osaka City Univ.)*, **and Shinichi KAWAGUCHI** *(Kinki Univ.)*

[*Bull. Chem. Soc. Jpn.*, **62**, 1802 (1989)]

The oxidative addition of 2-(chloromethyl) pyridine to tetrakis(triphenylphosphine)palladium (0) in toluene at 100 °C gave $[\{PdCl(C_5H_4N\text{-}2\text{-}CH_2)PPh_3\}_2]$ (**1**), which was characterized by analytical, molecular weight, and IR data as well as ^1H, ^{31}P, and ^{13}C NMR spectroscopy. The chloride ligand was readily replaced by other halides, whereas tertiary phosphines such as diphenylmethyl-, phenyldimethyl-, and triethylphosphines cleaved the bridge after substitution of triphenylphosphine to result in the monomeric trans-$[PdCl(C_5H_4N\text{-}2\text{-}CH_2)(PR_3)_2]$ complexes. Reactions of **1** with carbon monoxide and other reagents are also reported. The corresponding 3-picolyl complex $[\{PdCl(C_5H_4N\text{-}3\text{-}CH_2)PPh_3\}_n]$ was also prepared, but could not be well characterized because of lower stability and solubility.

V-E-2 Reaction of Pentamethylcyclopentadienyltetrachloromolybdenum(V). Synthesis, Structure and Electrochemical Properties of $[(\eta^5\text{-}C_5Me_5)MoOCl]_2O$

Keisuke UMAKOSHI and Kiyoshi ISOBE

Reaction of $[(\eta^5\text{-}C_5Me_5)MoCl_4]$ with Na_2WO_4 in THF gives red-brown $[(\eta^5\text{-}C_5Me_5)MoOCl]_2O$, while the reaction with Na_2MoO_4, Na_2WO_4, or $NaVO_3$ in water gives yellow $[(\eta^5\text{-}C_5Me_5)MoO_2]_2O$. The structure of $[(\eta^5\text{-}C_5Me_5)MoOCl]_2O$ has been investigated by X-ray diffraction (Figure 1). Each of molybdenum atoms with chloride ligand is linearly bridged by oxygen atom. $[(\eta^5\text{-}C_5Me_5)MoOCl]_2O$ shows reversible cyclic voltammogram in CH_2Cl_2 centered at -0.70 V vs Ag/AgCl. Crystal data: monoclinic, space group $P2_1/n$, a=10.621(1), b=14.371(3), c=7.689(1) Å, β=93.24(2)°, Z=2.

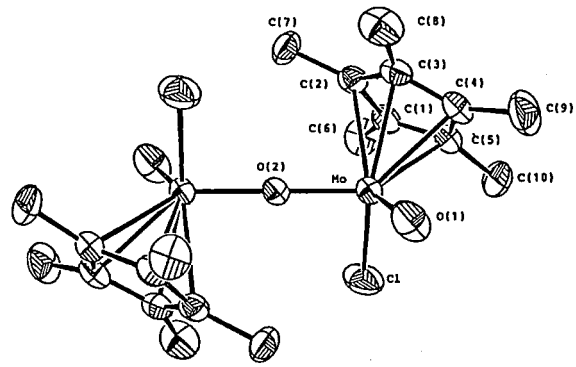

Figure 1. ORTEP diagram of $[(\eta^5\text{-}C_5Me_5)MoCl]_2O$. Thermal ellipsoids are drawn at the 50% probability level.

V–F Halogen-Bridged M^{II}-X-M^{IV} Mixed-Valence Compounds

In the past ten years, the series of halogen-bridged M^{II}-X-M^{IV} mixed-valence compounds (M=Pt, Pd, and Ni) has attracted much interest from solid-state physicists and chemists as one-dimensional materials having strong electron-lattice interaction. Their structures are well described as Peierls distorted linear chains with repeating unit $\cdots M^{II}\cdots X\text{-}M^{IV}\text{-}X\cdots$, in which the Peierls distortion is defined by the displacement of the bridging halogen atom, X, from the midpoint between the two metal atoms toward the M^{IV} atom. They show characteristic physical properties, such as the strong intervalence charge-transfer absorption and the luminescence with large Stokes shift. The solid-state properties can be interpreted by using an extended Peierls-Hubbard model which incorporates the electron-electron correlation on intermetal sites.

Recently, we succeeded in the preparation of halogen-bridged Ni^{III}-X-Ni^{III} compounds, which have a similar structure to the M^{II}-X-M^{IV} mixed-valence compound but have no Peierls distortion. The solid-state properties show the semiconductive character and the strong antiferromagnetic interaction between Ni^{III} atoms.

V-F-1 Crystal Structures and Solid State Properties of One-Dimensional Halogen-Bridged Ni^{III}-X-Ni^{III} Compounds (X=Cl and Br)

K. TORIUMI, M. YAMASHITA,[a] H. OKAMOTO, Y. WADA,[b] T. MITANI, S. BANDOW, Y. FUJII,[c] R.J.H. CLARK,[d] D.J. MICHAEL,[d] A.J. EDWARD,[e] D. WATKIN,[d] M. KURMOO,[d] and P. DAY[d] *([a]Nagoya Univ., [b]Nat. Inst. Res. Inorg., [c]Ibaraki Univ., [d]Univ. College London, [e]Oxford Univ.)*

[*J. Am. Chem. Soc.*, **111**, 2341 (1989)]

Halogen-bridged Ni^{III}-X-Ni^{III} linear-chain compounds, $\{[Ni(R,R\text{-chxn})_2X]X_2\}_\infty$ (X=Cl **1** and Br **2**), were synthesized and their structures have been determined by the low-temperature X-ray diffraction method. Crystal data for **2** are: orthorhombic, I222, Z=2, a=23.975(5), b=4.894(1), c=6.913(1) Å, V=811.1(3) Å^3 at -151 °C, and final R=0.032 and R_W=0.048 for 1974 reflections. The novel one-dimensional Ni^{III}-X-Ni^{III} structure with no Peierls distortion is an extreme limit of the M^{II}-X-M^{IV} mixed-valence structure. The optical energy gaps (1.3 eV for **1**

and 1.9 eV for **2**), electrical conductivities (1×10^{-3} $\Omega^{-1}cm^{-1}$ and 0.19 eV for **1**, and 2×10^{-2} $\Omega^{-1}cm^{-1}$ and 0.11 eV for **2**), and magnetic susceptibility data revealed the semiconductive character. The crystal structure analyses also revealed the characteristic hydrogen-bond network in the crystals [see *IMS Ann. Rev.* 120 (1988)].

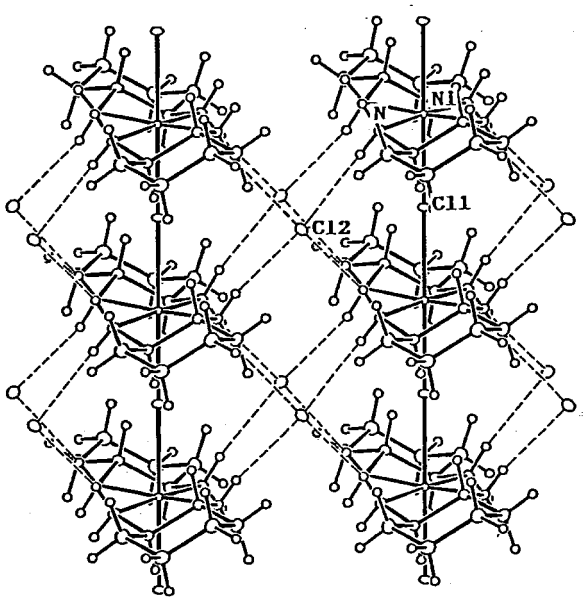

Figure 1. *ORTEP* drawing of a portion of the infinite chains along *b* with surrounding Cl^- ions of $\{[Ni(R,R\text{-}chxn)_2Cl]Cl_2\}_\infty$ at −151 °C. The dashed lines correspond to hydrogen bonds. The thermal ellipsoids are 50% probability surfaces.

V-F-2 Crystal Structure of Linear-Chain Chloro-Bridged Binuclear Platinum Complex, $(NH_4)_4[Pt_2(P_2O_5H_2)_4Cl]$

K. TORIUMI, M. YAMASHITA *(Nagoya Univ.)*, **SONGCHUN JIN** *(Tohoku Univ. and Changchun Inst. Appl. Chem.)*, **and T. ITO** *(Tohoku Univ.)*

[*Acta Cryst.*, **C45**, 1415 (1989)]

The title compound is one of a series of one-dimensional halogen-bridged mixed valence compounds which are of interest in the strong electron-lattice interaction. Crystal data are: orthorhombic, Pnnm, a=9.660(5), b=14.959(7), c=8.215(4) Å, V=1187(1) $Å^3$, Z=2, and R=0.025 for 1507 reflections. The structure consists of a linear chain with a $\cdots Pt^{II}\text{-}Pt^{II}\cdots Cl\text{-}Pt^{III}\text{-}Pt^{III}\text{-}Cl\cdots$ repeating unit along the c axis. Two Pt atoms are bridged by four $P_2O_5H_2^{2-}$ ligands and the Pt-Pt separation is 2.830(1) Å. The Pt-Pt distance is intermediate between the Pt^{II}-Pt^{II} distance (2.925(1) Å) observed for $K_4[Pt_2(P_2O_5H_2)_4]\cdot2H_2O$[1] and the Pt^{III}-Pt^{III} distance (2.695(1) Å) for $K_4[Pt_2(P_2O_5H_2)Cl_2]\cdot2H_2O$.[2] The bridging Cl atom is disorderd over two sites, giving short Pt-Cl (2.363(4) Å) and long Pt-Cl (3.022(4) Å) distances in the chain. The bridging O atoms of $P_2O_5H_2^{2-}$ ligands deviate 0.298(6) Å and 0.548(5) Å from the planes defined by two Pt atoms and two P atoms of the ligand, respectively.

References

1) C.-M. Che, F.H. Herbstein, W.P. Schaefer, R.E. Marsh, and H.B. Cray, *J. Am. Chem. Soc.*, **105**, 4604 (1983).
2) R.E. Marsh and F.H. Herbstein, *Acta Cryst.*, **B39**, 280 (1983).

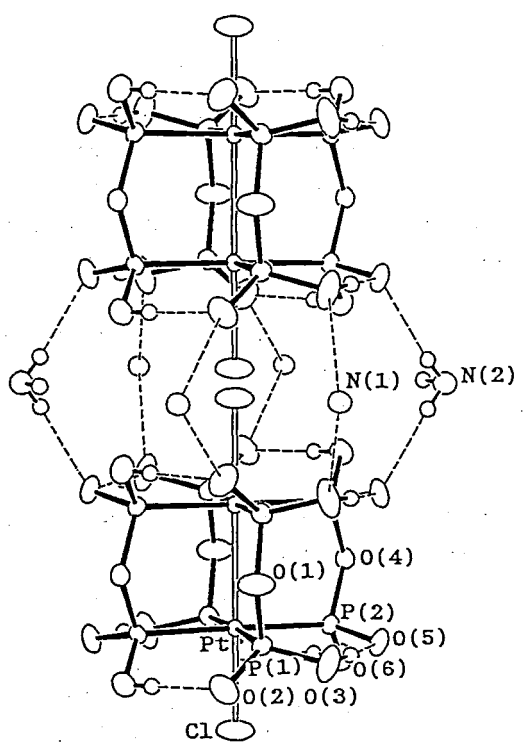

Figure 1. *ORTEP* drawing of a portion of the infinite chain along the *c* axis; thermal ellipsoid at 50% probability level; hydrogen bond by a broken line; binuclear complex lying on a 2/m site.

V-G New Reactive Intermediates Serving for Carbon-Carbon Bond Formation Reactions

Discovery of new reactive intermediates represents an ever-lasting challenge for chemists. In the past several decades, organometallic compounds have attracted particular interests as reactive intermediates that are important not only by themselves but for their use in organic chemistry. In the title area of research, we have placed a particular emphasis on the search for the "environment" wherein organometallic species may exhibit their greatest power in effecting formation of new carbon-carbon bonds.

V-G-1 Synthesis of Propellanes by "Exocyclic" Transannular Cycloaddition of Olefinic Methylenecyclopropanes

Shigeru YAMAGO *(Tokyo Inst. of Tech.)* **and Eiichi NAKAMURA** *(Tokyo Inst. of Tech. and IMS)*

[*Tetrahedron*, **45**, 3081 (1989)]

Olefinic methylenecyclopropanes (**1**) undergo quantitative transannular ring closure in the presence of Group 10 metal catalyst (e.g., $Ni(COD)_2/Ph_3P$, $PdCl_2(Ph_3P)_2$/DIBAL) to give [3.3.3]propellanes through cycloaddition of a trimethylenemethane-like intermediate. Synthesis of 12-nor-13-acetoxymodhephene (**2**) has been achieved in high overall yield using this new synthetic strategy.

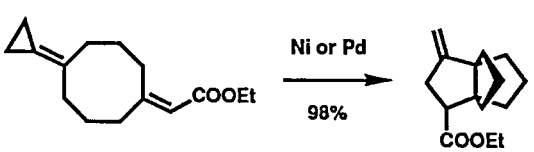

1

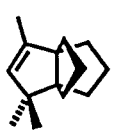

2

V-G-2 Use of Methylenecyclopropanone Ketals for Cyclopentane Synthesis. A New Efficient Thermal [3+2] Cycloaddition

Shigeru YAMAGO *(Tokyo Inst. of Tech.)* **and Eiichi NAKAMURA** *(Tokyo Inst. of Tech. and IMS)*

[*J. Am. Chem. Soc.* in press]

A ketal of methylenecyclopropanone (**1**) undergoes thermal [3+2] cycloaddition with a wide range of electron-deficient olefins to give five-membered carbocycles(**2**) in nearly quantitative yields. The cycloaddition proceeds with high retention of the stereochemistry of the olefinic acceptor and provides a viable synthetic route to functionalized bicyclo[3.n.0]alkanes.

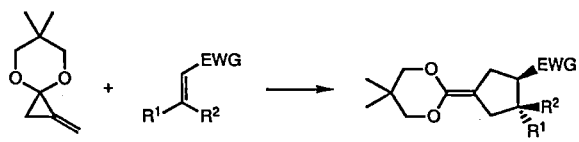

1 2

V-H Magnetic and Electronic Interactions through Organic Ligands in Dinuclear Copper(II) Complexes

Control of electronic and magnetic interactions between metal ions through an organic ligand in multi-nuclear coordination compounds is important to synthesize a molecule or molecular assembly which has interesting physical properties. In this project, new pyrazine bridged-dinuclear copper(II) compounds were synthesized and their the magnetic and electronic properties were studied.

V-H-1 Synthesis, Crystal Structure, and Electrochemical Property of Dichloro-μ-{2,5-bis[*N*,*N*-bis(2′-pyridylmethyl)aminomethyl]pyrazine}dicopper(II) perchlorate

Hiroki OSHIO, Koshiro TORIUMI, and Yoshihito HAYASHI

[*J. Chem. Soc., Dalton Trans.*, in press]

Reaction of octadentate ligand 2,5-bis[*N*,*N*-bis(2′-pyridylmethyl)aminomethyl]pyrazine (bpmpz) and copper(II) salt produces a dinuclear complex, which crystallized in green complexes $[Cu_2(bpmpz)Cl_2](ClO_4)_2$. The structure of the complexes has been determined by X-ray analysis. Crystallographic data are: triclinic, $P\bar{1}$, Z=1, a=10.004(1), b=12.212(2), c=7.791(1)Å, α=100.99(1), β=86.26(1), γ=111.76(1)°, R=0.036 for 2343 reflections. The complex cations in the crystals have centrosymmetric dinuclear structures with copper atoms in distorted square-pyramidal geometries. E.p.r. and magnetic susceptibility data of the compound do not show a strong magnetic interaction between copper atoms. The compound in acetonitrile shows a quasi-reversible cyclic voltammogram(CV) and the CV was interpreted to the two-step reduction whose potentials to the Cu(II)-Cu(I) and Cu(I)-Cu(I) from the Cu(II)-Cu(II) were estimated to be −0.14 and −0.26 V, respectively.

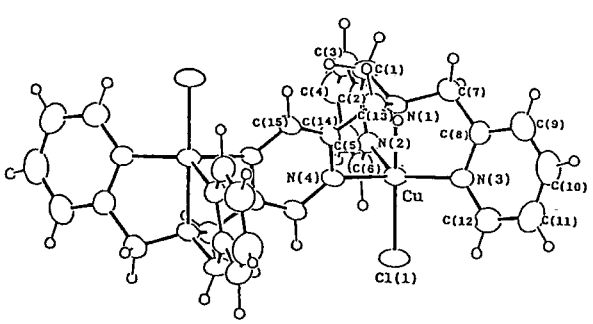

Figure 1. Molecular Structure of $[Cu_2(bpmpz)Cl_2]^{2+}$

V-H-2 Magnetic Property of Pyrazine-Bridged Dinuclear Copper(II) Compound. X-ray Structure of μ-2,5-Bis[{(dimethylamino)methyl}-pyrazine]-bis[(diethylenetriamine)copper(II)] perchlorate

Hiroki OSHIO and Umpei NAGASHIMA

Crystal structure and magnetic property of $[Cu_2(dapz)(dien)](ClO_4)_4$ where dapz is 2,5-bis[(dimethylamino)methyl]pyrazine and dien is diethylenetriamine are described. The crystal structure has been determined by X-ray diffractometry and crystallographic data are: monoclinic Z=2, a=15.441(3), b=14.519(2), c=7.954(2)Å, β=100.15(2)°, V=1755.4(6)Å^3, R=0.0386 for 3197 reflections. The compound is a ClO_4^- salt of a pyrazine-bridged, centrosymmetric Cu(II) dimeric cation with a distorted trigonal-bipyramidal symmetry around copper atom. An antiferromagnetic interaction was deduced from an EPR spectrum that shows the Δm=2 transition at 1600 G and the interaction is weak (J=−1.7 cm^{-1} and g=2.106) in spite of the fact that the unpaired electron, which reside in the d_{z^2} orbital, is almost directed at the nitrogen atom of bridged pyrazine ligand. From the extended Hückel MO studies for the compounds, it is suggested that direct or through ligand charge transfer characters between metal ions and a spin polarization mechanism through π-electrons play an important role to propagate an magnetic superexchange interaction in addition to the σ-orbitals pathway.

V–I Thermodynamic Stabilities of Carbocations in the Gas Phase

Studies on ion-molecule reactions in the gas phase provide an important basis for separation of the intrinsic structural effects from solvent effects. In this project, gaseous thermodynamic stabilities of carbocations were determined for a series of benzylic systems, $Ar\text{-}C^{+}(R^{1})R^{2}$, by measuring equilibrium constants of proton- or chloride-transfer reactions using a pulsed ion cyclotron resonance spectrometer. Inherent delocalization of the charge in a cation was explored by analysis of the substituent effects on intrinsic stabilities of carbocations based on the Yukawa-Tsuno LArSR equation.

$$\delta\Delta G^{\circ} = \rho(\sigma^{\circ} + r\,\Delta\bar{\sigma}_{R}^{+})$$

The r value is a parameter characteristic of a given system, measuring the resonance demand, the degree of π-interaction between the aryl π-system and reaction site. Comparison of gas-phase results with those for S_N1 solvolysis provided a new insight into the concept for relating the solvolysis transition states to their carbocationoid intermediates.

V-I-1 Stabilities of α-Cumyl Cations in the Gas Phase

Masaaki MISHIMA, Satoshi USUI *(Kyushu Univ.)*, **Hiroki INOUE** *(Kyushu Univ.)*, **Mizue FUJIO** *(Kyushu Univ.)*, **and Yuho TSUNO**

[*Nippon Kagaku Kaishi*, Special Articles on Structure and Reaction of Unstable Species, 1262 (1989)]

The gas-phase basicities (GB) of 2-(*m,p*-substituted phenyl)propenes were determined based on proton-transfer equilibrium method using a pulsed ion cyclotron resonance (ICR) spectrometer. The substituent effect on GB was linearly correlated with σ^{+}, giving a ρ of -13.0. The excellent correlation which covers a range of 35 kcal mol^{-1} reveals that σ^{+} values determined in solution are applicable to the gas-phase substituent effects without modification accounting for solvation of substituents, and suggests that the resonance demand for the α-cumyl cation stability is identical with an r of 1.00 for the solvolysis of α-cumyl chlorides. The identity of the r value between in gas phase and in solution leads to a conclusion that the degree of π-delocalization of the positive charge into aryl ring is independent of solvation effects. That is, the solvation of cation causes the dispersion of the central charge into solvent, resulting in the lower response of substituent effects, essentially without change in intramolecular charge delocalization.

V-I-2 Substituent Effect on the Stability of 1-Phenylethyl Cation in the Gas Phase

Masaaki MISHIMA, Satoshi USUI *(Kyushu Univ.)*, **Mizue FUJIO** *(Kyushu Univ.)*, **and Yuho TSUNO**

[*Nippon Kagaku Kaishi*, Special Articles on Structure and Reaction of Unstable Species, 1269 (1989)]

The gas-phase basicities were determined for a series of styrenes based on proton-transfer equilibrium method. The LArSR analysis of the substituent effect gave an r of 1.14 and a ρ of -13.6. The r value higher than unity indicates clearly a greater resonance demand for 1-phenylethyl cation than that for α-cumyl cation while the ρ value is in agreement with that of the latter. The exalted resonance demand might be attributed to the lower stability of 1-phenylethyl cation than α-cumyl cation. This trend in the r value is consistent with the observations for the relevant benzylic carbocations. Most importantly, the r value for gas-phase stability has been found to be identical in magnitude with the corresponding value for the solvolysis of 1-phenylethyl chlorides (r=1.15), supporting that the r value for the solvolysis is not a correlational artifact arising as a result of the non-linearity caused from mechanistic transition with change of substituent but intrinsic resonance demand characteristic of the parent 1-phenylethyl cation itself.

V-I-3 Gas Phase Substituent Effects in a Highly Electron Deficient System. Intrinsic Resonance Demand of 1-Aryl-1-(trifluoromethyl)ethyl Cation

Masaaki MISHIMA, Hiroki INOUE *(Kyushu Univ.)*, **Mizue FUJIO** *(Kyushu Univ.)*, **and Yuho TSUNO**

[*Tetrahedron Lett.* **30**, 2101 (1989)]

Gas phase stabilities of 1-aryl-1-(trifluoromethyl)ethyl cations as a highly electron-deficient carbocation system were determined by measuring equilibrium constants of proton transfer reactions of 1-aryl-1-(trifluoromethyl)ethylenes with appropriate reference cations by means of a pulsed ICR spectrometer. The substituent effect for stabilities of 1-aryl-1-(trifluoromethyl)ethyl cations was linearly correlated in terms of the LArSR equation with a ρ of -14.0 and a unique r value of 1.40 remarkably higher than unity for α-cumyl cation. The exalted resonance demand must be caused from strong destabilization of the charge in a cation by the electron-withdrawing CF_3 group. Clearly, this system with a high resonance demand r=1.4 is far beyond the applicability of the simple Brown σ^+ analysis. The identity of the r value between gas-phase carbocation stability and S_N1 solvolysis was observed, suggesting that the charge delocalization in the solvolysis transition state must be quite close to that of the carbocation intermediate.

V-I-4 Gas Phase Substituent Effects. Stabilities of 1-Aryl-2-,2,2-trifluoroethyl Cations

Masaaki MISHIMA, Hiroki INOUE *(Kyushu Univ.)*, **Mizue FUJIO** *(Kyushu Univ.)*, **and Yuho TSUNO**

[Submitted to *Tetrahedron Lett.*]

Gas-phase stabilities of 1-aryl-2,2,2-trifluoroethyl cations were determined based on chloride-transfer equilibria by the pulsed ion cyclotron resonance spectrometer. Chloride ion affinity of 1-phenyl-2,2,2-trifluoroethyl cation was higher by 7.0 kcal mol^{-1} than the corresponding benzyl cation. Combining with relevant results, it is found that the stability of the parent benzylic carbocation (ring substituent=H) significantly depends on electronic effects of α-substituent(s) linked to the central carbon. The effects of ring-substituent on the stability of 1-phenyl-2,2,2-trifluoroethyl cation have been analyzed based on the LArSR Eq., giving a remarkably high r of 1.53. The less stable carbocation should have substantially the higher resonance demand. The plots of the r values against the relative stabilities of the respective parent carbocations give a good linear relationship as shown in Figure 1. There is a continuous spectrum of varying resonance demands characteristic of the stabilities of parent carbocations. The degree of the π-delocalization of the charge in a cation into aryl π-system reflects the stabilization from α-substituent(s).

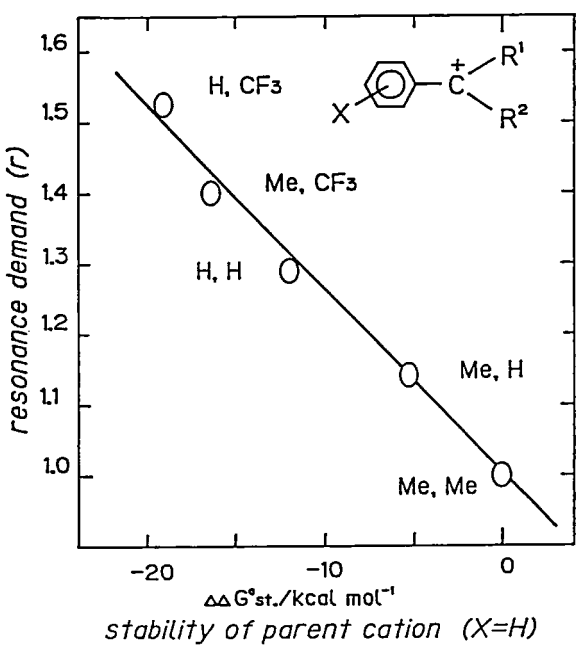

Figure 1. Relationship between resonance demands (r) and the stabilities of parent carbocations.

V–J Structure-Reactivity Relationship in Solvolysis

The substituent effect in the systems where the direct π-interaction between the aryl and carbocationic center is possible, can be generally described by the LArSR equation.

$$\log k/k_o = \rho(\sigma^o + r\Delta\bar{\sigma}_R^+)$$

What we have envisaged in the LArSR Eq. is to introduce the concept of varying resonance demands of reactions into the substituent effect analysis. The significance of r value will be examined by exploring the substituent effects on the system whose r value is significantly different from unity. In this project, we investigated extensively the solvolysis of neophyl brosylates as a model system giving a lower r value, and 1-aryl-1-(trifluoromethyl)ethyl tosylates giving a higher resonance demand, in addition to α-t-butylbenzyl tosylates as a model of the ordinary solvolysis of σ^+ category. The LArSR Eq. was successfully applied to other systems with a unique r value characteristic of the system.

V-J-1 The Resonance Demand in the Acetolysis of Neophyl Brosylates

Mizue FUJIO *(Kyushu Univ.)*, **Mutsuo GOTO** *(Kyushu Univ.)*, **Masaaki MISHIMA, and Yuho TSUNO**

The substituent effect in the acetolysis of neophyl brosylates was analyzed statistically based on the LArSR equation. The Brown $\rho^+\sigma^+$ equation did not provide a linear correlation but the LArSR equation gave an excellent linear correlation with an r value of 0.57, substantiating our basic LArSR concept of varying resonance demands with different systems. For statistical examination of the reliability of r value, the change in the standard deviation of the LArSR correlation was followed as a function of varying r by the iterative least-squares method. The r value of the neophyl solvolysis must be statistically significant enough to distinguish between the LArSR and simple Brown $\rho^+\sigma^+$ correlations of this system. The significance of the best-fit correlation was found to depend strongly upon the number and combination as well as the range of effective substituents. The study was extended to various β-aryl-assisted processes of complex mechanisms. Precise dissection analysis into two non-crossover k_Δ an k_s processes has been realized by the Gauss-Newton type non-linear least-squares method based on the assumption of LArSR correlations for both processes. The generality of the unique r_Δ value of neophyl solvolysis was verified to these β-aryl-assisted processes. The substituent effect on the k_Δ process can be characterized far more appropriately in terms of the $\bar{\sigma}_\Delta$ of r=0.6 rather than σ^+ of r=1.00.

V-J-2 Solvolysis of 1-Aryl-1-(trifluoromethyl)-ethyl Tosylates

Akihisa MURATA *(Kyushu Univ.)*, **Mutsuo GOTO** *(Kyushu Univ.)*, **Ryoji FUJIYAMA** *(Kochi Univ.)*, **Masaaki MISHIMA, Mizue FUJIO** *(Kyushu Univ.)*, **and Yuho TSUNO**

The rates of solvolysis of 1-aryl-1-(trifluoromethyl)ethyl tosylates were determined in 80% aqueous ethanol for a series of substituents. The Brown $\rho^+\sigma^+$ treatment fails to give a simple linear plot but all the p-π-donors deviate upward from the meta-correlation line. On the other hand, the LArSR Eq. gives a linear correlation for the whole range of substituents,

$$\log (k/k_o) = -6.287(\sigma^o + 1.388\Delta\bar{\sigma}_R^+)$$

with excellent precision. Strong destabilization of the carbocation intermediate by α-CF_3 appears to be reflected only in the extremely high r value, but not in the ρ value of the substituent effect. This conflicts seriously with the conclusion in the literature given for this reaction based on the simple Brown σ^+ treatment. This reaction having an extremely high resonance demand r=1.4 should be far beyond the scope of the simple Brown σ^+ analysis. Varying resonance demand should be a basic requirement for adequately describing the substituent effect on conjugative carbocation reactions.

V-J-3 Solvolysis of α-t-Butylbenzyl Tosylates

Yutaka TSUJI *(Kyushu Univ.)*, **Mizue FUJIO** *(Kyushu Univ.)*, **and Yuho TSUNO**

Rates of solvolysis of α-t-butylbenzyl tosylates were determined in 80% aqueous acetone (80A), 80% aqueous ethanol (80E), and 97%(w/w) aqueous trifluoroethanol (97Tw) for an extended series of substituents. The substituent effect can be linearly correlated in terms of the LArSR relationship, with a ρ value of −5.521 and an r value of 1.097 in 80A, and −5.650 and 1.106 in 80E, respectively. The same r value was obtained in 97Tw although serious deviations due to solvent effects on particular substituents were observed. The identity of r value in all solvents reveals that the r of 1.10 is characteristic of this system independent of solvents. The large negative ρ and exalted r values suggest the operation of the k_c mechanism in this secondary benzylic solvolysis without any nucleophilic solvent assistance and methyl participation. From the comparison of the substituent effects, the exalted r value of 1.15 in the solvolysis of α-methylbenzyl chlorides can be attributed to the enhanced resonance demand characteristic of secondary benzylic system rather than to a correlational artifact arising from non-linearity due to S_N1-S_N2 mechanistic change.

V−K Detailed Reaction Mechanisms of Solvolyses and Their Transition States

V-K-1 Non-Destructive Detection of Ion-Pair Return in Acetolysis of ^{13}C and ^{18}O Doubly Labeled β-Arylalkyl Tosylates. Quantitative ^{13}C-NMR Spectrometry by Using ^{18}O Isotope Effect

Mizue FUJIO *(Kyushu Univ.)*, **Futoshi SANEMATSU** *(Kyushu Univ.)*, **Yuho TSUNO, Masami SAWADA** *(Osaka Univ.)*, **and Yoshio TAKAI** *(Osaka Univ.)*

[*Nippon Kagaku Kaishi*, Special Articles on Structure and Reaction of Unstable Species, 1371 (1989)]

New non-destructive methodology to study the return process in the acetolysis of aralkyl benzenesulfonate esters was developed based upon ^{13}C NMR determination of oxygen-18 label scrambling within sulfonate moiety. The splitting in the ^{13}C NMR signals, induced by isotopic oxygen substitution $^{16}O/^{18}O$, was utilized successfully to determine quantitatively the extent of ^{18}O scrambling within three oxygens in the sulfonate moiety. ^{13}C-enrichment of the target carbon permitted direct determination of the signal intensities in situ. The method was applied to the investigation of return process in the acetolysis of neophyl, 2-phenylpropyl, and 2-arylethyl tosylates. In the acetolysis of neophyl tosylate, no ^{18}O-scrambling at the alkoxy oxygen of the starting tosylate was detected at all, affording the first experimental evidence for the absence of internal ion-pair return. The acetolysis of 2-(*p*-MeO-phenyl)ethyl tosylate gives the rearranged tosylates with complete randomization of the three oxygens. The acetolyses of 2-phenylpropyl and 2-phenylethyl tosylates also give the rearranged tosylates of two signals, accompanying the incomplete oxygen equilibration. The different scrambling behaviors for substituted phenylethyl tosylates may be arrtibutable to the nature of the ion-pairs. In the acetolysis of 2-phenylethyl tosylate, parallel runs of (1-*C)-OTs* and (2-*C)-OTs* indicate the equivalence of two methylene carbons for ^{18}O-incorporation from sulfonyl oxygens in the return process. This provides strong evidence that the ^{18}O scrambling occurs only after the formation of symmetrical phenonium-ion species.

V-K-2 Solvolysis of Benzyl Tosylates

Mizue FUJIO *(Kyushu Univ.)*, **Mutsuo GOTO** *(Kyushu Univ.)*, **Toshihiro SUSUKI** *(Kyushu Univ.)*, **Masaaki MISHIMA, and Yuho TSUNO**

The rates of solvolyses of a series of substituted benzyl tosylates were determined in 80% aqueous

acetone, and the substituent effect was analyzed in detail. The LArSR Eq. as well as Hammett-Brown treatment failed to give any simple linear plot for the effect of the full range of substituents, suggesting significant mechanistic shift. The σ^+ plot gave a split pattern of parallel curvatures with significant gaps for strong π-donors, weak π-donors, and non-conjugative substituents, respectively. The widely split σ^+ plot conflicts with the widely accepted interpretation in terms of k_c-k_s mechanistic transition, since the k_c-k_s mechanistic change should result in a single smooth-curved plot, only if plotted against an appropriate substituent constant scale. The plots of para π-donors against an appropriate $\bar{\sigma}^+$ scale with r=1.3 coalesced into a single smooth curve including the meta correlation curve. A sufficiently linear LArSR plot with r=1.3 for the reactive substituents down to m-methyl group can be referred to the substituent effect correlation for the k_c mechanism of this system. The result of correlation analysis confirmed this conclusion, giving a best ρ value of -5.24 and an r value of 1.28 for the range of substituents more activating than 4-MeS-3-CN.

RESEARCH ACTIVITIES VI
Coordination Chemistry Laboratories

In order to change the cycle of the term of adjunct professors and associate professors of the Coordination Chemistry Laboratories, Professor Akira Uehara and Associate Professor Hisashi Okawa retired their adjunct positions and went back to Kanazawa University and Kyushu University, respectively, and Dr. Masanobu Hidai of the University of Tokyo and Dr. Toshio Yamaguchi of Fukuoka University have been appointed to be a new Adjunct Professor and a new Adjunct Associate Professor, respectively, instead. Professor Hidai is a well-known scientist in the field of organometallic chemistry and Associate Professor Yamaguchi is a young and active solution chemist.

A technical assistant, Dr. Atsushi Yagasaki and an IMS fellow, Dr. Yusuke Tamura recently joined us to study coordination chemistry in the solid and solution states. Professor Georg Johansson of the Royal Institute of Technology in Stockholm, Sweden has been invited as a Guest Professor of the Coordination Chemistry Laboratories and is staying until the end of September, 1990.

The most noticeable occasion in the Coordination Chemistry Laboratories in this year is that a new laboratory of functional coordination chemistry has been established. Selection of the best person as the professor is going on now.

VI-A Structural Studies of Liquids

Structures of liquids and liquid mixtures are investigated by the X-ray diffraction method.

VI-A-1 Intramolecular and Liquid Structure of 2,2,2-Trifluoroethanol by X-Ray Diffraction

Tamas RADNAI*, Shin-ich ISHIGURO* *(*Tokyo Inst. of Tech.)*, **and H. OHTAKI**

[*J. Solution Chem.*, **18**, 771 (1989)]

Intramolecular and liquid structures of 2,2,2-trifluoroethanol (TFE) have been investigated by the X-ray diffraction method at 25°C. The structural parameters for the skeleton of the molecules in the liquid phase are similar to those in the gas phase. The conformers of TFE molecules in the liquid phase are discussed. The O...O distance at about 284 pm and additional F...O distance of about 302 pm were found to be characteristic for the first neighbor interactions. Various models (dimers and trimers) have been examined for analyzing the first negihbor structure of the liquid. The liquid structure was explained in terms of small clusters containing two to three molecules rather than a more extended polymer network.

VI-B Structure of Hydrated Metal Ions in Solution

Structures of hydrated ions in aqueous solutions have been studied by the X-ray diffraction, EXAFS and Raman spectroscopic methods.

VI-B-1 A Raman Investigation of the Hydration of Scandium (III) Ions

Hitoshi KANNO *(The National Defence Academy)*, **Toshio YAMAGUCHI** *(Fukuoka Univ.)*, **and Hitoshi OHTAKI**

[*J. Phys. Chem.*, **93**, 1695 (1989)]

Raman spectra were measured for aqua-Sc^{3+} ions in aqueous $ScCl_3$ and $Sc(ClO_4)_3$ solutions in both the liquid state at room temperature and the glassy state at liquid nitrogen temperature. Four Raman bands, inconsistent with octahedral symmetry, were observed for aqua-Sc^{3+} ions in the glassy $ScCl_3$ solution. It is concluded that the inner-sphere hydration number of all-aquated Sc^{3+} ions is other than six, probably seven.

VI–C Structural Studies of Ionic Melts

The liquid structure of ionic melts has been studied by the pulsed neutron diffraction method.

VI-C-1 Structural Study on Molten (^{7}Li, K)Cl and (^{7}Li, Na, K)Cl of the Eutectic Composition by Pulsed Neutron Diffraction

Akira ENDOH*, Toshio YAMAGUCHI*, Yusuke TAMURA*, Osamu ODAWARA*, Isao OKADA* *(*Tokyo Inst. of Tech.)*, **Hitoshi OHTAKI, and Masakatsu MISAWA** *(National Lab. for High Energy Physics)*

[*Z. Naturforsch.* **43a**, 961 (1988)]

Pulsed neutron diffraction measurements have been performed on molten (^{7}Li, K)Cl and (^{7}Li, Na, K)Cl mixtures of the eutectic composition to determine the nearest neighbour distance between Li^+ and Cl^- ions. Owing to the negative scattering length of the ^{7}Li nucleus, this contribution becomes negative in the radial distribution function and can be separated from the other contributions. The nearest neighbour distance between Li^+ and Cl^- ions is found to be 240 pm in both the binary and ternary mixtures.

VI–D Thermodynamic and Spectroscopic Studies of Metal Complexes in Nonaqueous Solutions

Formation constants, enthalpies, and entropies of complex formation reactions and structures of the complexes formed in nonaqueous solvents have been investigated by calorimetric and spectrophotometric methods.

VI-D-1 Calorimetric and Raman Spectroscopic Studies of Cadmium(II) Thiocyanato Complexes in *N,N*-Dimethylformamide

Shin-ich ISHIGURO*, Toshiyuki TAKAMUKU* *(*Tokyo Inst. of Tech.)*, **and Hitoshi OHTAKI**

[*Bull. Chem. Soc. Jpn.*, **61**, 3901 (1988)]

Formation of thiocyanato complexes of cadmium(II) ion has been calorimetrically studied in *N,N*-dimethylformamide(DMF) at 25°C. Calorimetric data obtained were well explained in terms of the formation of a series of four mononuclear $[CdX_n]^{(2-n)+}$ (n=1-4, X=SCN) complexes, and their formation constants, enthalpies and entropies were determined. Raman band shifts for the C-S stretching vibration of SCN^- ion indicated that SCN^- ion binds to cadmium(II) ion only with the N end within the mono- and dithiocyanato complexes, $[Cd(NCS)]^+$ and $[Cd(NCS)_2]$. Within the tri- and tetrathiocyanato complexes, thiocyanate ions bind with both the N and S ends, and the coordination modes, $[Cd(NCS)_2(SCN)]^-$ and $[Cd(NCS)_3(SCN)]^{2-}$, were suggested. The coordination modes for the di- and tetrathiocyanato complexes in DMF, $[Cd(NCS)_2]$ and $[Cd(NCS)_3(SCN)]^{2-}$, respectively, are different from those in water, $[Cd(NCS)(SCN)]$ and $[Cd(NCS)_2(SCN)_2]^{2-}$, respectively. It is thus shown that the N-bonding becomes more favorable in DMF than in water. Such a result may mainly be ascribed to relative weakened solvation of the SCN^- ion in DMF, especially at the N atom site which is hydrogen-bonded with water molecules but not with DMF.

VI-D-2 Solvent Effect on the Formation of Copper(II) Chloro Complexes in Acetonitrile-Dimethyl Sulfoxide Mixtures

Shin-ichi ISHIGURO*, Honoh SUZUKI*, Bojana G. JELIAZKOVA* *(*Tokyo Inst. of Tech.)*, **and Hitoshi OHTAKI**

[*Bull. Chem. Soc. Jpn.*, **62**, 39 (1989)]

Complexation of copper(II) with chloride ions has been studied calorimetrically and spectrophotometrically in various acetnitrile(AN)-dimethyl sulfoxide(DMSO) mixtures at 25°C. Complexation of copper(II) ion with DMSO as a ligand in AN has also been investigated calorimetrically. It is indicated that the solvent effect on the thermodynamic parameters of the complexation is dominated by two factors: (1) the preferential solvation of copper(II) ion with DMSO that mainly affects the enthalpies, and (2) the change in solvent-solvent interactions in the bulk that strongly affects the corresponding entropies.

VI-D-3 Spectrophotometric and Calorimetric Studies on the Formation of Binary (2,2′-Bipyridine)nickel(II) and Ternary (2,2′-Bipyridine)chloronickel(II) Complexes in *N*,*N*-Dimethylformamide

Shin-ichi ISHIGURO*, Kazuhiko OZUTSUMI*, Laszlo MAGY* *(*Tokyo Inst. of Tech.)*, **and Hitoshi OHTAKI**

[*J. Chem. Soc. Dalton Trans.* 655 (1989)]

Formation of binary (2,2′-bipyridine)nickel(II) and ternary (2,2′-bipyridine)chloronickel(II) complexes has been studied by spectrophotometry and calorimetry in *N*,*N*-dimethylformamide (DMF) at 25°C. Both spectrophotometric and calorimetric data obtained were well explained in terms of the formation of binary $[Ni(bipy)]^{2+}$ (bipy = 2,2′-bipyridine), $[Ni(bipy)_2]^{2+}$ and $[Ni(bipy)_3]^{2+}$ and ternary $[NiCl(bipy)]^{+}$, $[NiCl(bipy)_2]^{+}$, $[NiCl_2(bipy)]$, and $[NiCl_2(bipy)_2]$ complexes, and their formation constants, enthalpies, and entropies were determined. Electronic spectra of the individual complexes suggest that all the ternary complexes have an octahedral six-coordinate structure, as have the binary complexes in solution.

VI-E Synthesis, Characterization and Structural Effects on Chemical Properties of Novel Macrocyclic Polyamine Ligands and Their Complexes

A novel functionalized macrocyclic polyamines are synthesized by renovating the classical structure of macrocyclic polyamines; (1) conversion of amines into amides; (2) replacement of N donors for S donors; (3) replacement of skeletonic C-H for C-F; (4) attachment of intramolecular $[Ru(bpy)_3]^{2+}$ pendant.

VI-E-1 A New Tetradentate $(N^-)_2S_2$ Macrocyclic Ligand which is Highly Selective for Platinum(II) and Palladium(II)

Eiichi KIMURA, Yasuhisa KUROGI*, Senji WADA*, and Mitsuhiko SHIONOYA *(*Hiroshima Univ.)*

[*J. Chem. Soc., Chem. Commun.*, 781 (1989)]

Earlier, we designed 'dioxocyclams' (**1a-c**) as hybrid ligands of oligopeptides and cyclam for selective uptake of Cu^{II}, Ni^{II}, Pd^{II}, Pt^{II} or Co^{II} against other metal ions. Although both (**1**) and (**3**) enclose M^{II} ions to yield 1:1

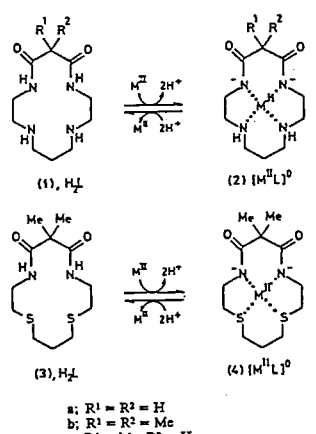

complexes with a common formula, $[M^{II}L]^0$ (2) and (4), respectively, the new sulphur ligand (3) shows high selectivity and efficiency for complex formation with Pt^{II} and Pd^{II} over Cu^{II}, Ni^{II} and Co^{II}.

VI-E-2 Novel Fluorinated Dioxocyclams and Cyclam Complexes: Synthesis, Characterization, X-Ray Structure, and Structural Effects on Chemical Properties

Mitsuhiko SHIONOYA, and Eiichi KIMURA

[submitted to *J. Am. Chem. Soc.*]

Following an earlier report of mono- and difluorinated dioxocyclams (**1b** and **1c**) and cyclams (**2b** and **2c**),[1] we now have succeeded in the synthesis of tetrafluorinated counterparts, **1d** and **2d**.

The effects of the successive F substitutions are illustrated by the protonation constants (pK_a) and redox potentials $E_{1/2}$ of their Cu^{II} and Ni^{II} complexes, as summarized in Table. The Ni(II)-**2d** complex takes nearly 100% high spin state (blue, λ_{max} 517 nm, ε7) in aq.0.1 M $NaClO_4$ at 25°C, while with the nonfluorinated cyclam (**2a**) counterpart, 29% in high spin and 71% in low spin states.[2] X-ray structure of Ni(II)-**2d** complex was also determined.

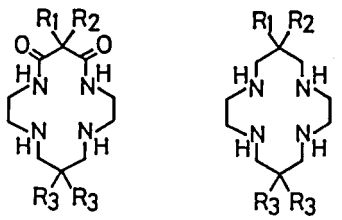

Dioxocyclams (1) Cyclams (2)

a; $R_1=R_2=R_3=H$
b; $R_1=F$, $R_2=R_3=H$
c; $R_1=R_2=F$, $R_3=H$
d; $R_1=R_2=R_3=F$

References

1) E. Kimura, M. Shionoya, M. Okamoto and H. Nada, *J. Am. Chem. Soc.*, **110**, 3679 (1988).
2) L. Fabbrizzi *et al.*, *J. Chem. Soc. Dalton Trans.*, 1857 (1979).

Table. Some Properties of Fluorinated Cyclams.

Ligand	pK_1 (0.1M $NaClO_4$)	pK_2	$E_{1/2}$(V *vs* SCE at pH=7, 25°C) $Cu^{III/II}$	$Ni^{III/II}$	$Ni^{III/I}$
1a	9.6	5.9	+0.64		
b	9.4	5.7	+0.69		
c	9.2	5.2	+0.83		
d	6.1	<2	>+1.0 (0.5M Na_2SO_4)		
2a	11.8	10.6		+0.50	−1.56
b	11.0	9.4		+0.52	−1.52
c	10.8	7.5		+0.63	−1.46
d	8.2	6.7		+0.81 (0.5M Na_2SO_4)	−1.40 (0.1M $NaClO_4$)

VI-E-3 A Novel Cyclam-Ni(II) Complex Appended with Tris-(2,2′-bipyridine) Ruthenium(II) Complex

Eiichi KIMURA, Senji WADA*, Mitsuhiko SHIONOYA, Toshikazu TAKAHASHI*, and Yoichi IITAKA** *(*Hiroshima Univ., **Teikyo Univ.)*

[submitted to *J. Am. Chem. Soc.*]

Synthesis, X-ray structure and some novel chemical properties of a new supermolecular ligand $[Ru^{II}(bpy)_2(bpy\text{-}cyclam)]^{2+}$ (**2**), and a resulting heterometallo-binuclear complex $[Ru^{II}(bpy)_2(bpy\text{-}cyclam)Ni^{II}]^{4+}$ (**3**) are reported as a new candidate of photocatalysts (for example, the reduction of CO_2 to CO). A remarkable feature of (**3**) in crystal and solution is a close contact between H_5 of the pendant bpy and Ni^{II} in the cyclam. Optical absorption, emission quenching and electrochemical studies of (**3**) suggested certain efficient interaction between the Ni^{II}-cyclam and the $Ru^{II}(bpy)_3$ units.

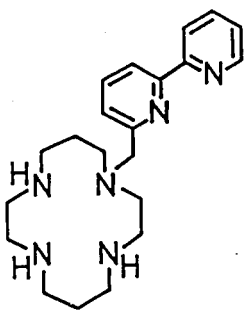

L

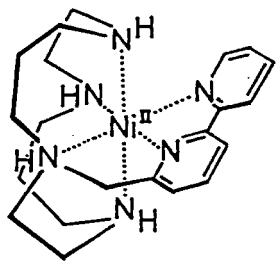

1

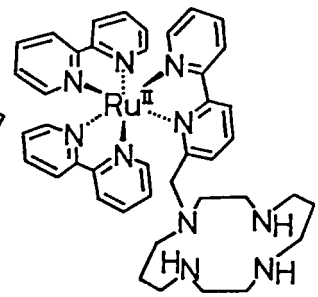

2

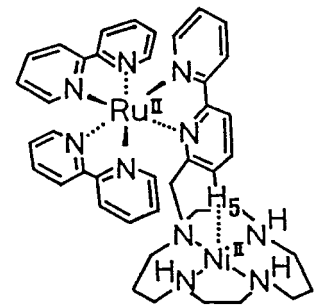

3

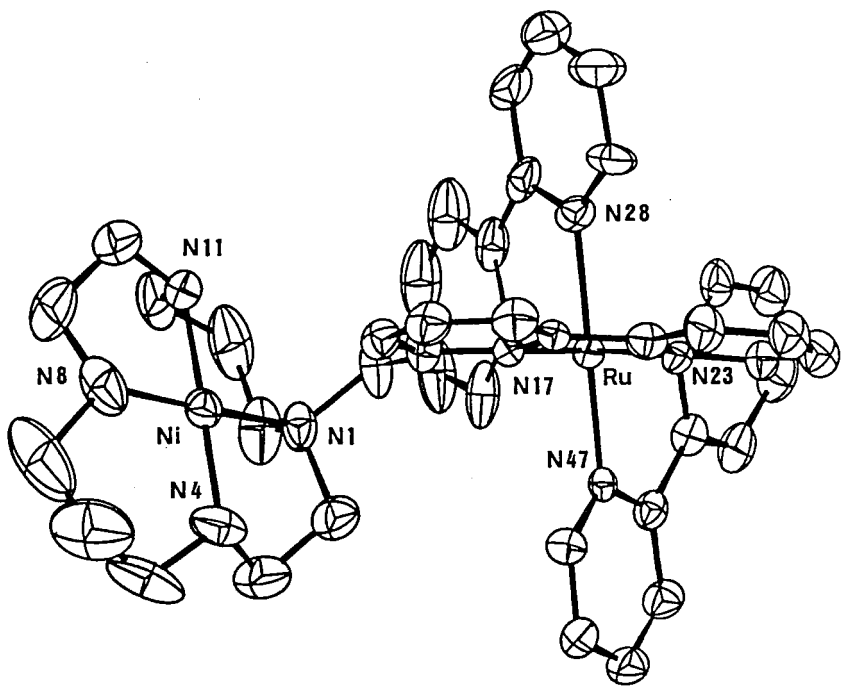

VI-E-4 A Copper(I) *N,N,N′,N″,N″*-Pentamethyldiethylenetriamine Complex and Its Carbon Monooxide Adduct in Aqueous Solutions

Eiichi KIMURA, Tohru KOIKE*, Mutsuo KODAMA, and Dan MEYERSTEIN***** *(*Hiroshima Univ., **Hirosaki Univ., ***Ben Gurion Univ.)*

[*Inorg. Chem.*, **28**, 2998 (1989)]

Copper(I) ion forms a stable 1:1 complex with pmdien (2,5,8-trimethyl-2,5,8-triazanonane) (**7**) in CO-saturated or CH_3CN-containing *aqueous* solutions, due to the formation of a stable 1:1 CO or CH_3CN adduct. The formation constants of $[Cu(pmdien)(CO)]^+$ (**8**) and $[Cu(pmdien)(CO)]ClO_4$ has been established by the pH-metric titration and polarographic methods. Moreover, crystalline $[Cu(pmdien)(CO)]ClO_4$ has been isolated from CO-saturated *aqueous* solution. The observed ν bands of the CO adduct (**8**) at 2082 cm^{-1} (KBr pellet) and 2088 cm^{-1} (aqueous solution) agree with the end-on CO coordination.

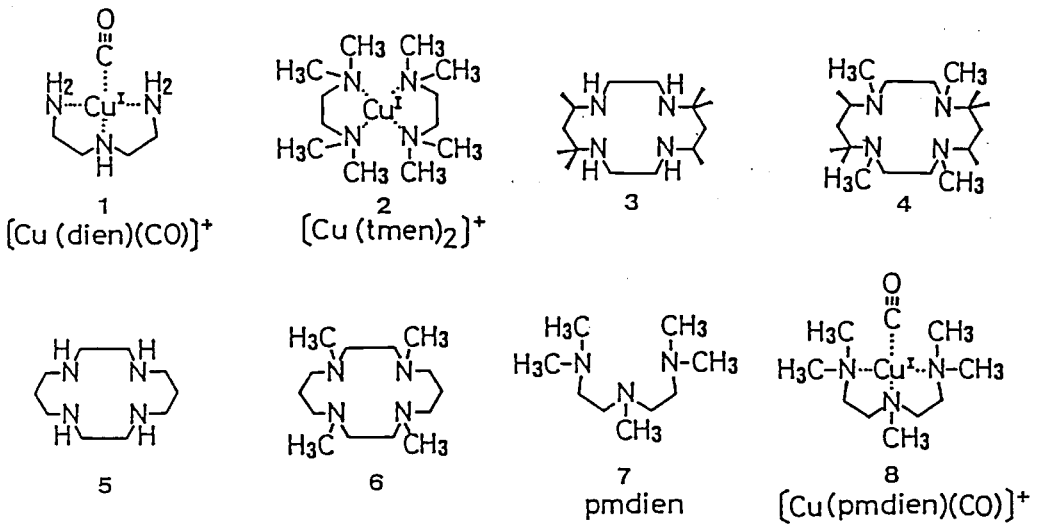

VI-E-5 A Convenient Synthesis of a Macrocyclic Dioxo Pentaamine and X-ray Crystal Structure of Its Monohydrazoic Acid Salt

Eiichi KIMURA, Hideki ANAN*, Tohru KOIKE*, and Motoo SHIRO** *(*Hiroshima Univ., **Shionogi Research Labs)*

[*J. Org. Chem.*, **54**, 3998 (1989)]

We have discovered a much more practical synthetic route to **1c**, whose Ni^{II} complex **2c** shows an even lower E^0 value of +0.17 V *vs* SCE, indicating more promising properties for O_2 activation. We also conducted an X-ray crystal structure analysis of **1c**·HN_3. The complex consists of two macrocyclic cations and two N_3^- anions, where the protonation is occurring at the N(4) atom which may be the most basic nitrogen in (**1**). The proton affinity in the macrocyclic dioxo pentaamine is determined primarily by its easiness to form intramolecular hydrogen bond.

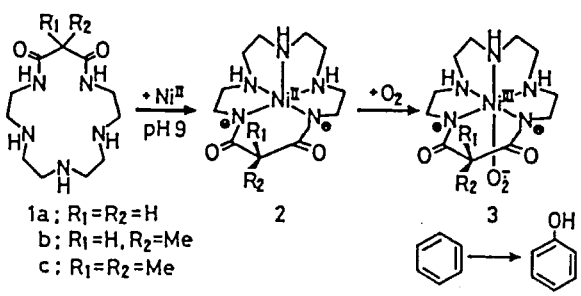

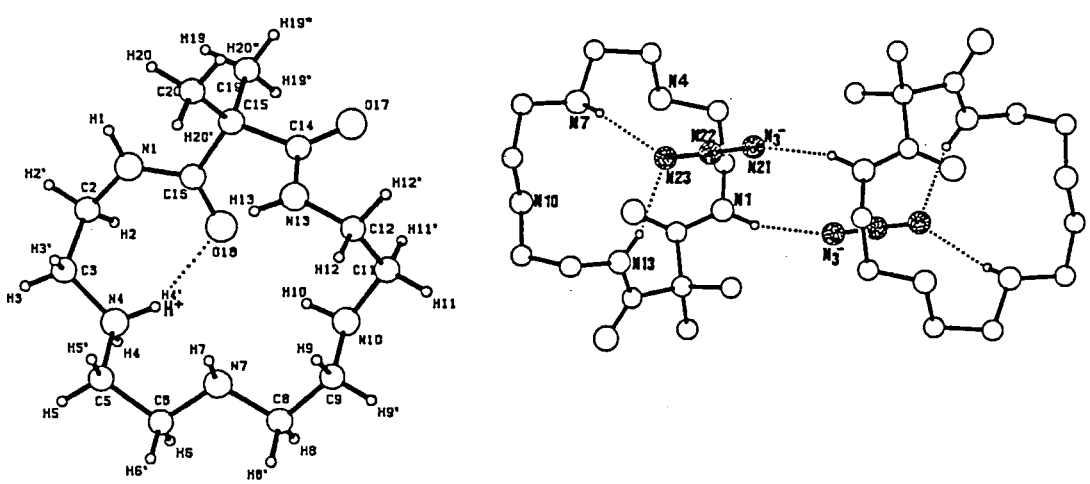

Figure 1. Structure of **1c**·HN_3: an upper figure shows intramolecular hydrogen bond between ionic amine proton and amide oxygen (N_3^- ion was omitted for clarity); lower figures show intermolecular hydrogen bonds with bridged N_3^- ions (nonbonding hydrogens were omitted for clarity).

VI-E-6 Isolation and Unusual stability of a New Macrocyclic Polyamine Containing a Phthalimidine

Eiichi KIMURA, Yukari YOSHIYAMA*, Mitsuhiko SHIONOYA, and Motoo SHIRO** *(*Hiroshima Univ., **Shionogi Research Labs)*

[*J. Org. Chem.*, in press]

The present study is concerned with an unexpected isolation of a new macrocyclic polyamine containing phthalimidine (**4**) during attempts to synthesize (**3**). The unique structure of (**4**) is identified by X-ray crystal structure analysis. The failure of (**3**) and unusual stability of (**4**) indicates the unusual reactivity of the carbonyl in (**3**) with the adjacent benzyl nitrogens.

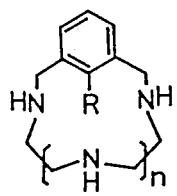

1: n=2, R=OH
2: n=3, R=OH
3: n=3, R=COOH

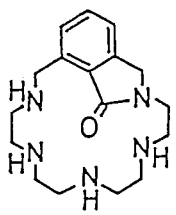

4

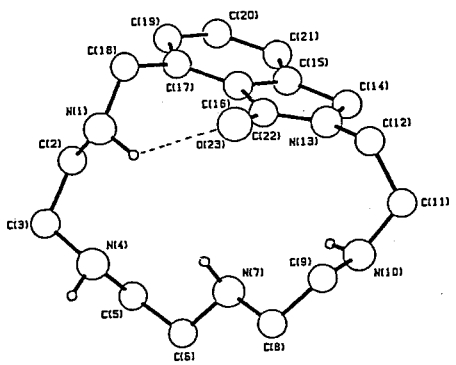

VI-E-7 The Complexation Equilibria of Mercury(II) Ions with Macromonocyclic 16-Membered Dioxopentaamine, 18-Membered Dioxohexaamine, and Their Related Compounds

Mustuo KODAMA*, and Eiichi KIMURA *(*Hirosaki Univ.)*

[*Bull. Chem. Soc. Jpn.*, **62**, 3093 (1989)]

We have investigated the equilibria of complexation reactions of mercury(II) ions with 16-membered macrocyclic dioxopentaamine (dioxo[16]aneN_5), 18-membered macrocyclic dioxohexaamine (dioxo[18]aneN_6) and their related compounds by employing a polarographic method and pH-metric titration. Dioxo[16]aneN_5, dioxo[18]aneN_6, and other dioxo ligands except dioxotetraamines were found to form solely 1:1 ratio mercury(II) complexes designated as $HgH_{-1}L^+$ with displacement of one amide proton, while the macrocyclic 16-membered monooxopentaamine (monooxo[16]aneN_5) forms HgL^{2+} in addition to $HgH_{-1}L^+$. The substitution of amine nitrogen of dioxo[16]aneN_5 by the sulfur donor unexpectedly gave no increase in the stability of mercury(II) complex of dioxo ligand, $HgH_{-1}L^+$.

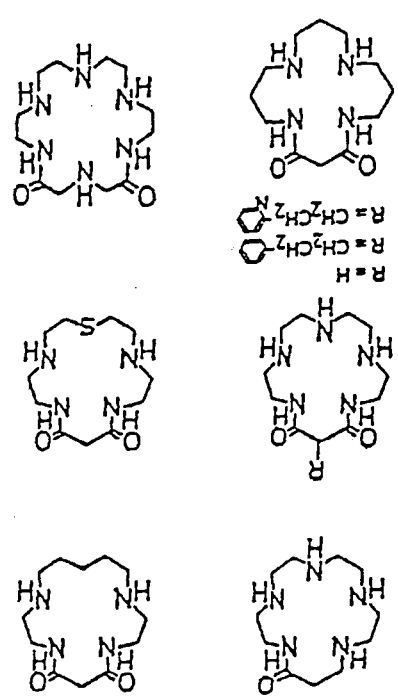

VI-E-8 Complexation Reactions of Copper(II) Ions with 16-Membered and 18-Membered Monocyclic Dioxopolyamines in an Aqueous Solution

Mutsuo KODAMA*, Hideki ANAN, Tohru KOIKE**, and Eiichi KIMURA** *(*Hirosaki Univ., **Hiroshima Univ.)*

[*Bull. Chem. Soc. Jpn.*, in press]

The equilibria of complexation reactions of dioxo[16]aneN$_5$, dioxo[18]aneN$_6$, and their related compounds with copper(II) ions were determined potentiometrically. Making a sharp contrast to the 13~15-membered monocyclic dioxotetraamine system, they interact with copper(II) ions on their neutral and doubly deprotonated forms, L and H$_{-2}$L^{2-}, yielding stable CuL^{2+} and CuH$_{-2}$L^0 complexes.

VI-F The Molecular Recognition Using Macrocyclic Polyamines

A lipophilic macrocyclic polyamine is developed for anion sensor of ATP^{4-} or dianions. Bis-macrocyclic polyamines are utilized as new ligands for inorganic and organic anions.

VI-F-1 Potentiometric Adenosine Triphosphate Polyanion Sensor Using a Lipophilic Macrocyclic Polyamine Liquid Membrane

Yoshio UMEZAWA*, Masamitsu KATAOKA*, Wako TAKAMI*, Eiichi KIMURA, Tohru KOIKE, and Hiroko NADA**** *(*Hokkaido Univ., **Hiroshima Univ.)*

[*Anal. Chem.*, **60**, 2392 (1988)]

A lipophilic macrocyclic polyamine, 15-hexadecyl-1,4,7,10,13-pentaazacyclohexadecane ($C_{16}H_{33}$-[16]-aneN$_5$), was used to construct a potentiometric liquid membrane sensor for adenosine triphosphate polyanion (ATP^{4-} and/or HATP^{3-}). The membrane potential was strongly dependent on the pH of the solution due to the proton uptake of [16]-aneN$_5$ at the membrane surface. This proton uptake seems prerequistie for the potential response for polyanions. The lineality of the log *C vs E* curve ranges from 10^{-7} to 10^{-3} M with a slope of -14.5 mV/decade in a HEPES buffer (pH 6.7). The extent of Nernstian or sub-Nernstian slopes of the present electrode toward ATP^{4-} and/or HATP^{3-}, ADP^{3-}, and AMP^{2-} was experimentally correlated with the association constants of each nucleotide with [16]aneN$_5$ and also with a solvent extraction sequence for the same system. Observed selectivities against ADP^{3-}, AMP^{2-}, HPO_4^{2-}, and monovalent of the formation of strong ion pairs between polyanions and the protonated [16]aneN$_5$ at the membrane surface.

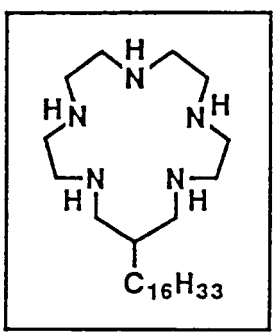

$C_{16}H_{33}$-[16]aneN$_5$

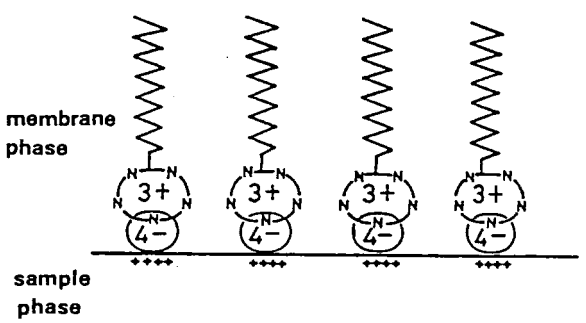

Figure A possible response model of lipophilic [16]aneN$_5$ liquid membrane electrode for ATP polyanions.

VI-F-2 Potentiometric Liquid Membrane Sensors that Discriminate Linear Homologs and Geometrical/Positional Isomers of Dicarboxylates

Masamitsu KATAOKA*, Ryuichi NAGANAWA*, Kazunori ODASHIMA*, Yoshio UMEZAWA*, Eiichi KIMURA, and Tohru KOIKE** *(*Hokkaido Univ., **Hiroshima Univ.)*

[*Anal. Lett.*, **22**, 1089 (1989)]

Potentiometric discrimination of series of linear homologs (**4-7**), geometrical isomers (**8,9**), and positional isomers (**10-12**) of dicarboxylate guests by a liquid membrane sensor containing lipophilic macrocyclic polyamine **1** as a sensory element is described. The pH conditions were carefully set so that the potentiometric response to the *dianionic* forms of the guests could be specifically observed. Whereas only small discrimination was observed for the flexible linear homologs (**4-7**), marked discrimination was observed for the geometrical isomers (**8,9**) and positional isomers (**10-12**) having rigid structures. The selectivities of the potentiometric response were found to correlate well with the reported selectivities of host-guest complexation in water displayed by macrocyclic polyamines having the structures related to **1**.

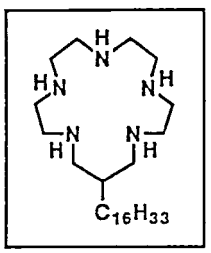

$C_{16}H_{33}$-[16]aneN$_5$
(1)

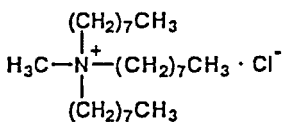

Capriquat®
(2)

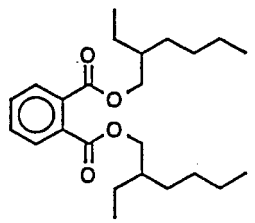

DOP (3)

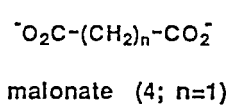

malonate (4; n=1)
succinate (5; n=2)
glutarate (6; n=3)
adipate (7; n=4)

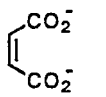

maleate
(8)

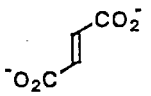

fumarate
(9)

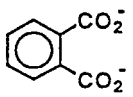

phthalate
(10)

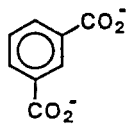

isophthalate
(11)

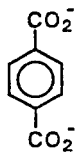

terephthalate
(12)

VI-F-3 Study of New Bis(Macrocyclic Polyamine) Ligands as Inorganic and Organic Anion Receptors

Eiichi KIMURA, Yasuhiro KURAMOTO*, Tohru KOIKE*, Haruto FUJIOKA, and Mutsuo KODAMA***** *(*Hiroshima Univ., **Fukuyama Univ., ***Hirosaki Univ.)*

[*J. Org. Chem.*, in press]

A propylene-bridged bisdioxo[16]aneN$_5$, (**4**), and diether-bridged (**2**) and propylene-bridged (**3**) bis[16]aneN$_5$ ligands [bis(macrocyclic pentaamine)] were synthesized as host molecules for inorganic and organic anion guests. By the polarographic and potentiometric methods, **1** as di- and tetra- protonated forms, and **2** and **3** as tetra- and hexa-protonated forms were demonstrated to yield stable 1:1 complexes with citrate^{3-}, AMP^{2-}, ATP^{4-}, HPO_4^{2-}, $[Fe(CN)_6]^{4-}$, and

$[Fe(CN)_6]^{3-}$ anions. Comparison of these association constants (K) with those of the parent monomeric polyamines reveals that the attachment of the second polyamine moiety always enhances their anion encapsulating abilities, suggesting the formation of sandwich type complexes.

VI-G Biomimetic Studies Using Polyamine Complexes

Active sites of metalloenzymes(*e.g.* Zn^{II}-containing carbonic anhydrase) and an anti-cancer drug(bleomycin) have been mimicked by synthetic polyamine ligands.

VI-G-1 Novel Macrocyclic Polyamine Zn(II) Complexes: For Study of Inherent Zn(II) Properties in Enzymes

Tohru KOIKE*, Takeshi SHIOTA*, and Eiichi KIMURA *(*Hiroshima Univ.)*

We present Zn(II)-macrocyclic polyamine complexes as a suitable probe for a model study of Zn(II)-containing enzymes. These studies have reproduced not only the nature of the coordinate environment around Zn(II) in enzymes, but also have served to spotlight the intrinsic characteristics of Zn(II) (*e.g.* Lewis acidity). First, we have measured the pK_a values for H_2O coordinated to various Zn(II)-macrocyclic triamines.[1] Zn(II) complex with the 12-membered N_3 **4** has the same H_2O acidity (pK_a = 7.4) to that of carbonic anhydrase. Second, we could incorporate Zn(II) into macrocyclic monooxo-polyamine **2**,[2),3)] and **3** by the so strengthened acidity. The mechanism of these amide deprotonation must be highly relevant to the Zn(II) acidity in the enzymes. The first Zn(II)-deprotonated amide complex with five coordinate **5**, was analyzed by X-ray study. These macrocycles were successfully used to distinguish Zn(II) from Cd(II).

References
1) E. Kimura, T. Koike, K. Toriumi, *Inorg. Chem.*, **27**, 3687 (1988).
2) E. Kimura, T. Koike, *et al.*, *Inorg. Chem.*, **27**, 1036 (1988).
3) E. Kimura, T. Koike, *et al.*, *Inorg. Chem.*, **26**, 2975 (1987).

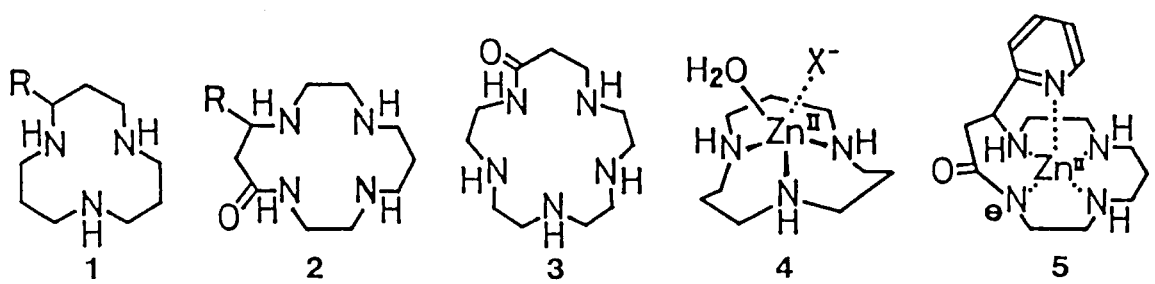

VI-G-2 Study on Bleomycin Active Centre by Model Ligands

Eiichi KIMURA, Hiromasa KUROSAKI, Tohru KOIKE*, and Motoo SHIRO** *(*Hiroshima Univ., **Shionogi Research Labs)*

Some ambiquities persist regarding the key metal ion (Fe^{II} or Cu^{I}) for anticancer activity of bleomycin (BLM).[1] The structure of the Cu^{I} complex remains unanswered. A more precise study will be possible only with appropriately designed small molecular BLM-mimic ligands. We have synthesized a peptide ligand **1** which was proven to be an ideal model.[2] The structure of its Cu^{I} complex, as shown by X-ray crystal analysis,

is very similar to that of Cu^{II}-BLM. From the titration results for Cu^{I} and Cu^{II} with **1**, we have established the structural change (**2** ⇌ **3**) upon redox of Cu. The spin-trapping technique found generation of · OH from O_2 by the Cu^{I} complex **2**, as Cu^{I}-BLM complex. Under identical conditions, Fe^{II}-**1** also generates · OH, but its activity is only 10% as much as that of Cu^{I}-**1**. These our data imply *higher O_2-activation by Cu^{I} than Fe^{II} with BLM, too.*

References

1) J. Stubbe and J.W. Kozarrich, *Chem. Rev.*, **87**, 1107 (1987).
2) H. Kurosaki, H. Anan, E. Kimura, *J. Chem. Soc., Jpn.*, 691 (1988).

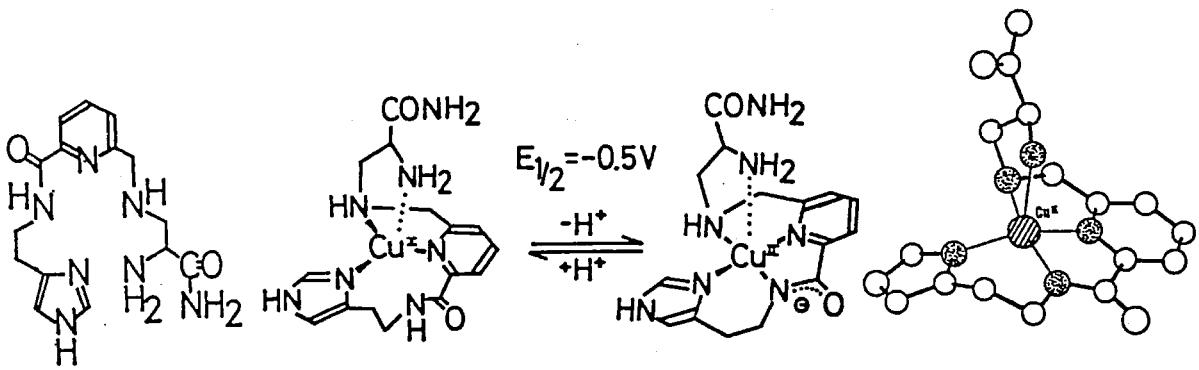

1 **2** **3** **4**

VI-H Dynamic Behavior of Ions and Electrons in Crystals

Diffusional and reorientational motions of molecular ions and electron migration in crystals have been studied by nuclear magnetic resonance and nuclear quadrupole resonance techniques. Dynamic parameters for the ions and electrons in these motional states were determined and their relationships with macroscopic phenomena such as electrical conductivity, plastic nature of crystals, and structural phase transitions are discussed for tetra- and hexahalogen metal complexes, halogen-bridged one-dimensional mixed-valence complexes, and n-alkylammonium halides of a two-dimensional lamellar structure.

VI-H-1 Phase Transition and Anionic Dynamics of Dimethylammonium Hexachlorotellurate(IV) as Studied by Pulsed Nuclear Quadrupole Resonance of Chlorine

Atsushi ISHIKAWA*, Keizo HORIUCHI*, Ryuichi IKEDA, and Daiyu NAKAMURA* *(*Nagoya Univ.)*

[*J. Mol. Struct.* **192**, 237 (1989)]

The temperature dependence of ^{35}Cl NQR frequencies was reinvestigated for dimethylammonium hexachlorotellurate(IV) by use of an FT NQR spectrometer. A new line was observed just above the lowest-frequency line already reported for the intermediate-temperature phase. In the lowest-temperature phase, the temperature dependence was definitely determined by finding new lines. The NQR frequencies could be precisely measured even in the vicinity of the phase transitions. The temperature dependence of the nuclear quadrupole relaxation time, T_{1Q} of ^{35}Cl and ^{37}Cl nuclei was also observed. In a temperature range 64-160 K, the isotope ratio, $T_{1Q}(^{37}Cl)/T_{1Q}(^{35}Cl)$ was 1.5 for each line, suggesting that the quadrupolar relaxation arises mainly from the libration of the complex anion. Above 160 K, T_{1Q} decreased very rapidly with increasing temperature for each line. This can be interpreted in terms of the onset of the reorientation of the anion as a whole, which is responsible for the fade-out phenomenon of the two lines occurring near 220 K. The nature of the phase transitions and the anionic dynamics are discussed in detail. Especially, the phase transition at 96 K was rather unusual and was explained through softening of the librations and the rotational displacement of the anions successively operated.

VI-H-2 Nuclear Magnetic Resonance Studies on Cationic Reorientation and Translational Self-Diffusion in Two Solid Phases Including the New High-Temperature Phase of Methylammonium Sulfate

Hiroyuki ISHIDA*, Noritoshi MATSUHASHI, Ryuichi IKEDA, and Daiyu NAKAMURA**** *(*Okayama Univ., **Nagoya Univ.)*

[*J. Chem. Soc. Faraday Trans.* 1, **85**, 111 (1989)]

Temperature dependence of the proton spin-lattice and spin-spin relaxation times, and also the second moment of ^1H n.m.r. absorptions of $(CH_3NH_3)_2SO_4$ and its partially deuterated analog, were observed in a wide temperature range including the new high-temperature solid phase obtainable above 428 K. The X-ray powder patterns taken at about 450 K revealed that the crystal in this phase has a hexagonal structure isomorphous with the α-form of K_2SO_4. From ^1H n.m.r. experiments, it was found that the cations in the high-temperature phase undergo overall reorientation as well as translational self-diffusion. Presence of these motions suggests that this new phase is in a state resembling to the plastic phase of molecular crystals. In the low-temperature phase, the reorientation of the CH_3 and NH_3^+ groups of the cation about the C-N bond axis was observed. The motional parameters were evaluated for these motional modes.

VI-H-3 Structural Phase Transitions in Solid tert-Butylammonium Nitrate as Studied by Differential Thermal Analysis and ^1H NMR

Hiroyuki ISHIDA*, Tadashi IWACHIDO*, Naomi HAYAMA*, Miyuki HASHIMOTO, Ryuichi IKE-**

DA, and Daiyu NAKAMURA** (*Okayama Univ., **Nagoya Univ.)

[Z. Naturforsch. 44a, 71 (1989)]

Seven solid phases including three metastable phases of $(CH_3)_3CNH_3NO_3$ were revealed by differential thermal analysis in the temperature range between 80 K and the melting point (418 K), and cationic dynamics in each phase was studied by use of ^1H NMR techniques. The highest-temperature solid phase obtainable above 412 K was found to be an ionic plastic phase, where the cations perform rapid translational self-diffusion and overall rotation about their center of gravity.

VI-H-4 Ionic Dynamics in $[(CH_3)_4N]SbF_6$ Crystals as Studied by the Temperature Dependence of ^1H and ^{19}F NMR Spin-Lattice Relaxation Times

Setsuko SATO*, Miyuki KONDO, Ryuichi IKEDA, and Daiyu NAKAMURA**** (*Gifu Univ., **Nagoya Univ.)

[*Ber. Bunsenges. Phys. Chem.*, **93**, 450 (1989)]

The temperature dependence studies of ^1H and ^{19}F NMR spin-lattice relaxation times (T_1) as well as differential thermal analysis measurements were carried out for $[(CH_3)_4N]SbF_6$ crystals. A phase transition assignable to the second order one was located at 200 K, above which temperature the temperature gradient of ^1H T_1 and ^{19}F T_1 curves became slightly gentler. The appearance of the ^1H T_1 curve was BPP like one although a maximum was detected at ca. 110 K. The ^1H T_1 minimum was explained as resulting from the CH_3 C_3 reorientation and the overall reorientation of the cation activated at almost the same temperature. The ^{19}F T_1 curves observed at 19.5 and 32 MHz were somewhat complicated. On the high temperature region above ca. 120K, ^{19}F T_1 was determined mainly by the motion of the cation activated at higher temperatures than that of the anion through ^1H-^{19}F magnetic dipolar interactions. On the other hand, ^{19}F T_1 observed below 120 K have a broad minimum attributable to the overall reorientation of the complex anion. The motional parameters for the above motions were derived. On the analysis of the T_1 curves observed, cross relaxation mechanism operative between ^1H and ^{19}F nuclei is fully considered.

VI-H-5 A Study of Anionic Motion in Solid Rubidium and Cesium Tetrachloroaurates(III) by Measuring the Temperature Dependence of Chlorine Nuclear Quadrupole Relaxation Times

Atsushi ISHIKAWA*, Tetsuo ASAJI*, Daiyu NAKAMURA*, and Ryuichi IKEDA (*Nagoya Univ.)

[*Z. Naturforsch.* **44a**, 125 (1989)]

The temperature dependence of ^{35}Cl NQR frequencies and ^{35}Cl nuclear quadrupole relaxation times T_{1Q} and T_{2Q} were determined above 82 K for $Rb[AuCl_4]$ and $Cs[AuCl_4]$ up to ca. 340 K and 320 K, respectively. Below these temperatures, two ^{35}Cl NQR frequencies were observed for each complex whereas no resonance could be detected above the respective temperatures. For both complexes, T_{1Q} observed below ca. 270 K was interpreted as mainly determined by the rotary lattice vibration around the pseudo-C_4(C_4') axis and each Cl-Au-Cl diagonal axis of the square planer complex anion, whereas T_{1Q} observed above 270 K was definitely shown to be determined through the reorientation of the anions about their C_4 axis. The activation energies for the C_4 reorientation of the anions was evaluated to be 71 and 53 $kJmol^{-1}$ for the rubidium and cesium salts, respectively. The anionic dynamics are discussed by assuming the motion of the anions within and out of the C_4 potential wells at lower and higher temperatures, respectively.

VI-H-6 Structural Phase Transitions and Ionic Motions in Pyridinium Hexachlorotellurate(IV), Hexachlorostannate(IV), and Hexabromostannate(IV) Crystals as Studied by ^1H NMR

Yutaka TAI*, Tetsuo ASAJI*, Ryuichi IKEDA, and Daiyu NAKAMURA* (*Nagoya Univ.)

[*Z. Naturforsch.* **44a**, 300 (1989)]

^1H NMR second moment M_2 and the spin-lattice relaxation time T_1 were determined for pyridinium hexachlorotellurate(IV), hexachlorostannate(IV), and

hexabromostannate(IV) at various temperatures above ca. 140 K. The phase transition temperatures already reported from the experiments of halogen NQR were accurately determined as 272, 331, and 285 K by differential thermal analysis (DTA) for the above complexes listed in the same order. From the DTA experiments as well as differential scanning calorimetry measurements, the above phase transitions were revealed to bear second-order nature. For pyridinium hexachlorotellurate(IV) and hexabromostannate(IV), a sharp ^1H T_1 dip was observed at each transition temperature. This is interpreted in terms of a phenomenon related to critical fluctuation of an order parameter. From the measurements of ^1H M_2 performed at various temperatures, 60° two-site jump (60° flip) motions around pseudo C_6 axis of the cation were suggested to occur in each high temperature phase of the complexes. Modulation of X...^1H (X = Cl, Br) magnetic dipolar interactions due to the reorientational motion of the complex anions was considered as a possible relaxation mechanism in each high temperature phase.

VI-H-7 The Highest-Temperature Crystalline Phas of Tetramethylammonium Thiocyanate with the Cations Performing Three-Dimensional Self-Diffusion as Revealed by Differential Thermal Analysis and Proton Magnetic Resonance Experiments

Toshitaka TANABE*, Ryuichi IKEDA, and Daiyu NAKAMURA* *(*Nagoya Univ.)*

[*Phys. Stat. Sol.* (a), **114**, K143 (1989)]

A new high-temperature solid phase of tetramethylammonium thiocyanate was found above 455 K by measuring differential thermal analysis. Above this phase transition temperature, the second moment of ^1H NMR absorption became vanishingly small (less than 0.01 G^2) indicating the presence of rapid 3D translational self-diffusion as well as overall reorientation of the cations. These experimental results suggest that ionic plastic phase is realized above the transition point.

VI-H-8 Self-Diffusion and Reorientation of Methylammonium Ions in $(CH_3NH_3)_2ZnCl_4$ Crystals as Studied by ^1H-NMR

Hiroyuki ISHIDA*, Tadashi IWACHIDO*, Naomi HAYAMA*, Ryuichi IKEDA, Mifune TERASHIMA, and Daiyu NAKAMURA**** *(*Okayama Univ., **Nagoya Univ.)*

[*Z. Naturforsch.* **44a** in press]

Differential thermal analysis, differential scanning calorimetry, and the temperature dependence of ^1H spin-lattice relaxation times as well as the second moments of ^1H-NMR absorptions in methylammonium tetrachlorozincate(II) crystals were observed over a wide temperature region. A solid-solid phase transition was located at 477 K in this complex. From ^1H-NMR experiments, it was found that the cations undergo overall reorientation as well as three dimensional translational self-diffusion in the high-temperature phase. In the low-temperature phase, a 120° reorientational motion of the CH_3 and NH_3^+ groups was detected for the cation about its C-N bond axis. The motional parameters for each motional mode of the cations in the crystal were evaluated from the analysis of ^1H-NMR experimental results obtained.

VI-H-9 Structural Phase Transitions and Cationic Motions in Pryidinium Dichloroiodate(I) as Studied by ^1H NMR, Differential Thermal Analysis, and Powder X-Ray Diffraction

Reiko WATANABE*, Tetsuo ASAJI*, Yoshihiro FURUKAWA*, Daiyu NAKAMURA*, and Ryuichi IKEDA *(*Nagoya Univ.)*

[*Z. Naturforsch.* in press]

The temperature dependences of ^1H NMR spin-lattice relaxation time T_1 and of the ^1H second moment M_2 were determined for the crystals of pyridinium dichloroiodate(I), $(pyH)ICl_2$. The small M_2 values around 1 G^2 observed above room temperature indicate that the cations perform rapid reorientational motion in crystals about their pseudohexad axis perpendicular to the cationic plane. ^1H T_1 minimum values observed were unusually long for the above motion.

This is explained in terms of the above cationic motion taking place in the local environments having a low symmetry. Phase transitions between stable solid phases were revealed at 282 and 373 K by the measurements of ^{1}H NMR and differential thermal analysis. The highest-temperature phase was supercooled unusually down to low temperatures and behaved as a metastable phase. The supercooled phase was transformed reversibly to and from another metastable phase on cooling and warming, respectively, at almost the same temperature of 138 K. The kinetics of the phase transition from the supercooled phase to the stable phase at room temperature was analyzed using the Avrami type relation. The growth time of the stable phase was estimated as ca. 14 h at room temperature.

VI-H-10 Two-Dimensional Ionic Diffusion of n-Alkylammonium Chlorides in the Rotator Phase

Mineyuki HATTORI*, Shigehiko IWAI*, Ryuichi IKEDA, and Daiyu NAKAMURA* *(*Nagoya Univ.)*

Crystalline n-alkylammonium chlorides ($C_nH_{2n+1}NH_3Cl$) with longer alkyl-chains n>5 perform three-step melting which can be observed in a wide temperature range between room temperature and 500-550 K. The low temperature phase containing the alkyl-chains of the ordered arrangements in crystals is transformed around room temperature into "rotator phase" characterized by dynamically disordered cationic orientation about the long chain axis.

Uniaxial rotation and conformational disorder of the alkyl-chains in the rotator phase have been studied by ^{1}H NMR. The onset of higher-order ionic motions is expected in this phase because macroscopic plastic nature of the crystal was observed even at room temperature. We measured ^{1}H NMR spin-lattice relaxation time in the whole temperature range of the rotator phase for C_4 to C_{10} alkylammonium chlorides and found the excitation of a new cationic motion with high activation energies (50-80 kJ mol^{-1}) in the high-temperature region (T>400 K). This motion can be assigned to the 2D translational self-diffusion of the cations in the lamellar type double-layered structure formed by the cations and anions stacked alternately. The two dimensional behavior of the diffusive motion was proved by electrical conductivity measurement on single crystals of n-butylammonium chloride. Jumping rates of the ionic diffusion are discussed in general including the data of 3D-diffusing methylammonium cations in the ionic plastic phase.

VI-H-11 Thermal and ^{1}H NMR Studies on a New Metastable Solid Phase of CH_3NH_3Br Transforming Gradually into Liquid

Masataka TANSHO*, Ryuichi IKEDA, and Daiyu NAKAMURA* *(*Nagoya Univ.)*

The highest-temperature solid phase of CH_3NH_3Br attainable above 483 K has been shown to be an ionic plastic phase by observing cationic translational self-diffusion and overall reorientation by ^{1}H NMR and from the bcc crystal structure determined by X-ray diffraction. This plastic phase was proved to transform into liquid when kept for a long time at a constant temprature even far below its melting point (510 K). The time for this transformation was determined to be ca. 35h at 483 K just above the transition temperature into this phase. These results indicate that the plastic phase is a metastable state and the stable phase in the same temperature range is liquid. The melting at 510 K observed as an endothermic anomaly on the DTA curve is not a usual phase transition between the thermodynamically stable states, but a transition from a over-heated state to liquid.

VI-H-12 Soliton-like Electron Diffusion in Halogen-Bridged Mixed-Valence Platinum Complexes with 1D Linear Chain Structure Studied by ^{1}H NMR Relaxation

Ryuichi IKEDA, and Masahiro YAMASHITA *(Nagoya Univ.)*

^{1}H NMR spin-lattice relaxation time T_1 in $[Pt(en)_2][PtX_2(en)_2](ClO_4)_4$ (X: Cl, Br, I) was measured between 100 K and room temperature. The absence of marked molecular motions in the ethylendiamine ligands was shown by observing a constant second moment of ^{1}H NMR absorptions up to room temperature for the chloro- and bromocomplexes. Steep T_1 decrease with increasing temperature observed above

200 K for these three complexes can be assigned to the fluctuation of magnetic dipolar and/or contact interactions between the protons and the unpaired electrons diffusion along the -Pt-X-Pt-chain. This interpretation agrees well with the narrowing of the ESR spectrum widths with increasing temperature for these complexes already reported. The activation energies for the electron hopping were roughly evaluated.

VI–I Bioinorganic Studies on Electronic and Molecular Structures of Metal Complexes as a Model for Active Site in Some Metalloproteins

Metal-containing proteins have been found to be widely distributed in both plants and animals and have been related to such metabolic processes as hydroxylation, oxygen transport, electron transfer, oxidative catalysis, and so on. In this project the electronic and molecular structures for several metal complexes are studied as a model of several metallo-proteins or metallo-enzymes by some physico-chemical methods.

VI-I-1 Aromatic Ring Stacking in Ternary Copper(II) Complexes, [Cu(histamine)(L-AA)(ClO_4)] (AA=phenylalaninate or tyrosinate). Structural Evidence for Intramolecular Stacking Involving a Coordinated Imidazole Ring

Osamu YAMAUCHI*, Akira ODANI* *(*Nagoya Univ.)*, **Takamitsu KOHZUMA, Hideki MASUDA, Koshiro TORIUMI, and Kazuo SATIO**

[*Inorg. Chem.*, in press]

Two ternary copper(II) complexes comprising histamine and an aromatic amino acid, Cu(hista)(L-Phe)ClO_4 (1) and Cu(hista)-(L-Tyr)ClO_4 (2) have been prepared and investigated by the X-ray diffraction method. Both complexes crystallized in the monoclinic space group, $P2_1$, with a unit cell of dimensions a=9.142(1), b=16.469(2), and c=5.889(1)Å, and β=92.55(2)° for 1 and a=9.186(1), b=16.394(2), and c=5.976(1)Å, and β=90.35(1)° for 2. Complexes 1 and 2 have almost the same square-pyramidal structures with the nitrogen atoms of hista and the nitrogen and oxygen atoms of Phe and Tyr coordinated at the equatorial positions and an oxygen atom of the perchlorate ion at an axial position, the two amino groups occupying equatorial cis positions. The side-chain aromatic ring of Phe and Tyr is located above the coordiantion plane and involved in the stacking interaction with the hista imidazole ring with the closest C···C distances of 3.49 and 3.45A for 1 and 2, respectively. Close contact between Cu(II) and the aromatic ring of Phe and Tyr has also been detected with the shortest Cu···aromatic ring distance of 3.14-3.20Å. The polycrystalline ESR spectra of 1 and 2 measured at 77K gave exactly the same parameters, indicating that the Cu(II) environment is the same for both complexes in aqueous solution.

VI-I-2 Intermolecular Interactions between Indole and Copper(II)-Coordinated Aromatic Rings. Model for Face-to-face and Edge-to-face Ring Orientations in Proteins

Hideki MASUDA, Akira ODANI*, Tamotsu SUGIMORI*, and Osamu YAMAUCHI* *(*Nagoya Univ.)*

Interactions between aromatic rings play important roles in stabilizing the protein structure and in the processes of biological recognition of molecules and subsequent specific reactions. Interring geometries found in many protein structures range from parallel face-to-face orientation. As an extension of the studies on weak interactions aimed at understanding molecular recognitions in biological systems, we investigated the intermolecular interactions between free and coordinated aromatic rings by synthetic, spectroscopic, and X-ray diffraction methods. Addition of excessive indole(in) to Cu(phen)(L-ala)NO_3 (phen=1,10-phenanthroline, L-ala=L-alanine) in aqueous methanol shifted the electronic absorption peak in the d-d region from 608 nm to 601 nm, and a complex with the

composition Cu(phen)(L-ala)$(in)_{2.5}NO_3$ was isolated as green needles. The crystal has the monoclinic space group $P2_1$ with four Cu(phen)(L-ala)NO_3 and ten indole molecules in the unit cell. The geometry around the Cu(II) ion is four-coordinate distorted square-planar. The most interesting structural feature of the crystal is the presence of both face-to-face and edge-to-face ring orientations. The indoles are positioned directly above and below the Cu(II) coordination plane and almost parallel to coordinated phen, the crystal structure showing alternating phen-indole stacking (-phen-in-phen-in-) with the face-to-face separation of about 3.6Å along the b-axis. Another indole is located nearly perpendicular to the plane of phen, whose proton projects towards the electron-rich five-membered ring of indole at the distance of 3.2Å from the mean plane. This is regarded as a manifestation of the edge-to-face interaction of aromatic rings as has been observed in proteins. In line with these structrural properties, the ESR as well as electronic spectra indicate the existence of the intermolecular interactions between the phen and indole rings in aqueous methanol. Molecular orbital calculations of $[Cu(phen)(L\text{-}ala)]^+$ and indole molecules by the Extended Huckel method suggest that the face-to-face interactions are dominated by the HOMO-LUMO interaction between the rings and the edge-to-face interactions by the electrostatic interaction between the positively charged H atom of coordinated phen and the HOMO of the negatively charged five-membered ring of indole. The present findings add to evidence for the significance of the aromatic ring orientations in proteins which may reflect their role as the electron transfer pathway.

VI-I-3 Synthesis and Structural Study of (2,2'-Bipyridine)-perchlorato(styrene)copper(I)

Hideki MASUDA, Katsunosuke MACHIDA *(Kyoto Univ.)*, **Megumu MUNAKATA*, Susumu KITAGAWA*, and Hisao SHIMONO*** *(*Kinki Univ.)*

[*J. Chem. Soc. Dalton. Trans.*, 1907 (1988)]

The reduction of $Cu(ClO_4)_2 \cdot 6H_2O$ with copper wire in the presence of styrene and 2,2'-bipyridine(bipy) gave the complex $[Cu(bipy)(CH_2{=}CHPh)(ClO_4)]$ in methanol. The complex has been characterized by spectroscopic and X-ray diffraction studies. Crystals of the complex are monoclinic, space group $P2_1/n$, with a=12.154(3), b=14.796(4), c=10.361(2)Å, β= 111.04(2)°, and Z=4. The geometry about the copper(I) atom is trigonal pyramidal, involving two nitrogen atoms of bipy and two carbon atoms of the olefinic moiety of styrene at equatorial positions in an approximately planar fashion and weak co-ordination to an oxygen atom of the perchlorate anion at the axial position. The olefinic C=C bond distance of the co-ordinated styrene molecule, 1.358(10)Å, is slightly longer than those reported for other free olefin molecules. This slight lengthening is reflected in the ^1H nmr spectrum of the olefinic protons and the C=C stretching frequency of the co-ordinated styrene in the Raman spectrum and suggests the importance of $d\pi(metal) \rightarrow \pi^*(styrene)$ back donation in the copper(I)-olefin bonding.

VI-I-4 Nuclear Magnetic Resonance Studies of Dicopper(II) Complexes with Binucleating Ligands Containing Imidazoles

Masahiko MAEKAWA*, Susumu KITAGAWA*, Megumu MUNAKATA* *(*Kinki Univ.)*, **and Hideki MASUDA**

[*Inorg. Chem.*, **28**, 1904 (1989)]

^1H NMR spectra of aqueous and nonaqueous solutions of $[Cu_2LX]Y_2$ (L=2,6-bis[((4-imidazolylethyl)methyl]-4-methylphenolate, 2,6-bis[((4-imidazolylethyl)amino)methyl]-4-methylphenolate; $X=OH^-$, Cl^-; $Y=ClO_4^-$, Cl^-) have been observed, together with the measurements of their solution magnetic susceptibilities. The obtained signals are narrow enough to characterized the species in solution. It has been found that both observed chemical shifts and line widths of ^1H NMR signals are controlled by the population distribution in singlet and triplets of the complexes. Methanol solutions of $[Cu_2L(OH)]^{2+}$ showed equilibria that are associated with the apical coordination of water molecules: in addition to the water-free complex, two species, $[Cu_2L(OH)(H_2O)]^{2+}$ and $[Cu_2L(OH)(H_2O)_2]^{2+}$, are found by ^1H NMR spectra. One of these species was crystallized from methanol solution. The crystal and molecular struc-

tures of $[Cu_2L(OH)(H_2O)_2](ClO_4)_2$ have been determined: space group $P2_1/c$, a=7.354(4), b=21.781(19), c=16.175(8)Å, β=90.70(4)å, Z=4, R=0.111, R_w=0.095. The two Cu atoms in this copper(II) complex are bridged by the oxygen atoms of the phenolate and hydroxy groups. The axial position at one Cu atom is occupied by a water molecule, while another Cu has no apical ligand. The coordinate geometries around the two Cu atoms are distorted tetragonal-pyramidal and square-planar.

VI-I-5 Raman Spectra of Cu(I) and Ag(I) Complexes with 1,5-Cyclooctadiene and the Nature of Metal-olefin Bonding. Possibility of Cu(I)-olefin Bonding in Cytochrome Oxidase

Hideki MASUDA

[submitted to *J. Organometal. Chem.*]

Raman spectra of copper(I) and silver(I) complexes with 1,5-cyclooctadiene(cod), $[Cu(cod)_2]ClO_4$ and $[Ag(cod)_2]ClO_4$, have been studied to examine the nature of the d^{10} metal ion-olefin bonding. Judging from the slight lowering of ν(C=C) stretching frequencies upon coordination of olefin to metal ions, the nature of the metal-olefin bondings in $[Cu(cod)_2]ClO_4$ and $[Ag(cod)_2]ClO_4$ seems to be dominated by σ-bonding from olefin π-orbital to metal dσ-orbital. Two strong vibrations appearing at the range from 420 to 350 cm^{-1} are assigned to the metal-olefin stretching ones, and their lower wavenumbers compared with those in isoelectronic series of d^8 and d^{10} metal complexes with cod support also the σ-bonding nature between metal and cod. Similar lowering of ν(C=C) stretching region(1650-1600 cm^{-1}) upon to the reduction of oxidized cytochrome oxidase may suggest that the peripheral 1-hydroxy-5,9,13-trimethyl-4,8,12-trans, trans-tetradecatrienyl substituent(trienyl group) on the heme a may form part of the Cu(I) ligation environment in the reduced copper-heme binuclear center.

VI-I-6 Indole Nitrogen-Palladium(II) Bonding. Chemical and Structural Characterization of Palladium(II) Complexes of Alkylindoles and Intermediacy of 3H-Indole Ring

Osamu YAMAUCHI *(Nagoya Univ.)*, **Masako TAKANI***, **Kazuo TOYODA*** *(*Kanazawa Univ.)*, **and Hideki MASUDA**

[submitted to *J. Am. Chem. Soc.*]

First palladium(II) complexes of alkylindoles (2-methylindole (MI) and 2,5-dimethylindole(DMI)) coordinating through the nitrogen atom in the 3H-indole form have been isolated and characterized by X-ray crystal structure analysis and ^1H NMR, ^{13}C NMR, ^{13}C CP/MAS NMR, and UV absorption spectra. The complexes $[Pd(MI)_2Cl_2]$(1) and $[Pd(DMI)_2Cl_2]$(2) were obtained as pale brown crystals from methanol solutions. Both complexes crystallized in the monoclinic space group $P2_1/c$ and Z=2. They have a square-planar structure with two indole molecules coordinating to Pd(II) in the trans geometry with two chloride ions occupying the remaining positions. The indole ring is bound to Pd(II) through the sp^2 nitrogen atom (N(1)) and nearly perpendicular to the Pd(II) coordination plane. The N(1)-C(2) bond length (1.305(12)Å) in 1 is much shorter than that found for 2,3-diphenylindole (1.392(2)Å), and the C(2)-C(3) (1.516(12)Å) and C(3)-C(3a) (1.469(15)Å) bonds are nearly equal to single bonds, indicating that the indole ring assumes the 3H-indole form. The ^1H NMR spectra of 1 in $CDCl_3$ exhibited CH_2 signals at 3.9 ppm but no C(3) and N(1) proton signals observed for MI, and ^{13}C NMR and ^{13}C CP/MAS NMR spectra of 1 exhibited 3-C signal at aliphatic carbon region, which are in accord with the 3H-indole structure. The results establish the coordination of the indole ring through the "pyridine-like" nitrogen and the intermediacy of the 3H-indole structure in the course of reactions catalyzed e.g. by metal ions having strong affinity toward nitrogen donors.

VI–J Synthesis of Optically Active Complexes and Their Catalytic Use in the Asymmetric Oxidation

The enantioselective synthesis of organic compounds using chiral transition-metal complexes has received attention. We are interested in the asymmetric epoxidation of olefins and oxidation of prochiral sulfides. In this project, the synthesis of new optically active complexes and their catalytic activities on the asymmetric oxidation reactions are investigaed.

VI-J-1 Crystal Structures of [VO(sal-L-ala)-(OCH_3)(CH_3OH)](sal-L-ala = *N*-salicylidene-L-alaninate) and {[VO(sal-L-ala)]$_2$O}$_2$·2CH_2Cl_2, and the Catalytic Activity of These and Related Complexes on Asymmetric Oxidation of Methyl Phenyl Sulfide with *t*-Butyl Hydroperoxide

Kiyohiko NAKAJIMA, Masaaki KOJIMA*, Koshiro TORIUMI, Kazuo SAITO, and Junnosuke FUJITA***
*(*Nagoya Univ., **ICU)*

[*Bull. Chem. Soc. Jpn.*, **62**, 760 (1989)]

A reddish brown oxovanadium(V) complex, [V^{V}O(sal-L-ala)(OCH_3)(CH_3OH)] (**2a**, sal-L-ala=*N*-salicylidene-L-alaninate) was formed by dissolving [V^{IV}O(sal-L-ala)(H_2O)] (**1a**) in methanol. Treatment of **2a** with wet dichloromethane yielded deep blue crystals of {[V^{V}O(sal-L-ala)]$_2$O}$_2$·2CH_2Cl_2 (**3a**). The structures of **2a** and **3a** have been determined by X-ray analyses. Crystal data are: (**2a**), monoclinic, C2, a=19.621(6), b=6.734(1), c=12.059(4)Å, β=117.72(2)° and Z=4. (**3a**), orthorhombic, $P2_12_12_1$, a=19.938(4), b=23.854(5), c=11.526(2)Å, and Z=4. In **2a**, the tridentate sal-L-ala ligand and a methoxide ion occupy the basal positions, and form distorted octahedral geometry around the vanadium(V) ion together with one methanol molecule (V-O distance: 2.384(4)Å) and the oxide ion of oxovanadium(V). The tetranuclear complex (**3a**) consists of two μ-oxo dinuclear vanadium(V) complexes, and each vanadium(V) ion has a distorted octahedral coordination. The Schiff base coordinates equatorially to each vanadium(V) ion, of which one axial site is occupied by O^{2-} and the other is weakly linked to the carboxylate O atom of a nearby Schiff base (V-O distance: 2.34-2.56Å). Octahedral coordination on each vanadium(V) is achieved by sharing an equatorial O^{2-} ligand. The brown complexes, [VO(sal-L-aa)(OCH_3)(CH_3OH)] (**2**, sal-L-aa=*N*-salicylidene L-amino carboxylate) catalyze the oxidation of methyl phenyl sulfide with *t*-butyl hydroperoxide in dichloromethane at 4°C to give (*R*)-methyl phenyl sulfoxide with optical yields (e.e.) of 8-14%.

VI–K Photoexcitation of Hexamolybdenum Cluster

In relation to the projects VI-J and VI-L in the 1988 Issue of this Annual Review, electron transfer reactions of metal cluster complexes have been studied with reference to the influence of pressure.

VI-K-1 Solvent Effect on the Emission Lifetime and its Quantum Yield of $[(Mo^{II}_6Cl_8)Cl_6]^{2-}$

Hideaki K. TANAKA*, Yoichi SASAKI*, Masahiro EBIHARA, and Kazuo SAITO *(*Tohoku Univ.)*

[*Inorg. Chim. Acta*, **161**, 63 (1988)]

Emission lifetime and quantum yield of this complex was measured in 6 solvents, CH_3CN, DMF, CH_3OH, 6 M HCl, 2 M HCl and 0.2 M HCl. It was found that the radiative rate constants are similar (0.00137 to 0.068 s^{-1}) in these solvents, but non-radiative rate constants are different (4.51×10^3 to 2.70×10^5 s^{-1}). Solvent effect on the vibrational decay process and on the excited state energy levels cannot account for the result. Solvent-assisted photo-dissociation of terminal

chloride seems responsible for the solvent effect.

VI-L Novel Reactivity of Molybdenum(0) Dinitrogen Complex of Crown Thioether

A molybdenum(0) dinitrogen complex containing sulfur coligands only, trans-$Mo(N_2)_2Me_8[16]aneS_4$ (1), has been suggested theoretically to be more electron rich than the well studied phosphine analogues due to p_π donor ability of the crown thioether. To delineate the electronic feature of this macrocycle and to clarify the difference in reactivity between **1** and the phosphine analogues, reactions of **1** with organic halides and isocyanides have been examined.

VI-L-1 N-Arylation and N,N-Dibenzylation of Coordinated N_2 with Organic Halides; Differences in the Reactivity of trans-$Mo(N_2)_2Me_8[16]aneS_4$ and Its Phosphine Analogues

Toshikatsu YOSHIDA *(Univ. Osaka Pref. and IMS)*, **Tomohiro ADACHI*, Tatsuo UEDA*, Manabu KAMINAKA*, Nobuyoshi SASAKI*, Taiichi HIGUCHI** *(Osaka City Univ.)*, **Takayuki AOSHIMA**, Izumi MEGA**, Yasushi MIZOBE**, and Masanobu HIDAI** *(Univ. Tokyo and IMS) (*Univ. Osaka Pref., **Univ. Tokyo)*

[*Angew. Chem.*, in press]

The electron richness of trans-$Mo(N_2)_2Me_8[16]aneS_4$ (**1**) was manifested by unprecedented N-arylation of the coordinated N_2 with ArX under ambient conditions to give trans-$MoX(N_2Ar)Me_8[16]aneS_4$ (**2**, Ar=Ph, X=Br; **3**, Ar=Ph, X=I; **4**, Ar=p-$C_6H_4CO_2Me$, X=I). Formation of the aryldiazenido complexes was confirmed by transformation of **3** into trans-$\{MoI(N_2MePh)Me_8[16]aneS_4\}I$ (**5**) and by an X-ray structural analysis of **4**. N,N-dibenzylation of **1** with $PhCH_2Br$ also proceeded readily in toluene under ambient conditions to give trans-$\{MoBr[N_2(CH_2Ph)_2]Me_8[16]aneS_4\}Br$ (**6**). A radical process for the first N-benzylation may be suggested from the reaction of **1** with MeI in toluene to produce trans-$\{MoI[N_2Me(CH_2Ph)]Me_8[16]aneS_4\}I$ (**7**) together with the expected N,N-dimethylhydrazido compound. Apparently the N_2 ligand in **1** is reactive enough to be attacked by such a stable radical as $PhCH_2\cdot$. Neither of these C-N bond forming reactions has been achieved with the phosphine analogues. **1** liberates NH_3 and acetone azine on treating with MeOH and MeOH/acetone at 50°C, respectively; the phosphine analogues are again completely inactive for such generation of nitrogen compounds under similar conditions.

VI-L-2 Reaction of a Molybdenum(0) Dinitrogen Complex Containing a Crown Thioether with Isocyanides. Formation of the Extensively Bent PhNC Complex trans-$Mo(PhNC)_2Me_8[16]aneS_4$ and Facile Dealkylation of t-BuNC to Give trans-$Mo(CN)_2Me_8[16]aneS_4$

Tomohiro ADACHI*, Nobuyoshi SASAKI*, Tatsuo UEDA*, Manabu KAMINAKA*, and Toshikatsu YOSHIDA *(Univ. Osaka Pref. and IMS) (*Univ. Osaka Pref.)*

[*J. Chem. Soc. Chem. Commun.*, in press]

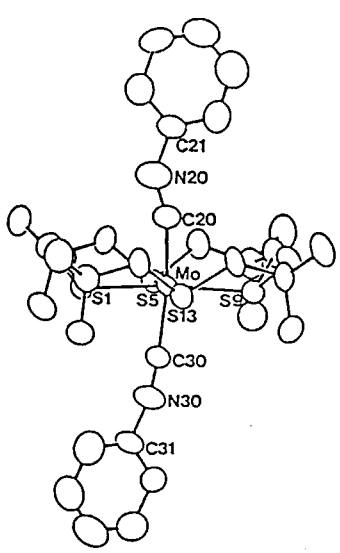

Figure 1. Mol. Structure of **2**.

Reaction of trans-$Mo(N_2)_2Me_8$[16]aneS_4 (**1**) with PhNC gave trans,syn-$Mo(PhNC)_2Me_8$[16]aneS_4, which contains both extensively bent and essentially linear PhNC coordination; the respective angles at the N atoms are 139 and 167°, respectively (Figure 1). EHMO calculations on trans-$Mo(HNC)_2(SH_2)_4$ suggest that the deviation of the Mo atom from 4S plane (0.110 Å) is responsible for the coexistence of both types of PhNC coordination. **2** represents the first well characterized example of extensively bent arylisocyanide complex. A similar reaction of **1** with t-BuNC afforded the paramagnetic trans,anti-$Mo(CN)_2Me_8$[16]aneS_4 (**3**). The facile dealkylation of t-BuNC is rather remarkable since the corresponding reaction of trans-$Mo(N_2)_2$-$(dppe)_2$ has been shown to give trans-$Mo(t\text{-}BuNC)_2(dppe)_2$.

VI–M Syntheses and Some Reactions of Trimethylsilylated Dinitrogen Complexes of Tungsten and Molybdenum

Keiko KOMORI*, Seiya SUGIURA*, Yasushi MIZOBE*, Masaki YAMADA* *(*Tokyo Univ.)*, **and Masanobu HIDAI** *(Tokyo Univ. and IMS)*

[*Bull. Chem. Soc. Japan.*, in press]

A series of new trimethylsilyldiazenido complexes $[MX(NNSiMe_3)(L)_4]$ (M = Mo: X = I; M = W: X = CF_3SO_3; L = PMe_2Ph or 1/2 dpe; dpe = $Ph_2PCH_2CH_2PPh_2$) and trimethylsilylhydrazido(2-) complexes $[MX_2$-$(NNHSiMe_3)(PMe_2Ph)_3]$ (M = Mo: X = I or Br; M = W: X = CF_3SO_3) and $[MX(NNHSiMe_3)(dpe)_2]X$ (M = Mo: X = I; M = W: W = CF_3SO_3) were prepared by treatment of dinitrogen complexes cis-$[M(N_2)_2(PMe_2Ph)_4]$ or trans-$[M(N_2)_2(dpe)_2]$ with Me_3SiX in benzene. The trimethylsilyl groups on the terminal nitrogen atoms were easily replaced by hydrogen by the reaction with MeOH or H_2O, affording, for example, diazenido and hydrazido(2-) complexes such as $[WI(NNH)(dpe)_2]$ and $[WI_2(NNH_2)(PMe_2Ph)_3]$ from $[WI(NNSiMe_3)(dpe)_2]$ and mer-$[WI_2(NNHSiMe_3)(PMe_2Ph)_3]$, respectively. When reduced with excess Na in THF under Ar, complexes trans-$[MI(NNSiMe_3)(PMe_2Ph)_4]$ (M = Mo or W) and mer-$[WI_2(NNHSiMe_3)(PMe_2Ph)_3]$ gave $(Me_3Si)_2NH$ and NH_3 in substantial yields, accompanied by the evolution of N_2 gas. Additional amount of NH_3 was obtained by the hydrolysis of the evaporated reaction mixture residue. When this reaction was performed under N_2, the parent dinitrogen complexes were regenerated in moderate yields.

VI–N Nucleic Aicd Structure and DNA–Ligand Interactions at the Molecular Level

DNA recognition by ligands plays a key role in various biological processes, whether the ligands are large proteins or small molecules. Many of the DNA – ligand interactions are DNA base-sequence specific. We have been designing and synthesizing novel compounds which can interact with DNA in specific manner, in order to understand the mechanism of the DNA – ligand interactions. The compounds we have been looking at include intercalators which insert themselves between the DNA base-pairs, DNA groove binders and the compounds which cleave DNA strands either by oxidation or uv/vis irradiation. For the analyses, we have been employing various methodology, such as X-ray crystallography, spectroscopy, enzymology and computer graphics.

VI-N-1 DNA Binding by Novel Metal Porphyrin Complexes: Importance of Charges on the Porphyrin on Sidechains

Eitaro TAKAHASHI *(Tokyo Univ.)*, **Reiko KURODA** *(Tokyo Univ. and IMS)*, **Toschitake IWAMOTO** *(Tokyo Univ.)*, **and L. Mark Fisher** *(Univ. London)*

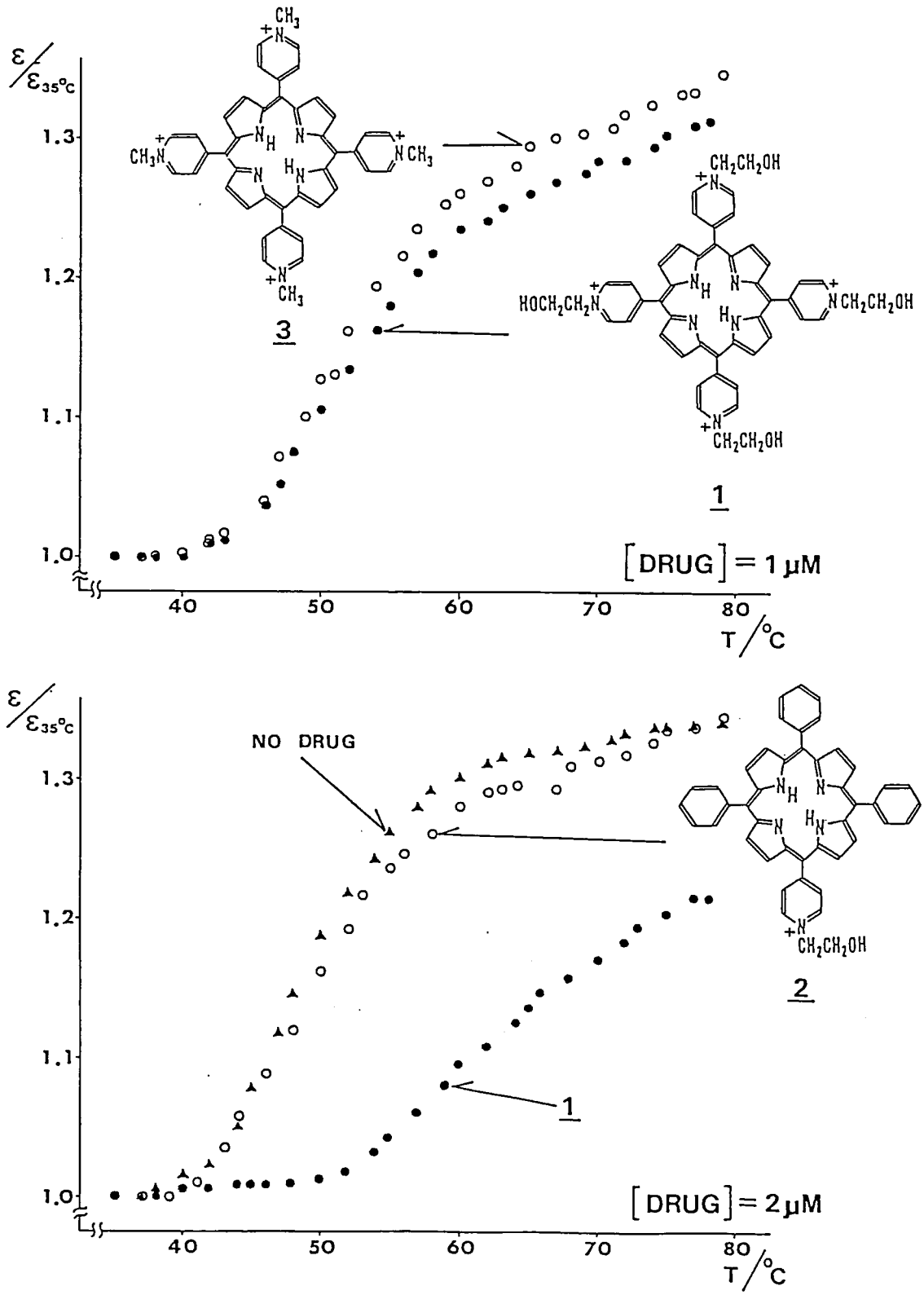

Figure 1. Calf thymus DNA melting curves with and without porphyrin compounds **1**, **2** and **3**.

We have synthesized (by Rothemund method) several new porphyrins containing sidechains, and their metal complexes in order to understand DNA – porphyrin interactions. The binding affinity and mode of interactions of 5,10,15,20-tetra(4′-N-(2″-hydroxyethyl)pyridiniumyl)porphyrin chloride, **1**, 5,10,15-triphenyl-20-(4′-N-(2″-hydroxyethyl)pryidiniumyl)porphyrin chloride, **2**, and their metal complexes were compared with known no-sidechain compound, 5,10,15,20-tetra(4-N-methylpyridiniumyl)-porphyrin chloride, **3**. DNA melting curves as well as spectrophotometric titrations with DNA in the region of Soret band showed intercalative binding mode for the free base and the Cu and Ni complexes of **1** and **3**. Mn complex of **1** and **2** with axial ligands did not show a substantial red shift of the Soret band, however, the stabilization of the double stranded DNA was observed in the melting curve($\Delta T_m = 5°$), suggesting an outside binding mode for the complex. The binding constants determined using Scatchard plots are $3.1 \times 10^6\ M^{-1}$ and $1.5 \times 10^7\ M^{-1}$ for **1** and **3**, respectively. The four sidechains of **1** seem to produce steric hindrance for the binding to DNA. In contrast, mono-sidechain compound, **2**, which has much less steric hindrance has very low affinity to DNA (Figure 1). Positive charges, only one for **2** as compared with four for **1** and **3** seem to be a key factor governing hte binding to DNA. DNA unwinding by topoisomerase I supports the result.

VI-N-2 Photocleavage of DNA by the *p*-Nitrobenzoyl Group: Selective Attack in the Major or the Minor Groove of DNA

Reiko KURODA *(Tokyo. Univ. and IMS)*, **and Miho HAMAGUCHI** *(Tokyo Univ.)*

DNA recognition plays a key role in DNA breakage by proteins and by small DNA ligand such as antibiotics. In the present study, we have designed and synthesized a series of new DNA photocleaving compounds which control the site of attack on DNA. These compound have a *p*-nitrobenzoyl group linked by a polymethylene chain to an acridine intercalator (Figure 1). The *p*-nitrobenzoyl group mediates DNA breakage on UV irradiation by an oxidative mechanism *via* singlet oxygen and/or *via* electron transfer. The incorporation of one of various acridine derivaties controls and enhances the binding of the compounds to DNA. **1a,b** are expected to place their sidechain and hence the photocleaver in the major groove of DNA, whereas **2a,b** in the minor groove. These compounds were characterized by elemental analysis, ^{1}H-NMR and UV-visible absorption spectroscopy.

Intercalation of the acridine moiety between the base-pairs of DNA was checked by absorption spectroscopy and DNA unwinding study using calf thymus topoisomerase I. Binding constants determined by Scatchard plot are similar for all the compounds.

The photocleavage efficiency was determined by the degree of nicking of supercoiled pBR322 DNA. Completely different photocleavage activity was observed depending on the choice of acridine and the group linking the *p*-nitrobenzoyl group to the polymethylene chain.

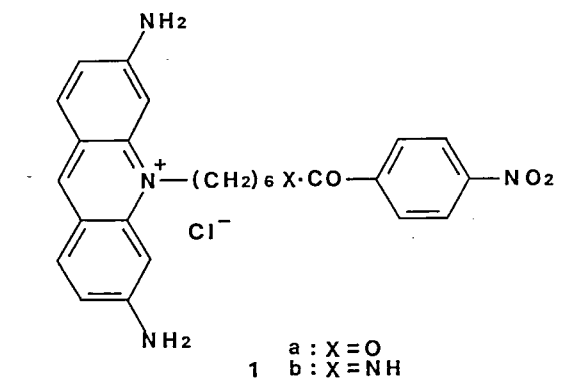

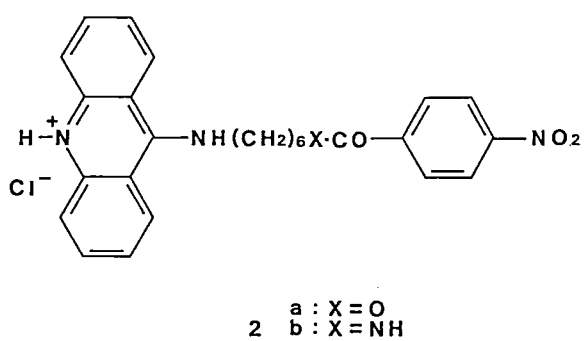

Figure 1. Molecular structure of novel photocleaving agents.

VI-N-3 Crystal of a DNA Binding Compound: 3,6-bis(dimethylamino)-10-[6-(4-nitrobenzoyloxy)-hexyl]acridinium chloride monohydrate

Reiko KURODA *(Tokyo Univ. and IMS)*, **and Miho HAMAGUCHI** *(Tokyo Univ.)*

The title compound which has been recently synthesized by us cleaves strands of DNA on UV irradiation, possibly by way of abstracting hydrogen atoms from the deoxyribose. In order to understand the mechanism of DNA – ligand interactions, we have determined the crystal structure of the compound.

Crystals were obtained from 1:1 aceton/ethanol solution. It was difficult to obtain a large crystal suitable for X-ray diffraction study, hence a rotating anode Cu source was employed. Crystal data: $C_{30}H_{37}N_4O_5Cl_1$, F.W. = 569.09, triclicic, a = 10.512(2), b = 11.203(2), c = 14.469(2)Å, α = 111.49(1), β = 105.74(1), γ = 95.82(1)°, U = 1487.4(5)Å^3, Space group $P\bar{1}$ (No. 2), $Z = 2$, $\mu = 31.25$ cm^{-1}. Intensity data were collected on a Rigaku AFC5R, using Cu Kα radiation (λ = 1.5418 Å). 2θ-ω scan mode was employed, up to $2\theta = 72°$. The structure was difficult to solve. Neither the heavy atom method based on the chloride or standard direct methods were successful. The structure was eventually solved by a direct method using a program MITHRIL. Final R factor was 0.1153 for 3100 reflections observed with $I>3\sigma(I)$. The chloride ion is disordered in the crystal lattice. The structure is highly planar: the polymethlene chain as well as para-nitro phenyl group are almost coplanar with the acridine moiety (Figure 1).

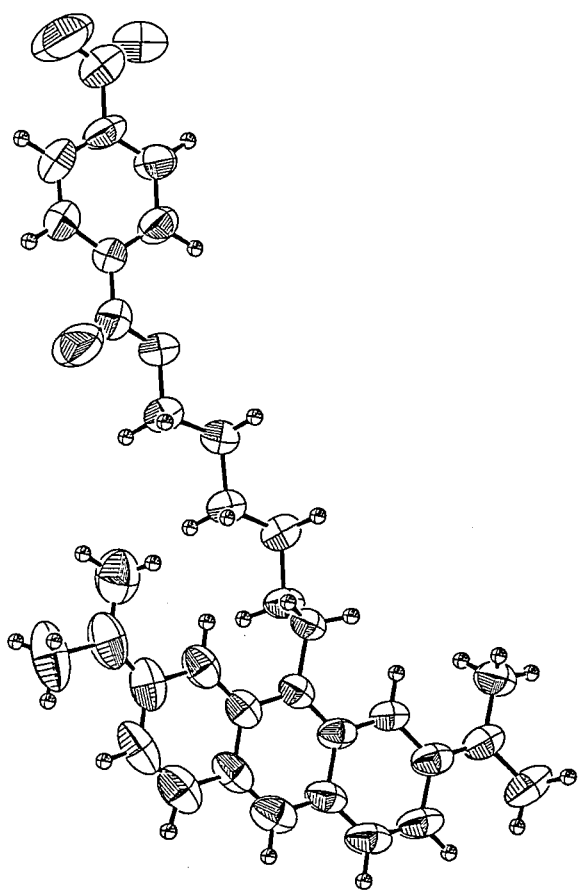

Figure 1. ORTEP drawing of 3,6-bis(dimethylamino)-10-[6-(4-nitrobenzoyloxy)hexyl]acridinium chloride monohydrate.

VI-N-4 Structure of Three DNA Cross-Linking Agents, Ethane-1,2-di(methylsulfonate), Propane-1,3-di(methylsulfonate) and *n*-Butane-1,4-di-(methylsulfonate)

Robert MCKENNA *(Inst. Cancer Res.)*, **Stephen. NEIDLE** *(Inst. Cancer Res.)*, **Reiko KURODA** *(Tokyo Univ. and IMS)*, **and Brian W. FOX** *(Patterson Inst. Cancer Res.)*

[*Acta Crysta.* **C45**, 311 (1989)]

(I)$C_4H_{10}O_6S_2$, M_r = 218.25, $P2_1/c$, a = 7.2611(9), b = 5.8726(4), c = 10.6628(19)Å, β = 103.95(1)°, V = 441.3(2)Å^3, Z = 2, D_m = 1.65, D_x = 1.642 Mg m^{-3}, λ(Cu Kα) = 1.54184Å, μ = 4.43 mm^{-1}, $F(000)$ = 228, R = 0.0336 and ωR = 0.0346 for 745 unique reflections with $F \geqq 3\sigma(F)$, T = 298 K.

(II)$C_5H_{12}O_6S_2$, M_r = 232.28, $P2_1/c$, a = 11.030(1), b = 8.452(1), c = 11.162(1)Å, β = 104.75(1)°, V = 1006.8(3)Å^3, Z = 4, D_m = 1.54, D_x = 1.532 Mg M^{-3}, λ(Cu Kα) = 1.54184Å, μ = 4.799 mm^{-1}, $F(000)$ = 488, R = 0.0418 and ωR = 0.0430 for 1666 unique reflections with $F \geqq 3\sigma(F)$, T = 298 K.

(III)$C_6H_{14}O_6S_2$, M_r = 246.30, $P1$, a = 5.6147(9), b = 6.8343(6), c = 7.5434(6)Å, α = 110.61(1), β = 92.08(1), γ = 76.15(1)°, V = 262.7(3)Å^3, Z = 1, D_m = 1.56, D_x = 1.557 Mg m^{-3}, λ(Cu Kα) = 1.54184Å, μ = 4.79 mm^{-1}, $F(000)$ = 130, R = 0.0397 and ωR = 0.0425 for 907 unique reflections with $F \geqq 3\sigma(F)$, T = 298 K.

All three compounds have a common conformation in the C.O.SO_2.CH_3 part of the molecules due to weak O...H interactions. Compounds (I) and (III) have a *trans* conformation about the central C – C bond, whereas (II) is *cis*.

VI-N-5 Isolation and Characterization of the Diastereoisomers of a Series of Phosphate-Ethylated Dinucleoside Monophosphates

Michael WEINFELD *(Imperial Cancer Research Fund)*, **Alex F. DRAKE** *(Univ. London)*, **Reiko KURODA** *(Inst. Cancer Research, Tokyo Univ. and IMS)*, **and David C. LIVINGSTONE** *(Imperial Cancer Research Fund)*

[*Analytical Biochem.*, **178**, 93 (1989)]

Internucleotide phosphate esterification is a common reaction of many potent carcinogenic alkylating agents. It can give rise to two stereochemically distinct molecules about a triesterified phosphorus atom. The eight individual diastereoisomers derived from phosphate ethylation of d-ApT, d-CpT, d-GpT, and d-TpT were prepared from *o*-chlorophenyl phosphotriester intermediates and isolated by reverse-phase HPLC. Each pair of isomers, together with its parent analog, was examined by variable temperature circular dichroism. The results are interpreted in terms of secondary structure changes from which the absolute configurations of the ethylated phosphate groups can be inferred. These configurational assignments were confirmed by ^{31}P NMR.

VI-N-6 Cloning and Characterization of a DNA Gyrase A Gene from *Escherichia coli* that Confers Clinical Resistance to 4-Quinolones

Martin E. CULLEN *(Univ. London)*, **A.W. WYKE** *(Glaxo Group Res.)*, **Reiko KURODA** *(Tokyo Univ. and IMS)*, **and L.M. FISHER** *(Univ. London)*

[*Antimicrobial Agents and Chemotherapy*, **33**, 886 (1989)]

Nalidixic acid, enoxacin, and other antibacterial 4-quinolones inhibit DNA gyrase activity by interrupting DNA breakage and reunion by A subunits of the A_2B_2 gyrase complex. Despite clinical importance, the mode of quinolone action and mechanisms of resistance are poorly understood at the molecular level. Using a DNA fragment enrichment procedure, we isolated the *gyrA* gene from a uropathogenic *Escherichia coli* strain that encodes a gyrase A protein cross-resistant to a variety of quinolones. When complemented with gyrase B subunit, the purified A protein reconstituted DNA supercoilling activity~100-fold more resistant to inhibition by enoxacin than the susceptible enzyme and failed to mediate quinolone-dependent DNA cleavage. The 875-amino-acid residue-resistant gyrase A protein differed at three positions from its wild-type *E. coli* K-12 counterpart: tryptophan, glutamate, and serine replaced serine, aspartate, and alanine residues at positions 83, 678, and 828, respectively. By genetic analysis of chimeric *gyrA* genes in a *gyrA*(T_s) background, we showed that the Ser-83 → Trp mutation in the gyrase A protein was solely responsible for high-level bacterial resistance to nalidixic acid and fluoroquinolones.

VI–O Synthesis, Structure and Properties of Transition Metal Complexes with Sugar Type Ligands

Sugar and sugar-type compounds form complexes with metal ions. The metal-sugar complexes play an important biological role in the transport phenomena of vital metal ions across cell membranes. The structure and properties of the metal-sugar complexes are investigated by electronic spectra, ESR, and X-ray absorption spectroscopy.

VI-O-1 Structure of Copper(II) Complexes of D-Ribose and D-Glucosamine. Electronic, ESR, and EXAFS Spectral Studies

Lászlo NAGY*, Toshio YAMAGUCHI, Masaharu NOMURA, and Hitoshi OHTAKI** *(*A József Univ., **Fukuoka Univ. and IMS, ***KEK-PF)*

[*Inorg. Chim. Acta*, submitted]

Interactions between D-ribose or D-glucosamine and copper(II) ion have been studied by electronic spectra, ESR, and Cu *K*-XANES and -EXAFS measurements. All data have shown that (1:1) copper(II)-sugar complexes are formed in aqueous

solution at a high pH. The ESR spectra of the two copper(II)-sugar complexes have indicated the presence of a dimeric species *via* hydroxide oxygen atoms in the solution. From the analysis of the EXAFS spectra the oxygen coordination geometry around copepr(II) ion and the copper(II)-oxygen bond lengths within the copper(II)-sugar complexes are not very different from those of the hexaaqua copper(II) ion. EXAFS Fourier transforms have clearly shown a peak ascribed to non-bonded Cu(II)···C interactions, indicating the formation of chelate rings of the sugar-ligand around the copper(II) ion. The most likely structure of the copper(II)-sugar complexes is proposed.

VI–P Structure and Properties of Hydrate Melts

Hydrate melts, which are classified between aqueous solutions and anhydrous molten salts, have recently attracted the attention of people in the fields of both fundamental and applied chemistry; interest includes the basic physicochemical properties of the solutions, crystallization of the salts, supercooling of the solutions, and various technological applications in thermal energy storage.

VI-P-1 X-ray Diffraction and Raman Studies of Zinc(II) Chloride Hydrate Melts, $ZnCl_2 \cdot RH_2O$ (R=1.8, 2.5, 3.0, 4.0 and 6.2)

T. YAMAGUCHI*, S. HAYASHI, and H. OHTAKI**
*(*Fukuoka Univ. and IMS, **Tokyo Inst. of Tech.)*

[*J. Phys. Chem.*, **93**, 2620 (1989)]

X-ray and Raman scattering measurements have been performed at 25 °C on solutions of $ZnCl_2 \cdot RH_2O$ with R = 1.8, 2.5, 3.0, 4.0 and 6.2. Analysis of the X-ray radial distribution functions and model fittings revealed that tetrahedral species $[ZnCl_x(OH_2)_{4-x}]^{(2-x)+}$ are predominantly formed in the solutions and that the average number of Zn-Cl interactions changes from ~2.4 for the solution of R = 6.2 to ~3.4 for the saturated solution of R =1.8. Both X-ray scattering and Raman data confirmed an aggregate of tetrahedral species linked via Cl atoms at a corner of the tetrahedra in solutions of solute concentrations above about 10 mol dm^{-3}, the nearest-neighbor Zn···Zn distance was ~395 pm. Anomalies in the physicochemical data of the $ZnCl_2$-H_2O system are discussed from a structural point of view.

VI-P-2 X-ray Diffraction Study of Calcium(II) Chloride Hydrate Melts: $CaCl_2 \cdot RH_2O$ (R=4.0, 5.6, 6.0, 8.6)

T. YAMAGUCHI*, S. HAYASHI, and H. OHTAKI**
*(*Fukuoka Univ. and IMS, **Tokyo Inst. of Tech.)*

[*Inorg. Chem.*, **28**, 2434 (1989)]

X-ray scattering measurements have been performed on calcium(II) chloride hydrate solutions, $CaCl_2 \cdot RH_2O$, with R = 4.0 (120 °C), 5.6 (72 °C), 6.0 (33 °C), and 8.6 (25 °C). The analysis of the radial distribution functions and model fittings revealed that in the solution of $CaCl_2 \cdot 8.6H_2O$ a Ca^{2+} ion is surrounded by six water molecules, the Ca^{2+}-OH_2 distance being 245 pm. With decreasing H_2O concentration a direct Ca^{2+}-Cl^- correlation owing to the formation of contact ion pairs appears at 270 pm. About one Cl^- ion binds to a Ca^{2+} ion in the $CaCl_2 \cdot 6H_2O$ melt, whereas about two Cl^- ions coordinate to a Ca^{2+} ion in the $CaCl_2 \cdot 4.0H_2O$ melt, whose structure is similar to that found in the crystal structure of $CaCl_2 \cdot 4H_2O$. The structure of the $CaCl_2 \cdot 6H_2O$ melt, which always yields supercooling, was investigated at 15 °C below the melting point (29.9 °C) and 80 °C. The structure in the supercooled state is similar to that found at 33 °C but different from that of $CaCl_2 \cdot 6H_2O$ crystal. A tendency of further Cl^- ion coordination to the Ca^{2+} ion with increasing temperature was observed.

VI–Q Studies on Dinuclear and Polynuclear Complexes

New dinuclear and polynuclear metal complexes have been synthesized and their physicochemical properties, of particular spin-exchange interactions, were investigated.

VI-Q-1 Dinuclear Copper(II) Complexes of New Dinucleating Ligands with Pyrazolate Group as Endogenous Bridge. Effects of Exogenous Azide and Acetate Bridges on Magnetic Properties

Toshiro KAMIUSUKI*, Hisashi ŌKAWA *(Kyushu Univ. and IMS)*, **Eiji KITAURA*, Masayuki KOIKAWA*, Naohide MATSUMOTO*, Hiroki OSHIO** *(IMS)*, **and Sigeo KIDA*** *(*Kyushu Univ.)*

[*J. Chem. Soc. Dalton*, in press]

New dinucleating ligands containing pyrazole as an endogenous bridging group, 3,5-bis[N-{(2-pyridyl)-methyl}carbamoyl]-pyrazole (H_3L^1), 3,5-bis[N-{2-(N,-N-diethylamino)ethyl}carbamoyl]pyrazole (H_3L^2), and 3.5-bis[N-{3-(N,N-dimethylamino)-propyl}carbamoyl]-pyrazole (H_3L^3), and their dinuclear copper(II) complexes with azide or acetate ion as an exogenous bridge have been obtained. Cryomagnetic investigations (5-300 K) have revealed a significant antiferromagnetic spin-exchange for the azide-bridged complexes of L^1-L^3 (-J: 371-297 cm^{-1}) whereas a ferromagnetic spin-exchange (J: +8.9 cm^{-1}) for the acetatebridged complex of L^1. The acetate-bridged complex gave ESR signals characteristic of spin-triplet state. ESR simulations gave the parameters g_{zz}=2.533, g_{xx}=2.055, A_{zz}=0.0103 cm^{-1}, D=0.210 cm^{-1}, and E=0.020 cm^{-1}.

VI-Q-2 Synthesis, Structure, and Spectral and Magnetic Properties of Trinuclear Copper(II) Complexes Bridged by Glyoximate Group

Hisashi ŌKAWA *(Kyushu Univ. and IMS)*, **Dominique LUNEAU** *(IMS)*, **Hiroki OSHIO** *(IMS)*, **Masayuki KOIKAWA*, and Sigeo KIDA*** *(*Kyushu Univ.)*

[*J. Chem. Soc. Dalton*, in press]

Copper(II) complexes of the composition $Cu_3(dioxim)_2(L)_2X_2$ have been obtained, where dioxim=dimethylglyoximate, diphenylglyoximate, or o-benzoquinonedioximate dianion, L=bipy or phen, and X=ClO_4^- or NO_3^-. X-ray structure analyses have revealed that the complexes are linearly trinuclear bridged by the deprotonated glyoxime oxygens, with the coordination of L (bipy or phen) to the terminal copper as "end-cap" ligand. Magnetic investigations (80-300 K) demonstrate the operation of a very strong antiferromagnetic spin-exchange through the oximate bridges to cause a complete or nearly complete spin-coupling even at room temperature.

VI-Q-3 Synthesis, Structure, and Redox Property of Dicopper(II,II) Complexes of N-(2-Hydroxyphenyl)salicylamide and Homologs. Facile Oxidation to Cu_2(II,III) and Cu_2(III,III) Species

Masayuki KOIKAWA*, Hisashi ŌKAWA *(Kyushu Univ. and IMS)*, **Naohide MATSUMOTO*, Mikio GOTOH*, Sigeo KIDA*, and Takamitsu KOHZUMA** *(IMS) (*Kyushu University)*

[*J. Chem. Soc. Dalton*, in press]

Dicopper(II,II) complexes of N-(2-hydroxyphenyl)salicylamide (H_3L^1) and its homologs with a substituent on the "2-hydroxyphenyl" moiety (4-CH_3, H_3L^2; 4-Cl, H_3L^3; 4-NO_2, H_3L^4) have been obtained as tetrabutylphosphonium (TBP) salts. Single crystal X-ray analysis for $(TBP)_2[Cu_2(L^1)_2]$ demonstrates that two copper ions are bridged by the phenolic oxygen of the "aminophenol" moiety with the Cu-Cu separation of 3.035(2) A. There operates a significant antiferromagnetic spin-exchange between a pair of copper ions (-2J: 393.4-448.8 cm^{-1}). The Cu_2(II,II) complexes are reduced electrochemically or chemically to Cu_2(II,III) and then to Cu_2(III,III) species. The mixed-valence species of L^1-L^3 are characterized by an intense visible absorption attributable to intervalence transition band.

VI-Q-4 Synthesis and Magnetism of Homo and Hetero Dinuclear Complexes with Bridging Diimine-Dioxime

Dominique LUNEAU, Hiroki OSHIO, Hisashi ŌKAWA *(Kyushu Univ. and IMS)*, **and Sigeo KIDA** *(Kyushu Univ.)*

Copper(II) and nickel(II) complexes of bis-(diacetylmonooxime)-1,3-propanediimine (H_2dopn) and bis-(diacetylmonooxime)-1,2-ethanediimine (H_2doen) react with copper(II) or nickel(II) ion to afford homo and hetero dinuclear complexes, [Cu(dopn)Cu(L)]X_2, [Cu(doen)Cu(L)]X_2, [Ni(dopn)-Cu(L)]X_2 and [Ni(dopn)Ni(L)$_2$]X_2 where X is ClO_4^- or NO_3^- and L is 2,2′-bipyridyl or 1,10-phenanthroline. All the Cu-Cu complexes are practically diamagnetic at room temperature, demonstrating that complete spin-coupling is attained even at room temperature. The Ni-Cu complex (μ_{eff}=1.80μ_B per molecule at room temperature) is found to contain low-spin nickel(II) ion. The Ni-Ni complex is a rare mixed-spin dinuclear complex comprised of a high-spin and a low-spin nickel(II) ion.

VI-Q-5 Synthesis, Structure, and Magnetism of [Cu{Cu(dopn)}$_2$](ClO$_4$)$_2$ (H_2dopn=bis-(diacetyl-monooxime)-1,3-propanediimine)

Dominique LUNEAU, Hiroki OSHIO, Hisashi ŌKAWA *(Kyushu Univ. and IMS)*, **and Sigeo KIDA** *(Kyushu Univ.)*

The title complex has been prepared by the reaction of bis-(diacetylmonooxime)-1,3-propanediiminato-copper(II) perchlorate [Cu(Hdopn)](ClO$_4$), copper(II) perchlorate hexahydrate and NaOH (in a 2:1:2 stoichiometry) in methanol. The crystal structure has been determined by single-crystal X-ray diffraction study. The complex consists of [{Cu(dopn)}$_2$Cu]$^{2+}$ trinuclear cation and perchlorate anions (Figure 1). The central copper Cu(1) bridges two [Cu(dopn)]$^{2-}$ ions through their deprotonated oxime oxygens with the Cu(1)–Cu(2) distance of 3.5516(2)Å. The configuration around the central copper is of a flatted tetrahedron. Each terminal copper Cu(2) with N_4 donor atoms in the equatorial plane is also bonded to an oxime oxygen of an adjacent molecule to form infinite chains (Figure 2).

This complex shows a magnetic moment of 2.00 μ_B per molecule at room temperature, indicating the operation of a very strong anti-ferromagnetic spin-exchange to cause an almost complete spin-coupling at room temperature.

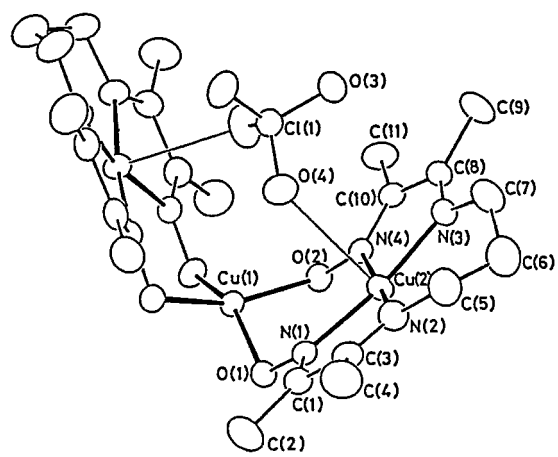

Figure 1. Structure of the trinuclear cation [{Cu-(dopn)}$_2$Cu]$^{2+}$

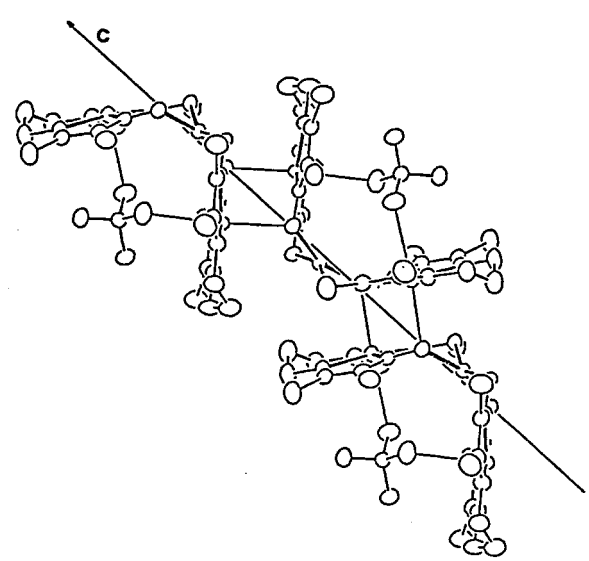

Figure 2. Polynuclear chains formed by [Cu{Cu-(dopn)}$_2$](ClO$_4$)$_2$.

RESEARCH ACTIVITIES VII
Computer Center

VII-A Theoretical Investigations of Metal Complex by the Ab Initio SCF MO Method

Metal complexes are interesting polyatomic systems because of their complicated electronic structure and their catalytic functions. In this project the electronic structure and the fundamental functions are studied for several complexes by using the *ab initio* SCF MO program JAMOL4 and a newly developed MCSCF program JASON2.

VII-A-1 CASSCF Study on Fe-O_2 Bond in Dioxygen Heme Complex

Shigeyoshi YAMAMOTO and Hiroshi KASHIWAGI

[*Chem. Phys. Lett.* **161**, 85 (1989)]

Ab initio complete active space self-consistent field (CASSCF) calculations have been performed to elucidate the electronic structure of the Fe-O_2 bond in an oxyheme model compound. The molecular structure is shown in Figure 1. This compound is a model for oxyhemoglobin. The main configuration in the CASSCF ground state wave function is designated $^1A'$ Fe(II)(S=0)-O_2(S=0), $(d\varepsilon)^6(\pi_g{}^a)^2$. This electronic configuration was originally proposed by Pauling, but the weight of this main configuration is quite small (0.641). The Fe-O_2 bond cannot be described with the Pauling model only. Two-electron excitations, $(d_\pi)^2 \rightarrow (\pi_g{}^b)^2$ and $(\pi_g{}^a)(d_\pi) \rightarrow (\pi_g{}^b)(d_\sigma)$, mix into the dominant configurations.

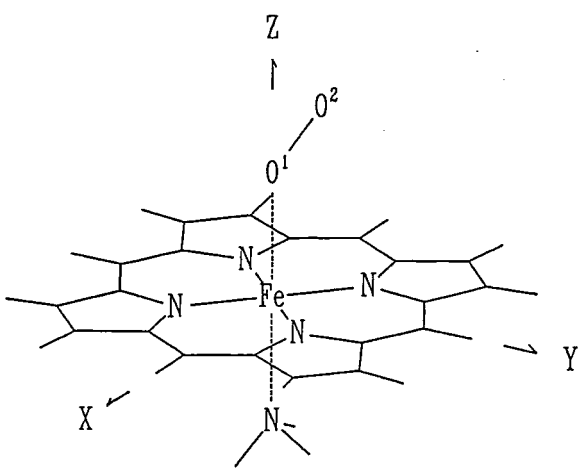

Figure 1. Assumed geometry of the oxyheme model.

VII-A-2 *Ab Initio* MO Study on Electron Correlation Effects in CuO_6 Cluster Relating to High-T_c Superconductivity

Shigeyoshi YAMAMOTO, Kizashi YAMAGUCHI *(Osaka Univ.)*, **and Keiichiro NASU**

Ab initio molecular orbital (MO) calculations for CuO_6 cluster have been performed to investigate the electronic structure of undoped and doped copper oxides which are received current interest in relation to the high-T_c superconductivity. The electron correlation effects are considered with full-valence configuration interaction (FVCI) method and complete active space self-consistent field (CASSCF) method. The electron correlation is rather simple for σ hole, but in-plane π hole, pair excitations and spin-flip excitations give great contribution to the configuration interaction.

VII-A-3 Structures and Properties of Molecular Assemblies

Kazuo KITAURA

A project will be started for studying structures and properties of molecular assemblies such as molecular clusters, liquids, solutions and solids. The molecular dynamics and the Monte Carlo technique will be employed with a new intermolecular potential functions proposed by us. The potential function is expressed by overlap integrals between molecules and point charge interactions. The potential function is easy to generate and reproduces *ab initio* potential surfaces in reasonable accuracy.

A general computer program will be developed for

generating the potential functions and for calculating structures and properties of molecular assemblies.

VII-A-4 Atomic Dynamics on the First Ionic State of o-Hydroxybenzaldehyde (OHBA)

Umpei NAGASHIMA and Shin-ichi NAGAOKA

The ground state geometry of OHBA are intramolecularly hydrogenbonded closed conformers. In the first excited state, the intramolecular proton transfer takes place and enol tautomer is formed. In the first ionic state the proton transfer to yield the enol tautomer does not take place, although the potential energy surface is slightly distorted from that of the ground state. To analyse the dynamic process in the first stage after ionization, we calculated a classical trajectory. In the calculation, it was assumed that each atoms move as classical particles on a potential energy surface which is made by the motion of electron and is evaluated by *ab initio* molecular electronic structure theory. All degrees of freedom (3N-6) are considered. The classical equation of motion is solved by using the Runge-Kutta method. The ground state geometry was used as the initial geometry in order to corresponding to a vertical ionization. In each Runge-Kutta step, *ab initio* energy gradients were evaluated by using STO-3G basis set.

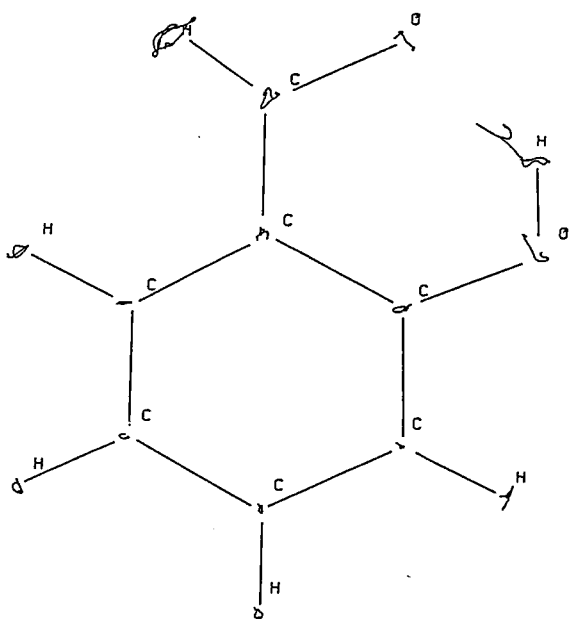

Figure 1. The classical trajectory of OHBA on the first ionic state within 0.2 pico sec. from vertical ionization.

The calculated trajectory until 0.2 pico second is shown in Figure 1. Within this time, the benzene part oscillates almost 3 times. The displacement of benzene part is small and ground state geometry is kept. However, the oscillation of O-O is not completed within this time and the displacement is bigger than that of benzene part. The displacement of proton hydrogen-bonded is big and vibration concerned to C-C-O angular distortion is strongly coupled to the OH stretching. The motion to the out of plane is very small.

VII-A-5 Structure and Stability of $H_3^+(H_2)_n$ Clusters (n=1~16)

Umpei NAGASHIMA, Keiji MOROKUMA, and Hideki TANAKA

The standard statistical mechanical Classical Monte Carlo simulation have been carried out to investigate molecular structure and stability of large hydrogen cluster ions, $H_3^+(H_2)_n$ (n=3~16), by using two-body potential functions, which have made by fitting the results of *ab initio* SCF MO MP4SDTQ with (4s2p) basis set.

The n dependence of dissociation energy ($\delta E_{n-1,n}$) is in good agreement with the experiment. Molecular structure and stability is mainly determined by an ionic interaction between H_3^+ and H_2. The H_2-H_2 interaction seems to give small effect to the structure and stability of cluster. Strong stabilization has been observed at n=6,9 and 12 where optimized structure has three hold symmetry and distinct coordination spheres seem to exist. The structure of $H_3^+(H_2)_3$ cluster is quite stable because the structure of this molecule held even in a bigger size cluster.

Chemical Materials Center

VII-B Preparation and Properties of Novel Heterocyclic Compounds

Heterocyclic compounds are useful as components of functional materials such as organic conductors since heteroatoms in their rings are helpful to stabilize ions or ion-radical species. In this project novel electron acceptors and donors containing heterocycles were synthesized and the properties including the charge-transfer complexes or ion-radical salts were investigated in detail.

VII-B-1 p-Quinodimethane Analogues of Tetrathiafulvalene

Yoshiro YAMASHITA, Yasuo KOBAYASHI *(Tohoku Univ.)*, **Tsutomu MIYASHI** *(Tohoku Univ.)*

[*Angew. Chem.*, in press]

Bis(1,3-dithiole) derivatives containing quinodimethane structures are promising electron donors for organic metals due to the extended conjugation to decrease Coulomb repulsion. However, the parent compound, 2,2′-p-quinobis(1,3-dithiole) **1** was hitherto unknown, and the reported examples of derivatives as neutral donors were limited to the dibenzo derivatives, although some dication salts were known. We have found a simple synthesis of **1** using a retro-Diels-Alder reaction of **2** which was obtained by a Wittig-Horner reaction of 2-dimethoxyphosphinyl-1,3-dithiole with a cyclopentadiene adduct of p-benzoquinone. This method was applied to syntheses of the various derivatives. The oxidation potentials of the donors obtained here are much lower than that of TTF. The difference between the first and the second oxidation potential in **1** is very small and two-electron oxidation waves are observed in the other new donors, indicating that the donors with quinoid structures form dications more readily upon oxidation due to the decreased Coulombic repulsion. The donors gave charge-transfer complexes with TCNQ which exhibit good conductivities.

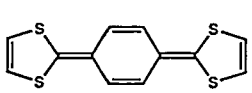

1

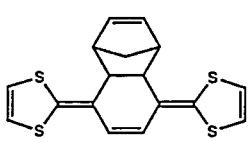

2

VII-B-2 Preparation, Properties, and Crystal structures of [1,2,5]Thiadiazolotetracyanoquinodimethane

Takanori SUZUKI *(Tohoku Univ.)*, **Yoshiro YAMASHITA, Chizuko KABUTO** *(Tohoku Univ.)*, **Tsutomu MIYASHI** *(Tohoku Univ.)*

[*J. Chem. Soc., Chem. Commun.*, in press]

Electron acceptors containing chalcogen atoms are of interest since the interheteroatom interactions may suppress the metal insulator transitions. Bisthiadiazolo-TCNQ (BTDA) **1** shows interesting properties, which are not seen in TCNQ itself, due to the fused thiadiazole rings. However, **1** does not form highly conductive complexes with TTF and its derivatives because **1** incorporates them in the cavity formed by the strong S---N interaction. In order to overcome this disadvantage, monothiadiazolo-TCNQ (TDA) **2** was prepared by reaction of 4,7-dibromo-2,1,3-benzothiadiazole with malononitrile anion followed by oxidation with PbO_2. **2** was a stronger acceptor than **1** and gave highly conductive complexes with TTF. **2** forms a coplanar dyad in the crystal by hydrogen bonding.

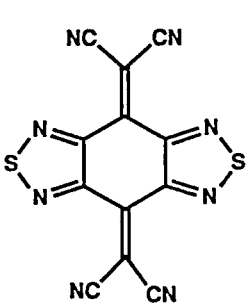

1

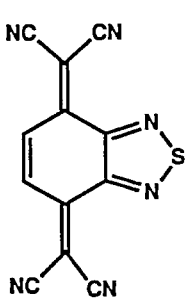

2

VII-B-3 2,2′-(5,8-Dihydroquinoxaline-5,8-diylidene)bis(1,3-benzodithiole)s. A New Type of Electron Donors.

Yoshiro YAMASHITA, Takanori SUZUKI *(Tohoku Univ.)*, **and Tsutomu MIYASHI** *(Tohoku Univ.)*

[*Chem. Lett.*, 1607 (1989)]

One of the important strategies for the design of components giving organic metals is to extend conjugation to decrease on-site Coulomb repulsion. TTF analogues containing quinoid structures are interesting from this viewpoint. However, such compounds are generally unstable and readily decomposed in solvents. Therefore, we designed pyrazine-fused quinodimethane analogues **1**, in which the electron withdrawing heterocycle is expected to play a role in the stabilization. **1** were prepared from quinoxaline-5,8-diones by using a Wittig-Horner reaction and a retro-Diels-Alder reaction. They are stronger donors than dibenzo-TTF and formed conducting complexes with TCNQ and iodine.

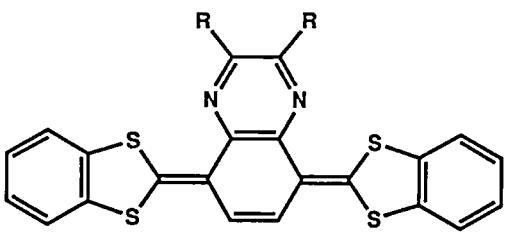

1 R=H,Me,Ph

VII-B-4 Electronic and Molecular Structure of 3,6-Di-t-butyl-1,4-diazapentalene

Shoji TANAKA *(IMS)*, **Akira KIYOMINE*, Takanori SUZUKI*, Chizuko KABUTO*, Tsutomu MIYASHI*** *(*Tohoku Univ.)*, **Tsunetoshi KOBAYASHI** *(Keio Univ.)*, **and Toshio MUKAI** *(Nihon Univ.)*

The resonance stability and bonding character of aza analogues of pentalene have been important subject in the field of physical organic chemistry. Recently we have synthesized the titled compound **1**, which is the first kinetically stabilized diazapentalene. In this article we report the structural characters of this compound.

We first carried out the X-ray structure analysis of **1**. The results are summarized in Figure 1. The compound **1** has a planar bicyclic ring system with C_{2h} symmetry. There exists strong double-bond alternation in the perimeter. The aromaticity index based on double-bond fixation suggests the 'antiaromatic' nature of this compound as predicted previously. We then investigated the electronic structure of **1** on the basis of the He(I) photoelectron spectroscopic study. There exist four ionization bands at low-energy region (8.43–9.95 eV). The orbital energies derived by the SCF MO calculations (MNDO, STO-3G, and 4-31G) correlate reasonably well with the observed ionization energies. In conclusion, these bands are assigned, from the top, to the ionization from the $\pi_4(a_u)$, $\pi_3(b_g)$, $n_+(a_g)$, and $n_-(b_u)$, orbitals, respectively.

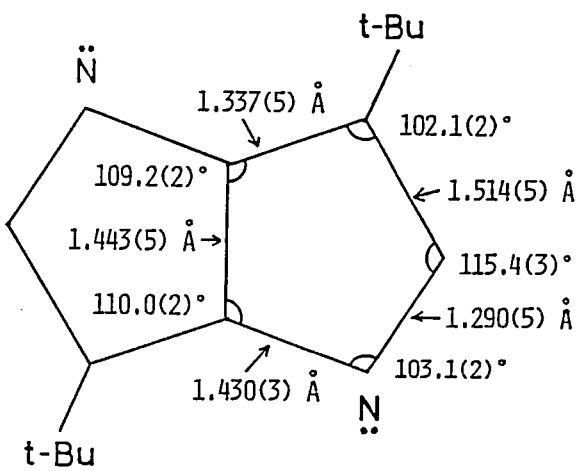

Figure 1. Bond lengths and bond angles of **1**.

Instrument Center

VII-C Reaction of Gas-Phase Metal Clusters

Reactions of neutral and ionic metal clusters with small molecules have grown as a new field of chemistry that bridges the gap between molecular and surface sciences. A new technique of synthesizing isolated clusters, that of sudden condensation of laser-produced metal vapor, has made possible the study of gas-phase clusters of virtually any material. Using this technique, we have made the study of the elementary chemical properties of gas-phase metal clusters.

VII-C-1 Reaction of Aluminum Clusters, Al_n (n = 7–24), with Oxygen and Ammonia

Kiyokazu FUKE, Shinji NONOSE*, Noriyoshi KIKUCHI*, and Koji KAYA* *(*Keio Univ.)*

[*Chem. Phys. Lett.*, **147**, 479 (1988)]

The reaction of aluminum clusters, Al_n (n = 7–24), formed by laser vaporization, with oxygen and ammonia was studied by using a fast flow reactor. It was found that the oxygen reacts strongly with aluminum clusters to form chemisorbed products while ammonia is adsorbed weakly with Al_n in a physisorbed form. In the reaction with oxygen under multiple collision conditions, a mixed cluster, Al_9O_7, was found to be formed selectively.

VII-C-2 Reaction of Vanadium and Cobalt Clusters with Ethylene and Acetylene

Shinji NONOSE*, Yasutomo SONE*, Noriyoshi KIKUCHI*, Kiyokazu FUKE, and Koji KAYA* *(*Keio Univ.)*

[*Chem. Phys. Lett.*, **158**, 152 (1989)]

The reactions of vanadium and cobalt clusters, generated by laser vaporization, with ethylene and acetylene were studied by using a fast flow reactor. In the reaction of small V_n with C_2H_4, the dehydrogenated products V_nC_2, $V_nC_2H_2$ were observed. Upon increasing the cluster number, the intensities of those products decrease monotonically, while those of $V_nC_2H_4$ increase. Similar results were observed in the reaction of V_n with C_2H_2. On the other hand, only non-dehydrogenated products were observed in the reaction of small Co_n with C_2H_4, but for larger clusters ($n \geq 9$) the dehydrogenated products Co_nC_2 and $Co_nC_2H_2$ appeared. The contrast between the reaction of V_n and Co_n is related to the heat of adsorption and the structure of adsorbed products.

VII-D Dynamics of Proton-Transfer Reaction in a Model Hydrogen-Bonded Base Pairs

A purpose of this study is to understand the dynamics and the interplay between molecular structure and reactivity of intermolecular proton-transfer reaction.

VII-D-1 Dynamics of Double-Proton-Transfer Reaction in the Excited-State Model Hydrogen-Bonded Base Pairs

Kiyokazu FUKE and Koji KAYA *(Keio Univ.)*

[*J. Phys. Chem.*, **93**, 614 (1989)]

The absorption and emission behaviors of model hydrogen-bonded base pairs such as 7-azaindole and 1-azacarbazole dimers and their heterodimer were studied in a supersonic jet by using a laser induced fluorescence method. These dimers were found to exist as the two conformational isomers, and one of the

isomers, which has a nearly coplanar structure, selectively undergoes the double-proton-transfer reaction (DPTR) in the excited state. In these dimers, DPTR occurs even from the zero vibrational level of the S_1 state and the rate of DPTR were affected substantially by deuterium substitution. We found that the symmetric stretching vibration in the hydrogen bond promotes pronouncedly the DPTR of these dimers. Moreover, the fluorescence excitation and dispersed fluorescence spectra of the jet-cooled tautomer of 7-azaindole were measured by a two-step laser excitation, and the double minimum potential of the dimer was experimentally elucidated. On the basis of these results, the dynamics of DPTR was discussed in terms of a dynamic coupling of proton motion with the intermolecular vibration.

VII-D-2 Excited-State Double Proton Transfer in Solid 1-Azacarbazole

Kiyokazu FUKE, Takaya YAMANAKA, Hiroyuki YAMADA*, and Koji KAYA* *(*Keio Univ.)*

In our previous works[1,2], the jet-cooled 1-azacarbazole (1-AC) dimers were found to exist as the two conformational isomers, and one of the isomers, which has a coplanar structure, selectively undergoes the double-proton-transfer reaction (DPTR): the rate of DPTR is affected extraordinarily by a subtle change in the structure of dimer. In order to gain more insight into the interplay between molecular structure and reactivity for these dimers, the static and transient fluorescence spectroscopy of solid 1-AC, consisting of nearly coplanar, double hydrogen-bonded dimers, are investigated as a function of temperature and deuteration of the pyrrole group. Large H/D isotope effects are observed for the decay rate of initially excited dimer, which corresponds approximately to the rate of DPTR (shown in Figure 1). The temperature dependence of DPTR rate is interpreted by a kinetic model, which includes two cyclic dimers structurally related to the conformational isomers found in a jet.

References

1) K. Fuke, T. Yabe, N. Chiba, T. Kohida, and K. Kaya, *J. Phys. Chem.* **90**, 2309 (1986).
2) K. Fuke and K. Kaya, *J. Phys. Chem.* **93**, 614 (1989).

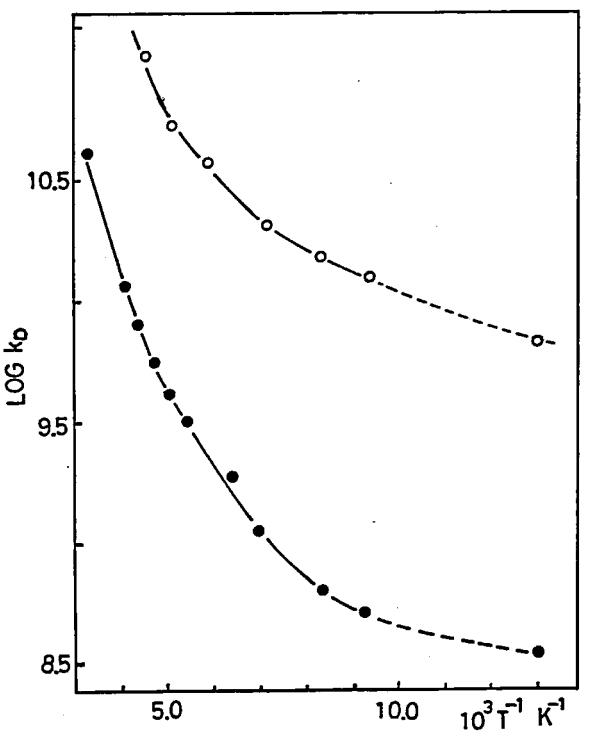

Figure 1. A plot of log k_D versus T^{-1} for 1-A (○) and 1-AC-d (●), where k_D is the decay rate of the initially excited dimer.

VII-E Studies of Ultrafine Particles

The physical properties of fine particles the size of which is less than ten nm, are affected by the quantum size effect, surface effect and a fluctuation of a thermodynamical property due to low dimensionality. These effects were studied as functions of particle species, supporting organic liquids and preparation techniques.

VII-E-1 ^{27}Al NMR Study of AlF_3 Ultrafine Particles

Naoki SATOH and Keisaku KIMURA

High resolution ^{27}Al nuclear magnetic resonance spectra of AlF_3 ultrafine particles (UFP's) were obtained by means of motional narrowing caused by Brownian motions of UFP's in a liquid phase. The NMR spectra observed were resolved in five signals, 10, −5, −8, −12 and −16 ppm quoted from a $Al^{3+}(H_2O)_6$ standard. UFP's were fractionated by their sizes using an ultrafiltration technique. From the NMR measurements of fractionated colloidal solutions, the five peaks were classified into three groups by their origins, i.e., the peak at −16 ppm is from larger UFP's (diameter D, 9 nm), the peaks at −5, −8 and −12 ppm from smaller UFP's ($1<D<3$ nm) and the peak at 10 ppm from free ions. Line widths of larger and smaller UFP's were about 10 ppm (1 kHz) and 4 ppm (0.4 kHz), respectively. The observed line widths were considerably larger than the calculated values taking into account only dipole-dipole interactions. The quadrupole interaction was suggested to be the origin of this discrepancy. Further, the signal at −8 ppm was assigned to Al ions at surfaces of UFP's. The size dependence of chemical shifts was ascribed to changes in the degree of ionicities of Al-F bonds, which is a function of the particle size. This interpretation was supported by the measurements of X-ray photoelectron spectroscopy.

VII-E-2 The Shape Effect on the Quantum Size Effect of Cu Small Particles

Keisaku KIMURA

In finite metallic particles, the energy levels are no longer continuous, exhibiting remarkable deviation of electronic properties from those in bulk. The size as well as shape of a particle are responsible to this deviation. As a typical example, the Knight shift data of Cu small particles were analyzed by proposed formula. It was concluded that the shape of particles are not random but regular inconsistent with commonly accepted assumptions. The influence of the spin-orbit interaction and the Zeeman effect on the magnetic susceptibility was also discussed. A possible energy level statistics for the small particles was suggested.

VII-E-3 Preparation of Colloids made of Metals and Semiconductive Materials by Sputtering

Shunji BANDOW and Keisaku KIMURA

[*Nippon Kagaku Kaishi*, **11**, 1957 (1989)]

Ultrafine particles (UFP's) of metals and semiconductive materials were prepared by the gas-flow sputtering method. This is a versatile method applicable for metals and other materials with high melting temperature. Production rates of UFP's were of the order of a few μg/min cm^2 W. With the combination of this method and the particle collection technique called as solution trap method, a colloidal solution was obtained. Very stable colloids made of metals and semiconductive materials including Pt, Fe, Ag and Si were obtained in an ethanol solution. Diameter of colloidal particles was varied in the range from 6 to 180 nm by changing the pressure of sputtering gas (He + 40 % H_2).

VII-E-4 ESR Study of Spin Assembly in a Finite System: Disappearance of Long Range Ordering in Ultrafine Magnetite Particles

Shunji BANDOW and Keisaku KIMURA

It is well known that the superparamagnetism is observed when ferromagnetic materials are finely devided. Limit of the division is confined by an atom or a molecule which shows paramagnetic properties. Hence, a question is posed on the states of superparamagnetism and paramagnetism, that is, how the spin state changes in a microscopic level. There is a long range spin ordering in a superparamagnetic state and not in a paramagnetic state. We focused our attention to this point and studied by ESR. Samples of strongly interacting spin-assembly were prepared by vacuum evaporation technique using electron beam heating. Iron metal was deposited on an evaporated quartz film with a thickness of a few sub-nm. Through this process, very small particles (usually called as ultrafine particles;

UFP's) of Fe were grown on the quartz film. After evaporation of Fe, 2.7 × 10^2 Pa of pure O_2 was introduced into a chamber to oxidize Fe UFP's. Quartz was again evaporated to isolate UFP's and prevent further oxidation. Above processes were repeated several times to make a multilayered film which gives a good ESR signal to noise ratio. Iron-oxide UFP's were found to be magnetite (Fe_3O_4) by the electron diffraction. Mean diameter was determined both by the width of Debye-Scherrer rings and by the real images of transmission electron microscopy. In magnetite UFP's with a mean diameter less than 3.4 nm, ferromagnetic resonance (FMR) could not be detected as shown in Figure 1. This is same down to 3 K. This is a very interesting result suggesting that the magnetite UFP's whose sizes are less than 3.4 nm do not exhibit long range spin ordering.

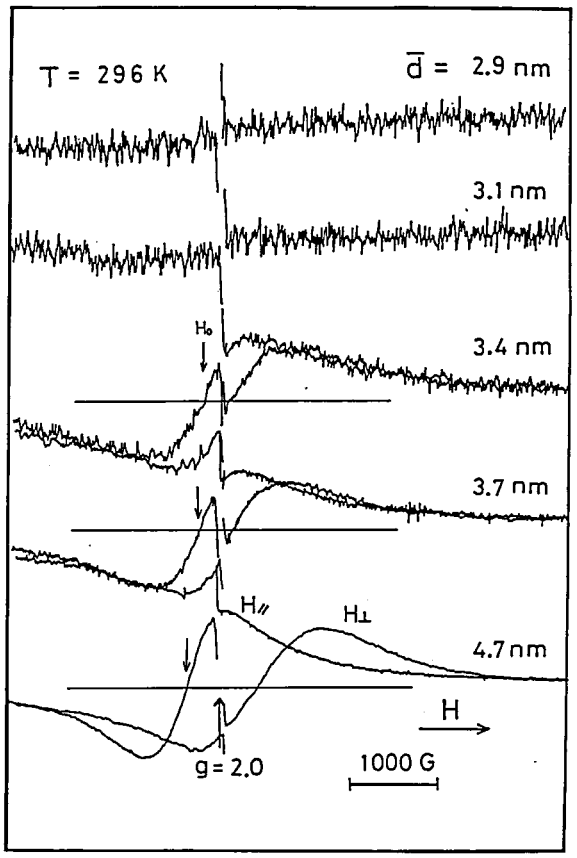

Figure 1. ESR spectrum of ultrafine magnetite particles. Mean diameters of UFP's are represented by *d*. $H_{//}$ and $H_{\perp}$ mean the direction of applied magnetic fields parallel and perpendicular to the film. H_0 is the center of resonance field in the case of $H_{//}$ and gradually decreases with increasing particle size. ESR spectrum of the samples with *d* being larger than 3.4 nm exhibited a characteristic of FMR.

Low-Temperature Center

VII-F Instrumentation for Low Temperature Experiments

VII-F-1 Liquid Helium Levelmeter by Audio-Sound Detection

Kiyonori KATO

[*Rev. Sci. Instrum.* **60**, pp.1345 (1989)]

A new audible liquid helium level detector using the thermal oscillations of helium gas has been developed. A liquid level can be easily detected by a clear sound change of a vibrating plastic film which is fixed on top of a stainless steel tube. This levelmeter is very simple, but more convenient and economical compared with commercial electronic type of levelmeters.

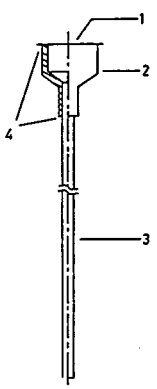

Figure 1. Cross section view of a typical audio-sound detectable levelmeter: 1. A piece of plastic film (Kapton, polyimide film)
thickness 50 μm. 2. Machined reducer, maximum o.d. and i.d. are 18mm, 22mm, respectively. Minimum i.d. must be fitted to the o.d. of the tube. 3. Stainless steel tube. A 4mm o.d. and length 1.2m. 4. Adhesive, epoxy adhesive for low temperature use, Oxford instruments co., Inc.

VII-G Ferromagnetic Interaction in Molecular Crystals

The study of the ferromagnetic intermolecular interaction in organic molecular solids should bring us important knowledge, not only to the establishment of molecular ferromagnet but also to the understanding about the radical reactions. In the present project, we investigate the factors controlling ferromagnetic and antiferromagnetic behaviors in solids.

VII-G-1 Ferromagnetic Intermolecular Interaction of the Organic Radical, 2-(4-Nitrophenyl)-4,4,5,5-tetramethyl-4,5-dihydro-1*H*-imidazolyl-1-oxy 3-Oxide

Kunio AWAGA and Yusei MARUYAMA

[*Chem. Phys. Lett.* **158**, 556 (1989)]

α-Nitronyl nitroxides are known to be stable radicals of S=1/2, and to have strong spin polarization. The temperature dependence of the magnetic susceptibility and the magnetization curve of the organic free radical, 2-(4-nitrophenyl)-4,4,5,5-tetramethyl-4,5-dihydro-1*H*-imidazolyl-1-oxy 3-oxide, have been measured. It is found that ferromagnetic intermolecular interaction obtains in the crystal of this compound. The Curie and Weiss constants are 0.375 emu K mol^{-1} and +0.9 K, respectively. The magnetization curve at about 2 K almost corresponds to the theoretical one for the S=2, indicating that the ferromagnetic interaction covers more than four radicals.

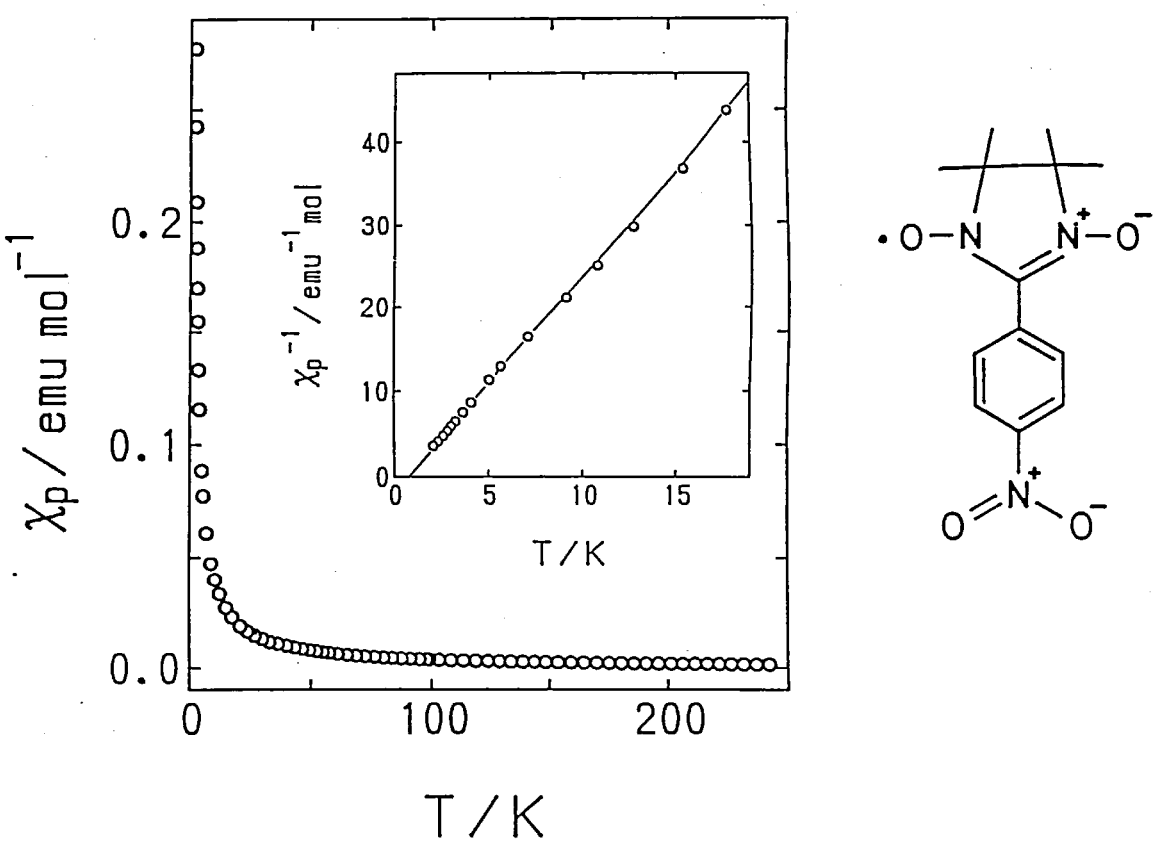

Figure 1. The temperature dependence of the magnetic susceptibility of 2-(4-nitrophenyl)-4,4,5,5-tetramethyl-4,5-dihydro-1*H*-imidazolyl-1-oxy 3-oxide. The inset shows the reciprocal susceptibility below 20 K. The straight line in the inset is calculated by the Curie-Weiss law.

VII-G-2 Ferromagnetic and Antiferromagnetic Intermolecular Interactions of Organic Radicals, α-Nitronyl Nitroxides.

Kunio AWAGA and Yusei MARUYAMA

[*J. Chem. Phys.* **91**, 2743 (1989)]

The temperature dependence of the magnetic susceptibilities and the magnetizations for the three kinds of α-nitronyl nitroxides, 2-R-4,4,5,5-tetramethyl-4,5-dihydro-1*H*-imidazolyl-1-oxy 3-oxide [with R= phenyl (I), 3-nitrophenyl (II) and 4-nitrophenyl (III)] have been measured. It is found that the intermolecular spin interaction is ferromagnetic in the crystal of III, while it is antiferromagnetic in I or II. UV-Vis absorption spectra suggests the enhancement of the π-electron delocalization in III in comparison with the others. The difference in the magnetic coupling between I or II and III is interpreted based on this effect.

VII-G-3 Two-Dimensional Network of the Ferromagnetic Organic Radical, 2-(4-Nitrophenyl)-4,4,5,5-tetramethyl-4,5-dihydro-1*H*-imidazolyl-1-oxy 3-Oxide

Kunio AWAGA, Tamotsu INABE, Umpei NAGASHIMA, and Yusei MARUYAMA

[*J. Chem. Soc. Chem. Commun.* in press]

The X-ray crystal analysis and the molecular orbital calculation have been carried out on the ferromagnetic radical, 2-(4-nitrophenyl)-4,4,5,5-tetramethyl-4,5-dihydro-1*H*-imidazolyl-1-oxy 3-oxide. This radical forms a 2-D network by the contacts between the O-atoms in the NO groups and the N-atoms in the NO_2 groups. MNDO calculation indicates that the unpaired electron occupying SOMO is localized on the side of the nitronyl nitroxide and has little population in the nitrophenyl ring, whereas NHOMO and NLUMO are distributed mainly in the nitrophenyl ring. At the contact point in the 2-D network, the intermolecular overlap between SOMO's could be much smaller than those between SOMO-NHOMO and/or between SOMO-NLUMO. The ferromagnetic interaction would originates in the intermolecular SOMO-NHOMO and/or SOMO-NLUMO interaction and the intramolecular strong spin-polarization of this radical.

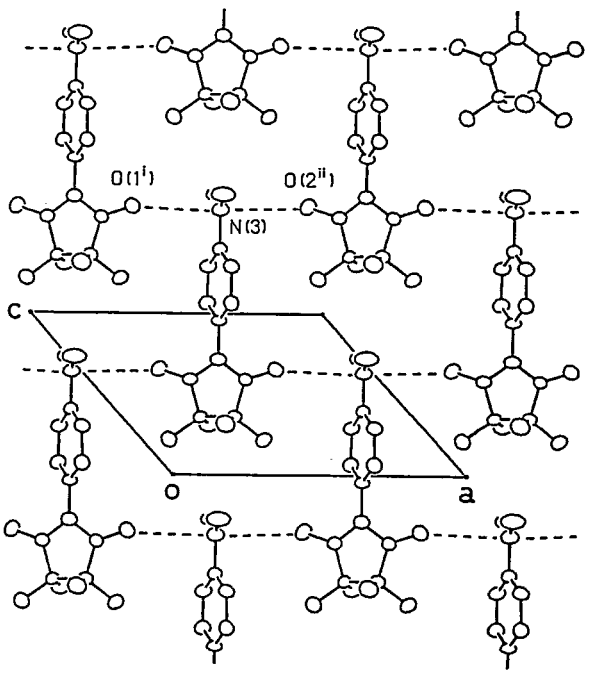

Figure 1. The 2-D network of 2-(4-nitrophenyl)-4,4,5,5-tetramethyl-4,5-dihydro-1*H*-imidazolyl-1-oxy 3-oxide, projected to the *ac* plane.

VII-G-4 Spin-Soliton Excitation in One-Dimensional Alternating Antiferromagnetic System of Galvinoxyl Single Crystal

Kunio AWAGA, Hiroshi OKAMOTO, Tadaoki MITANI, Yusei MARUYAMA, Tadashi SUGANO *(ISSP, Univ. Tokyo)*, **and Minoru KINOSHITA** *(ISSP, Univ. Tokyo).*

[*Solid State Commun.* in press]

EPR studies have been carried out on the alternating antiferromagnetic chain appearing in the low-temperature phase of the galvinoxyl radical (S=1/2). The EPR spectrum of the single crystal consists of the line due to the doublet state and the lines due to the triplet excitons of radical pairs. The temperature dependence of the doublet state absorption is interpreted as due to overlapping of the Curie spins and the thermally-excited doublet spins (doublet excitons). The

doublet exciton can be assigned to a spin-soliton which is created by switching of the bond alternation. The activation energy of the soliton is 12 meV, 27 % of that of the triplet exciton.

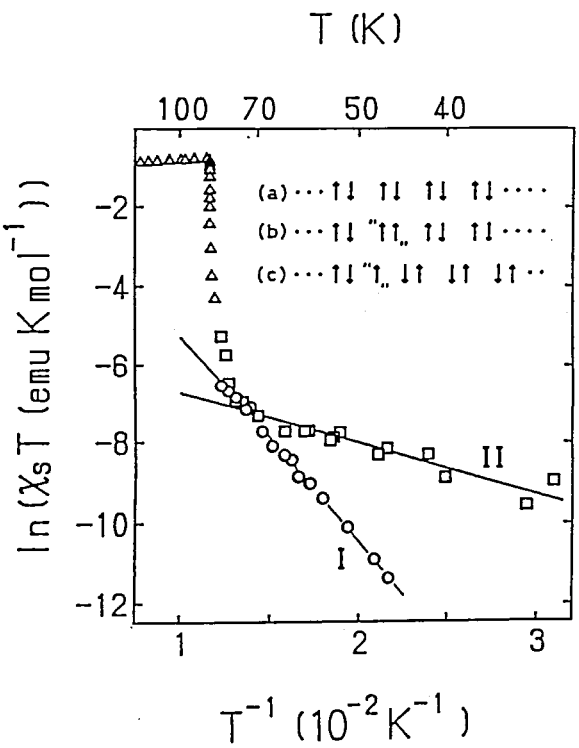

Figure 1. The spin susceptibility of the triplet exciton (circles) and the spin soliton (squares). The triangles show the static magnetic susceptibility of galvinoxyl in the high-temperature phase. The inset shows the schematic representation of the magnetic excitons in an alternating antiferromagnetic chain. (a) is the ground state, (b) is the triplet exciton, and (c) is the spin soliton.

Equipment Development Center

VII-H Studies of Quasi-1-D Organic Semiconductors

VII-H-1 A New Approach to Protonics in the H-bonded CT Complexes

Tadaoki MITANI, Hiroshi OKAMOTO, and Kaoru OKANIWA

[*Mol. Cryst. Liq. Cryst.* **171**, 343 (1989)]

Our recent study of interacting protons in H-bonded organic molecular crystals including derivatives of quinhydrone and N-salicylideneaniline has been reviewed, together with several other related topics, i.e. the neutral-to-ionic phase transition and the photochromism in the CT complexes. Several suggestions were proposed for design of a new molecular function in conductive CT complexes, by controlling dynamics of protons focusing on the excess π-electron effect on the hydrogen bonding in the CT complexes.

VII-H-2 Development of Halogen-Bridged Metal Complexes by Chemical Modifications.

Hiroshi OKAMOTO, Tadaoki MITANI, Kaoru OKANIWA, Koshiro TORIUMI, and Masahiro YAMASHITA *(Nagoya Univ.)*

The 1-D electronic state of halogen-bridged mixed-valence metal complexes has been found fairly to depend on the nature of interchain hydrogen bondings linking ligands to counter anions. Changing counter anions from ClO_4^- to a harogen ion (Br^- or I^-), the hydrogen bondings are strengthened, where quenching of luminescence, enhancement of photoconductivity, and increase of number of paramagnetic defects were observed. These features are explained as a result of considerable suppression of the Peierls distortion by introducing strong hydrogen bondings. By further modification, which gives rise to an increase of the

on-site electron repulsive energy in the chain, the Peierls distortion disappears and the electronic system is transformed into the Mott insulator as demonstrated by replacing M=Pt, or Pd with M=Ni in $\{[M(R,R\text{-}chxn)_2Br]Br_2\}_\infty$ [see V-F-1]. In Figure 1, the absorption spectra of the CT transition in these complexes are presented for M=Pt, Pd, and Ni at R. T. The remarkably sharp structure observed in the Ni complex reflects weak electron-lattice coupling, in contrast to the broad bands of Pt and Pd complexes in the Peierls phases.

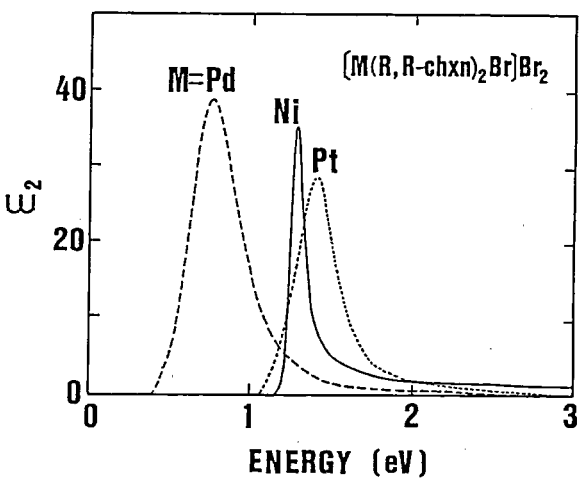

Figure 1. Imaginary parts of the dielectric constant ε_2 transformed from polarized reflectance spectra of $\{[M(R,R\text{-}chxn)_2Br]Br_2\}_\infty$ (M=Pt, Pd and Ni) with an electric vector parallel to a 1-D chain.

VII-H-3 Pressure-Induced Neutral-to-Ionic Phase Transition in Organic Charge-Transfer Crystals of Tetrathiafulvalene-p-Benzoquinone Derivatives

Hiroshi OKAMOTO, Takao KODA*, Yoshinori TOKURA*, Tadaoki MITANI, and Gunzi SAITO* *(*Univ. of Tokyo)*

[*Phys. Rev.* **B39**, 10693 (1989)]

Infrared and visible absorption spectra have been measured on three kinds of mixed-stack organic charge-transfer crystals of tetrathiafulvalene (TTF)-p-benzoquinone derivatives under hydrostatic pressures up to about 50 kbar. In TTF-tetrachloro-p-benzoquinone and TTF-trichloro-p-benzoquinone crystals, the regularly stacked quasineutral phase at ambient pressure undergoes a change to the dimerized quasi-ionic phase under the increasing pressure, passing through an inhomogeneous mixed state where the quasineutral molecular region and the quasi-ionic molecular region are spatially separated. On the other hand, in TTF-2,5-dichloro-p-benzoquinone, a continuous increase in the degree of charge transfer is observed under increasing pressure up to about 50 kbar. The nature of these pressure-induced neutral-to-ionic transitions in the respective TTF-complex crystals is discussed.

VII-H-4 Anomalous Dielectric Response in Tetrathiafulvalene-p-Chloranil as Observed in Temperature and Pressure-Induced Neutral-to-Ionic Phase Transition

Hiroshi OKAMOTO, Tadaoki MITANI, Yoshinori TOKURA*, Sinya KOSHIHARA*, Takashi KOMATSU*, Yoshihiro IWASA*, Takao KODA*, and Gunzi SAITO* *(*Univ. of Tokyo)*

Temperature and pressure-dependences of dielectric constants have been measured on a mixed-stack organic charge-transfer crystal tetrathiafulvalene (TTF)-p-chloranil in a frequency range from 100 Hz to 10 MHz. The dielectric response is remarkably increased with decreasing temperature down to T_c=81K where the neutral-to-ionic (NI) phase transition occurs. On the other hand, with applying pressure at room temperature, the change in strength of dielectric response is not so remarkable, whereas the dc conductivity σ_{dc} considerably increases. Such dynamical responses are explained by a Debye-type relaxation model. It turns out that the strength of dielectric response is closely correlated with both the relaxation time τ and σ_{dc}. A possible mechanism of these anomalous dielectric response is discussed in terms of dynamics of the NI domain wall pairs and ionic domains in the neutral lattice.

VII-I Development of Nonlinear Technique for Ultrafast Spectroscopy

VII-I-1 Two-Photon Absorption Sampling Spectroscopy for Fast Transient Luminescence Measurements

Yoshihiro TAKAGI and Keitaro YOSHIHARA

[*Ultrafast Phenomena VI*, pp.407–409 Springer, 1988]

A novel fast sampling spectroscopy based on two-photon absorption has been proposed. Fast transient fluorescence from an organic dye solution has been gated both in time and spectral domain with time and spectral resolution determined by the excitation laser pulse. Various atomic vapors showed excellent characteristics as a nonlinear device for two-photon resonant transition using one photon from the laser pulse and one photon from the fluorescence to be measured.

VII-I-2 Multi-Quantum Transition Sampling Spectroscopy for Fast Transient Luminescence Measurement

Yoshihiro TAKAGI, Thoru KOBAYASHI, and Keitaro YOSHIHARA

[*Laser Spectroscopy IX*, pp.185–187 Springer, 1989]

Two-photon-excited photoelectron emission in various solids has been used for the first time for high time-resolution sampling spectroscopy of short-lived UV luminescence and UV laser pulse measurement. Alkali-halide and silver halide have shown a typical quadratic power dependence due to two-photon photoelectric effect, which was successfully applied to an autocorrelation pulse-width measurement in UV spectral region. Pulse-width of the third-harmonic (355 nm) and fourth-harmonic (266 nm) of a mode-locked Nd:YAG laser was measured using an ordinary autocorrelator based on Michelson interferometer, in which the crystal for second-harmonic generation was replaced by a vacuum chamber containing an evaporated film of cesium iodide and an electron multiplier. A slight modification of this optical arrangement has provided a new sampling method for highly time-resolved fluorescence measurement.

VII-I-3 Application of Two-Photon-Excited Photoconductivity in GaAsP and GaP Photodiodes to Ultrashort IR Laser Pulse-Width Measurement

Yoshihiro TAKAGI

A quadratic dependence of the photoconductivity on the incident light power density has been observed and applied for the first time to the autocorrelation pulse-width measurement using inexpensive commercial GaAsP and GaP photodiodes (Hamamatsu Photonics). In a Michelson-type autocorrelator a nonlinear crystal for second-harmonic generation was replaced by a GaAsP (or GaP) photodiode with an external inverse voltage of 1.5 volts. An incident light with wavelength 1064 nm, single pulse of a passively mode-locked Nd:YAG laser, was split into two beams, one going through a variable optical delay and the other through a fixed optical delay, and the beams were overlapped again on the photodiode with an angle of a few degrees between the two beams. Figure 1 shows an input power dependence and a delay time dependence of the photocurrent. The photodiode used in the experiment has a spectral response in the wavelength range 200–680 nm. A clear quadratic characteristics in Figure 1 indicates the photoconductivity due to the two-photon excitation. This is confirmed by a clear second-order autocorrelation signal. The pulse-width is nearly the same as that obtained by the ordinary second-harmonic generation method. An autocorrelator using a photodiode is useful as a simple device for pulse-width measurements and optical alignment in ultrashort time scale.

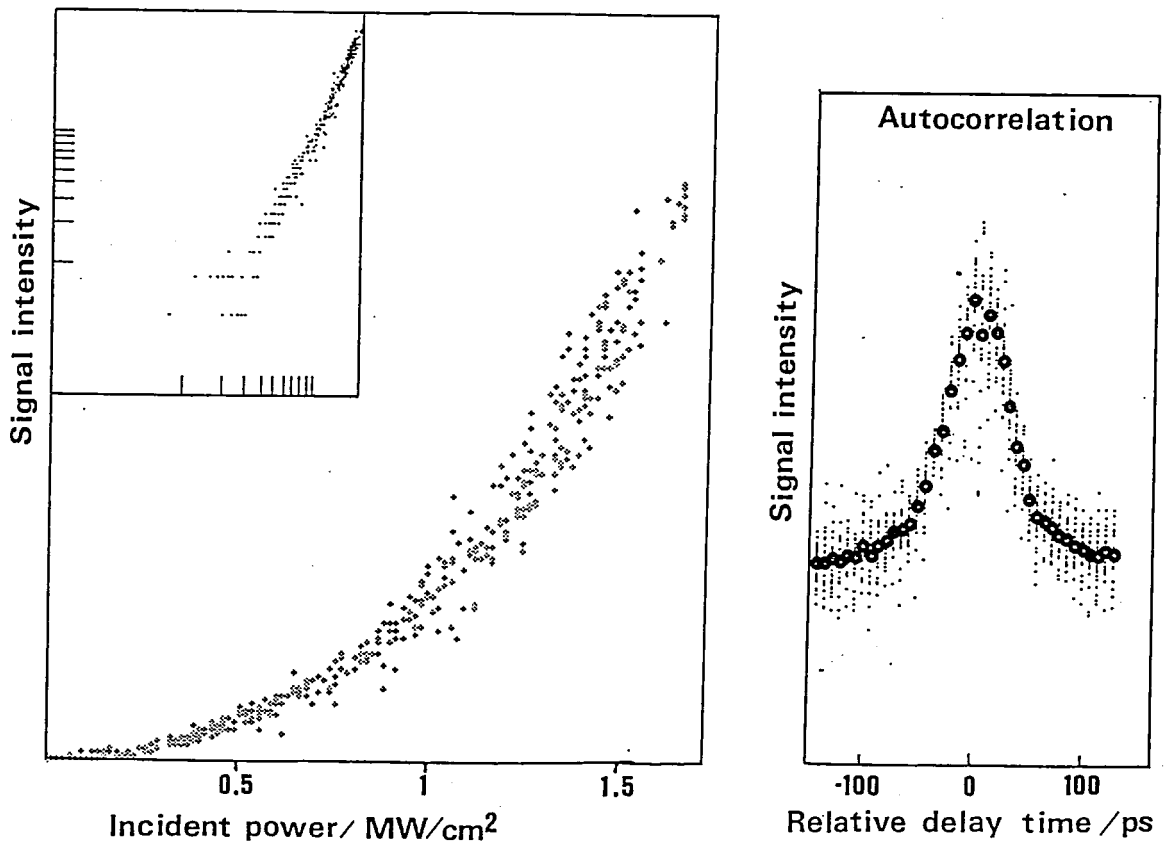

Figure 1. Input power dependence (left) and delay time dependence of a photocurrent of GaAsP photodiode.

VII-J Development of Experimental Devices

VII-J-1 Development of GP-IB Interface Using Logic Cell Array

Hisashi YOSHIDA, Kazuo HAYAKAWA, and Kouichi UCHIYAMA

Electronics development section has introduced a commercial LCA (Logic Cell Array) logic circuit development system that provides a great simplification and reliability in logic circuit boards by replacement of SSI/MSI devices with a single user-programmable LSI chip. The LCA, an array of 1,200 gates, controls three functions: I/O blocks, configurable logic blocks, and user-programmable interconnections. Using the LCA, we have developed an interface circuit to provide a GP-IB listener function to a printer. Figure 1 shows a block diagram of GP-IB listener interface. Components indicated by solid lines were designed internally in the LCA and broken lines show external devices. The listener consists of a decoder of the controller commands, a handshake control for accepting talker data, and another handshake control for data-transfer to the printer. Use of one LCA chip has reduced the number of TTL chips by a factor 15. Furthermore, reprogrammable characteristics of the LCA simplified debugging of the circuit.

As a result, the present work suggests that not only a simple replacement of TTLs with one LCA chip, but also somewhat large scale logic circuits can be well designed by the LCA. By using the LCA adequately, hereafter, we hope to increase efficiency of circuit designing as well as the reduction of the number of electric devices.

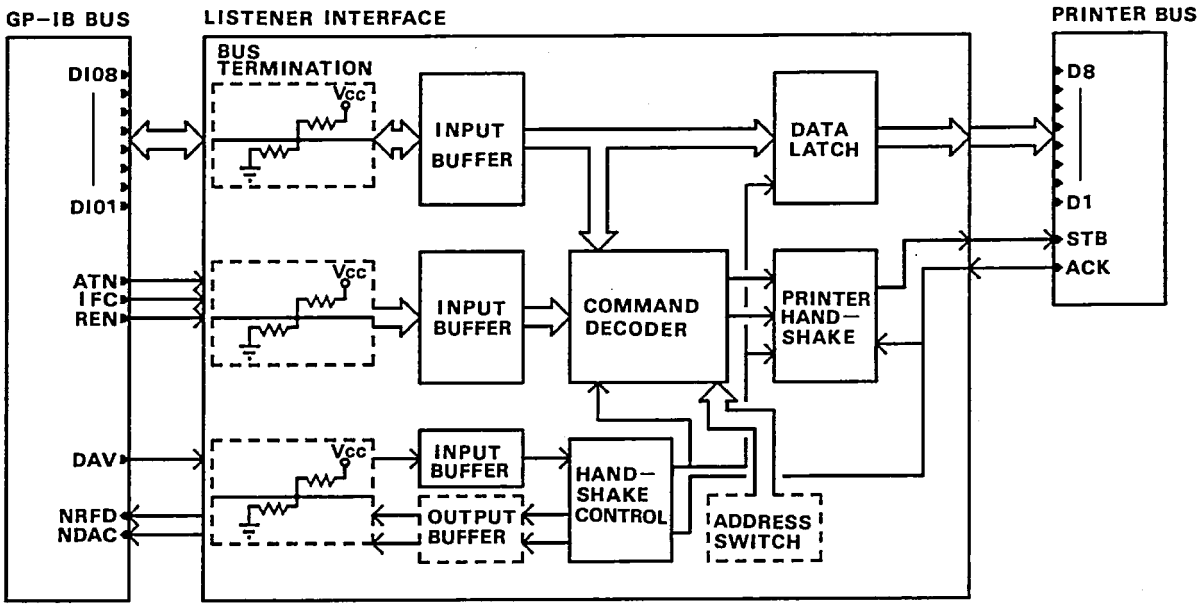

Figure 1. Block diagram of GP-IB listener interface.

VII-J-2 Construction of an IR Liquid Helium Cryostat

Norio OKADA and Toshio HORIGOME

A compact liq. He cryostat with CaF_2 optical windows has been constructed, which can be used at low temperatures below the λ point of Liq. He (ca. 2K) with a large optical aperture of ca. 60°, and in a wide spectral region from 150 nm to 10000 nm. Figure 1 (A) shows a cross section of a optical part of the cryostat, in which three types of CaF_2 window, a, b, and c are attached. The inside CaF_2 windows (a) are directly attached to a liquid helium reservoir. The technique of vacuum-sealing of CaF_2 windows at low temperatures has been reported in Ann. Rev. '88 in detail by authors. The CaF_2 windows (b) are settled on an radiation shield (d) which is thermally contacted to liq. N_2 reservoir. Due to experimental restrictions of size of cryostat, a content of the liquid helium reservoir was limited to ca. 800ml, which permits ca. 1.5 hour operation at low temperatures below 2K. Some improvements of the cryostat, e.g. suppression of heat leak from the Liq. He reservoir and extension of an applicable spectral region down to far IR frequency, are now in progress.

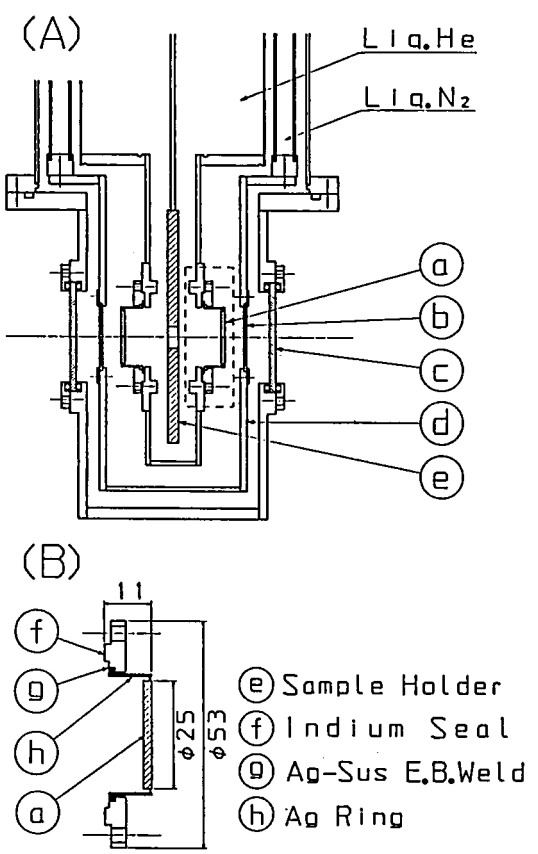

Figure 1. Cross sections of IR Liq. He cryostat; (A) a optical part of the cryostat and (B) an inner window (see text).

Ultraviolet Synchrotron Orbital Radiation Facility

VII-K Construction of UVSOR Light Source

VII-K-1 Increase in Impurity in Single Bunch Mode of UVSOR Storage Ring

Toshio KASUGA *(Hiroshima Univ.)*, **Hiroto YONEHARA, Masami HASUMOTO, and Toshio KINOSHITA**

The UVSOR storage ring is a synchrotron radiation light source and the pulsed light is supplied with the period of 11 ns for the researchers. Recently, the requests for single bunch mode operation have gradually increased. The impurity, that is the rate of electrons in buckets following the single bunch, is important in this mode. An impurity below 10^{-3} is currently required by the researchers, however, more stringent conditions will be required in the near future. We installed a photon counting system for the impurity measurement and found that the impurity increases gradually with the passage of time after the beam injection. This phenomenon is explained: Electrons thrown out of the bucket by the Touschek effect are captured in following buckets again by the radiation damping. The trajectory of the electron thrown out of the bucket in the longitudinal phase space is illustrated in Figure 1. The measured rate of the impurity increase is about two-thirds of the estimated value. Considering the errors in the measurements of the machine parameters (usually 20 %), the agreement between the measurement and the estimation is not so bad. To cure the impurity increase, a beam scraper system was installed at the non-zero dispersion section of the ring and completely suppresses the growth of the impurity in the single bunch mode.

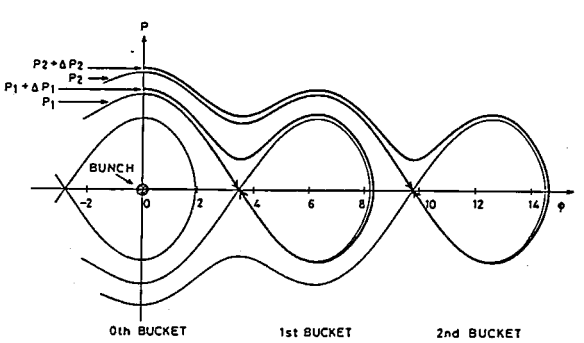

Figure 1. The trajectory of the electron thrown out of the bucket in the longitudinal phase space. An electron with momentum gain between p_1 and $p_1+\Delta p_1$ is captured by the bucket 1.

VII-K-2 Orbit Distortion due to UVSOR Wiggler

Hiroto YONEHARA, Toshio KASUGA *(Hiroshima Univ.)*, **Toshio KINOSHITA, and Masami HASUMOTO**

The critical wavelength of the UVSOR synchrotron radiation from the bending magnets at the beam energy of 600 MeV is 5.7 nm. In order to extend the coverage of the wavelength, a superconducting wiggler, which maximum magnetic field of the wiggler was decided to be 4 T to reach the critical wavelength of 2 nm, was installed in the ring in 1984. The insertion effect of the wiggler on the stored electron beam, is not negligibly small, therefore the tune values and the closed orbit distortion (COD) have to be compensated. The tune shifts due to the wiggler were measured and are in good agreement with the expected values which are obtained with the magnetic field measurement.

The closed orbit distortions due to the wiggler were measured at the wiggler field of 3 T and 3.9 T. The horizontal COD can be corrected by two auxiliary coils, which are placed at the both sides of the main coils, and the maximum displacement is less than 0.2 mm. To compensate the vertical COD due to the wiggler, a vertical steering magnet are placed at the downstream side of the wiggler. In lower excitation of the wiggler for example 3 T, the vertical COD can be compensated with the steering magnet. The COD at the field of 4 T, is not corrected perfectly with it. Two vertical steering magnets must be placed at the upstream and downstream sides of the wiggler to suppress the vertical COD in full range of the wiggler excitation.

VII-L Development of Equipments for UVSOR

VII-L-1 Radiometric Calibration System at BL5B

M. SAKURAI[a)], S. MORITA[a)], J. FUJITA[a)], H. YONEZU[a)], K. FUKUI, K. SAKAI, E. NAKAMURA, M. WATANABE, E. ISHIGURO[b)], and K. YAMASHITA[c)] *(a) Nat. Inst. for Fusion Sci., b) Osaka City Univ. and c) Osaka Univ.)*

At BL5B a new plane-grating monochromator (PGM) and calibration chamber were installed. It is used for the radiometric calibration of plasma diagnostic devices as well as optical components and detectors used therein. Figure 1 shows an experimental setup of the whole beamline. The PGM is designed to cover a wavelength range of 1.8–238 nm with the resolving power of 500 ± 200. Synchrotron radiation of 10 mrad (horizontal) × 3 mrad (vertical) is made parallel by two premirrors M_0 and M_1, and diffracted by one of the three gratings. Negative first order light is focused by one of seven mirrors (M_{20}-M_{26}) onto the exit slit S_2. Divergent light from S_2 is focused onto point Q by the toroidal mirror M_3. The gratings and focusing mirrors are interchangeable in vacuum. The calibration chamber contains a goniometer for the characterization of optical components, and is equipped with a four-stage differential pumping system which enables the measurement of absolute intensity of the beam by use of a windowless rare-gas ionization chamber. The pressure rise at the PGM due to a gas flow from the ionization chamber is suppressed by a factor of 10^{-4}.

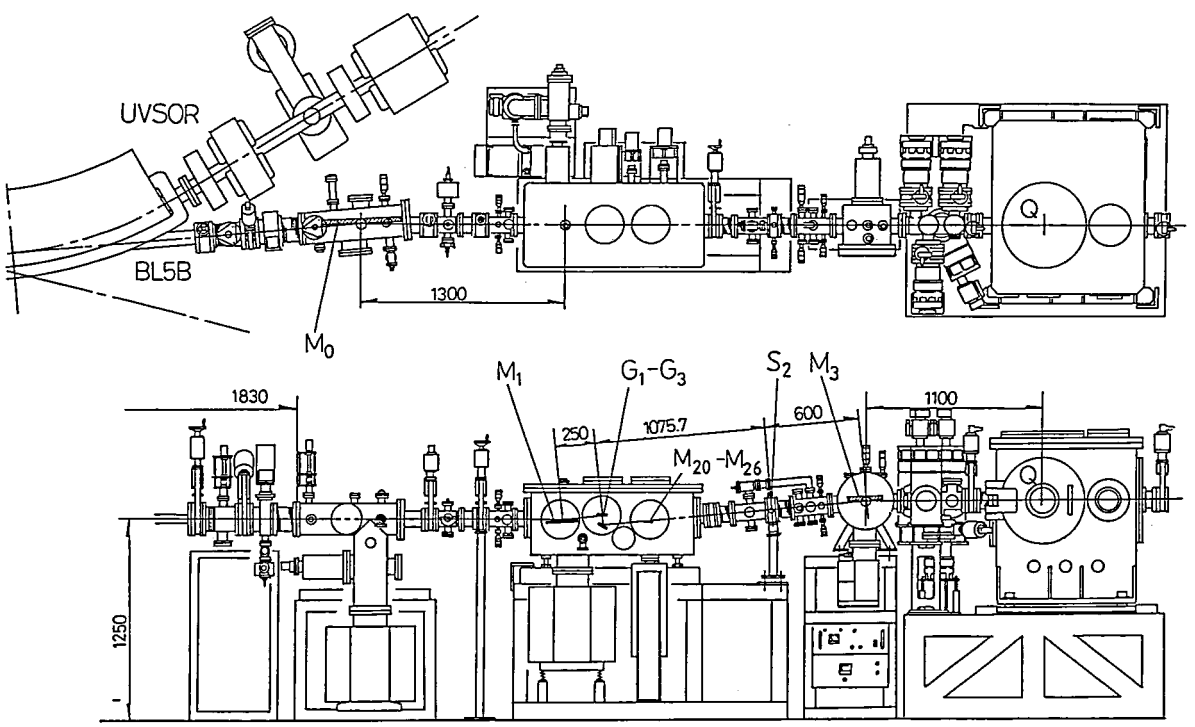

Figure 1. Schematic drawing of the PGM and calibration chamber at BL5B.

VII-M Researches by the Use of UVSOR

Researches of IMS staff other than UVSOR staff are reported at some other places in this issue. Details of all researches preformed by inside and outside users will be reported in UVSOR Activity Report 1989.

VII-M-1 K Absorption Spectrum of Solid Neon

Atsunari HIRAYA, Kazutoshi FUKUI, Poh-Kun TSENG *(National Taiwan Univ.)*, **Takatoshi MURATA** *(Kyoto Univ. of Education)*, **and Makoto WATANABE**

Absorption measurement was made on solid neon in the 850–1300 eV region at BL7A. The obtained spectrum is shown in Figure 1. The width of the first peak becomes broader (~1 eV) in solid neon, in comparison with that in gaseous neon (0.7 eV).[1] The separation between the first peak and the second peak in gaseous neon becomes small in solid neon (1.7 → 1.4 eV). The XANES structure of the solid neon above 880 eV seems to be due to the solid effect. The band calculation shows that the minimum of the conduction band in solid neon is Γ_1.[2] Therefore the transition from the 1s state to the minimum of the conduction band is forbidden. In the Na-K absorption spectrum of NaCl, a weak peak is observed at the lower energy side of the first peak, which is attributed to the forbidden transition from 1s to s-like conduction band (Γ_1).[3] However, in the solid neon, such a weak band could not be observed. The first peak seems to be due to excitonic peak associated with the transition to the p-like conduction band. A very weak EXAFS structure was observed above 980 eV. At present, the analysis of the EXAFS structure is under way.

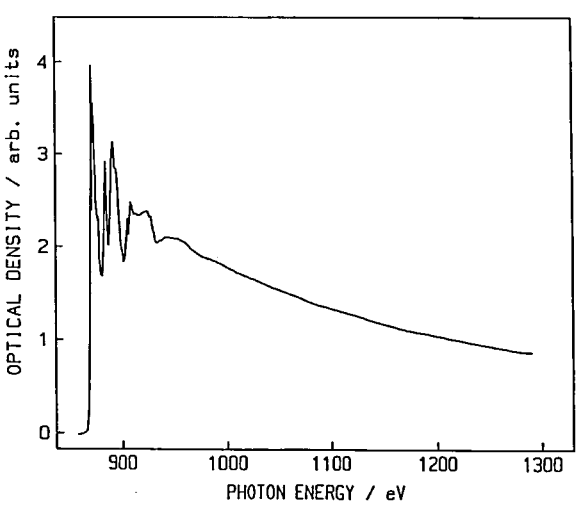

Figure 1. K absorption spectrum of solid neon.

References

1) F. Wuilleumier, *J. Phys, (Paris), Colloq. C4, Supp. 10*, **32**, 88 (1971).
2) A. B. Kunz and D. J. Mickish, *Phys. Rev. B* **8**, 779 (1973).
3) T. Murata, T. Matsukawa and S. Naoe, *Solid State Commun.* **66**, 787 (1988).

VII-M-2 Core Excitation in GeTe both in Amorphous and Crystalline Phases

Kazutoshi FUKUI, Tadaaki SAITO *(Fukui Univ.)*, **Shin-ichi KONDO** *(Fukui Univ.)*, **and Makoto WATANABE**

Crystalline group IV Tellurides (GeTe, SnTe and PbTe) are all semiconductor but their electric properties are metallic. On the other hand, as-deposit films evaporated on the substrates below critical temperature are amorphous and their electric properties are

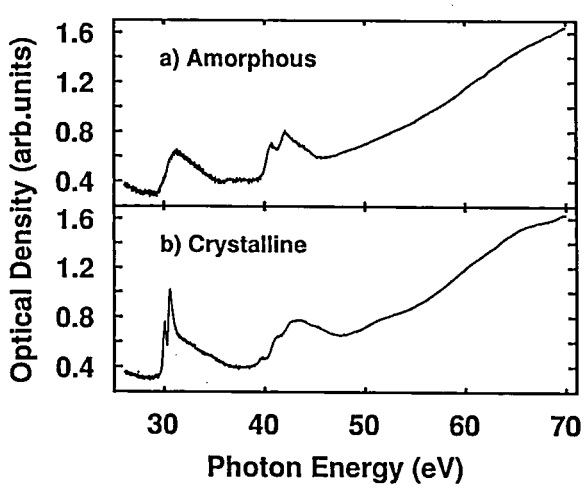

Figure 1. Absorption spectra of GeTe film at 80 K both in the amorphous and the crystalline phases.

insulator-like. Core absorptions from Ge 3d level and Te 4d level were studied for both phases. Figure 1 shows the absorption spectra of GeTe in both amorphous(a-) and crystalline(c-) phases in the energy region from 27 to 70 eV. The structures around 30 eV and 40 eV correspond to the transitions from Ge 3d level and Te 4d level to the conduction bands, respectively. The line shapes are different not only between a- and c-phases but also between initial Ge 3d level and Te 4d level. The sharp doublet peaks at around 30 eV in the c-phase due to the transition from Ge 3d levels are probably due to the excitonic transitions. We calculated the intensity ratio and the energy splitting of the peaks using atomic model with the intermediate coupling scheme. Calculation results are in agreement with experimental results. A small peak appears at about 40 eV after crystallization which is the lowest energy peak due to the transition from Te 4d level. A similar small peak was also observed in the case of SnTe. Since Fermi energy is located in the valence band (v.b.) in p-type degenerate semiconductor and the present SnTe and GeTe samples are p-type, states near the top of the v.b. are probably unoccupied. Therefore, the small peaks at 40 eV seems to be due to the transition from Te 4d core level to the top of the v.b. Similar experiments on PbTe are under way.

VII-M-3 Ionization Energies of Free Molecules and Molecular Solids

Kazuhiko SEKI *(Hiroshima Univ. and IMS)*

[*Mol. Cryst. Liq. Cryst.*, **171**, 255 (1989)]

Gas phase ionization energies I_g for compounds of interest from electrical and electronic viewpoints can be determined using photoemission techniques. Also reasonably good estimation can be obtained from oxidation potential and energy of charge-transfer absorption in solution. Photoemission techniques are also used for determining ionization energies of molecular solids I_s. These methods are reviewed, and a table of ionization energies for 120 compounds are given. The difference Δ between I_g and I_s can be ascribed to the polarization of surrounding molecules and, in some cases, intermolecular band formation. The trends in I_g, I_s, and Δ for various compounds are discussed. Finally, information from I_g and I_s is surveyed for the energetics of ionized states and the electronic structure of binary systems.

RESEARCH FACILITIES

For the sake of brevity the present issue includes only the newly installed facilities and the activities since September 1988. Concerning the activities and facilities before September 1988, please refer to older IMS Annual Review issues (1978～1988).

Computer Center

The main computers at the Center are a supercomputer HITAC S-820/80 and a general purpose computer HITAC M-680H. S-820, with a peak speed of 3 GFLOPS, has a 256 mega byte main memory and a 4 giga byte extended strage (solid state disk), while M-680H has a 128 mega byte main memory with a speed of about 14 MFLOPS. The disk memory has been expanded in June 1989 from 85 to 140 giga byte. In July 1989, the computers have been linked to the Japanese inter-university network, through which users can have access to them as well as through an existing commercial packet exchange network. The Center is equipped with a few workstations including a Silicon Graphics IRIS-4D/70GT. The Center also provides a BITNET service (nodename: JPNONRI) for in-house staff members via a VAX at NIBB.

The Computer Center has been supporting development, porting and improvement of computer programs for molecular science. About 200 programs are available for immediate execution. Recent additions include JAMOL4, KAMUY, HONDO7, PSI and CCP5.

Databases in molecular science are also available at the Computer Center. These include the Quantum Chemistry Literature Database (QCLDB), Carnegie-Mellon Quantum Chemistry Archive Index (CMQCA), Infrared Spectra Database (IR2), Steric Chemical Calculation Database (STERIC) and Quatum Chemistry Basis Function Database (QCBDB). QCLDB, which has been developed by the Center in collaboration with the QCDB Group and had in the past been distributed only to academic institutions on a trial basis, is now available to all the interested organizations throughout the world including industrial laboratories.

About 35% of the computer time is used by the research staff at IMS, and the remaining 65% is given out as research grants free of charge to scientists outside the Institutes in related fields. As of March 1989, the number of project group was 231, consisting of 652 users.

It is a great loss to the center that Prof. Hiroshi Kashiwagi, who had been the principal driving force of all our activities, moved to the Kyushu Institute of Technology in April 1989. Dr. kazuo Kitaura, formerly Research Associate at the Osaka City University after serving as JSPS Postdoctral Fellow and Research Associate at IMS, has been appointed in July 1989 as new Associate Professor at the Center.

Chemical Materials Center

The Chemical Materials Center plays an important role in the synthesis and purification of chemical substances in IMS. The scientists and technical associates of this facility support other people in IMS to carry out the above works. Upon request, technicians carry out elemental and mass spectrometric analyses of new compounds prepared at IMS. They also carry out their own researches on synthesis of new interesting compounds, developments of new selective chemical transformations, elucidation of reaction mechanisms, and application of new methodologies developed in IMS to the analysis of chemical substances and reactions. Parts of the scientific activities are presented in the Section VII.

Instrument Center

For the efficient use of instruments, the Center is equipped with various types of instruments for general use.[1] One instrument has been newly installed in 1989.

Scanning Electron Microscope (HITACHI S-900)
Surface image of organic, inorganic, and biological substances can be observed with a resolution of 0.7 nm. The system is composed of a computer-controlled electron optics, a field-emission type electron gun, a SE detector, and an EP-1040 image processors.

Research associate Naoto Tamai moved to Department of Chemical Process Engineering, Faculty of Engineering, Hokkaido University on October, 1988. Dr. Kiyokazu Fuke was appointed an associate professor as a new staff member of the center at November, 1988. In June, 1989, Mr. Fuminori Misaizu was also appointed a research associate as a new staff member of the center.

Reference
1) *List of Instruments*, No.7, *IMS Instrument Center* (1989).

Low Temperature Center

1. The new helium liquefier system has been completed in March, 1989. The newly installed machines in 1988 fiscal year are (1) a helium compressor (oil-cooling screw-type, 15.5 kg/cm^2), (2) a liquid helium reservoir (3,000 ℓ), (3) a delivery tube, (4) a transfer tube, (5) recovery and ballast tanks, (6) a helium gas recovery system (recovery manifold, dryer), and (7) utilities (water, air, electricity). Schematic arragement of the system is shown in the figure. The liquefying rate of the main liquefier is about 150 ℓ/h under internal purifying operation.

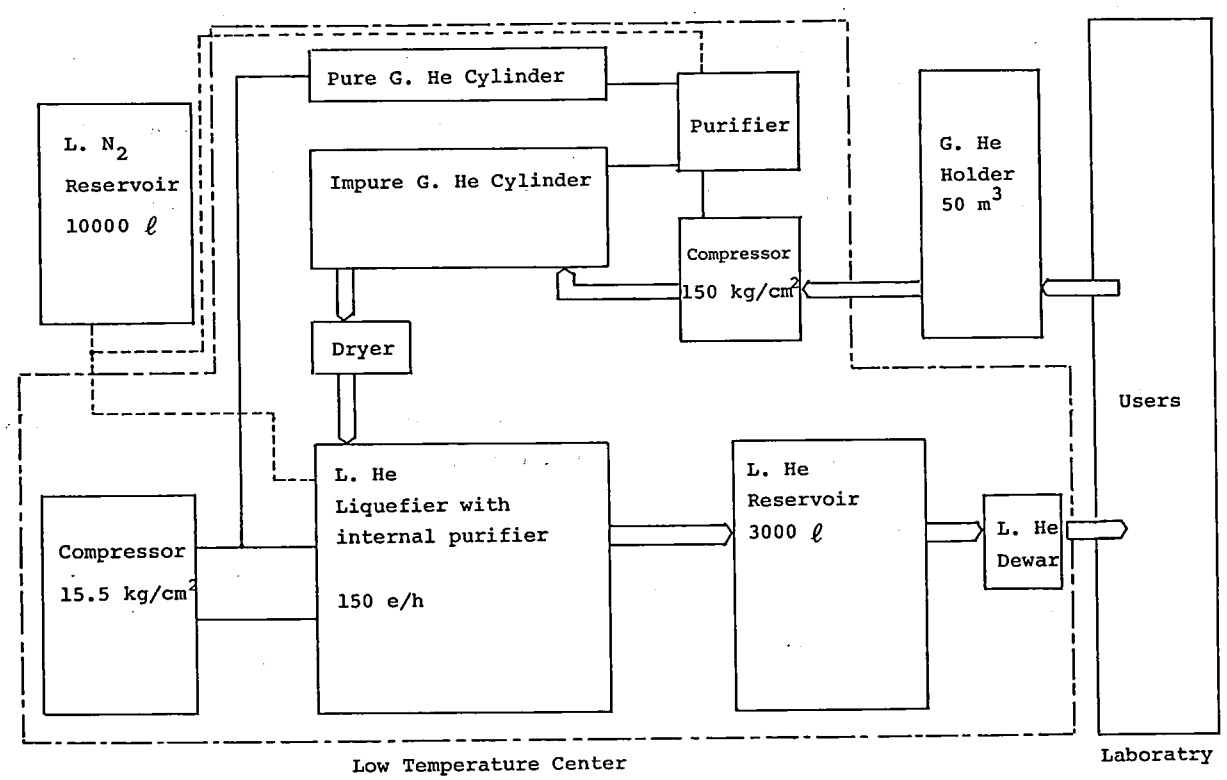

2. The supplied amount of liquid helium in 1988 was 18.242 ℓ in the same level as in 1987.

Equipment Development Center

A number of research instruments have been designed and constructed by making use of the mechanical, electric and glass-blowing technologies at this Facility. Representative instruments developed during this fiscal year of 1988 are listed below.

Specific Heat Cryostat.
Inner-Dewar of Superconducting Magnet.
Cryostat for Magnetization.
Threshold Electron Analyzer with Capillary Array Plate.
Ellipsoidal Mirror.
Supersonic Jet Apparatus for Cluster beam.
Flow Cell for Photoacoustic Spectroscopy.
Liq. He Cryostat for Electrical Conductivity.
Improvement of Magnetic Bottle Electron Spectrometer.
Faraday balance Jacking System.
IR Liq. He Cryostat.
Fast Signal Averager.
Video Image Degitizer.
Programmable Pulse Train Generator for NMR.
Transient Degitizer.
High Precision Gauss Meter.
MCS for Pseude-Random Chopper.
Molecular Beam Valve Controller.
Jet Nozzles for Dye Laser.
Capillary for Raman Scattering.

Ultraviolet Synchrotron Orbital Radiation Facility

The UVSOR light source is usually operated at an electron energy of 750 MeV with an initial current of 120 mA. Single bunch operation has been performed with a frequency of 1 week per 2 months. An RF cavity and a wiggler used so far had been replaced by new ones. A new beam line, BL4A has served as a irradiation port for photo-catalysis experiments. The Activity Report 1988 has been published in this April.

SPECIAL RESEARCH PROJECTS

IMS has special research projects supported by national funds. Three projects presently in progress are:

(1) Development and evaluation of molecular synergistic systems and their application to chemical energy conversion (1985–1990).

(2) Fundamental research of molecular devices (1985–1990).

(3) Molecular science of primordial chemical evolution and selforganization (1987–1991).

These projects are being carried out with close collaboration between research divisions and facilities. Collaborators from outside also make important contributions. Research fellows join these projects. The results in 1988 are reviewed in this report.

(1) Development and Evaluation of Molecular Synergistic Systems and their Application to Chemical Energy Conversion

Dynamical Molecular Structure and Control of Reactive Molecules

Eizi HIROTA*, Chikashi YAMADA, Yasuki ENDO *(Univ. Tokyo and IMS)*, **Kentarou KAWAGUCHI, Hideto KANAMORI, Masaharu FUJITAKE, Haruhiko ITO, Eberhard TIEMANN** *(Univ. Hannover and IMS)*, **Edward A. COHEN** *(Jet Propulsion Lab. and IMS)*, **and Toshinori SUZUKI**

Microwave kinetic spectroscopy was combined with the 193 nm photolysis of SO_2 to investigate $O(^3P)$ + C_2H_4 or C_3H_6, the former being previously studied by generating $O(^3P)$ with Hg-sensitization (II-A-15). Infrared diode laser kinetic spectroscopy was employed to unveil the mechanisms of $O(^1D)$ + CH_4 (II-A-12) and $O(^1D)$ + SiH_4 (II-A-16), where $O(^1D)$ was generated by the 193 nm photolysis of N_2O and OH and CH_3 or SiH_3 were monitored. Infrared kinetic spectroscopy was also employed to generate C_2H_3 (II-A-3), C_3 (II-A-4), SiH_2 (II-A-5), and SCl (II-A-7).

A laser induced fluorescence spectrometer was constructed to study simple reactive molecules and also more complicated free radicals cooled in the molecular beam (II-B-1).

Studies on Structure and Dynamical Processes of Highly Excited Atoms and Molecules

Norio MORITA, Toshifumi SUZUKI, and Mitsutaka KUMAKURA

The observation of high-lying doubly excited states of Ca atoms has been continued. In addition to the *msns* $^1S^e$ and *mdns* $^1D^e$ ($m \leq n$) doubly excited states observed in the previous studies, many resonances of the *msnd* $^1D^e$ ($m \leq n$) and *mdnd* $^1D^e$, $^1G^e$ states have successfully been observed. The quantum defects and the electron correlation effects of those states have been studied in comparison with the previously observed states.

The R-matrix calculation as well as the large-scale CI-calculation have also been executed successfully to reproduce the spectra of the doubly excited states so far observed. The behavior of the electron correlation has been investigated extensively by drawing charge density plots. Some quite unusual angular-correlation patterns have been observed and discussed from a viewpoint of configuration-mixing.

Finally, it has been tried to observe two-photon resonances of highly excited states (~700Å) of some rare-gas dimers by using a coherent VUV source so far constructed. This trial, however, has not been successful yet.

Construction of Small Angle X-ray Scattering System

Hisashi HAYASHI, Kazuyuki TOHJI, and Yasuo UDAGAWA

Small angle x-ray scattering is a valuable tool to obtain structural information about non-crystalline materials including liquids and amorphous solids. A new system for small angle x-ray scattering, whose schematics is shown in Fig. 1, is now being constructed. It features the following;

1. A use of a rotating anode x-ray generator with a point focus target
2. A use of a doubly bent LiF(200) crystal to monochromatize and to focus Cu $K\alpha_1$ radiation
3. Long focal length (70cm) to completely reject $K\alpha_2$ radiation
4. PSPC (position sensitive proportional counter) for an effective collection of data

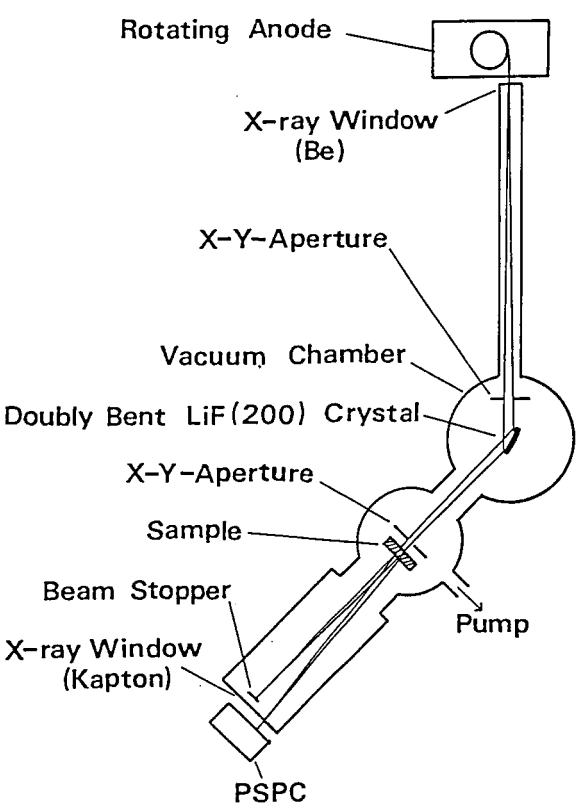

Figure 1. A schematic diagram of the small angle x-ray scattering system.

Construction of a Femtosecond Dye Laser System for Studies on Ultrafast Phenomena

Hiromi OKAMOTO, Yoshihiro TAKAGI, and Keitaro YOSHIHARA

A laser system for studies on ultrafast phenomena in femtosecond time scale has been constructed. The time scale corresponds to the period of molecular vibration and is an ultimate one for chemistry as a molecules is vibrating entity. A system with two dye lasers was constructed for the studies on coherent anti-Stokes Raman (CARS) spectroscopy. A home-made CW mode-locked YAG laser [average power > 1 W at 532 nm, pluse with 70 ps, and repetition rate 81 MHz] excites two dye lasers. The first dye laser is hybridly mode-locked with linear cavity configuration and produces ultrashort light pulses with width as short as 80 fs at 585 nm, for example. The second dye laser produces ordinary picosecond pulses of ca. 10 ps and tunable between 600 and 700 nm. The first laser pulse which is split into two halves, serves as ω_1 and ω_3 and the second one as ω_2 in CARS. The light with ω_3 is delayed relative to that with ω_1 and CARS signal is recorded as a function of the delay time. The system has been applied to CARS of neat benzene for non-resonant condition, of β-carotene for pre-resonance condition, and of cyanine dyes for rigorous resonance condition. The details are described in III-C-1, 2, and 3.

Effect of Water Vapor on the Energy-Gap Dependence of the Electron Transfer from Rhodamine B to Semiconductors

Kazuhito HASHIMOTO and Tadayoshi SAKATA

We reported the new energy-gap (ΔE) dependence of the photo-induced electron transfer (ET) *in vacuo* from adsorbed dye to oxide semiconductors (SC). ΔE was defined as the energy difference between oxidation potential of the excited state dye and flat-band potential of SC. It was found that the ET rate *in vacuo* is proportional to the state density of the conduction band of SC. Here the effect of solvent molecule on the energy-gap dependence of the ET was studied; water vapor was introduced into the systems, in which rhodamine B is adsorbed on various oxide SC, resulting

the formation of water drop on the SC surfaces. In most cases, the ET rate became slower by the introduction of water vapor. However, the ratio of the ET rates in the absence (K_{et}(vac)) and in the presence of water (k_{et}(wet)) decreased by increasing ΔE. This is shown in Figure 1. As we reported previously, the ET rate from molecule to SC is expressed as

$$k_{et} = (2\pi/\hbar)V(R)^2\int\rho(E)D_-(E)dE \qquad (1).$$

Here, $\rho(E)$ and $D_-(E)$ represent the state density of the conduction band of the SC and the distribution function of electron in the excited state dye, respectively. By using above equation, the ratio of (k_{et}(vac)) and (k_{et}(wet)) was numerically calculated to fit the experimental data. Here the energy gap, ΔE, and reorganization energy were the parameters. The best fit curve was shown in the figure. This indicates that energy gap does not change by water but reorganization energy increases from 0.3 eV to 0.43 eV.

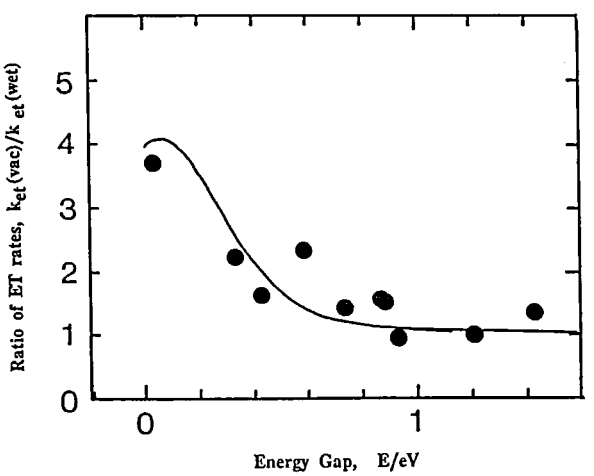

Figure 1. The ratio of the electron transfer rates in the absence and presence of water as a function of energy gap. Solid line represents the theoretical curve calculated using eq. 1.

External Magnetic Field Effects upon Chemical Reactions

Haruo ABE *(Inst. of Phys. Chem. Res. and IMS)*, **Ryoichi NAKAGAKI, Minoru SUMITANI, and Saburo NAGAKURA**

In the present research project, we have investigated magnetic field effects on photo-redox reactions involving biradical reaction intermediates for a series of bichromophoric chain species. Since extremely small interactions such as the Zeeman energy and hyperfine interaction may give rise to a remarkable change in the product distribution, the magnetic field effects have some potential for application, *e.g.*, control of reaction yields or selection of reaction pathways. The relative yield of the escape to the cage process, Φ(escape)/Φ(cage), is appreciably varied by an external magnetic field (0.6 T) in the case of 4-O_2N-$C_{10}H_6$-1-O$(CH_2)_8$-NHC_6H_5.

We have also observed a conspicuous magnetic field effects upon the emission intensity of NO in the $B^2\Pi_r$ excited state, which is populated through collisions between N and O atoms generated by microwave discharge.

Dynamics of Ion-Molecule Reactions

Shinzo SUZUKI , Takashi IMAMURA, and Inosuke KOYANO

The TESICO technique (see IV-E) has been applied to the reactions of the type $MH^+ + MH \rightarrow MH_2^+ + M$H, for which two direct-type reaction mechanisms, *i.e.*, proton transfer and hydrogen atom abstraction, generally exist. The technique is capable of distinguishing these two mechanisms utilizing the difference in the time-of-flight between the MH_2^+ ions produced by proton transfer and those produced by hydrogen atom abstraction. The reactions studied in detail during the last year include $CH_4^+ + CH_4 \rightarrow CH_5^+ + CH_3$, $CH_3Cl^+ + CH_3Cl \rightarrow CH_4Cl^+ + CH_2Cl$, $CH_3F^+ + CH_3F \rightarrow CH_4F^+ + CH_2F$ (IV-E-1), and $D_2^+ + D_2 \rightarrow D_3^+ + D$ (IV-E-2). The relative cross sections have been determined for each microscopic reaction mechanisms as a function of internal and collision energy of reactants.

In order to probe transition states in ion-molecule reactions, various photo-induced processes are being investigated (IV-F). Collisional deactivation of photo-excited $CO^+ A^2\Pi$ ions has been studied with the aim of observing laser absorption by or emission from colliding ion-molecule pairs (IV-F-1).

Excited-State Photoelectron Spectroscopy for Studying Photophysical and Photochemical Behaviors of Molecules and van der Waals Complexes

Katsumi KIMURA, Katsuhiko OKUYAMA, Masatoshi TAKAHASHI, and Hiroyuki OZEKI

Excited-state photoelectron spectroscopy combining a UV/visible pulse laser technique and a supersonic molecular beam technique has been developed in this Institute since 1980 (IMS Annual Review, 1980–88). The method which is often called "MPI or REMPI photoelectron spectroscopy" has made it possible to study dynamic behavior of excited-state species which include nonradiative electronic states. Photoelectron spectra originating from various molecular excited states have been investigated from photophysical and photochemical points of view. The information deduced from excited-state photoelectron spectra have been found to be unique and important.

In this project, with this technique we have being studying not only single molecules but also van der Waals molecules (or molecular clusters) produced in supersonic jet, and we have demonstrated some typical applications in the following several subjects: (1) ionization selectivity, (2) autoionization, (3) intramolecular vibrational redistribution, (4) photodissociation, and (5) excited states of van der Waals molecules (see IV-J).

Synthesis and Properties of New Types of Transition Metal Cluster Compounds

Kiyoshi ISOBE, Yoshiki OZAWA, and Yoshihito HAYASHI

Research in the area of the cluster compounds has showed us their beautiful gigantic molecular structures and unique chemical properties due to multimetal center frameworks. Still in many cases, formation of a particular framework of cluster is fortuitous in nature. We have recently shown that some rational control of charge, steric factors and the number of the available coordination site on organometallic groups and oxometalates gives integrated cubane types of clusters having three-dimensional framework of mixed-metals and mixed-valence centers.

We have applied this potential method to the control of the framework architecture in sulfide cluster compounds, and have found novel clusters, $[(IrCp^*)WO(\mu\text{-}S)_2(S_2)]_2$(**1**), $[(RhCp^*)_3W_2O(\mu_3\text{-}S)_3(\mu_3\text{-}S_2)(\mu\text{-}S)_2(S_4)]$ (**2**). X-ray analysis of these clusters revealed that cluster **1** has an incomplete double cubic framework and cluster **2** has a single cubic framework with a variety of coordination modes of sulfur ligands.

Construction of a Molecular Beam Apparatus for the Research of Solvated Metal Clusters

Kiyokazu FUKE and Fuminori MISAIZU

Metal ions are intimately involved in chemistry and biochemistry and play a crucial role in many reactions. Although there has been extensive progress in the thermodynamic and kinetic studies of solvated metal ions, the study of microscopic aspect of solvation dynamics has been rather limited. Spectroscopic studies of the solvated metal ion clusters as a specific function of cluster size can provide detailed information on energetic and dynamics of solvation and can play an important role in elucidating the transition between the

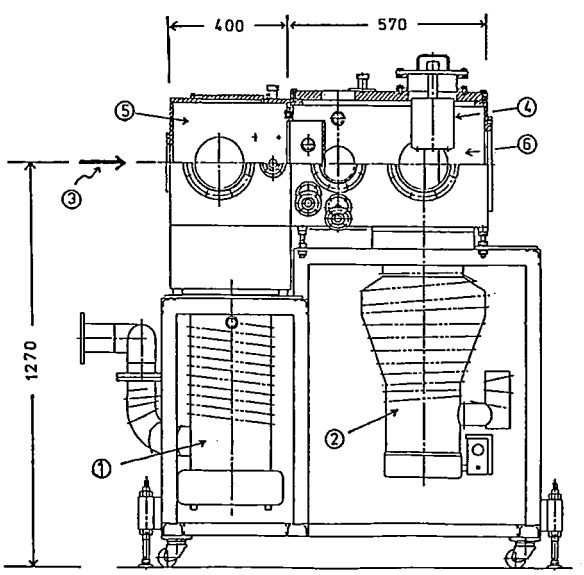

Figure 1. A schematic side view of a molecular beam apparatus.
1. two 10″ diffusion pumps, 2. "diffstak" (2000 l/s), 3. molecular beam axis, 4. liq. N_2 trap, 5. beam source chamber, 6. main chamber.

gas and condensed states. The advent of mass spectrometer and metal cluster beam techniques in conjunction with laser probes now allow an attack on the problem for the solvation of metal atoms and clusters through studies that probe energy levels and dynamical processes occurring in solvated metal clusters.

In order to investigate the solvation dynamics of metal clusters, we are constructing a molecular beam apparatus (shown in Figure 1) in collaboration with the Equipment Development Center of IMS. We adopt a recently developed laser vaporization technique to produce metal clusters. The system is still being developed and the performances will be reported in a near future.

(2) Fundamental Research of Molecular Devices

Study of Molecular Fastener

Hiroo INOKUCHI

We are studying novel single component organic semiconductors. In this study, we apply a new strategy for the fabrication of molecular assemblies in such a fashion that organic π-molecules can pile up one upon after another so tight that the system shows a high conductivity. Thus, we found that alkylchalcogeno-substituted tetrathiafulvalenes show a fairly high electrical conductivity and also high electron mobility. The cause of these high conduction is as follows; the central skeleton has been "fastened" together strongly with the four long alkyl chains. We call this type of organic semiconductor by the name, molecular fastener. In these series, we also found a new organic semiconductor, tetrakis(methyltelluro)tetrathiafulvalene ($TTeC_1$-TTF), of electrical resistivity 8.1×10^4 Ωcm having high charge mobility, 20 - 30 $cm^2C^{-1}S^{-1}$.

Resonance Raman Study on Vectorial Proton Transfer by Bacteriorhodopsin

Teizo KITAGAWA, Masashi NAKAGAWA, Takashi OGURA and Akio MAEDA *(Kyoto Univ.)*

Bacteriorhodopsin (BR) is a retinoid protein found in the purple membrane of a light-harvesting bacterium, *H. halobium*. This protein transforms light energy into electrochemical energy by transporting protons across the membrane. The proton transfer is vectorial. Light-adapted BR_{568} has all-*trans* retinal bound to Lys-216 via a protonated Schiff base and upon absorbing light it undergoes a cyclic reaction involving the *trans* to *cis* isomerization at $C_{13}=C_{14}$ bond and subsequent deprotonation of the Schiff base; $BR_{568} \rightarrow K_{590} \rightarrow L_{550} \rightarrow M_{412} \rightarrow N \rightarrow O_{640} \rightarrow BR_{568}$. Ejection of protons from the membrane to the outside takes place at a rate comparable to that for the formation of M_{412} and the uptake of protons occurs in the decaying process of M_{412}. In order to elucidate the gating mechanism of the proton translocation, we have investigated transient resonance Raman spectra of L_{550} and M_{412} in a time range of 15 to 1200 μs by using a double-beam flow apparatus. We noticed the presence of a very fast decaying M_{412} at alkaline pH (τ=0.39 ms) in addition to the reported ms decaying component. This species did not give the N intermediate. The efficiency for the practical photoreaction appeared 1.6 times higher at pH 10.5 than at pH 7.0 and the increment was ascribed to generation of the very fast M_{412}. On the other hand, we demonstrated that the L′ species found in the spinning cell experiment at alkaline pH was the same as that of N intermediate. We also examined transient Raman spectra of lysine-acetylated BR.

Fabrication of Novel Organic Molecular Assemblies with the Use of the Molecular Beam Epitaxy Technique

Yusei MARUYAMA, Hajime HOSHI, Anthony John DANN *(Univ. of Nottingham and IMS)*, **and Tamotsu INABE**

In order to prepare new materials which could be useful for molecular devices elements, we have started to design and fabricate ultra-thin organic multi-layered systems. After the trial for TCNQ and TTF-TCNQ films, we are now preparing ultra-thin μ-bridged (-F-) metallo (Al) phthalocyanine polymer mono-films on several kinds of substrates. Fairly well oriented, uni-or bi-directionally, crystalline films are obtainable on the alkali halide substrates. Based on this kind of mono-film, we are going to fabricate a multi-layered system.

Besides the conventional MBE evaporation, highly-regulated deposition with the use of a high power laser and high electric field will be challenged to fabricate more highly-oriented thin films.

Fabrication of High T_c Metal Oxide-Superconducting Films by Layer-by-Layer Deposition from Multi-Electron-Beam-Gun Sources

Yusei MARUYAMA, Toshifumi TERUI, and R. J. FLEMING *(Monash Univ, and IMS)*

Successive deposition of each component of metal

oxides has been undertaken to achieve the layer-by-layer construction for high T_c oxide superconductors. The high vacuum evaporation machine is equiped with three electron-beam guns and it can be operated under a differential pumping when oxygen inclusion is required. As an initial trial, La-Sr-Cu-O system is now investigated.

Coupled Proton and Electron Transfer in the Crystals of Salicylideneaniline Derivatives and their Complexes

Tamotsu INABE, Isabelle GAUTIER-LUNEAU, Naomi HOSHINO *(Hokkaido Univ.)*, **Kaoru OKANIWA, Hiroshi OKAMOTO, Tadaoki MITANI, and Yusei MARUYAMA**

Our interest in this particular area of research on molecular devices lies in the possibility of furnishing molecular assemblies with novel physical properties through an appropriate modification of the constituent molecules. Proton-transfer process was chosen as the molecule-based function, and its coupling to the assemble-based properties has been investigated. A framework of salicylideneaniline has such a function of intramolecular proton transfer. The thermochromic behavior observed in many of the derivatives gives a clue for changes in the π-electron state accompanying the proton transfer. Thus, the work has been devoted to the crystal structure determination at varied temperature and elucidation of possible cooperation in proton- and electron-transfer processes in the crystal of these compounds by means of optical measurements. Since the assembly-based properties depend largely on the intermolecular interaction, some derivatives have been employed as a donor component of the charge-transfer complexes with various acceptors in order to introduce stronger intermolecular interaction. The structural and optical studies of the complexes have provided the information about the correlation between the proton motion and the electronic state, which suggests possibilities of constructing a novel type of electrical conductors.

Similarly, the structures and the optical and electrical properties of some charge-transfer complexes with intermolecular hydrogen-bonds have been studied. Details of the work are given in Section IV-Q.

High Temperature Oxide Superconductors

Masatoshi SATO, Masafumi SERA, Masashige ONODA, Shin-ichi SHAMOTO, Kenji FUKUDA, Shinji KONDOH, Yoshiyasu ANDO and Shin-ichi YAMAGATA

Based on our experimental results taken at the very beginning of the study on high-T_c oxides, we had an idea that the BCS's mean field theory would still be valid to describe the high temperature superconductivity and it seemed to be quite tough task to get the key information to extract the essential distinction of the properties between usual superconductors and high-T_c oxides. Therefore, continuous effort has been made to accumulate various kinds of experimental results on the detailed properties of the high-T_c oxides by applying various experimental methods such as transport, thermal, magnetic, optical and neutron scattering measurements. In each experiment, samples which were most suitable for its purpose(s) were selected among the sintered pellets and the single crystals, which were prepared and well charaterized here. As a result of these studies, the electronic natures and the characteristic behaviors have essentially been, at least experimentally, understood. Our recent studies seem to have revealed certain difference of the superconducting properties between usual superconductors and the high -T_c oxides and we feel it is an important future step for the understanding on the mechanism of the superconductivity to carry the detailed and careful experimental studies on the superconducting properties of the high -T_c oxides. No distinction can be made between our usual activities and the special research project. Therefore please refer Research Activities IV-U.

Research of Phenomena associated with the Electron-Proton Interaction in H-bonded Molecular Crystals

Tadaoki MITANI and Hiroshi OKAMOTO

The dynamics of interacting protons in H-bonded systems has been the subject of prolonged interest. Particularly, the motion of protons in H-bonded charge-transfer (CT) complexes has attracted much attentions due to the presence of strong cooperation of

electron and proton transfer in the CT processes between D-A molecules.

In the present project, (i) quinhydrone, (ii) N-salicylideneaniline, and (iii) halogen-bridged mixed-valence Pt-complex have been chosen as a starting material for design and creation of a new molecular function associated with the electron-proton cooperation. By chemical modifications of these complexes, unusual behaviors have been revealed in semiconducting transport, optical and magnetic properties.[1] In addition, it is worth to note that the Peirls distortion has been completely suppressed for the first time in the series of the (iii) complexes by introducing strong interchain H-bondings (see VII-H-2). The electric and optical properties of this phase are now in investigation.

Reference

1) T. Mitani, Mol. Cryst. Liq. Cryst. **171,** 343 (1989).

Study of Ultrafine Particles

Keisaku KIMURA and Shunji BANDOW

Small particles are produced by the gas evaporation method and by the sputtering method conbined with a solution trap giving a dispersion in organic liquids. The ratio of the number of atoms at surface to the total atoms in nm particles exceeds 50 % resulting in the enhanced surface effects. We have observed that the NMR line width of ionic crystals of AlF_3 sample was split lines. The smaller the particles, the lower field the chemical shift position becomes. This finding meets the fact that the chemical bonding of ultrafine particles are somewhat covalent and was susbstantiated by the X-ray photoelectron spectroscopic observation. The sputtering method gave many kinds of ultrafine particles with high melting points.

Ferromagnetism in Organic Molecular Solids

Kunio AWAGA and Yusei MARUYAMA

The study of ferromagnetic interaction in organic molecular solids is basically important to develope organic ferromagnets. We have chosen single crystal systems of organic radicals in which the ferromagnetic interaction is involved and of which structure can be well defined.

Details of the work are described in VII-G section.

(3) Molecular Science of Primordial Chemical Evolution

Uncatalyzed Chemical Oscillations during Oxidation of Rhodamine B Base / Rhodamine B with Acidic Bromate

Prem. K. SRIVASTAVA, Yoshihito MORI and Ichiro HANAZAKI

Uncatalyzed temporal chemical oscillations have been investigated in laser dyes, Rhodamine B Base and Rhodamine B in oxidation with acidic bromate in a batch reactor. These oscillations occur in a concentration range of dyes, bromate and sulfuric acid. The induction time, time period, life time and number of oscillations were found to be sensitive to the initial conditions. These oscillation can be monitored by platinum redox or with bromide-ion sensitive electrode. Typical results are shown in Figure 1. Two optically dectactable intermediates were found by the absorption spectrum measurement of oscillating reaction mixture, out of which the band appearing at 518 nm increased and then decreased its intensity. However the other at 350 nm appeared instantaneously after the addition of bromate and its intensity decreased during a course of reaction. Although these intermediates were not oscillating, its appearance coincided with oscillating period, suggesting these intermediates to have a close relationship with mechanistic features of the temporal oscillation.

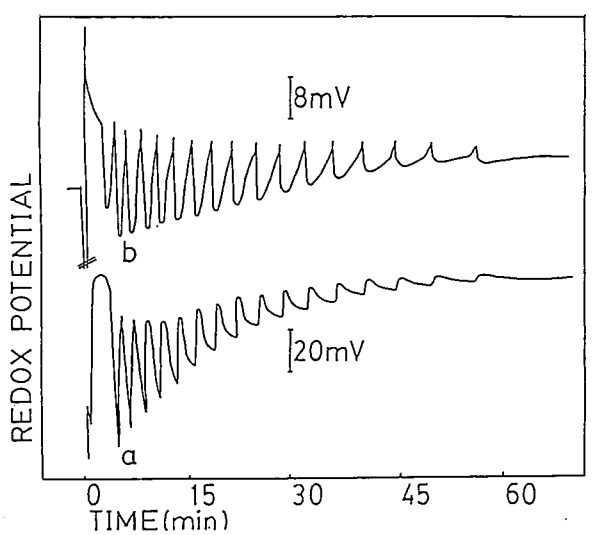

Figure 1. Uncatalysed chemical oscillation for Rhodamine B Base at 25°C ± 0.1°C: Rhodamine B Base (2.87×10^{-3}M), BrO_3^- (2.65×10^{-2}M) and H_2SO_4 (1.5M). The time scale is measured from the time of addition of the BrO_3^- solution.
(a) platinum electrode
(b) Ag/AgBr electrode

A Dual Frequency Oscillator: *o*-Hydroxyacetophenone - Ce^{+4} - BrO_3^- - H_2SO_4 System

Prem. K. SRIVASTAVA, Yoshihito MORI and Ichiro HANAZAKI

The experimental behavior of cerium-catalyzed Belousov-Zhabotinskii oscillating chemical reaction with *o*-hydroxyacetophenone (OHAP) as organic substrate has been investigated in batch and continuously stirred tank reactors. Under certain conditions, the system displays two types of temporal oscillation in a batch reactor which are characterized as high and low frequency oscillations. These oscillations can be recorded by platinum redox or bromide-ion sensitive

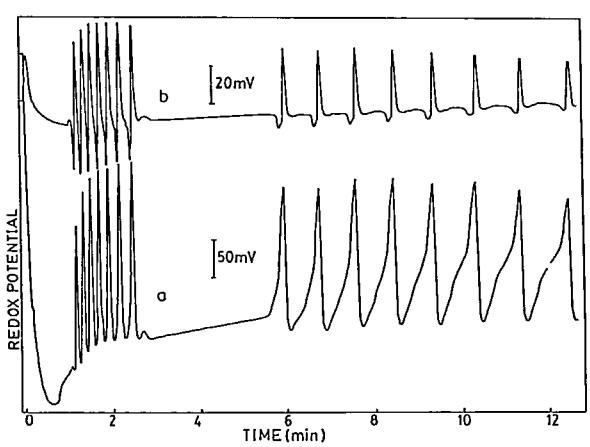

Figure 1. Dual frequency oscillations in batch reactor for the reaction mixture containing OHAP(0.0139M), BrO_3^-(0.035M), Ce^{+4}(0.0005M), H_2SO_4(2.5M) and at 25°C ± 0.1°C.
The time scale is measured from the time of addition of the BrO_3^- solution.
(a) Platinum electrode
(b) Ag/AgBr electrode

electrodes. The high frequency oscillation appears after a short time of induction upon the addition of sodium bromate. Subsequently the system comes to a non-oscillatory regime. The system then bifurcates to the low frequency oscillating regime, where the period of oscillation increases with time and bifurcates finally to a stable branch once again. Typical results are shown in Figure 1. It was observed that the higher-frequency oscillation disappeared first, and then the lower-frequency oscillation appeared when the OHAP concentration approached its higher limit, whereas to the lower limits, the lower-frequency oscillation disappeared first.

Self-association and Self-organization of Alkyl Carboxylic Acids and Alcohols in Aqueous Solution in the Presence of Ions

Nobuyuki NISHI and Kazunori YAMAMOTO

Due to the second law of the thermodynamics, most of solute molecular species are never mixed homogeneously with the solvent molecules in the course of temperature change. Despite of the increasing entropy in binary solutions, quite ordered structures of molecular associates were found in the various binary or ternary aqueous solutions. Just the distribution of the size of the associates became increasingly broader, and the molecular compositional variation was also increasing. Through the project of this year, we studied these three subjects: 1) effect of ionic species on the association of alkyl carboxylic acids in relation to lipid bilayer membrane formation, 2) origin of self association of alkyl carboxylic acids in aqueous solution, and 3) generation of macroscopic ordered structure in various alcohol-water binary systems due to large cluster formation. We analyzed the molecular composition of liquid fragments isolated as molecular clusters by adiabatic expansion of liquid jets in vacuum. In the first subject, we found that, since ionic species such as amino acids attract solvent water molecules strongly, the addition of small amount of amino acids to the solution of alkyl carboxylic acid accelerated the mutual association of alkyl compounds. This is due to the breaking of hydrophobic hydration networks around the alkyl groups and also related to the "salting-out"phenomenon of non-electrolyte compounds. The mechanism of formation and evolution of solute complexes is now under investigation at molecular level.

OKAZAKI CONFERENCES

"Okazaki Conferences" are principal symposia at IMS, which are held on the subjects related to the "Special Research Projects". They are held two or three times a year, with a moderate number of participants around 50, including several invited foreign speakers. The formal language for the conference is English. Outlines of the thirty-second to thirty-fifth conferences are as follows.

The Thirty-second Okazaki Conference

Theoretical Chemistry of Excited Molecules
(September 27–29, 1988)

Organizers: T. FUENO *(Osaka Univ.)* **and K. MOROKUMA** *(IMS)*
Invited Speakers: R.J. BUENKER *(Univ. Wuppertal)*, **S. R. LANGHOFF** *(NASA Ames Res. Center)*, **J.P. MALRIEU** *(CNRS, Toulouse)*, **R. SCHINKE** *(Max Planck Inst. f. Stroemungsforschung)*, **M. SHAPIRO** *(Weizmann Inst.)*, **and D.R. YARKONY** *(Johns Hopkins Univ.)*.

The conference was focused on the theoretical study of chemical behavior of excited molecules. Recent advances in experiment, aided in particular by laser and beam techniques, have made the cooperation between the experimentalists and theoreticians indispensable to interpretation, understanding and design of experiments. Main themes of the Conference were 1. Electronic structure of excited molecules, 2. Dynamic behavior of excited molecules, 3. Transfer and conversion of excitation energy. In addition to six invited lectures, seventeen oral presentations and thirteen posters were presented. The total attendance was approximately 75.

The Thirty-third Okazaki Conference

Prebiotic Syntheses of Biomolecules and the Origins of Chirality

(December 1–3, 1988)

Organizers: K. HARADA *(Tsukuba Univ.)*, **A. SHIMOYAMA** *(Tsukuba Univ.)*, **I. HANAZAKI** *(IMS)* **and N. NISHI** *(IMS)*
Invited Speakers: J.R. CRONIN *(Arizona State Univ.)*, **L. BARRON** *(Univ. Glasgow)*, **W. THIEMANN** *(Univ. Bremen)*, **G.E. TRANTER** *(Wellcome Res. Lab.)*, **and A.W. SCHWARTZ***(Univ. of Nijmegen)*

A contemplative and critical attitude is now prevailing among a significant number of the current generation of experimentalists (Prof. Schwartz). The problem has been complicated by newer models of the evolution of Earth's atmosphere. Geophysical studies on radioisotope abundances suggested that organic compounds would have been transported to the Earth by comets and meteorites where the synthesis processes had no selection on the chirality of biological molecules. Clearly, selection mechanisms would have been necessary to permit chemical evolution to proceed, whether from a rich or a meager supply of starting materials. Based on this situation, the conference was organized for the discussion on (1) Organic compounds found in carbonaceous condrites and other meteorites, (2) Origin of molecular chirality and parity violation, and (3) Experimental study of abiotic synthesis of biomolecules. The discussion was highly activated by the participation of theoreticians who were interested in the origin of molecular chirality. The conference was also successful in helping communication among the people in various interdisciplinary fields.

The Thirty-fourth Okazaki Conference

Chemical Kinetics in Combustion
(December 20–22, 1988)

Organizers: H. JINNO *(Kyoto Univ.)*, **S. KODA** *(Univ. Tokyo)*, **K. HAYASHI** *(Nagoya Univ.)*, **and I. KOYANO** *(IMS)*

Invited Speakers: J. WOLFRUM *(Univ. Heidelberg)*, **D. GUTMAN** *(Catholic Univ. America)*, **L.B. HARDING** *(Argonne National Lab.)*, **Th. JUST** *(Inst. Phys. Chem. Verbrennung)*, **C.K. WESTBROOK** *(Lawrence Livermore National Lab.)*, **and R.K. HANSON** *(Stanford Univ.)*

The purpose of this conference was to discuss the complicated combustion phenomena based on the recent growing body of detailed information obtained on various aspects of it, in hope of gaining a unified viewpoint. For this purpose, about sixty scientists involved in different areas of combustion study got together to discuss the following subjects actively: (1) Elementary chemical reactions in combustion, (2) Potential energy surfaces and the theory of reaction rates, (3) High temperature kinetics and the mechanisms of combustion, (4) Visualization of combustion phenomena and spectroscopic tracing of chemical reactions.

The Thirty-fifth Okazaki Conference

Rational Synthesis of Metal Cluster Compounds and Cooperative Phenomena of Multinuclear Frameworks

(May 23–25, 1989)

Organizers: T. SAITO *(The Univ.of Tokyo)*, **H. YAMAZAKI** *(Riken)*, **T. ITO** *(Tohoku Univ.)* **and K. ISOBE** *(IMS)*
Invited Speakers: B.F.G. JOHNSON *(The Univ. of Cambridge)*, **A. SIMON** *(Max-Planck-Institute)*, **R.D. ADAMS** *(The Univ. of South Carolina)* **and J.K. BURDETT** *(The Univ. of Chicago)*

Metal cluster compounds are today recognized as a bridge between molecules and more extended arrays. Rational assembly of cluster frameworks is one of the most interesting and important subjects not only for production of particular geometric shapes but also for yield of cooperative effects due to multimetal- and mixed valence-centers.

This conference was held to discuss the following topics: (1) Catalysis of carbonyl clusters, (2) Relations between electroconductive solids and cluster compounds of oxides, sulfides and halides, (3) Bonding theories of molecular cluster, extended solid clusters and microclusters of metal, (4) Magnetic interaction of polynuclear complexes, and (5) Rational synthesis of cluster compounds. There were 34 contributions including 20 oral (6 contributions from foreign chemists) and 14 poster presentations to the conference. All of them were eagerly discussed by about 80 participants.

JOINT STUDIES PROGRAMS

As one of the important functions of an inter-university research institution, IMS undertakes joint studies programs for which funds are available to cover research expenses as well as travel and living expenses of individuals. The proposals from domestic scientists are reviewed and controlled by the inter-university committee. The programs are carried out under one of five categories:

1) Joint Studies on special projects (a special project of significant relevance to the advancement of molecular science can be carried out by a team of several groups of scientists).
2) Research Symposia (on timely topics in collaboration with both outside and IMS scientists).
3) Cooperative Research (carried out in collaboration with both outside and IMS scientists).
4) Use of Facility (the Computer Center, Instrument Center and other research facilities at IMS are open to all researchers throughout the country).
5) Joint studies programs using UVSOR facilities.
   a) Special Project, b) Cooperative Research, c) Use of UVSOR Facility.

In the fiscal year 1988, numbers of joint studies programs accepted amounted to 3, 10, 147 and 239 for categories 1)–4), respectively and 3, 20 and 89 for 5a)–5c), respectively.

1) Special Projects

A Studies of Elementary Chemical Reaction Processes by Development of New Spectroscopic Methods

Coordinators: **Soji TSUCHIYA** *(Univ. Tokyo)*, **Seiichiro KODA** *(Univ. Tokyo)*, **Okitsugu KAJIMOTO** *(Univ. Tokyo)*, **Yasuki ENDO** *(Univ. Tokyo and IMS)*, **Kaoru YAMANOUCHI** *(Univ. Tokyo)*, **Eizi HIROTA, and Hiroki NAKAMURA**

This research project aims at development of new spectroscopic methods to clarify basic aspects of chemical reactions. Two spectroscopic methods are chosen to be developed and applied to kinetic studies.

A-1 Generation of Tunable Vacuum Ultraviolet (VUV) Laser and Its Application to Spectroscopic and Kinetic Studies.

Intense and tunable VUV laser has been generated by 2-photon resonant 4-wave mixing of visible or ultraviolet laser beams in a non-linear medium. We have found that the convenient non-linear media for the 200-170 nm, 170-145 nm, and 145-125 nm regions are Sr, Mg, and Kr, respectively.[1)]

In the lowest optically allowed state $1^1\Sigma_u^+$ of Cl_2 located in the VUV(130 nm) region, a double minimum potential is predicted due to mixing of the Rydberg and the ion-pair state. The present VUV laser makes it possible to resolve the rotational structure, and based on its analysis, it is concluded that only one vibrational level(v'=39) is localized in a shallow well in the Rydberg side.[2)]

The spin-orbit state distribution of $O(^3P_J)$ produced by photodissociation of NO_2 is determined by LIF spectroscopy of $O(^3P_J)$ atoms. The population ratio of the J=2, 1, and 0 states is 0.81:0.16:0.03 for the 355, 337, and 266 nm excitation, while it is 0.70:0.25:0.05 for the 212 nm excitation. This result is attributable to the difference in the primarily excited electronic states.

A-2 Microwave Kinetic Spectroscopy of Reaction Kinetics of Atomic Oxygen with Olefins.

In the reaction of $O(^3P) + C_2H_4$, the branching ratio of the reactions to produce C_2H_3O + H and CHO + CH_3 offers an important basis for discussion of the mechanism of the singlet-triplet potential surface crossing. In the present project, the reaction yields of C_2H_3O and CHO are directly determined by the time-resolved microwave spectroscopy of these radicals. Our main concern is to discuss the dependence of the branching ratio on the kinetic energy of O atoms. Hot O atoms produced by photodissociation of SO_2 at

193 nm shows the branching ratio similar to the thermal atoms.

References
1) K. Yamanouchi, T. Tsuchizawa, J. Miyawaki, and S. Tsuchiya, *J. Spectrosc. Soc. Jpn.* (in Japanese) **37**, 110 (1978).
2) K. Yamanouchi, T. Tsuchizawa, J. Miyawaki, and S. Tsuchiya, *Chem. Phys. Lett.* **156**, 301 (1989).

B Molecular Mechanism of the Electron and Proton Transfers by Proteins and Their Coupling

Teizo KITAGAWA and Takashi OGURA *(IMS)*, **Akio MAEDA** *(Kyoto Univ.)*, **Nobuhito SONE** *(Jichi Medical School)*, **Yutaka ORII** *(Kyoto Univ.)*, **Kohki OHNO** *(Jichi Medical School)*, **Hideo AKUTSU** *(Yokohama National Univ.)*, **Shin'ya YOSHIKAWA** *(Himeji Inst. of Tech.)*, **and Masamitsu FUTAI** *(Osaka Univ.)*

The vectorial proton translocation across the energy transducing membrane is known to be essential to produce biological energy, but its molecular mechanism remains to be explored. This project aims to elucidate a mechanism of the proton translocation by proteins for three representative cases; 1) the light-driven proton pump, 2) the electron-driven proton pump, 3) passive proton translocation. This is the last year of the 3 years projects and the results from IMS are contained in the publication list.

The first system is seen in light-harvesting bacteria and we selected bacteriorhodopsin which involves the *cis-trans* isomerization of the retinal Schiff base and the subsequent deprotonation of the Schiff base. Drs. Kitagawa, Maeda, Ogura and Ohno are involved in this subject and our group at IMS has observed transient resonance Raman spectra by using the pump-probe flow-cell apparatus. The second system is seen in the respiratory chain of aerobic organisms, and out of three pumping sites we have picked up Site III, where cytochrome *c* oxidase pumps protons when electrons are transferred from cytochrome *c* to oxygen molecules. The Raman group at IMS and Dr. Yoshikawa have explored transient states for reduction of dioxygen by constructing a device for measuring Raman and absorption spectra simultaneously and an artificial cardiovascular system which enables us to regenerate the enzyme during the sample circulation through the cell and thus to accumulate the data for a long time with a small amount of sample (see II-F-3). The timing of the proton ejection induced by the electron transfer will be determined with the time-resolved fluorescence spectra and a pH indicating fluoro-dye. Drs. Ogura, Sone, and Orii are involved in this project. The electron transfer through proteins is investigated with a multiheme cytochrome *c*, namely, cytochrome c_3. Drs. Akutsu and Kitagawa are studying it with NMR and resonance Raman techniques, respectively. The third system intends to study a molecular mechanism of the H^+-ATPase, which catalyzes the formation of ATP from ADP and P_i upon passive proton translocation. Drs. Futai, Sone and Ohno are involved in this project.

C A New Approach to Study Photodynamic Processes of Isolated Molecular Assemblies

The aim of our one-year special project was to explore hitherto unknown photodynamic processes in isolated molecular assemblies produced in supersonic free jets. Even for complex organic molecules and their van der Waals (vdW) complexes it was possible to excite them at their single vibronic levels and to follow the resulting emission decays ranging from 2 to 110 ns. The detailed analysis of these decay curves allowed us to examine the excess-energy dependence of electronic relaxation, role of dark levels in radiationless transitions, photofragmentation of weakly bonded complexes, refractive index dependence of the natural radiative lifetime, etc., none of which could be studied without accurate decay-time measurements. To achieve higher time resolution, a newly developed optical oscilloscope was tested for its capability of monitoring emission decays of molecules in supersonic free jets.

C-1 Electronic Relaxation in Isomers of 9,10-dimethoxyanthracene and their Rare-Gas Complexes

Satoshi HIRAYAMA *(Kyoto Institute of Technology)*, **Fujio TANAKA** *(University of Osaka Prefecture)*, **and Kosuke SHOBATAKE** *(IMS)*

[*J.Phys.Chem.*, in press]

Two types of red shift observed upon complexation

of the title compound (DMEOA) with the rare-gas atoms (Ar, Kr and Xe) have revealed the existence of two stereo isomers (cis and trans) of DMEOA. The main vibronic bands of the uncomplexed DMEOA in the range 25790 to 28630 cm^{-1} can be assigned to either isomer. The fluorescence lifetime of the uncomplexed trans isomer is 28.1±0.1 ns in the electronic origin and is rather insensitive to the excess energy, being 15.9±0.1 ns even at the excess energy of 2835 cm^{-1}. For the 12_0^1 or 12_0^2 band DMEOA exhibits isomer-dependent fluorescence lifetimes or intensities, but, for the other main vibronic levels, there is no significant difference in τ_f. Although both isomers form 1:1 complexes with rare-gas atoms in comparable yields, the formation of higher coordination complexes is less feasible for the cis isomer. In contrast to 9-methoxyanthracene (MEOA),[1] all the rare-gas complexes have fluorescence lifetimes lying between 25 and 33 ns and no external heavy atom effect is found at any main vibronic level examined. The photodissociation of the vdW complexes and energy redistribution after dissociation will also be discussed in relation to the greatly shortened fluorescence decays in thermalized states of DMEOA and the rather insensitive excess-energy dependence of the fluorescence lifetime of the supercooled bare molecule.

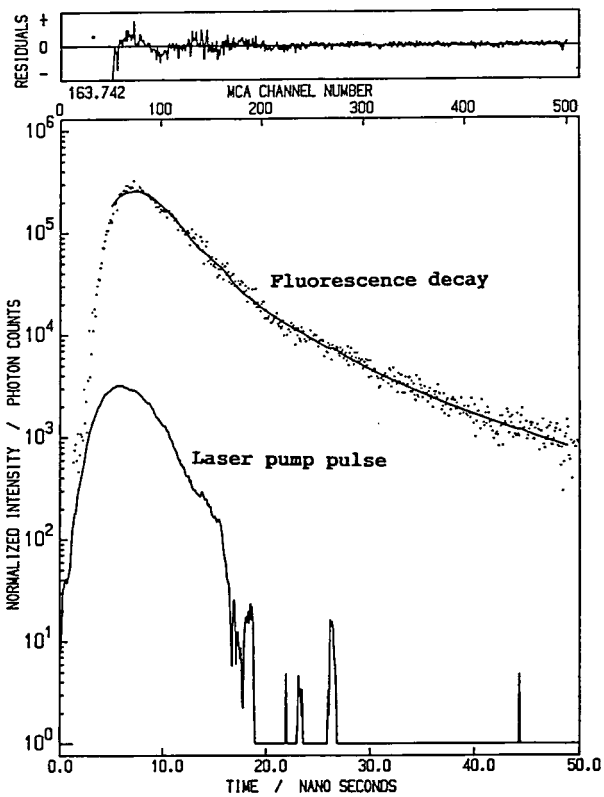

Figure 1. Non-exponential fluorescence decay curve observed with a Hamamatu OO-01 optical sampling oscilloscope for DMEOA in the gas phase. The quality of the data is high enough to allow three-exponential analysis.

Reference

1) S. Hirayama, F. Tanaka and K. Shobatake, *Chem. Phys. Lett.*, **153**, 112 (1988).

C-2 Vibrational Predissociation of Rare-gas van der Waals Complexes of 9-Methoxyanthracene

Satoshi HIRAYAMA *(Kyoto Institute of Technology)*, **Fujio TANAKA** *(University of Osaka Prefecture)*, **and Kosuke SHOBATAKE** *(IMS)*

The energy redistribution which may occur upon vibrational predissociation of vdW complexes between rare-gas atoms and large organic molecules has attracted much interest recently because the fragmented parent molecules can be used to probe the mechanism of the energy redistribution. The non-exponential fluorescence decays which are recorded for the fragmented molecules show clearly that the dissociation from the vibronic level of 12_0^2 results in relatively high yields of vibrationless MEOA. The short-lived component becomes dominant upon increasing the excess energy of excitation. A comparison of the relative fluorescence quantum yields, calculated by using the fluorescence decay parameters, with the relative band intensities suggests that dissociation of the Ar and Kr complexes occurs in much shorter periods of time than the radiative lifetimes of the corresponding complexes. However, an appreciable fraction of the Xe complexes decays from the 8_0^1 vibronic level via a nonradiative pathway in which dissociation does not occur. The substantial reduction in the fluorescence lifetime of the insufficiently colled states of MEOA, together with the data obtained from the photodissociation of complexes of 9,10-dimethoxyanthracene with rare-gas atoms, indicates that the residual energies of the vibrational predissociation are not distributed significantly among optically inactive modes. To achieve higher time resolution, a newly developed optical oscilloscope was tested as is shown in Figure 1.

C-3 Fluorescene Decays in van der Waals Complexes of 9-Cyanoanthracnene studied in Supersonic Free Jets

Satoshi HIRAYAMA and Akiho ADACHI *(Kyoto Institute of Technology)*, **Fujio TANAKA** *(University of Osaka Prefecture)*, **Kosuke SHOBATAKE and Kyung-Hoon Jung** *(IMS)*

[*J.Chem.Soc.Faraday Trans. 2,* **84** 1927 (1988).]

van der Waals (vdW) complexes of 9-cyanoanthracene (9CNA) with ligands of various types have been generated in supersonic free jets and studied by laser-induced fluorescence (l.i.f) spectroscopy and nanosecond fluorescence lifetime measurements. Depending on the nature of the ligand molecules, four different types of decay have been observed. (i) After the complexation of 9CNA with water, ammonia and ethanol, the emission decay process is unaltered in the complexes's vibrationless and vibrationally excited states. (ii) Carbon disulphide and triethylamine (TEA) form vdW complexes with 9CNA whose fluorescence lifetimes are less than one half of that of the uncomplexed 9CNA. Furthermore, the intramolecular vibrational excitation of the 9CNA moiety in these two complexes appears to lead to almost total fluorescence quenching, since no l.i.f. excitation bands are observed at the expected wavelengths. This contrasts sharply with the vdW clusters mentioned above. (iii) For complexes with benzene, much longer lifetimes (36-48 ns) than that of the uncomplexed 9CNA are found, although no new type of emission is detected. (iv) N,N-Dimethylaniline (DMA) yields an exciplex with a lifetime of 110 ns, which might be formed directly from the vdW complex in the ground state. The effect of complexation on the fluorescence lifetimes is also discussed in relation to the fluorescence quenching observed in solution.

C-4 Microscopic Solvent Effects on the S_1 - T_2 Intersystem Crossing of 9,10-Diphenylanthracene in Supersonic Free Jets

Fujio TANAKA *(University of Osaka Prefecture)*, **Satoshi HIRAYAMA** *(Kyoto Institute of Technology)*, **and Kosuke SHOBATAKE** *(IMS)*

Fluorescence excitation spectra and fluorescence decays were measured for isolated 9,10-diphenylanthracene (DPA) and its van der Waals (vdW) complexes with Ar and Xe atoms. The fluorescence lifetime of DPA at the S_1 origin is significantly shorter than the pure radiative lifetime. In contrast to the condensed phase, the intersystem crossing from S_1 to T_2 occurs in the isolated state because S_1 is located above as a result of the absence of solvation. However, it is proposed that S_1 lies below T_2 when the number of Xe atoms coordinated to DPA is increased, since the heavy-atom effect of Xe on the fluorescence lifetime which is observed for the 1:1 vdW complex disappears in the highly coordinated complexes.[1)]

Reference

1) F. Tanaka, S. Yamashita, S. Hirayama, A. Adachi and K. Shobatake, *Chem.Phys.*, **131** 435 (1989).

C-5 Natural Radiative Lifetimes of Anthracene Derivatives and their Dependence on Refractive Index

Satoshi HIRAYAMA *(Kyoto Institute of Technology)*, **Fujio TANAKA** *(University of Osaka Prefecture)*, **and Kosuke SHOBATAKE** *(IMS)*

Fluorescence lifetimes of the electronic origins of S_1 are measured in supersonic free jets for nine anthracene derivatives. For most of the meso di-substituted derivatives, these lifetimes are virtually equal to the natural radiative lifetimes in vacuum and they are satisfactorily related to the radiative lifetimes determined in n-hexane through a factor of n^2 (n: refractive index). This unambiguous relationship found for the anthracene derivatives will bring a long-standing debate on the refractive index dependence of the radiative lifetime to an end. It will also provide a basis for the discussion of the dependence of the radiative lifetime on single vibronic levels (SVL).

2) Research Symposia

1. Electron-transfer in Electrode-catalysis Systems
   (September 19th – 20th, 1988)
   Organizer: T. Sakata (IMS)

2. New Developments in Spin-chemistry
   (December 6th – 8th, 1988)
   Organizer: N. Hirota (Kyoto Univ.)
3. Approach to Biological-function in the Manner of Molecular Science
   (January 12th – 14th, 1989)
   Organizer: A. Imamura (Hiroshima Univ.)
4. Manifestation of Multiple-function by Polymerization and Intelligentization of Complexes
   (January 27th – 28th, 1989)
   Organizer: N. Tojima (Tokyo Univ.)
5. Symposium on Theoretical Chemistry for the Younger Researchers of Molecular Science
   (May 30th, 1989)
   Organizer: K. Kajimoto (Tokyo Univ.)
6. Mechanisms of Relaxation of Molecular Excited States in Solids
   (June 6th – 3rd, 1989)
   Organizer: A. Matsui (Konan Univ.)
7. Molecular Processes under Non-linear and Non-equilibrium Conditions
   (June 5th – 7th, 1989)
   Organizer: K. Yoshikawa (Nagoya Univ.)
8. Synthesis and Properties of Assembly of Metal Complex Molecules
   (June 29th – July 1st, 1989)
   Organizer: I. Shirotani (Muroran Inst. of Tech.)

3) Cooperative Research

This is one of the most important programs IMS undertakes for conducting its own research of the common interest to both outside and IMS scientists by using the facilities at IMS. During the first half of fiscal year of 1988 ending on September 30, 75 outside scientists including 4 invited collaborated with IMS scientists; and during the second half of the fiscal year, 72 outside scientists including 2 invited worked in collaboration with IMS scientists, the names and the affiliations of these collaborators are found in the Research Activities.

4) Use of Facility

The number of projects accepted for the Use of Facility Program of the Computer Center during the fiscal year of 1988 amounted to 150 (471 users), and the computer time spent for these projects is 4566 hours (converted to the HITAC M-680 time), and amounts to 47% of the total annual CPU time used.

Sixty five projects (213 users) were accepted for the Use of Facility Program of the Instrument Center during the fiscal year of 1988.

5) UVSOR

Joint studies programs using UVSOR facilities are carried out under one of three categories: 5-a) UVSOR Special Project, 5-b) UVSOR Cooperative Research, and 5-c) Use of UVSOR Facility.

The 10th UVSOR Research Symposium, organized by K. Kimura (IMS), was held during December 9th – 10th, 1988.

5-a) UVSOR Special Project

Analysis of the Electronic Structures of Molecular Assemblies with Photoelectron Spectroscopy Using Synchrotron Radiation

Coordinators: **Kazuhiko SEKI** *(Hiroshima Univ. and IMS)*
Makoto WATANABE *(UVSOR Facility)*

Angle-resolving photoelectron spectrometer at the BL 11B2 has been used for studying the electronic structures of several organic molecular and polymeric solids.

Among the continued works from last year, the studies of oligothiophenes as model compounds of poly(2,5-thienylene) have been completed, and it has been extended to the studies of thienylthiophenes and poly(thienylenevinylene). Also the studies of long alkyl compound n-$C_{16}H_{33}(CO)C_{16}H_{33}$ has been continued as a model of polyethylene with a structural defect.

Several new subjects also started. (i) the electronic structure of poly(tetrafluoroethylene) was studied by using evaporated films of short chain model compounds and oligomers. The results were analyzed in a detailed way, in combination with band calculations, vuv absorption spectra, and XANES measurements. (ii)

liquid thin film samples of poly(dimethylsiloxane) was studied under ultrahigh vacuum, and the results were analyzed in comparison with related compounds such as polysilanes and SiO_2, with the aid of band calculations. (iii) Tetrathianaphthacene was studied for probing the intermolecular band dispersion. (iv) Measurements of ring alkanes $(CH_2)_n$ with n = 32, 48, and 64 were tried as an extension of the studies of linear alkanes, but sofar the measurements are not successful due to the difficulty in sample preparation.

Far Infrared Spectroscopy under High Pressure using Synchrotron Radiation

Coordinators: **Takao NANBA*** *(Tohoku Univ.)*
Makoto WATANABE *(UVSOR)*

The change in the phonon spectrum of alkali halide crystals due to the pressure-induced phase transition from the B1 phase (rock salt) to the B2 phase (cesium chloride) was observed by the absorption measurement using a diamond anvil cell at BL6A1. The pressure is available up to 5 GPa at room temperature.

The experimental results were obtained with KI, KBr, RbI and RbBr crystals. In these crystals, the phonon energy of the transverse optic (TO) mode was observed to make a blue shift with the increase of the pressure in the B1 phase and show a sudden decrease at the pressure which the pressure-induced phase transition occurs. In the B2 phase the TO phonon energy also shifted linearly to the higher energy with the pressure. From the results, the TO phonon energy of KI, KBr, RbI and RbBr in the B2 phase was found to be 106, 118, 73 and 90 cm^{-1}, respectively.

Reference

* present address: Department of Physics, Kobe Univ.

Photoinduced Transient Phenomena in Organic Crystals

Tadaoki MITANI, Hiroshi OKAMOTO, and Youji ACHIBA

A new system for photoinduced absorption spectroscopy has been constructed for the first time by using a CW mode-locked picosecond Nd:YAG laser synchronized with the synchrotron radiation pulses.[1] By an application of the delay-time modulation technique, the measurements on polyacetylene films under irradiation of the laser has been successfully made in a time resolution of ca. 0.5 ns in a wavelength region from UV to near IR. In IR and far IR regions, however, precise data could not be obtained due to the weak photon-flux of the SR pulses. To improve this experimental situation, we are now constructing the FT-IR spectrometer, which leads to an increase of two order magnitudes of the effective strength of the SR pulses. In parallel, the construction of a time-resolved photoelectron spectrometer using the synchronized laser pulses is now in progress.

Reference

1) T. Mitani, H. Okamoto, Y. Takagi, M. Watanabe, K. Fukui, S. Koshihara, and C. Ito, *Rev. Sci, Instrum.* **60**, 1569 (1989).

5-b) UVSOR Cooperative Research

During the first half of fiscal year of 1988, 10 outside scientists including 3 invited collaborated with IMS scientists; and during the second half of the fiscal year, 10 outside scientists including 2 invited worked in collaboration with IMS scientists.

5-c) Use of UVSOR Facility

The number of projects accepted for the Use of UVSOR Facility Program during the fiscal year of 1988 amounted to 89.

FOREIGN SCHOLARS

Visitors from abroad play an important role in research activities and are always welcome at IMS. The following is the list of foreign scientists who visited IMS in the past year (Aug. 1988 – July 1989). The sign *1 indicates an attendant to an Okazaki Conference, *2 an IMS or Japan Society for the Promotion of Science Invited Foreign Scholar (period of stay is from 3 to 6 months), *3 an IMS councillor, *4 an IMS visiting scientist and *5 an IMS adjunct professor or associate professor from abroad (period of stay is from 9 to 12 months). Scientists who wish to visit IMS under programs 2 and 5 are invited to make contact with an IMS faculty in a related field.

Dr. A.E. Dorigo*2	UCLA	(USA)	Feb. 1988 –
Dr. P. Knowles	Cambridge Univ.	(UK)	Aug. 1988
Prof. A. Enflo	Univ. of Stockholm	(Sweden)	Aug. 1988
Prof. A.J. Egginton		(UK)	Aug. 1988
Prof. H.S. Sun	Pusan Natl. Univ.	(Korea)	Aug. 1988
Dr. Fu, Shaojun	HESYRL, Univ. Sci. & Tec., China	(China)	Aug. 1988
Prof. Bao, Zhongmou	HESYRL, Univ. Sci. & Tec., China	(China)	Aug. 1988
Prof. Pei, Yuanji	HESYRL, Univ. Sci. & Tec., China	(China)	Aug. 1988
Prof. J. Troe*2	Univ. of Göttingen	(FRG)	Aug. 1988
Dr. G. Graner	Univ. Paris-Sud	(France)	Aug. 1988
Prof. V.V. Mikhailin	Moscow State Univ.	(USSR)	Sep. 1988
Dr. E.S. Gluskin	Inst. of Nuclear Phys.	(USSR)	Sep. 1988
Prof. J.A.R. Samson	Univ. of Nebraska	(USA)	Sep. 1988
Dr. K.B. Lee	POSTECH	(Korea)	Sep. 1988
Dr. P.H. Elleaume	European Synchrotron Radiation Facility	(France)	Sep. 1988
Dr. R.P. Madden	NIST	(USA)	Sep. 1988
Dr. G.P. Williams	NSLS, Brookhaven Natl. Lab.	(USA)	Sep. 1988
Prof. A. Mitsui	Univ. of Miami	(USA)	Sep. 1988
Prof. I. H. Munro	Daresbury Lab.	(UK)	Sep. 1988
Dr. I. Nenner	Centre d'Etudes Nucleaires de Saclay	(France)	Sep. 1988
Dr. C.D. Hall*2	King's Coll London Univ. of London	(UK)	Sep. 1988
Dr. T.W. Ebbeson	NEC	(Norway)	Sep. 1988
Dr. K.C. Kim	Los Alamos Natl. Lab.	(USA)	Sep. 1988
Dr. H.J. Dewey	Los Alamos Natl. Lab.	(USA)	Sep. 1988
Prof. R.J. Buenker*1	Wuppertal Univ.	(FRG)	Sep. 1988
Dr. S.R. Langhoff*1	NASA Ames Lab.	(USA)	Sep. 1988
Dr. J.P. Malrieu*1	CNRS, Toulouse	(France)	Sep. 1988
Dr. R. Schinke*1	Max-Planck-Inst.	(FRG)	Sep. 1988
Dr. M. Shapiro*1	Weizmann Inst.	(Israel)	Sep. 1988
Prof. D.R. Yarkong*1	Johns Hopkins Univ.	(USA)	Sep. 1988

Prof. W.T. Borden*[2]	Univ. of Washington	(USA)	Sep. – Dec. 1988
Dr. E.A. Cohen*[2]	JPL	(USA)	Sep. – Dec. 1988
Dr. A. Seidle	3M Research Lab.	(USA)	Oct. 1988
Prof. A. San Pietro	Indian Univ.	(USA)	Oct. 1988
Dr. E. Amouyal	CNRS, Univ. Paris-Sud	(France)	Oct. 1988
Dr. R. Bensasson	CNRS, Museum d'Histoire Naturelle Paris	(France)	Oct. 1988
Dr. R. Bonneau	CNRS, Bordeaux	(France)	Oct. 1988
Prof. J. Delaire	Univ. Paris-Sud	(France)	Oct. 1988
Prof. J. Faure	Univ. Paris-Sud	(France)	Oct. 1988
Dr. J. Kossanyi	CNRS, Thiais	(France)	Oct. 1988
Prof. R. Marx	Univ. Paris-Sud	(France)	Oct. 1988
Prof. J. Pete	Univ. Reims	(France)	Oct. 1988
Dr. P. Pichat	CNRS, Lyon	(France)	Oct. 1988
Prof. G. R. DeMare	Univ. Libre de Bruxelles	(Belgium)	Oct. 1988
Prof. A. Lablache-Combier	Univ. of Lille	(France)	Oct. 1988
Prof. J. Wirz	Univ. of Basal	(Switzerland)	Oct. 1988
Prof. S. Rosenwaks	Ben Grion Univ.	(Israel)	Oct. 1988
Prof. J. Webb	Murdock Univ.	(Australia)	Oct. 1988
Prof. L. Krause*[2]	Univ. of Windsor	(Canada)	Oct. 1988
Prof. R.L. Kay	Carnegie-Mellon Univ.	(USA)	Oct. 1988
Dr. W. Lepkowski	American Chemical Society	(USA)	Oct. 1989
Prof. R. Holroyd	Brookhaven Natl. Lab.	(USA)	Oct. 1988
Dr. Y. Li	Inst. Chem., Acad. Sin.	(China)	Oct. 1988
Dr. P. Seta	CNRS, Montpellier	(France)	Oct. – Nov. 1988
Prof. X.Q. Song	Tsinghua Univ.	(China)	Nov. 1988
Prof. Er-Jian Wang	Inst. of Photographic Chem. Acad, Sinica	(China)	Nov. 1988
Prof. S.K. Wu	Inst. of Photographic Chem. Acad. Sinica	(China)	Nov. 1988
Dr. Qun Bai	Inst. of Photographic Chem. Acad. Sinica	(China)	Nov. 1988
Prof. C. Ping Zhen	Inst. of Photographic Chem. Acad. Sinica	(China)	Nov. 1988
Prof. Yi Cao	Inst. of Photographic Chem. Acad. Sinica	(China)	Nov. 1988
Dr. L. Jorissen	Univ. Giesen	(FRG)	Nov. 1988
Prof. H. Staab*[3]	Max-Planck-Gesellschaft	(FRG)	Nov. 1988
Ms. P. Wang*[2]	Inst. Chem., Acad. Sin.	(China)	– Nov. 1988
Prof. D.D. Eley	Univ. of Nottingham	(UK)	Nov. 1988
Prof. L.E. Lyons	Univ. of Queensland	(Australia)	Nov. 1988
Prof. M. Pope	New York Univ.	(USA)	Nov. 1988
Prof. M.M. Labes	Temple Univ.	(USA)	Nov. 1988
Prof. F. Wudl	Univ. of California	(USA)	Nov. 1988
Prof. K. Bechgaard	Univ. of Copenhagen	(Denmark)	Nov. 1988
Prof. N. Karl	Univ. of Stuttgart	(FRG)	Nov. 1988

Prof. M.R. Willis	Univ. of Nottingham	(UK)	Nov. 1988
Dr. G. Denninger	Univ. of Bayreuth	(FRG)	Nov. 1988
Prof. R. Qian	Inst. Chem., Acad. Sin.	(China)	Nov. 1988
Prof. J. Sworakowski	Tech. Univ. of Wroctow	(Poland)	Nov. 1988
Dr. E.A. Silinsh	Inst. Phys. & Energ., Acad. Sci. Latovian SSR	(USSR)	Nov. 1988
Prof. E.C.M. Chen	Univ. of Houston	(USA)	Nov. 1988
Dr. Z.D. Popovic	Xerox Res. Center, Canada	(Canada)	Nov. 1988
Dr. J.T. Hougen	NIST	(USA)	Nov. – Dec. 1988
Prof. J.R. Cronin*[1]	Arizona State Univ.	(USA)	Nov. – Dec. 1988
Dr. G.E. Tranter*[1]	Wellcome Res. Lab.	(UK)	Nov. – Dec. 1988
Prof. W. Thiemann*[1]	Univ. Bremen	(FRG)	Nov. – Dec. 1988
Prof. L. Barron*[1]	Univ. of Glasgow	(UK)	Nov. – Dec. 1988
Prof. A.W. Schwartz*[1]	Univ. of Nijmegen	(Netherlands)	Nov. – Dec. 1988
Dr. P. vanden Hoek	Vrije Univ.	(Netherland)	Nov. 1988
Prof. C.P. Casey	Univ. of Wisconsin	(USA)	Nov. 1988
Dr. Y. Xie	Fudan Univ.	(China)	Nov. 1988 – Mar. 1989
Prof. H.S. Sun	Pusan Natl. Univ.	(Korea)	Dec. 1988 – Feb. 1989
Prof. D. Gutman*[1]	Catholic Univ. of America, Washington, D.C.	(USA)	Dec. 1988
Dr. L.B. Harding*[1]	Argonne Natl. Lab.	(USA)	Dec. 1988
Prof. R.K. Hanson*[1]	Standard Univ.	(USA)	Dec. 1988
Prof. Th. Just*[1]	Deutsche Forschungs-und Versuchsanstalt fur Luft-und Raumfahrt e. V.	(FRG)	Dec. 1988
Dr. C.K. Westbrook*[1]	Lawrence Livermore Natl. Lab.	(USA)	Dec. 1988
Prof. J. Wolfrum*[1]	Univ. of Heidelberg	(FRG)	Dec. 1988
Prof. R.J. Fleming*[5]	Monash Univ.	(Australia)	Jan. 1989 –
Dr. J.H.D. Eland*[5]	Univ. of Oxford	(UK)	Jan. – Aug. 1989
Dr. E.I. von Nagy-Felsobuki*[5]	Univ. of Newcastle	(Australia)	Jan. – Aug. 1989
Dr. S.N. Rai*[2]	North Eastern Hill Univ.	(India)	Jan. 1989 –
Prof. S.C. Park	Kangweon Natl. Univ.	(Korea)	Feb. 1989
Prof. I. Bertini	Florence Univ.	(Italy)	Feb. 1989
Dr. J.M. Williams*[2]	Argonne Natl. Lab.	(USA)	Feb. 1989
Prof. R.D. Levine	Hebrew Univ. of Jerusalam	(Israel)	Mar. 1989
Prof. J. Pfab*[2]	Heriot-Watt Univ.	(UK)	Mar. 1989
Dr. P. Smith	Harvard-Smithsonian Center for Astrophysics	(USA)	Mar. 1989
Prof. R.W. Field	MIT	(USA)	Mar. 1989
Prof. M.P. Sue	Seoul Natl. Univ.	(Korea)	Mar. 1989
Prof. Chi-Ming Che	Hong Kong Univ.	(Hong Kong)	Mar. 1989
Prof. Chung-Sun Chung	Tsing Hua Univ.	(Taiwan)	Mar. 1989
Prof. D. Phillips	Royal Inst.	(UK)	Mar. 1989
Dr. A.J. Stace	Univ. Sussex	(UK)	Mar. 1989
Dr. I. Powis	Nottingham Univ.	(UK)	Mar. 1989

Dr. D.V. Brumbaugh	Eastman Kodak	(USA)	Mar. 1989
Prof. S.H. Bauer	Cornell Univ.	(USA)	Mar. 1989
Prof. R.J. Donovan	Univ. of Edinburgh	(UK)	Mar. – May 1989
Dr. C. Jansen	Univ. of Georgia	(USA)	Mar. 1989
Dr. Y. Yamaguchi	Univ. of Georgia	(USA)	Mar. 1989
Dr. S. Mathieu*2	Univ. of Toulouse	(France)	Mar. 1989 –
Mr. F. Maseras	Univ. of Barcelona	(Spain)	Apr. – Aug. 1989
Prof. Looi Eng Choon	Univ. Singapore	(Singapore)	Apr. 1989
Dr. Chang, Cheng-Hsiang	Synchrotron Radiation Research Center (SRRC), Taiwan	(Taiwan)	Apr. 1989
Dr. Haung, Ching-Shiang	SRRC, Taiwan	(Taiwan)	Apr. 1989
Dr. A. Lin	SRRC, Taiwan	(Taiwan)	Apr. 1989
Prof. Tseng, Poh-Kun	SRRC, Taiwan	(Taiwan)	Apr. 1989
Dr. Jen-Chun Lee	SRRC, Taiwan	(Taiwan)	Apr. 1989
Prof. F. Wilkinson	Loughborough Univ. of Tech.	(UK)	Apr. 1989
Dr. D. Kim	Korea Stand. Res. Inst.	(Korea)	Apr. 1989
Prof. T. Yonetani	Univ. of Pennsylvania	(USA)	Apr. – May 1989
Mr. Y. Ding*4	Beijing Normal Univ.	(China)	Apr. – Aug. 1989
Dr. M. Inokuti*2	Argonne Natl. Lab.	(USA)	May 1989
Prof. J.H. Penn	West Viginia Univ.	(USA)	May 1989
Prof. B.F.G. Johnson*1	Cambridge Univ.	(UK)	May 1989
Prof. B.T. Heaton*1	Univ. of Liverpool	(UK)	May 1989
Prof. Lu Jiaxi*1	Chinese Acad. Sci.	(China)	May 1989
Dr. A. Simon*1	Max-Planck-Inst.	(FRG)	May 1989
Prof. R.D. Adams*1	Univ. of South Calorina	(USA)	May 1989
Prof. J.K. Burdett*1	Univ. of Chicago	(USA)	May 1989
Prof. J.F. Ojo*1	Obafemi Awolowo Univ.	(Nigelia)	May 1989
Prof. J.H. Futrell	Univ. of Delaware	(USA)	Jun. 1989
Dr. K. Kemnitz	ERATO	(FRG)	Jun. 1989
Prof. W.C. Stwalley	Univ. of Iowa	(USA)	Jun. 1989
Dr. S.R. Meech*4	Heriot-Watt Univ.	(UK)	Jun. – Oct. 1989
Prof. B.J. Yoon	Kangreung Univ.	(Korea)	Jun. 1989 –
Prof. W. Lewis-Bevan*2	Southern Illinois Univ.	(USA)	Jul. 1989 –
Prof. Tseng, Poh-Kun*2	SRRC, Taiwan	(Taiwan)	Jul. 1989 –
Dr. J. Eric	French Emrbassy in Tokyo	(France)	Jul. 1989
Prof. K.A. Burkov	Leningrad Univ.	(USSR)	Jul. 1989
Dr. Du-Jeon Jang	Korea Stand. Res. Inst.	(Korea)	Jul. 1989
Prof. M. Onellion	Univ. of Wisconsin-Madison	(USA)	Jul. 1989
Prof. E.J. Nordgren	Uppsala Univ.	(Sweden)	Jul. 1989
Prof. G. Schoenhense	Univ. of Bielefeld	(FRG)	Jul. 1989
Prof. P. Zimmermann	Technische Univ. Berlin	(FRG)	Jul. 1989
Dr. O. Dutuit	Univ. Paris-Sud	(France)	Jul. 1989
Dr. A. Gerschel	Univ. Paris-Sud	(France)	Jul. 1989
Prof. P. Woodruff	Univ. of Warwick	(UK)	Jul. 1989
Prof. H. Kroto	Univ. of Sussex	(UK)	Jul. 1989
Prof. K. Codling	Univ. of Reading	(UK)	Jul. 1989

Prof. J. Bordas	Daresbury Lab.	(UK)	Jul. 1989
Prof. I.H. Munro	Daresbury Lab.	(UK)	Jul. 1989
Dr. B.T. Sutcliffe	Univ. of York	(UK)	Jul. 1989
Dr. B.J. Howard	Oxford Univ.	(UK)	Jul. 1989
Dr. N.-S. Lee	Chungbuk Natl. Univ.	(Korea)	Jul. 1989
Prof. P. Rosmus	Univ. of Frankfurt	(FRG)	Jul. 1989 –

AWARD

Professor Inokuchi's Scientific Achievements

Professor Hiroo Inokuchi was awarded the 1989 Fujihara Prize for his outstanding contributions to research on organic semiconductors, conductors and superconductors.

Prof. Inokuchi is one of the pioneers in the study of electrical conductivity in solid state organic materials, and during the last 40 years has proposed several important new ideas in this field and played a leading role in its development.

His main contributions are as follows:

1) Discovery of Organic Semiconductors.

Extending his work with Professor Akamatu on the electrical conductivity of graphite, Professor Inokuchi found that condensed polycyclic aromatic hydrocarbons such as violanthrone exhibited semiconducting characterisitcs (1950). Following a wide range of measurements including the photoelectric effect, charge carrier drift mobility and pressure-dependence of semiconductivity, by 1965 he had confirmed the occurrence of semiconductivity in organic compounds, originating in the transport of electrons and holes through overlapping intermolecular π-orbitals.

2) Synthesis of Novel Organic Semiconductors.

In 1979 Professor Inokuchi discovered unusually high conductivity in the hemoprotein cytochrome c_3, and in 1986 he synthesized a range of "molecular fasteners" based on tetrakis(alkylthio)-tetrathiafulvalene(TTC_n-TTF). The latter demonstrates very strikingly the effects of additive intermolecular van der Waals forces between long alkyl chains. In 1987 Professor Inokuchi also showed that charge-carriers in the related tellurium compound $TTeC_1$-TTF have a relatively high mobility of order 30 $cm^2/Vsec$.

3) Discovery of Highly Conductive Charge-Transfer Complexes.

Professor Inokuchi, Matsunaga and Akamatu together discovered a range of extremely highly conductive charge-transfer-complexes based on perylene-iodine (1954). This was the stimulus for the synthesis of organic metals and superconductors in many loboratories around the world in later years.

4) Measurement of Ionization Potentials and Polarizabilities of Organic Solids.

Professor Inokuchi has measured the ionization potentials and polarizabilities of many organic solids. This reliable body of data has proved extremely useful in the study of the electronic structure of these materials, and an invaluable guide in the synthesis of novel compounds.

Professor Ohtaki's Scientific Achievements

Professor H. Ohtaki received the Tejima Prize for Scientific Research, together with Dr. Ishiguro (Associate Professor at Tokyo Institute of Technology and a previous adjunct Associate Professor of IMS), for their contribution to "Thermodynamic and Structural Investigations of Divalent Metal Complexes in Non-aqueous Solutions".

The Tejima Prize is given by the Tejima Foundation of Science and Technology to persons who made a remarkable progress in their work at the Tokyo Institute of Technology or those who are related to the university. Professor Ohtaki and Dr. Ishiguro have achieved a remarkable success in the field of thermodynamic and spectroscopic studies of complex formation reactions in combination with the X-ray diffraction method in solution in various nonaqueous solution systems.

LIST OF PUBLICATIONS

S. NAKAMURA and K. MOROKUMA, "Theoretical Investigation of the Platinum Ketene Complex $Pt(PR_3)_2(CH_2=C=O)$ and Carbene Complex $Pt(PR_3)_2(CH_2)(CO)$", *Organometallics,* **7**, 1904 (1988).

S. YABUSHITA and K. MOROKUMA, "Potential Energy Surfaces for Rotational Excitation of CH_3 Product in Photodissociation of CH_3I", *Chem. Phys. Lett.* **153**, 517 (1988).

S. SAKAKI, T. AIZAWA, N. KOGA, K. MOROKUMA and K. OHKUBO, "Electronic Structure and Enhanced Reactivity of Carbon Dioxide Coordinated with a Rhodium(I) Complex. An ab Inition MO Study", *Inorg. Chem.* **28**, 103 (1989).

P.N. SKANCKE, N. KOGA and K. MOROKUMA, "A Theoretical Study of the Thermal Degenerate Rearrangement in Methylenecyclobutane", *J. Am. Chem. Soc.* **111**, 1559 (1989).

Y. AOKI, A. IMAMURA and K. MOROKUMA, "Self-Consistent-Field Variational Approach to the Interaction between a Polymer and a Small Molecule", *Theo. Chim. Acta* **75**, 247 (1989).

A.E. DORIGO and K. MOROKUMA, "Theoretical Studies of Nucleophilic Additions of Organocopper Reagents to Acrolein. Rationalization of the Differences in Regioselectivity in the Reactions of Methylcopper and Methyllithium", *J. Am. Chem. Soc.* **111**, 4635 (1989).

A.E. DORIGO and K. MOROKUMA, "Stereoselectivity of the Nucleophilic Addition of Organocopper Reagents to Chiral α, β-Unsaturated Carbonyl Compounds. *Ab Initio* Molecular Orbital Studies of Steric and Electronic Effects", *J. Am. Chem. Soc.* **111**, 6524 (1989).

I. OHMINE, H. TANAKA and P.G. WOLYNES, "Large Local Energy Fluctuations in Water, II. Cooperative Motions and Fluctuations", *J. Chem. Phys.* **89**, 5852 (1988).

A. OHSAKI, H. NAKAMURA and M. BAER, "Chemical-reaction-theoretical Approach to the Muon-transfer Process", *Phys. Rev.* **A38**, 2798 (1988).

A. OHSAKI, H. NAKAMURA and S.C. PARK, "On the Evaluation of Cross Section and Rate Constant of Atom-Diatom Reactions in the Sudden and Adiabatic Approximations", *Comp. Phys. Commun.* **52**, 291 (1989).

M. NAKAMURA and H. NAKAMURA, "Theory of Rotational Transition in Atom-Diatom Chemical Reaction", *J. Chem. Phys.* **90**, 4835 (1989).

K. NAKASHIMA, H. NAKAMURA, Y. ACHIBA and K. KIMURA, "Autoionization Mechanism of NO Molecule: Calculation of Quantum Defect and Theoretical Analysis of Multiphoton Ionization Experiment", *J. Chem. Phys.* **91**, 1603 (1989).

M. IWAI and H. NAKAMURA, "Generator-coordinate Representation of the O(4) Supermultiplets of Doubly Excited States", *Phys. Rev.* **A40**, 2247 (1989).

K. YAMAGUCHI, Y. TAKAHARA, T. FUENO and K. NASU, "Ab Initio MO Studies of Hole Delocalization in Copper Oxides and Related Species: Necessity of the Extended Hubbard Model", *Jpn. J. Appl. Phys.* **27**, L509 (1988).

K. YAMAGUCHI, Y. TAKAHARA, T. FUENO and K. NASU, "Ab Initio Molecular Orbital Calculations of Effective Exchange Integrals for Transition Metal Oxides and Halides: Strong Superexchange Interactions and High Tc Superconductivity", *Physica* **C153-155**, 1213 (1988).

K. NASU, "Superconductivities of a Quasi Two-Dimensional Peierls-Hubbard Model", *Physica* **C153-155**, 231 (1988).

K. NASU and A. MISHIMA, "Nonlinear Lattice Relaxation Process of Charge-Transfer Exciton in Quasi One-Dimensional Halogen-Bridged Mixed-Valence Metal Complexes, —Self-Trapped Excitons, Solitons and Polarons in CDW—", *Reviews of Solid State Science* (World Scientific, Singapore) **2**, 539 (1988).

A. MISHIMA and K. NASU, "Nonlinear Lattice Relaxation of Photo-Generated Charge-Transfer Excitation in Halogen-Bridged Mixed-Valence Metal Complexes I, — Soliton and Self-Trapped Exciton —", *Phys. Rev.* **B39**, 5758 (1989).

A. MISHIMA and K. NASU, "Nonlinear Lattice Relaxation of Photo-Generated Charge-Transfer Excitation in Halogen-Bridged Mixed Valence Metal Complexes II, — Polaron Channel —", *Phys. Rev.* **B39**, 5763 (1989).

A. MISHIMA and K. NASU, "Pair-Creation Path of Doubly Charged Spinless Soliton through Photoexcitation in Halogen-Bridged Metal Complexes", *Synthetic Metals* **29**, F175 (1989).

K. YAMAGUCHI, S. YAMAMOTO and K. NASU, "Electronic States of Cu-O Clusters by Ab Initio Calculations", *Solid State Physics* (AGUNE GIJUTSU CENTER, TOKYO, in Japanese) **24**, 353 (1989).

T. MOTOYAMA, N. KOYAMA and M. MATSUZAWA, "Electron-Impact Excitation of Atoms in High-lying Doubly Excited States: Correlation Effects in Collision Dynamics", *Phys. Rev.* **A32**, 670 (1988).

N. KOYAMA, A. TAKAFUJI and M. MATSUZAWA, "High-Lying Doubly Excited States of H^- and He: II $^1P^o$ States", *J. Phys. B At. Mol. Opt. Phys.* **22**, 553 (1989).

M. MATSUURA and Y. SHINOZUKA, "Excitons in Type II Quantum-Well Systems: Binding of the Spatially Separated Electron and Hole", *Phys. Rev.* **B38**, 9830 (1988).

M. MATSUURA and Y. SHINOZUKA, "Excitons in Type II Superlattice Systems", Proc. Int. Conf. on Electronic Materials '88.

H. KANAMORI and E. HIROTA, "Infrared Diode Laser Kinetic Spectroscopy of the CCD Radical ν_3 Band", *J. Chem. Phys.* **88**, 6699 (1988).

C. YAMADA and E. HIROTA, "Infrared Diode Laser Spectroscopy of Lithium Hydride", *J. Chem. Phys.* **88**, 6702 (1988).

T. SUZUKI and E. HIROTA, "Optical-Optical Double Resonance (Stimulated Emission Pumping) Spectroscopy of HCF", *J. Chem. Phys.* **88**, 6778 (1988).

N. ITABASHI, K. KATO, N. NISHIWAKI, T. GOTO, C. YAMADA and E. HIROTA, "Measurement of the SiH_3 Radical Density in Silane Plasma Using Infrared Diode Laser Absorption Spectroscopy", *Jpn. J. Appl. Phys.* **27**, L1565 (1988).

H. KANAMORI, E. TIEMANN and E. HIROTA, "Infrared Diode Laser Spectroscopy of SO in the $a^1\Delta$ State Generated by the Photolysis of Cl_2SO at 193 nm", *J. Chem. Phys.* **89**, 621 (1988).

K. KATO, N. ITABASHI, N. NISHIWAKI, T. GOTO, C. YAMADA and E. HIROTA, "Measurements of SiH ($X^2\Pi$: v=0) Radicals in Ar/SiH_4 Plasma Using an Infrared Diode Laser", *Proc. Jpn. Symp. Plasma Chem.* **1**, 11 (1988).

N. TANAKA, Y. HAMADA, C. YAMADA and E. HIROTA, "Molecular Parameters of the ν_2 Band of $^{15}N^{16}O_2$", *J. Mol. Spectrosc.* **131**, 44 (1988).

K. MATSUMURA, H. KANAMORI, K. KAWAGUCHI, E. HIROTA and T. TANAKA, "Infrared Diode Laser Spectroscopy of Triacetylene by the Source and the Stark Modulation Techniques", *J. Mol. Spectrosc.* **131**, 278 (1988).

K. MATSUMURA, H. KANAMORI, K. KAWAGUCHI and E. HIROTA, "Infrared Diode Laser Kinetic Spectroscopy of the ν_3 Band of C_3", *J. Chem. Phys.* **89**, 3491 (1988)..

H. KANAMORI and E. HIROTA, "Vibronic Bands of the CCH Radical Observed by Infrared Diode Laser Kinetic Spectroscopy", *J. Chem. Phys.* **89**, 3962 (1988).

K. KAWAGUCHI, T. AMANO and E. HIRORA, "Infrared Diode Laser Spectroscopy of the $\nu_2+\nu_3$ Band of CCH", *J. Mol. Spectrosc.* **131**, 58 (1988).

E. HIROTA, Y. ENDO, M. FUJITAKE, E.W. DELLA, P.E. PIGOU and J.S. CHICKOS, "Development of Millimeter- and Submillimeter-Wave Spectroscopy and its Application to Isotopically-Substituted Nonpolar Molecules, Deuterated Cubane and Deuterated Cyclobutanes", *J. Mol. Structure* **190**, 235 (1988).

K. TANAKA, M. FUJITAKE and E. HIROTA, "Submillimeter Wave Spectrum of the Vibrationally Induced Rotational Transitions of Allene in the Degenerate Vibrational States", *Chem. Phys. Lett.* **153**, 237 (1988).

Y, KAWASHIMA, Y. ENDO and E. HIROTA, "Microwave Spectrum, Molecular Structure, and Force Field of HBO", *J. Mol. Spectrosc.* **133**, 116 (1989).

N. ITABASHI, K. KATO, N. NISHIWAKI, T. GOTO, C. YAMADA and E. HIROTA, "Diffusion Coefficient and Reaction Rate Constant of the SiH_3 Radical in Silane Plasma", *Jpn. J. Appl. Phys.* **28**, L325 (1989).

C. YAMADA, M. FUJITAKE and E. HIROTA, "Detection of the NaO Radical by Microwave Spectroscopy", *J. Chem. Phys.* **90**, 3033 (1989).

A.L. VERMA, K. KIMURA, A. NAKAMURA, T. YAGI, H. INOKUCHI and T. KITAGAWA, "Resonance Raman Studies of Hydrogenase-catalyzed Reduction of Cytochrome c_3 by Hydrogen; Evidence for Heme-Heme Interactions", *J. Am. Chem. Soc.* **110**, 6617 (1988).

J. DE GROOT, R.E. HESTER, S. KAMINAKA and T. KITAGAWA, "Functional Activity of Haemoglobins Adsorbed on Colloidal Silver: A SERRS Study", *J. Phys. Chem.* **92**, 2044 (1988).

K. HOSOI, J. UTSUMI and T. KITAGAWA, "Structural Characterization of Fibroblast Human Interferon-β_1", *J. Interferon Res.* **8**, 375 (1988).

M. NAKAGAWA, T. OGURA, A. MAEDA and T. KITAGAWA, "Transient Resonance Raman Spectra of Neutral and Alkaline Bacteriorhodopsin Photointermediates by Using Double-Beam Flow Apparatus: Presence of Very Fast Decaying M_{412}", *Biochemistry* **28**, 1347 (1989).

P.K. KHULBE, A. AGARWAL, G.S. RAGHUVANSHI, H.D. BIST, H. HASHIMOTO, T. KITAGAWA, T.S. LITTLE and J.R. DURIG, "Raman Studies of the Vibrational Dynamics and Phase Transitions in Uranyl Nitrate Hexahydrate", *J. Raman Spectrosc.* **20**, 283 (1989).

Y. MIZUTANI, K. KAMOGAWA and K. NAKANISHI, "Effect of Urea on Hydrophobic Interaction: Raman Difference Spectroscopy on the C-H Stretching Vibration of Acetone and the C-H Stretching Vibration of Urea", *J. Phys. Chem.* **93**, 5650 (1989).

M. NAKAGAWA, A. MAEDA, T. OGURA and T. KITAGAWA, "Origin of Raman Spectral Difference Between the Spinning-cell and Flow-cell Measurements for Bacteriorhodopshin Photointermediates", *J. Raman Spectrosc.* **20**, 303 (1989).

S. KAMINAKA, T. OGURA, K. KITAGISHI, T. YONETANI and T. KITAGAWA, "Resonance Raman Spectra of Intermediate Ligated Forms of Hemoglobin: The $\nu_{Fe\text{-}His}$, $\nu_{Fe\text{-}CO}$, δ_{FECO}, and ν_{OO} Modes of Cross-Linked Fe-CO Hybrid Hemoglobins", *J. Am. Chem. Soc.* **111**, 3787 (1989).

M. NAGAI, Y. YONEYAMA and T. KITAGAWA, "Characteristic in Tyrosine Coordination of Four Hemoglobins M Probed by Resonance Raman Spectroscopy", *Biochemistry* **28**, 2418 (1989).

Y. OZAKI, K. AOYAGI, K. IRIYAMA, H. OGOSHI and T. KITAGAWA, "Resonance Raman Characteristics of N-Methyl-Octaethylporphyrinatocobalt (II)", *J. Phys. Chem.* **93**, 3842 (1989).

S. HASHIMOTO, R. NAKAJIMA, I. YAMAZAKI, T. KOTANI, S. OHTAKI and T. KITAGAWA, "Resonance Raman Characteristics of Hog Thyroid Peroxidase: A SERRS Study", *FEBS Lett.* **248**, 205 (1989).

A.L. VERMA, K. KIMURA, T. YAGI, A. NAKAMURA, H. INOKUCHI and T. KITAGAWA, "SERR Evidence for Enzymic Reduction of Cytochrome c_3 Adsorbed on Ag Colloids", *Chem. Phys. Lett.* **159**, 189 (1989).

T. MIZUSHIMA, K. TOHJI, Y. UDAGAWA, M. HARADA, M. ISHIKAWA and A. UENO, "Characterization of Silica Supported Bimetallic Iron-Nickel Catalysts by EXAFS", *J. Catal.* **112**, 282 (1988).

T. KUGITA, K. MOCHIDA, K. TOHJI and Y. UDAGAWA, "Unusual Long Distances of Germanium-Carbon Bond of Organogermyl-alkali Metal Probed by EXAFS", *Chem. Lett. 501*, (1989).

T. MIZUSHIMA, K. TOHJI and Y. UDAGAWA, "An EXAFS Study on the Morphology Change of Ru/Al_2O_3 by CO Adsorption", *Physica* **B158**, 195 (1989).

K. TOHJI and Y. UDAGAWA, "A Double Crystal Spectrometer for EXAFS Spectroscopy", *Physica* **B158**, 332 (1989).

Y. UDAGAWA and K. TOHJI, "Observation of X-ray Raman Scattering", *Physica* **B158**, 550 (1989).

F. OKUMURA, N. KAKUTA, A. UENO, R. MORIMO, T. MIZUSHIMA, Y. UDAGAWA and H. NAMIKAWA, "Preparation and Characterization of Aluminum-doped SiO_2:Sm^{+3} Phosphor", *Chem. Lett. 829*, (1989).

K. TOHJI and Y. UDAGAWA, "X-ray Raman Scattering as a Substitute for Soft X-ray EXAFS", *Phys. Rev.* **B39**, 7590 (1989).

H. PETEK, Y. FUJIWARA, D. KIM and K. YOSHIHARA, "Observation of a Local Minimum on the S_1 Surface of cis-Stilbene Solvated in Inert Gas Clusters.", *J. Am. Chem. Soc.* **110**, 6269 (1988).

N. IKEDA, M. KOSHIOKA, H. MASUHARA and K. YOSHIHARA, "Picosecond Dynamics of Excited Singlet States in Organic Microcrystals: Diffuse Reflectance Laser Photolysis Study.", *Chem. Phys. Lett.* **150**, 452 (1988).

H. NAKAMURA, H. FUJII, H. SAKAGUCHI, T. MATSUO, N. NAKASHIMA, K. YOSHIHARA, T. IKEDA and S. TAZUKE, "Laser-Induced Electron Liberation from Carbazole-Containing Bilayer Membranes in Aqueous Systems.", *J. Phys. Chem.* **92**, 6151 (1988).

A. GRABOWSKA, A. MORDZINSKI, N. TAMAI and K. YOSHIHARA, "Picosecond Kinetics of the Excited-State Intramolecular Proton Transfer Reaction: Confirmation of the Intrinsic Potential Barrier in 2,5-Bis-(Benzoxazolyl)-Hydroquinone.", *Chem. Phys. Lett.* **153**, 389 (1988).

S. MEECH and K. YOSHIHARA, "Picosecond Dynamics of Adsorbates by Time-Resolved Surface Second-Harmonic Generations." *Chem. Phys. Lett.* **154**, 20 (1988).

N. SHIMO, N. NAKASHIMA and K. YOSHIHARA, "Laser-Ignited Explosive Decomposition of Organometallic Compounds.", *Chem. Phys. Lett.* **156**, 31 (1988).

Y. TAKAGI and K. YOSHIHARA, "Two-Photon Absorption Sampling Spectroscopy for Fast Transient Luminescence Measurements.", in "Ultrafast Phenomena VI", T. Yajima, K. Yoshihara, C.B. Harris, and S. Shionoya Eds. Springer, Berlin, 407 (1988).

N. IKEDA, M. KOSHIOKA, H. MASUHARA, N. NAKASHIMA and K. YOSHIHARA, "Direct Observation of Photophysics in Opaque Organic Microcrystals: A Picosecond Diffuse Reflectance Laser Photolysis Study.", in "Ultrafast Phenomena VI", T. Yajima, K. Yoshihara, C.B. Harris and S. Shionoya Eds. Springer, Berlin, 428 (1988).

D. KIM, K. YOSHIHARA and I. IKEGAMI, "Picosecond Photochemistry of P700-Enriched and Vitamin K_1-Depleted Photosystem I Particles Isolated from Spinach.", *Plant Cell Physiol.* **30**, 679 (1989).

T. EBBESEN, K. TOKUMARU, M. SUMITANI and K. YOSHIHARA, "Charge Transfer and Cis-Trans Isomerization.", *J. Phys. Chem.* **93**, 5453 (1989).

N. NAKASHIMA and K. YOSHIHARA, "Role of Hot Molecules Formed by Internal Conversion in UV Single-Photon and Multiphoton Chemistry.", *J. Phys. Chem.* **93**, 7763 (1989). A Feature Article.

M. AZUMA, K. HASHIMOTO, M. HIRAMOTO, M. WATANABE and T. SAKATA, "Carbon Dioxide Reduction at Low Temperature on Various Metal Electrodes", *J. Electroanal. Chem.* **260**, 441 (1989).

H. SHINOHARA, N. NISHI and N. WASHIDA, "Experimental Evidence of the Magic Number Stability of the Hydrated Ammonia Cluster Ions $(H_2O)(NH_3)_{0-4}NH_4^+$", *Chem. Phys. Lett.* **153**, 417 (1988).

M. KAWASAKI, H. SATO and N. NISHI, "Laser Photodissociation of Chlorine and Methylchloride on Low-temperature Silicon Substrates", *J. Appl. Phys.* **65**, 792 (1988).

H. SHINOHARA and N. NISHI, "Higher Electronically Excited States of Benzene Clusters", *Chem. Phys.* **129**, 149 (1989).

N. NISHI and H. SHINOHARA, "Intra-cluster Ion-molecule Reactions and Photodissociation of Molecular Clusters", *Z. Phys. D.* **12**, 269 (1989).

F. MISAIZU, P.L. HOUSTON, N. NISHI, T. KONDOW and M. KINOSHITA, "The Dissociation Dynamics and Multiphoton Ionization Mechanism of Ammonia Clusters", *J. Phys. Chem.* **93**, 5224 (1989).

R. NAKAGAKI, K. MUTAI, M. HIRAMATSU, H. TUKADA and S. NAGAKURA, "Magnetic Field Effects upon Photochemistry of Bichromophoric Chain Molecules Containing Nitro-aromatic and Arylamino Moieties: Elucidation of Reaction Mechanism and Control of Reaction Yields", *Can. J. Chem.* **66**, 1989 (1988).

R. NAKAGAKI, K. MUTAI and S. NAGAKURA, "Photochemistry of Chain Molecules Containing 4-Nitro-1-naphthoxyl and Anilino Chromophores. Switching of Reaction Pathways due to Methylene Chain Length and Magnetic Field Effects", *Chem. Phys. Lett.* **154**, 581 (1989).

Y. TANIMOTO, K. HASEGAWA, N. OKADA, M. ITOH, K. IWAI, K. SUGIOKA, F. TAKEMURA, R. NAKAGAKI and S. NAGAKURA, "Magnetic Field Effects on the Intra- and Intermolecular Exciplex Fluorescence of Phenanthrene and Dimethylaniline", *J. Phys. Chem.* **93**, 3586 (1989).

Y. TANIMOTO, C. JINDA, Y. FUJIWARA, M. ITOH, K. HIRAI, H. TOMIOKA, R. NAKAGAKI and S. NAGAKURA, "Laser Flash Photolysis Studies of the Magnetic Field Effects on the Hydrogen Abstraction Reaction of 2-Naphthylphenylcarbene in Micellar Solution", *J. Photochem. Photobiol.* **A47**, 269 (1989).

T. IMAMURA, S. NAGAKURA, H. ABE, Y. FUKUDA and H. HAYASHI, "External Magnetic Field Effect on CS_2 Banded Emission. Laser Excitation in the Wavelength Region of a Nitrogen Laser", *J. Phys. Chem.* **93**, 69 (1989).

M. BABA, M. KIMURA, T. TSUBOI, H. KATO and S. NAGAKURA, "The Magnetic Predissociation of the $B^3\Pi_{ou}^+$ State of the Iodine Molecule", *Bull. Chem. Soc. Jpn.* **62**, 17 (1989).

A. UGAWA, G. OJIMA, K. YAKUSHI and H. KURODA, "Optical and Electrical Properties of an Organic Superconductor, di[bis(ethylenedithio)tetrathiafulvalenium] dithiocyanocuprate(I), $(BEDT\text{-}TTF)_2[Cu(SCN)_2]$", *Phys. Rev.* **B38**, 5122 (1988).

A. UGAWA, Y. OKAWA, K. YAKUSHI, H. KURODA, A. KAWAMOTO, J. TANAKA, M. TANAKA, Y. NOGAMI, S. KAGOSHIMA, K. MURATA and T. ISHIGURO, "Physical Properties of β''-$(BEDT\text{-}TTF)_2ICl_2$", *Synth. Met.* **27**, A407 (1988).

A. UGAWA, G. OJIMA, K. YAKUSHI and H. KURODA, "Infrared Properties of a Novel Organic Superconductor, $(BEDT\text{-}TTF)_2[Cu(SCN)_2]$", *Synth. Met.* **27**, A445 (1988).

H. KURODA, K. YAKUSHI, H. TAJIMA, A. UGAWA, M. TAMURA, Y. OKAWA, A. KOBAYASHI, R. KATO, H. KOBAYASHI and G. SAITO, "Reflectance Spectra of β-, θ-, and $\varkappa$-$(BEDT\text{-}TTF)_2I_3$, and β''- and β'-$(BEDT\text{-}TTF)_2ICl_2$: Relation between the Interband Transition and the Dimeric Structure", *Synth. Met.* **27**, A491 (1988).

K. YAKUSHI, G. OJIMA, A. UGAWA and H. KURODA, "Spectroscopic Evidence for the Inter-Chain Charge-Transfer Interaction in Copper-bis(2,5-dimethyl-*N,N'*-dicyanoquinonediimine), $Cu(2,5\text{-}DM\text{-}DCNQI)_2$", *Chem. Lett.* **95**, (1988).

K. YAKUSHI, M. YOSHITAKE, H.KURODA, A. KAWAMOTO, J. TANAKA, T. SUGANO and M. KINOSHITA, "Preparation and Characterization of (Tetrabenzoporphyrinato)-nickel Hexafluoroarsenate, $(NiTBP)_3(AsF_6)_2(C_{10}H_7Cl)$. A New Type of Metallomacrocyclic Radical Salts", *Bull. Chem. Soc. Jpn.* **61**, 1571 (1988).

K. YAKUSHI, H. YAMAKADO, M. YOSHITAKE, N. KOSUGI, H. KURODA, T. SUGANO, M. KINOSHITA, A. KAWAMOTO and J. TANAKA, "Electrochemical Preparation and Characterization of the Radical Salts of (Phthalocyaninato)nickel, $NiPc(SbF_6)_{0.5}$, and $NiPc(AsF_6)_{0.5}$", *Bull. Chem. Soc. Jpn.* **62**, 687 (1989).

K. YAKUSHI, H. YAMAKADO, M. YOSHITAKE, N. KOSUGI, H. KURODA, A. KAWAMOTO, J. TANAKA, T. SUGANO, M. KINOSHITA and S. HINO, "Preparation and Characterization of the Cation Radical Salts of Phthalocyanine and Tetrabenzoporphyrin", *Synth. Met.* **29**, F95 (1989).

H. YAMAKADO, K. YAKUSHI, N. KOSUGI, H. KURODA, A. KAWAMOTO, J. TANAKA, T. SUGANO, M. KINOSHITA and S. HINO, "Preparation, Crystal Structure, and Solid State Properties of Highly Conductive (Phtalocyaninato)platinum Radical Salts: $PtPc(ClO_4)_{0.5}$ and $PtPc(AsF_6)_x$", *Bull. Chem. Soc. Jpn.* **62**, 2267 (1989).

S. TOMODA, S. SUZUKI and I. KOYANO, "State Selected Ion-Molecule Reactions by the TESICO Technique. XV. Hydrogen Atom Abstraction as an Electron Jump Followed by Proton Transfer in the $ND_3^+(v) + NH_3$ and $NH_3^+(v) + ND_3$ Reactions", *J. Chem. Phys,* **89**, 7268 (1988).

T. MASUOKA, T. HORIGOME and I. KOYANO, "Construction of a New Apparatus for Angle and Energy Resolved Measurements of Photoelectrons and Photoions", *Rev. Sci. Instrum.* **60**, 2179 (1989).

S. SUZUKI, T. IMAMURA, I. KOYANO and K. OKUNO, "Performance of a Dodecapole Collision Chamber for the Study of Ion-Molecule Reactions Using Synchrotron Radiation", *Rev. Sci. Instrum.* **60**, 2186 (1989).

S. NAGAOKA, S. SUZUKI, U. NAGASHIMA, T. IMAMURA and I. KOYANO, "Investigation of Fragmentation Processes Following Core Photoexcitation of Trimethylgallium in the Vapor Phase", *Rev. Sci. Instrum.* **60**, 2201 (1989).

T. IMAJO, T. IMAMURA and I. KOYANO, "Collisional Quenching of the CO^+ $A^2\Pi(v=1)$ State by He, Ne, Ar, N_2 and CO", *Chem. Phys. Lett.* **160**, 143 (1989).

K. HONMA, K. TANAKA, S. SUZUKI and I. KOYANO, "A TPEPICO Study of Dissociative Photoionization of $C_2H_2D_2$ Isomers", *Int. J. Mass Spectrom. Ion Process.* **93**, 1 (1989).

K. UEDA, E. SHIGEMASA, Y. SATO, S. NAGAOKA, I. KOYANO, A. YAGISHITA, T. NAGATA and T. HAYAISHI, "Ionic Fragmentation Following the 3d Core Excitation of $Sn(CH_3)_4$ by Soft X-rays", *Chem. Phys. Lett.* **154**, 357 (1989).

S. NAGAOKA, I. KOYANO, K. UEDA, E. SHIGEMASA, Y. SATO, A. YAGISHITA, T. NAGATA and T. HAYAISHI, "Site-Specific Fragmentation Following Inner-Core Level Excitation of $Pb(CH_3)_4$ in the Vapor Phase", *Chem. Phys. Lett.* **154**, 363 (1989).

K. KIMURA, K. SATO, K. OKUYAMA and M. TAKAHASHI, "Picosecond Pulse Laser Photoelectron Spectra of Some Molecular Excited States", in *"Ultrafast Phenomena", Vol. VI, ed. by T. Yajima et al., (Springer-Verlag, New York, 1988),* p.483.

Y. ACHIBA and K. KIMURA, "Optical-Optical Double Resonance MPI Photoelectron Spectroscopy of the NO Molecule via the $C^2\Pi$ (v=4) State: *n*s and *n*d Rydberg Series", *Chem. Phys.* **129**, 11 (1989).

H. SHIROMARU, H. SUZUKI, H. SATO, S. NAGAOKA and K. KIMURA, "Synchrotron Radiation Study on Small Binary Molecular Clusters. Ar-Water and CO_2-Water Systems", *J. Phys. Chem.* **93**, 1832 (1989).

K. NAKASHIMA, H. NAKAMURA, Y. ACHIBA and K. KIMURA, "Autoionization Mechanisms of NO Molecule: Calculation of Quantum Defect and Theoretical Analysis of REMPI Experiment", *J. Chem. Phys.* **91**, 1603 (1989).

S. HIRAYAMA, F. TANAKA and K. SHOBATAKE, "Vibronic-level Specific Heavy Atom Effect on the Fluorescence Decays of the Rare Gas Complexes of 9-Methoxyanthracence", *Chem. Phys. Lett.* **153**, 112 (1988).

S. HIRAYAMA, A. ADACHI, F. TANAKA, K. SHOBATAKE and K.-H. JUNG, "Fluorescence Decays in a Wide Variety of van der Waals Complexes of 9-Cyanoanthracene in Supersonic Free Jets", *J. Chem. Soc. Faraday Trans. 2*, **84**, 1927 (1988).

I. TOKUE, A. HIRAYA and K. SHOBATAKE, "Photoabsorption Spectra and Photodissociation of S_2Cl_2 in the Vacuum Ultraviolet", *Chem. Phys. Lett.* **153**, 346 (1988).

F. TANAKA, S. YAMASHITA, S. HIRAYAMA, A. ADACHI and K. SHOBATAKE, "Fluorescence Decays of 9, 10-Dichloroanthracene and its van der Waals Complexes with Rare Gas Atoms in Supersonic Free Jets", *Chem. Phys.* **131**, 435 (1989).

I. TOKUE, A. HIRAYA and K. SHOBATAKE, "Photoexcitation of Dimethyl Disulfide in the Vacuum Ultraviolet Region: Rydberg States and Photofragment Emissions", *Chem. Phys.* **130**, 401 (1989).

T. IBUKI, A. HIRAYA and K. SHOBATAKE, "Photoabsorption Spectrum and $CCl_2(A^1B_1)$ Radical Formation via VUV Excitation of C_2Cl_6", *Chem. Phys. Lett.* **157**, 521 (1989).

T. IBUKI, A. HIRAYA and K. SHOBATAKE, "Photochemistry of CCl_3F and CCl_2F_2 in the 106-200 nm region", *J. Chem. Phys.* **90**, 6290 (1989).

S. HIRAYAMA, F. TANAKA and K. SHOBATAKE, "Vibrational Predissociation of Rare-gas van der Waals Complexes of 9-Methoxyanthracene", *J. Chem. Soc. Jpn.* (in Japanese), **1989**, 1217 (1989).

T. IBUKI, A. HIRAYA, K. SHOBATAKE, Y. MATSUMI and M. KAWASAKI, "He(I) Photoelectron Spectra and VUV Absorption Cross Sections of $Ga(CH_3)_3$ and $In(CH_3)_3$", *Chem. Phys. Lett.* **160**, 152 (1989).

I. TOKUE, A. HIRAYA and K. SHOBATAKE, "Vacuum Ultraviolet Absorption Spectra of Thiirane and Thietane", *J. Chem. Phys.* **91**, 2808 (1989).

N. HOSHINO, T. INABE, T. MITANI and Y. MARUYAMA, "Structure and Optical Properties of a Thermochromic Schiff Base. Thermally Induced Intramolecular Proton Transfer in the *N,N'*-Bis(salicylidene)-*p*-phenylenediamine Crystals.", *Bull. Chem. Soc. Jpn.* **61**, 4207 (1988).

T. INABE, T. MITSUHASHI and Y. MARUYAMA, "Charge Transfer Complexes Based on the Twin-TCNQ-Type Acceptor 11,11,12,12,13,13,14,14-Octacyano-1,4:5,8-anthradiquinotetramethane (OCNAQ).", *Bull. Chem. Soc. Jpn.* **61**, 4215 (1988).

H. URAYAMA, H. YAMOCHI, G. SAITO, S. SATO, T. SUGANO, M. KINOSHITA, A. KAWAMOTO, J. TANAKA, T. INABE, T. MORI, Y. MARUYAMA, H. INOKUCHI and K. OSHIMA, "Crystal and Electronic Structures and Physical Properties of T_c=10.4K Superconductor, $(BEDT\text{-}TTF)_2Cu(NCS)_2$.", *Synth. Met.* **27**, A393 (1988).

T. INABE and Y. MARUYAMA, "Crystal Structure of the Electrochemical Product of Potassium Dicyanophthalocyaninatocobalt (III). Novel Two-Dimensional Stacking Interaction of Phthalocyanine.", *Chem. Lett.* **1989**, 55.

Y. MARUYAMA, T. INABE, T. NISHII, L. HE, A.J. DANN, I. SHIROTANI, M.R. FAHY and M.R. WILLIS, "Electrical Conductivity of Black Phosphorus-Silicon Compound.", *Synth. Met.* **29**, F213 (1989).

Y. KAWAI, Y. MARUYAMA, T. TERUI and I. SHIROTANI, "Thin Films of the Y-Ba-Cu-O System Prepared by RF-Magnetron Sputtering.", *Synth. Met.* **29**, F685 (1989).

T. INABE, N. HOSHINO, T. MITANI and Y. MARUYAMA, "Structure and Optical Properties of a Thermochromic Schiff Base. Low-Temperature Structural Studies of the *N,N'*-Disalicylidene-*p*-phenylenediamine and *N,N'*-Disalicylidene-1,6-pyrenediamine Crystals.", *Bull. Chem. Soc. Jpn.* **62**, 2245 (1989).

S. SUGAI, S. SHAMOTO and M. SATO, "Two Magnon Raman Scattering in $(La_{1-x}Sr_x)_2CuO_4$.", *Phys. Rev.* **B38**, 6436 (1988).

R. J. BIRGENEAU, D.R. GABBE, H.P. JENSSEN, M.A. KASTNER, P.J. PICONE, T.R. THURSTON, G. SHIRANE, Y. ENDOH, M. SATO, K. YAMADA, H. HIDAKA, M. ODA, Y. ENOMOTO, M. SUZUKI and T. MURAKAMI, "Antiferromagnetic Spin Correlation in Insulating, Metallic and Superconducting $La_{2-x}Sr_xCuO_4$.", *Phys. Rev.* **B38**, 6614 (1988).

M.A. KASTNER, R.J. BIRGENEAU, T.R. THURSTON, P.J. PICONE, H.P. JENSSEN, D.R. GABBE, M. SATO, K. FUKUDA, S. SHAMOTO, Y. ENDOH, Y. YAMADA and G. SHIRANE, "Neutron Scattering Study of the Transition from Antiferromagnetic to Weak Ferromagnetic Order in La_2CuO_4.", *Phys. Rev.* **B38**, 6636 (1988).

Y. ANDO, K. FUKUDA, S. KONDOH, M. SERA, M. ONODA and M. SATO, "Study on Normal and Superconducting Properties of $Bi_4Sr_3(Ca_{1-x}Y_x)_3Cu_3O_y$.", *Solid State Commun.* **67**, 815 (1988).

J.P. POUGET, S. GIRAULT, A.H. MOUDDEN, B. HENNION, E. ESCRIBE-FILLIPPINI and M. SATO, "Structural Aspects of Charge Density Waves in the Blue Bronzes.", *Physica Scripta* **T25**, 58 (1989).

M. SERA, S. SHAMOTO and M. SATO, "Anisotropic Thermoelectric Power of $YBa_2Cu_3O_{7-\delta}$ and $(La_{1-x}Sr_x)_2CuO_4$ Single Crystals.", *Solid State Commun.* **68**, 649 (1988).

M. SERA, S. KONDOH and M. SATO, "Thermoelectric Power of Superconducting Ba-K-Bi-O with Perovskite Structure.", *Solid State Commun.* **68**, 647 (1988).

T.R. THURSTON, R.J. BIRGENEAU, D.R. GABBE, H.P. JENSSEN, M.A. KASTNER, P.J. PICONE, N.W. PREYER, J.D. AXE, P. BÖNI, G. SHIRANE, M. SATO, K. FUKUDA and S. SHAMOTO, "Neutron Scattering Studies of Magnetic Excitations in $La_{2-x}Sr_xCuO_4$.", *Proc. Int. Symp. on the Electronic Structure of the High-T_c Superconductors* 1988 *Rome.*

M. SATO, M. SERA, S. SHAMOTO, M. ONODA, S. KONDOH, K. FUKUDA and Y. ANDO, "Recent Experimental Studies on High-T_c Oxides at IMS.", in "Mechanisms of High Temperature Superconductivity", edited by H. Kamimura and A. Oshiyama, Springer Verlag, p.275.

M. SERA, Y. ANDO, S. KONDOH, K. FUKUDA, M. SATO, I. WATANABE, S. NAKASHIMA and K. KUMAGAI, "Transport and Magnetic Anomalies in $La_{2-x}Sr_xCuO_4$.", *Solid State Commun.* **69**, 851 (1989).

H. FUJISHITA, S. SHAMOTO, M. ONODA and M. SATO, "Crystal Structure of Superconducting $LnBaAeCu_3O_y$ (Ln=La, Nd; Ae=Ca, Sr).", *Jpn. J. Appl. Phys.* **28**, 754 (1989).

S. KONDOH, M. SERA, Y. ANDO and M. SATO, "Normal State Properties and Oxygen Isotope Effect of $(Ba,K)BiO_3$.", *Physica* **C157**, 469 (1989).

M. ONODA and M. SATO, "EPR Study on Dynamics of Electrons in Superconducting and Normal Metallic $(La_{1-x}Sr_x)_2CuO_{4-\delta}$ System.", *Solid State Commun.* **70**, 309 (1989).

T. TAKAHASHI, H. MATSUYAMA, H. KAYATAMA-YOSHIDA, Y. OKABE, S. HOSOYA, K. SEKI, H. FUJIMOTO, M. SATO and H. INOKUCHI, "*Proc. 1st. Int. Symp. on Superconductivity* 1988 *Nagoya,* Springer Verlag, p.175.

M. ONODA, S. KONDOH and M. SATO, "Oxygen Isotope Effect of Superconducting $(Nd_{1-x}Ce_x)_2CuO_{4-\delta}$ System.", *Solid State Commun.* **70**, 1141 (1989).

S. SUGAI and M. SATO, "Magnon and Phonon Raman Scattering in $Bi_2Sr_2Ca_{1-x}Y_xCu_2O_{8+y}$.", *Phys, Rev.* **B40**, 9292 (1989).

J. M. TRANQUADA, G. SHIRANE, B. KEIMER, S. SHAMOTO and M. SATO, "Neutron Scattering Study of Magnetic Excitations in $YBa_2Cu_3O_{6+x}$.", *Phys. Rev.* **B40**, 4503 (1989).

M. SATO, S. KONDOH and M. SERA, "Physical Properties of $(Ba,K)BiO_3$.", *Proc. IBM-Japan Symp. on Strong Correlation and Superconductivity* 1989 *Hakone,* Springer Verlag, p.341.

M. ONODA and M. SATO, "Anomaly of Magnetoresistance in Normal State of $(Nd_{1-x}Ce_x)_2CuO_4$ System.", *Solid State Commun.* **72**, 537 (1989).

H. FUJISHITA and M. SATO, "Comparison of the Normal State Properties between the Superconducting and the Nonsuperconducting Metallic Phases in $La_{2-y}Sr_yCu_{1-x}Ni_xO_4$.", *Solid State Commun.* **72**, 529 (1989).

T. MATSUSHIMA, "Anisotropic Angular Distribution of Desorption of CO_2 Produced on Pd(110) Surfaces", *Chem. Phys. Lett.* **155**, 313 (1989).

T. MATSUSHIMA, "Angular Distribution of the Desorption of Carbon Monoxide and the Exchange Reaction over Alkali-Covered Noble Metal Surfaces", *Z. Phys. Chem. N.F.* **162**, 1 (1989).

T. MATSUSHIMA, "Adsorption and Dissociation of Oxygen Molecules on Palladium (110) Surfaces at Low Temperatures", *Surface Science* **217**, 155 (1989).

Z.R. SHI, T. ENOKI, K. IMAEDA, K. SEKI, P.J. WU, H. INOKUCHI and G. SAITO, "Thermal Properties of Tetrakis(alkylthio)tetrathiafulvalene (TTC_n-TTF)", *J. Phys, Chem.* **92**, 5044 (1988).

N. SATO, G. SAITO and H. INOKUCHI, "Ultraviolet Photoelectron Spectra of Hexamethylenetetratellurafulvalene (HMTTeF) in the Gaseous and Solid State", *Chem. Phys.* **126**, 395 (1988).

M. MITSUYA, K. SEKI and H. INOKUCHI, "Ultraviolet Photoelectron Spectroscopic Study of Perfluorinated Carboxylic Acid Monolayer Films Prepared by Vacuum Deposition", *J. Appl. Phys.* **64**, 4150 (1988).

T. TAKAHASHI, H. MATSUYAMA, H. KATAYAMA-YOSHIDA, Y. OKABE, S. HOSOYA, K. SEKI, H. FUJIMOTO, M. SATO and H. INOKUCHI, "Photoemission Study of Single Crystal $Bi_2Sr_2CaCu_2O_8$", Proceedings of the 1st International Symposium on Superconductivity (ISS '89), Nagoya, August 28-31 1988, "*Advances in Superconductivity*" (K. Kitazawa and T. Ishiguro eds.) p.175 Springer-Verlag Tokyo (1989).

T. TAKAHASHI, H. MATSUYAMA, H. KATAYAMA-YOSHIDA, Y. OKABE, S. HOSOYA, K. SEKI H. FUJIMOTO, M. SATO and H. INOKUCHI, "Band Structure of $Bi_2Sr_2CaCu_2O_8$ Studied by Angle-Resolved Photoemission", *Phys. Rev.* **B39**, 6636 (1989).

T.B. TANG, H. YAMAMOTO, H. INOKUCHI, K. SEKI, M. OKAZAKI and T. TANI, "Electronic Structure of Thiacyanine Dyes in the Solid State", *J. Phys. Chem.* **93**, 3970 (1989).

U. NAGASHIMA, H. FUJIMOTO, H. INOKUCHI and K. SEKI, "Electronic and Geometric Structures of Oligothiophenes", *J. Mol. Struct.* **197**, 265 (1989).

P. WANG, T. MORI, C. NAKANO, Y. MARUYAMA, H. INOKUCHI, N. IWASAWA, H. YAMOCHI, H. URAYAMA and G. SAITO, "Crystal Structures and Electrical Properties of $TSeC_n$-TTF (n=2 and 4)", *Bull. Chem. Soc. Jpn.* **61**, 3455 (1988).

P. WANG, T. INABE, C. NAKANO, Y. MARUYAMA, H. INOKUCHI, N. IWASAWA and G. SAITO, "Crystal Structures and Electrical Properties of Tetrakis(methylseleno)tetrathiafulvalene ($TSeC_1$-TTF) and Two Phases of $(TSeC_1\text{-TTF})I_3$", *Bull. Chem. Soc. Jpn.* **62**, 2252 (1989).

P. WANG, T. ENOKI, K. IMAEDA, N. IWASAWA, H. YAMOCHI, H. URAYAMA, G. SAITO and H. INOKUCHI, "Thermal and Electrical Properties of Tetrakis(alkylseleno)tetrathiafulvalenes ($TSeC_n$-TTF, n=1-18)", *J. Phys. Chem.* **93**, 5947 (1989).

H. YAMAMOTO, K. SEKI, T. ENOKI and H. INOKUCHI, "Ultraviolet Photoelectron Spectroscopy of Ternary Graphite Intercalation Compound C_8KH_x", *Solid State Commun.* **69**, 425 (1989).

K. OSHIMA, T. MORI, H. INOKUCHI, H. URAYAMA, H. YAMOCHI and G. SAITO, "Shubnikov-de Haas Effect and the Fermi Surface in an Ambient-Pressure Organic Superconductor [Bis(ethylenedithio)tetrathiafulvalene]$_2$Cu(NCS)$_2$", *Phys. Rev.* **B38**, 938 (1988).

K. OSHIMA, T. MORI, H. INOKUCHI, H. URAYAMA, H. YAMOCHI and G. SAITO, "Fermi Surface and Pressure Effect in (BEDT-TTF)$_2$Cu(NCS)$_2$", *Synth. Met.* **27**, A165 (1988).

H. KOBAYASHI, R. KATO, A. KOBAYASHI, T. MORI, H. INOKUCHI, Y. YOSHINO, K. KAJITA and W. SASAKI, "Molecular Design and Solid State Properties of New Superconductors and Molecular Metals with Ordered Spin Structures", *Synth. Met.* **27**, A289 (1988).

T. MORI, P. WANG, K. IMAEDA, T. ENOKI, H. INOKUCHI, F. SAKAI and G. SAITO, "An Organic Superconductor, (BEDT-TTF)$_3$Cl$_2$(H$_2$O)$_2$, and Some Other BEDT-TTF Conductors", *Synth. Met.* **27**, A451 (1988).

T. MORI, H. INOKUCHI, A. KOBAYASHI, R. KATO and H. KOBAYASHI, "Coexistence of a Magnetic Order and Metallic Conduction in an Organic System, (DMDCNQI)$_2$Cu", *Synth. Met.* **27**, B237 (1988).

R. KATO, H. KOBAYASHI, A. KOBAYASHI, T. MORI and H. INOKUCHI, "Preparation and Structure of Highly Conductive Anion Radical Salts, M(2,5-R_1, R_2-DCNQI)$_2$ (DCNQI=*N,N'*-dicyanoquionediimine; R_1, R_2=Me, MeO, halogen; M=Ag, Li, Na, K. NH_4)", *Synth. Met.* **27**, B263 (1988).

A. KOBAYASHI, T. MORI, H. INOKUCHI, R. KATO and H. KOBAYASHI, "The Organic π-Electron Metal System with Interaction through Mixed-Valence Metal Cation: Electronic and Structural Properties of Highly Conducting Anion Radical Salts (2,5-R_1, R_2-DCNQI)$_2$Cu (DCNQI=*N,N'*-dicyanoquinonediimine; R_1, R_2=CH_3, CH_3O, Cl, Br)", *Synth. Met.* **27**, B275 (1988).

R. KATO, H. KOBAYASHI, H. KIM, A. KOBAYASHI, Y. SASAKI, T. MORI and H. INOKUCHI, "Structual and Electrical Properties of a New Two-Dimensional Molecular Metals, $Et_2Me_2N[Ni(dmit)_2]_2$", *Synth. Met.* **27**, B359 (1988).

N. IWASAWA, H. URAYAMA, H. YAMOCHI, G. SAITO, K. IMAEDA, T. MORI, Y. MARUYAMA, H. INOKUCHI, T. ENOKI, Y. HIGUCHI and N. YASUOKA, "Preparation, Structure, and Physical Properties of a Series of Uncapped $C_6X_4Y_4$ (X, Y=Sulfur, Selenium, Tellurium) Compounds", *Synth. Met.* **27**, B463 (1988).

T. MORI and H. INOKUCHI, "Thermoelectric Power of Organic Superconductors-Calculation on the Basis of the Tight-Binding Theory", *J. Phys. Soc. Jpn.* **57**, 3674 (1988).

T. MORI and H. INOKUCHI, "Metal-to-Semiconductor Transition of an Organic Metal, (EDT-TTF)$_2$AuBr$_2$", *Solid State Commun.* **70**, 823 (1989).

K. IMAEDA, T. ENOKI, T. MORI, H. INOKUCHI, M. SASAKI, K. NAKASUJI and I. MURATA, "Electronic Properties of New Organic Conductors Based on 2,7-Bis(methylthio)-1,6-dithiapyrene (MTDTPY) with TCNQ and p-Benzoquinone Derivatives", *Bull. Chem. Soc. Jpn.* **62**, 372 (1989).

M. TANAKA, H. TAKEUCHI, M. SANO, T. ENOKI, K. SUZUKI and K. IMAEDA, "Electrical and Magnetic Properties of (BEDT-TTF)$_4$Ni(CN)$_4$ Complex", *Bull. Chem. Soc. Jpn.* **62**, 1432 (1989).

Y. HAYASHI, Y. OZAWA, and K. ISOBE, "The First "Vanadate Hexamer" Capped by Four Pentamethylcyclopentadienyl-rhodium or -iridium Groups.", *Chem. Lett.* 425 (1989).

K. ISOBE, Y. NAKAMURA, and S. KAWAGUCHI, "Preparation and Properties of the σ-Picolyl Complexes of Palladium(II), [{PdCl(C$_5$H$_4$N-2-CH$_2$)PPh$_{3-n}$Me$_n$}$_2$] (n=0,1, and 2).", *Bull. Chem. Soc. Jpn.* **62**, 1802 (1989).

Y. HAYASHI, K. MATSUMOTO, Y. NAKAMURA, and K. ISOBE, "Synthesis, Characterization, and Thermolytic Behaviour of η^3-Allyl(methyl)(tertiary phosphine)palladium(II), and X-Ray Structure of the Cluster [Pd$_4$(μ-C$_3$H$_5$)$_2$(μ-Cl)$_2$(μ-dppm)$_2$]·4C$_4$H$_8$O (dppm=Ph$_2$PCH$_2$PPh$_2$).", *J. Chem. Soc. Dalton Trans.* 1519 (1989).

N. MATSUMURA, M. TOMURA, O. MORI, Y. TSUCHIYA, S. YONEDA, and K. TORIUMI, "Synthesis and Structure of 6,7-Dihydro-2,3-disubstituted 5H-2a-Thia(2a-S^{IV})-2,3,4a,7a-tetraazacyclopent[cd]indene-1,4(2H,3H)-dithione.", *Bull. Chem. Soc. Jpn.* **61**, 2419 (1988).

K. TORIUMI, Y. WADA, T. MITANI, S. BANDOW, M. YAMASHITA, and Y. FUJII, "Synthesis and Crystal Structure of a Novel One-Dimensional Halogen-Bridged Ni^{III}-X-Ni^{III} Compound, {[Ni(*R,R*-chxn)$_2$Br]Br_2}.", *J. Am. Chem. Soc.* **111**, 2341 (1989).

SANG-OH OH, K. TORIUMI, and K. SAITO, "Trans-Dichlorobis(cyclohexylamine)palladium(II).", *Acta Cryst.* **C45**, 1213 (1989).

SONGCHUN JIN, T. ITO, K. TORIUMI, and M. YAMASHITA, "Structure of Linear-Chain Chloro-Bridged Binuclear Platinum Complex, $(NH_4)_4[Pt_2(P_2O_5H_2)_4Cl]$.", *Acta Cryst.* **C45**, 1415 (1989).

N. HARADA, J. KOHORI, H. UDA, and K. TORIUMI, "Synthesis, Absolute Stereochemistry, and Circular Dichroism of Chiral 1,8a-Dihydroazulene Derivatives.", *J. Org. Chem.* **54**, 1820 (1989).

H. OSHIO, K. TORIUMI, and S. BANDO, "Preparation and Crystal Structure of a New Hetero-Metal Mixed Valence Cu^{II}-Pt^{IV} Complex with One Dimentional Chain Structure $[Cu(en)_2][PtCl_2(en)_2](ClO_4)_4$", *Chem. Lett.* 1713 (1988).

M. MISHIMA, S. USUI, H. INOUE, M. FUJINO, and Y. TSUNO, "Stabilities of α-Cumyl Cations in the Gas Phase", *Nippon Kagaku Kaishi*, Special Articles on Structure and Reaction of Unstable Species (in Japanese), 1262 (1989).

M. MISHIMA, S. USUI, M. FUJIO, and Y. TSUNO, "Gas Phase Substituent Effect on the Stability of 1-Phenylethyl Cation in the Gas Phase", *Nippon Kagaku Kaishi*, Special Articles on Structure and Reaction of Unstable Species (in Japanese), 1269 (1989).

M. FUJIO, F. SANEMATSU, Y. TSUNO, M. SAWADA, and Y. TAKAI, "Non-Destructive Detection of Ion-Pair Return in Acetolysis of ^{13}C and ^{18}O Doubly Labeled β-Arylalkyl Tosylates. Quantitative ^{13}C-NMR Spectrometry by Using ^{18}O Isotope Effect", *Nippon Kagaku Kaishi*, Special Articles on Structure and Reaction of Unstable Species (in Japanese), 1371 (1989).

M. MISHIMA, H. INOUE, M. FUJIO, and Y. TSUNO, Gas Phase Substituent Effects in a Highly Electron Deficient System. Intrinsic Resonance Demand of 1-Aryl-1-(trifluoromethyl)ethyl Cation", *Tetrahedron Lett.* **30**, 2101 (1989).

S.-D. YOH, Y. TSUNO, M. FUJIO, M. SAWADA, and Y. YUKAWA, "Multiple Structure-Reactivity Relationships for a Menschutkin-type S_N2 Reaction", *J. Chem. Soc. Perkin Trans. 2*, 7 (1989).

N. SHIMIZU, T. MIYAHARA, M. MISHIMA, and Y. TSUNO, "Photolysis of Alcohols and Alkanones in Acetone Solutions. Photochemical [2+2] Cycloaddition Reaction between Acetone and Aliphatic Enols", *Bull. Chem. Soc. Jpn.* **62**, 2032 (1989).

M. GOTO, K. FUNATSU, N. ARITA, M. MISHIMA, M. FUJIO, and Y. TSUNO, "The Substituent Effect on Solvolyses of 2-Aryl-1-methylethyl Tosylates", *Mem. Fac. Sci., Kyushu Univ., Ser. C,* **17 (1)**, 123 (1989).

Y. TSUJI, M. FUJIO, and Y. TSUNO, "Substituent Effect on the Solvolysis of α-t-Butylbenzyl Tosylates. Solvent Modification of Substituent Effects", *Mem. Fac. Sci., Kyushu Univ., Ser. C,* **17 (1)**, 139 (1989).

M. MISHIMA, T. TERASAKI, T. ARIGA, M. FUJIO, and Y. TSUNO, "Gas Phase Basicities of Substituted Benzenes. Intrinsic Resonance Demand of Benzenium Ion", *Mem. Fac. Sci., Kyushu Univ., Ser. C,* **17 (1)**, 159 (1989).

T. RADNAI, S. ITOH and H. OHTAKI, "Liquid Structure of *N,N*-Dimethylformamide, Acetonitrile, and Their 1:1 Molar Mixture", *Bull. Chem. Soc. Jpn.* **61**, 3845 (1988).

S. ISHIGURO, T. TAKAMUKU and H. OHTAKI, "Calorimetric and Raman Spectroscopic Studies of Cadmium(II) Thiocyanato Complexes in *N,N*-Dimethylformamide", *Bull. Chem. Soc. Jpn.* **61**, 3901 (1988).

T. YAMAGUCHI, M. NOMURA, H. WAKITA and H. OHTAKI, "An Extended X-Ray Absorption Fine Structure Study of Aqueous Rare Earth Perchlorate Solutions in Liquid and Glassy States", *J. Chem. Phys.* **89**, 5153 (1988).

A. ENDOH, T. YAMAGUCHI, Y. TAMURA, O. ODAWARA, I. OKADA and H. OHTAKI, "Structural Study on Molten (^{7}Li,K)Cl and (^{7}Li,Na,K)Cl of the Eutetic Composition by Pulsed Neutron Diffraction", *Z. Naturforsch.* **43a**, 961 (1988).

S. ISHIGURO, H. SUZUKI, B.G. JELIAZKOVA and H. OHTAKI, "Solvent Effects on the Formation of Copper(II) Chloro Complexes in Acetonitrile-Dimethyl Sulfoxide Mixtures", *Bull. Chem. Soc. Jpn.* **62**, 39 (1989).

H. OHTAKI and N. FUKUSHIMA, "Dissolution of an NaCl Crystal with the (111) and (-1-1-1) Faces", *Pure & Appl. Chem.* **61**, 179 (1989).

H. KANNO, T. YAMAGUCHI and H. OHTAKI, "A Raman Investigation of the Hydration Number of Scandium(III) Ions", *J. Phys. Chem.* **93**, 1695 (1989).

T. YAMAGUCHI, S. HAYASHI and H. OHTAKI, "X-Ray Diffraction and Raman Studies of Zinc(II) Chloride Hydrate Melts, $ZnCl_2 \cdot RH_2O$ (R=1.8, 2.5, 3.0, 4.0, and 6.2)", *J. Phys. Chem.* **93**, 2620 (1989).

S. ISHIGURO, K. OZUTSUMI, L. NAGY and H. OHTAKI, "Spectrophotometric and Calorimetric Studies on the Formation of Binary (2,2'-Bipyridine)nickel(II) and Ternary (2,2'-Bipyridine)chloronickel(II) Complexes in *N,N*-Dimethylformamide", *J. Chem. Soc. Dalton Trans.* 655 (1989).

T. RADNAI, S. ISHIGURO and H. OHTAKI, "Intramolecular and Liquid Structure of 2,2,2-Trifluoroethanol by X-Ray Diffraction", *J. Solution Chem.* **18**, 771 (1989).

L. NAGY, T. YAMAGUCHI, M. NOMURA and H. OHTAKI, "EXAFS Study of Iron(III) Complexes of Sugar Type Ligands.", *Inorg. Chim. Acta.* **159**, 201 (1989).

T. YAMAGUCHI, S. HAYASHI and H. OHTAKI, "X-Ray Diffraction Study of Calcium(II) Chloride Hydrate Melts: $CaCl_2$:RH_2O (R=4.0, 5.6, 6.0, 8.6).", *Inorg. Chem.* **28**, 2434 (1989).

E. KIMURA, Y. KUROGI, S. WADA and M. SHIONOYA, "A New Tetradentate $(N^-)_2S_2$ Macrocyclic Ligand which is Highly Selective for Platinum(II) and Palladium(II).", *J. Chem. Soc., Chem. Commun.* 781 (1989).

E. KIMURA, T. KOIKE, M. KODAMA and D. MEYERSTEINE, "A Copper(I) *N,N,N',N'',N''*-Pentamethyldiethylenetriamine Complex and Its Carbon Monooxide Adduct in Aqueous Solutions.", *Inorg. Chem.* **28**, 2998 (1989).

E. KIMURA, H. ANAN, T.KOIKE and M. SHIRO, "A Convenient Synthesis of a Macrocyclic Dioxo Pentaamine and X-Ray Crystal Structure of Its Monohydrazoic Acid Salt.", *J. Org. Chem.* **54**, 3998 (1989).

M. KODAMA and E. KIMURA, "The Complexation Equilibria of Mercury(II) Ions with Macromonocyclic 16-Membered Dioxopentaamine, 18-Membered Dioxohexaamine, and Their Related Compounds.", *Bull. Chem. Soc. Jpn.* **62**, 3093 (1989).

Y. UMEZAWA, M. KATAOKA, W. TAKAMI, E. KIMURA, T. KOIKE and H. NADA, "Potentiometric Adenosine Triphosphate Polyanion Sensor Using a Lipophilic Macrocyclic Polyamine Liquid Membrane.", *Anal. Chem.* **60**, 2392 (1988).

M. KATAOKA, R. NAGANAWA, K. ODASHIMA, Y. UMEZAWA, E. KIMURA and T. KOIKE, "Potentiometric Liquid Membrane Sensors that Discriminate Linear Homologs and Geometrical/Positional Isomers of Dicarboxylates.", *Anal. Lett.* **22**, 1089 (1989).

Y. TAI, A. ISHIKAWA, K. HORIUCHI, T. ASAJI, D. NAKAMURA and R. IKEDA, "^{35}Cl Nuclear Quadrupole Relaxation in Pyridinium Hexachlorostannate(IV)", *Z. Naturforsch.* **43a**, 1002 (1988).

A. ISHIKAWA, K. HORIUCHI, R. IKEDA and D. NAKAMURA, "Phase Transitions and Anionic Dynamics of Dimethylammonium Hexachlorotellurate(IV) as Studied by Pulsed Nuclear Quadrupole Resonance of Chlorine", *J. Mol. Struct.* **192**, 237 (1989).

H. ISHIDA, N. MATSUHASHI, R. IKEDA and D. NAKAMURA, "^{1}H Nuclear Magnetic Resonance Studies on Cationic Reorientation and Translational Self-Diffusion in Two Solid Phases Including the New High-Temperature Phase of Methylammonium Sulfate", *J. Chem. Soc. Faraday Trans.1,* **85**, 111 (1989).

H. ISHIDA, T. IWACHIDO, N. HAYAMA, M. HASHIMOTO, R. IKEDA and D. NAKAMURA, "Structural Phase Transition in Solid tert-Butylammonium Nitrate as Studied by Differential Thermal Analysis and ^{1}H NMR", *Z. Naturforsch.* **44a**, 71 (1989).

S. SATO, M. KONDO, R. IKEDA and D. NAKAMURA, "Ionic Dynamics in $[(CH_3)_4N]SbF_6$ Crystals as Studied by the Temperature Dependence of ^1H and ^{19}F NMR Spin-Lattice Relaxation Time", *Ber. Bunsenges.Phys. Chem.* **93**, 450 (1989).

A. ISHIKAWA, T. ASAJI, R. IKEDA and D. NAKAMURA, "A Study of Anionic Motion in Solid Rubidium and Cesium Tetrachloroaurates(III) by Measuring the Temperature Dependence of Chlorine Nuclear Quadrupole Relaxation Times", *Z. Naturforsch.* **44a**, 125 (1989).

Y. TAI, T. ASAJI, R. IKEDA and D. NAKAMURA, "Strucrural Phase Transitions and Ionic Motions in Pyridinium Hexachlorotellurate(IV), Hexachlorostannate(IV), and Hexabromostannate(IV) Crystals as Studied by ^1H NMR", *Z. Naturforsch.* **44a**, 300 (1989).

T. TANABE, R. IKEDA and D. NAKAMURA, "The Highest-Temperature Crystalline Phase of Tetramethylammonium Thiocyanate with the Cations Performing Three-Dimensional Self-Diffusion as Revealed by Differential Thermal Analysis and Proton Magnetic Resonance Experiments", *Phys, Stat. Sol. (a),* **114**, K143 (1989).

K. NAKAJIMA, M. KOJIMA, K. TORIUMI, K. SAITO and J. FUJITA, "Crystal Structure of [VO(sal-L-ala)$(OCH_3)(CH_3OH)$](sal-L-ala=*N*-salicylidene-L-alaninate) and $\{[VO(sal\text{-}L\text{-}ala)]_2O\}_2\cdot 2CH_2Cl_2$, and the Catalytic Activity of These and Related Complexes on Asymmetric Oxidation of Methyl Phenyl Sulfide with *t*-Butyl Hydroperoxide", *Bull. Chem. Soc. Jpn.* **62**, 760 (1989).

H. MASUDA, K. MACHIDA, M. MUNAKATA, S. KITAGAWA and H. SHIMONO, "Synthesis and Structural Study of (2,2′-Bipyridine)perchlorato(styrene)copper(I).", *J. Chem. Soc. Dalton Trans.* 1907 (1988).

M. MUNAKATA, S. KITAGAWA, H. SHIMONO and H. MASUDA, "Structure of Bis(2,6-dimethylpyridine)-copper(I) Perchlorate. The Relationship Between the Cu-N(pyridine) Distance and Cu···CH_3(methyl group) Contacts.", *Inorg. Chim. Acta* **158**, 217 (1989).

H. MASUDA, A. ODANI and O. YAMAUCHI, "Structure of an L-Tyrosyl-L-histidine-Copper Complex Involving an Axial Copper(II)-Phenol OH Bonding. Implication for Substrate Binding at the Active Site of Tyrosinase.", *Inorg. Chem.* **28**, 624 (1989).

T. KOHZUMA, H. MASUDA and O. YAMAUCHI, "Structure and Properties of a Pterin-Containing Ternary Copper(II) Complex, $[Cu(bpy)(PC)(H_2O)]\cdot 3H_2O$(bpy=2,2′-Bipyridine; PC=Pterin-6-carboxylate). Implications for the Active-Site Copper-Cofactor Bonding in *Chromobacterium violaceum* Phenylalanine Hydroxylase.", *J. Am. Chem. Soc.* **111**, 3431 (1989).

M. MAEKAWA, S. KITAGAWA, M. MUNAKATA and H. MASUDA, "Nuclear Magnetic Resonance Studies of Dicopper(II) Complexes with Binucleating Ligands Containing Imidazoles.", *Inorg. Chem.* **28**, 1904 (1989).

H. SHIMOISHI, S. TERO-KUBOTA, K. AKIYAMA and Y. IKEGAMI, "Influence of Solvent Polarity on the Excited Triplet States of Nonphosphorescent 1,2-Naphthoquinone and Phosphorescent 9,10-Phenanthrenequinone: Time-Resolved Triplet ESR and CIDEP Studies", *J. Phys. Chem.* **93**, 5410 (1989).

H. TOFTLUND and S. ISHIGURO, "Surprisingly High Stability of Alkali-Metal Complexes of Ligand. Tris(2-pyridylmethyl)-amine(T.PA)", *Inorg. Chem.* **28**, 2236 (1989).

M. SUZUKI, H. OSHIO, A. UEHARA, K. ENDO, M. YANAGA, S. KIDA and K. SAITO, "Synthesis and Characterization of Dinuclear High-Spin Iron(II,III) and (III,III) Complexes with 2,6-Bis[bis(2-benzimidazolylmethyl)aminomethyl]-4-methylphenolate(1-).", *Bull. Chem. Soc. Jpn.* **61**, 3907 (1988).

M. JOHODA, M. SUZUKI and A. UEHARA, "Preparation of μ-Cyano Dinuclear Chromium(III) Complexes $M^I[F(en \text{ or } tn)_2Cr(NC)Cr(CN)_5]$ from the Doubly Complexed Salts of the Form $M^I[CrF(H_2O)(en \text{ or } tn)_2][Cr(CN)_6]$.", *Bull. Chem. Soc. Jpn.* **62**, 738 (1989).

M. SUZUKI, T. SUGISAWA, H. SENDA, H. OSHIO and A. UEHARA, "Synthesis and Characterization of a Novel Tetranuclear Manganese(II,III,III,II) Mixed Valence Complex.", *Chem. Lett.* 1091 (1989).

N. MATSUMOTO, N. TAKEMOTO, A. OHYOSHI and H. ŌKAWA, "Crystal Structure of the Imidazole and the 1,4-Di(imidazolyl)butane Adducts of N,N′-Ethylenebis(salicylideneamino)maganese(III) Perchlorate", *Bull. Chem. Soc. Jpn.* **61**, 2984 (1988).

M. SAKAMOTO, T. ISHIMORI and H. ŌKAWA, "Specific Binding of Substrates Containing Nitrogen and Oxygen Donor Groups to Copper(II)-Gadolinium(III) Hetero-Metal Center", *Bull. Chem. Soc. Jpn.* **61**, 3319 (1988).

M. HANDA, H. ŌKAWA and S. KIDA, "Dinuclear Cobalt(II), Iron(II), and Manganese(II), and Trinuclear Manganese(II) Complexes with Tridentate Ligands of NNS-Donor Set Derived from 2-Amino-ethanethiol", *Bull. Chem. Soc. Jpn.* **61**, 3353 (1988).

M. HANDA, M. MIKURIYA, Z.J. ZHONG, H. ŌKAWA and S. KIDA, "Synthesis, Properties, and Crystal Structure of Binuclear Nickel(II) and Palladium(II) Complexes of Tridentate Thiolic Ligands with NNS-Donor Set", *Bull. Chem. Soc. Jpn.* **61**, 3883 (1988)

T. AKUI, A. OHYOSHI, N. MATSUMOTO and H. ŌKAWA, "The Synthesis and Characterization of Manganese(III) Complexes with the General Formula of $[Mn(X)(L)]^{n+}$ (n=0, 1) (X=Cl^-, N_3^-, Pyridine, N-Methylimidazole, L=*N,N'*-[(Methylimino)bis(trimethylene)]bis(salicylideneaminate): The X-Ray Crystal Structure of $[Mn(N\text{-}MeIm)(L)][BPh_4]$", *Bull. Chem. Soc. Jpn.* **61**, 4155 (1988).

M. HANDA, M. MIKURIYA, H. ŌKAWA and S. KIDA, "Thiolate-Bridged Binuclear Nickel(II) Complex with Thioether Pendant Group", *Chem. Lett.* 1555 (1988).

M. MATSUMOTO, S. YAMASHITA, A. OHYOSHI, S. KOHATA and H. ŌKAWA, "Synthesis and X-Ray Crystal Structures of an Imidazolate-bridged Polynuclear Copper(II) Complex Exhibiting a Unique Helicoid Structure and its Precursor Mononuclear Complex", *J. Chem. Soc., Dalton Trans.* 1943 (1988).

H. ŌKAWA, H. TOKUNAGA, T. KATSUKI, M. KOIKAWA and S. KIDA, "Noncovalent Interactions in Metal Complexes. 16. Stereoselectivity of 1:3 Complexes of Sc, Y, La, Al, Ga, In Ions with 4-(*ℓ*-Menthyloxy)-1-phenyl-1,3-butanedione and 4-(*ℓ*-Menthyloxy)-1-p-tolyl-1,3-butanedione", *Inorg. Chem.* **27**, 4373 (1988).

M. TOMITA, N. MATSUMOTO, H. AKAGI, H. ŌKAWA and S. KIDA, "Metal Complexes (Co^{3+}, Fe^{3+}, Mn^{3+}) of the Quinquedentate Salen Analogue, 2-Methyl-4-benzylthio-*N,N'*-butane-1,2-diylbis(salicylideneimine): Crystal Structure and Sulphur Coordination Effect", *J. Chem. Soc., Dalton Trans.* 179 (1989).

D. LUNEAU, H. OSHIO, H. ŌKAWA and S. KIDA, "Synthesis and Structure of Completely Spin-coupled Trinuclear Copper(II) Complex, $[Cu(dmg)_2\{Cu(bipy)(CH_3OH)\}_2](NO_3)_2$, Bridged by Bis(dimethylglyoximato)cuprate(II) Dianion", *Chem. Lett.* 443 (1989).

N. MATSUMOTO, Z.J. ZHONG, H. ŌKAWA and S. KIDA, "Crystal Structure and Magnetic Property of the Binuclear Manganese(III) Complex $[Mn(L)H_2O]_2(ClO_4)_2$ (L=N-(acetylacetonylidene)-*N'*-(*α*-methylsalicylidene)ethylenediamine)", *Inorg. Chim. Acta* **160**, 153 (1989).

N. MATSUMOTO, Y. MAEDA, H. ŌKAWA, T. AKUI, T. KAWAJI, A. OHYOSHI, M. KODERA, H. OSHIO and S. KIDA, "Synthesis and Characterization of Imidazolate-bridged Iron(III)-Copper(II) and Manganese(III)-Copper(II) Binuclear Complexes", *J. Chem. Soc., Dalton Trans.* 943 (1989).

H. ŌKAWA, T. KATSUKI, M. NAKAMURA, N. KUMAGAI, Y. SHUIN, T. SHINMYOZU and S. KIDA, "Enantioselective Reduction of Ketones on Sterically-controlled Lanthanoid(III) Complexes", *J. Chem. Soc., Chem. Commun.* 139 (1989).

M. MIKURIYA, K. KUSHIDA, H. ŌKAWA and H. OSHIO, "Preparation, Electronic Properties and Crystal Structure of Imidazolebis-(1,10-phenanthroline)copper(II) Bis(hexafluorophosphate)", *Inorg. Chim. Acta* **159**, 149 (1989).

N. MATSUMOTO, K. INOUE, H. ŌKAWA and S. KIDA, "Ferromagnetic Interaction of Imidazolate-Bridged Copper(II)-Chromium(III)-Copper(II) Complex", *Chem. Lett.* 1251 (1989).

P. BISCARINI and R. KURODA, "Stereoselective Synthesis and Characterization of the Optically Labile Chiral Cr(III) Complex $\Delta\text{-}(+)_{589}\text{-}\{Cr[(-)bdtp]_3\}$.", *Inorg. Chim. Acta* **154**, 209 (1988).

R. MCKENNA, S. NEIDLE, R. KURODA and B.W. FOX, "Structures of Three DNA Cross-linking Agents, Ethane-1,2-di(methylsulfonate), Propane-1,3-di(methylsulfonate) and *n*-Butane-1,4-di(methylsulfonate).", *Acta Crystallogr.* **C45**, 311 (1989).

M.E. CULLEN, A.W. WYKE, R. KURODA and L.M. FISHER, "Cloning and Characterization of a DNA Gyrase A gene from *Escherichia coli* that Confers Clinical Resistance to 4-Quinolones.", *Antimicobial Agents and chemotherapy* **33**, 886 (1989).

M. WEINFELD, A.F. DRAKE, R. KURODA and D.C. LIVINGSTONE, "Isolation and Characterization of the Diastereoisomers of a Series of Phosphate-Ethylated Dinucleoside Monophosphates.", *Anal. Biochem.* **178**, 93 (1989).

S. NISHIKIORI, T. KITAZAWA, R. KURODA and T. IWAMOTO, "Orientation of Guest Benzene Molecules in Hofmann-Type and Related Clathrates by Molecular Mechanics Calculation.", *J. Inclusion Phenomena and Molecular Recognition in Chemistry* **7**, 369 (1989).

S. YAMAMOTO, U. NAGASHIMA, T. AOYAMA and H. KASHIWAGI, "Development of a Program for MCSCF Calculations with Large Basis Sets", *J. Comput. Chem.* **9**, 627 (1988).

M. SAITO and H. KASHIWAGI, "An *ab initio* MO Study on the Structure Dependence of Mössbauer Spectra in Iron Porphyrin Complexes", *Chem. Phys. Lett.* **155**, 557 (1989).

K. OHNO, J. MOROKUMA, H. HOSOYA, F. HIROTA, S. IWATA, Y. OSAMURA, H. KASHIWAGI, S. YAMAMOTO, K. KITAURA, H. NAKATSUJI, S. OBARA, K. TANAKA. M. TOGASI and S. YAMABE, "Quantum Chemistry Literature Data Base Supplement 7", *J. Mol. Struct. (Theochem)* **182**, 1 (1988).

Y. MOCHIZUKI, K. TANAKA, K. OHNO, H. TAKEWAKI and S. YAMAMOTO, "*Ab initio* CASSCF/MRSDCI Study of the $CuCH_2$ Cluster", *Chem. Phys. Lett.* **152**, 457 (1988).

U. NAGASHIMA, H. FUJIMOTO, H. INOKUCHI and K. SEKI, "Electronic and Geometric Structures of Origothiophenes", *J. Mol. Struct.* **197**, 265 (1989).

Y. YAMASHITA, Y. SUZUKI and T. MIYASHI, "2,2'-(5,8-Dihydroquinoxaline-5,8-diylidene)bis(1,3-benzodithiole)s. A New Type of Electron Donors.", *Chem. Lett.* 1607 (1989).

N. OYAMA, T. OHSAKA, H. MIYAMOTO, S. TANAKA, A. KIYOMINE, Y. KUMAGAI, T. MIYASHI and T. MUKAI, "Electropolymerization of Fused Pyrroles as New Heteroaromatic Polymers", *Synth. Metals* **28**, C193 (1989).

K. OZAWA, T. ISHIDA, K. FUKE and K. KAYA, "Electronic Spectra of Jet-cooled Phenyl Nitrene", *Chem. Phys. Lett.* **150**, 249 (1988).

K. FUKE, S. NONOSE, N. KIKUCHI and K. KAYA, "Reaction of Aluminum Clusters, Al_n (n=7-24), with Oxygen and Ammonia", *Chem. Phys. Lett.* **147**, 479 (1988).

S. NONOSE, Y. SONE, N. KIKUCHI, K. FUKE and K. KAYA, "Reaction of Vanadium and Cobalt Clusters with Ethylene and Acetylene", *Chem. Phys. Lett.* **158**, 152 (1989).

K. FUKE and K. KAYA, "Dynamics of Double-Proton-Transfer Reaction in the Excited-State Model Hydrogen-Bonded Base Pairs", *J. Phys. Chem.* **93**, 614 (1989).

K. KIMURA and N. SATOH, "High Resolution Solid State NMR of $^{27}AlF_3$ Particles Observed by a Conventional Fourier-Transform Spectrometer", *Chem. Lett.* 271 (1989).

K. KIMURA, "Shape Effect and Quantum Size Effect on Small Metal Particles", *Z. Phys.* **D11**, 327 (1989).

N. SATOH and K. KIMURA, "Metal Colloids Produced by Means of Gas Evaporation Technique. V. Colloidal Dispersion of Au Fine Particles to Hexane, Poor Dispersion Medium for Metal Sol", *Bull. Chem. Soc. Jpn.* **62**, 1758 (1989).

N. SATOH, S. BANDOW and K. KIMURA, "Dispersibility of Fine Metal Particles in Organic Solvents", *J. Colloid & Interface Sci.* **131**, 874 (1989).

K. AWAGA, T. SUGANO and M. KINOSHITA, "Ferromagnetic Intermolecular Interaction of Organic Radical, Galvinoxyl", *Synth. Metals* **27**, B631 (1988).

K. AWAGA and Y. MARUYAMA, "Ferromagnetic Intermolecular Interaction of the Organic Radical, 2-(4-Nitrophenyl)-4,4,5,5-tetramethyl-4,5-dihydro-1H-imidazolyl-1-oxy 3-oxide", *Chem. Phys. Lett.* **158**, 556 (1989).

K. AWAGA and Y. MARUYAMA, "Ferromagnetic and Antiferromagnetic Intermolecular Interactions of Organic Radicals, α-Nitronyl Nitroxides. II", *J. Chem. Phys.* **91**, 2743 (1989).

K. KATO, "Liquid Helium Level Meter by Audio-sound Detection.", *Rev. Sci. Instrum.* **60**, 1343 (1989).

T. MITANI and G. SAITO, "Cooperative Phenomena associated with Electron- and Proton-Transfer in Charge Transfer Crystals", *Shyth. Metals.* **27**, B499 (1988).

T. MITANI, H. OKAMOTO, Y. TAKAGI, I. YAMAZAKI, M. WATANABE, K. FUKUI, S. KOSHIHARA and C. ITO, "Application of the Time Characteristics of Synchrotron Radiation to Transient Spectroscopy", Springer Ser. Chem. Phys. **48** (Springer, 1988) pp.410.

T. MITANI, H. OKAMOTO, Y. TAKAGI, M. WATANABE, K. FUKUI, S. KOSHIHARA and C. ITO, "Delay-Time Modulation Spectroscopy Using a CW Mode-Locked Nd:YAG Laser Synchronized with the Synchrotron Radiation Pulses", *Rev. Sci. Instrum.* **60**, 1569 (1989).

H. OKAMOTO, T. KOMATSU, Y. IWASA, T. KODA, Y. TOKURA, S. KOSHIHARA, T. MITANI and G. SAITO, "Dynamical Aspect of Neutral-to-Ionic Phase Transition in Organic Charge-Transfer Complex Crystals", *Synth. Metals* **27**, B189 (1988).

H. OKAMOTO, T. KODA, Y. TOKURA, T. MITANI and G. SAITO, "Pressure-Induced Neutral-to-Ionic Phase Transition in Organic Charge-Transfer Crystals of Tetrathiafulvalene-p-Benzoquinone Derivatives", *Phys. Rev.* **B39**, 10693 (1989).

Y. WADA, T. MITANI, K. TORIUMI and M. YAMASHITA, "Optical Properties of Halogen-Bridged Mixed Valence Complexes, $[M(en)_2][PtX_2(en)_2](ClO_4)_4$, (M=Pt, Pd and N; X=Cl, Br and I): Effects of Metal-Atrernation", *J. Phys. Soc. Jpn.* **58** (1989).

Y. TAKAGI and K. YOSHIHARA, "Two-Photon Absorption Sampling Spectroscopy for Fast Transient Luminescence Measurements", *Ultrafast Phenomena VI,* pp.407-409 Springer, 1988.

Y. TAKAGI, T. KOBAYASHI and K. YOSHIHARA, "Multi-Quantum-Transition Sampling Spectroscopy for Fast Transient Luminescence Measurement", *Laser Spectroscopy IX*, pp.185-187 Springer, 1989.

T. KASUGA, H. YONEHARA, M. HASUMOTO and T. KINOSHITA, "Suppression of Longitudinal Coupled-Bunch Instability by Decoupling Method", *Jpn. J. Appl. Phys.* **27**, 1976 (1988).

T. KASUGA, H. YONEHARA, M. HASUMOTO and T. KINOSHITA, "Increase in Impurity in Single Bunch Mode of UVSOR Storage Ring", *Jpn. J. Appl. Phy.* **28**, 541 (1989).

H. YONEHARA, T. KASUGA, M. HASUMOTO and T. KINOSHITA, "Orbit Distortion due to UVSOR Wiggler", (Proc. 3rd Int. Conf. Synchrotron Radiation Instrumentation, 1988) *Rev. Sci. Instrum.* **60**, 1849 (1989).

T. MATSUKAWA, S. NAOE, T. MURATA and M. MORI, "Cationic Core Excitons in NaBr and $MgBr_2$", *J. Phys. Soc. Jpn.* **57**, 2916 (1988).

S. NAOE, T. MURATA and T. MATSUKAWA, "Mg K-XANES Studies in Magnesium Halides", *Physica* **B158**, 615 (1989).

T. NANBA and M. WATANABE, "Direct Observation of the Change in the Phonon Spectrum of KI due to the B1-B2 Phase Transition", *J. Phys. Soc. Jpn.* **58**, 1535 (1989).

M. WATANABE, K. SAKAI, E. NAKAMURA, J. YAMAZAKI, O. MATSUDO, K. FUKUI, E. ISHIGURO and S. MITANI, "2.2-m Rowland-circle Grazing-incidence Monochromator", *Rev. Sci. Instrum.* **60**, 2081 (1989).

M. SAKURAI, S. MORITA, J. FUJITA, H. YONEZU, K. FUKUI, K. SAKAI, E. NAKAMURA, M. WATANABE, E. ISHIGURO and K. YAMASHITA, "A Plane-grating Monochromator for Radiometric Calibration", *Rev. Sci. Instrum.* **60**, 2089 (1989).

E. ISHIGURO, M. SUZUI, Y. YAMAZAKI, E. NAKAMURA, K. SAKAI, O. MATSUDO, N. MIZUTANI, K. FUKUI and M. WATANABE, "Constant Deviation Monochromator for the Range 100 Å $\leq \lambda \leq$ 1000 Å", *Rev. Sci. Instrum.* **60**, 2105 (1989).

T. MASUJIMA, H. YOSHIDA, H. KAWATA, Y. AMEMIYA, T. KATSURA, M. ANDO, T. NANBA, K. FUKUI and M. WATANABE, "Photoacoustic Detector for Synchrotron-radiation Research", *Rev. Sci. Instrum.* **60**, 2318 (1989).

H.NAKAGAWA, T. DEGUCHI, H. MATSUMOTO, T. MIYANAGA, M. FUJITA, K. FUKUI, E. ISHIGURO, I.H. MUNRO, T. KATO and M. WATANABE, "Formation of CN^--Centers on KCl from Gaseous N_2 and CO_2 with Undulator Light", *J. Phys. Soc. Jpn.* **58**, 2605 (1989).

Review Articles and Textbooks

N. KOGA and K. MOROKUMA, "Potential Energy Surface of Olefin Hydrogenation by Wilkinson Catalyst: Comparison Between trans and cis Intermediates", in "The Challenge of d and f Electrons: Theory and Cumputation", ed. by R. Salahub and M.C. Zerner, *Am. Chem. Soc. Series* No.394, p.77 (1989).

K. MOROKUMA, K. YAMASHITA and S. YABUSHITA, "Potential Energy Surfaces of Several Elementary Chemical Reactions", in "Supercomputer Algorithms for Reactivity, Dynamics and Kinetics of Small Molecules", ed. by A. Lagana, NATO ASI Series, (Kluwer, Dordrecht), p.37 (1989).

I. OHMINE, "Molecular Dynamics and Chemical Reactions in Liquid" (in Japanese), in "The Year Book of High Technology & Science '89", Gijutsu-Shuppan, Tokyo (1989).

H. NAKAMURA, H. TAKAGI and K. NAKASHIMA, "Theoretical Study of Dissociative Recombination of Electrons", in "Dissociative Recombination: Theory, Experiment and Applications", ed. by J.B.A. Mitchell and S.L. Guberman (World Scientific, Singapore) p.73-83 (1989).

M. MATSUZAWA, "High-Rydberg Atoms" Butsurigaku Saizensen (Frontiers in Physics) (in Japanese) Vol. 24, ed. Y. Ohtsuki (Kyoritsu Shuppan) pp.119-198 (1989).

S. WATANABE and M. MATSUZAWA, "The Molecular Model and Dynamics of Multiply Excited States" *Butsuri (Proc. Phys. Soc. Jpn.)* (in Japanese) **44**, 500 (1989).

Y. SHINOZUKA, "On the Configuration Coordinate Model for Deel-Levels in Semiconductors" *Oyo Buturi* (in Japanese). **57**, 1877 (1988).

E. HIROTA, "High-Resolution Infrared Laser Spectroscopy and its Applications to Photochemistry", *Optronics* (in Japanese) **7**, 113 (1988).

E. HIROTA, "Laser High-Resolution Spectroscopy", in "Laser Handbook (in Japanese)", T. Yajima, K. Shimoda, F. Inaba, S. Namba Eds., Asakura, pp.363-367 (1989).

E. HIROTA, "Large-Amplitude Motions in Short-Lived Molecules", *Chemistry* (in Japanese) **44**, 558 (1989).

N. MORITA, "Laser Multiphoton Excitation of Doubly Excited States of Ca Atom and Study of Their Electron Correlation", *Oyo Buturi* (in Japanese) **58**, 1737 (1989).

T. KITAGAWA, "Structural Chemistry of Heme Proteins Probed by Resonance Raman Spectroscopy", in "Spectroscopic and Structural Studies of Biomedical Materials", J. Twardowski Ed. Sigma Press, pp.113-123 (1988).

K. KAMOGAWA and T. KITAGAWA, "Application of Raman Difference Spectroscopy to Solution Chemistry" in "Vibrational Spectra and Structure", J.R. Durig Ed. **17B**, pp.447-472, Elsevier (1989).

Y. UDAGAWA, "X-ray Raman Scattering – A Substitute for Soft X-ray EXAFS (in Japanese)", *Nihon Kinzoku Gakkai Kaihou* **27**, 878 (1988).

Y. UDAGAWA, "A Glance at the World of Catalysis (in Japanese)", *Shokubai* **30**, 620 (1988).

Y. UDAGAWA, "Local Structure Analysis by X-ray Raman Scattering (in Japanese)", *Nihon Kesshou Gakkaishi* **31**, 24 (1988).

Y. UDAGAWA, "An Introduction to In-house EXAFS Facilities", *Rigaku Journal* **6**, 20 (1989).

H. PETEK and K. YOSHIHARA, "Investigation of Ultrafast Radiationless Process in Isolated Molecules.", in "Ultrafast Phenomena in Spectroscopy", Z. Rudzikas, A. Piskarskas, and B. Battramiejunas Eds., World Scientific, London, 339 (1988).

Y. TAKAGI and K. YOSHIHARA, "Ultrashort Light Pulses and Ultrafast Phenomena." *Math. Sci.* (in Japanese) **306**, 46 (1988).

K. YOSHIHARA, N. NAKASHIMA and K. KEMNITZ, "Surface Energy and Electron Transfer Dynamics of Submonolayer Dyes on Organic Crystals.", in "Lasers in Atomic, Molecular, and Nuclear Physics", V.S. Letokhov Ed., World Scientific, London, 239 (1989).

K. KEMNITZ, N. NAKASHIMA and K. YOSHIHARA, "Electron Transfer between Adsorbed Dye Molecules and Organic Crystals: Model Character of the Adsorption System for Certain Aspects in Photosynthesis.", in "Photochemistry on Solid Surfaces", M. Anpo and T. Matsuura Eds., Elsevier, Amsterdam, 236 (1989).

K. YOSHIHARA, "Characteristics of Laser Chemistry.", in "Laser Handbook", New Edition (in Japanese), T. Yajima, K. Shimoda, F. Inaba, and S. Namba Eds., Asakura, Tokyo, 351 (1989).

K. YOSHIHARA, "Relaxation of Excited States.", in "Laser Handbook", New Edition (in Japanese), T. Yajima, K. Shimoda, F. Inaba, and S. Namba Eds., Asakura, Tokyo, 383 (1989).

N. NISHI and S. SAITO, "Interstellar Molecules", in "*Chemistry Today*" (Gendai Kagaku, in Japanese) **218**, 31 (1989).

N. NISHI and S. SAITO, "Comets: Snowballs of Interstellar Molecules", in "*Chemistry Today*", (Gendai Kagaku, in Japanese) **219**, 31 (1989).

R. NAKAGAKI, H. SAKURAGI and K. MUTAI, "Switching of Reaction Pathways due to Methylene Chain Length Effects", *J. Phys. Org. Chem.* **2**, 187 (1989).

K. KIMURA, "Dynamic Aspect of Excited-State Photoelectron Spectroscopy. Some Small Molecules", in "*The Structure of Small Molecules and Ions", ed. by R. Naaman and Z. Vager, (Plenum, New York, 1988),* p.173.

K. KIMURA and Y. ACHIBA, "Resonant MPI Photoelectron Study on Direct Ionization and Autoionization of Nitric Oxide Molecule", in "*Advances in Multi-Photon Processes", ed. by S.H. Lin (World Scientific, 1989),* p.317.

K. KIMURA, "Synchrotron Radiation Facility of the Institute for Molecular Science" (in Japanese), *Purometeusu, No. 69, p.34 (1989).*

K. SHOBATAKE, "Resonance in Chemical Reactions – Spectroscopy of Transition State", *Chemistry* (in Japanese), **44**, 72 (1989).

Y. MARUYAMA, "Charge-Carrier Mobilities in Organic Molecular Solids.", *Mol. Cryst. Liq. Cryst.* **171**, 287 (1989).

M. SATO and K. KUMAGAI, "New Structural Phase of $(La,Ba)_2CuO_4$", *Parity* (in Japanese) 1989 February issue.

M. SATO, "Present Status of the Experimental Studies on High-T_c Oxides", *Butsuri* (in Japanese) 1989 June issue.

M. SATO, "On the Physical Properties of the High-T_c Oxides", *Parity* 1989 *2nd Special issue on high-T_c oxides.*

M. SATO, M. SERA, M. ONODA, S. SHAMOTO, S. KONDOH, K. FUKUDA, Y. ANDO and S. Yamagata, "Broad Experimental Studies on High-T_c Oxides", *Research Report on Mechanism of Superconductivity March* 1989.

K. SEKI, "Ionization Energies of Free Molecules and Molecular Solids", *Mol. Cryst. Liq. Cryst.* **171**, 255 (1989).

H. INOKUCHI, "Studies of Organic Semiconductors for 40 Years – II. Polycyclic Aromatics as Organic Semiconductors", *Mol. Cryst. Liq. Cryst.* **171**, 23 (1989).

H. INOKUCHI, "New Organic Superconductors", *Angew. Chem.* **100**, 1817 (1988).

T. ENOKI and H. INOKUCHI, "Novel Electronic Structure and a Two-Dimensional Lattice of Hydrogen in Potassium-Hydrogen-Graphite Ternary Intercalation Compounds", *Butsuri* (in Japanese) **43**, 858 (1988).

T. MORI, "Charge Transfer Complexes of π-Acceptor/Ligand DCNQI's", *Kotai Butsuri* (in Japanese) **24**, 113 (1989).

H. OHTAKI, "Structure and Properties of Water", *Kagaku Kogyo* (in Japanese), No.9, 17 (1989).

H. OHTAKI, "Coordination Chemistry – The Eye-Appealing Field –", *Nikkei Sangyo Shinbun* (in Japanese), March 2nd (1988).

H. OHTAKI, "Transfiguration of Solution Chemistry", *Kagaku* (in Japanese), **44**, 356 (1989).

T. YAMAGUCHI, "Structure and Dynamic Properties of Liquid Water in Micropores.", *Denki Kagaku oyobi Kogyou Butsuri Kagaku* (in Japanese), **157**, 632 (1989).

E. KIMURA, "Developments in Functionalization of Macrocyclic Polyamines.", *Pure & Applied Chemistry,* **61**, 823 (1989).

E. KIMURA, "Future Development of Host-guest Chemistries.", *Yuuki Gousei Kyoukai-shi,* **583**, (1989).

E. KIMURA and M. SHIONOYA, "Enzyme Activities and Metal Ions", *Chemical Education,* **37**, 370 (1989).

E. KIMURA and T. KOIKE, "The Chemistry of Biological Metal Complexes", (Hirokawa Publishing Co.) **Chapter 12**, 236 (1989).

R. KURODA, "Host-Guest Chemistry in Biological Systems: Molecular Basis of DNA-Ligand Interactions.", *Yuki Gohsei Kagaku Kyohkai-shi* (in Japanese), **47**, 547 (1989).

H. KASHIWAGI, "Computation in Chemistry and Supercomputer System", in *"The Year Book of High Technology and Science"*, p.180 (Gijutsu Shuppan 1989).

K. YAMAGUCHI, S. YAMAMOTO and K. NASU, "Ab Initio Studies on the Electronic Structures of Copper Oxide Clusters", *Solid State Physics* (in Japanese), **24**, 350 (1989).

K. KIMURA, "To Microclusters beyond Ultrafine Particles", *Kagaku* (Iwanami, in Japanese), **59**, 153 (1989).

K. KIMURA, "Shape and Solid State Properties of Ultrafine Metal Particles", *Hyomen* (in Japanese), **27**, 733 (1989).

K. KIMURA, "High Resolution Solid State NMR of Ultrafine Particles", *Suuri Kagaku* (in Japanese), **316**, 52 (1989).

K. KATO, "Liquid Helium Sonic Level Detecter.", *Kotai Butsuri* (in Japanese), **23**, 843 (1988).

T. MITANI, T. INABE and H. OKAMOTO, "Control of Electron and Proton Transfer in Organic Crystals – Approach to Protonics –", *Oyo Buturi* (in Japanese) **58**, 1014 (1989).

T. MITANI, "Synchrotron Radiation and Its Application: SOR Spectroscopy", *Optoronics* (in Japanese) No. 87, 111 (1989).

T. MITANI, "A New Approach to Protonics in the H-Bonded Charge-Transfer Crystals", *Mol. Cryst. Liq. Cryst.* **177**, 343 (1989).

M. WATANABE, K. SHOBATAKE and T. MITANI, "Synchrotron Radiation Research in Molecular Science – Current Topics at UVSOR –", *Butsuri* (in Japanese) **43**, 775 (1988).

E. ISHIGURO and M. WATANABE, "Grazing Incidence Monochromators at the UVSOR Facility", *Hoshako* (in Japanese) **2**, 5 (1989).

Institute for Molecular Science, Myodaiji, Okazaki 444, Japan